97-4010
Vol 1 of 3

384001

CRA EXPLORATION PTY. LIMITED
ACN 000 057 125

Seventh Annual Report
For The Period Ending 1 March 1997
EL 38/89 Zeehan No. 4, Tasmania

Volume I of III

Author: SJ Tear
SAJ Russell

Date: March 1997

Licence Holder: CRA Exploration Pty. Limited

Submitted to: Chief Geologist, SE District

Copies to: Mineral Resources Tasmania
CRAE - SE District
CRAE - Zeehan
CRAE - ETIG
Allegiance Mining NL

Submitted by: A Jacross (for SA Russell / SJ Tear)

Accepted by:

97-4010

CRAE Report No. 22210

ANNUAL REPORT - EL 38/89
CRA - S TEAR/S RUSSELL
VOL 1 0F 3

Abstract

Exploration has continued on EL 38/89 (Zeehan 4) for carbonate hosted base-metal deposits within the Gordon Limestone of the Zeehan area, West Tasmania. Analogies with Irish-style carbonate hosted base metal deposits are being used to guide exploration.

Work undertaken in the 12 month period to 1/3/1997 consisted of diamond drilling (1 hole for 242.5m), zinc recovery bench tests on drillcore, a basin analysis study and an honours project on the Grieves area.

DD96ZG416 was designed to test the down dip extent of mineralisation in DD93ZG107 and DD95ZG406 on section 47900N. Only sub-economic mineralisation was intersected.

1.3m	@	3.35% Zn	from	184.5m	
2.8m	@	2.17% Zn	from	190.4m	
7.4m	@	2.58% Zn	0.31% Pb	from	216m

(Cut off grades are 1.0% Zn and 0.1% Pb).

Results from the detailed helimag survey were interpreted and incorporated into the geological map. Delineation of argillaceous units within the limestone was possible along with the recognition of major structures. Siderite alteration at Grieves Siding is also recognisable in the magnetics.

A study by CRA-ATD on zinc recoveries from Grieves drillcore concluded that the ore will be difficult to process on account of oxidation and fine grained nature of the material.

A basin analysis study was completed by Geosea Consultants (Dr Clive Burrett). Three formations were recognised in the Gordon Limestone corresponding to differing carbonate depositional environments. It was inferred that there are truncated sequences within the limestone of the Grieves area. In conjunction with the above mentioned honours project, the basin analysis study has provided a detailed stratigraphic reconstruction of depositional environments for the Grieves area during the Ordovician.

Results from the honours project also indicated multi-phase dissolution and re-precipitation of sphalerite during weathering. Lead isotope data suggests a Cambrian source to the mineralisation with the timing of emplacement at or around the late Ordovician.

The conclusion of the 1996 drilling programme is that sphalerite mineralisation and siderite alteration are replacing the dolomitised Oolite Unit. It occurs in two bands with the lower horizon having a lead enrichment of at least one or two orders of magnitude. The possibility of palaeo-weathering having reconstituted the mineralisation is still feasible.

Recommendations are for further diamond drilling down-dip or along strike from DD956ZG416 including up to 1-2 km to the north. It is also recommended to diamond drill test the mineralised structure of Grieves South.

Environmental rehabilitation consisted of ripping compacted ground around drill-sites and access tracks and the removal of rubbish and cuttings. Care has been taken to avoid unnecessary damage to vegetation.

Expenditure for the 12 month period was $114,957.

Total expenditure for this licence to 1/3/1997 is $1,040,287.

A joint venture partner is currently being sought.

Contents

Plans

Plan No.	Title	Scale
Tv 1105	EL 38/89 Zeehan 4 Location Plan	1:100,000
Tv 1022	Zeehan Project Target Plan	1:50,000
Tv 964	EL 38/89 Zeehan 4 Geology and Drillhole Location Plan	1:2,500
Tv 1040	EL 38/89 Zeehan 4 Zeehan Carbonate Grieves Prospect Cross Section : 47900N.	1:1,000
Tv 1030	EL 38/89 Zeehan 4 Zeehan Carbonate Grieves Prospect Cross Section : 47600N	1:1,000
Tv 1031	EL 38/89 Zeehan 4 Zeehan Carbonate Grieves Prospect Cross Section : 47800N	1:1,000
Tv 1042	EL 38/89 Zeehan 4 Zeehan Carbonate Grieves Prospect Cross Section : 48225N	1:1,000

Appendices

Appendix I	The Gordon Limestone Lithostratigraphy
Appendix II	Summary of Previous Exploration - Competitor and CRAE
Appendix III	Grieves - DD96ZG416. Diamond Drill Logs and Assay Results
Appendix IV	Flow Sheet for Diamond Drillcore Analysis
Appendix V	Grieves Prospect Characterisation (CRA-ATD)
Appendix VI	Detailed Helimag Data
Appendix VII	Basin Analysis Report
Appendix VIII	The Timing and Style of Pb/Zn Mineralisation at Grieves Siding, Western Tasmania.
Appendix IX	Nanotem Work
Appendix X	Zinc Mineralisation in the Gordon Limestone

1. Conclusions and Recommendations

The diamond drill hole DD96ZG416 intersected three mineralised horizons (>1% Zn), hosted within two distinct siderite zones; 179.8-193.5m and 215.4-222.6m. These horizons occur at the top and bottom of the dolomitised Oolite Unit. The zinc mineralisation is present as sphalerite within siderite both having replaced the Oolite Unit. Drilling downgraded potential for a CRA size orebody. It was decided to seek a joint venture partner.

Zinc recoveries on drillcore from Grieves were poor due to oxidation effects and the fine grained nature of the ore material.

The basin analysis study has confirmed some structural complexity within the Grieves Siding area, including the suggestion of truncated sequences due to faulting.

The detailed helimag survey has delineated the siderite zone associated with the Grieves Siding mineralisation. Several other anomalies with similar amplitudes occur in what is considered as non-prospective limestone areas. Argillaceous units in the limestone and surrounding clastic formations are well defined as magnetic lows, in particular the Siltstone Unit. Several subtle magnetic features coincide with geochemical anomalies, and are thought to be mineralised structures. Some structures transect the limestone.

An honours project on the 'Timing and Style of Pb/Zn Mineralisation of the Grieves Siding area, Western Tasmania' has shown that the mineralisation is Ordovician aged. Mineral bearing fluids were introduced via structures tapping the underlying Cambrian Mount Read Volcanics sequence. There is evidence of multiple sphalerite dissolution and re-precipitation.

The collection and compilation of data over the past two years has greatly increased the understanding of the geology of the Ordovician/Silurian sequence. Prior to further drilling or surface work, greater effort should be put into the three dimensional geometry of the limestone and reference made to the unique pattern of carbonate deposition.

Considerations for further work include:-

- Continue down-dip diamond drill tests of the Grieves mineraliation. This can be along strike north and south from DD96ZG416 or drill down to greater depths (e.g. 400m).
- The northern area of Grieves Siding is poorly understood, therefore diamond drill testing of the base of the Gordon Limestone should be undertaken.
- Diamond drill test the mineralised structure where it cuts across the Siltstone Unit at Grieves South.

2. Introduction

EL 38/89 was granted to Major Mining Ltd. on the 30th March 1990. CRAE Pty. Ltd. entered into a Joint Venture Agreement with Major on the 23rd April 1991. In late 1993 Major Mining divested its interest in the Joint Venture to Allegiance Mining, with the exploration tenements transferred to CRAE (90%) and Allegiance (10%) as tenants in common on 22nd January 1994.

EL 38/89 covers 9 km^2 located 12 km south of Zeehan on the Tasmanian West Coast (Plan Tv 1105). During the period under review, the seventh year of tenure, CRAE has a statutory requirement to spend $18,000.

CRAE's principal commodity of interest is zinc within the Ordovician Gordon Limestone.

The main prospect is at Grieves Siding, which commanded all the undertaken work for 1996. The other area of interest is Grieves South, which occurs approximately 1 km south of Grieves Siding.

This report details all exploration conducted within EL 38/89 by CRAE for the period 1/3/96 to 1/3/1997. This work consisted of 1 diamond drill hole (242.5m).

A description of the regional geology is given in Parkinson (1994).

Sub-divisions of the Gordon Limestone are made on a lithologic/lithostratigraphic basis for utilisation in drill hole logging. Explanation of formation codes is in Appendix 1.

3. Review of Previous Work

See Appendix II.

4. Exploration Completed in the 12 Month Period Ending 1 March 1997

Exploration was confined to a single diamond drill hole at Grieves, zinc recovery tests on drillcore and an honours project on the 'Timing and Style of Pb/Zn Mineralisation of the Grieves Siding area' by Darren Glover at the University of Tasmania.

See Appendix IV for the drillcore analysis routine.

4.1 Diamond Drilling (Plan Tv 964)

Grieves Siding

DD96ZG416 85° to 143° (AMG) TD 242.5m Drillrig: LY38
(Diamond Drilling of Tasmania Pty. Ltd).

Aim of Hole

The target was to test the down-dip extension of high grade zinc mineralisation associated with DD93ZG107 and DD95ZG406.

Results

This drill hole intersected two mineralised siderite horizons: 184.5m to 193.2m and 216m to 223.4m (Plan Tv 1040) that occur at the top and bottom of a dolomitised equigranular bioclastic unit - the Oolite Unit, - towards the base of the Gordon Limestone (Appendix III).

The upper horizon yielded two intercepts using a 1% Zn cut off grade.

- 1m @ 3.35% Zn (Pb 56 ppm) from 184.5m
- 2.8m @ 2.2% Zn (Pb 25 ppm) from 190.4m

The lower contact yielded:-

- 7.4m @ 2.58% Zn (0.31% Pb) from 216m

Using simple mass balance calculations it is inferred that most zinc occurs as sphalerite in the lower horizon, whilst the upper zone is a mixture of zinc siderite, sulphide and silicate.

Copper, arsenic and silver are enhanced within the lower zone up to 946 ppm, 1790 ppm and 13.2g/t respectively.

Manganese assays show a correlation with dolomitisation.

Additional cross sections showing previous drilling information have been completed - plans Tv 1030, Tv 1031 and Tv1042

4.2 Zinc Recoveries from Drillcore

CRA-ATD (Melbourne) undertook bench tests for zinc recoveries on drillcore from the Grieves Prospect. Two samples 5471296 and 5471297 were sent for characterisation. The former from DD932G107 - 154 to 163m and the latter from DD96ZG406 - 115 to 126m. Both samples are metallurgically complex, different in character and will be difficult to process. A copy of the full report is included in Appendix V.

Significantly the iron carbonate (siderite) appears to be an end member for a solid solution series, with smithsonite being the other end member. Text references to zincian siderite may in fact refer to weathering products of sphalerite (smithsonite is an acknowledged zinc secondary mineral).

Factors inhibiting recovery are:

- oxidation coatings on sulphide grains
- fine grained nature and thus poor liberation

4.3 Detailed Helimag Survey

The Gordon Limestone of the Zeehan area was flown over as part of a detailed sub-regional helicopter-borne magnetic survey. Line spacing was approximately 60m with an average flight height of 30m and sampling intervals were approximately every 3-4m. A feature of this innovative survey was that the flight lines were aimed at being perpendicular to the strike of the limestone which resulted in time consuming and complex processing.

Relevant parts of the initial report (CRAE report 22222) including the Grieves area are included in Appendix VI. Interpretation of the data has been incorporated into the geological map. Significant features include:-.

- Accurate definition of the boundaries of the Gordon Limestone with respect to the underlying and overlying clastic sequences.
- Delineation of argillaceous limestone horizons, in particular the Siltstone Unit.
- As a result of the lithological segregation, inference of fault structures can be made.
- Identification of the siderite zone at Grieves Siding. Unfortunately this anomaly is similar in amplitude and dimensions to numerous other anomalies generally in non-prospective limestone areas.
- The Upper Dolomite Unit with its inferred mineralised fluid interaction is highlighted.

4.4 Basin Analysis Study

Dr Clive Burrett of Geosea Consultants was contracted to provide a stratigraphic study of the Zeehan carbonate drill holes to establish:-

- a stratigraphic column for the Zeehan carbonate sub-basin including identification of formational boundaries.
- a measure of the variability of carbonate depositional environments and the possible inference of syn-sedimentary faults.

This was achieved successfully and a copy of the full report is included as Appendix VII.

The work has established sub-divisions of the Gordon Limestone, the Blackjacks, Myrtle and Ugbrook Formations which are recognisible throughout the Zeehan area. Some discrepancies remain, such as whether there are fault truncated sequences and the exact recognition of the facies variable Siltstone Unit (re the Lord's Siltstone in the Florentine Valley).

Drill holes viewed from EL 38/89 were DD95ZG406, DD95ZG405, DD95ZG403, DD95ZG410, DD95ZG413 and ZB1007.

4.5 Honours Project

This report details stratigraphic correlations of all the Grieves and Grieves South drill core (including previous competitor's drilling). The results have been incorporated within the sub-regional setting as produced by Geosea. The study also contains details of a microscopic examination of the zinc mineral-bearing species found within the area (Appendix VIII). In addition, a detailed examination of the paragenetic sequence is presented. It is proposed that siderite occurs as an early and as a later phase than the main zinc mineralisation.

The main conclusions of the study are:-

- Carbonate deposition has occurred at four main sites within the carbonate platform, similar to the Great Bahaman Bank and the Persian Gulf of today.
- Sulphide oxidation, dolomite dissolution and remobilisation of HCO_3- resulted in the precipitation of smithsonite, rhodochrosite and magnesite with a later hemimorphite overprint.
- Textural features of the mineralisation show evidence for repeated sphalerite dissolution and re-precipitation.
- A manganese and barium halo is associated with the main mineralised zone.
- Lead isotope ratios for galena plot close to the edge of the Cambrian field; well away from the Devonian field.
- Two possible scenarios for the fluid characteristics and source are proposed for the mineralisation at Grieves:-

  1. non magmatic, low temperature, low salinity basinal or connate brine

  and/ or;

  2. modified seawater hydrothermal fluid derived from compaction of Ordovician and Cambrian sediments by the Late Ordovician Benambran Orogeny .

5. Discussion of Results

The preferred stratigraphic horizon for zinc mineralisation at Grieves is the dolomitised Oolite Unit. This Oolite Unit has considerable strike extent throughout the Grieves area and beyond. Its thickness is generally of the order of 30m. The underlying argillaceous bioclastic unit may also be mineralised.

In DD95ZG406 and DD93ZG107, two mineralised zones are found associated with siderite alteration, dark grey clay and ferruginous clay. Generally the upper zone is lead deficient whilst the lower zone is lead enriched. This pattern of mineralisation is matched in DD96ZG416 except that in this hole, the unit between the mineralised siderite zones is the dolomitised Oolite Unit. Weathering of the dolomitic Oolite Unit is likely to remove the calcium (and magnesium) leaving behind dark grey clay minerals i.e.the Dark Grey Clay Unit, whilst recent weathering of the Siderite Unit is likely to produce the Ferruginous Clay Unit.

A very argillaceous bioclastic unit often lies beneath the Oolite Unit, particularly in the non-mineralised holes e.g. DD95ZG405. Weathering of this unit is also thought to produce dark grey clay. This unit may also have had mineralisation which on weathering converts to the lower, more clay rich sulphidic mineralised zone. Other permutations of weathering, faulting and sediment cyclicity may produce variations on this theme. Weathering is also believed to have caused the dissolution, movement and reprecipitation of sphalerite in the near surface environment. This is chemically possible in very acid, peat rich soils with a high rainfall and cold climatic conditions. Some Iberian pyrite belt discoveries have secondary siderite which is slightly magnetic (+/- secondary (weathering induced) galena).

Is it possible that the siderite of Grieves represents weathered massive pyrite and thus the siderite is not a product of the Heemskirk Granite mineralising episode?

Dolomitisation also appears to be related to faulting e.g. the dolomitic zone 60.9m - 71.7m coincides with zones of broken core and evidence of shearing.

The dolomitistion of the Oolite Unit may be the result of precursory and prevasive fluids acting prior to the main mineral-bearing phase.

6. Environment and Rehabilitation

A number of activities conducted during 1996 have impacted on the environment. These include:

- diamond drilling at Grieves

Rehabilitation of surface disturbance included:-

- capping of diamond drill hole collars
- raking of drill sites
- removal of rubbish and cuttings

All exploration work is discussed on site with Department of Industry Safety and Mines personnel prior to it being undertaken. Their advice allows for environmental impact of the proposed work to be kept to a minimum.

The drill site will naturally revegetate. No permanent new access tracks were created. Where possible, low-impact technologies were employed in exploration.

7. References

Parkinson, R G	1993	Zeehan No 4 EL 38/89, Tasmania. Report on Exploration for the Third Year of Tenure 1/3/92 to 28/2/93. CRAE Report No. 18647.
Parkinson, R G	1994	Zeehan No 4 EL 38/89, Tasmania. Report on Exploration for the Fourth Year of Tenure 1/3/93 to 28/2/94. CRAE Report No. 19635.
Parkinson, R G	1995	Zeehan No 4 EL 38/89, Tasmania. Report on Exploration for the Fifth Year of Tenure 1/3/94 to 28/2/95. CRAE Report No. 20613.
Tear S J	1996	Zeehan No 4 EL 38/89, Tasmania. Report on Exploration for the Sixth Year of Tenure 1/3/95 to 28/2/96. CRAE Report No. 21169.

8. Location

Queenstown	SK55-5	1:250,000
Pieman	7914	1:100,000
Zeehan	7914-S	1:50,000

9. Keywords

Tasmania, Ordovician, Gordon Limestone, Zeehan, Siderite, Zinc,

Helicopter-borne Magnetics, Syn-sedimentary faulting, Basin Analysis.

Diamond drilling

10. DPO Register

CRA Exploration Pty Limited
DPO Register

EL 38/89 Zeehan 4

DPO Number	LAB Batch Number	Lab Name	DPO Location	Office Date	Geologist	Tenement Number	Tenement Name	Sample Type	Number of Samples	250,000 Map Sheet	100,000 Map Sheet
77400	11709	Analabs	Zeehan	3/7/96	S. Tear	38/88	Grieves	½ DDHQ/NQ	70	SK55-5	7914

384012

97-4010

ANNUAL REPORT - EL 38/89
CRA - S TEAR/S RUSSELL
VOL 1 0F 3

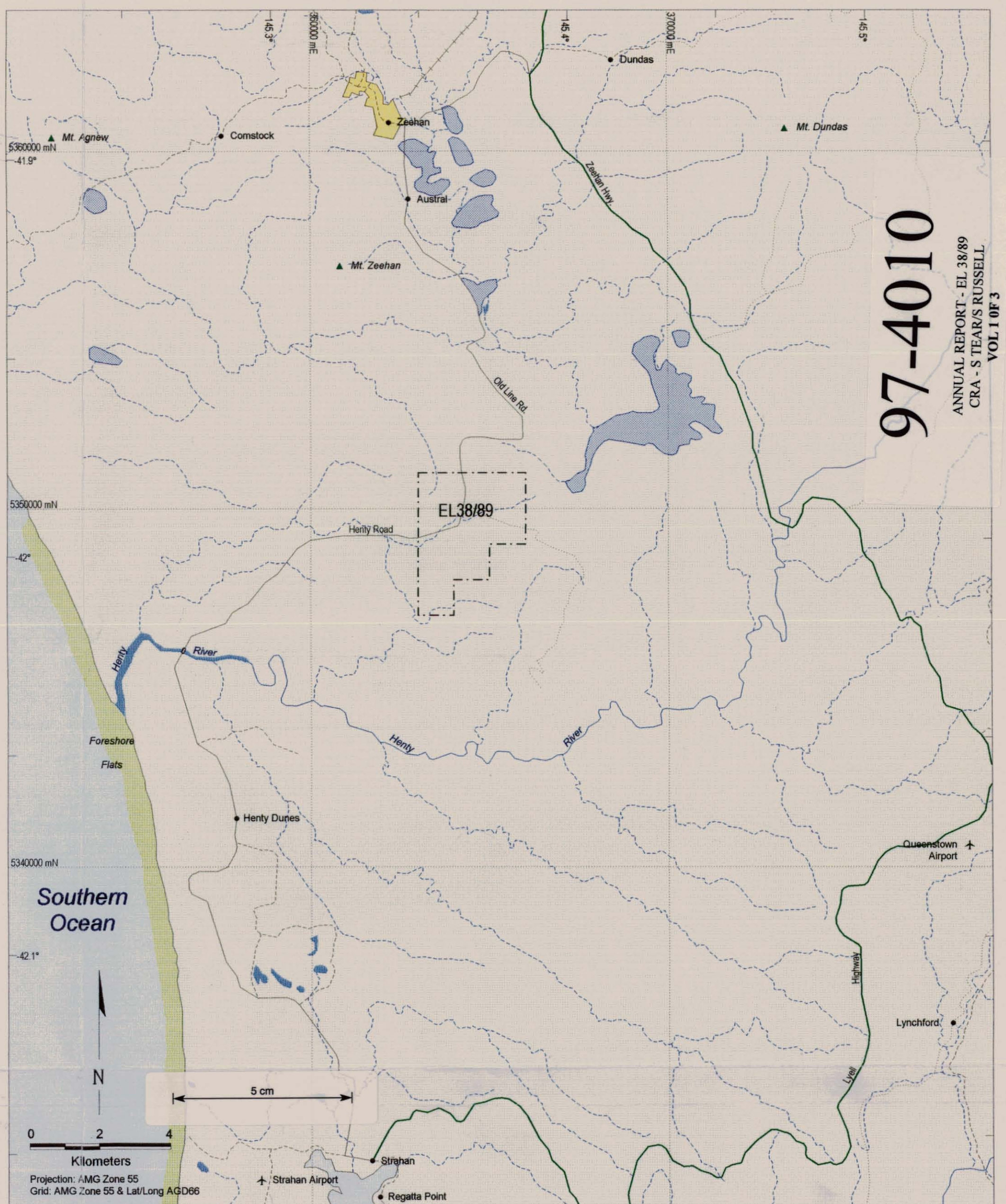

Location Diagram

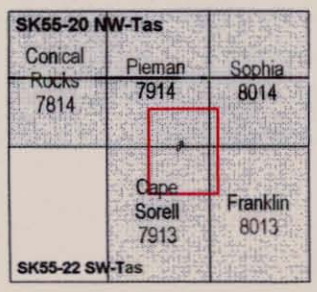

Mapsheet Reference

Legend

- Town
- Mountain
- EL Boundary
- Perennial Drainage
- Non-Perennial Drainage
- Highway
- Secondary Road
- Minor Road
- Track
- Railway
- Lake
- Swamp
- Urban

CRA EXPLORATION PTY. LIMITED

384013

EL38/89 Zeehan 4

Location Plan

Author: Simon Tear	Reference: SW Tasmania SK55-22
Drawn: Tony Sargeant	File Name: Tv1105.wor
Date: December 1995	Report No: 22210
Scale: 1:100,000	Plan No: Tv1105

360 000mE
5 370 000mN
370 000mE
380 000mE
5 370 000mN
340 000mE
5 360 000mN
350 000mE
5 360 000mN
5 350 000mN
340 000mE
5 350 000mN
350 000mE
360 000mE
370 000mE
380 000mE
5 340 000mN

EL 43/92
EL 28/88
EL 45/92
EL 38/89
EL 34/88

TENTH LEGION FAULT
FIREWOOD SIDING
LITTLE HENTY FAULT
FAULT

ZEEHAN
Sassafrass
Black Jacks
Stonehenge
Mariposa
Austral
Sunny Corner–Bahnockburn
Westerway
Avebury
Oceana
McLean Creek
Pyramid
Fan Creek
Remine
Myrtle
Professor Range
Amber Creek
King Billy
Leatherwood
Grieves
Firewood Siding
Rose Valley
Bovra
Queenstown Aerodrome

SOUTHERN OCEAN

Diamond Drillhole – CRAE 1995
Diamond Drillhole – CRAE Pre 1995
Diamond Drillhole – Other
Major Faults
CRAE Tenement Boundaries
Ordovician Gordon Limestone (usually covered by peat and gravels)

5cm
0 1 2 3 4kilometres

North

384014

97-4010

ANNUAL REPORT - EL 38/89
CRA - STEARS/RUSSELL
VOL 1 OF 3

CRA EXPLORATION PTY. LIMITED

ZEEHAN PROJECT
Target Plan

Ref.: SK55 – 5	File: Tv1022.dwg
Scale: 1 : 50000	Date: November 1995
Author: Simon Tear	Report No.: 22210
Drawn: T. Sargeant	Plan No.: Tv 1022

97-4010

ANNUAL REPORT - EL 38/89
CRA - S TEAR/S RUSSELL
VOL 1 0F 3

GRIEVES SOUTH GRID
60900E = 362 961E
46500N = 5 349 045N
GN = 071° AMG

GRIEVES GRID
60900E = 364 580E
48200N = 5 349 830N
GN = 053° AMG

GRIEVES BASE LINE 60900E

Old mine workings

Dip of beds.
Devonian cleavage.
Pre-Devonian cleavage
F— —F Fault
Sc Silurian Crotty Quartzite
Og Ordovician Gordon Limestone
Ogud upper dolomite
Ogsi carbonaceous/calcareous siltstone marker
Ogdl Undifferentiated dolomite
Ogul undifferentiated limestone
Oglz Lower Zone: undifferentiated altered carbonate and stratabound clays
Ogsd Lower Zone: siderite alteration
Om Ordovician Moina Sandstone
Diamond Drillhole
•125 Geochemical sample location and Zn result in ppm
110 • Geochemical sample location and Pb result in ppm

5 cm

0 50 100 150 200
metres

AMG North
Mag. North
12°

384015

CRA EXPLORATION PTY. LIMITED

ZEEHAN 4 EL 38/89
GRIEVES PROSPECT
COMPILATION MAP
With Zinc & Lead Geochemistry

Ref.: SK 55-05	File: Tv964
Scale: 1 : 2,500	Date: July 1995
Author: Simon Tear	Report No.: 22210
Drawn: T. Sargeant	Plan No.: Tv964

60800 E | 60900 E | 61000 E | 61100 E | 61200 E | 61300 E | 61400 E | 61500 E

200m RL

100m RL

0m

-100m RL

-200m RL

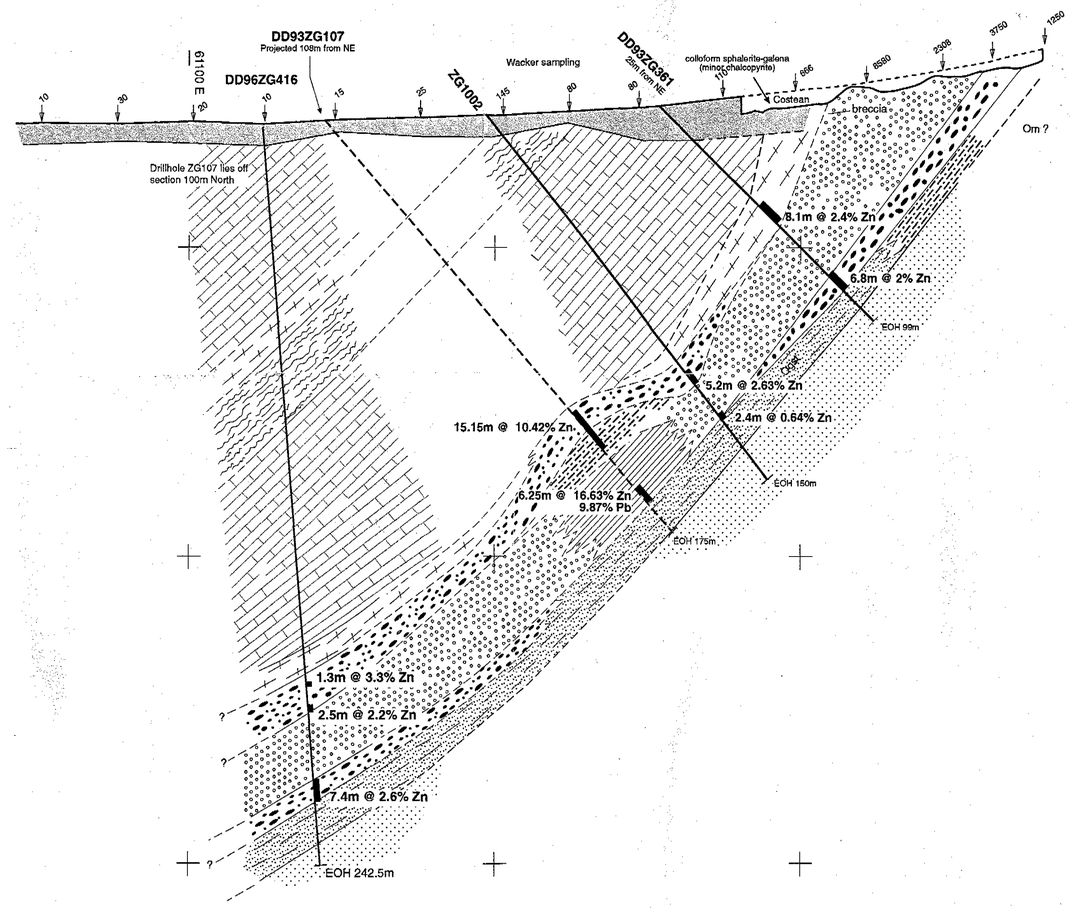

Sc	Crotty Quartzite	Silurian
Ogud	Upper Dolomite Unit	Gordon Limestone
Ogsl	Siltstone Unit	
Ogul	Undifferentiated limestone	
Ogdl	Undifferentiated dolomite	
Ogmu	Laminated Micrite Unit	
Ogoo	Oolite Unit	
Ogsd	Siderite Unit	
Ogdc	Dark grey/black clay Unit	
Ogfc	Ferruginous Clay Unit	
Ogms	Massive Sulphide Unit	
Ogst	Silty Transition Unit	
Ogfz	Fault zone	
Ogbr	Carbonate breccia	
Om	Moina Sandstone	Ordovician
Oc	Owen Conglomerate	
Ed	Dundas Group (undifferentiated)	Cambrian

Drillhole Intercept Mineralisation Styles

- Zinc as Sphalerite
- Zinc as mixed sphalerite, zinc rich siderite and zinc silicates (+carbonates)
- Zinc as zinc rich siderite

- Bedrock sampling (aircore EOH / wacker) Hole no / Zn : ppm
- Strong siderite in aircore holes
- Moderate siderite in aircore holes
- Elevated Zn in aircore holes

384016

97-4010

ANNUAL REPORT - EL 38/89
CRA - S TEAR/S RUSSELL
VOL 1 0F 3

5 cm

0 10 20 30 40 50 60m

CRA EXPLORATION PTY LIMITED

EL38/89 Zeehan 4
ZEEHAN CARBONATE
GRIEVES PROSPECT
Section : 47900 N

Author:	S J Tear	Reference:	SK5425 Queenstown
Drawn :	D Oliva	File Name :	Tv1040
Date :	Jun 1996	Report No:	22270
Scale :	1:1000	Plan No :	Tv1040

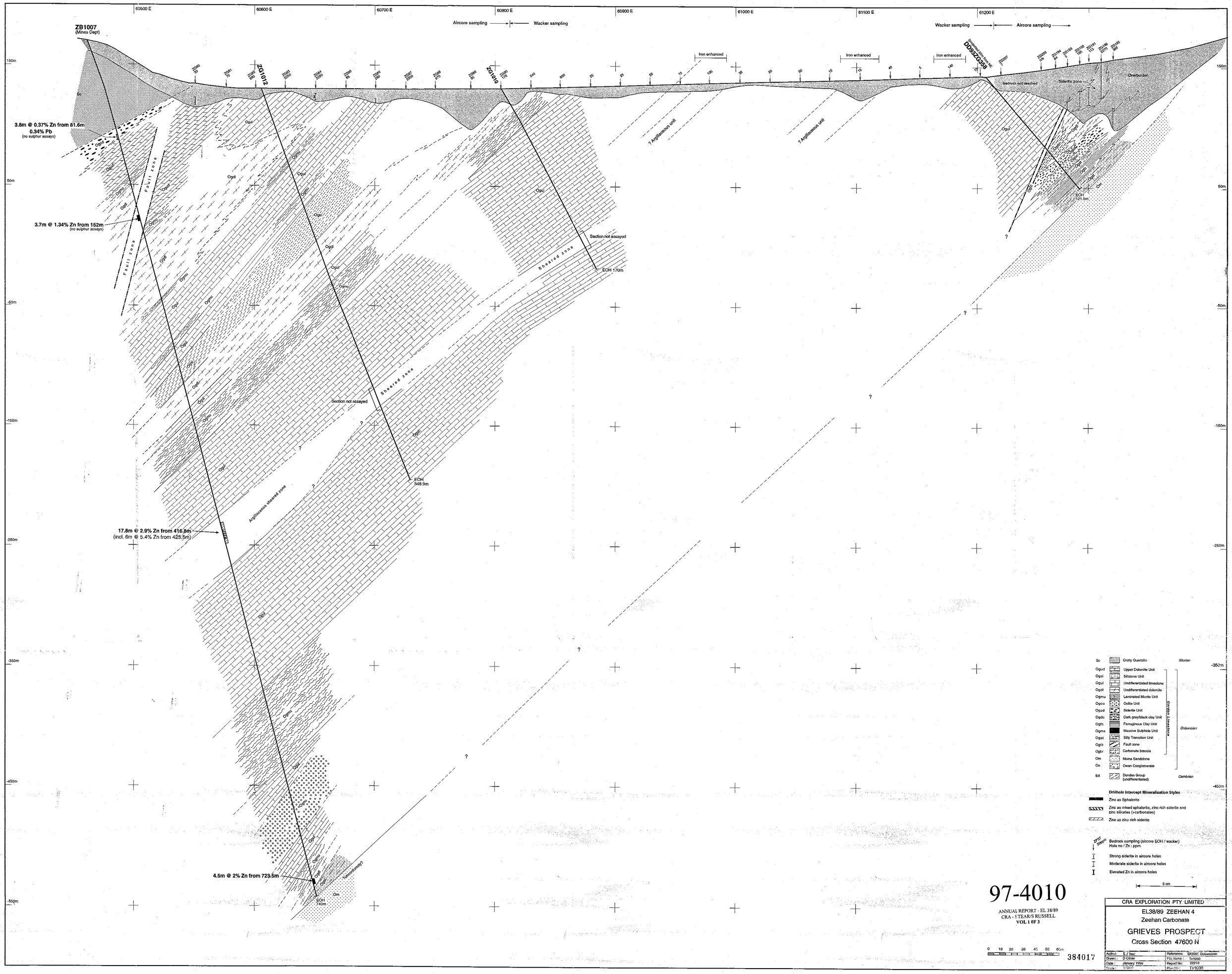

97-4010

ANNUAL REPORT - EL 38/89
CRA - S TEAR/S RUSSELL
VOL 1 OF 3

384017

CRA EXPLORATION PTY LIMITED

EL38/89 ZEEHAN 4

Zeehan Carbonate

GRIEVES PROSPECT

Cross Section 47600 N

Author:	S.J Tear	Reference:	SK9501 Grievesxsec
Drawn:	D Oliver	File Name:	Tv1030
Date:	January 1996	Report No:	22210
Scale:	1:1000	Plan No:	TV1030

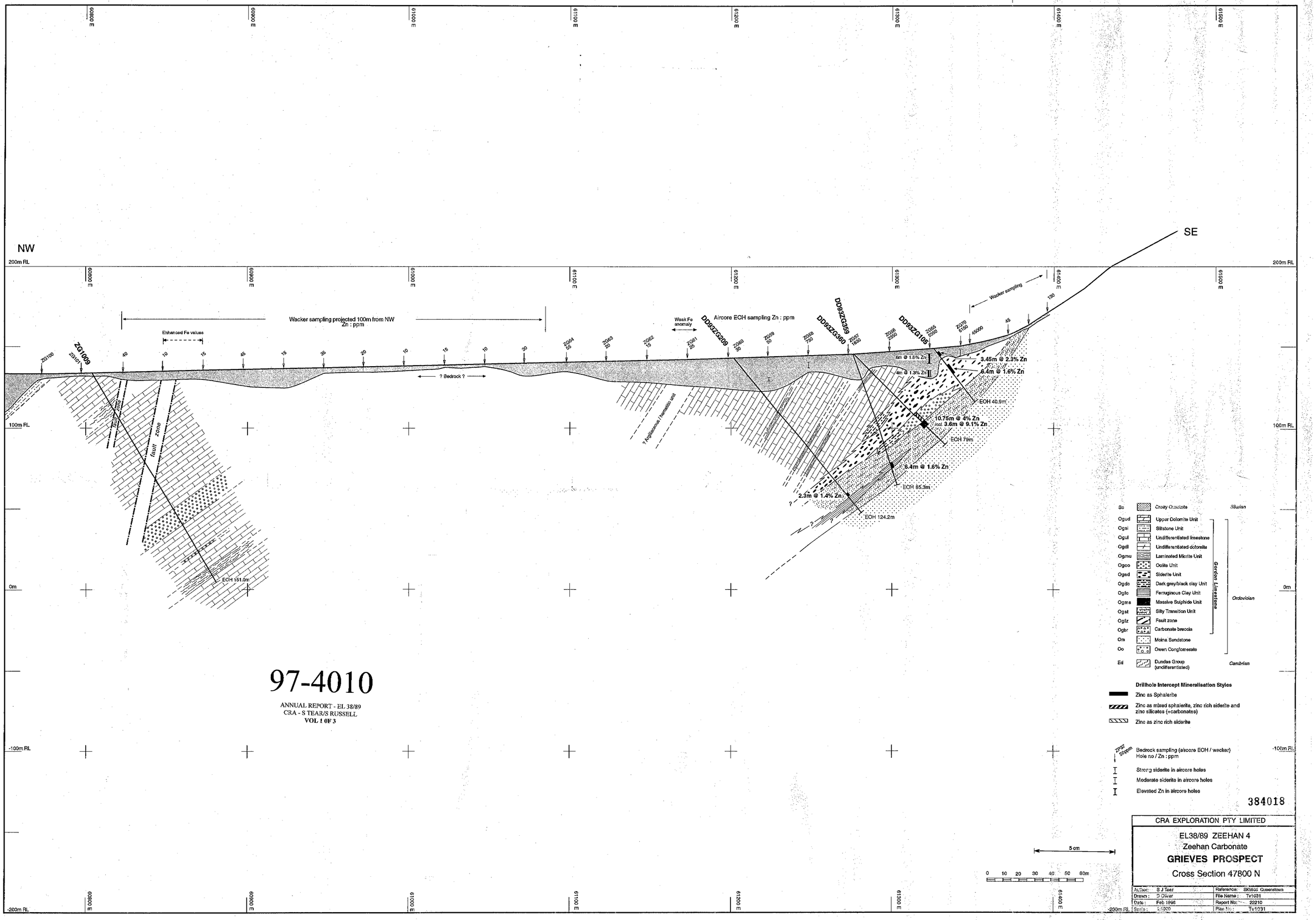

97-4010

ANNUAL REPORT - EL 38/89
CRA - S TEAR/S RUSSELL
VOL 1 0F 3

384018

CRA EXPLORATION PTY LIMITED

EL38/89 ZEEHAN 4
Zeehan Carbonate
GRIEVES PROSPECT
Cross Section 47800 N

Author:	S J Tear	Reference:	SK5866 Queenstown
Drawn:	D Oliver	File Name:	Tv1031
Date:	Feb 1996	Report No:	22210
Scale:	1:1000	Plan No:	Tv1031

60800 E | 60900 E | 61000 E | 61100 E | 61200 E | 61300 E | 61400 E | 61500 E

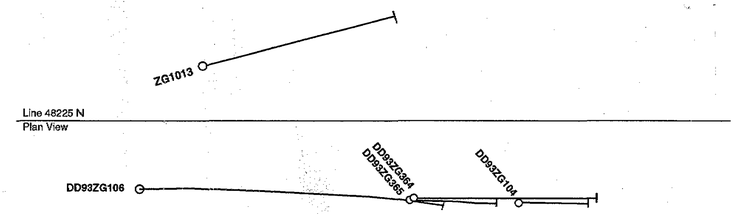

200m RL

60800 E | 60900 E | 61000 E | 61100 E | 61200 E | 61300 E | 61400 E | 61500 E

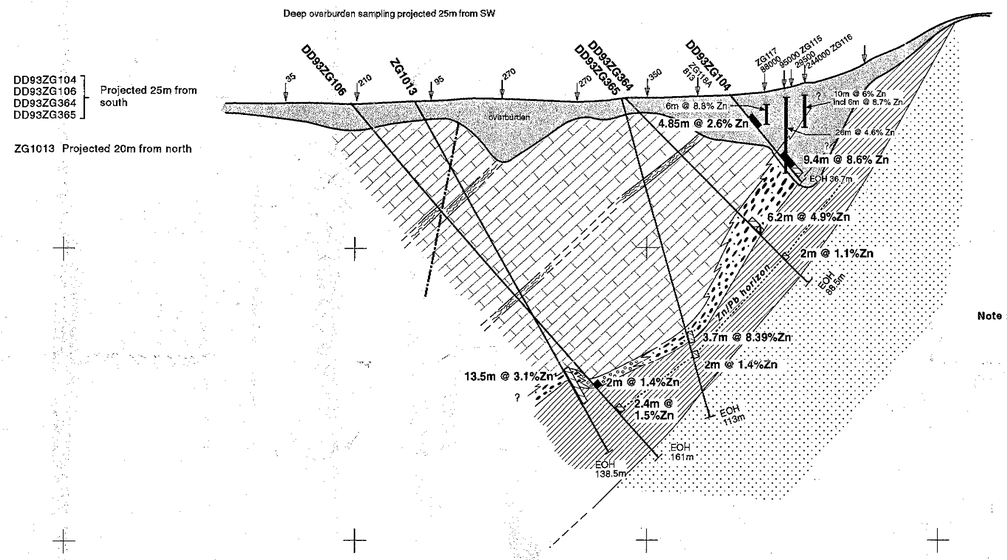

100m RL

0m

-100m RL

-200m RL

60800 E | 60900 E | 61000 E | 61100 E | 61200 E | 61300 E | 61400 E

Note : The zinc siderite zone is devoid of significant lead values

Sc	Crotty Quartzite	Silurian
Ogud	Upper Dolomite Unit	Ordovician Gordon Limestone
Ogsl	Siltstone Unit	
Ogul	Undifferentiated limestone	
Ogdl	Undifferentiated dolomite	
Ogmu	Laminated Micrite Unit	
Ogoo	Oolite Unit	
Ogsd	Siderite Unit	
Ogdc	Dark grey/black clay Unit	
Ogfc	Ferruginous Clay Unit	
Ogms	Massive Sulphide Unit	
Ogst	Silty Transition Unit	
Ogfz	Fault zone	
Ogbr	Carbonate breccia	
Om	Molna Sandstone	
Oo	Owen Conglomerate	
Ed	Dundas Group (undifferentiated)	Cambrian

Drillhole Intercept Mineralisation Styles

- Zinc as Sphalerite
- Zinc as mixed sphalerite, zinc rich siderite and zinc silicates (+carbonates)
- Zinc as zinc rich siderite

Bedrock sampling (aircore EOH / wacker)
Hole no / Zn : ppm

- Strong siderite in aircore holes
- Moderate siderite in aircore holes
- Elevated Zn in aircore holes

5 cm

0 10 20 30 40 50 60m

97-4010

ANNUAL REPORT - EL 38/89
CRA - S TEAR/S RUSSELL
VOL 1 0F 3

384019

CRA EXPLORATION PTY LIMITED

EL38/89 Zeehan 4
Zeehan Carbonate
GRIEVES PROSPECT
Section : 48225 N

Author:	S J Tear	Reference:	SK0505 Queenstown
Drawn :	D Oliver	File Name :	Tv1042
Date :	Feb 1996	Report No:	25210
Scale :	1:1000	Plan No :	Tv1042

97-4010
384020 Vol 2 of 3

CRA EXPLORATION PTY. LIMITED
ACN 000 057 125

Annual Report
For The Period Ending 1 March 1997
EL 38/89 Zeehan No. 4, Tasmania

Volume II of III

Author: SJ Tear
SAJ Russell

Date: March 1997

Licence Holder: CRA Exploration Pty. Limited

Submitted to: Chief Geologist, SE District

Copies to: Mineral Resources Tasmania
CRAE - SE District
CRAE - Zeehan
CRAE - ETIG
Allegiance Mining NL

97-4010

CRAE Report No. 22210

ANNUAL REPORT - EL 38/89
CRA - S TEAR/S RUSSELL
VOL 2 0F 3

Appendix I

The Gordon Limestone Lithostratigraphy

In the Zeehan sub-basin the Gordon Limestone has a thickness of 500m (DDH ZB1007). Drilling by CRAE has subdivided this formation into lithologic and lithostratigraphic units. These subdivisions have been utilised in the drillhole logging and are displayed below.

Drill Hole Logging Formation / Lithology Codes

Sc	=	Crotty Quartzite		**SILURIAN**
Ogud	=	Upper Dolomite	**GORDON LIMESTONE**	**ORDOVICIAN**
Ogsi	=	Siltstone Unit		
Ogul	=	Undifferentiated limestone		
Ogdl	=	Undifferentiated dolomite		
Ogmu	=	Laminated Micrite Unit		
Ogoo	=	Oolite Unit		
Ogsd	=	Siderite Unit		
Ogdc	=	Dark Grey / Black Clay Unit		
Ogfc	=	Ferruginous Clay Unit		
Ogms	=	Massive Sulphide Unit		
Ogst	=	Silty Transition Unit		
Om	=	Moina Sandstone		
Oo	=	Owen Conglomerate		
Ed	=	Dundas Group (undifferentiated)		**CAMBRIAN**

An explanation for the sub-divisions is given below.

1) The Crotty Quartzite

This formation is a sequence of deltaic quartzites of Silurian age. However in drillcore there appears to be no consistency in lithologies at its base which is perhaps to be expected. The question of a faulted contact is brought to mind and thus the unit has not been subdivided. In DD95ZM190 the sequence passes from white massively bedded sandstone into interbedded/interlaminated sands, shales and silts before finally passing into dark shales (fissile) and clays (possible fault gauge). This is possibly matched in DD95DS98 but there are considerable thickness variations.

2) The Upper Dolomite Unit (Ogud)

This is a dolomitised limestone unit that always occurs beneath the Crotty Quartzite contact. Its thickness is variable, up to 100m in DD95ZR104 and down to 25m in DD95ZM190. It is possible that the dolomitisation is fault related, the fault being the Crotty Quartzite/Gordon Limestone Contact.

3) The Siltstone Unit (Ogsi)

This is an argillaceous calcsiltite with bands of bioclastic calcarenite and nodular calcsiltite. Locally it is unreactive to dilute HCL. It generally occurs at the base of the top third of the stratigraphic column and has an average thickness of 15m.

There is a transitional upper and lower sequence to the main Siltstone Unit.

4) Undifferentiated Limestone (Ogul)

This is a bucket term to fit all limestones that do not separate out into any distinctive lithology subdivision

5) Undifferentiated Dolomite (Ogdl)

Localised zones of dolomitised limestone occur within various parts of the stratigraphic column. Unless it is part of the Upper Dolomite, it is referred to as undifferentiated dolomite. The dolomitisation is attributable to faults and/or due to mineralisation as Ogdl units often have elevated base metal values.

6) Laminated Micrite Unit (Ogmu)

This is a distinctive lithofacies comprising of banded and stylolitic fine grained calcarenites and micrites. Sometimes the laminae consist of argillaceous material. The units have an upper thickness limit of generally <3m except in specific circumstances (DD95ZP63). Birds eye micrite units are often associated with the laminated zones. The unit is not a marker horizon but occurs with sufficiently regularity in drillcore as to be able to assist stratigraphic correlations.

7) Oolite Unit (Ogoo)

This unit occurs in outcrop at Grieves Prospect as a dolomitised equigranular calcarenite unit - believed to be an oolite. It is believed that this well sorted, clean, medium grained bioclastic calcarenite unit, locally oolitic, is really part of a package of well sorted calcarenites seen towards the base of the limestone sequence.

8) Siderite Unit (Ogsd)

The Siderite Unit is an alteration facies imposed on and replacing limestone (?dolomitised) at the base of the Gordon Limestone. It is regarded as being part of the alteration associated with the replacement Zn/Pb mineralisation.

Siderite alteration also occurs at Grieves in the middle of the limestone sequence.

Siderite is also present at the upper sandstone/limestone contact at Blackjacks (DD95DB110) and Myrtle (DD95ZM190).

9) Dark Grey/Black Clay Unit (Ogdc)

These clays are encountered at surface and in drill core above 300m vertical depth. They generally are to be found at the base of the limestone, although they can occur at the top contact (DD95DB110). Dark clays can also be found in the top of drillholes where surficial weathering of the limestones has produced a black pug - depths of 45 vertical metres have been recorded (DD95ZR103). The exact nature of the clays at the basal part of the limestone is unclear. They always underlie the Oolite Unit, often can be intermixed with siderite zones of the Siderite Unit and can be part of the underlying Silty Transition Unit. Whether they are products of deep surface weathering, palaeo-weathering, fault zones or mineral-related alteration remains to be resolved.

10) Ferruginous Clay Unit.

These are light grey, orange, yellow, brown and red coloured clays, often banded. They generally occur beneath the Dark Clay Unit, although at Grieves they can be intermixed with the Dark Clays. In some instances they are sericitic, in others they can be sandy (fine grained quartz grains). They are heavily limonitic and their exact nature is unsure. It is possible that the clays are part of the Silty Transition Unit or even the underlying Moina Sandstone. Alternatively they could be weathering products of mineralisation associated with the dark clay unit.

11) Silty Transition Unit

This is the basal unit of the Gordon Limestone. It comprises of a series of partly dolomitised limestones and fine grained arenaceous units with black siltstones. It appears to have a well defined thickness of between 12-16m and in some instances overlies the Moina Sandstone conformably. Mineralisation would appear to lie immediately above the top contact of the Silty Transition Unit.

12) *Moina Sandstone*

This sandstone formation is characterised by a silicic quartzite with localised conglomerate bands, often becoming a pink silicic quartzite.

384025

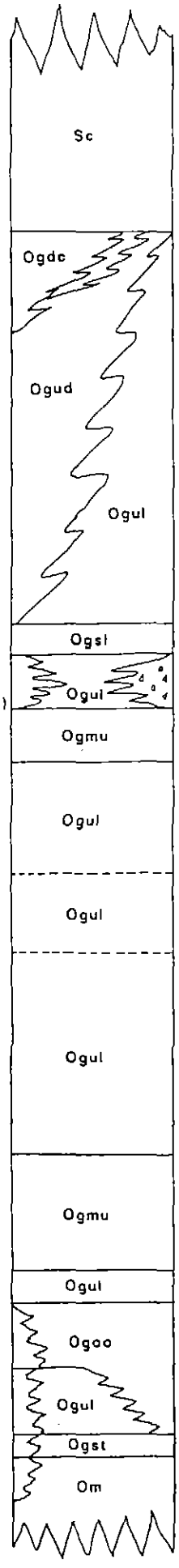

CROTTY QUARTZITE

SIDERITE ALTERATION (Ogsd)

DARK GREY CLAYS

MINERALISATION (WEAK)

UPPER DOLOMITE

UNDIFFERENTIATED LIMESTONE

SILTSTONE UNIT

Ogdl) DOLOMITE
Coarse bioclastic unit)

DOLOMITIC BRECCIA (Ogbr)

MINERALISATION

MICRITE UNIT

?ARGILLACEOUS UNIT

UNDIFFERENTIATED LIMESTONE

MINERALISATION

5 cm

EQUIGRANULAR BIOCLASTIC UNIT → OOLITE UNIT → OFFSHORE BAR

SIDERITE ALTERATION (Ogsd)

MINERALISATION

DARK GREY CLAY ALTERATION (Ogdc)

ARGILLACEOUS BIOCLASTIC UNIT

SILTY TRANSITION UNIT

FERRUGINOUS CLAY ALTERATION (Ogfe)

MOINA SANDSTONE

CRA EXPLORATION PTY. LIMITED

SEMI-SCHEMATIC

GORDON LIMESTONE STRATIGRAPHY

Ref.:	Scale:
Author: S.J.TEAR	Report No.:
Drawn: A.JELEN	Plan No.:

384026

Appendix II

Summary of Previous Exploration

Competitor and CRAE

Year 1 Activities by Major Mining prior to CRAE's involvement are detailed in the relevant statutory reports.

Year 2 Exploration by CRAE on EL 38/89 prior to 1/3/92 focussed on a compilation and review of existing open-file data. These initial activities lead to a concentration of effort on adjacent tenements EL 28/88 and EL 34/88, at that time considered to be more prospective.

Year 3 Parkinson (1993). Compilation of open-file wacker and costean geochemistry lead to the recognition that significant amounts of Zn were accumulating in surficial black pug (decomposed limestone), above apparently weakly mineralised carbonates at Grieves prospect. Wacker sampling defined three separate targets; an 1100m linear zone at the upper contact of the limestone, a 700m linear trend at the base of the limestone, and a highly conspicuous single point anomaly in the middle of the limestone.

It was thought that there may be potential for sufficient metal accumulations to justify evaluation. Rock sampling of infilled costeans, mineralogical studies, and reverse-circulation aircore drilling traverses were completed in an effort to identify areas of substantial secondary near-surface mineralisation.

Year 4 Parkinson (1994). Additional detailed aircore traverses were completed at Grieves to identify the extent of mineralised surficial clays. Significant intersections were made over 500m of strike length at the lower Gordon Limestone - Moina Sandstone contact. Better results included:-

48250N	ZG123	5.5m to 24m EOH	18.5m @ 4.5% Zn
48200N	ZG115	2.8m to 28.5m EOH	25.7m @ 4.8% Zn
48150N	ZG352	8.0m to 28.7m EOH	20.7m @ 3.6% Zn
47850N	ZG180	2.5m to 16.0m	13.5m @ 8.5% Zn
47800N	ZG54	6.0m to 22.0m	16.0m @ 13.7% Zn
47750N	ZG181	1.5m to 20.0m	18.5m @ 3.4% Zn

Diamond drilling confirmed the surface zone is the manifestation of underlying primary stratabound Zn mineralisation. Better diamond holes returned:-

48200N	ZG365	79.1m to 88.0m	8.9m @ 4.5% Zn
48000N	ZG107	123.95m to 139.1m	15.15m @ 10.4% Zn
and			
47800N	ZG359	52.75m to 63.5m	10.75m @ 4.0% Zn

Initial interpretations showed the mineralisation to have several components:-

- surficial "black-pug" style, related to geochemical dispersion and enrichment by near-surface processes.
- stratabound mineralisation associated with siderite alteration
- mineralisation within stratabound clays adjacent to the ankerite alteration zone.

Year 5 Parkinson (1995). Continuation of detailed aircore drilling ZG366-ZG400 amount to 35 holes for 312m including the following results:-

Moina Sandstone - Gordon Limestone contact - Grieves Siding

Additional 10m-spaced aircore drilling at Grieves on line 47700N returned:-

ZG368	2.0m to 12.1m EOH	10.1m @	12.9% Zn	2.6% Pb
ZG370	2.5m to 14.0m	11.5m @	6.0% Zn	
and				
ZG371	18.0m to 30.5m EOH	12.5m @	2.9% Zn	
ZG372	28.0m to 34.0m	6.0m @	3.5% Zn	

Middle portion of the limestone - Grieves South

Aircore drilling at 10m spacing around 47100N in the middle section of the limestone where hole ZG36 in early 1993 intersected 6.2m @ 5.4% Zn returned best values of:-

ZG374	0.0m to 4.8m EOH	4.8m @	14.2% Zn	3.7% Pb
ZG395	4.0m to 12.0m	8.0m @	2.0% Zn	1.0% Pb

Diamond drilling at Grieves prospect consisted of two holes (ZG364 and 365) totalling 201.5m. Additional diamond drilling results not previously reported are included here:-

Intervals exceeding 1% Zn for results received during the period are:-

47800N	ZG359	52.7m to 63.5m	10.8m	@	4.0% Zn
47800N	ZG360	71.1m to 74.8m	3.7m	@	2.3% Zn
47900N	ZG361	46.4m to 54.5m	8.1m	@	2.4$ Zn
	and	78.6m to 85.4m	6.8M	@	2.0% Zn
48000N	ZG362	18.1m to 54.0m	35.9m	@	2.8% Zn
	and	78.4m to 86.0m	7.6m	@	3.6% Zn
48000N	ZG363	41.3m to 101.0m	59.7m	@	4.0% Zn
48200N	ZG364	54.0m to 65.2m	11.2m	@	3.5% Zn
482000N	ZG365	79.1m to 88.0m	8.9m	@	4.5% Zn

Sulphur analyses indicate sphalerite to be present but probably subordinate to Zn clay and Zn-Fe-Mn carbonate.

All altered and mineralised sections from Grieves boreholes drilled by EZ were relogged. Any altered, mineralised or clay zones not previously sampled by EZ were resampled.

Best results in previously unsampled zones include (>1% Zn):-

48250N	ZG1013	105.5m to 119.0m	13.5m	@ 3.3% Zn
48400N	ZG1015	110.8m to 112.7m	1.9M	@ 1.5% Zn
	and	121.7m to 125.6m	3.9m	@ 1.1% Zn

Additional mineralogical work included XRD analysis of high zinc yielding core pulps and petrological inspections of selected altered limestones.

Other work consisted of a 'back of the envelope' study into the economics of a predicted CRA-style orebody. Magnetic susceptibility studies on core samples highlighted the weakly magnetic properties of the siderite. Reprocessing of Amoco's gravity data was also undertaken.
Further groundwork comprised:-

1. 57 wacker samples at 200 x 25m intervals - sampling concentrated on areas outside of Grieves Siding.
2. 36 decomposed organic material samples - results were regarded as unreliable.

Year 6 (Tear 1996) Diamond Drilling consisted of 8 holes for 1317.6m at Grieves South. The significant intercepts are shown below.

Hole No.	from (m)	Interval (m)	Zn %	Pb%	Ag ppm	S%	Comment
DD95ZG402	8.95	2.55	2.47	4.03	6.2	3.97	Sphalerite in dark grey/black clays
DD95ZG402	27.5	2.5	1.88	0.36	<0.5	3.58	Sphalerite in dark grey/black clays
DD95ZG403	134	1.5	0.56	0.14	1	1.8	Probable sphalerite in a dolomitised oolite unit
DD95ZG404	151	1.65	0.82	1.68	3.1	5.16	Probable sphalerite and galena in dark grey/black clays
DD95ZG406	115	10.6	14.1	<0.1	<0.5	1.63	Possibly secondary zinc (smithsonite); no siderite visible.
DD95ZG406	162	1	7.8	8.2	66	12.9	Sphalerite and galena in dark grey clays
DD95ZG406	164.3	1.7	2.1	1.7	7	1.63	Zincian siderite and sphalerite/galena in dark grey/black clays
DD95ZG407	99	5	4.8	<0.1	<0.5	4.3	Mixture of zincian siderite and sphalerite? in dark grey clay
DD95ZG408	109.1	0.3	0.94	<0.1	1	0.36	Zincian siderite?
DD95ZG412	39.4	0.8	3.39	1.27	1.7	0.35	Zincian siderite in possible fault zone
DD95ZG414	60.7	1.1	0.84	<0.1	0.7	0.65	Possible sphalerite in dolomitised oolite unit
DD95ZG415	84.6	0.95	1.92	<0.1	5.2	3.48	Possible sphalerite in dolomitised oolite unit

The holes at Grieves Siding prospect designed to test the down dip plunge of near surface mineralisation previously intersected. Overall, the results were disappointing. Despite the high values in DD96ZG406 the zinc is believed to be in the form of zinc aluminium silicate which is not easily processed.

Two zinc rich horizons occur in drillholes. The lower zone is characterised by elevated lead values. Mineralisation is thought to be a replacive style - replacing dolomitised Oolite Unit.

At Grieves South 3 drillholes (DD95ZG409, DD95ZG410, DD95ZG412) aimed to test the lower sandstone/limestone contact along strike from Grieves Siding. No significant mineralisation was intersected, although minor siderite alteration was recorded.

DD95ZG402 confirmed that a 3% Zn wacker bedrock anomaly was due to sphalerite in dark grey clays.

A detailed helimag survey was flown over the Gordon Limestone of the Zeehan area. Line spacing was approximately 60m with an average flight height of 30m and sampling intervals were approximately every 3-4m. The flight lines were flown perpendicular to the strike of the limestone.

Appendix III

Grieves -DD96ZG416 Diamond Drill Logs and Assay Results

CRA EXPLORATION PTY. LIMITED

DRILL-HOLE SUMMARY LOG

384031

HOLE NAME: DD96ZG446 AMG EAST 364487 NORTH 5349450

PROSPECT GRIEVES. GRID EAST 61150 NORTH 47900.

EL: ZEEHAN 4 EL3889 RL 140m. DEPTH 242.5m

DATE DRILLED: 6/2/1996

LOGGED BY: S. RUSSELL

DRILLING CO.: DDTAS.

DRILL TYPE: DD

DRILL RIG: LY38.

LOC DRILL CORE: ZEEHAN.

SURVEYS:

DEPTH	AZIM (AMG)	DIP	DEPTH	AZIM (AMG)	DIP
51	160	-86.5°			
101	167	-86.5°			
155	175	-86°			
207	192	-86°			
240.	193	-87°			

OBJECTIVES OF HOLE:

TEST DOWN-DIP EXTENSION OF MINERALISATION IN DD93ZG107 AND DD95ZG406.

LITHOGICAL SUMMARY:

FROM	TO	FORM CODE	COMMENTS
0	4.3	Qha.	overburden.
4.3	9.1.	Ogul.	Calcarenite + occasional bioclasts.
9.1	14.1	Ogmu.	Laminated bioclastic micrite
14.1	61.8	Ogul.	Calcarenite + argillaceous material, + burrowing/bioturbation
61.8	70.6	Ogdl.	Medium to coarse grained dolomitised calcarenite.
70.6	75.8	Ogul.	Calcarenite, locally micritic + bands of argillaceous calcarenite
75.8	81.0	Ogmu.	Fenestral limestone (micritic).
81.0	82.0	Ogdl.	Dolomitised calcarenite.
82.0	94.0	Ogmu.	Laminated micrite.
94.0	119.5	Ogul.	Calcarenite + argillaceous content + variable bioclasts.
119.5	135.2	Ogmu.	Micrite unit.
135.2	179.8	Ogul.	Calcarenites with variable argillaceous content + some red beds
179.8	193.5	Ogsd.	Siderite zone.
193.5	194.4	Ogdl.	Shear zone of extensively dolomitised calcarenite
194.4	215.4	Ogoo	Oolite unit - equigranular, bioclastic.
215.4	222.6	Ogsd.	Siderite zone.
222.6	229.1	Ogdc.	Dark grey/black clays
229.1	239.1	Ogst	Silty transition = clays + white sst fragments.
239.1	242.5	Oqa	Grey quartzite.

MINERALISATION SUMMARY:

FROM	TO	COMMENTS
184.5	185.8	3.35% Zinc in siderite
190.4	193.2	2.17% Zinc in siderite
216.0	223.4	2.58% Zinc } in siderite
		0.31% Lead }

COG = 1% Zn
0.1% Pb.

CONCLUSIONS:

Two mineralised horizons either side of the Oolite Unit.
No ferruginous clays in between the two horizons.
Lower horizon is lead-enriched.

Graphic Log

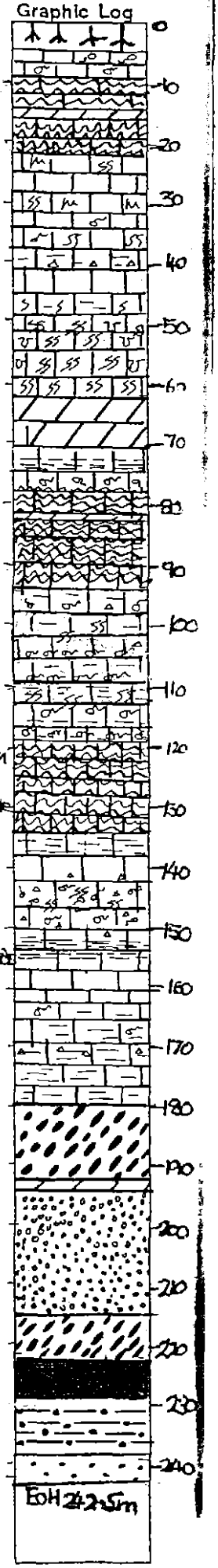

AMG: 364487 E 6115OE Local Grid
3349450 N

C.R.A. EXPLORATION PTY. LIMITED
DRILL CORE LOG

SHEET No. 1/11

TENEMENT NAME GRIEVES No. EL 3889

PLAN – MAP REFERENCE Zeenan 4 DD96

CO-ORDINATES 47900N AZIMUTH 131(Mag) DRILLERS DDTAS COMMENCED 6/2/1996 DEPTH 242.5m HOLE No. ZG416

RL COLLAR 140m INCLINATION 85° DRILL TYPE LY38 COMPLETED 6/3/1996 CASING LEFT DPO No(s) 77400

DEPTH To(M)	REC %	RQD	Graphic Log	CORE DESCRIPTION	SPECIAL FEATURES Weath, Alteration, Fracturing, Veining, Mineralization	Sample No.	From (M)	To (M)
4.3	0	–	Cha	No Recovery	–			
9.1	100	2F	Cgul	Grey, fine grained calcarenite, locally micritic. Approx. 10% interstitial argillaceous calcarenite. Occasional bioclasts (dominantly bivalves) up to 2cm Ø.	- Fine calcite veinlets. - Local syngedimentary deformation / brecciation.	5471201	4.3	6.0
12.6	60	3F	Cgmu	Laminated, fine-medium grained lmst/calcarenite grading into a coarse bioclastic base (gastropods + bivalves) up to 2cm diameter	More pronounced calcite veining + replacement of bioclasts. C/A = 45° Bedding. PAC.			
14.19	0	2F	Cgmu	As above - with smaller/ less coarse bioclastic unit @ base. The laminated calcarenite has disturbed + burrowed (?) laminae. Minor compactional stylolites.	(C/A = angle to long core axis)			
16.3	100	2F	Cgul	Grey fine grained calcarenite, locally micritic. Occasional bioclasts (up to 1cm) Grades into an interlaminated calcarenite (grey) + argillaceous calcarenite (dk grey) unit. Possible hardgrounds (?) or exploitation of weaknesses by calcite veinlets. Terminated by a medium-coarse bioclastic unit. Heavy/bioturbation. Intense	Fairly regular contact / abrupt termination by bioclastic unit above. C/A of contact = 30° Local syngedimentary breccias present.	5471202	15.0	17.1

ASSAY VALUES (Analysed by .....) MAG SUS

DEPTH	VALUE	REC From	REC To	REC (m)	REC %
4.5	0	0	4.3	0	0
5.0	0	4.3	6.0	1.65	97
5.5	8	6.0	9.0	2.80	93
6.0	0	9.0	12.0	1.80	60
6.5	6	12.0	13.7	1.25	74
7.0	5	13.7	15.0	1.30	100
7.5	0	15.0	17.1	1.90	90
8.0	0	17.1	18.9	1.60	89
8.5	0	18.9	21.2	2.20	100
9.0	0	21.2	22.7	1.50	100
9.5	6	22.7	25.5	2.25	80
10.0	5	25.5	27.0	1.40	93
10.5	0	27.0	30.0	3.0	100
10.0	5	30.3	33.0	2.6	87
11.5	7	33.0	35.8	1.7	94
12.0	5	35.8	38.9	2.3	74
12.5	8	38.9	42.0	2.6	84
13.0	0	42.0	43.2	1.2	100
13.5	15	43.2	44.6	1.2	86
14.0	10	44.6	45.9	1.1	85
14.5	10	45.9	48.0	1.9	90
15.0	6	48.0	49.3	1.1	85
15.5	7	49.3	50.9	1.4	88
16.0	9	50.9	52.5	1.3	81
16.5	5	52.5	54.0	1.6	100
18.0	9	54.0	54.7	0.7	100
17.5	5	54.7	55.7	0.9	90
18.0	5	55.7	58.7	3.0	100
18.5	8	58.7	60.9	2.0	91
19.0	9	60.9	62.1	1.2	100
19.5	7	62.1	63.7	1.3	81

3644876E } AMG
S349450N.J
61150E Local Grid

C.R.A. EXPLORATION PTY. LIMITED
DRILL CORE LOG

SHEET No. 2/4

TENEMENT NAME GRIEVES No. 38/89

PLAN – MAP REFERENCE

CO-ORDINATES 47900N AZIMUTH 131 (Mag) DRILLERS ODTAS COMMENCED 6/2/1996 DEPTH 242.5m HOLE No. ZG 416

RL COLLAR 140m INCLINATION 85° DRILL TYPE LY38 COMPLETED 6/3/96 CASING LEFT DPO No(s) 77400

DEPTH From (M)	DEPTH To(M)	Rec %	RQD	Graphic Log	CORE DESCRIPTION	SPECIAL FEATURES Weath, Alteration, Fracturing, Veining, Mineralization	Sample No.	From (M)	To (M)
16.3	22.7	90	1F	Ogul	Grey laminated medium grained calcarenite with local micrites. Discrete dk grey-black 2-3cm argillaceous bands of calcarenite. Occassional bioclasts up to 1cm diameter + local compactional synsedimentary stylolites. Some (= 5-10%) interstitial argillaceous calcarenite.	Regular contact with above unit parallel to bedding (C/A = 45°) Local pyrite mineralisation exploiting argillaceous unit adjacent to contact. C/A bedding = 90° at 16.7m + returns to 45° @ 17.1m			
22.7	29.1	95	1F	Ogul	Intermixed medium grained grey calcarenite with dk grey argillaceous calcarenite. Grades into a zone of discrete layers where argillaceous calcarenite can occur in bands up to 4-5cm. Occassional bioclasts, increasing in size and occurrence towards the base of the unit.		5471203	24.0	25.5
29.1	31.7	100	1F	Ogul	Course bioclastic, high energy unit. Contains bivalves (up to 2 cm) + gastropods (up to 2 cm). Medium grained, grey calcarenite. Rare corals (2cm Ø). Intense bioturbation + occurrence of discrete argillaceous bands.	C/A 45° bedding.			

ASSAY VALUES (Analysed by MAG SUS)

Depth	Value	Rec From	Rec To	Rec (m)	Rec %
20.0	10	63.7	65.2	1.3	87
20.5	11	65.2	66.5	1.3	100
21.0	9	66.5	67.8	1.2	92
21.5	9	67.8	69.0	1.2	100
22.0	8	69.0	70.5	1.5	100
22.5	6	70.5	71.7	1.1	92
23.0	10	71.7	73.2	1.3	87
23.5	qc	73.2	74.7	1.5	100
24.0	9	74.7	76.4	1.6	94
24.5	10	76.4	77.9	1.8	100
25.0	10	77.9	79.7	1.6	89
25.5	9	79.7	81.0	1.3	100
26.0	5	81.0	82.4	1.2	86
26.5	7	82.4	84.0	1.5	94
27.0	6	84.0	85.6	1.3	81
27.5	qc	85.6	88.5	2.9	100
28.0	qc	88.5	90.0	1.5	100
28.5	5	90.0	90.9	0.9	100
29.0	5	90.9	92.3	1.4	100
29.5	9	92.3	93.7	1.4	100
30.0	5	93.7	95.0	1.2	92
30.5	8	95.0	96.5	1.5	100
31.0	8	96.5	98.0	1.5	100
31.5	5	98.0	99.6	1.6	100
32.0	10	99.6	101.2	1.6	100
32.5	5	101.2	102.7	1.5	100
33.0	2	102.7	104.4	1.7	100
33.5	5	104.4	106.4	2.0	100
34.0	9	106.4	107.9	1.4	93
34.5	10	107.9	109.5	1.6	100
35.0	5	109.5	111.0	1.5	100

3840333

C.R.A. EXPLORATION PTY. LIMITED
DRILL CORE LOG

SHEET No. 3/11

364487 E } AMG
5349450 N
61150 E Local Grid
47900 N

TENEMENT NAME GRIEVES No. 38/89
PLAN – MAP REFERENCE
CO-ORDINATES AZIMUTH 131 (Mag) DRILLERS DDTAS COMMENCED 6/2/1996 DEPTH 242.5m HOLE No. DD96 ZG416
RL COLLAR 140m INCLINATION 85° DRILL TYPE LY38 COMPLETED 6/3/1996 CASING LEFT DPO No(s) 77400

DEPTH From (M)	DEPTH To(M)	Rec. %	RQD	Graphic Log	CORE DESCRIPTION	SPECIAL FEATURES Weath, Alteration, Fracturing, Veining, Mineralization	Sample No.	From (M)	To (M)	ASSAY VALUES (Analysed by.....) Mag Sus Depth	Mag Sus Value	Rec From	Rec To	Rec (m)	Rec %
31·7	33·6	70	5F	Ogfz	Possible Fracture Zone	Fracture zone.	6471204	32·2	33·5	35·5	9	111·0	112·5	1·5	100
					Broken core - medium grained					36·0	5	112·5	115·5	3·0	100
					grey calcarenite containing					36·5	5	116·5	117·4	1·6	84
					large amnt of clays.					37·0	4	117·4	118·4	1·0	100
33·6	37·5	90	1F	Ogwl	Intermixed / Interstitial	Discrete shear zone parallel				37·5	5	118·4	120·5	1·75	83
					(30-40% argillaceous)	to length of core.				38·0	2	120·5	121·3	0·7	88
					grey medium/fine calcarenite	Minor calcite veining.				38·5	8	121·3	123·2	1·2	63
					+argillaceous calcarenite.					39·0	7	123·2	124·5	1·1	85
					large degree of fracturing					39·5	5	124·5	125·9	1·45	100
					Some bioturbation + occasional					40·0	5	125·9	128·0	1·2	57
					bioclasts (up to 1cm)					40·5	6	128·0	129·6	1·5	94
37·5	38·9	95	5F	Ogfz	Broken core as above.	Fracture zone				41·0	11	129·6	130·1	0·5	100
38·9	39·9	85	2F	Ogwl	As for 33·6 - 37·5 - with					41·5	9	130·1	130·9	0·8	100
					less argillaceous material		5471205	39·6	40·6	42·0	4	130·9	132·1	1·0	83
					(5-10% interstitial)					42·5	9	132·1	133·6	0·5	33
39·9	42·5	100	3F	Ogwl	Grey fine grained	Possibly partial / slight				43·0	4	133·6	135·0	1·1	79
					calcarenite - micrite, with	dolomitisation.				43·5	2	135·0	136·4	1·2	86
					some birdseye textures.					44·0	5	136·4	138·2	1·2	67
					10-15% interstial argillaceous					44·5	4	138·2	139·8	0·7	44
					material. Intensely					45·0	5	139·8	141·0	1·1	92
					bioturbated.					45·5	6	141·0	144·0	3·0	100
42·5	43·6	90	5F	Ogfz	Fracture zone - medium -	Fracture zone				46·0	4	144·0	146·3	2·2	96
					fine grained calcarenite +	Calcite veining/replacement				46·5	5	146·3	149·5	2·4	75
					10-20% argillaceous dk grey	of argillaceous units. Minor				47·0	5	149·5	152·0	2·8	100
					calcarenite. Minor - no bioclasts	pyrite contained within				47·5	5	152·0	152·9	0·9	100
					present.	calcite veins/replacements.				48·0	4	152·9	155·7	2·8	100
43·6	45·6	95	3F	Ogwl	As above, with more					48·5	8	155·7	158·3	2·6	100
					pronounced replacement of arg.					49·0	9	158·3	161·0	2·7	100
					material by calcite.					49·5	7	161·0	161·9	0·9	100
45·6	46·1	100	5F	Ogfz	As above - fracture zone.	Fracture zone.				50·0	6	161·9	163·5	1·6	100
										50·5	5	163·5	164·9	1·4	100

C.R.A. EXPLORATION PTY. LIMITED

DRILL CORE LOG

SHEET No. 4/4

TENEMENT NAME GRIEVES No. 38/89

PLAN – MAP REFERENCE

AMG: 364487E

CO-ORDINATES 5344850N AZIMUTH 131 (Mag) DRILLERS DOTAS COMMENCED 6/2/1996 DEPTH 242.5m HOLE No. ZGR16

RL COLLAR 140m INCLINATION 85° DRILL TYPE LY38 COMPLETED 6/3/96 CASING LEFT DPO No(s) 77400

DEPTH From (M)	DEPTH To (M)	Rec. %	RQD	Graphic Log	CORE DESCRIPTION	SPECIAL FEATURES Weath, Alteration, Fracturing, Veining, Mineralization	Sample No.	From (M)	To (M)
46.1	48.7	90	8F	Ogwl	Discrete 1-2cm argillaceous dk grey calcarenite in fine grained calcarenite. Some burrowing + local synsedimentary brecciation	Minor calcite veins c/A BPs = 40° Some shear on calcite veins = mineral lineations	5471206	48.0	49.3
48.7	60.4	90	2F	Ogwl	Intensely burrowed + bioturbated grey fine grained calcarenite - locally micritic	Calcite veins up to 1.5cm wide increasing towards base of unit. dominantly @ 90° to core	5471207	58.7	60.0
							5471208	60.0	60.9
60.4	61.8	95	4F	Ogwl	Medium grained calcarenite (dk grey) - no obvious argillaceous layers. Possible partial dolomitisation	Minor → intense calcite veining (coarsely crystalline	5471209	60.9	62.1
61.8	65.5	85	4F	Ogdl	Fractured medium to coarse grained calcarenite with partial - extensive dolomitisation.	Fracture zone. Calcite veins contain small angular fragments of host rock. Pyrite present in some calcite veins.	5471210	62.1	63.7
							5471211	63.7	65.2
65.5	66.9	100	2F	Ogdl	Medium grained grey - dk grey calcarenite Minor dolomitisation.	Zone of medium to intense calcite veining (@ 90° ^ to core) Local hydrothermal breccias in veins ≥ 4cm diameter.	5471212	65.2	66.5
66.9	70.6	90	3F	Ogdl	Medium - coarse grained calcarenite; partial - extensive dolomitisation Local bioturbated units.	Calcite veins with angular fragments of host rock common Core heavily fractured towards base	5471213	66.5	67.8
							5471214	67.8	69.0
							5471215	69.0	70.5
70.6	71.7	75	5F	Ogwl	Dk grey rotted limstone with high clay content + calcite veining	Calcite + pyrite veining	5471216	70.5	71.7
71.7	73.0	90	3F	Ogwl	As above - some fresh calcite veining. Occasional bleb sh angle to long axis of 30°	Secondary(?) pyrite @	5471217	71.7	73.2

ASSAY VALUES (Analysed by .....)

Mag Sus Depth	Mag Sus value				Rec From	Rec To	Rec (m)	Rec %
51.0	6				164.9	165.7	0.8	89
51.5	5				165.7	168.0	2.1	91
52.0	6				168.0	170.2	2.2	100
52.5	8				170.2	171.0	0.8	100
53.0	5				171.0	174.0	3.0	100
53.5	10				174.0	176.7	2.7	100
54.0	5				176.7	179.7	2.5	83
54.5	6				179.7	180.6	0.6	67
55.0	5				180.6	184.5	0.2	5
55.5	6				184.5	185.8	0.7	54
56.0	10				185.8	187.4	0.9	56
56.5	6				187.4	188.9	1.5	100
57.0	8				188.9	190.4	0.9	60
57.5	20				190.4	191.9	1.5	100
58.0	9				191.9	193.2	1.1	92
58.5	5				193.2	195.7	2.5	100
59.0	10				195.7	196.9	1.2	100
59.5	9				196.9	198.5	1.2	75
60.0	10				198.5	201.0	0	0
60.5	5				201.0	203.1	0.8	38
61.0	21				203.1	205.1	1.6	80
61.5	14				205.1	206.9	1.6	89
62.0	5				206.9	208.5	1.6	100
62.5	30				208.5	210.0	1.5	100
63.0	20				210.0	213.0	3.0	100
63.5	5				213.0	216.0	2.7	90
64.0	5				216.0	218.3	1.9	83
64.5	15				218.3	221.6	2.5	76
65.0	25							
65.5	5							
66.0	5							

C.R.A. EXPLORATION PTY. LIMITED

DRILL CORE LOG

SHEET No. 5/11

TENEMENT NAME GRIEVES No. 38189

PLAN – MAP REFERENCE

AMG: 364487E

CO-ORDINATES 5349450N AZIMUTH 131 (Mag) DRILLERS DOTAS COMMENCED 6/2/1996 DEPTH 242.5m HOLE No. ZGH16

RL COLLAR 140m INCLINATION 85° DRILL TYPE LY38 COMPLETED 6/3/96 CASING LEFT DDH6 DPO No(s) 77400

DEPTH From (M)	DEPTH To (M)	Rec. %	RQD	Graphic Log	CORE DESCRIPTION	SPECIAL FEATURES Weath, Alteration, Fracturing, Veining, Mineralization	Sample No.	From (M)	To (M)	Rec (M)	ASSAY VALUES (Analysed by) Mag SUS. Depth	Value	Rec (From)	Rec (To)	Rec (m)	Rec %
73.0	75.8	100	1F	Ogul	Fine grained calcarenite - locally micritic with bands of ag. calcarenite (dk grey) up to 3cm wide. Grades into a heavily bioturbated/burrowed calcarenite	Very minor calcite veinlets B/Ps @ 45° C/A. Some shearing/shear planes.					66.5	25	221.6	222.4	0.4	50
											67.0	10	222.4	226.2	1.9	50
											67.5	24	226.2	227.6	1.4	100
											68.0	19	227.6	229.1	1.85	100
											68.5	15	229.1	230.6	1.2	80
75.8	78.3	100	1F	Ogul	Fenestral limestone/calcarenite Dominantly micritic with argillaceous filled fenestrae occasional bioclasts.	Little - no calcite veining					69.0	22	230.6	234.0	1.7	50
											69.5	23	234.0	236.6	1.8	70
											100	22	236.6	239.5	2.0	69
											70.5	10	239.5	240.8	0.3	22
78.3	81.0	90	2F	Ogmu	Main micrite unit. Pale grey, v. fine grained with anastomosing compactional stylolites.	Little to no veining Some pyrite on fracture surface.					71.0	26	240.8	242.5	0.5	30
											71.5	10				
											72.0	5				
											72.5	5				
81.0	82.0	80	5F	Ogdl	Fracture zone - broken core Extensive dolomitisation: more coarsely grained angular core fragments	Fracture zone					73.0	10				
											73.5	10				
											74.0	6				
											74.5	10				
82.0	82.4	70	4F	Ogmu	Micrite Unit: As for 78.3-82m	Minor calcite veinlets.					75.0	15				
82.4	84.3	60	3F	Ogmu	Broken core - (as 81-82m) Significant clays (drillers mud?) towards base. Micrite.	Fracture zone					75.5	18				
											76.0	14				
											76.5	10				
84.3	88.9	90	2F	Ogmu	Laminated micrite (pale grey) with common calcite filled birdseyes.	Minor calcite veining laminations @ 90° C/A.	547128	84.2	85.6		77.0	5				
											77.5	10				
											78.0	5				
88.9	90.3	95	4F	Ogmu	Pale grey micrite with some sand filled cavities (birdseyes). Significant fracturing of core	Fracture zone					78.5	6				
											79.0	10				
											79.5	9				
											80.0	6				
90.3	92.2	95	3F	Ogmu	Laminated pale grey micrite with variable fracturing Small calcite veinlets. (< 1cm)	Some shearing + presence of clays.					80.5	9				
											81.0	11				
											81.5	10				

3840360

C.R.A. EXPLORATION PTY. LIMITED
DRILL CORE LOG

SHEET No. 6/11
TENEMENT NAME GRIEVES No. 3889
PLAN – MAP REFERENCE
CO-ORDINATES AMG 364487E 5349450N AZIMUTH 131° (Mag) DRILLERS DOTAS COMMENCED 6/2/1996 DEPTH 242.5m HOLE No. DD96ZG416
RL COLLAR 140m INCLINATION 85° DRILL TYPE LY38 COMPLETED 6/3/96 CASING LEFT DPO No(s) 77400

DEPTH From (M)	DEPTH To (M)	Rec. %	RQD	Graphic Log	CORE DESCRIPTION	SPECIAL FEATURES Weath, Alteration, Fracturing, Veining, Mineralization	Sample No.	From (M)	To (M)	Rec (M)	ASSAY VALUES (Analysed by) Mag Sus Depth	Value
92.2	94.0	70	4F	Ogmw	broken micrite - some 'rotted' surfaces. Compactional stylolites common	Fracture zone					82.0	10
											82.5	5
											83.0	5
94.0	95.1	90	3F	Ogwl	Fine grained calcarenite locally micritic with ≈ 20% interstitial argillaceous calcarenite	Significant syn sedimentary deformation on local scale (1cm displacement)					83.5	5
											84.0	0
											84.5	4
											85.0	6
95.1	98.2	90	2F	Ogwl	Fine-medium grained darker grey calcarenite, occasionally micritic. ≈ 5% interstitial argillaceous calcarenite. Occassional bioclasts + calcite filled birdseyes	Calcite filled vugs + rare calcite veinlets. Pyrite occurs on some fracture surfaces.	5471219	95.0	96.5		85.5	4
											86.0	7
											86.5	10
											87.0	9
											87.5	10
											88.0	6
											88.5	10
98.2	101.2	100	1F	Ogwl	Intensely burrowed + bioturbated fine grained calcarenite, with ≈ 25% argillaceous calcarenite occassional bioclasts (gastropods < 1cm)	Calcite veinlets					89.0	11
											89.5	10
											90.0	10
											90.5	5
											91.0	6
											91.5	5
101.2	104.6	100	1F	Ogwl	Variably bioturbated grey calcarenite with common bivalves + gastropods (< 1cm) + large colonial corals (BRYOZOAN) (up to 6cm diameter)	Colonial corals = possible marker horizon.	5471220	104.4	106.4		92.0	11
											92.5	6
											93.0	6
											93.5	8
											94.0	10
104.6	106.0	90	2F	Ogwl	Medium grained calcarenite, with 3 bands 1-2cm wide containing abundant bioclasts (< 1cm) (gastropods + bivalves). Partial dolomitisation.	Minor calcite veining.					94.5	6
											95.0	6
											95.5	10
											96.0	10
											96.5	10
											97.0	9

384037

C.R.A. EXPLORATION PTY. LIMITED
DRILL CORE LOG

SHEET No. 7/4

TENEMENT NAME Grieves No. 3809

PLAN – MAP REFERENCE

AMG 364487E

CO-ORDINATES 5349450N AZIMUTH 131° (Mag) DRILLERS ODTAS COMMENCED 6/2/1996 DEPTH 242.5m HOLE No. JD96 2GT416

RL COLLAR 140m INCLINATION 85° DRILL TYPE LY 38 COMPLETED 6/3/96 CASING LEFT DPO No(s) 77400

DEPTH From (M)	DEPTH To(M)	Rec. (%)	RQD	Graphic Log	CORE DESCRIPTION	SPECIAL FEATURES Weath, Alteration, Fracturing, Veining, Mineralization	Sample No.	From (M)	To (M)	Rec (M)	ASSAY VALUES (Analysed by .....) mag sus Depth	Value
106.0	107.1	95	2F	Ogul	Intermixed arg. calcarenite + some micrites. Small (<1cm) bioclasts - possibly some tetradiums.						97.5	9
											98.0	5
											98.5	6
											99.0	6
107.1	109.4	95	2F	Ogul	Laminated medium grained calcarenite + common bioclastic units =5cm wide =5% argillaceous calcarenite	Bips @ C/A 45°					99.5	5
											100.0	10
											100.5	5
											101.0	10
109.4	111.7	90	2F	Ogul	Intensely bioturbated unit - pale grey calcarenite + 35% interstitial arg. calcarenite. Contains colonial corals (typical) bivalves + gastropods (up to 2cm ø) Grains become equigranular towards base.	Common calcite veins.					101.5	9
											102.0	6
											102.5	6
											103.0	6
											103.5	5
											104.0	9
											104.5	4
											105.0	5
111.7	113.5	95	1F	Ogul	Intercalated burrowed calcarenites/micrites with laminited calcarenites Occasional bioclasts (tetradiums + small bivalves)	Anastamosing calcite veins Contacts between burrowed/ intermixed zones with laminated zones = C/A 30°	547221	117.4	118.4	105.5	105.5	5
											106.0	4
											106.5	5
											107.0	6
											107.5	5
113.5	114.6	100	2F	Ogul	Broken core: grey medium grained calcarenite with discrete 1-2cm arg. calcarenite layers. Possible partial dolomitisation.	Fracture zone					108.0	2
											108.5	2
											109.0	9
											109.5	0
											110.0	10
114.6	117.4	95	2F	Ogul	Medium grained calcarenite + discrete arg. calcarenite bands. Local syndepositional deformation common. Minor bioclastic bands present throughout	Arg. units @ 45° C/A.					110.5	4
											111.0	4
											111.5	5
											112.0	5
											112.5	7

3840038

C.R.A. EXPLORATION PTY. LIMITED
DRILL CORE LOG

SHEET No. 8/11

TENEMENT NAME GRIEVES No. 38189

AMG 364487 E

PLAN – MAP REFERENCE DP96

CO-ORDINATES 5349450N AZIMUTH 131 (Mag) DRILLERS DOTAS COMMENCED 6/2/1996 DEPTH 242.5m HOLE No. ZG416

RL COLLAR 140m INCLINATION 85° DRILL TYPE LY38 COMPLETED 6/3/96 CASING LEFT DPO No(s) 77400

DEPTH From (M)	DEPTH To (M)	Rec. (%)	RQD	Graphic Log	CORE DESCRIPTION	SPECIAL FEATURES Weath, Alteration, Fracturing, Veining, Mineralization	Sample No.	From (M)	To (M)	Rec (M)
117.4	119.5	70	5F	ogfz	Dominantly broken core; Grey calcarenite with 30-40% interstitial argillaceous calcarenite. Numerous bioclasts (dominantly bivalves up to 0.5cm) replaced by calcite. Local micritic units present.	Fracture zone. Little - no calcite veining				
119.5	126.0	90	2F	ogmu	Micrite unit, locally fine grained calcarenite with variable interstitial arg. calcarenite. Rare bioclasts.	Faulted clay zone from 122.3m → 123.3m				
126.0	135.2	80	2F	ogmu	Pale grey micrite unit with compactional stylolites + laminations. Rare - no bioclasts	Minor calcite veins. Common fracturing + presence of clays/sands	5471222	130.1	132.1	
135.2	136.8	85	2F	ogul	Grey calcarenite + locally micrite unit, with increasing clays towards base. ≈ 20% interstitial argillaceous calcarenite. Rare bioclasts.	Minor calcite veins + veinlets				
136.8	140.0	65	5X	ogul	Pale pink/brown calcarenite medium grained. Local pale grey micrite units. Significant core loss (erosional surface)	Significant calcite veins towards base. ~ Typical emergent conditions (TOP OF PAC).	5471223	136.4	139.8	
							5471224	139.8	141.0	
140.0	145.3	95	2X	ogul	Grey calcarenite, locally micritic with increasing argillaceous calcarenite content downwards. large component of clays. Occasional birdseyes (calcite filled). Increased bioclasts (<0.5cm) + minor bioturbation at base.	Minor calcite veins with common 0.5 - 1cm displacements.	5471225	141.0	144.0	
							5471226	144.0	145.2	

ASSAY VALUES (Analysed by .....)

Mag Sus Depth	Mag Sus Value	Mag Sus Depth	Mag Sus Value
113.0	6	128.5	0
113.5	5	129.0	0
114.0	10	129.5	0
114.5	5	130.0	5
115.0	5	130.5	5
115.5	5	131.0	3
116.0	6	131.5	0
116.5	5	132.0	2
117.0	5	132.5	5
117.5	5	133.0	c/L
118.0	7	133.5	5
118.5	9	134.0	5
119.0	9	134.5	c/L
119.5	4	135.0	5
120.0	5	135.5	15
120.5	2	136.0	0
121.0	6	136.5	2
121.5	6	137.0	4
122.0	5	137.5	c/L
122.5	4	138.0	15
123.0	6	138.5	c/L
123.5	9	139.0	c/L
124.0	6	139.5	0
124.5	4	140.0	0
125.0	5	140.5	0
125.5	4	141.0	6
126.0	0	141.5	9
126.5	0	142.0	4
127.0	5	142.5	12
127.5	4	143.0	11
128.0	0	143.5	5

384039

C.R.A. EXPLORATION PTY. LIMITED

DRILL CORE LOG

SHEET No. 9/11

TENEMENT NAME GRIEVES. No. 38189

PLAN – MAP REFERENCE

364487E ?AMG
5349450N

CO-ORDINATES 611500E 4790N AZIMUTH 131 (Mag) DRILLERS ODTAS COMMENCED 6/2/1996 DEPTH 242.5m HOLE No. QD96ZG416

RL COLLAR 140m INCLINATION 85° DRILL TYPE LY38 COMPLETED 6/3/1996 CASING LEFT DPO No(s) 77400

DEPTH From (M)	DEPTH To(M)	Core Rec. (M)	Core Size	Graphic Log	CORE DESCRIPTION	SPECIAL FEATURES Weath, Alteration, Fracturing, Veining, Mineralization	Sample No.	From (M)	To (M)	Rec (M)	ASSAY VALUES (Analysed by.....) Mag depth	Mag value	SUS	Mag depth	Mag value	SUS	Mag depth	Mag value	SUS
145.3	152.0	95	3X	Qgul	Grey calcarenite - (fine grained) capped	- Significant fracturing of core	5471227	145.2	146.3		144.0	15		159.5	4		175	4	
					by pink coloured calcarenite	- Calcite veining.	5471228	146.3	149.5		144.5	15		160.0	8		175.5	4	
					at top of interval (20cm).	- Possible fracture zone.	5471229	149.5	151.7		145.0	15		160.5	15		176	3	
					Some elongated calcite filled		5471230	151.7	152.9		145.5	15		161.0	7		176.5	2	
					birdseye structures are present.						146.0	9		161.5	10		177	13	
					occasional bioclasts.	Fractures along b/ps. @ 45°	5471231	152.9	154.0		146.5	8		162.0	13		177.5	3	
152.0	156.0	100	3F	Qgul	Dark grey argillaceous	angle to core axis.					147.0	9		162.5	20		178	10	
					calcarenite - rare to no	Minor calcite veining.					147.5	12		163.0	14		178.5	15	
					macroscopic bioclasts.	Some shearing surfaces					148.0	c/L		163.5	11		179	40	
156.0	166.2	95	2	Qgul	Grey calcarenite - fine -	Minor calcite veining					148.5	c/L		164.0	5		179.5	c/L	
					medium grained, with	Bedding = ≃45°/A.					149.0	0		164.5	4		180	20	
					30-40% interstitial argillaceous						149.5	0		165.0	9		180.5	75	
					calcarenite. Occasional						150.0	5		165.5	26		181	c/L	
					birdseyes + rare bioclasts.						150.5	4		166.0	19		181.5	c/L	
166.2	167.2	100	3X	Qgul	Bedded clay zone		5471232	165.7	168.0		151.0	0		166.5	4		182	c/L	
					(possibly represents						151.5	18		167.0	60		182.5	c/L	
					top of PAC)						152.0	18		167.5	5		183.0	c/L	
167.2	172.5	100	2F	Qgul	Intermixed grey fine grained	Fine calcite veinlets +					152.5	10		168.0	0		183.5	13	
					calcarenite + argillaceous dk	occasional argillaceous horizons					153.0	15		168.5	8		184	c/L	
					grey calcarenite. Occasional	replaced by calcite. May also					153.5	10		169.0	5		184.5	c/L	
					calcite filled birdseye features	contain red (ferruginous?)					154.0	11		169.5	11		185	65	
					towards base	material. B/Ps @ 45° c/A.					154.5	2		170.0	25		185.5	47	
172.5	176.8	100	2F	Qgul	Grey, medium grained	Minor 10cm clay zone @	5471233	174.0	176.0		155.0	4		170.5	7		186	65	
					calcarenite containing	174m.					155.5	22		171.0	5		186.5	42	
					abundant bioclasts (<0.3cm)	Calcite veining.					156.0	5		171.5	3		187	35	
					+ birdseye structures. Large						156.5	10		172.0	0		187.5	c/L	
					(8cm ø) clast of red siltstone						157.0	c/L		172.5	0		188	96	
					/ calcisiltite within calcarenite						157.5	10		173.0	0		188.5	70	
					@ 176.4m, indicative of shallow						158.0	10		173.5	3		189	50	
					marine / emergent conditions (PAC ?? BAC).						158.5	8		174.0	5		189.5	25	
											159.0	0		174.5	3		190.	55	

3840440

C.R.A. EXPLORATION PTY. LIMITED

DRILL CORE LOG

SHEET No. 10/11

TENEMENT NAME GREVES No. 38/89

PLAN – MAP REFERENCE

CO-ORDINATES 364487E 5349450N AMG AZIMUTH 131 (Mag) DRILLERS DOTAS COMMENCED 6/2/96 DEPTH 242.5m HOLE No. DD96 ZG446

RL COLLAR 140m INCLINATION 85° DRILL TYPE LY38 COMPLETED 6/3/96 CASING LEFT DPO No(s) 77400

DEPTH From (M)	DEPTH To(M)	Core Rec. (M)	Core Size	Graphic Log	CORE DESCRIPTION	SPECIAL FEATURES Weath, Alteration, Fracturing, Veining, Mineralization	Sample No.	From (M)	To (M)	Rec (M)	ASSAY VALUES (Analysed by .....) MAG SUS Depth	MAG SUS Value	MAG SUS Depth	MAG SUS Value
176·8	177·0	100	3F	Ogwl	Medium grained grey calcarenite		5471234	176·0	178·0		190·5	c/L	206	18
					with discrete 0·5cm horizons						191	38	206·5	11
					of argillaceous calcarenite.						191·5	45	207	37
177·0	178·6	90	3X	Ogwl	Grey medium grained	Minor calcite veining	5471235	178·0	178·7		192	180	207·5	28
					calcarenite + 5-10% interstitial	Significant fracturing of					192·5	78	208	46
					argillaceous calcarenite.	core.					193	75	208·5	40
178·6	179·8	20	3X	Ogwl	Red medium grained calcisiltite		5471236	178·7	179·7		193·5	60	209	12
					(top of PAC) - undergone subaerial		5471237	179·7	180·6		194	27	209·5	9
					exposure.		5471238	180	184·5		194·5	38	210	20
179·8	193·3	52	2X	Ogsd	Zone of sideritic alteration.	Possible shear zone causing	5471239	184·5	185·8		195	30	210·5	20
					Partially rotted, with slight	siderite alteration.	5471240	185·5	187·4		195·5	23	211	20
					reaction with acid. Remnant	- Grey/Brown/colouration.	5471241	187·4	188·9		196	18	211·5	22
					red-bed @ 190·4m.	Olive Green	5471242	188·9	190·4		196·5	65	212	33
193·3	193·5	100	2F	Ogsd	Non calcareous red siltstone/		5471243	190·4	191·9		197	50	212·5	180
					sandstone, with sharp		5471244	191·9	193·2		197·5	75	213	15
					upper contact - possibly sheared		5471245	193·2	194·4		198	25	213·5	8
193·5	194·4	100	3X	Ogdl	Sheared zone of calcarenite,	Shear zone	5471246	194·4	195·7		198·5	30	214	5
					extensively dolomitised.		5471247	195·7	196·9		199	c/L	214·5	4
					Significant clay component		5471248	196·9	198·5		199·5	c/L	215	21
					(Grey/DK Grey colouration.		5471249	201·0	203·1		200	c/L	215·5	55
194·4	215·0	95	2F	Ogoo	Equigranular grey bioclastic	Calcite veining.	5471250	203·1	205·1		200·5	c/L	216	c/L
					unit - (oolitic + calcareous).	Siderite alteration	5471251	205·1	206·9		201	c/L	216·5	250
					Extensive dolomitisation,	(more minor than above	5471252	206·9	208·5		201·5	28	217	240
					(areas of white matrix	unit) increases density	5471253	208·5	210·0		202	20	217·5	220
					brecciation). Areas of	of core.	5471254	210·0	211·5		202·5	85	218	110
					red haematitic staining		5471255	211·5	213·0		203	c/L	218·5	200
215·0	215·4	100	2X	Ogoo	Shear zone - brecciated	Shear zone	5471256	213·0	213·9		203·5	25	219	210
					dolomitised equigranular		5471257	213·9	215·7		204	0	219·5	150
					bioclastic unit		5471258	215·7	216·0		204·5	15	220	140
215·4	222·6	60	4X	Ogsd	DK green/grey sideritic alteration	Pyrite present in some regions	5471259	216·0	218·3		205	8	220·5	240
					zone, partially rotted. Significant	clays. Brick red alteration	5471260	218·3	221·6		205·5	10	221	160

@ 221m.

384041

C.R.A. EXPLORATION PTY. LIMITED

DRILL CORE LOG

SHEET No. 1 of 11

TENEMENT NAME Zeehan 4 No. 38/89

PLAN – MAP REFERENCE GRIEVES

CO-ORDINATES 364487 E AMG 5349450N AZIMUTH 131° (mag) DRILLERS DDTAS COMMENCED 6/2/96 DEPTH 242.5m HOLE No. DD96 ZG416

RL COLLAR 140m INCLINATION 85° DRILL TYPE LY38 COMPLETED 6/3/96 CASING LEFT DPO No(s) 77400

DEPTH From (M)	DEPTH To(M)	Core Rec. (M)	Core Size	Graphic Log	CORE DESCRIPTION	SPECIAL FEATURES Weath, Alteration, Fracturing, Veining, Mineralization	Sample No.	From (M)	To (M)	Rec (M)
222.6	229.1	75	5x	Ogdc	Dark grey/black clay – possible sheared zone.	Heavily pyritic as blebs and disseminations – localised	547126	221.6	222.6	
							62	222.6	223.4	
							63	223.4	226.2	
229.1	236.45	69	5x	Ogst	Dark grey/black clay with qtz sand grains – locally sandstone. Bedding 50° to c/A	?Magnetite grains @ 230.1m. minor dissem of pyrite.	64	226.2	227.6	
							65	227.6	229.1	
							66	229.1	230.6	
							67	230.6	234	
236.45	239.1	66	8x	Ogst	White/grey sandstone clay with white silt fragments. Possible bedding 60° to c/A.		68	234	236.45	
							69	236.45	239.5	
							70	239.5	242.5	
239.1	242.5	50	5x	Om	White/grey silicic massive looking quartzite; broken core + core loss Upper contact preserved. 60° to c/A.	V. minor hematite alteration at top of unit.				
					END OF HOLE	242.5m.				

ASSAY VALUES (Analysed by .....)

MAG Depth	MAG Value	SUS Depth	SUS Value
221.5	c/L	237	0
222	c/L	237.5	c/L
222.5	200	238	0
223	0	238.5	c/L
223.5	c/L	239	c/L
224	c/L	239.5	0
224.5	0	240	0
225	c/L	240.5	c/L
225.5	c/L	241	c/L
226	0	241.5	c/L
226.5	5	242	c/L
227	c/L	242.5	0
227.5	0		
228	0		
228.5	0		
229	0		
229.5	0		
230	c/L		
230.5	0		
231	c/L		
231.5	c/L		
232	c/L		
232.5	0		
233	c/L		
233.5	c/L		
234	0		
234.5	c/L		
235	40		
235.5	c/L		
236	c/L		
236.5	0		

384042

bhole	fulldh	DPO	smpno	Prospect	EL	afrom	ato	aag	aal	aas	aba	aca	acu	afe	ak	amg	amn	apb	azn	as	MRTLlh
bhole	fulldh	DPO	smpno	Prospect	EL	afrom	ato	aag	aal	aas	aba	aca	acu	afe	ak	amg	amn	apb	azn	as	MRTLlh
ZG416	DD96ZG416			Grieves	38/89	0	4.3														Oha
ZG416	DD96ZG416	77400	5471201	Grieves	38/89	4.3	6	1.9	0.58	-5	36	30	-5	0.34	0.3	0.45	83	13	15		Ogul
ZG416	DD96ZG416			Grieves	38/89	6	12														Ogul
ZG416	DD96ZG416			Grieves	38/89	12	15														Ogmu
ZG416	DD96ZG416	77400	5471202	Grieves	38/89	15	17.1	1.2	1.19	-5	52	26.7	-5	0.93	0.59	1.01	112	12	15		Ogmu
ZG416	DD96ZG416			Grieves	38/89	17.1	24														Ogmu
ZG416	DD96ZG416	77400	5471203	Grieves	38/89	24	25.5	1.1	0.9	7	39	26.5	-5	0.87	0.47	2.98	126	-10	19		Ogmu
ZG416	DD96ZG416			Grieves	38/89	25.5	32.2														Ogmu
ZG416	DD96ZG416	77400	5471204	Grieves	38/89	32.2	33.5	1	0.96	14	40	23.4	-5	3.13	0.47	1.97	91	10	20		Ogfz
ZG416	DD96ZG416			Grieves	38/89	33.5	39.6														Ogfz
ZG416	DD96ZG416	77400	5471205	Grieves	38/89	39.6	40.6	1.8	0.81	-5	37	28.4	-5	0.68	0.42	1.98	111	-10	13		Ogfz
ZG416	DD96ZG416			Grieves	38/89	40.6	48														Ogfz
ZG416	DD96ZG416	77400	5471206	Grieves	38/89	48	49.3	1.2	1.59	-5	68	23.3	-5	1.06	0.8	3.23	203	14	13		Ogul
ZG416	DD96ZG416			Grieves	38/89	49.3	58.7														Ogul
ZG416	DD96ZG416	77400	5471207	Grieves	38/89	58.7	60	-0.5	1.98	6	87	25.3	-5	1.16	1.01	2.68	321	15	10		Ogul
ZG416	DD96ZG416	77400	5471208	Grieves	38/89	60	60.9	-0.5	2.03	-5	80	21.4	-5	1.63	0.97	3.29	561	11	428		Ogul/Ogdl
ZG416	DD96ZG416	77400	5471209	Grieves	38/89	60.9	62.1	-0.5	1.64	23	58	18.4	-5	4.16	0.75	5.73	1220	18	19		Ogdl
ZG416	DD96ZG416	77400	5471210	Grieves	38/89	62.1	63.7	-0.5	1.11	-5	41	19.6	-5	3.96	0.5	5.66	1510	-10	88		Ogdl
ZG416	DD96ZG416	77400	5471211	Grieves	38/89	63.7	65.2	-0.5	0.89	-5	28	23.5	-5	3.04	0.38	5.21	1120	12	31		Ogdl
ZG416	DD96ZG416	77400	5471212	Grieves	38/89	65.2	66.5	-0.5	1.93	-5	49	19.3	-5	3.36	0.64	5.96	1270	12	33		Ogdl
ZG416	DD96ZG416	77400	5471213	Grieves	38/89	66.5	67.8	-0.5	1.6	-5	43	20.4	-5	3.7	0.55	7.4	1340	13	44		Ogdl
ZG416	DD96ZG416	77400	5471214	Grieves	38/89	67.8	69	0.8	0.81	-5	30	18.4	-5	2.91	0.39	8.37	1020	-10	10		Ogdl
ZG416	DD96ZG416	77400	5471215	Grieves	38/89	69	70.5	0.6	0.92	-5	34	19	-5	3.41	0.39	8.79	1210	-10	10		Ogdl
ZG416	DD96ZG416	77400	5471216	Grieves	38/89	70.5	71.7	-0.5	0.86	-5	31	19.7	-5	3.6	0.41	8.49	1330	13	10		Ogdl
ZG416	DD96ZG416	77400	5471217	Grieves	38/89	71.7	73.2	1.3	1.27	29	51	26.1	-5	1.41	0.59	1.86	115	13	108		Ogdl/Ogmu
ZG416	DD96ZG416			Grieves	38/89	73.2	84.2														Ogmu
ZG416	DD96ZG416	77400	5471218	Grieves	38/89	84.2	85.6	1.4	0.6	-5	28	32.1	-5	0.36	0.26	0.7	48	14	34		Ogmu
ZG416	DD96ZG416			Grieves	38/89	85.6	95														Ogmu
ZG416	DD96ZG416	77400	5471219	Grieves	38/89	95	96.5	1.3	0.65	-5	29	33.4	-5	0.61	0.34	1.32	129	15	30		Ogmu
ZG416	DD96ZG416			Grieves	38/89	96.5	98.3														Ogmu
ZG416	DD96ZG416			Grieves	38/89	98.3	104.4														Ogul
ZG416	DD96ZG416	77400	5471220	Grieves	38/89	104.4	106.4	1.2	0.4	-5	15	30.1	-5	0.8	0.2	2.84	131	11	18		Ogul
ZG416	DD96ZG416			Grieves	38/89	106.4	117.4														Ogul
ZG416	DD96ZG416	77400	5471221	Grieves	38/89	117.4	118.4	1.4	1.12	-5	44	26.8	-5	0.9	0.52	1.04	279	13	24		Ogfz
ZG416	DD96ZG416			Grieves	38/89	118.4	123.2														Ogfz
ZG416	DD96ZG416			Grieves	38/89	123.2	130.1														Ogmu
ZG416	DD96ZG416	77400	5471222	Grieves	38/89	130.1	132.1	2.2	0.22	76	10	32.4	-5	2.12	0.11	0.79	65	-10	3580		Ogmu
ZG416	DD96ZG416			Grieves	38/89	132.1	136.4														Ogmu
ZG416	DD96ZG416	77400	5471223	Grieves	38/89	136.4	139.8	-0.5	1.79	7	61	24	17	1.84	0.51	3.02	400	30	774		Ogmu
ZG416	DD96ZG416	77400	5471224	Grieves	38/89	139.8	141	1.6	0.72	-5	25	30	-5	1.22	0.24	1.54	252	27	3760		Ogmu
ZG416	DD96ZG416	77400	5471225	Grieves	38/89	141	144	0.6	1.03	18	35	25.9	-5	2.23	0.35	2.59	490	14	1960		Ogul
ZG416	DD96ZG416	77400	5471226	Grieves	38/89	144	145.2	0.8	0.87	-5	36	24.3	-5	2.12	0.39	3.8	588	11	674		Ogul
ZG416	DD96ZG416	77400	5471227	Grieves	38/89	145.2	146.3	-0.5	1.25	-5	47	21.1	-5	2.77	0.48	3.94	699	18	1500		Ogdl
ZG416	DD96ZG416	77400	5471228	Grieves	38/89	146.3	149.5	1	0.92	-5	38	25.8	-5	1.16	0.4	1.59	298	15	715		Ogul
ZG416	DD96ZG416	77400	5471229	Grieves	38/89	149.5	151.7	0.8	1.39	-5	63	25.2	-5	0.98	0.67	0.85	310	12	71		Ogul
ZG416	DD96ZG416	77400	5471230	Grieves	38/89	151.7	152.9	1.1	1.31	-5	58	28.4	-5	1.06	0.64	0.73	465	11	19		Ogul
ZG416	DD96ZG416	77400	5471231	Grieves	38/89	152.9	154	1.2	1.4	-5	62	28.5	6	0.76	0.69	0.62	224	13	17		Ogul
ZG416	DD96ZG416			Grieves	38/89	154	165.7														Ogul
ZG416	DD96ZG416	77400	5471232	Grieves	38/89	165.7	168	0.5	2.3	-5	80	22.1	-5	2.84	0.82	3.53	1370	38	1490		Ogdl
ZG416	DD96ZG416			Grieves	38/89	168	172.4														Ogul
ZG416	DD96ZG416			Grieves	38/89	172.4	174														Ogoo
ZG416	DD96ZG416	77400	5471233	Grieves	38/89	174	176	1	0.55	-5	19	29.3	-5	0.79	0.22	1.44	302	28	373		Ogoo
ZG416	DD96ZG416	77400	5471234	Grieves	38/89	176	178	0.7	0.93	-5	29	26.3	-5	2.06	0.34	2.62	900	33	436		Ogoo
ZG416	DD96ZG416	77400	5471235	Grieves	38/89	178	178.7	-0.5	7	22	251	11.8	12	3.05	2.24	2.57	242	54	516		Ogfz
ZG416	DD96ZG416	77400	5471236	Grieves	38/89	178.7	179.7	0.9	2.03	-5	65	26.9	-5	1.66	0.68	1.66	406	78	1170		Ogfz
ZG416	DD96ZG416	77400	5471237	Grieves	38/89	179.7	180.6	0.9	0.58	-5	21	14.6	-5	17.4	0.23	2.42	5790	53	2110		Ogsd
ZG416	DD96ZG416			Grieves	38/89	180.6	183														Ogsd
ZG416	DD96ZG416	77400	5471238	Grieves	38/89	183	184.5	-0.5	1.2	11	36	11.8	57	13.1	0.4	6.19	6730	31	4880		Ogsd
ZG416	DD96ZG416	77400	5471239	Grieves	38/89	184.5	185.5	-0.5	0.5	59	20	10.2	-5	15	0.21	5.55	5220	56	33500	2.6	Ogsd
ZG416	DD96ZG416	77400	5471240	Grieves	38/89	185.5	187.4	-0.5	0.58	-5	20	12.9	46	12.1	0.27	7.17	5730	23	8500	0.44	Ogsd
ZG416	DD96ZG416	77400	5471241	Grieves	38/89	187.4	188.9	-0.5	1.81	17	60	10.7	-5	16.3	0.83	5.55	5960	22	6300	0.54	Ogsd
ZG416	DD96ZG416	77400	5471242	Grieves	38/89	188.9	190.4	-0.5	1.52	9	51	10.9	-5	16.5	0.67	5.69	5080	22	6130	0.75	Ogsd
ZG416	DD96ZG416	77400	5471243	Grieves	38/89	190.4	191.9	-0.5	0.88	-5	32	7.2	-5	23.4	0.34	3.39	12100	24	22900	0.49	Ogsd
ZG416	DD96ZG416	77400	5471244	Grieves	38/89	191.9	193.2	-0.5	0.81	-5	28	11.7	-5	15.1	0.37	6.92	9740	26	20400	0.59	Ogsd
ZG416	DD96ZG416	77400	5471245	Grieves	38/89	193.2	194.4	0.6	2.78	15	97	13.3	15	6.27	0.9	6.99	2680	165	7960	0.87	Ogfz
ZG416	DD96ZG416	77400	5471246	Grieves	38/89	194.4	195.7	0.6	0.7	-5	20	19.6	7	5.28	0.17	10.7	2000	78	3890		Ogoo

bhole	fulldh	DPO	smpno	Prospect	EL	afrom	ato	aag	aal	aas	aba	aca	acu	ale	ak	amg	amn	apb	azn	as	MRTLith
ZG416	DD96ZG416	77400	5471247	Grieves	38/89	195.7	196.9	0.9	0.31	-5	16	20.2	6	5.21	0.08	11	1780	71	3910		Ogoo
ZG416	DD96ZG416	77400	5471248	Grieves	38/89	196.9	198.5	-0.5	0.53	-5	74	16.6	9	6.53	0.5	11.6	3190	89	6330	0.25	Ogoo
ZG416	DD96ZG416			Grieves	38/89	198.5	201														Ogoo
ZG416	DD96ZG416	77400	5471249	Grieves	38/89	201	203.1	-0.5	0.46	-5	22	19.5	25	6.13	0.13	10.6	2300	81	2850		Ogoo
ZG416	DD96ZG416	77400	5471250	Grieves	38/89	203.1	205.1	0.6	0.14	-5	6	22.9	7	1.55	-0.05	13.6	744	54	919		Ogoo
ZG416	DD96ZG416	77400	5471251	Grieves	38/89	205.1	206.9	-0.5	0.96	-5	33	19	-5	4.5	0.26	10.8	1840	55	2550		Ogoo
ZG416	DD96ZG416	77400	5471252	Grieves	38/89	206.9	208.5	1.1	0.32	-5	7	19.6	-5	5.37	0.05	11.7	2310	49	3940		Ogoo
ZG416	DD96ZG416	77400	5471253	Grieves	38/89	208.5	210	0.9	0.13	-5	-5	20.9	5	2.5	-0.05	11.9	1350	34	2010		Ogoo
ZG416	DD96ZG416	77400	5471254	Grieves	38/89	210	211.5	0.5	0.04	-5	6	20.8	-5	1.99	-0.05	12.4	1010	87	2250		Ogoo
ZG416	DD96ZG416	77400	5471255	Grieves	38/89	211.5	213	-0.5	0.08	-5	-5	19.6	6	4.63	-0.05	11.3	2260	44	3650		Ogoo
ZG416	DD96ZG416	77400	5471256	Grieves	38/89	213	213.9	-0.5	0.11	-5	5	20.9	5	1.1	-0.05	12.7	603	76	835		Ogoo
ZG416	DD96ZG416	77400	5471257	Grieves	38/89	213.9	215.7	1.2	1.94	-5	73	17.9	8	4.29	0.57	9.8	1840	325	5130	0.5	Ogoo/Ogsc
ZG416	DD96ZG416	77400	5471258	Grieves	38/89	215.7	216	0.6	1.11	37	38	14.7	-5	8.89	0.46	8.03	4550	269	8540	0.98	Ogsd
ZG416	DD96ZG416	77400	5471259	Grieves	38/89	216	218.3	0.6	1.72	36	64	3.71	90	26.3	0.74	1.56	13100	1370	19400	1.2	Ogsd
ZG416	DD96ZG416	77400	5471260	Grieves	38/89	218.3	221.6	8.2	3.23	100	92	1.09	641	31.1	1.1	0.63	15800	4060	33900	2.5	Ogsd
ZG416	DD96ZG416	77400	5471261	Grieves	38/89	221.6	222.6	13.2	2.32	128	77	0.7	946	32.9	0.77	0.44	15000	3390	21900	1	Ogsd
ZG416	DD96ZG416	77400	5471262	Grieves	38/89	222.6	223.4	11	6.36	1790	224	0.08	918	7.08	2.28	0.34	1230	3520	16000	6.1	Ogdc
ZG416	DD96ZG416	77400	5471263	Grieves	38/89	223.4	226.2	-0.5	7.59	161	344	0.07	59	3.11	3.15	0.36	103	1610	7930	3.6	Ogdc
ZG416	DD96ZG416	77400	5471264	Grieves	38/89	226.2	227.6	-0.5	7.95	57	360	0.15	20	1.76	3.11	0.43	70	284	2400		Ogdc
ZG416	DD96ZG416	77400	5471265	Grieves	38/89	227.6	229.1	-0.5	8.34	55	380	0.05	21	2.88	3.31	0.45	61	92	1450		Ogdc
ZG416	DD96ZG416	77400	5471266	Grieves	38/89	229.1	230.6	-0.5	5.65	121	246	0.05	19	3.13	2.19	0.34	68	154	2730		Ogsl
ZG416	DD96ZG416	77400	5471267	Grieves	38/89	230.6	234	-0.5	4.95	132	180	-0.05	24	2.02	1.86	0.23	34	2370	4330		Ogsl
ZG416	DD96ZG416	77400	5471268	Grieves	38/89	234	236.5	-0.5	7.37	178	303	-0.05	42	2	3.15	0.36	31	160	4670		Ogsl
ZG416	DD96ZG416	77400	5471269	Grieves	38/89	236.45	239.5	-0.5	6.31	16	229	-0.05	17	0.52	2.54	0.31	21	100	64		Om
ZG416	DD96ZG416	77400	5471270	Grieves	38/89	239.5	242.5	-0.5	1.23	-5	47	-0.05	7	0.26	0.5	0.06	23	40	25		Om

384044

Appendix IV

Flow Sheet for Diamond Drillcore Analysis

384046

Diamond Drillcore Sampling Flowsheet

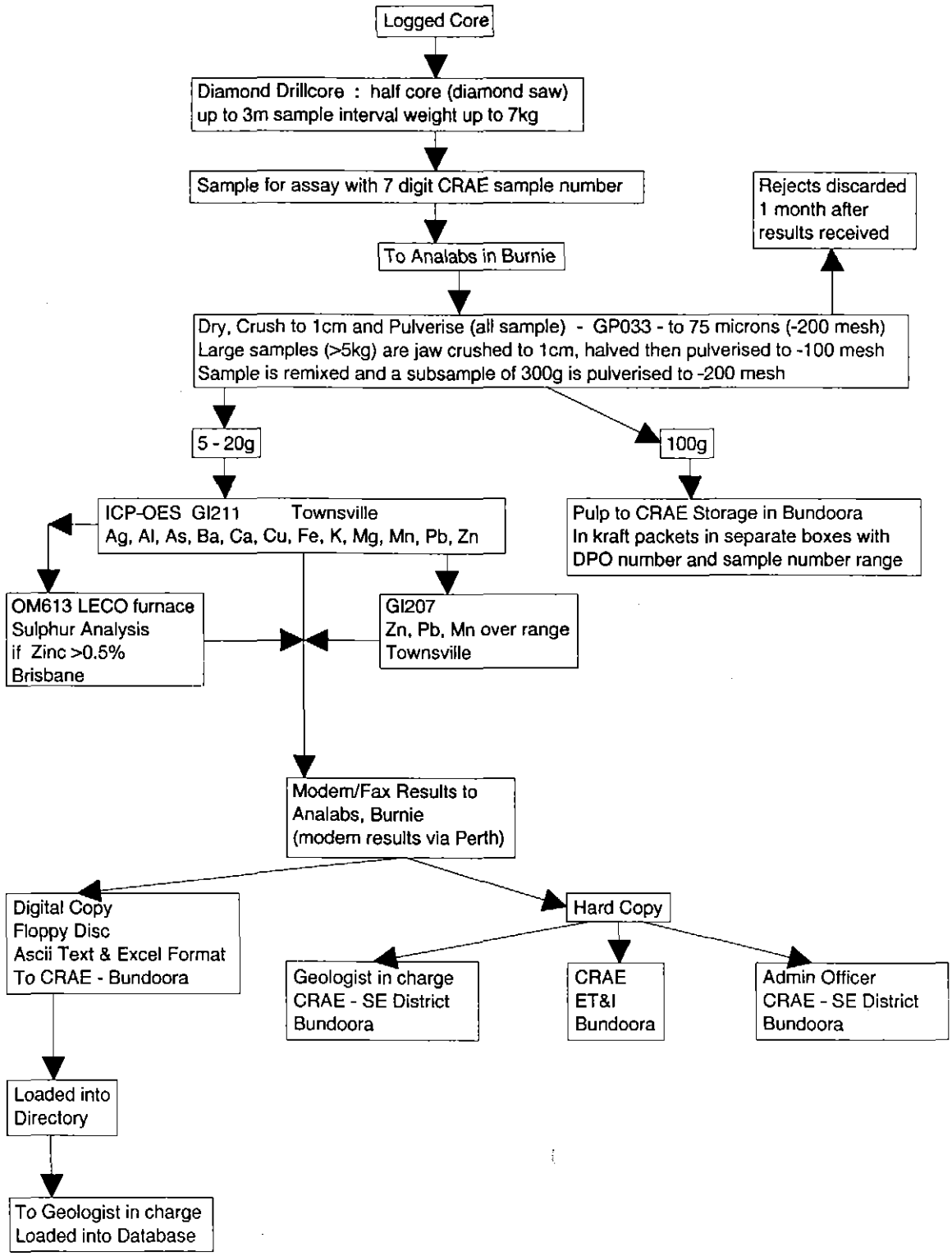

GI211 - Aqua Regia/Perchloric/hydrofluoric acid : acid digest
GI207 - Aqua Regia/Perchloric/hydrofluoric acid : acid digest

S.J.Tear August 1996

Appendix V

Grieves Prospect Characterisation (CRA-ATD)

CRA ATD Technology for CRA

384048

A Report prepared for
CRA Exploration

Grieves Prospect Characterisation

CONFIDENTIAL

30 October 1996

Client: Simon Tear
CRA Exploration

CONFIDENTIAL

Grieves Prospect Characterisation

Author: Rob Walker
03 9242 3180

Contributors: Susan Headberry
Jason Silverstein

Responsible Manager: Mark Stokes
03 9242 3220

Internal copy to: B Kelley/File

Date: 30 October 1996

CONTENTS

DETAILS

Project Focus

CRA Exploration commissioned ATD to undertake a mineralogical and metallurgical characterisation of the Grieves zinc prospect in Tasmania. The objective of the research was to provide an evaluation of the processing potential of the ore, to assist CRAE in theIR efforts to joint venture the prospect with other exploration companies. Two samples of high grade ore were subjected to a range of mineralogical and metallurgical testwork and evaluation.

What is the processing potential of the Grieves ore?

Research Conducted

Two samples - 5471296 and 5471297 were received for characterisation. Sample 5471296 was obtained from drill hole ZG107 at a depth of 154 to 163 metres, while sample 5471297 was obtained from drill hole ZG406 at a depth of 115 to 126 metres.

Each sample was prepared by drying at 70° C and crushed to 100% passing 2mm. A representative sample was extracted from each and pulverised for subsequent chemical analysis and x-ray diffraction for mineral identification.
A separate subsample was extracted from each sample, ground to eighty percent passing 200μm and screened at 38,75 and 150μm respectively. All of the plus 38μm size fractions were prepared as polished thick sections for subsequent mineralogical examination by both optical and scanning electron microscopy.

Mineralogical characterisation using the techniques mentioned above resulted in mineral identity, liberation, association and grain size being quantified. These properties directed the metallurgical research program and aided the evaluation of the processing potential of these ore samples. Mineralogical examination of metallurgical products was conducted on appropriate samples to aid our understanding of the metallurgical performance.

Eight metallurgical bench tests were undertaken to assess the processing potential of the Grieves ore. These included sulphide flotation, acid leaching and gravity concentration techniques. Flotation and leaching were performed on finely ground ore (<100μm) while gravity concentration was performed on relatively coarse samples (<500μm).

Findings

The Grieves ore is metallurgically complex

Both samples are metallurgically complex, different in character and will be difficult to process. Because of this significant difference in character each ore will be reported separately.

Sample 5471296

This sample contains the minerals Quartz,Galena,Sphalerite, Fraipontite $(Zn,Al)_3(Si,Al)_2O_5(OH)_4$ and Anglesite ($PbSO_4$) and assays 12.2wt%Zn, 7.1wt%Pb and 3.1wt%S. The mineralogy is shown in the x-ray diffractogram (XRD) shown as graph No1 below.

Graph No 1 XRD mineralogy - 5471296

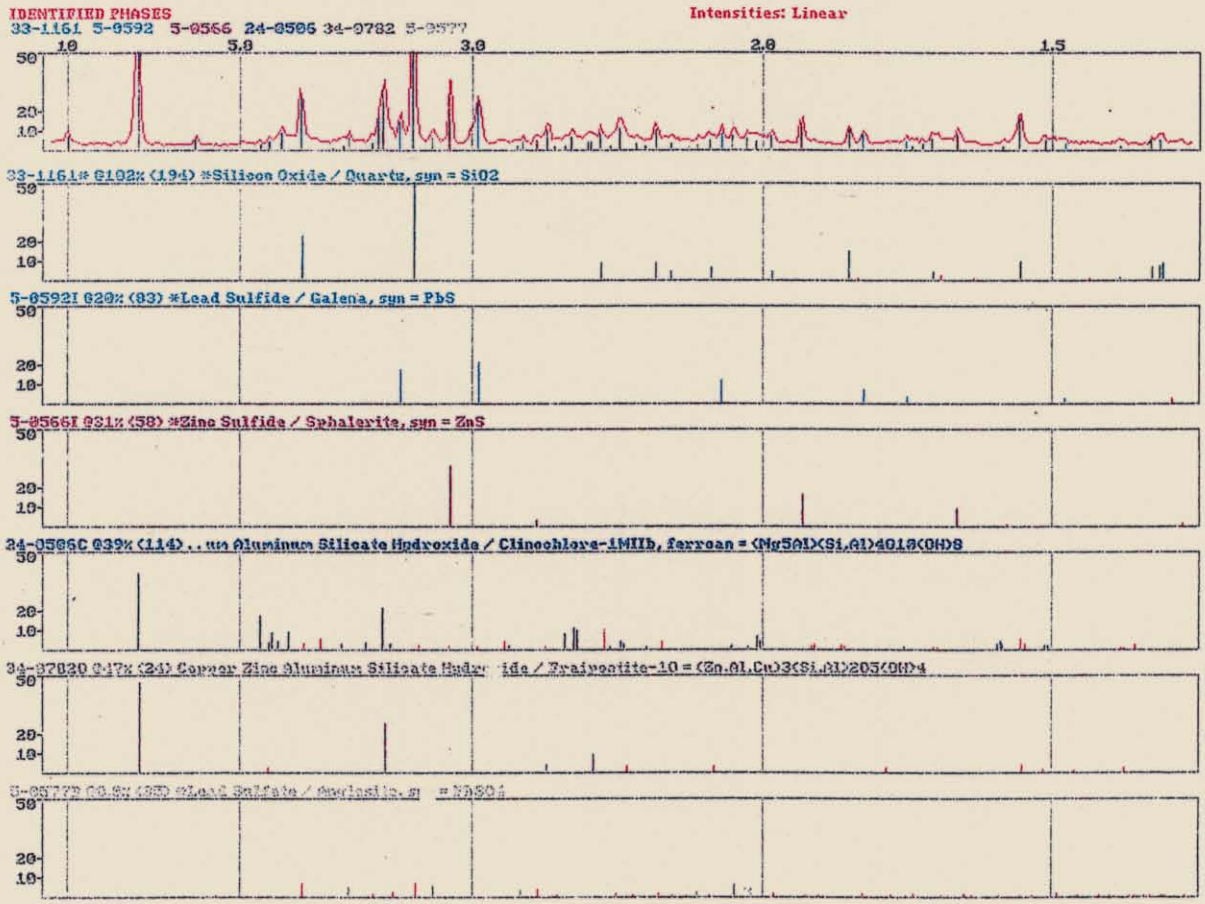

This graph shows quartz to be the dominant mineral in terms of abundance, followed closely by fraipontite and moderate amounts of sphalerite and galena and minor anglesite. Fraipontite is the only complex silicate in this sample. Although clinochlore is suggested by XRD, it was not observed by electron microscopy.

Photomicrographs No1 and No2 show backscattered electron images of this sample for a -150μm +75μm size fraction. The brightest phase is galena with bright grey phase being sphalerite. The most abundant mineral, fraipontite is grey, while the darkest grains are quartz. All minerals with the exception of galena are intimately associated with each other (poorly liberated) and are fine grained.

Photomicrograph No1 - 5471296

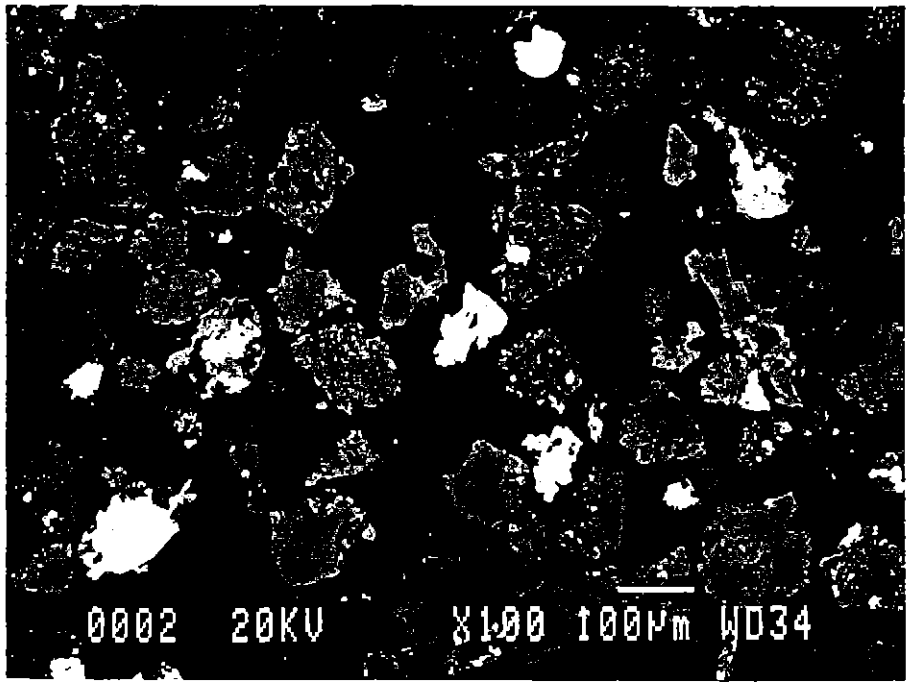

White - Galena/Anglesite Bright grey - Sphalerite
Grey - Fraipontite Dark grey - Quartz

Photomicrograph No2 - 5471296

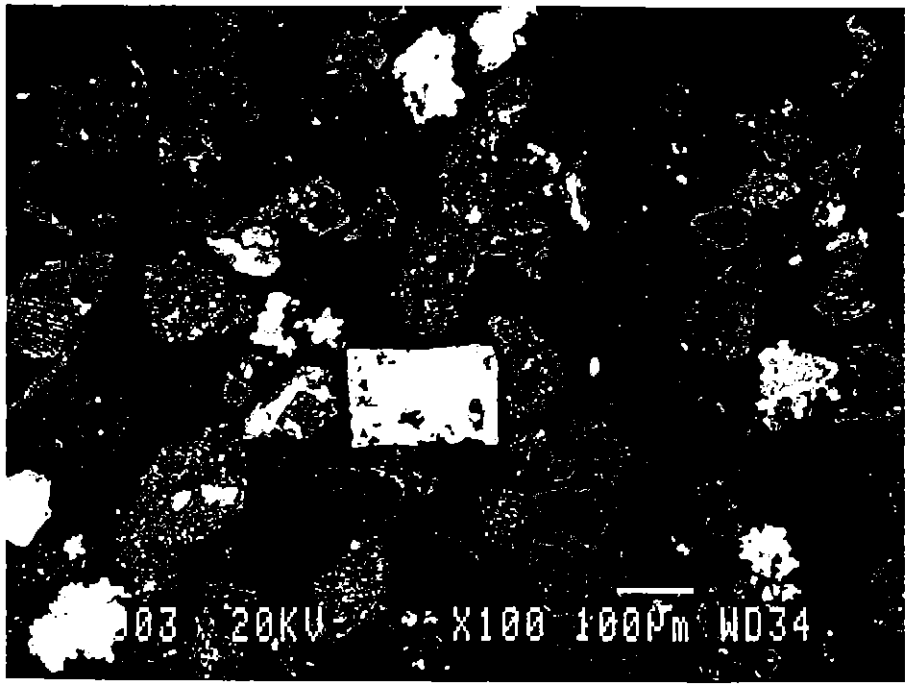

Sulphide flotation resulted in very poor lead and zinc recovery at low metal grades. Using a flotation scheme based on the Century flowsheet, maximum lead recovery to the concentrate was 15 % at an assay of 10wt % Pb while maximum zinc recovery was only 7% at 13 wt% Zn grade. These grades and recoveries show little if any selectivity for galena and sphalerite. The likely causes of this poor metallurgical performance are ore oxidation, reagent absorption onto fraipontite and poor liberation.

Gravity processing at a density of 3.3g/cc appears promising as a preconcentration procedure as 32 % of this sample reported to the gravity concentrate. Sphalerite and galena predominantly reported to the concentrate (85% and 75% recovery respectively), however fraipontite recovery was only 40%. As fraipontite is the dominant zinc mineral in this sample, only 55% of the total zinc reported to the concentrate.

Sulphuric acid leaching resulted in partial leaching of the sphalerite, however fraipontite appears to be refractory to acid leaching. Zinc recovery to the leach liquor was only 3%. A combination of all three metallurgical techniques is unlikely to result in high lead and zinc recovery. This ore is very soft and has a tendency to overgrind.

Sample 5471297

This sample contains the minerals Quartz, Illite, Sphalerite, Smithsonite/Siderite and Hemimorphite and assays 17.9wt%Zn, <0.01wt%Pb and 1.8wt%S. The mineralogy is shown in the x-ray diffractgram (XRD) graph No2 below

Graph No2 XRD mineralogy - 5471297

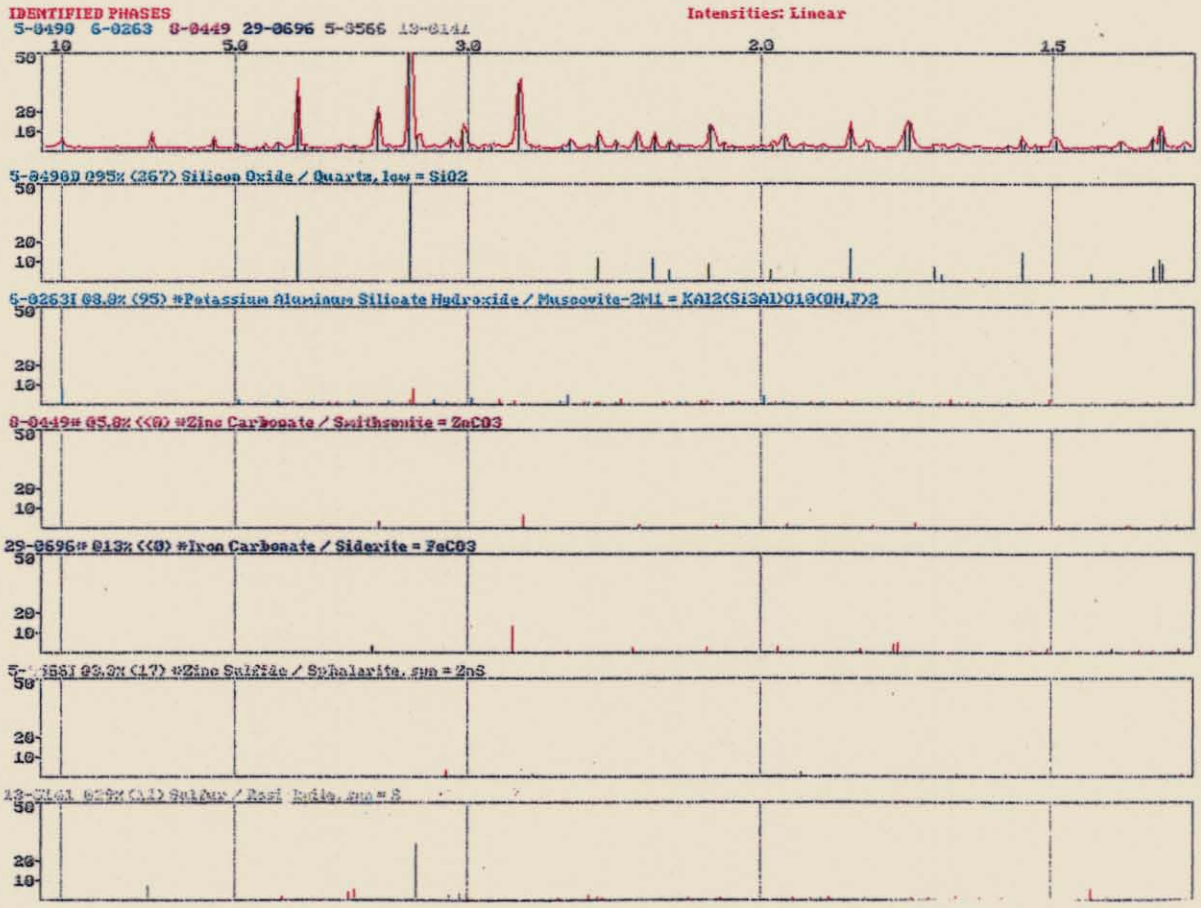

This graph shows quartz to be the dominant mineral in terms of abundance, followed by smithsonite/siderite and minor amounts of illite and sphalerite. Electon microscope examination of this sample shows the carbonate to be neither smithsonite nor siderite but a solid solution mineral intermediate between the two end members. Graph No3 shows the chemical composition of a carbonate grain. Both zinc and iron are clearly present with a minor concentration of manganese. The chemical composition of this carbonate is highly variable.

Graph No 3 - Chemical composition of smithsonite/siderite.

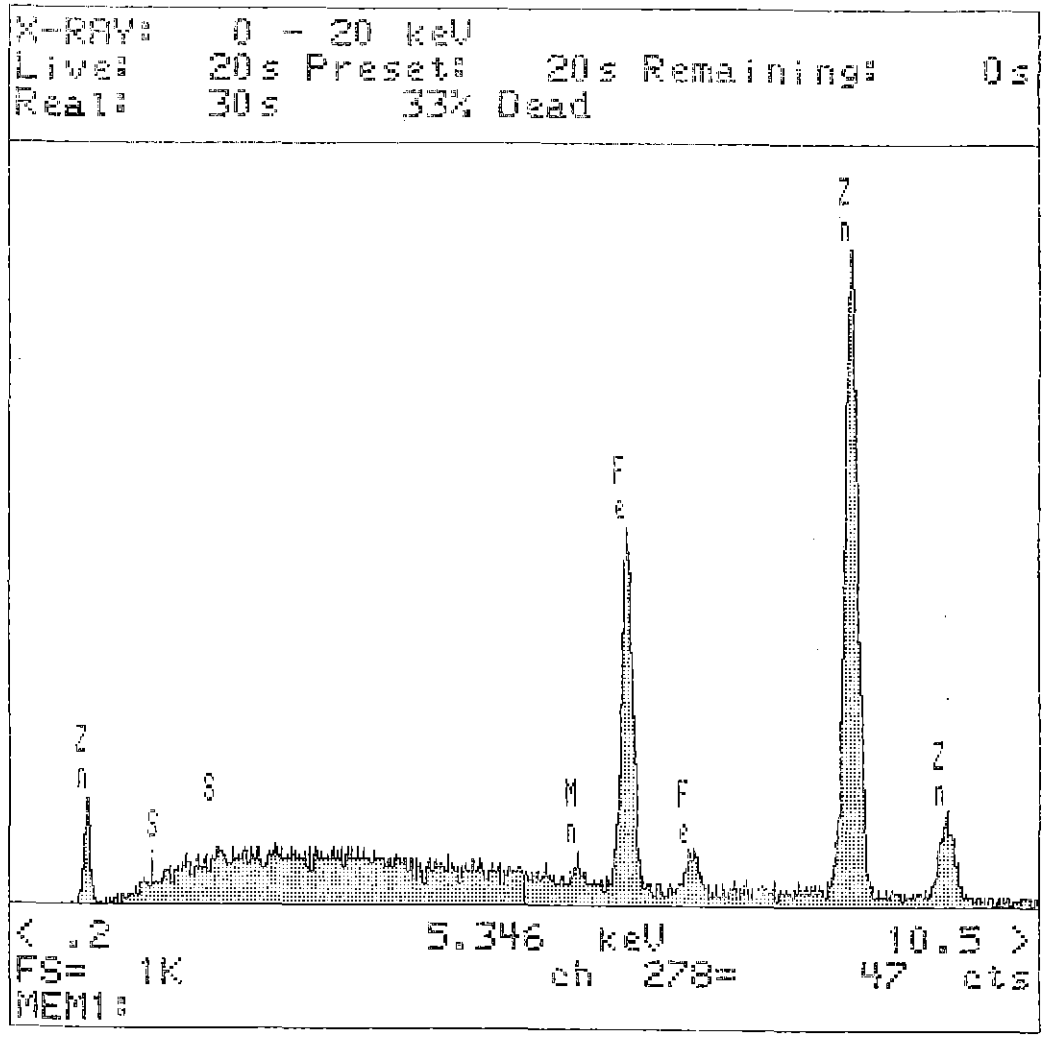

Photomicrograph No3 shows a backscattered electron image of this sample for a -150µm +75µm size fraction.The brightest phase is hemimorphite with the bright grey phase being smithsonite/siderite. The dark grey phase is predominantly quartz with minor calcite and illite. A significant proportion of the carbonate phase is locked with quartz.

Photomicrograph No3 - 5471297

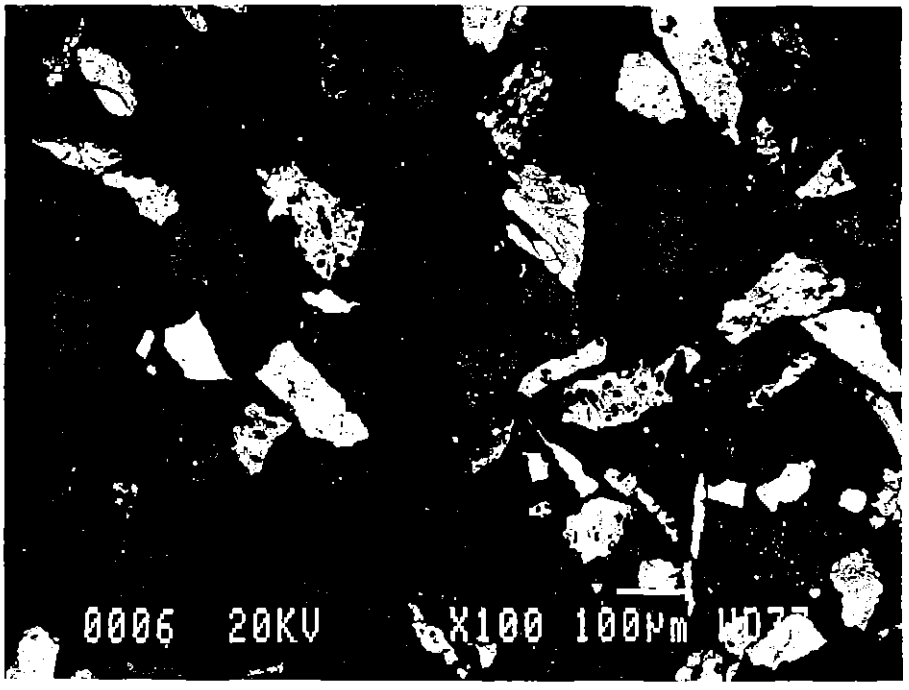

White- Hemimorphite Bright grey- Carbonates Grey- Quartz.

Sulphide flotation was not performed on this sample because of the lack of sulphides present and the existence of the mixed carbonate which was unlikely to respond to sulphidisation and subsequent flotation.

Gravity processing at a density of 3.3g/cc appears promising as a preconcentration procedure as 78% of the sample reported to the gravity concentrate. A high recovery of the zinc minerals was achieved to the concentrate (87%), however the zinc grade was low at 22% due mainly to the significant locking of quartz with the zinc carbonate. Gravity processing is therefore only likely to be of value as a preconcetration procedure.

Sulphuric acid leaching resulted in high zinc recovery to solution with both the carbonate and the hemimophite being leached. The major issues in leaching are the very high level of acid consumption and the need for extensive purification due to the high levels of both iron and silica leached.

Processing costs will be high.

Compared to conventional flotation, metallurgical extraction of lead and zinc from this prospect will be expensive due the the complex mineralogy and the need for multiple processing steps. High recoveries have not been achieved in this study putting more pressure on the cost of production per tonne of metal.

Implications

This ore will be difficult to process. There is no positive metallurgical information that will aid a potential joint venture proposal.

Appendix 1

XRD Mineralogy and assays

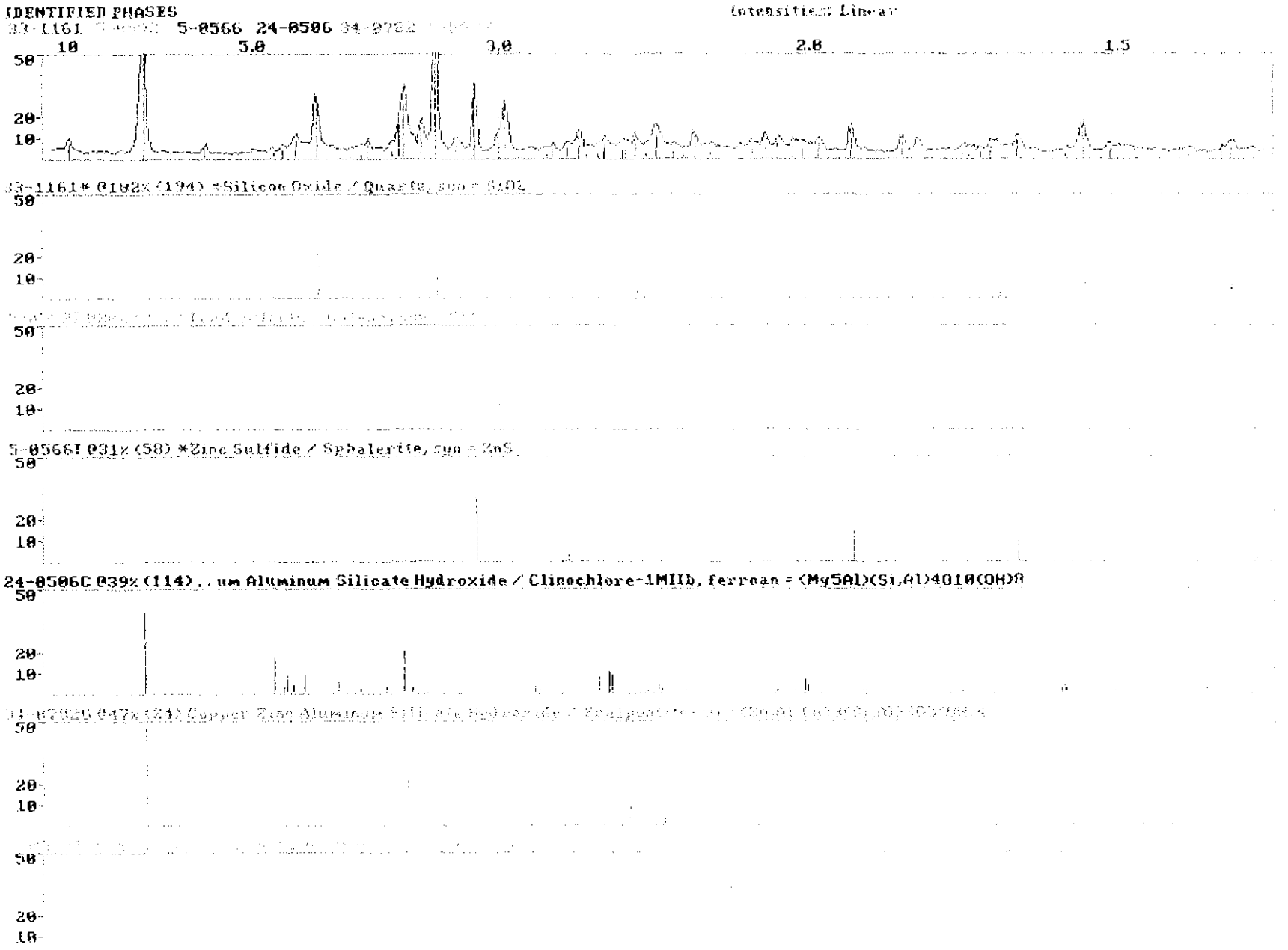
IDENTIFIED PHASES
Intensities: Linear
5-0566 24-0506
10
5.0
3.0
2.8
1.5
50
20
10
*Silicon Oxide / Quartz
5-0566
*Zinc Sulfide / Sphalerite
24-0506
Aluminum Silicate Hydroxide / Clinochlore-1MIIb

384060

μPDSM Report 10:43, 9/11/96

Input Pattern

~~1786~~
471296

06-Sep-1996 00:23:52

d	I	d	I	d	I	d	I	d	I	d	I
.05	7.2	3.633	2.7	2.7667	4.5	2.3951	11	2.0357	5.2	1.6342	7.5
.131	83	3.587	16	2.7050	4.5	2.3432	3.0	2.0169	3.9	1.5675	1.8
5.748	5.9	3.556	33	2.6600	9.8	2.3141	1.7	1.9812	6.8	1.5433	16
.751	2.4	3.436	14	2.6330	1.9	2.2844	9.8	1.9146	14	1.5099	4.4
.628	3.6	3.351	100	2.5917	1.7	2.2375	3.4	1.8198	10	1.4849	3.0
.478	8.6	3.231	6.2	2.5653	6.3	2.1893	1.3	1.7929	7.9	1.4193	1.9
4.269	28	3.129	34	2.5062	3.9	2.1647	2.2	1.7153	4.0	1.3836	4.9
.966	0.61	3.009	11	2.4940	3.5	2.1327	4.6	1.7061	1.5	1.3743	4.9
.865	1.8	2.9760	25	2.4617	7.8	2.1012	7.9	1.6888	2.7		
3.320	6.3	2.7945	1.6	2.4263	1.3	2.0723	6.7	1.6738	5.3		

58 lines in pattern.

Identified Phases:

JCPDS#	SI	ML/X	At%	Identity . . .
33-1161*	194	14/4	102	*Silicon Oxide / Quartz, syn = SiO2
	Ierr:50,150		derr:2.0	Bground:0.61 dmax/min:11.04/1.343
5-0592I	83	6/1	20	*Lead Sulfide / Galena, syn = PbS
	Ierr:50,150		derr:2.0	Bground:0.61 dmax/min:11.04/1.343
5-0566I	58	4/2	31	*Zinc Sulfide / Sphalerite, syn = ZnS
	Ierr:50,150		derr:2.0	Bground:0.61 dmax/min:11.04/1.343
24-0506C	114*	27/5	39	Magnesium Aluminum Silicate Hydroxide / Clinochlore-1MIIb, ferroan = (Mg5Al)(Si,Al)4O10(OH)8
	Ierr:50,150		derr:5.0	Bground:0.61 dmax/min:11.04/1.343
44-0782O	24	4/5	47	Copper Zinc Aluminum Silicate Hydroxide / Fraipontite-1O = (Zn,Al,Cu)3(Si,Al)2O5(OH)4
	Ierr:50,150		derr:2.0	Bground:0.61 dmax/min:11.04/1.343
5-0577D	35	9/8	8.0	*Lead Sulfate / Anglesite, syn = PbSO4
	Ierr:50,150		derr:2.0	Bground:0.61 dmax/min:11.04/1.343

Summary Report (Part 1 of 2):

	Full	Resid	33-1161:102%		5-0592: 20%		5-0566: 31%		24-0506: 39%	
d	I	I	d	I	d	I	d	I	d	I
.05	7.2	7.2								
.131	83	None							7.121	39
5.748	5.9	5.9								
.751	2.4	None							4.747	17
.628	3.6	None								

384061

.478	8.6	None								4.526	3.5
"	"									4.407	8.5
1.[illegible]69	28	None	4.257	23						[4.240	3.1]
										<4.075	5.0>
.966	0.61	0.61									
3.[illegible]65	1.8	None								3.885	2.3
[illegible]320	6.3	None									
.633	2.7	None								3.681	3.1
3.[illegible]587	16	None								3.560	21
3.[illegible]556	33	None								3.503	2.3*
.436	14	None			3.429	17					
3.[illegible]751	100	None	3.342	102						3.315	1.5
.231	6.2	None									
.129	34	None					3.133	31		[3.133	1.5]
3.[illegible]009	11	None									
3.[illegible]9760	25	None			2.969	20				[2.980	1.2]
										<2.848	3.5>
2.[illegible]7945	1.6	None								2.824	1.2
2.[illegible]7667	4.5	None									
.7050	4.5	None					2.705	3.1		[2.669	1.2]
.6600	9.8	6.1									
2.[illegible]6330	1.9	1.9									
.5917	1.7	None								2.593	7.4
2.[illegible]5653	6.3	None								2.554	1.5
"	"									2.545	8.9
.5062	3.9	3.9									
.4940	3.5	None									
2.[illegible]4617	7.8	None	2.457	8.2						[2.448	9.7]
.4263	1.3	None								2.427	0.77
.3951	11	None								2.393	3.5
"	"									2.384	2.3
.3432	3.0	3.0									
2.[illegible]3141	1.7	None								2.309	0.77
2.[illegible]2844	9.8	None	2.282	8.2						[2.265	3.9]
.2375	3.4	None	2.237	4.1							
.1893	1.3	None									
2.[illegible]1647	2.2	None									
.1327	4.6	None	2.127	6.1							
2.[illegible]1012	7.9	None			2.099	12					
2.[illegible]0723	6.7	None								2.077	0.77
"	"									2.072	1.2
2.[illegible]0357	5.3	None								2.035	0.77*
"	"										
.0169	3.9	None								2.013	6.2
"	"									2.005	3.9
1.[illegible]9812	6.8	None	1.9792	4.1							
.9146	14	None					1.912	16			
										<1.892	1.5>
										<1.8877	2.3>
.8198	10	None	1.8179	14						[1.8334	1.9]
"	"									[1.8262	1.2]
			<1.8021	1.0>							
.7929	7.9	None			1.790	7.1					
1.[illegible]7153	4.0	None			1.714	3.3					
.7061	1.5	None								1.7194	0.77
.6888	2.7	2.7									
1.[illegible]6738	5.3	None	1.6719	4.1						[1.6709	0.77]
"	"									[1.6647	0.77]
			<1.6591	2.0>							
.6342	7.5	None					1.633	9.3			
			<1.6082	1.0>							
.5675	1.8	None								1.5737	1.0

"	"							1.5667	1.9
						<1.561	0.62>		
.433	16	None	1.5418	9.2				[1.5424	5.4]
"	"							[1.5360	3.1]
.5099	4.4	None						1.5086	1.5
"	"							1.5063	1.5
.4849	3.0	None			1.484	2.0			
			<1.4536	1.0>					
.193	1.9	None	1.4189	1.0				[1.4172	0.77]
"	"							[1.4134	0.77]
								<1.4014	2.6>
.836	4.9	None	1.3820	6.1					
.3743	4.9	None	1.3752	7.2					
"	"		1.3718	8.2					
					<1.362	2.0>	<1.351	1.9>	

* = Obscured (...) = Missing [...] = Previously Removed

ummary Report (Part 2 of 2):

	Full	Resid	34-0782: 47%		5-0577: 6%	
	I	I	d	I	d	I
0.05	7.2	7.2				
.131	83	None	7.07	47		
.748	5.9	5.9				
.751	2.4	None				
.628	3.6	None	[4.65	2.3]		
"	"					
.478	8.6	None				
"	"					
4.269	28	None			[4.260	7.0]
.966	0.61	0.61				
.965	1.8	None				
3.320	6.3	None			3.813	4.6
.633	2.7	None			[3.622	1.8]
.587	16	None				
3.356	33	None	3.538	26		
					<3.479	2.6>
.436	14	None				
3.351	100	None			[3.333	6.9]
3.231	6.2	None			3.220	5.7
.129	34	None				
3.009	11	None			3.001	8.0
2.9760	25	None				
.7945	1.6	None				
2.7667	4.5	None			2.773	2.8
2.7050	4.5	None			[2.699	3.7]
.6600	9.8	6.1	2.661	3.7		
2.6330	1.9	1.9				
					<2.618	0.64>
.5917	1.7	None				
2.5653	6.3	None				
"	"					
.5062	3.9	3.9				
.4940	3.5	None	2.486	9.3		
2.4617	7.8	None				
2.4263	1.3	None				
.3951	11	None			[2.406	1.4]
"	"					
			<2.372	3.3>		
.3432	3.0	3.0				
.3141	1.7	None				
2.2844	9.8	None			[2.276	1.6]
2375	3.4	None			[2.235	0.40]
1893	1.3	None			2.193	0.56

384062

384063

.1327	4.6	None			[2.133	0.40]
			<2.120	2.8>		
2. 012	7.9	None				
.0723	6.7	None			2.067	6.1
"	"					
2. 0357	5.3	None			2.031	2.7
"	"				2.028	3.8
.0169	3.9	None				
"	"					
1. 9812	6.8	None				
					<1.973	1.7>
.9146	14	None				
.8198	10	None				
"	"					
.7929	7.9	None			[1.793	1.2]
			<1.749	2.3>	<1.741	0.64>
1. 7153	4.0	None			[1.716	0.24]
.7061	1.5	None			[1.703	1.3]
.6888	2.7	2.7				
1. 6738	5.3	None				
"	"					
1. 6342	7.5	None				
					<1.621	1.5>
					<1.611	0.80>
.5675	1.8	None			[1.571	0.48]
"	"					
"	"					
1. 5433	16	None	[1.539	3.7]	[1.542	0.16]
"	"					
.5099	4.4	None	[1.511	1.9]		
"	"					
					<1.493	1.2>
.4849	3.0	None				
			<1.472	0.93>	<1.441	0.64>
1. 4193	1.9	None				
"	"					
			<1.414	2.3>		
1. 3836	4.9	None			[1.385	0.16]
1. 3743	4.9	None			[1.371	0.48]
"	"					

* = Obscured <..> = Missing [..] = Previously Removed

IDENTIFIED PHASES

Intensities: Linear

5-0490 5-0566 8-0449 29-0696 5-0566

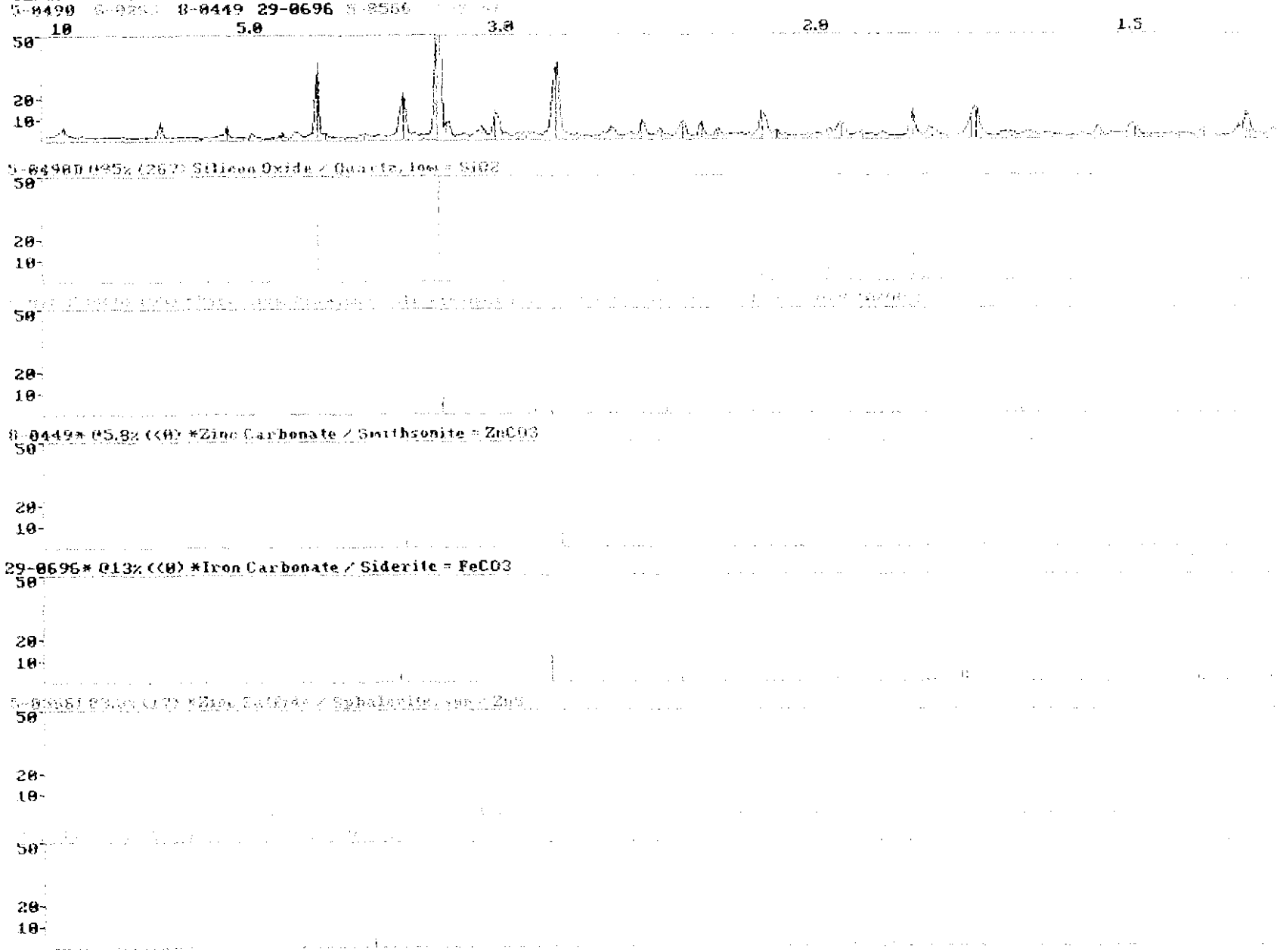

384065

...rDSM Report ... 10:57,Wed 11/06

...ut Pattern

...6-Sep-1996 9:48...

...11297

d	I	d	I	d	I	d	I	d	I	d	I
...995	4.9	3.849	2.5	2.8895	2.1	2.2115	1.6	1.7848	1.8	1.4975	5.2
...517	1.1	3.736	1.6	2.7677	.36	2.1804	1.1	1.7197	.11	1.4542	0.95
...596	8.4	3.569	.22	2.7103	1.3	2.1251	.12	1.7139	.14	1.4441	...
...357	5.9	3.486	1.5	2.6774	0.63	2.0911	2.8	1.6724	1.9	1.4294	...
...103	0.45	3.428	0.95	2.5885	1.8	2.0670	0.58	1.6597	1.9	1.4182	...
988	2.2	3.344	100	2.5580	5.2	2.0202	1.1	1.6338	1.9	1.3828	...
...221	0.45	3.288	7.4	2.4913	1.6	1.9975	1.0	1.6021	0.92	1.3750	...
...117	3.0	3.193	0.82	2.4564	8.0	1.9784	2.3	1.5622	2.0	1.3715	...
...663	3.0	3.102	5.1	2.3992	3.9	1.9524	6.7	1.5423	0.8	1.3498	...
...250	26	3.031	11	2.3342	8.6	1.9095	2.5	1.5378	3.3		
...185	2.3	2.9881	1.3	2.2814	7.8	1.8725	1.7	1.5227	1.6		
...109	0.82	2.9293	1.8	2.2364	4.0	1.8184	.13	1.5160	1.3		

...9 lines in pattern

Identified Phases:

...PDS#	Sl	ML/X	At%	Identity . . .
...-0490D	267	15/2	95	Silicon Oxide / Quartz, low = SiO2
	Ierr:50,150		derr:2.0	Bground:0.45 dmax/min:11.04/1.343
...-0263I	95	22/*	8.0	*Potassium Aluminum Silicate Hydroxide / Muscovite-2M1 = KAl2(Si3Al)O10(OH,F)2
	Ierr:50,150		derr:2.0	Bground:0.45 dmax/min:11.04/1.343
...-0449*	<0	2/6	5.8	*Zinc Carbonate / Smithsonite = ZnCO3
	Ierr:50,150		derr:2.0	Bground:0.45 dmax/min:11.04/1.343
...-0696*	<0	2/9	13	*Iron Carbonate / Siderite = FeCO3
	Ierr:50,150		derr:2.0	Bground:0.45 dmax/min:11.04/1.343
...-0566I	17	3/1	3.3	*Zinc Sulfide / Sphalerite, syn = ZnS
	Ierr:50,150		derr:2.0	Bground:0.45 dmax/min:11.04/1.343
...-0141	11	7/9	29	Sulfur / Rosickyite, syn = S
	Ierr:50,150		derr:2.0	Bground:0.45 dmax/min:11.04/1.343

...mmary Report (Part 1 of 2):

	Full	Resid	5-0490: 95%		6-0263: 8%		8-0449: 6%		29-0696: 1...	
d	I	I	d	I	d	I	d	I	d	I
9.995	4.9	None			9.95	7.6				
...517	1.1	1.1								
...596	8.4	None								
"	"									
...357	5.9	5.9								
...103	0.45	0.45								

384066

.721	0.45	0.45								
.617	3.0	3.0								
4.65	3.0	None			4.47	1.6				
.256	36	None	4.26	33						
4.185	2.3	2.3								
4.09	0.82	None			4.11	0.32				
					<3.95	0.48>				
					<3.88	1.1>				
3.49	2.3	2.3								
.736	1.6	None			3.73	1.4				
3.769	22	16					3.55	2.9*	3.593	3.2
.486	1.5	None			3.48	1.6				
.428	0.95	0.95								
3.344	100	None	3.343	95	[3.34	2.0]				
					<3.32	8.0>				
.288	7.4	None								
.193	0.82	None			3.19	2.4				
.02	5.1	None			3.12	0.16*				
031	13	10								
2.9881	1.3	None			2.987	2.8				
2.9293	1.8	1.8								
8895	2.1	2.1								
					<2.859	2.0>			<2.795	13>
					<2.789	1.6>				
.677	36	36								
							<2.75	5.8>		
2.7103	1.3	None								
2.6774	0.63	0.63								
5885	1.8	None			2.596	1.3				
2.5580	5.2	None			2.566	4.4			[2.564	0.13]
					<2.505	0.64>				
4913	1.6	None			2.491	1.1				
2.4564	8.0	None	2.458	11	[2.465	0.64]				
"	"				[2.450	0.64]				
3992	3.9	3.1			2.398	0.80				
					<2.384	2.0>			<2.346	2.6>
2.3342	8.6	7.1					2.327	1.5*		
2.2814	7.8	None	2.282	11						
					<2.254	0.80>				
2.2364	4.0	None	2.237	5.7	[2.236	0.32]				
2.2115	1.6	None			2.208	0.64				
2.1804	1.1	None			2.189	0.32				
					<2.149	1.3>				
2.1251	12	None	2.128	8.6	[2.132	1.6]			[2.134	2.6]
							<2.110	1.0>		
2.0911	2.8	2.8								
2.0670	0.58	None			2.070	0.32				
					<2.053	0.48>				
2.0202	1.1	1.1								
1.9975	1.0	None			1.993	3.6				
1.9784	2.3	None	1.980	5.7	[1.972	0.80]				
									<1.965	2.6>
1.9524	6.7	4.7			1.951	0.48*	1.946	1.5		
1.9095	2.5	None								
1.8725	1.7	None			1.871	0.32				
1.8184	13	None	1.817	16	[1.822	0.32]				
			<1.801	0.95>					<1.7968	1.5>
1.7848	3.8	2.7								
					<1.731	0.64>	<1.776	0.70>	<1.7382	3.8>
									<1.7315	4.5>
1.7197	11	11								
1.7139	14	14			1.710	0.48*				

.6724	1.9	None	1.672	6.7						
. 597	1.9	None	1.659	2.9	[1.662	0.96]				
					<1.646	2.0>				
.6338	1.9	None			1.631	0.48				
			<1.608	0.95>	<1.620	0.48>				
. 021	0.82	None			1.603	0.48				
5622	2.0	None			1.569	0.64				
.5423	6.8	None	1.541	14	[1.541	0.32]				
. 378	3.3	None	" "	"	" "	"				
5227	1.3	None			1.524	0.96				
5162	1.3	None					1.515	0.91		
					<1.504	2.4>			<1.5060	1.0>
976	5.2	5.2								
							<1.493	0.81>		
.4542	0.95	None	1.453	2.9	[1.453	0.32]				
. 441	1.5	1.5								
4294	0.88	None							1.4266	1.4
.4182	4.1	3.1	1.418	0.95						
							<1.411	0.58>	<1.3969	0.77>
0828	5.5	None	1.382	6.7					[1.3818	0.38]
.3750	11	None	1.375	10	[1.375	0.16]	[1.374	0.23]		
.3715	7.1	None	1.372	8.6	" "	"	" "	"		
									<1.4548	1.4>
3490	2.1	None			1.352	0.96				

* = Obscured <..> = Missing [..] = Previously Removed

384067

mmary Report (Part 2 of 2):

	Full I	Resid I	5-0566: d	3% I	13-0141: d	29% I
4. 995	4.9	None				
617	1.1	1.1				
.1596	8.4	None			6.65	7.2
"	"				6.63	1.1
057	5.9	5.9				
103	0.45	0.45				
1.0988	2.2	None				
0721	0.45	0.45				
617	3.0	3.0				
1.1465	3.0	None				
					<4.41	1.7>
256	36	None				
. 185	2.3	2.3				
1. 109	0.82	None				
3.0349	2.3	2.3				
					<3.79	4.0>
. 736	1.6	None			[3.74	5.7]
2.1569	22	16				
3. 186	1.5	None				
1 428	0.95	0.95				
344	100	None				
2 288	7.4	None			3.29	29
1 193	0.82	None				
			<3.123	3.3>		
3 102	5.1	None			3.10	2.9
1 031	13	10			3.04	3.4
2.9881	1.3	None			[3.00	1.1]
2 3293	1.8	1.8				
3895	2.1	2.1				
2 7677	36	36				

.6774	0.63	0.63				
.5885	1.8	None			[2.60	0.57]
[redacted]580	5.2	None				
.4913	1.6	None			[2.49	2.3]
[redacted]564	8.0	None			[2.46	1.7]
[redacted]	"	"				
					<2.44	1.1>
[redacted]3992	3.9	3.1				
[redacted]5342	8.6	7.1				
.2814	7.8	None				
[redacted]364	4.0	None				
.2115	1.6	None				
[redacted]1804	1.1	None			[2.18	1.1]
[redacted]1251	12	None				
					<2.10	0.57>
[redacted]911	2.8	2.8				
[redacted]670	0.58	None				
[redacted]202	1.1	1.1				
[redacted]975	1.0	None				
.9784	2.3	None				
[redacted]524	6.7	4.7				
					<1.932	0.57>
9095	2.5	None	1.912	1.7		
					<1.894	0.57>
[redacted]725	1.7	None			1.872	1.1
					<1.857	1.7>
[redacted]184	13	None				
7848	3.8	2.7			1.786	1.1
[redacted]197	11	11				
7139	14	14				
					<1.708	0.57>
					<1.679	0.57>
6724	1.9	None				
[redacted]597	1.9	None				
[redacted]338	1.9	None	1.633	0.99	[1.635	1.7]
[redacted]021	0.82	None			[1.599	0.57]
[redacted]622	2.0	None	[1.561	0.07]	[1.567	1.1]
5423	6.8	None				
[redacted]378	3.3	None				
[redacted]227	1.3	None				
5162	1.3	None				
[redacted]976	5.2	5.2				
4542	0.95	None			[1.452	5.2]
[redacted]441	1.5	1.5				
[redacted]294	0.88	None			[1.432	1.1]
4182	4.1	3.1				
[redacted]828	5.5	None				
3750	11	None				
[redacted]3715	7.1	None				
[redacted]490	2.1	None	[1.351	0.20]		

* = Obscured <..> = Missing [..] = Previously Removed

384069

CRA ADVANCED TECHNICAL DEVELOPMENT

Analytical Laboratory

Chemical Analysis Report

Report to: ROWLAND ONG

Department: MINERAL PROCESSING

Date Received: 03/09/96

Date Required: 13/09/96

Date Reported: 13/09/96

Project code: F857E

Request No's: B1148

Job : F857E11

Copy to Rob Walker

Invoice Amount $367.00

Unless otherwise specified, all results are reported on an "as-received" basis and to an accuracy and precision of ± 5%.

Authorised by: B O'Riordan

CRA ADVANCED TECHNICAL DEVELOPMENT

Analytical Laboratory

Project Code: F857E

Request number:B1148

Analytical Results

Final

	Analytes	Zn	Pb	SiO2	Fe
	Units	%	%	%	%
	Method	ICP2	ICP2	ICP2	ICP2
	Det Lim	0.01	0.01	0.01	0.01
	F14785	7.32	0.58	45.8	10.1
	F14786	12.1	7.09	42.8	3.20
	F14787	17.9	<0.01	34.5	8.80
	F14788	4.73	2.94	60.7	2.70
Dup	F14788	4.69	2.88	60.0	2.69

CRA ADVANCED TECHNICAL DEVELOPMENT

Analytical Laboratory

Project Code: F857E

Request number: B1148

Analytical Results

Final

	Analytes	S	C
	Units	%	%
	Method	CS1	CS1
	Det Lim	0.01	0.01
	F14785	4.67	3.70
	F14786	3.11	1.79
	F14787	1.76	5.74
	F14788	5.11	1.22
Dup	F14788	5.05	1.25

384072

CRA ADVANCED TECHNICAL DEVELOPMENT

Analytical Laboratory

Project Code: F857E

Request number: B1148

QC Check Results

Analytes	Zn	Pb	SiO2	Fe	S
Units	%	%	%	%	%
Method	ICP2	ICP2	ICP2	ICP2	CS1
Det Lim	0.01	0.01	0.01	0.01	0.01
CS5	--	12.7	--	14.5	--
Exp value	31.49	12.47	5.13	14.23	--
CS8	10.7	2.84	17.2	--	--
Exp value	10.44	2.76	16.49	28.97	--
CS14	--	--	64.9	--	--
Exp value	1.035	0.206	63.1	8.62	--

CRA ADVANCED TECHNICAL DEVELOPMENT

Analytical Laboratory

Project Code: F857E

Request number: B1148

QC Check Results

Analytes	C
Units	%
Method	CS1
Det Lim	0.01
CS5	--
Exp value	--
CS8	--
Exp value	--
CS14	--
Exp value	--

Appendix 2

Metallurgical testwork

amdel

A.C.N. 008 127 802

Amdel Limited
Mineral Services Laboratory
Osman Place
Thebarton SA 5031
AUSTRALIA

Telephone (08) 8416 5200
Facsimile (08) 8352 8243
Telex AA 82520

PO Box 338
Torrensville Plaza SA 5031

384075

30 September 1996

CRA ATD
1 Research Avenue
BUNDOORA VIC 3080

Attn: R Walker

REPORT G653600G/96

HEAVY LIQUID SEPARATION OF TWO SAMPLES

YOUR REFERENCE:	Note fro R Walker enclosed with samples
SAMPLE IDENTIFICATION:	5471296, 5471297
MATERIAL:	+20 μm particulate material
DATE SAMPLES RECEIVED:	19 September 1996
DATE AUTHORISATION RECEIVED:	19 September 1996
WORK REQUIRED:	Heavy liquid separation
INVESTIGATION AND REPORT BY:	Dr Keith J Henley

Keith Henley

Dr Keith J Henley
Manager, Mineralogical Services

cjc

HEAVY LIQUID SEPARATION OF TWO SAMPLES

1. INTRODUCTION

Two particulate samples (+20 μm) labelled 5471296 and 5471297 were submitted by CRA ATD (R Walker) for centrifugal heavy liquid separation.

2. PROCEDURE

Each sample was weighed and then separated centrifugally in a heavy liquid of specific gravity 3.3 using a density gradient and recycling the products according to the flowsheet given in Appendix 1. The products were weighed and returned to CRA ATD by courier on 24 September 1996.

3. RESULTS

Sample	Weight, g				Weight, %		
	<3.3 sp. gr.	>3.3 sp. gr.	Total	Initial	<3.3 sp. gr.	>3.3 sp. gr.	Total
5491296	6.73	3.21	9.93	10.20	67.72	32.28	100.00
5491297	8.02	28.09	36.11	36.45	22.22	77.78	100.00

APPENDIX 1
SEPARATION FLOWSHEET

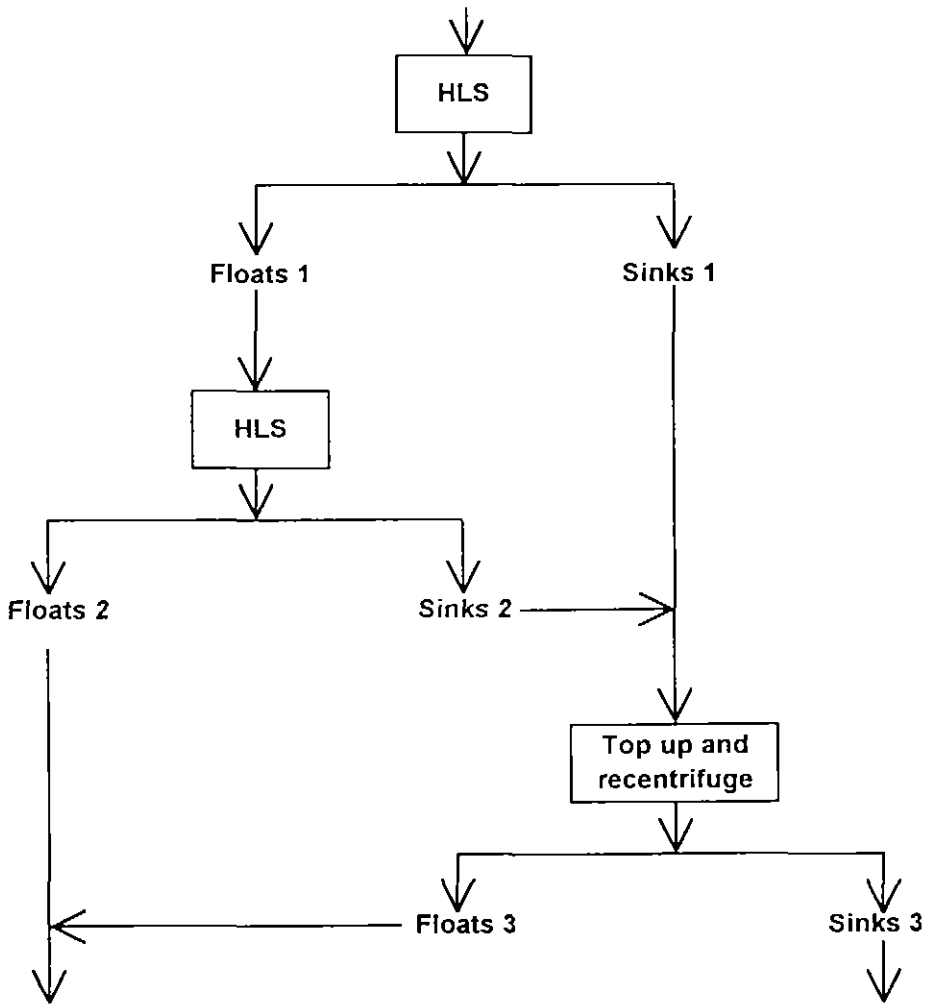

Note:
HLS means centrifugal heavy liquid separation with a density gradient

384079

Appendix VI

Detailed Helimag Data

CRA EXPLORATION PTY. LIMITED
ACN 000 057 125

Preliminary Notes and Observations of the Helicopter-borne Magnetic Survey Zeehan, Tasmania

Author: SJ Tear
J Tesselaar

Date: July 1996

Submitted to: Chief Geologist, Vic/Tas

Copies to: Mineral Resources Tasmania
CRAE - SE District
CRAE - ETIG
CRAE - Zeehan
Allegiance Mining NL

Submitted by:

Accepted by:

CRAE Report No. 22222

List of Figures

List of Appendices

1. Introduction

Drillcore from the Gordon Limestone of the Zeehan area shows zinc mineralisation being related to weakly magnetic siderite alteration. This alteration predominantly occurs at the base of the Limestone just above its contact with the underlying Moina Sandstone. Siderite alteration can occur at the limestone's upper contact with the overlying Crotty Quartzite eg at Blackjacks and Myrtle whilst intense alteration is also associated with limestones in the middle of the Gordon Limestone eg the Oceana Mine and the Grieves South area. The magnetic response of the siderite is weak, in the range of 50-200 x 10-5 SI, but is deemed detectable by an airborne magnetic survey. Forward modelling indicated that the siderite would give weak aeromagnetic anomalies (1-5nT). Thus a helimag survey was commissioned to fly over all the Gordon limestone outcrops of the Zeehan under licence to CRAE.

The aim of the survey was to identify mineral-related siderite zones for follow-up diamond drilltesting. The target is a stratabound zinc/lead orebody hosted by the Ordovician Gordon Limestone with analogies to Irish-type Zn/Pb orebodies.

A separate survey was flown over the Gordon Limestone of McLean Creek. This area is known to have a large magnetic anomaly - attributed to a magnetite skarn - known as the Avebury target. In addition the nickel target areas at Melba Flats were also flown.

This report provides technical details of the survey and processing as well as some geological interpretations of the results. Locations of the prospects are shown in plan Tv1022.

The survey was flown in March 1995 by Universal Tracking Systems Pty. Ltd. with initial results received in December 1995. Data processing and some interpretation was undertaken by Tony Doe and John Tesselaar (CRAE - Orange).

Sub-divisions of the Gordon Limestone for drillhole logging purposes have been made on a lithostratigraphic and lithologic basis and is included elsewhere in this report.

2. Flight Survey and Data Processing Details

The flight line height was a nominal 30m with the line spacing approximately 60m with readings taken every 4-5m. A total of 2400 line km was completed covering the following prospects :- Sassafras, Blackjacks-Mariposa-Sunny Corner-Pyramid, Professor Range-Amber Creek-King Billy-Leatherwood, Myrtle-Grieves-Baura-Firewood Siding-Rose Valley. New areas between Leatherwood and Mariposa were also investigated and this included the Westerway and Tom Creek areas. Flight line maps are shown in Appendix I.

The data from the helimag survey was obtained as an XYZ file of easting, northing and total magnetic intensity. No terrain clearance data was provided with the original XYZ file.

Over each area of Gordon Limestone to be interpreted, a small (<3km2) data subset was selected. These areas were designed to include all of the Gordon Limestone but as little as possible of the surrounding rocks, particularly the Dundas Group which tended to 'swamp' the more subtle magnetic data variations of the limestone. This data was then imaged.

The vertical derivative of the magnetic data was produced along the flight line using TRAKPAK. This data was then imaged with the previously existing geology data superimposed. Some of the small linear anomalies coincided with mapped siderite. Other lithological units were also mapped

eg the Moina Sandstone and the Crotty Quartzite.

Where applicable, magnetic inversion using MAGMOD was undertaken over the siderite-like anomalies. In most cases, anomalies over 1nT were able to be successfully inverted. These models should only be used as a guide as to the geometry of the source of the anomalies. This is due to :-

- There is no account of terrain clearance;
- The anomalies have small amplitudes;
- Not all lines were perpendicular to strike;
- The problem of "non-uniqueness" in magnetic inversion.

3. Magnetic Interpretations

Initial raster images failed to highlight major zones of inferred siderite alteration (plan Tv1026). Removal of regional gradients and the selective use of sub-area vertical derivative data greatly improved the resolution (plan Tv 1027). From the modelling it was impossible to distinguish between siderite zones and other stratabound weakly magnetic units.

As a result of this work a much better understanding was gained of the geology of the Ordovician-Silurian sequence in the Zeehan area.

The Gordon Limestone is relatively more magnetic than the surrounding clastic sequences whilst the Siltstone Unit of the limestone is less magnetic than the limestone. The high magnetic susceptibility of the surrounding Cambrian Dundas Group of sediments, volcaniclastics and basic intrusions caused imaging problems. Major units which appeared as magnetic highs included the Upper Dolomite Unit of the Gordon Limestone (possibly other dolomitic zones are relatively magnetic but lack of geochemical surface control could not confirm them) and the Amber Slate of the Silurian clastic sequence. Major structures are difficult to identify and follow. Interpreted linears deemed to represent faults show a lack of continuity eg the Firewood Siding Fault and the Little Henty Fault.

3.1 Grieves (plan Tv 1139)

- The clastic Siltstone Unit is a magnetic low compared to the surrounding limestone particularly the dolomitised units, which locally are enhanced magnetically eg. 364250mE, 5350000mN.

- Many weak anomalies occur including one associated with the siderite drill intercepts at the lower limestone contact at the Grieves Siding trial excavations (364500mE, 5349250mN). However this anomaly is no different to some of the sub-regionally enhanced Upper Dolomite Unit and the undifferentiated dolomite of the upper third of the Gordon Limestone sequence. Further interpretative work is required.

- The Crotty Quartzite at South Grieves/Baura appears to have a magnetically distinct sub-unit within it which is not seen elsewhere. This may reflect a change in the depositional environment in early Silurian times which is related to syn-depositional faulting (363350mE, 5349850mN).

- A cultural-looking anomaly occurs at South Grieves close to siderite intersections in drillcore including 7m @ 8% Zn. This anomaly lies close to an inferred E-W striking mineralised structure which also occurs in DD96ZG412. The anomaly is not attributed to drillhole casing (363630mE, 5348900mN).

4. General Geological Interpretation Summary

- The Amber Slate is a non-calcareous slate of Silurian age which is recognised in the dataset as a magnetic high.

- The Crotty Quartzite appears on the vertical derivative map as a magnetic low.

- The Gordon Limestone appears as a magnetic high except for the non-calcareous, argillaceous Siltstone Unit eg King Billy, Amber Creek, Grieves, Myrtle, Baura and Firewood Siding. The Siltstone Unit is not apparent in the magnetic data at Blackjacks, Mariposa, Sunny Corner Tom Creek and Pyramid.

- The Moina Sandstone is a magnetic low near the overlying Gordon Limestone. At Grieves this low unit is 200-300m thick before passing down sequence into a magnetic high. This high unit may be part of the Owen Conglomerate.

- The Owen Conglomerate is generally a magnetic high eg Professor Range and Pyramid.

- Major, brittle faults are not readily identifiable, often disappearing along strike eg the Balstrup Fault in the Pyramid and Tom Creek areas.

- Parts of the Gordon Limestone display more continuously intense magnetic zones eg at Grieves and Firewood Siding South. This may be a reflection on mineral fluids having altered the limestone particularly via dolomitisation. Alternatively these highs may be a reflection of powerful surface weathering producing surficial de-calcified clays. It is possible to say that the rotting of variably composed limestone may give rise to differential surface effects that have different magnetic susceptibilities.

- The diamond drilling identified siderite zones at Blackjacks, Mariposa and Grieves can be seen in the magnetic data. However numerous anomalies of a similar intensity occur elsewhere, generally in areas of the Gordon Limestone considered as non-prospective.

- There are several targets in the magnetic data that lie at the base of the Gordon Limestone which require drill testing.

Simon Tear
John Tesselaar

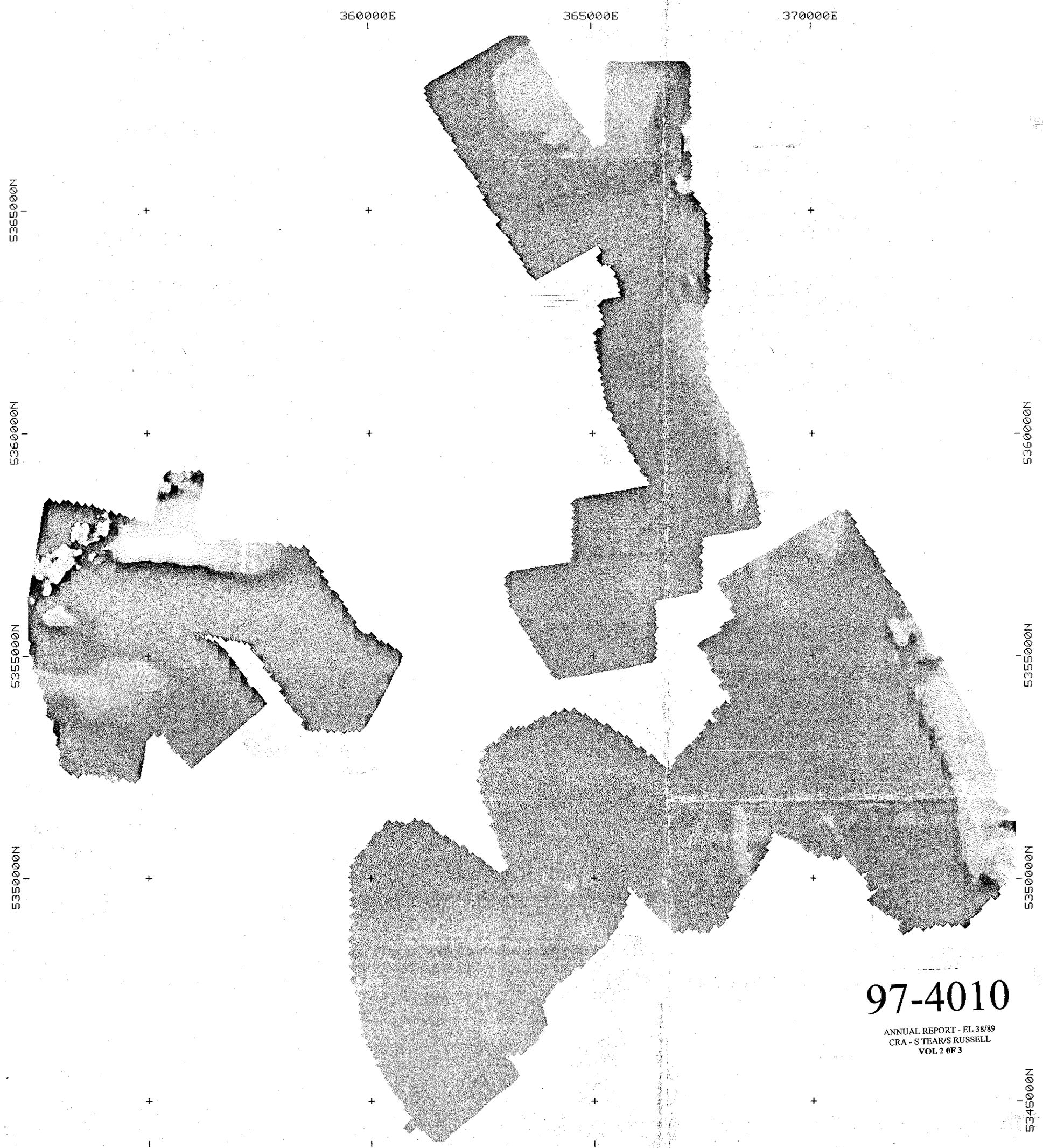

97-4010

ANNUAL REPORT - EL 38/89
CRA - S TEAR/S RUSSELL
VOL 2 OF 3

CRAE AIRBORNE MAGNETIC SURVEY, ZEEHAN AREA
TOTAL FIELD (GEOSOFT GRIDDING)
CRAE SURVEY NUMBER T27M AMG PROJECTION ZONE 55 DATUM AGD 66
CELL SIZE 20M RESAMPLED TO 10M PLOT NO QIP0496 1:50,000

CRA EXPLORATION PTY. LIMITED

384085

Zeehan Helimag Survey

Total Magnetic Intensity Map

Author: John Tesselaar	Reference: SK55-05
Drawn: John Tesselaar	File Name:
Date: July 1996	Report No: 22222
Scale: 1:50,000	Plan No: Tv1026

5 cm

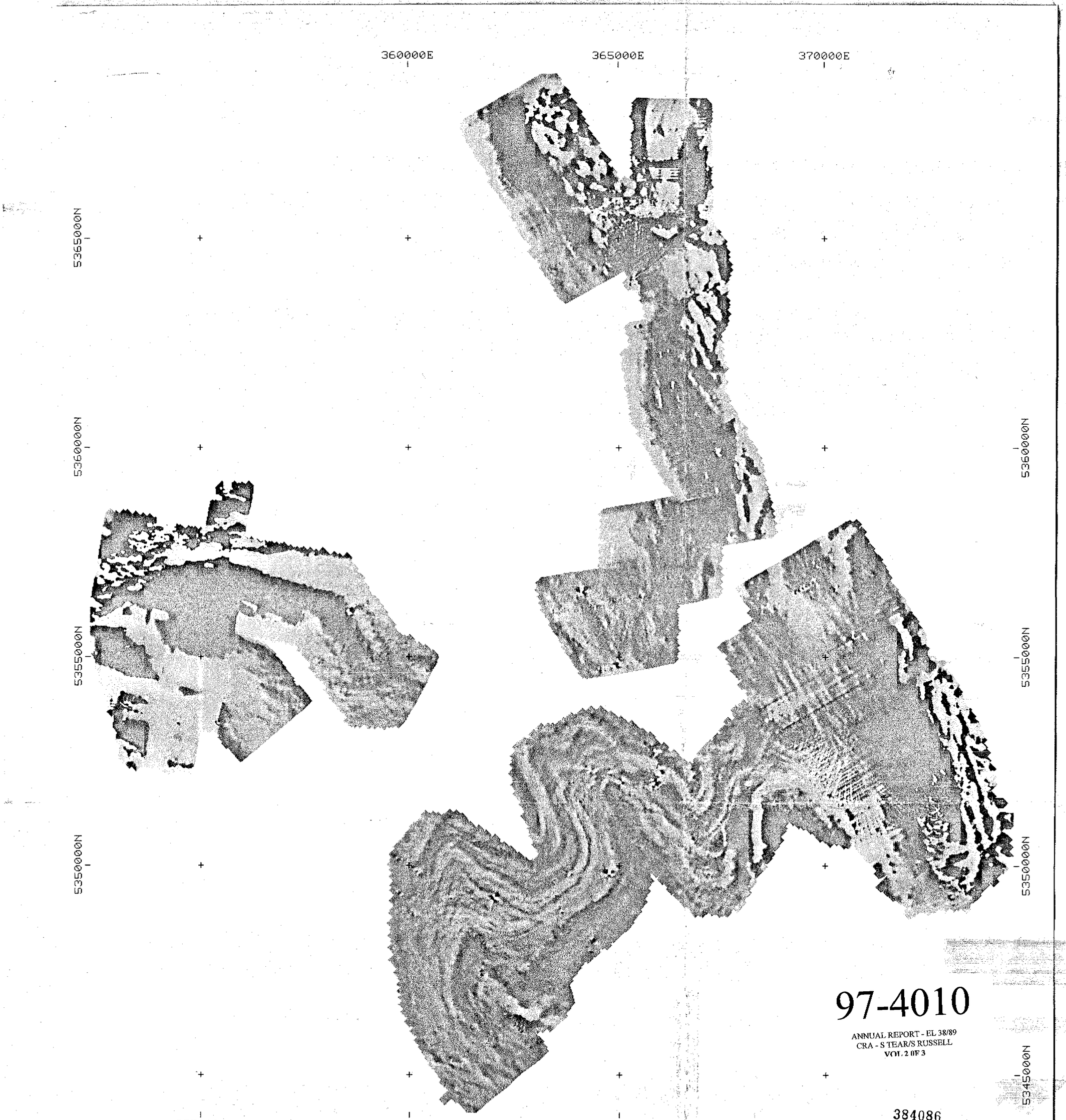

CRAE AIRBORNE MAGNETIC SURVEY, ZEEHAN AREA
VERTICAL DERIVATIVE (GEOSOFT GRID)
CRAE SURVEY NUMBER T27M AMG PROJECTION ZONE 55 DATUM AGD 66
CELL SIZE 20M RESAMPLED TO 10M PLOT NO QIP0497 1:50,000

97-4010

ANNUAL REPORT - EL 38/89
CRA - S TEAR/S RUSSELL
VOL 2 OF 3

384086

CRA EXPLORATION PTY. LIMITED

Zeehan Helimag Survey

Vertical Derivative Map

Author: John Tesselaar	Reference: SK55-05
Drawn: John Tesselaar	File Name:
Date: July 1998	Report No: 22222
Scale: 1:50,000	Plan No: Tv1027

5 cm

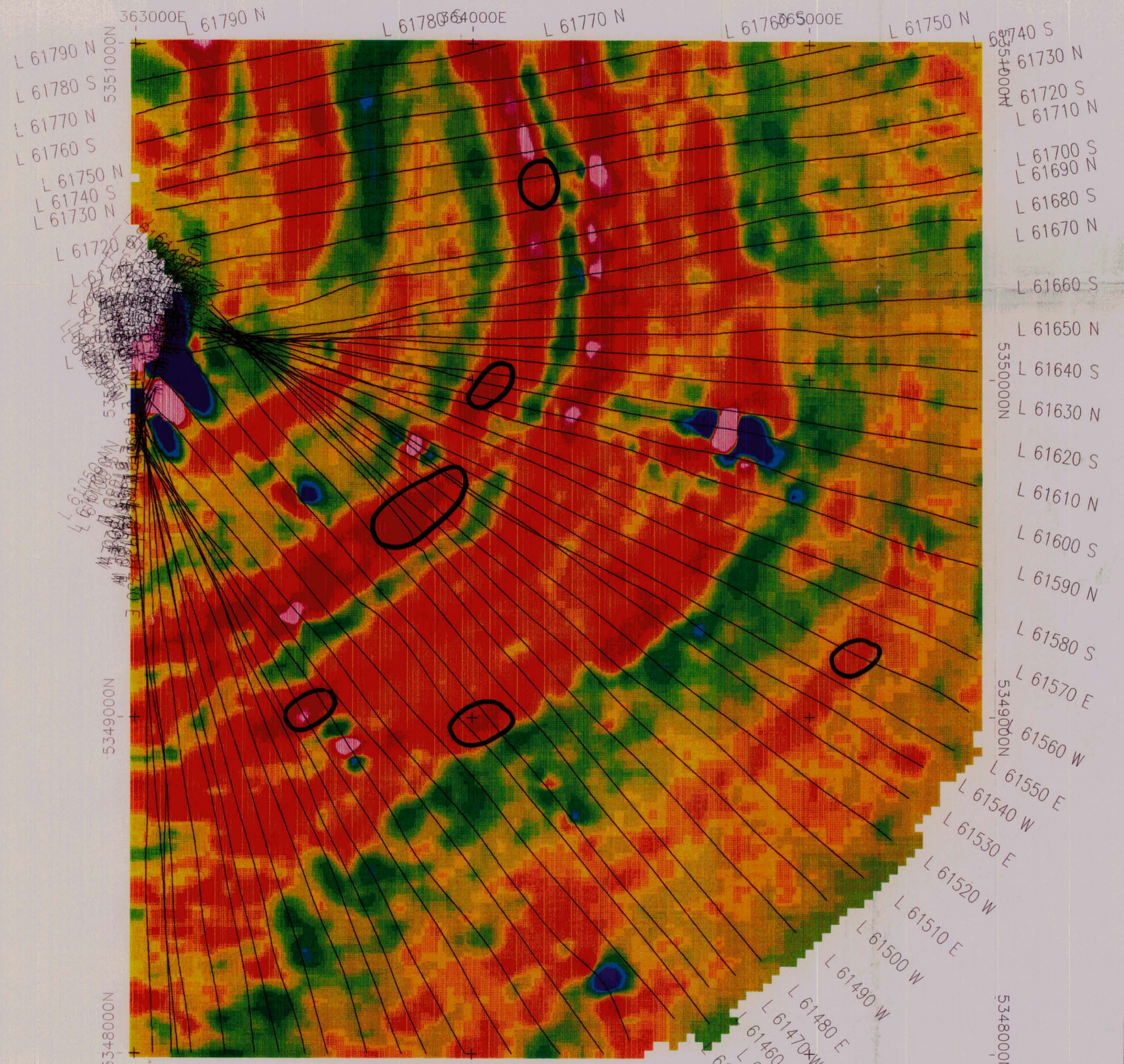

97-4010

ANNUAL REPORT - EL 38/89
CRA - S TEAR/S RUSSELL
VOL 2 OF 3

CRA EXPLORATION PTY. LIMITED

Zeehan Helimag Survey

EL38/89 Zeehan 4 - Grieves Prospect

Vertical Derivative Image, Flight Line Overlay & Modelled Anomalies

Author: John Tesselaar	Reference: SK55-05
Drawn: John Tesselaar	File Name:
Date: July 1996	Report No: 22222
Scale: 1:10,000	Plan No: Tv1139

Appendix VII

Basin Analysis Report

ORDOVICIAN GORDON GROUP CARBONATES, ZEEHAN REGION, TASMANIA, AUSTRALIA - STRATIGRAPHY AND PALAEOENVIRONMENTS

CLIVE BURRETT,
GEOSEA CONSULTANTS,
22 HINMAN DRIVE,
KINGSTON, TASMANIA,
AUSTRALIA, 7050

Final Report 15-11-1995

CONTENTS

ABSTRACT

The Gordon Group in the Zeehan area comprises 3 conformable formations; the Ugbrook, Myrtle (new) and Black Jacks (new). The Ugbrook Fm, first defined in the Mole Creek area, was deposited in protected shallow subtidal to low intertidal waters in an offshore bar to lagoonal to lagoonal-island environment during the Early Caradoc.

The basal Ugbrook interdigitates with the siliciclastic Moina Fm and suggests that the Early Caradoc shoreline was at or very close to Black Jacks. A transgression shifted these environments northwards and eastwards during the Caradoc and Ashgill.

The tidal flat complex of the Myrtle Fm developed throughout the area in the mid-Caradoc and consists of fifteen 1m to 4m thick Punctuated Aggradational Cycles (PACs) which can be correlated throughout the area. The Myrtle Fm is similar lithologically, environmentally and chronostratigraphically to the Lower Limestone Member of the Florentine Valley.

The Myrtle Fm is succeeded by mainly shallow to moderately deep subtidal alternating micrites and shales with minor PACs, belonging to the Black Jacks Fm which is similar to the Upper Limestone Member of the Florentine Valley. The lack of PACs in the Upper Black Jacks and the very common occurrence of coarse carbonates in the Myrtle stratigraphic drillcore suggests that the Myrtle area might have been in a slightly deeper and more rapidly subsiding region. The Lords Member of the Black Jacks Fm is present in several of the drillcores and, as is normal elsewhere in the state, varies in thickness and lithology from mudstones to coarse sandstones. Minor PACs and some faunal horizons help in the correlation of the Black Jacks.

INTRODUCTION

At the request of CRA, 8 full days in October 1995 were spent logging core through Ordovician sedimentary sequences from drillholes in the Zeehan area. An extra four days were allocated to plotting, drafting, report preparation and the examination of thin sections and fossils. Logging concentrated on the Gordon Group carbonates but short sections of the underlying Denison Group (Moina Fm) and overlying Eldon Group (Crotty Fm) siliciclastics were also examined.

The Gordon Group carbonates are deformed and the extent of stratigraphic loss or repetition is difficult to establish from the numerous veined and crushed intervals. In any sedimentary basin analysis it would be desirable to plot isopachs in order to define the basin shape and its evolution through time. Unfortunately, depending on the relation of bedding to the principal axis of the strain ellipsoid, bedding thickness may be increased or decreased substantially. Tectostylolites, which are pervasive in the Zeehan cores, will decrease stratigraphic thickness. They preferentially affect more argillaceous sections and the amount of section loss will (as with cleavage) depend on their angle of incidence with bedding. This problem is soluble but not within the confines of this study. A full palinspastic study would also need to remove, in map view, the Devonian folding and the thrust faulting.

LITHOSTRATIGRAPHY

Several major lithostratigraphic units are recognisable in the Zeehan cores. The Gordon Group comprises the Ugbrook Fm, the Myrtle Fm (new name) and the Black Jacks Fm (new name). The Black Jacks Fm includes the Lords Siltstone Member (Fig.1). The positions and suggested correlations of these units are shown in Fig. 5 (large diagram in pocket). All thicknesses are uncorrected downhole distances rather than dip-corrected stratigraphic thicknesses.

Denison Group, Moina Formation

The Moina Fm of the Denison Group underlies the Gordon Group in northern and western Tasmania (Fig. 2). The boundary between the Moina Fm and the Gordon Gp is everywhere marked by a siltstone-mudstone transitional zone that may be a metre thick or 30m thick. This transition is 200m thick in the Florentine Valley and is known as the Florentine Valley Fm. The separation between the Denison Gp and the Gordon Group is based on the dominance of siliciclastics (Denison Gp) and limestone (Gordon Gp). The siltstone-mudstone transition is therefore historically and pragmatically regarded as the topmost part of the Moina Fm and the base of the Gordon Gp is defined on the incoming of carbonates. However, where there is an interdigitation of siliciclastics and carbonates, as in DB111, or where the lowest limestones are replaced by siderite or are mineralised then the placement of the boundary may be arbitrary. In all sections, delineation of the boundary has to regarded as a matter of taste. In most sections I have taken the boundary to be the first obvious and definite limestone.

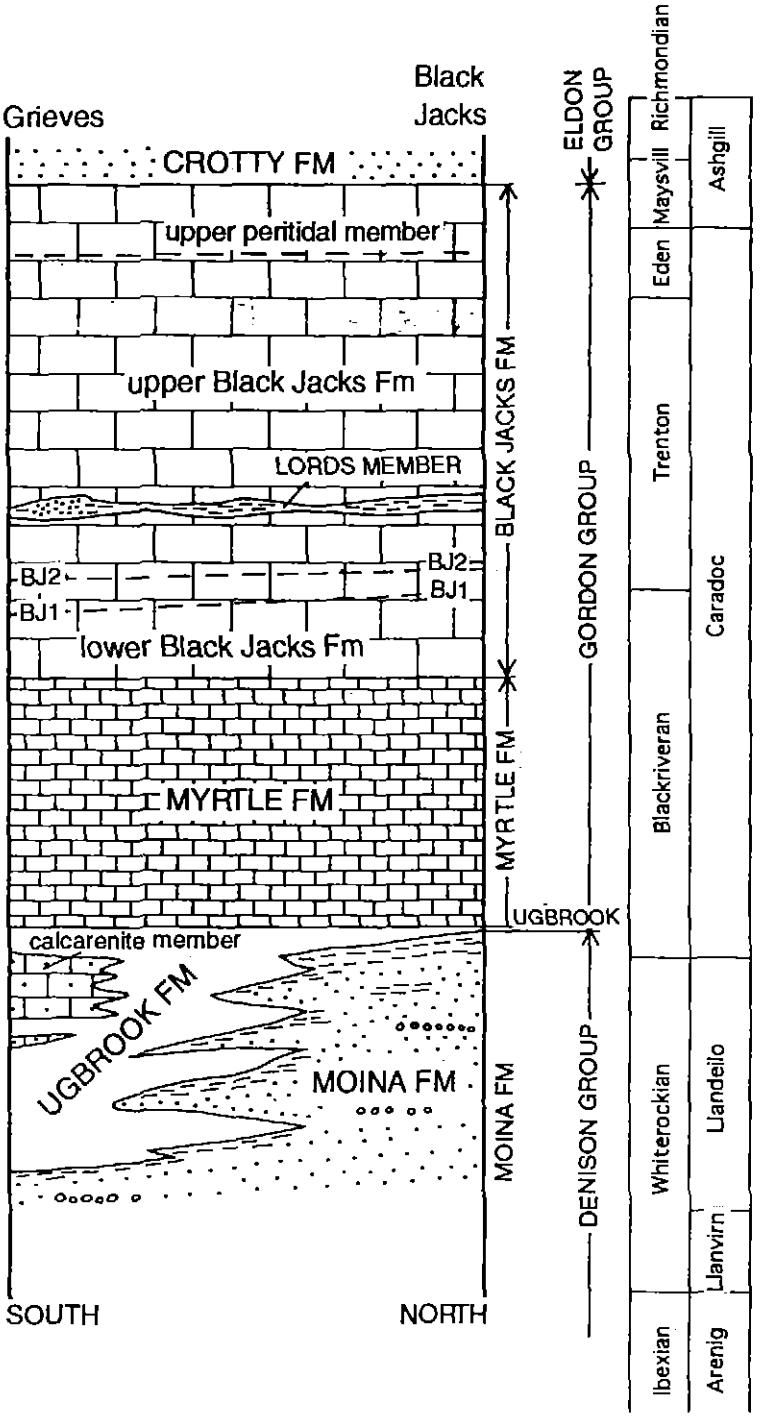

Fig.1 Summary of Ordovician lithostratigraphy in the Zeehan region.
Chronostratigraphic units are based on the standard North American scheme and the standard British scheme. Correlations are most easily made to the American scheme but the British scheme is used in the text because of its greater familiarity.

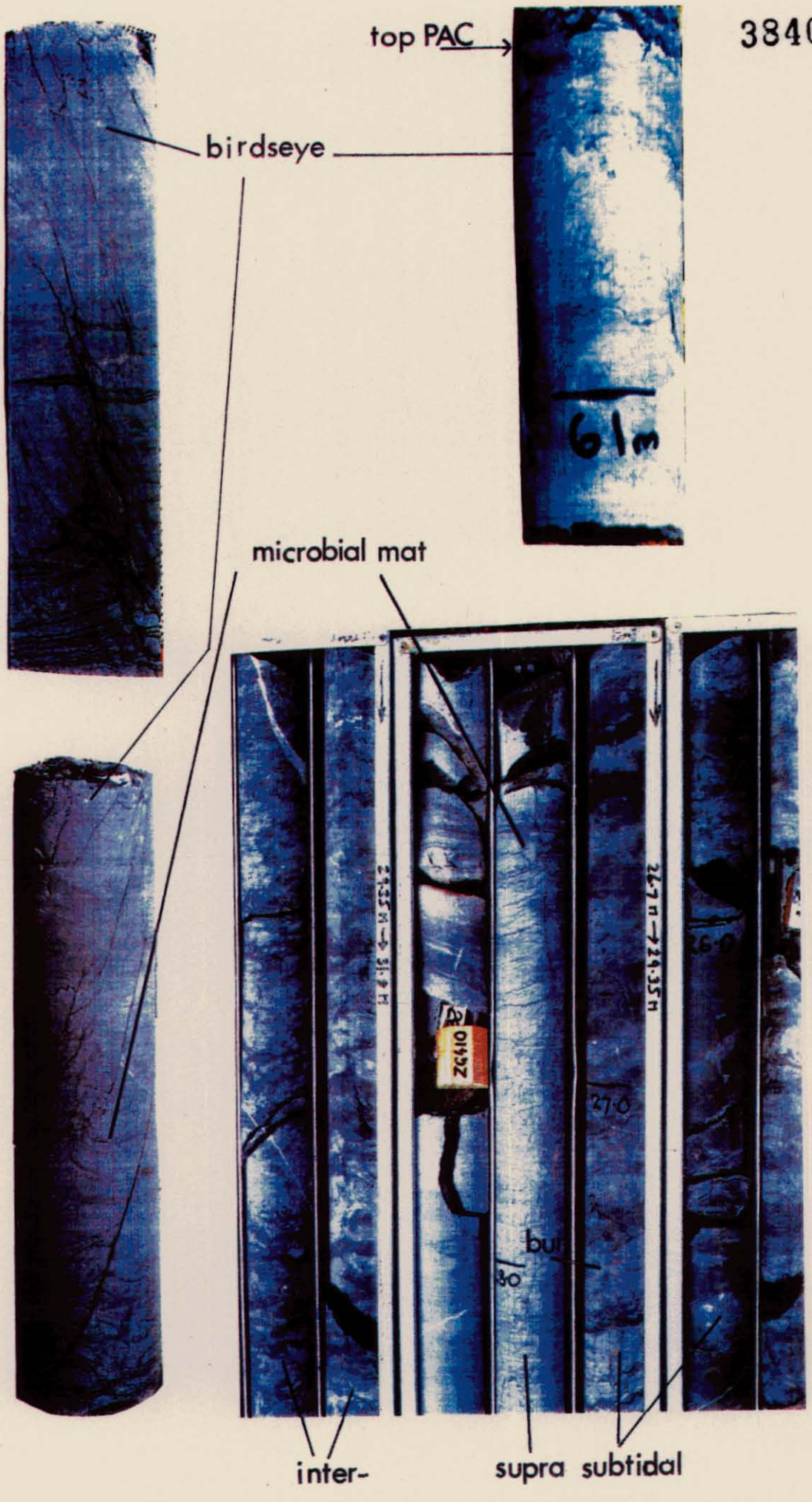

Plate 1 Typical PAC lithologies from ZG 410. Note darkening of limestone from shallow to deep.Core between 26.7m and 27m is typical subtidal alternation of argillaceous and micritic limestone and this lithology is typical of much of the Black Jacks Fm. but forms a small percentage of the Myrtle Fm. Boundary between Myrtle Fm and Black Jacks Fm is at 27.5m.

Ugbrook Formation (Burrett & Goede 1987, Burrett *et al.* 1989)

The siltstones of the upper part of the Moina Fm are succeeded by alternating thin micrites and shales with, in some cores, siltstones and sands (notably DB111). These centimetre-decimetre scale alternations are frequently bioturbated and often nodular (due to sedimentary boudinage). Pelloids and comminuted shells are very common. Asaphid trilobites are present but other identifiable fossils are rare. Several sections have developments of biocalcarenites and/or biosparites composed mainly of crinoidal debris. These sequences are very similar to the Ugbrook Fm in Mole Creek (Burrett *et al.* 1989; Appendix C) and, rather than erect a new name, I will use that term. This lithology is only a few metres thick in DB 110 (possibly 40m thick if a sideritised zone is included) and thickens towards Myrtle which also has a thick development of the crinoidal biospararenite member.

Myrtle Formation (new name)

The Myrtle Fm consists of between 40-170m of micrites, biomicrites, dolomitised micrites and minor calcarenites and shales deposited as upwardly shallowing tidal flat cycles known as Punctuated Aggradational Cycles (PACs). These were first recognised and used as a correlation tool by Calver (1977). Unfortunately, he did not publish and PACs have since been recognised worldwide as a useful correlation and palaeoenvironmental tool. The PAC concept is summarised in Appendix B and photographs of representative lithologies are shown on the attached photographs (Plate 1). Calver (1977) used PACs to correlate throughout the Florentine River Valley recognising 18 PACs in the Lower Limestone Member of the Benjamin Limestone. In the Florentine Valley, and in Zeehan, this correlateability is due to a basinwide or at least sub-basinwide response to changing sea level. PAC boundaries may therefore be regarded as essentially isochronous horizons. Fifteen PACs are recognised in the Myrtle Fm. and each section has most of them. The extent of faulting in ZG 403 is clear as only the first PAC is present.

Black Jacks Formation (new name)

The Myrtle Fm is succeeded by the Black Jacks Fm which consists of alternating micrites and shales with some biomicrites, calcarenites and calcisiltites. Two PACs occur in the Lower Black Jacks but are not present in every section. These are labelled BJ1 and BJ2 on Fig. 5. The Lords Member is a thin (1m-15m) siltstone-shale-sometime sandstone unit that is surprisingly variable on a kilometre scale for a unit that appears over most of western Tasmania from Precipitous Bluff on the south coast to the Florentine Valley to Zeehan to Mole Creek (Fig.2). The Lords Member equivalent at Mole Creek (the Mole Creek Fm) is discontinuous (see p.7 of Appendix C). A coarse, quartz sandstone occurs at the appropriate stratigraphic level in ZF 37 (Firewood Siding). The Lords Member is characterised, statewide, by a distinctive fauna consisting of abundant *Pliomerina* trilobites, strophomenid brachiopods (*Sowerbyites*) and the Tasmanian endemic ostracod *Dominina*.. The Lords Member lithology/fauna does not appear suddenly but is preceded by a gradual deepening of both biofacies and lithofacies.

The Upper Black Jacks Fm is completely dolomitised in some holes (ZR 104) and partially in others (DTM 84-6, DTB 84-1). Complete dolomitisation is unusual in the Gordon Group and increased porosity, including vuggy porosity, is evident in ZR 104 due to the 12% volume loss when calcite is replaced by dolomite. As dolomitised limestones are important petroleum reservoirs (and therefore porous for ore forming fluids) it might be useful to plot the distribution of dolomitisation within the Gordon Group at Zeehan (see Appendix A).

Where undolomitised, there is an abundant coral-stromatoporoid fauna, some of which is correlated to the widespread 'Den fauna'. A diverse trilobite-brachiopod-bryozoan fauna, which in previous studies has been called the 'Smelters fauna' (Zeehan Smelters fauna described by Pitt (1961) and mentioned by Banks and Burrett (1980), occurs below an 'upper peritidal member '. This 'upper peritidal member' occurs in ZF 37, DS 98, DTM 84-6 and DB 110 but is not obvious in ZM190.

PALAEOENVIRONMENTS

Most sections of the Gordon Group were deposited in predominantly very shallow subtidal to peritidal conditions on a mini-platform. due to a marine transgression from the south, west and east towards the Precambrian/Cambrian islands of the Tyennan and Rocky Cape regions (Fig. 3). Thick siliciclastic sandstone sequences, followed

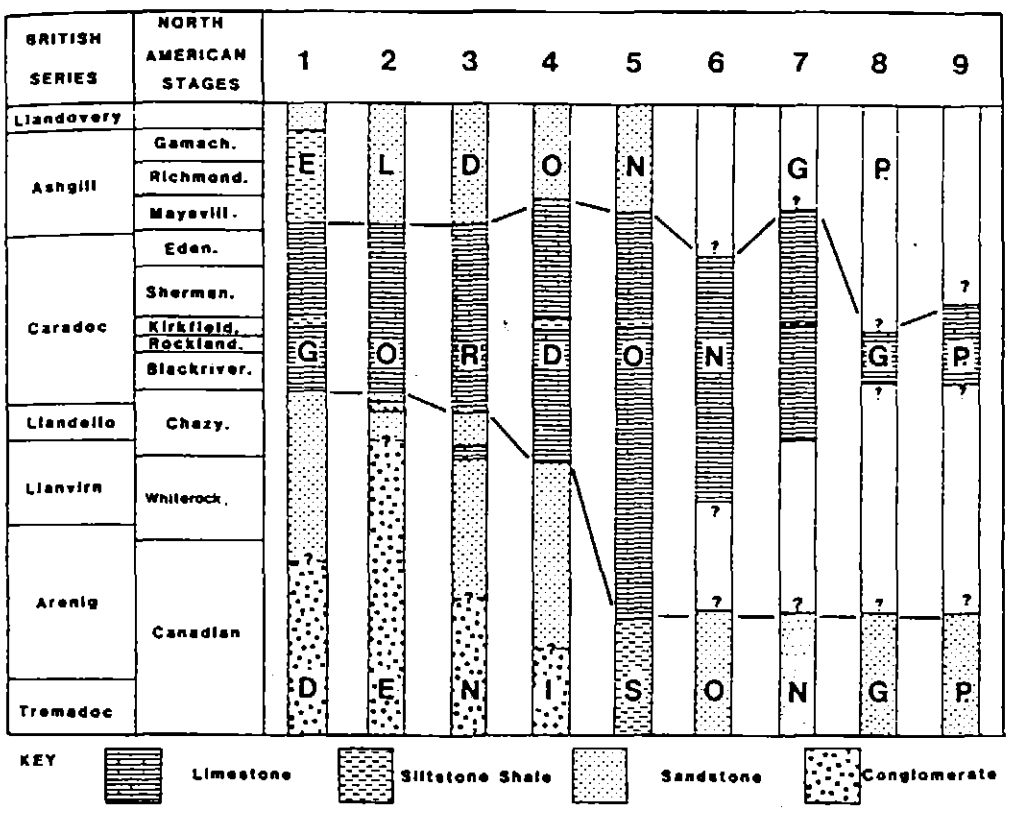

Fig.2. Simplified stratigraphic columns showing diachronous base of the Gordon Gp and of the Moina Fm. 1=Queenstown, 2=Vale of Belvoir, 3=Lower Gordon River,4=Mole Creek, 5=Florentine Valley, 6=Ida Bay, 7=Precipitous Bluff, 8=Point Cecil, 9=Surprise Bay. (Burrett *et al.* 1984).

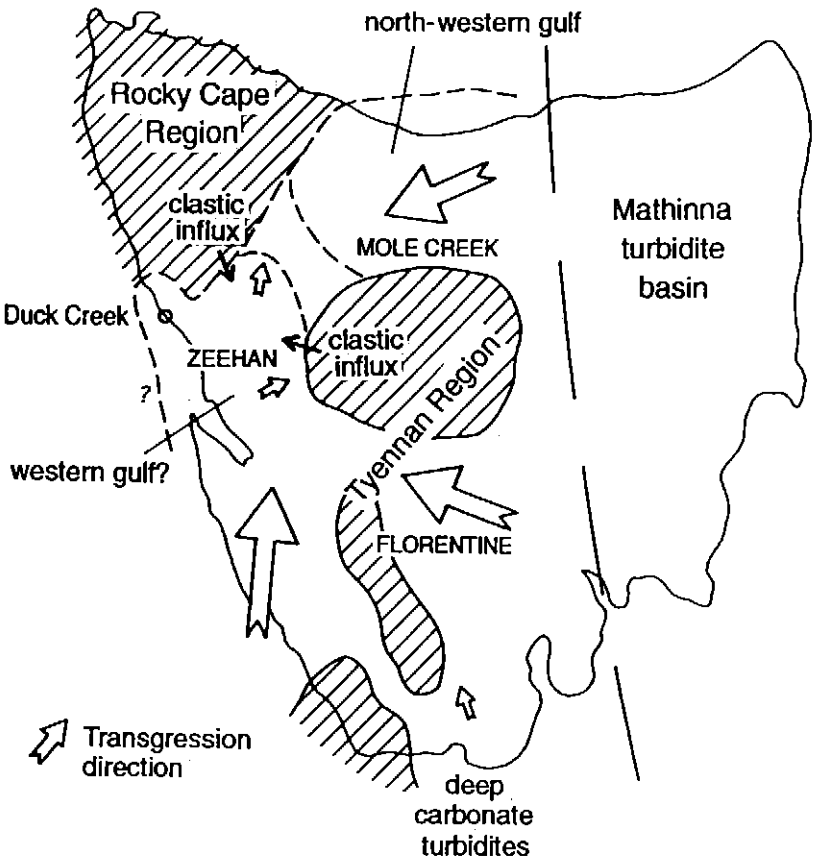

Fig.3. Generalised palaeogeography of the Tasmanian miniplatform in the Caradoc showing inferred directions of transgression. Dotted link between Tyennan and Rocky Cape regions may be an isthmus transgressed during Late Caradoc times.

by thick carbonate successions were gradually built up. This transgression started in the Tremadoc (in the Florentine Valley) and continued up to the Late Caradoc or even Early Ashgill (Figs.2-3). Probably much of the Tyennan and Rocky Cape regions were still emergent in the Late Ordovician (Ashgill). The timing of the transgression is mainly determined from conodont dates on the lowest Gordon Group carbonates with supplementary information from macrofossils in the underlying Denison Group siliciclastics (Fig.2). In the north of the state, the transgression moved towards the Tyennan and Rocky Cape regions from the north and east possibly forming an east-west aligned gulf (Burrett 1978). In the west, the transgression was from the south towards the west and north. Very thin sequences of the Gordon Group are found at Duck Creek (just to the north of the Heemskirk Granite) and at Heazlewood River. It is possible that a similar gulf to the one in the northwest existed in the west of the state. The siliciclastic sands at the Lords level in the Firewood Siding hole (ZF 37) also suggest proximity to land. A solution to this palaeogeographic problem depends on studies on the Ordovician around Queenstown, outcrops south of Grieves and the poor limestone outcrops between Zeehan and the Vale of Belvoir and south of Firewood Siding.

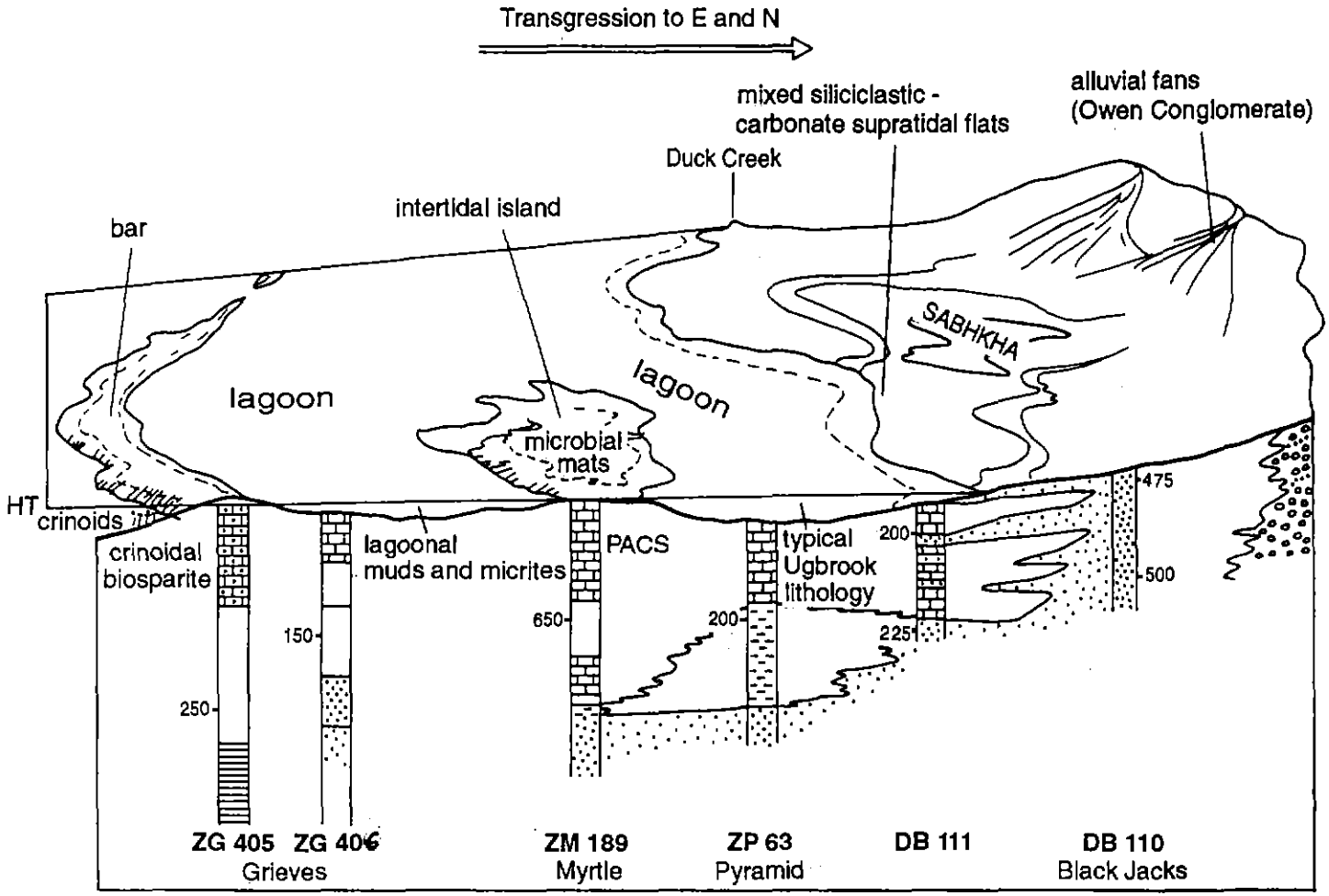

Fig. 4 Environmental reconstruction of the Zeehan area for early Ugbrook Fm times (about Early Caradoc) from the south of the area at Grieves to Black Jacks in the north. Shoreline is to the north (right) and east (behind the viewer). Not to scale. HT = normal high tide level. Numbers refer to down hole depth in m not stratigraphic thickness.

The Ugbrook Fm thins dramatically from DB111 to DB 110 and there is no suggestion that this is due to Devonian faulting. Unlike the other cores examined, the Ugbrook in DB 111 has several coarse siliciclastic interbeds as well as reddened tops to PACs in its basal part. The simplest explanation for this is that the (irregular) shoreline was between DB111 and DB 110 in early Ugbrook time (approximately mid-Caradoc or Blackriveran time) as shown in Fig.4, with clastic debris being derived from the Tyennan region to the east. This date, or a slightly younger one, also applies to the basal carbonates at Duck Creek and Heazlewood River. The typical Ugbrook micrites and pelloidal bioturbated shales were deposited in a lagoon formed behind (north of) a northerly or northeasterly migrating offshore carbonate bar with the minor PAC carbonates formed on intertidal islands within the lagoon (Fig.4). As the transgression continued, the carbonate bar moved from Grieves towards Myrtle during late Ugbrook time. Stabilisation occurred during Myrtle times (Upper Blackiveran) with the whole Zeehan area covered with waxing and waning PACs. Probably by that time, the shoreline (i.e. high supratidal limit) had moved north to Duck Creek and east onto the Tyennan region.

Deepening occurred after Myrtle Fm times, probably due either to the incapacity of the carbonate factory to keep-up with rising sea level or to an increased rate of basinal subsidence. Open subtidal sediments were deposited over the whole area with brief peritidal flat deposition (BJ 1 and BJ2) at Grieves, Myrtle (ZM189) and at Black Jacks (DB110).

The Myrtle core, ZM189, is unusual in that coarse grained carbonates including sparites, spararenites, calcarenites, biosparites are common through the section. This is presumably the consequence of the production of large bioclasts due to deposition further from the micrite producing tidal flats and due to the preponderance of a good subtidal fauna such as crinoids.

The Lords event appears to be isochronous across the whole Tasmanian miniplatform. It was a time of uplift in the Tyennan region leading to coarse quartzite conglomerates being deposited within the middle of the Benjamin Limestone Fm to the west of the Florentine Valley (in the Vale of Rasselas), a deepening in most sections but a shallowing in the deepwater Surprise Bay sequence (Burrett *et al.* 1984). The Lords event was clearly a significant but short lived epeirogenic episode during the mid-Trentonian (Late Caradoc). Normal shallow subtidal conditions resumed during the remainder of Black Jacks time except for a widespread peritidal interlude in late Black Jacks time (Late Trentonian/Early Ashgill). This upper peritidal interval is not found in the Upper Black Jacks Fm at Myrtle (ZM190) which again may suggest that Myrtle may have been in slightly deeper water. The upper peritidal member may correlate to a similar shallowing interlude recognised in the Overflow Creek Fm at Mole Creek.

CONCLUSIONS

The Gordon Group sequence at Zeehan, although starting later during the earliest Blackriveran rather than in the Chazyan, is similar to that at Mole Creek and dissimilar to that in the Florentine Valley. It lacks the oncolitic Standard Hill Fm but the fauna, lithofacies and interdigitation of the Ugbrook with the Moina is very similar. The Myrtle Fm has similarities with both the thicker Lower Limestone Member in the Florentine Valley and the Sassafras Creek Fm at Mole Creek. The generally subtidal Black Jacks Fm is, though, closer to that of the Upper Limestone Member of the Florentine Valley than to the dominantly peritidal Dogs Head and Overflow Creek Fms at Mole Creek.

Interdigitation of the Moina with the Ugbrook and a greatly thinned Ugbrook sequence at Black Jacks suggests that the Blackriveran (Early Caradoc) shoreline was at about the position of DB 110, moving eastwards onto the Tyennan region and northwards towards Duck Creek by the Late Blackriveran.

Identification of PACs or shallowing-upward sequences in the Myrtle Fm and in the Upper Black Jacks Fm allows correlation across the region.

There are several argillaceous horizons present in some sections and the identification of the Lords Member is helped by the identification of its characteristic fauna and by the lithofacies deepening prior to its deposition.

RECOMMENDATIONS

Chronostratigraphic correlations in the Zeehan area could be improved substantially by employing conodonts. Conodonts are rare in peritidal sections but this study has shown that there are sufficient subtidal intervals that would yield sufficient useable conodont elements per kilogram of core. If this was coupled with an intensive study of the macrofossils then very reliable chronostratigraphic correlations are possible. Conodonts also record the maximum temperature that they have experienced and, more importantly, are pitted in a characteristic manner by hydrothermal fluids. Such a study could define flowpaths of hydrothermal fluids.

There are sufficient drillholes to define the extent of any basin or basins by the use of isopachs. However, a complete palinspastic study is recommended that takes into account extension due to cleavage and stratigraphic loss due to tectostylolites as well as removing the effects of Devonian folding and thrusting.

The extent of pervasive dolomitisation in the Black Jacks Fm should be plotted. This might reveal a zone of enhanced porosity/ permeability within the Gordon Group into which hydrothermal fluids might have flowed (see Appendix A).

REFERENCES

Baillie, P., & Burrett, C., 1990. Conodonts as indicators of mineral prospectivity. Tasmanian Department of Mines Report 1990/4; 1-4.

Banks, C.F., Baillie, P., Calver, C. and Burrett, C.F., 1989. Upper Cambrian-Devonian. In Burrett, C. and Martin, E. (Eds.) Geology and Mineral Resources of Tasmania, Geological Society of Australia Special Publication 15. Hobart, 600pp .

Banks, M.R. and Burrett, C.F., 1980: A preliminary Ordovician biostratigraphy of Tasmania. Journal of the Geological Society of Australia 26:363-376.

Banks, M.R. and Burrett, C.F., 1986: Some Ordovician and Silurian rocks and fossils from the Huskisson River area, W. Tasmania 151-162 in Brown, A.V., Geology of the Mt. Lindsay-Youngbuck area, W. Tasmania. Dept. Mines Geol. Survey, Tasmanian Bulletin 62.

Bendall, M., Volkman,J., Leaman, D. & Burrett, C., 1991: Recent developments in oil exploration in Tasmania. Australian Petroleum Exploration Association Journal, 1991, 74-84.

Burrett, C.F., !978: Stratigraphy and conodonts of the Ordovician Gordon Group, Tasmania. Unpublished Ph.D. thesis, University of Tasmania.

Burrett C.F., 1979: Tasmanognathus a new Ordovician conodont genus from Tasmania. Geologica et Palaeontologica 13: 31-38.

Burrett, C., 1984: Early Devonian deformation and metamorphism of conodonts in western Tasmania - economic, theoretical and nomenclatural implications, p. 14-17 in Baillie, P. and Collins, P. (eds.) Mineral Exploration and tectonic processes in Tasmania. Geological Society Australia, Hobart.

Burrett, C., Sharples, C., Stait, B. and Laurie, J., 1984: A Middle-Upper Ordovician tropical carbonate platform to basin transition, southern Tasmania, Australia. In: Bruton, D. (ed.) Aspects of the Ordovician system. Universitetsforlaget, Oslo, 149-157.

Burrett, C.F. & Martin, E., (Eds.) 1989. Geology and Mineral Resources of Tasmania, Geological Society of Australia, Special Publication 15, Sydney, 603 pp.

Burrett, C.F. 1992. Conodont geothermometry in the Palaeozoic carbonate rocks of Tasmania and its economic implications. Australian Journal of Earth Science 39, 61-66.

Burrett, C.F., Banks, M., Clota, G. and Seymour, D. 1989. Stratigraphy and structure of the Ordovician of Mole Creek Synclinorium, N.W. Tasmania. Records of the Queen Victoria Museum Launceston 96, 1-14.

Burrett, C.F., Laurie, J. and Stait, B., 1981: Gordon Subgroup (Ordovician) carbonates at Precipitous Bluff and Pt. Cecil, South West Tasmania, Australia. Pap. Proc. Roy. Soc. Tasm. 115: 93-99.

Burrett, C.F., Stait, B. and Laurie, J., 1983: Trilobites and microfossils from the Middle Ordovician of Surprise Bay, southern Tasmania, Australia. Memoirs Australian Association of Palaeontologists, 1: 177-193.

Calver, C., 1977: Palaeoecology of the Lower Limestone member, Florentine Valley, Unpublished thesis, University of Tasmania.

Ellis, A.,1984: Mineralization and palaeoenvironments in Gordon Group sediments, south of Zeehan, western Tasmania. Unpublished thsis, University of Tasmania.

North, F.K., 1985: Petroleum Geology. Allen and Unwin. 607pp.

Pitt, R.P.B., 1961: The Geology of the Zeehan Area. Unpublished Thesis, University of Tasmania.

Webby, B.D., VandenBerg, A., Burrett, C., Laurie, J. and Stait, B., 1981: The Ordovician System in Australia, New Zealand and Antarctica. Correlation Chart and Explanatory Notes. IUGS, Canada.

Webby,B., Stait,B., Laurie, J., Cooper,I., Burrett,C.F. & Shergold, J., 1991: Subdivisions of the Ordovician System in Australia. In: Advances in Ordovician geology. Geological Survey Of Canada Paper 90-9, 47-58.

Appendix A

Dolomitization and its control on porosity and reservoirs in the Trenton Limestone
(from North, 1985 p.198-199).

Appendix B

Peritidal Carbonates from Walker and James Eds 1992. Facies Models. Geological Association of Canada.

Appendix C

Lithostratigraphy at Mole Creek , Burrett et al. 1989.

recrystallization, and most commonly of *dolomitization*. About 80 percent of all hydrocarbon reserves contained in carbonate reservoirs in North America are in essentially pure dolomites. This percentage is by no means representative of other regions of the world, and unquestionably reflects the number of North American carbonate reservoirs that are Paleozoic in age. In the Persian Gulf Basin, with the most prolific carbonate reservoirs in the world, the proportion of dolomite reservoirs is no more than 20 percent.

The replacement of $CaCO_3$ by dolomite involves a loss of volume of about 12.3 percent, and a consequent increase in porosity by that amount, if the replacement is molecule for molecule. It may not always be so, because volume for volume replacement is also possible. Yet it remains the case that in many fields having partially dolomitized carbonate reservoirs the oil is restricted entirely to the dolomitized portion. This portion is favorable because of *partial* dolomitization, preferentially of the finer-grained components of the limestone, and later leaching of the remaining calcitic parts which are more soluble. The most-quoted example of this phenomenon is the sprawling Lima–Indiana field south of the Great Lakes (Fig. 13.52). The oil is confined to porous dolomitic zones in the Ordovician Trenton Group where it passes over the axis of the broad, bifurcating Cincinnati Arch. Updip, porosity disappears in the unaltered limestone and only gas is recovered. Among the fields providing case histories for this book is the Jay field in Florida (Ch. 26), another example of restriction of oil to the dolomitized part of a carbonate formation. Up the dip, the undolomitized micritic limestone lacks porosity and is barren of oil. Most carbonate producing basins afford comparable examples.

An intriguing small example is provided by the Dover field, at the southwestern extremity of Ontario in Canada, like Lima–Indiana in the Ordovician Trenton Group. During the 1920s, articles on oil-bearing structures quoted Dover as an example of the rare synclinal trap. The syncline is controlled by an elongate fracture zone (Fig. 13.53) along which migrating waters have been able to dolomitize a considerable thickness of strata; the oil is restricted to the porous dolomite and therefore to the "syncline." The Albion–Scipio "trend", in Michigan's part of the same basin, is very similar and produces from the same formation (Fig. 13.52). From outside the normal concern of petroleum geologists comes the parallel case of Mississippi Valley-type lead–zinc deposits, in some of which it is established that the brines, derived from evaporite deposits, that deliver the metals also bring about dolomitization.

The selective nature of dolomitization extends to its

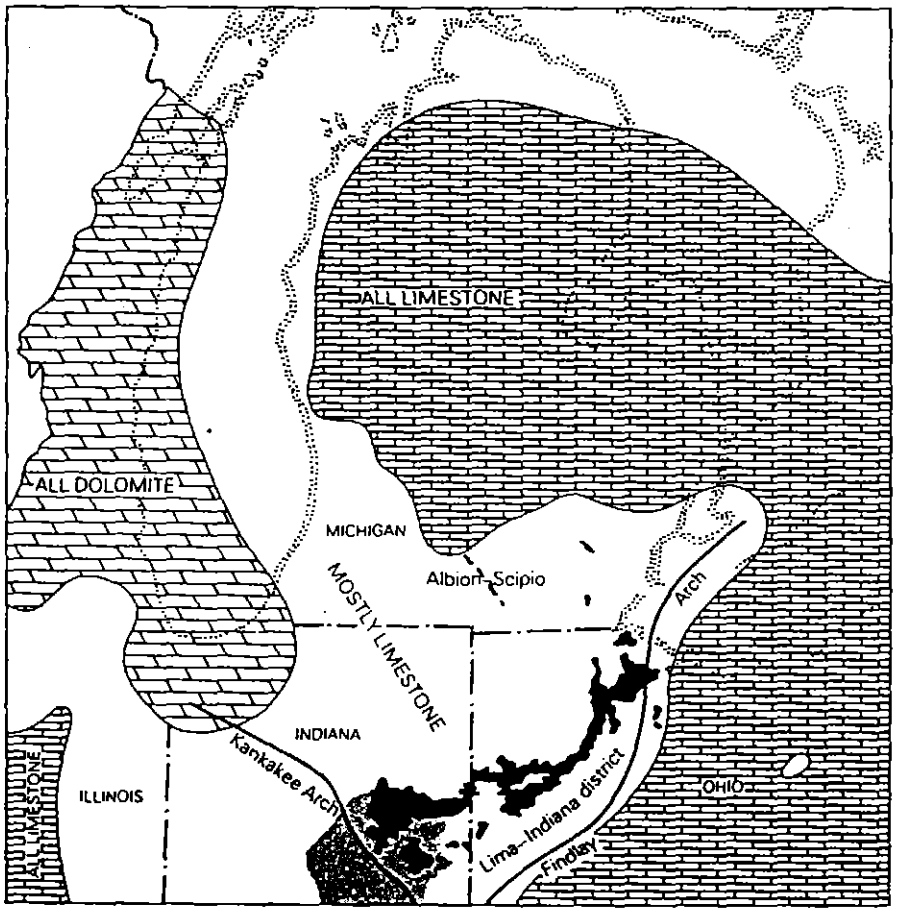

Figure 13.52 Michigan Basin in Middle Ordovician time, showing the Cincinnati Arch bifurcating into two arches as it crosses the basin from the south. The Trenton Group carbonates are dolomitized over the arches and along linear fracture zones; oil accumulations are restricted to the dolomitized portions. Dotted outlines on map delineate present Lakes Michigan and Huron. (After K. K. Landes, *Petroleum geology of the United States*, New York: Wiley–Interscience, 1970; and G. V. Cohee, US Geol. Survey Preliminary Chart no. 9, 1945.)

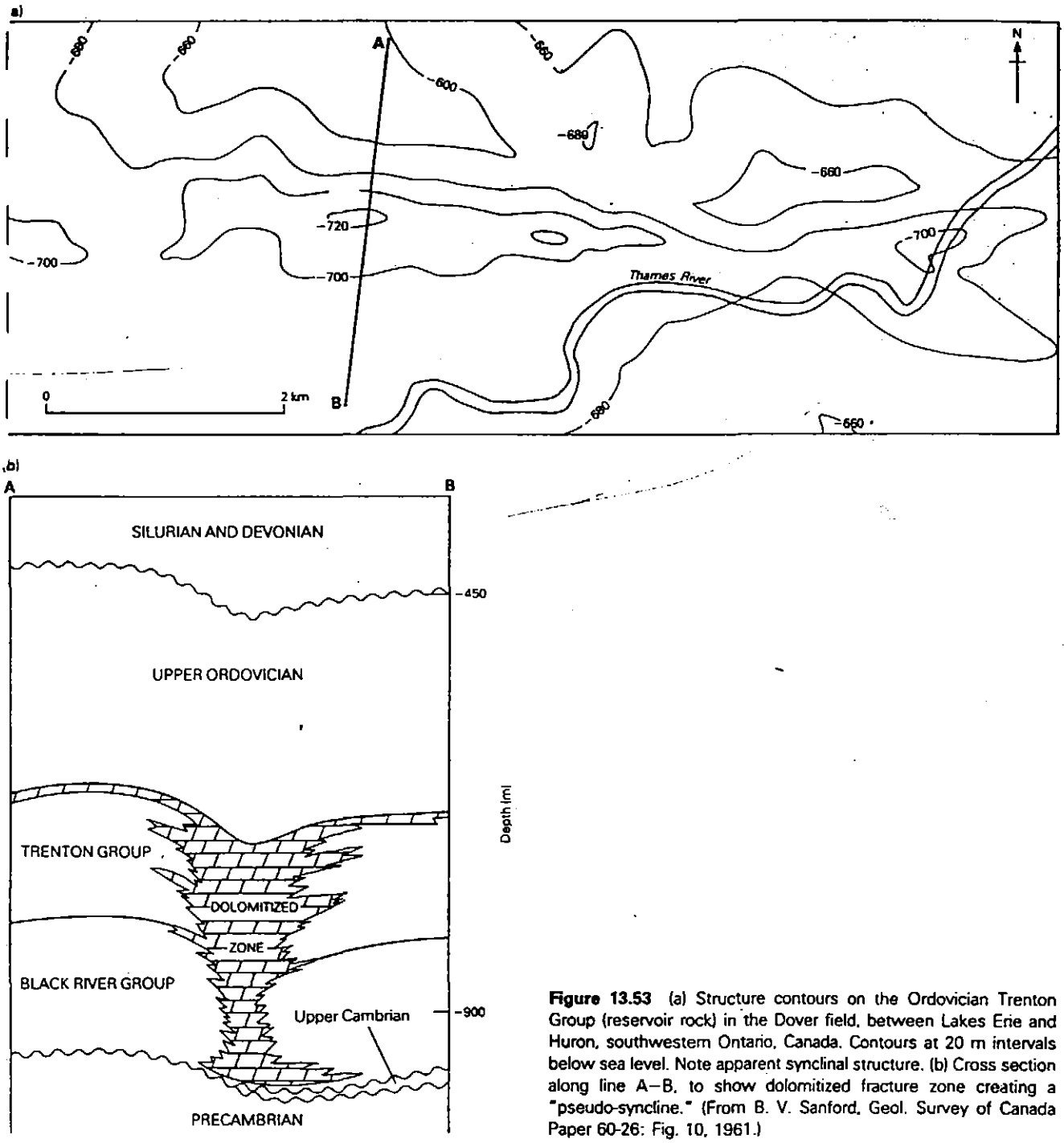

Figure 13.53 (a) Structure contours on the Ordovician Trenton Group (reservoir rock) in the Dover field, between Lakes Erie and Huron, southwestern Ontario, Canada. Contours at 20 m intervals below sea level. Note apparent synclinal structure. (b) Cross section along line A–B, to show dolomitized fracture zone creating a "pseudo-syncline." (From B. V. Sanford, Geol. Survey of Canada Paper 60-26: Fig. 10, 1961.)

effects on skeletal remains. Aragonite is much more easily dolomitized than is calcite, so shells of gastropods, cephalopods, and corals are dolomitized earlier than those of brachiopods, ostracodes, or echinoids. Well sorted crinoidal or shelly limestones are less dolomitized than surrounding rocks which contain less coarse material and more cement. Calcareous algae are easily dolomitized because high-magnesium calcite is deposited on them during their lives, and the algae themselves reduce sulfate which would otherwise inhibit dolomitization (especially of calcite). The vast mats of algae in the shallow epicontinental seas of the great Paleozoic transgressions are undoubtedly a factor in the prevalence of Paleozoic dolomites. There is very little dolomite in the stratigraphic record since the early Cretaceous, especially in the Northern Hemisphere. This may be because the present oceans, originating at that time, have a distribution and orientation different from those of earlier oceans, and epicontinental seas in low latitudes are highly restricted.

Appendix B

384106

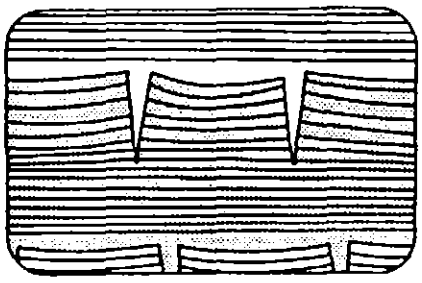

16. Peritidal Carbonates

Brian R. Pratt, Department of Geological Sciences, University of Saskatchewan, Saskatoon, Saskatchewan S7N 0W0

Noel P. James and Clinton A. Cowan, Department of Geological Sciences, Queen's University, Kingston, Ontario K7L 3N6

INTRODUCTION

Limestones and dolostones composed of calcareous sediment deposited in very shallow seawater and on muddy tidal flats are probably the most conspicuous carbonate facies in the rock record (Fig. 1). The term *peritidal* (from the Greek *peri*, meaning around or near, and tidal, relating to tides) was coined in passing by Folk (1973) and has proven a useful general name for the spectrum of nearshore and shoreline depositional environments and facies.

What distinguishes these rocks is their wide variety of features that can be compared directly with modern analogues, making them both easy to recognize in the field and important paleobathymetric indicators. The facies are generally arranged vertically in a *shallowing-upward sequence* (James, 1984), now referred to as a *shallowing-upward succession*, in which marine sediments are overlain successively by muddy carbonates deposited in paleoenvironments subject to varying periods of exposure. This vertical stacking of peritidal and related facies is a valuable record of the dynamics of carbonate platform development, on both large and small scales. It hints at extrinsic factors such as relative sea level change and climate, and records the effect on periodically exposed sediment of biotic evolution through geologic time. Peritidal carbonates are also economically important because they host Pb and Zn deposits and frequently form hydrocarbon reservoirs.

In this chapter, we first summarize the tidal flat environment from a Recent standpoint. We then discuss how the record of carbonate tidal flats may have changed through time in response to biological evolution and provide ancient examples of commonly encountered peritidal facies, with evidence for their interpretation. Finally, we outline how peritidal facies are preserved in the stratigraphic record, describe current hypotheses used to explain stratigraphic repetition and suggest how these facies can best be used in sequence stratigraphic analysis.

Figure 1 Panorama of Cambrian shallow water limestones and dolostones, Dezaiko Range, east-central British Columbia. Distinctive "stripy" bedding of lower unit, to the right of the small ice field, is from peritidal facies of the Snake Indian Formation. The unit in the middle of the photograph is the Eldon Formation, consisting of locally dolomitized subtidal limestones, and the left side comprises peritidal limestones of the Lynx Group.

THE PERITIDAL ENVIRONMENT

The understanding of tidal flat carbonate rocks underwent a dramatic boost with the largely petroleum company-funded research on Holocene tidal flats during the 1950s and 1960s. This produced comprehensive studies on shallow water sedimentation of south Florida (Ginsburg, 1956; Gebelein, 1977; Enos and Perkins, 1979), Andros Island of the northern Bahamas (Hardie, 1977), Belize (Wantland and Pusey, 1975), the Arabian (Persian) Gulf (Purser, 1973), and Shark Bay, Western Australia (Logan *et al.*, 1970, 1974). Observations from these areas were quickly applied to ancient examples (e.g., Beales, 1958; Roehl, 1967; Matter, 1967; Laporte, 1967; Ginsburg, 1975; Schwarz, 1975), which ushered in the modern era of carbonate sedimentological thinking. These Holocene examples, together with more recently studied flats in the Caicos Islands (Wanless *et al.*, 1988) and southern Australia (Burne and Colwell, 1982; Belperio *et al.*, 1988) are fundamental reference points for the interpretation of carbonate rocks and illustrate the wide variety of potentially preservable peritidal environments. The carbonate tidal flat is an easily accessible area and students are encouraged to explore for themselves a modern example.

Three bathymetric zones are recognized in the nearshore setting: subtidal, intertidal and supratidal (Fig. 2).

The subtidal zone is permanently submerged and ranges from low-energy, lagoonal environments to higher energy shoals. Semimonthly neap tides may briefly expose the shallowest portions. The intertidal, or littoral, zone lies between normal low- and high-tide levels and is therefore submerged on a diurnal or semidiurnal basis. It is generally dissected by subtidal creeks and dotted with brackish or saline ponds. The supratidal zone is above normal high tide, and is flooded only during storms and semimonthly spring tides. It may become evaporitic in semiarid and arid climates, and for these supratidal flats the Arabic word *sabkha* has been adopted by sedimentologists (Chapter 19).

The three-fold environmental subdivision is only an approximation, however, since tidal flats are often geographically complex, and tidal range can be modified by winds. While the environments are due to the variable submergence and emergence brought about by lunar tides, little sediment is transported onto the flats by the daily rise and fall in sea level. It is storms, which stir up the adjacent offshore sediments and drive sediment-laden waters up the tidal creeks and onto the flats, that result in sediment deposition. Even so, it is still the depositional environments, which are generated by daily lunar tides, that contain the distinctive sedimentary features that allow us to pinpoint facies so precisely. One approach to the analysis of environmental subdivision is to assign a specific, quantitative "exposure index" to lithologic features based on Holocene examples (see Hardie, 1977), but few ancient deposits have been described in this way (Smosna and Warshauer, 1981).

Marine coastlines can be separated into microtidal (<2 m), mesotidal (2-4 m) and macrotidal (>4 m) settings. Tidal range depends on basin shape and water depth. Strong tidal currents are generated when water is forced through relatively narrow straits or mouths of bays or over shallow shoals. Modern peritidal carbonate environments are exclusively microtidal. There is as yet no satisfactory way of judging ancient tidal range, but the scarcity of sedimentary structures formed by strong tidal currents suggests that most ancient carbonate peritidal settings were also microtidal.

Where do they form?

Carbonate sediment, generated mostly in the subtidal zone (the *carbonate factory*), can be subsequently transported and molded into tidal flats by physical processes. In this sense, tidal flats are repositories of allochthonous sediment, and accrete as wedges along shorelines (e.g., Qatar, Shark Bay, Spencer Gulf), in the lee of rocky islands (e.g., northern Bahamas, Caicos, Belize), spits (e.g., Florida) and reefs and shoals (e.g., Trucial Coast), and as discrete islands and banks in shallow seas (Fig. 3). This last setting is inferred from ancient examples because modern shelves are comparatively narrow and not directly analogous to the broad epeiric seas that were common in the past.

For muddy tidal flats to form they must be protected from open ocean swells and such protection can be provided by a platform rim or in the case of a ramp or unrimmed platform, by nearshore carbonate sand shoals (Fig. 4). Muddy tidal flats do not, therefore, generally occur in the facies spectrum of high-energy, unrimmed platforms, except behind nearshore shoals or islands.

Holocene carbonate tidal flat environments

Shallow subtidal and lower intertidal

The shallow seafloor oceanward of modern tidal flats is generally a bio-

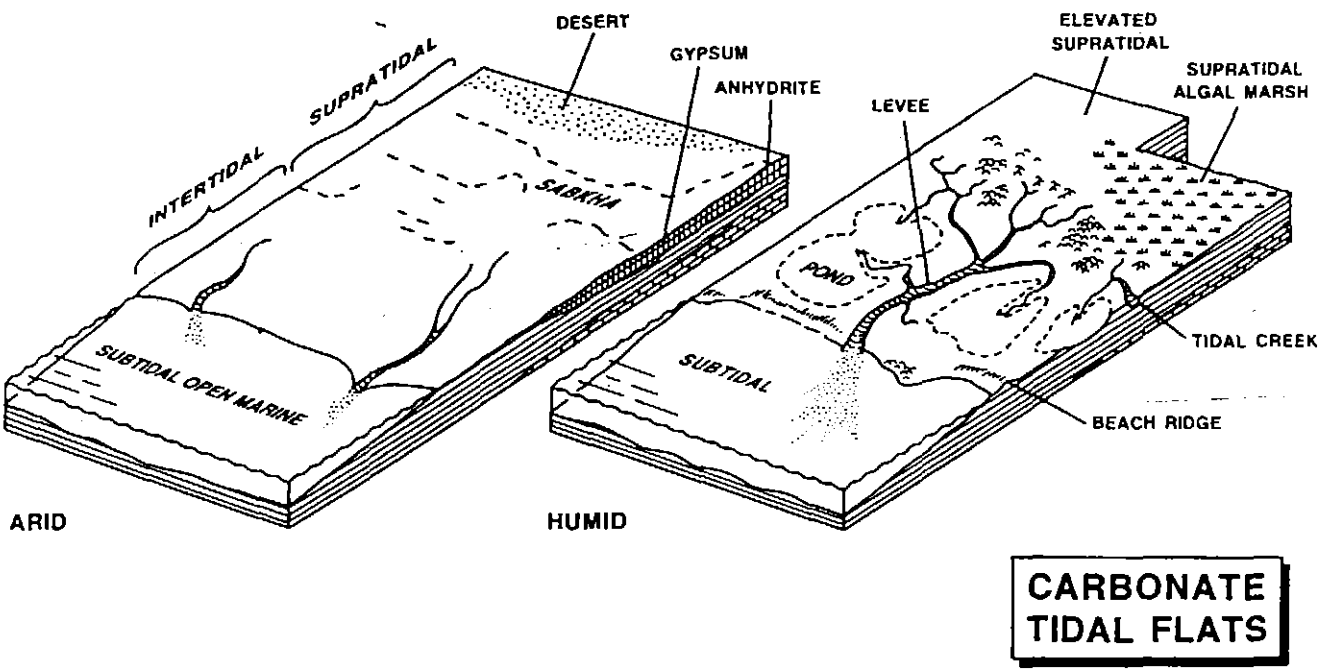

Figure 2 Block diagram showing the main morphological elements of a carbonate tidal flat. Left: a hypersaline tidal flat with few channels bordering a desert and developing evaporite deposits (based on modern Persian [Arabian] Gulf). Right: normal-marine tidal flat with many creeks, or channels, and ponds in a humid to sub-humid setting (based on modern Bahamas).

turbated and pelleted lime mud variably rich in shelly material from benthic oganisms, and commonly supports a cover of sediment-stabilizing sea grasses (Chapter 15). Protective low-relief banks of cross-stratified oolitic or bioclastic sand are present in some higher-energy nearshore areas where wave agitation is frequent.

In tranquil settings of normal salinity, the lowermost intertidal zone tends also to be a thoroughly bioturbated mixture of lime mud, pellets and bioclasts. This sediment is usually covered during low tide with an ephemeral microbial ("algal") slick that is the source of food for grazing organisms such as gastropods and worms. Crabs, shrimps, worms and fish are responsible for the bioturbation in the underlying sediment. Many low-energy flats are fronted by beaches of bioclastic sand winnowed from creeks and ponds or the adjacent seafloor during storms. Beach sands can be partially lithified by synsedimentary cement composed of aragonite fibres or bladed and micritic high-Mg calcite, forming gently seaward-dipping layers of beachrock. Beachrock tends to be crumbly and easily eroded, and supports a hard-substrate biota of encrusting and boring invertebrates, plants and microbes.

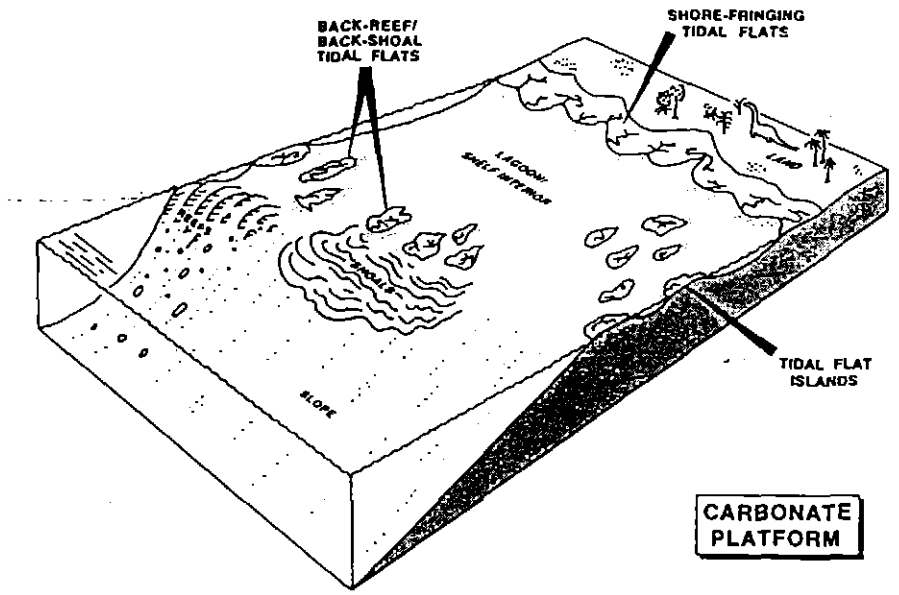

Figure 3 Block diagram of a carbonate platform, with basinward to left and landward to right, showing possible locations of tidal flats: in the lee of reefs and carbonate sand shoals, as islands, and as shoreline deposits.

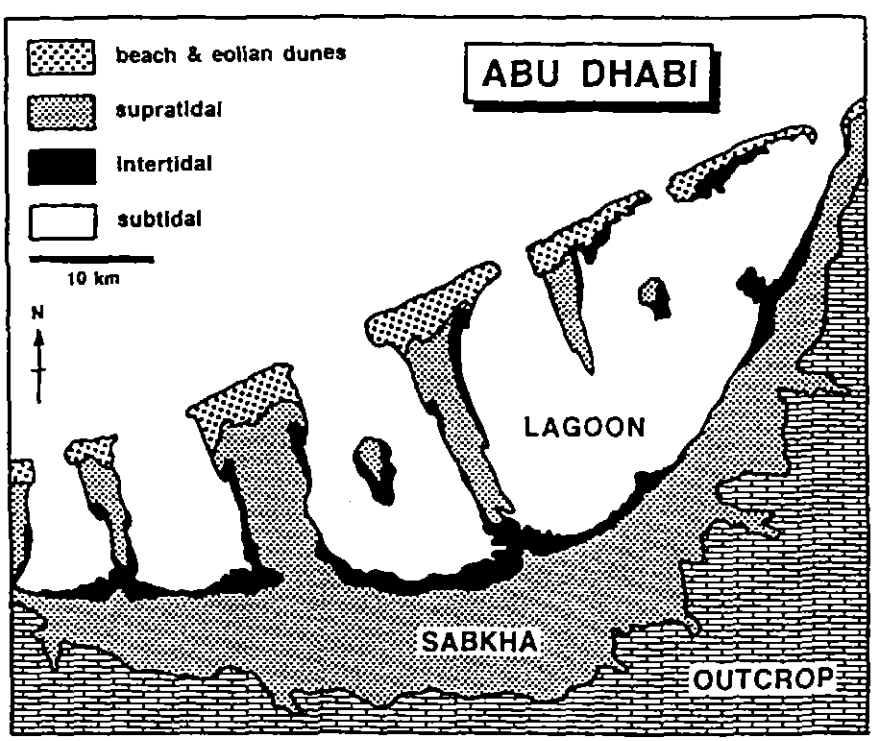

Figure 4 Simplified map of modern tidal flat areas near Abu Dhabi, Persian (Arabian) Gulf; based on Purser (1973).

Intertidal flats

Higher in the intertidal zone, microbial mat cover is more permanent, and forms thick, leathery carpets that can be locally shrunken, torn and folded over (Fig. 5). These exhibit various surface features such as pustules, blisters, wrinkles, crenulations or small, domical stromatolites. These mats are composed of a variety of filamentous and coccoid cyanobacteria ("blue-green algae") and bacteria, and are responsible for the millimetre-scale lamination exhibited by most of the sediment beneath them. The taxonomic makeup and surface appearance of such mats varies with degree of subaerial exposure and can be reflected in the microscopic nature of the underlying lamination. This type of lamination was called "algal" or "cryptalgal" before geologists became familiar with the detailed biological nature of the mats; "microbial" seems now to be the preferred adjective.

Ponds and creeks

Ponds containing brackish or hypersaline water are a common feature of the intertidal zone (Fig. 6), especially in more humid climates. These contain a restricted biota of microbial mats, foraminifera, gastropods, small bivalves, shrimps, ostracodes, and nematode and polychaete worms that is adapted to fluctuating salinity. This assemblage, living in a stressed environment, is typically one of high numbers of individuals but low species diversity, different from the immediate offshore

biota. Copses of mangroves are usually present, except in the most arid areas. Also characteristic of the intertidal zone are permanently submerged tidal creeks or channels that are the conduits for tidal flooding and draining (Fig. 6). Such tidal creeks (least common in arid settings) are up to several metres deep and tens of metres wide, and contain a basal lag of semilithified intraclasts eroded from the surrounding flats and flanking levees, and bars of bioclastic sand winnowed from the ponds. Supratidal levees protrude above high-tide level and are microbially laminated. Creeks migrate laterally, as they do in siliciclastic tidal flats, and leave behind a vertical succession of cross-stratified, intraclastic and bioclastic sand overlain in turn by bioturbated bioclastic and peloidal lime mud and microbially laminated sediment. The amount of lateral migration of creeks and the proportion of the internal facies mosaic of intertidal flats that is generated by such migration are not well understood, but studies of modern flats suggest that it may be considerable (Hardie, 1977).

Supratidal flats

Most of the sediment surface in the upper intertidal and supratidal zones is covered by microbial mats that are typically shrunken into desiccation polygons and commonly dislodged into chips or intraclasts. The laminated sediment beneath these mats is generally fine grained with occasional coarser intercalations that reflect deposition by exceptional storms and, in some regions, by winds blowing off the neighbouring land surface. Beds and nodules of anhydrite precipitate in these sediments in arid settings (Chapter 19). In many areas, the supratidal zone is the locus of widespread synsedimentary cementation by microcrystalline aragonite, high-Mg calcite, or dolomite. This forms lithified pavements a few centimetres thick that are usually broken into intraclasts by forces exerted during crystal growth, groundwater pore pressure, or the roots of halophytic (salt-tolerant) plants such as grasses and mangroves. Evaporating sea spray can be responsible in some arid areas for fans and isopachous layers of fibrous aragonite that encrust stable substrates such as beachrock and shells, forming objects termed coniatolites.

Landward parts of the supratidal zone grade into eolian deposits, soils or freshwater marshes and lakes, or onlap bedrock surfaces, depending on the region's geography and climate. Marshes and lakes, which exist in the more humid areas and have fluctuating water chemistry, are characterized by microbial mats and stromatolites; these are partially lithified by high-Mg calcite cement and calcification of organic substrates, and are interbedded with thin-bedded, locally bioturbated lime mud and bioclastic and peloidal carbonate sand deposited during storms. Much of the microbially laminated sediment shows fenestral fabric, i.e., the presence of millimetre-

Figure 5 Upper intertidal microbial mat mainly composed of filamentous cyanobacteria *(Microcoleus)* that has shrunken into desiccation polygons. Boca Jewfish, Bonaire; trowel is about 25 cm long.

Figure 6 Oblique aerial photograph of the tidal flats on the northeast coast of Andros Island, Bahamas, looking north. Offshore subtidal is to the left. The white areas along the channel edges are supratidal levees. The dark patches are intertidal microbial flats between the levees and around the periphery of the mainly subtidal ponds. The field of view is about 3 km across.

to centimetre-sized subhorizontal, sheet-like pores formed as voids bridged by microbial mats or as molds of degraded mats. Decimetre-scale tepee structures (Fig. 7), consisting of disrupted and overthrust crusts of lithified, tufa-like fenestral sediment giving an inverted V-shaped cross section, form in areas of groundwater discharge (Kendall and Warren, 1987). These also contain complex generations of internal sediment and aragonite and high-Mg calcite cements.

Geological evolution of peritidal facies

Biological and environmental developments through geologic time have exerted an important influence on the nature of carbonate tidal flats. This is manifest in several ways, via 1) the increase in diversity of carbonate-secreting organisms and consequent change in sediment type, 2) the evolution of bioturbating and herbivorous invertebrates, and 3) the evolution of angiosperms.

The subtidal carbonate factory was in its infancy during Precambrian time, when $CaCO_3$ was extracted from seawater by inorganic and microbial processes only. Peritidal strata during this phase in Earth's history are composed of ooids, intraclasts, stromatolites, supratidal tufas, and variable amounts of lime mud. Some subtidal units are entirely siliciclastic, and large-scale cyclicity of alternating calcareous and noncalcareous facies (e.g., Grotzinger, 1986; Bertrand-Sarfati and Moussine-Pouchkine, 1988) may have involved basin-wide, or greater, changes in carbonate saturation of seawater. The dramatic increase in skeleton-secreting and sediment-ingesting invertebrates beginning in Cambrian time meant that the carbonate factory changed in character and increased its output manyfold. New types of sedimentary particles appeared, in the form of abundant shells, fecal pellets, and carbonate mud from the breakdown of fragile skeletons and other biologically influenced precipitates. This no doubt changed the nature of tidal flats by causing increased mobility of the substrate, making it less and less likely to be cemented quickly or encrusted by stromatolite-forming microbial mats except in hypersaline areas (Pratt, 1982). It has been commonly held (Garrett, 1970) that grazing invertebrates such as gastropods caused intertidal stromatolites to become scarce after the Proterozoic, but the above sedimentary reasons rather than ecologic pressure seem likely to have been responsible for this decline.

Proterozoic tidal flat carbonates are distinctive too because, in comparison with other Precambrian carbonate facies and younger sediments, they were the preferred sites of diagenetic silica precipitation and formation of chert nodules (Maliva *et al.*, 1989). These cherts are important because they host the bulk of the Precambrian fossil record (Knoll *et al.*, 1991).

Bioturbation became a sediment-

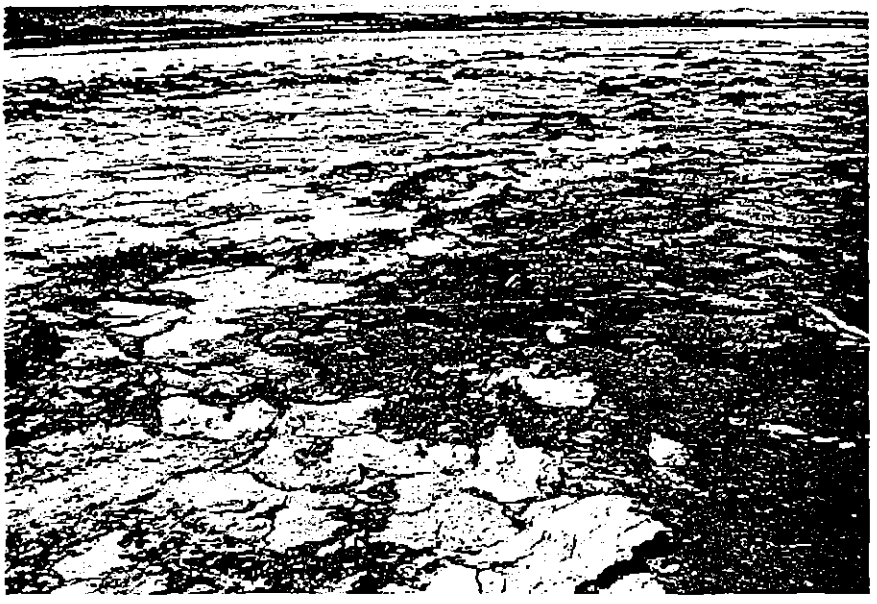

Figure 7 The supratidal flat at Fisherman Bay, Spencer Gulf, southern Australia. The polygonal crusts are lithified and have been thrust into teepees by episodic groundwater resurgence. Crusts in the foreground are roughly 30 cm across.

Figure 8 Outcrop of lenticular and wavy beds of wave-rippled peloidal grainstone (light coloured) in argillaceous dolostone (dark coloured), probably deposited in the lower intertidal zone. Petit Jardin Formation (Upper Cambrian), Port-au-Port Peninsula, western Newfoundland; lens cap is 6 cm across.

modifying process in Late Proterozoic time. Diversification of microbes, especially those involved in the breakdown of organic material, must have occurred in tandem with invertebrate diversification and the resulting appearance of new organic substances. The organic content and therefore the geotechnical properties of tidal flat sediments surely changed in the early Paleozoic. The effect of bioturbation seems to have increased dramatically after the late Paleozoic or earliest Mesozoic (Thayer, 1983; Bottjer and Ausich, 1986; Pratt, 1991). This was heralded by the evolution of a more diverse fauna including animals, such as certain shrimps and crabs, capable of burrowing as deeply as 1 m. Consequently, tidal bedding that would have been preserved in the Precambrian and early Paleozoic was commonly destroyed by infaunal activity, except in the upper intertidal and supratidal zones. Furthermore, intertidal to supratidal sedimentary and organosedimentary structures that escaped destruction were often subsequently bioturbated when buried by subtidal or lower intertidal sediments with an active deeply burrowing infauna.

Evolution of angiosperms since Cretaceous time has meant that the disruption of tidal flat sediments by halophytic plants has become a characteristic of Cenozoic deposits. In addition, shallow subtidal sea bottoms are especially well stabilized by the rhizomes (roots) of angiosperm sea grasses *(Thalassia, Posidonia, Cymodocea)*. Such grasses also support a prolific encrusting biota that supplies fine-grained carbonate sediment to the factory. These carpets of sea grasses, however, are disrupted only by intense storms, causing "blowouts" (Wanless, 1981), and we suggest that pre-Cenozoic subtidal sediments, especially silt- and sand-sized particles, might have been more readily moved onto tidal flats than they are now, because they were not bound by these grasses. This is analogous to the suggestion that the post-Devonian presence of widespread terrestrial plant cover, with its stabilizing, soil-forming and weathering attributes, affected the subaerial sedimentary system of the Earth. It may partly explain why some early Paleozoic intertidal carbonates look so much like siliciclastic counterparts from settings that lack significant seagrass communities.

Ancient peritidal carbonate facies

Environmental interpretation of peritidal limestones and dolostones is easily achieved in the broad sense, especially when they contain features unequivocally of subaerial origin. However, some facies cannot be assigned confidently to a bathymetric position, and for these Walther's Law must be invoked. Furthermore, tidal processes involve such a variety of energy regimes, sediment sizes and climates that there may be a limit as to

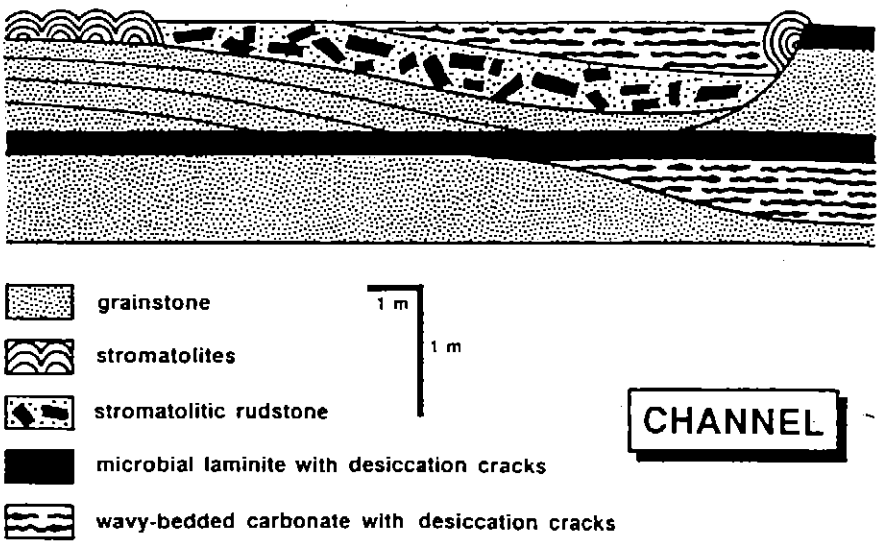

Figure 9 Simplified outcrop sketch of hypothetical channel or creek deposits cut into tidal flat facies, based on examples from the Waterfowl Formation (Upper Cambrian, Rocky Mountains, Alberta; Waters *et al.*, 1989) and Elbrook-Conococheague Formations (Middle and Upper Cambrian, Virginia; Koerschner and Read, 1989).

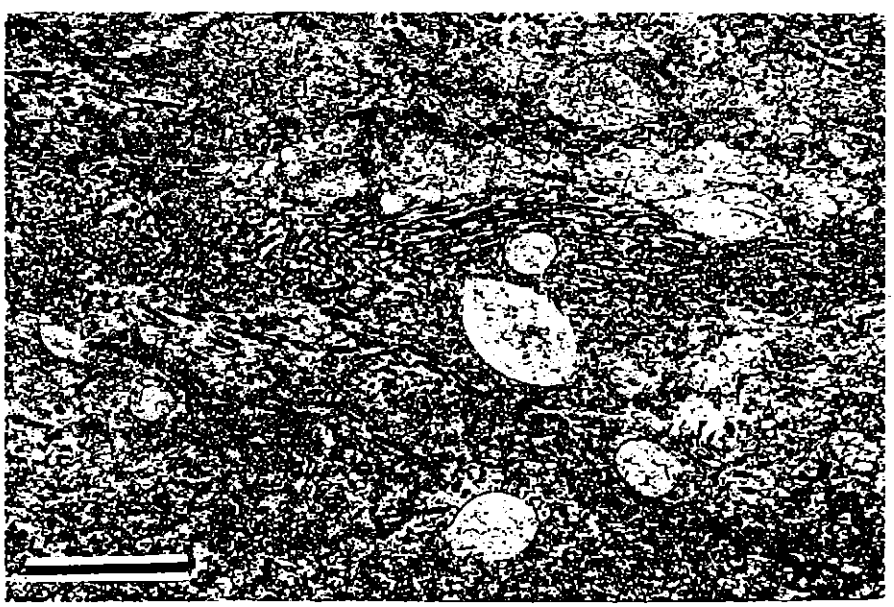

Figure 10 Thin section photomicrograph of limestone composed of loosely packed micrite, micrite peloids, articulated ostracode valves, and calcimicrobe *(Girvanella)* filaments with organic-rich walls. This sediment is interpreted to have been deposited in a tidal flat pond because of the low-diversity biota and the calcification of filamentous cyanobacterial thalli. Table Point Formation (Middle Ordovician), Port-au-Port Peninsula, western Newfoundland; scale bar is 1 mm.

how precise an interpretation one can make. The present level of detail is generally at the scale of units decametres to metres in thickness; few studies have gone down to the scale of individual beds and laminae.

Shallow subtidal and lowermost intertidal facies

Precambrian subtidal rocks are the most difficult to recognize, because the carbonate was produced by inorganic or microbially mediated precipitation, and there were no distinctive skeleton-secreting organisms. Such subtidal facies tend to be variably siliciclastic, or frequently dolomitized lime mudstone with local oolitic, peloidal or intraclastic beds. Nearshore limestones of Phanerozoic age are fossiliferous, commonly bioturbated to some degree, and may exhibit patch reefs and oolites. Units of thinly interbedded bioturbated lime mudstone and wackestone and ripple or dune cross-laminated grainstone that are overlain by rocks exhibiting clearly supratidal facies are typical. Subtidal and lower intertidal carbonates of Mesozoic and Cenozoic age are commonly thick bedded and totally bioturbated, reflecting the post-Paleozoic increase in the diversity and effect of the bioturbating fauna.

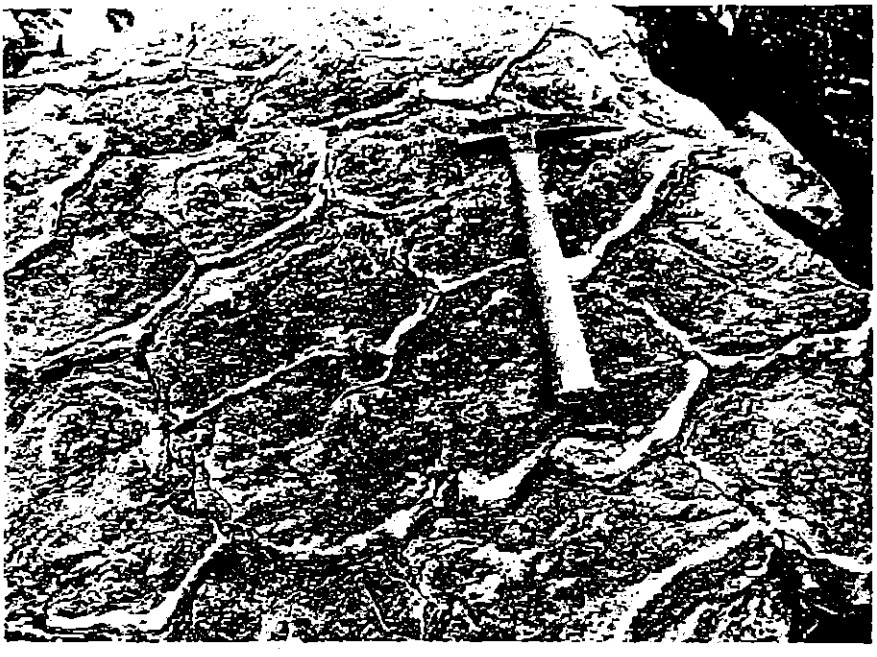

Figure 11 A bedding plane of desiccation-cracked polygons in which the edges of each polygon are curled up, probably because the original microbial mats shrivelled upon exposure. East Arm Formation, Upper Cambrian, Bonne Bay, western Newfoundland; hammer is 30 cm long.

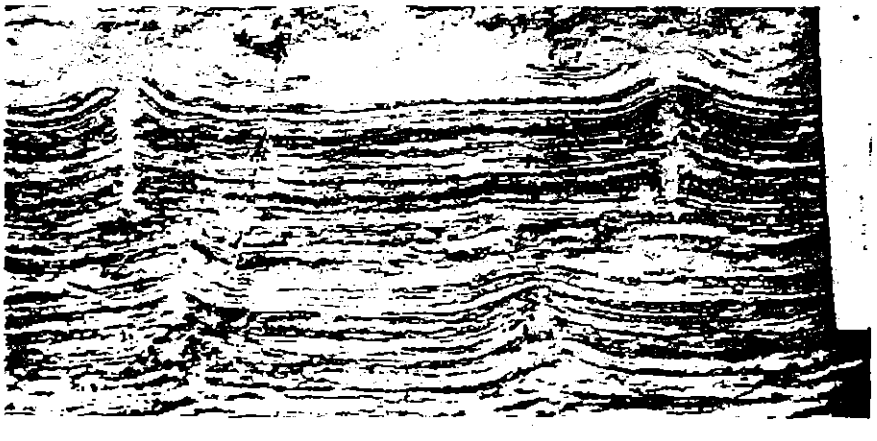

Figure 12 A cross section of desiccation cracks in microbially laminated peritidal dolostones; Providence Island Dolomite, Middle Ordovician, Lake Champlain, New York State.

Intertidal flat facies

Wavy-, lenticular- and flaser-bedded peloidal lime mudstone or grainstone (calcisiltite) and dolomitized argillaceous lime mudstone (sometimes interbedded with small hemispheroidal stromatolites), arising from the alternation between slack water and sediment transport by both unidirectional currents and waves under lower flow regime, are particularly distinctive of Precambrian and lower Paleozoic sequences (Fig. 8). This facies is directly comparable to the tidal bedding in siliciclastic peritidal deposits, including those forming in many modern settings (see Reineck and Singh, 1980). The carbonate strata, however, commonly contain intraclastic horizons which are absent in siliciclastic counterparts. Phanerozoic intertidal facies frequently have bioclastic layers. Well-sorted coquinas were likely washed in from the subtidal zone by storms, whereas poorly sorted shelly deposits containing a low-diversity assemblage of gastropods or bivalves probably represent the in situ intertidal fauna. Laminae that appear laterally continuous, undulating and uniform in thickness, are typically intercalated in this facies, and record periods of stabilization or binding of the substrate by a microbial mat. This tidal bedding can be burrowed in Phanerozoic sequences, and in the lower Paleozoic the trace fossil fauna is dominated by a low-diversity assemblage of horizontal burrows and U-shaped forms like *Arenicolites* and *Diplocraterion*. As with subtidal deposits, post-Paleozoic intertidal sediments are likely to be thoroughly churned; bioturbated, poorly fossiliferous lime mudstone units may be interpreted as intertidal if other criteria, such as vertically juxtaposed beds with desiccation cracks, are evident.

Tidal creek facies

Rocks specifically interpreted as having accumulated in tidal creeks or channels piercing intertidal flats are relatively uncommon. The reasons for this are mainly 1) the rarity of laterally

extensive exposures that intersect the possible margins of channels once they stop migrating laterally, 2) the difficulty in distinguishing creek fills from regressive packages with a basal, higher-energy component that resulted from tidal flat progradation, 3) the similarity between bedforms and lateral-accretion bedding from bar migration in channels and inclined and tabular cross stratification from migrating offshore carbonate sand shoals, and 4) the difficulty in separating creeks in tidal flats from channels between adjacent offshore islands or shoals. The presence of flat-pebble and blocky intraclasts derived from the surrounding flats and levees, respectively, along with bipolar (herringbone) cross stratification typically exhibiting reactivation surfaces and *tidal bundles* (couplets of sandy and muddy laminae), seem to be diagnostic of creek or channel deposits (e.g., Pratt and James, 1986). Grainstone beds with erosional bases and containing stromatolite or thrombolite mounds in some Proterozoic and Cambrian sequences are reasonably interpreted as channel deposits, (Koerschner and Read, 1989; Wright *et al.*, 1990). Waters *et al.* (1989) and Cloyd *et al.* (1990) have mapped Cambrian channels at least 10 m wide and 1 m deep with erosional bases, filled with lateral-accretion beds of individually graded, locally bipolar cross-laminated grainstone containing desiccation-cracked lime mud drapes and reactivation surfaces (Fig. 9). Care must be taken in late Proterozoic and early Paleozoic carbonates, however, to differentiate subaerial (desiccation) cracks and other cracks of submarine origin (Knoll and Swett, 1990; Cowan and James, 1992).

Beach facies

Beaches, which also have not been reported frequently from ancient tidal flat sequences, are characterized by seaward-dipping, low-angle laminae and thin beds of grainstone, often with hardgrounds exhibiting bored surfaces. This facies passes laterally to subtidal deposits in the seaward direction and tidal-bedded strata in the landward direction (e.g., Inden and Moore, 1983; Waters *et al.*, 1989). Steeper shorelines, such as Tertiary and Quaternary examples from the Mediterranean and Red seas, are often onlapped by gravelly beds of well-rounded pebbles and large shells.

Pond facies

Recognition of schizohaline pond deposits on humid intertidal flats may be impossible in most rock sequences unless the ponds were particularly long-lived. In one example (Pratt, 1979), burrowed wackestone containing ostracodes and horizontal meshes of *Girvanella* filaments with organic-rich walls (Fig. 10) are intercalated within burrowed and microbially laminated lime mudstone and tidal-bedded dolostone and lime mudstone. The restricted biota of this deposit, the well-preserved microbial remains, and its lenticular geometry within a peritidal sequence argue against a normal-marine subtidal environment.

Supratidal facies

Microbially laminated limestone or dolostone, usually with desiccation cracks and coarser rippled layers, is a common peritidal rock type (Figs. 11, 12); such rocks, however, may be

Figure 13 Polished slab of clotted and peloidal lime mudstone showing microbial lamination and fenestral fabric of laminoid, millimetre- to centimetre-sized, cement-filled pores. This distinctive fabric probably formed in the upper intertidal or lower supratidal zone. Eldon Formation (Middle Cambrian), Exshaw, Alberta; scale bar is 1 cm.

Figure 14 Thin section photomicrograph of peloidal and clotted micrite containing bioclasts (mainly ostracodes and gastropods) and exhibiting fenestral fabric. Upper parts of the laminoid fenestral pores have pendant fringes of fibrous calcite cement (grey coloured) suggesting that this sediment was deposited in the upper intertidal zone and that the fibrous calcite precipitated as marine or mixed waters percolated through the pores during low tides. Table Point Formation (Middle Ordovician), western Newfoundland; scale bar is 1 mm.

upper intertidal or supratidal in origin. In older Phanerozoic sequences, a supratidal setting might be inferred if bioturbation is rare or absent, or there is evidence for prolonged subaerial exposure such as evaporites, karst horizons or paleosols. Intercalated within many microbially laminated rocks are intraclastic horizons, which are analogous to pavements of microbial mat chips or fragments of cemented crusts in modern supratidal environments. Fenestral lime mudstone and peloidal grainstone (Fig. 13) are common (Shinn, 1983b) and, by analogy with tidal flats of Florida and the Bahamas, were probably deposited in moist supratidal "algal marshes" or around ponds. This facies sometimes exhibits features, such as pendant fibrous cement (Fig. 14), brecciated crusts and tepees, pisolites and pores with geopetal sediment floors, suggestive of flushing by downward-percolating seawater and rainwater and upward-flushing by groundwaters in a subaerial environment. Precambrian supratidal deposits often contain digitate stromatolites, millimetres to centimetres in diameter, which have been interpreted as supratidal, tufa-like aragonite precipitates (e.g., Grotzinger, 1986). Post-depositional leaching of evaporites causes collapse brecciation in supratidal facies.

THE PERITIDAL SHALLOWING-UPWARD SUCCESSION

Ancient peritidal carbonate lithofacies are characteristically organized stratigraphically into metre- to decametre-thick, shallowing-upward successions (Fig. 15) each with a basal subtidal unit, intermediate intertidal facies, and an upper supratidal unit with or without a terrestrial horizon on the top (James, 1984; Wright, 1984; Tucker and Wright, 1990). Contacts between the members are gradational or sharp and may show evidence of local synsedimentary scour. Walther's Law tells us that, if there are no major depositional breaks, we can reconstruct the ancient environmental mosaic by dealing out each facies like a deck of cards. There are departures from this ideal pattern, however, and it is not unusual to find the supratidal member overlain by intertidal facies, or components missing because of nondeposition or erosion.

Characteristics

The lithologic nature of the subtidal → intertidal → supratidal succession is variable, reflecting the broad spectrum of intertidal and supratidal depositional environments, the dictates of biotic evolution and past changes in ocean chemistry. Such peritidal shallowing-upward successions can be subdivided into two types, low energy (Figs. 16, 17) and high energy (beach; Fig. 18) , and both may show the effects of climate, such as thin beds of evaporites, especially anhydrite (Chapter 19).

In the simplest case, and referring only to the Phanerozoic, low-energy shallowing-upward successions have a burrow-mottled, variably argillaceous lime mudstone to wackestone or packstone lowest member, often with a basal bioclastic and intraclastic grainstone or rudstone as a transgressive lag on top of the pre-existing succession (Fig. 16). Patch reefs may be present in the subtidal member. The intertidal member exhibits thin-, lenticular- and wavy-bedded, variably bioturbated lime mudstone and bioclastic, peloidal and sometimes oolitic grainstone, locally with small domical stromatolites. This grades upward to an upper intertidal and supratidal member that is usually a microbially laminated, locally desiccation-cracked, slightly argillaceous lime mudstone frequently exhibiting fenestral fabric, with thin interbeds of intraclastic horizons and laminae of peloidal or bioclastic grainstone. If the sediments were laid down in an arid climate, nodular to wavy beds of anhydrite may displace and replace sediment of the intertidal and supratidal members (Fig.16). Higher-energy cycles (Fig. 18) also have a bioturbated subtidal bioclastic basal member, but the intertidal component is made up of bioclastic and/or locally oolitic grainstones representing beach deposits. These may exhibit inclined- and cross-stratification and hardgrounds. The upper intertidal and supratidal units are generally desiccation-cracked microbial laminites.

Both kinds of shallowing-upward successions can have a capping horizon of marsh sediments, paleosol or calcrete. Successions may be separated from overlying units by a karst surface caused by subaerial weathering, or an erosion surface formed during the environmental shift responsible for the next succession. Supratidal sediments may show the diagenetic effects of groundwater dis-

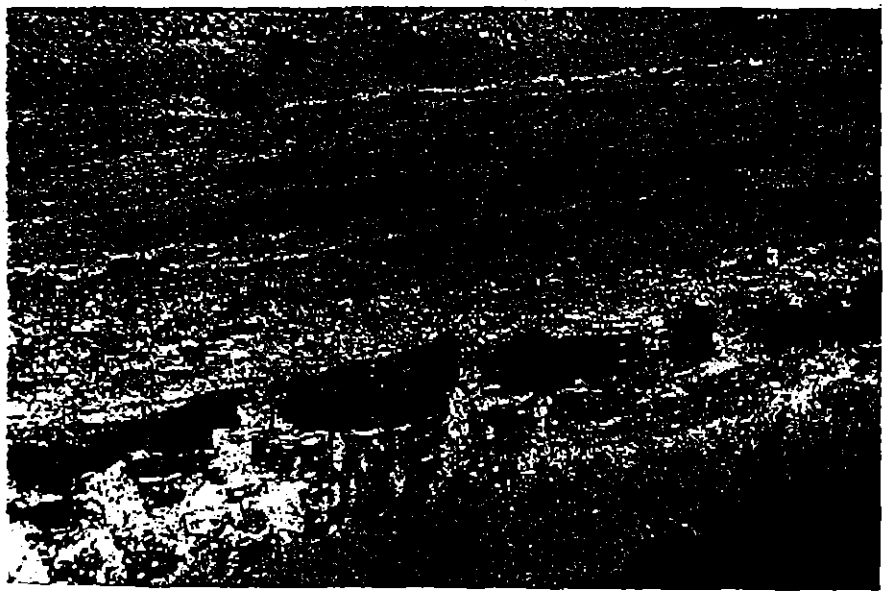

Figure 15 A shallow pit excavated on the Holocene sabkha; Abu Dhabi, United Arab Emirates. The roughly 1 m of section is composed of light-hued subtidal sediment at the base, overlain in turn by conspicuous black intertidal microbial mats with desiccation cracks and light-coloured supratidal sediment and capped by eolian quartz-rich sands. Photo courtesy P. Scholle.

charge, such as tepees, cements and leaching of evaporites.

A warning! Tidal creek or channel fills can look suspiciously like shallowing-upward successions produced by tidal flat progradation (Fig. 18). Predictably, they should be composed of a basal intraclastic, peloidal and bioclastic grainstone lag or bar facies, overlain by thin-bedded and bioturbated lime mudstone and wackestone, and capped by microbially laminated lime mudstone, recording waning energy conditions as the creek is abandoned (e.g., Waters *et al.*, 1989; Cloyd *et al.*, 1990). Unless a channel margin or lateral-accretion bedding is exposed, or blocky intraclasts from margin collapse are present, these deposits could easily be misunderstood.

Geometry

To interpret how any particular peritidal shallowing-upward succession may have developed there must be firm local and regional lateral control on the distribution of units; bed or event correlation must be demonstrable. Besides walking or tracing out individual beds, the lithologic features that may be widely correlatable in peritidal successions are subaerial exposure horizons (karst surfaces, collapse breccias and paleosols), evaporite beds and siliciclastic horizons resulting from sea level fall. We recognize two geometries. *Laterally continuous* metre-scale successions are widespread, possibly platform-wide, and correlatable. *Laterally discontinuous* metre-scale successions are local in extent and noncorrelatable and supratidal facies can be traced laterally into intertidal and/or subtidal facies over kilometre-scale distances.

Origin

An aspect of carbonate sedimentology that has become a maxim over the last decade, for Phanerozoic rocks at least, is that healthy carbonate platforms, i.e., those not stressed by environmental conditions like cold water, hypersalinity, turbidity or nutrient poisoning that hinder organism growth, can produce enough carbonate sediment to aggrade, and commonly a surplus, causing progradation, while relative sea level rises (Schlager, 1981). Shallow water sediments thus overlie deeper water facies. Each shallowing-upward peritidal succession records the vertical and lateral accretion of a single tidal flat to a level just exceeding high-tide mark; if there was no subsidence or sea level change, the thickness of the intertidal-supratidal component might approximate the tidal range, but if there was any relative sea level change, the thickness is no indication of this at all.

There are currently three models used to explain how a shallowing-upward succession forms 1) as a prograding wedge, 2) as a simultaneously

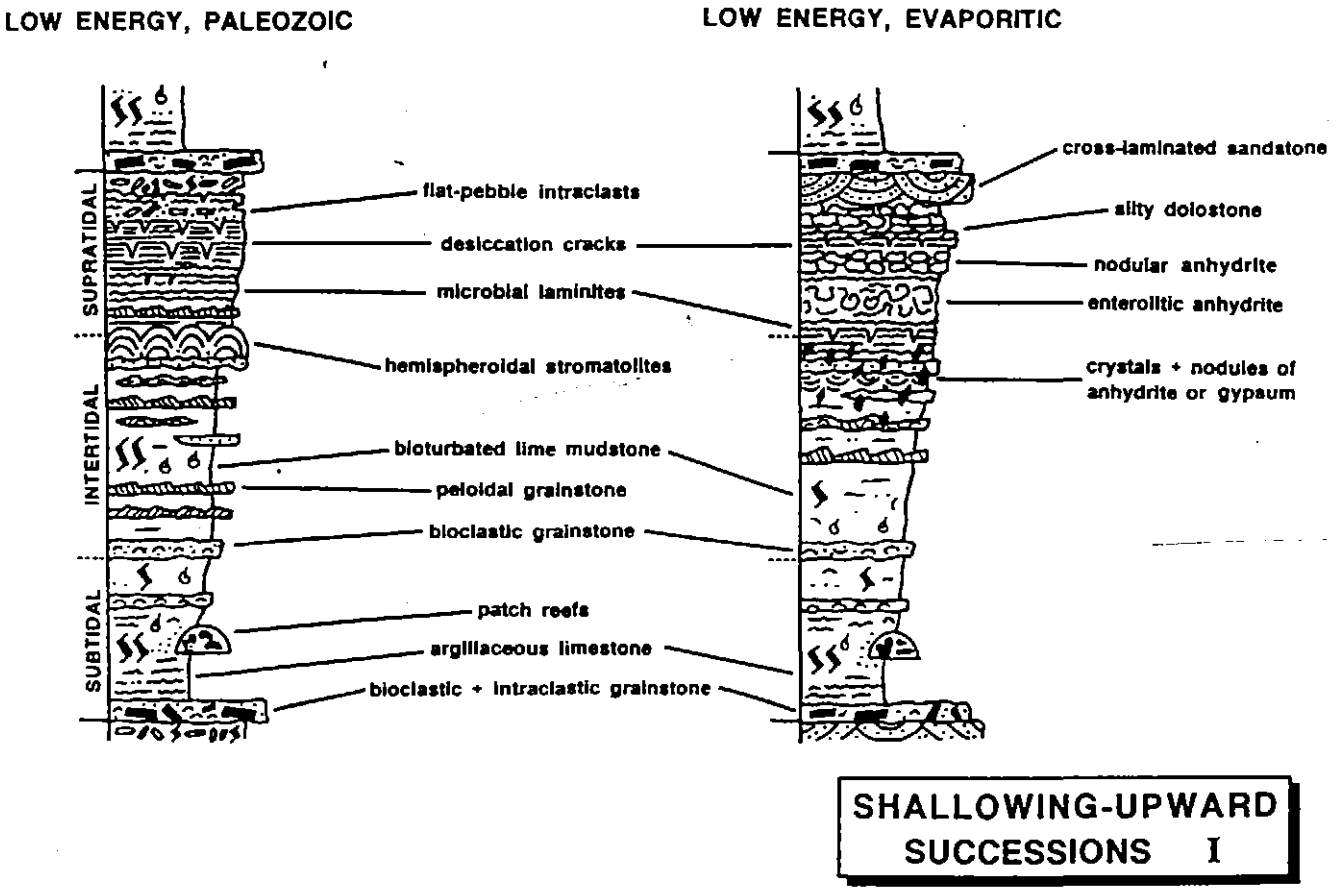

Figure 16 Hypothetical vertical profiles of individual low-energy, metre-scale, peritidal shallowing-upward successions. Left: from the lower Paleozoic; upper Paleozoic examples might exhibit calcretes at the top. Right: an evaporitic example (Chapter 19). No scale is implied, but each succession is typically 1-10 m thick.

aggrading sheet or, 3) as a mosaic of tidal flat islands (Fig. 19).

The prograding wedge

Holocene shallow-marine and peritidal environments are dynamic in that they shift geographically over geologically short periods of time in response to both local and regional changes in climate, prevailing wind direction, current pattern, and sediment supply. A single coastline, for example, may possess tidal flats that are accumulating and prograding, and tidal flats that are dormant or are eroding (e.g., Shinn *et al.*, 1969; Strasser and Davaud, 1986). Regardless, to generate a single, laterally extensive wedge that has peritidal, shallowing-upward attributes throughout, the tidal flat must prograde laterally from a nucleus. Such accretion can develop seaward from land, outward from islands, or shelfward from platform margin buildups and/or shoals. It must be stressed that deposition on the tidal flat is a physical process. Sediment generated on the platform is swept onto the flats by storms producing the gradually prograding tidal flat wedge. As such, the size and dynamics of the peritidal wedge are primarily a function of the health and nature of the source area (the subtidal carbonate factory) and the way in which sediment is redistributed on the platform (i.e., how much is transported to the flats, how much stays in place, how much is transported offshore into deep water).

The Holocene record of sea level change is one of rapid rise between 11 ka and 6 ka, followed by decelerated rise from 6 ka to the present. There are, unfortunately, few tidal flats that have been cored in enough detail to provide a good three-dimensional stratigraphic picture of deposition during this period. As a result of this small data base it is difficult to make generalizations. Nevertheless, at present there appear to be two styles of progradation (Fig. 20), *simple offlap* and *staggered offlap* (Hardie and Shinn, 1986). Simple offlap is typified by the gradually prograding wedge along the southern coast of the Persian (Arabian) Gulf. Staggered offlap is characterized by the northern Bahamas tidal flats. In the latter case the tidal flat does not seem to have prograded but instead aggraded behind a protecting beach ridge. The vertical succession is mainly burrowed sediment, reflecting deposition in a variety of pond, channel and intertidal flat environments, capped by laminated upper intertidal to supratidal sediments. It is thought that tidal flat sedimentation began only when the offshore carbonate sand bar emerged to become a barrier. Once the flat aggraded to sea level, progradation took place by a series of jumps followed by back filling (Hardie, 1986). Such successions in the rock record should

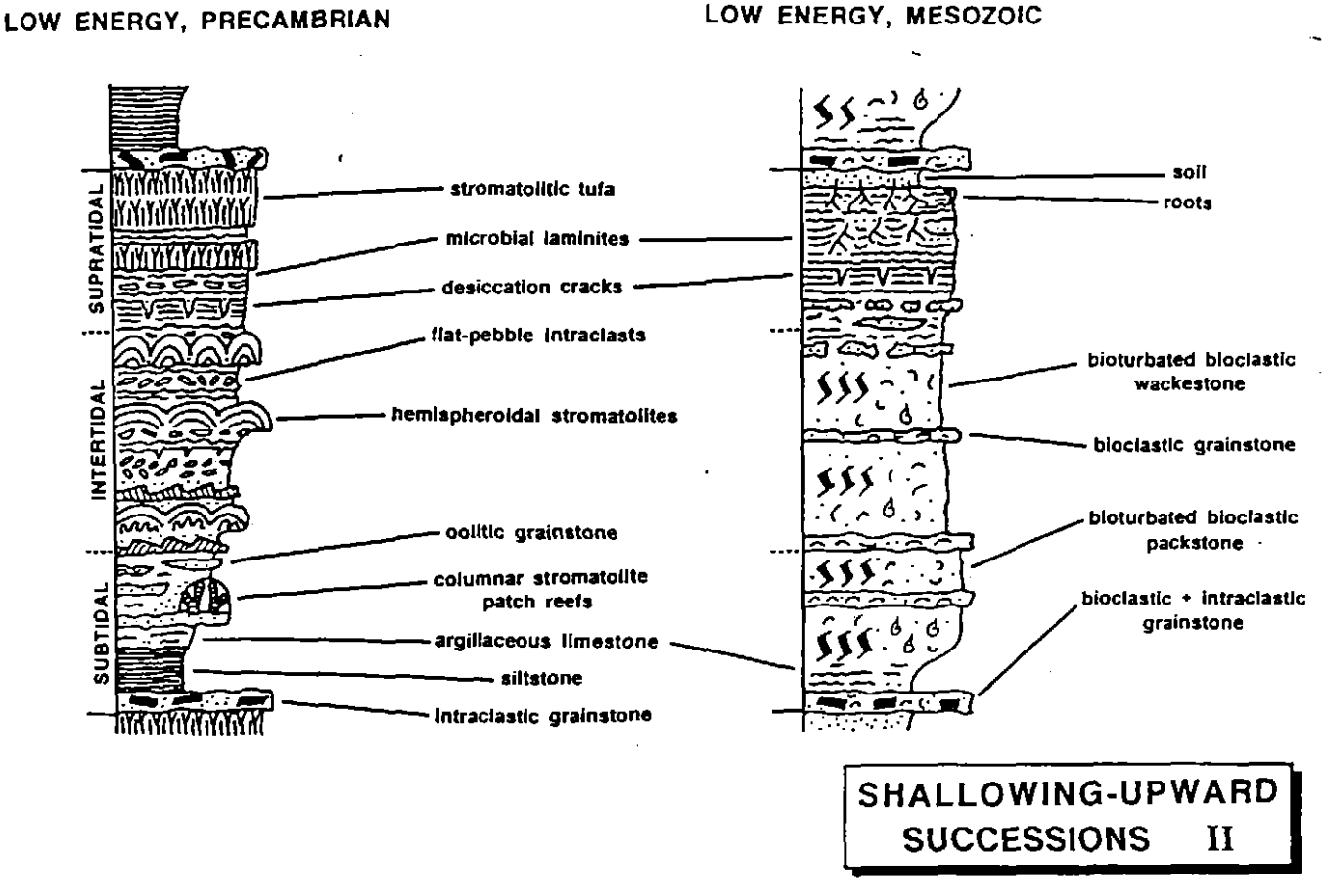

Figure 17 Hypothetical vertical profiles of individual low-energy, metre-scale, peritidal shallowing-upward successions from the Precambrian (left) and Mesozoic (right). A comparison of these with the Paleozoic example in Figure 16 shows some of the lithologic changes exerted by biotic evolution through geologic time.

contain remnants of these barriers. The Abu Dhabi sabkha is reported to have buried barriers (Warren and Kendall, 1985) and may have also developed, in part, through staggered offlap.

For a wedge of tidal flat sediment to prograde from the strandline across an entire platform, accumulation of sediment must occur under relatively stable hydrographic conditions (i.e., sea level and climate) for the length of time represented by progradation. A rapid rise in sea level would flood the broad supratidal flat and halt progradation, whereas any fall in sea level would strand the tidal flat before transplatform progradation was complete.

This style of accumulation has been proposed to explain the extensive Cambro-Ordovician peritidal strata of the southern Appalachians (Hardie, 1986). Metre-scale peritidal shallowing-upward successions of this epeiric platform have been correlated (but not traced) for distances greater than 100 km parallel and perpendicular to depositional strike. Progradation at this scale, however, would produce vast areas of abandoned supratidal flats behind the prograding shoreline, far distant from the subtidal source of sediment and exposed to protracted subaerial diagenetic effects. Since constant and uniform subsidence would inundate this supratidal surface, progradation must have taken place while relative sea level was stationary or gradually falling. If progradation was simple offlap, then successions will be laterally continuous. If progradation was staggered offlap, successions will be discontinuous and separated by lenticular beach deposits.

Simultaneously aggrading sheet

In this situation, continuous in situ carbonate sediment production results in aggradation of the seafloor steadily to sea level. The entire platform becomes intertidal and then supratidal, and can be completely exposed before flooding and deposition of the next overlying succession (Fig. 19). There are no Holocene analogues for this process; it is derived entirely from interpretation of the rock record, and therefore is poorly constrained. Platform-wide peritidal exposure under these circumstances cannot be *intertidal* per se, because it is unlikely that tides could operate across such a vast horizontal distance all at once. Instead, alternating flooding and exposure would have to be induced through the movement of the sea surface by periodic storm surges or persistent winds. Such a style of *occasional* exposure and submergence may be difficult to distinguish in the rock record from true *intertidal conditions*. This hypothesis demands that at least some sediment be produced on the flats when the whole platform is in the intertidal-supratidal environment. Such accretion could predictably produce platform-wide, laterally continuous, metre-thick shallowing-upward successions, such

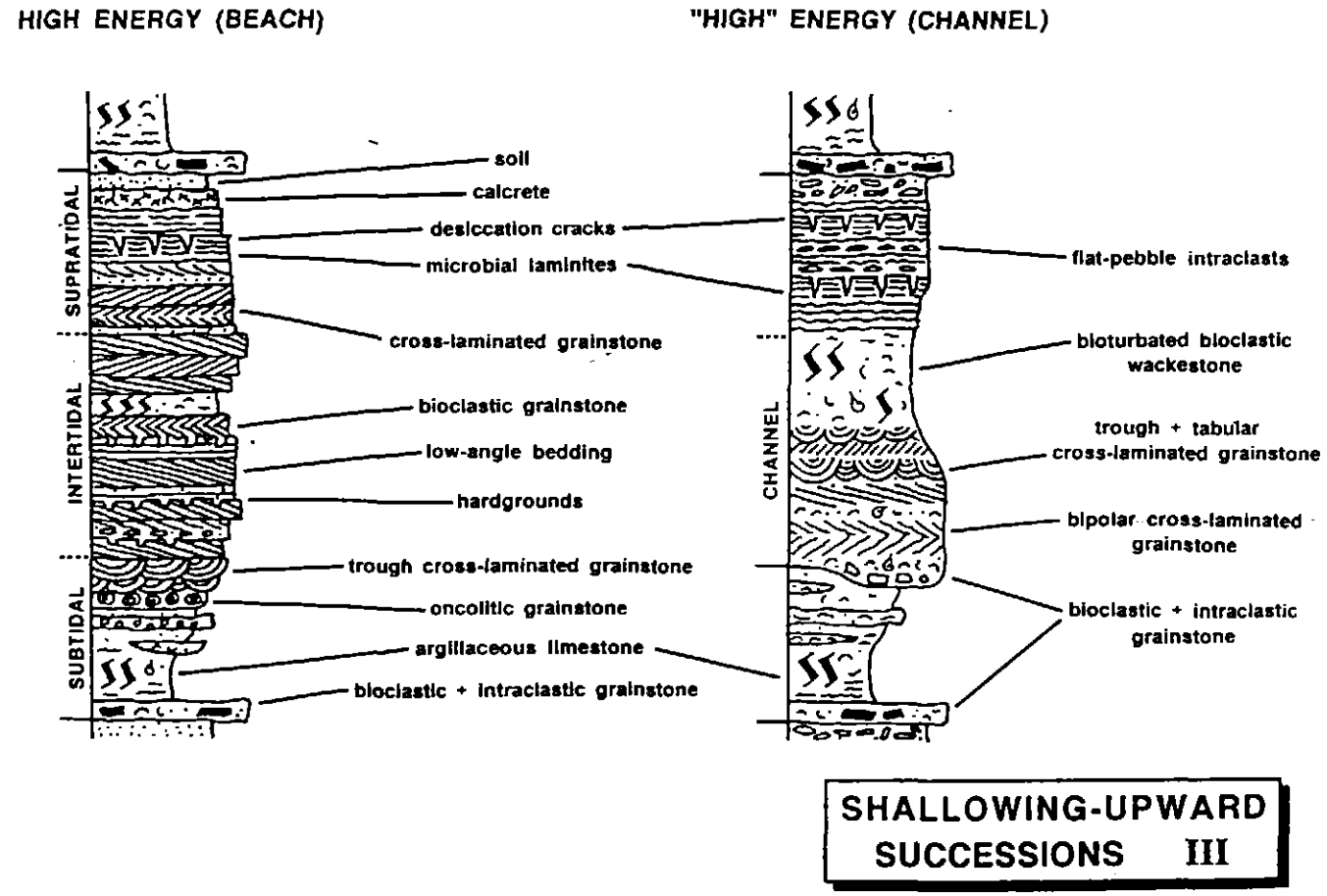

Figure 18 Hypothetical vertical profiles of individual high-energy, metre-scale, peritidal shallowing-upward successions, from a setting characterized by beach development (left) and a tidal flat penetrated by channels or creeks (right).

as those inferred from Cambrian strata by Koerschner and Read (1989).

Tidal flat islands

An alternative model has been postulated to explain shallowing-upward peritidal successions that are demonstrably laterally discontinuous (Pratt and James, 1986). In this *tidal flat island* model deposition is envisioned as taking place on a platform dotted by a mosaic of exposed low-relief islands and intertidal banks separated by subtidal source areas (Fig. 19), with the whole complex shifting laterally and vertically through time in response to a range of local and regional hydrographic conditions. Such islands are developed today in Florida Bay and illustrate two modes of Holocene accumulation, 1) physically deposited mud banks capped by prograding intertidal and supratidal sediments, and 2) entirely supratidal deposition of a coastal mud flat, later dissected by erosion (Enos and Perkins, 1979; Wanless and Tagett, 1989). These islands, however, have not migrated much during the relatively short period of Holocene flooding. If viable, this tidal flat island model severely limits the architectural predictability of ancient platforms, as the constituent facies, particularly the supratidal caps, are of inherently limited regional extent.

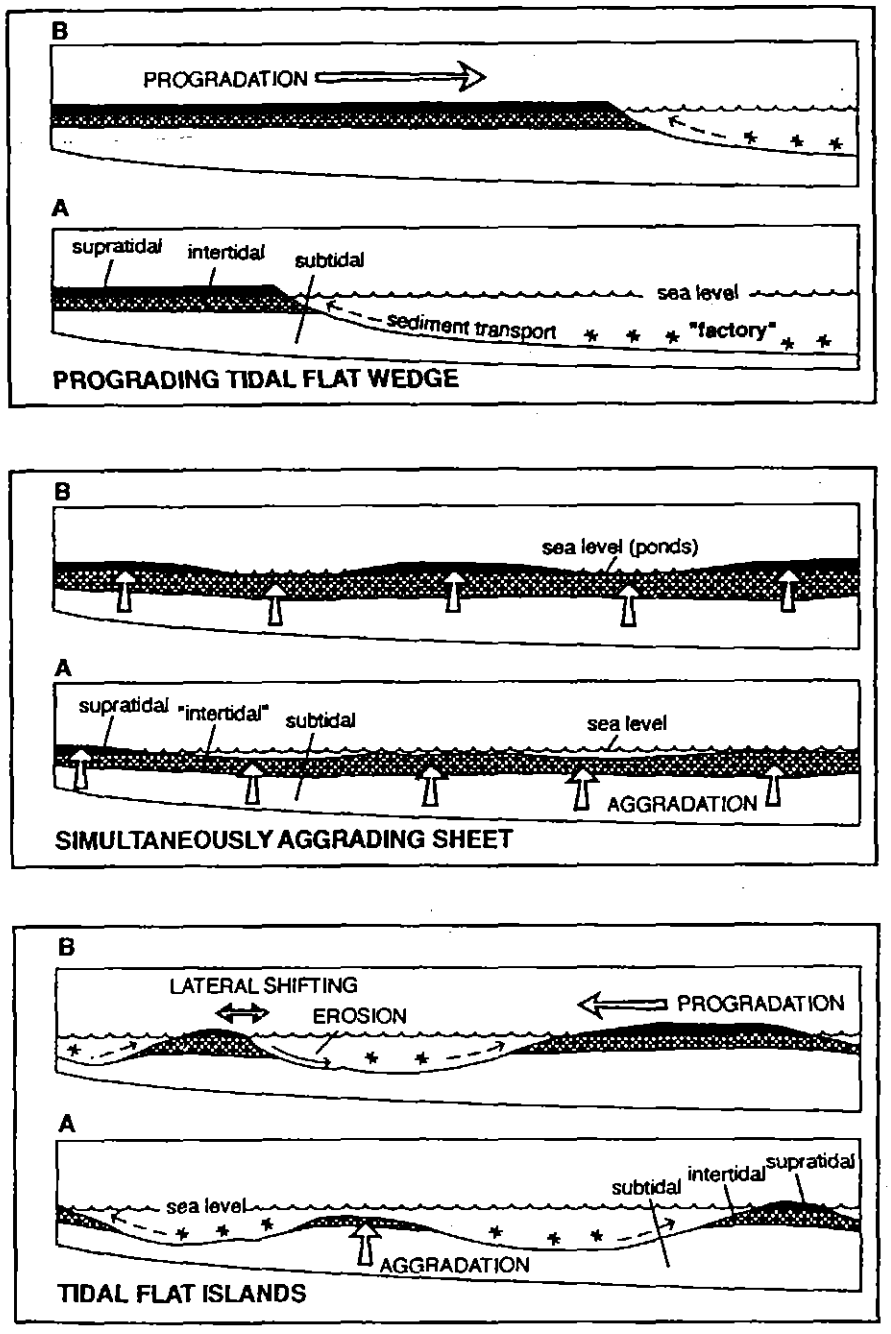

Figure 19 Diagrams illustrating various ways in which a metre-scale, peritidal, shallowing-upward succession can form. A prograding wedge is generated by sediment transported onto the tidal flat from the offshore carbonate factory. A simultaneously aggrading sheet accretes vertically to sea level and the whole platform becomes sequentially intertidal and then supratidal. Tidal flat islands nucleate and accrete by aggradation and progradation and shift in response to hydrographic forces.

Asymmetry

Why is a metre-scale, peritidal shallowing-upward succession asymmetric? The characteristic asymmetry of a typical shallowing-upward succession, i.e., subtidal (A), intertidal (B) and supratidal (C) stacked in ABC → ABC *hemicycles* (Figs. 16, 17, 18), as opposed to full CBABC cycles, is generally attributed to problems with the source area during platform inundation. If the flooding which begins a succession were gradual, then the seafloor during initial submergence is thought to have been too wave swept and/or too shallow or restricted to produce much carbonate sediment. Thus there is a "lag time" or "lag depth" (Hardie, 1986) before the seafloor becomes deep enough to actively produce sediment that is subsequently moved onto the tidal flats. In some successions this time interval is represented by a coarse-grained "transgressive" facies at the base, whereas in others there is no obvious record of this hiatus in deposition. Alternatively, if flooding was rapid, then supratidal facies (C) would be rapidly drowned and intertidal facies (B) would not have time to accumulate.

PERITIDAL CYCLOSTRATIGRAPHY

The stratigraphic record of ancient peritidal carbonates tends to be one of persistent repetition of the basic metre-scale, shallowing-upward succession, imparting a characteristic *cyclic* or, more appropriately, *rhythmic* appearance to the strata. While Holocene tidal flats sometimes provide an analogue for the generation of one

shallowing-upward succession, the cause of stratigraphic repetition must be derived from the rock record. The Pleistocene history of climate and sea level change, although the most detailed and best understood of past epochs, has left a stratigraphic record of limited usefulness because sea level fluctuations were so large that they did not result in stacked metre-scale shallowing-upward successions. Consequently, there is currently much discussion as to what causes the rhythmic stacking into thick stratigraphic packages of ancient shallowing-upward successions. Debate has centred around the question of whether the new space made available for each successive shallowing-upward succession is the result of 1) recurring sea level changes (perhaps eustatic) at the same scale and temporal rhythm as the lithologic packaging; or 2) a high-frequency packaging mechanism *intrinsic* to processes of carbonate sedimentation which are superimposed on a low-frequency or irregular sea level rise. These are the *allocyclic* and *autocyclic* mechanisms, respectively, (see also Wilkinson, 1982). The two stacking mechanisms are not necessarily mutually exclusive, and it is uncertain at the moment whether or not evidence for either mechanism can be isolated in the rock record (Hardie *et al.*, 1991; Read *et al.*, 1991).

There is good evidence that a typical shallowing-upward succession was deposited within a time span of 10-100 k.y. (Algeo and Wilkinson, 1988). This is a scale of resolution beyond that provided by biostratigraphic methods. Much of the time represented by stacked shallowing-upward successions, however, is accounted for by hiatuses. Thus the time of deposition for a given tidal flat succession may be only a small fraction of the total apparent stratigraphic time; Wilkinson *et al.* (1991) have suggested as little as 3-30 per cent for some successions.

Autocyclicity

The driving force behind autocyclicity is the dynamics of sedimentation on the platform. Assuming optimum conditions, production rates for shallow-marine carbonate detritus could potentially provide enough sediment over a period of 10-100 k.y. to account for tidal flat aggradation to sea level or progradation of many tens to perhaps hundreds of kilometres under essentially static sea level conditions on a gradient which experienced typical passive-margin rates of subsidence (see also Hardie and Shinn, 1986).

Progradation is inherently limited by the sediment budget of the carbonate platform. For example, in a model first proposed by Ginsburg (1971; see Bosellini and Hardie, 1973; Mossop, 1979), a tidal flat wedge is envisioned as prograding across a gently inclined, gradually subsiding platform under static or slowly changing sea level (Fig. 19). As progradation covers the platform, the subtidal source area for tidal flat sediments becomes increasingly smaller (and deeper). Eventually the source area is too small or too deep to provide sediment for the tidal flat, so sedimentation stops. If relative sea level continues to rise, however, soon the whole platform will once again be subtidal and, after a lag period, the carbonate factory will be robust enough for sediment production, and the cycle will begin again.

The meagre areal coverage of present-day tidal flats makes it difficult to envision a platform literally choking itself off through hundreds of kilometres worth of tidal flat progradation under steady-state sea level and subsidence conditions. Furthermore, it should be emphasized that interpretations of platform-wide progradation in ancient examples are usually based on correlation of strata assumed to be diachronous, not on continuous stratigraphic exposure.

Under conditions of platform-wide *aggradation* it is thought that, once flooded, a shallow platform could generate enough sediment in situ that the whole seafloor would inexorably build to sea level (Fig. 19). Fundamental to this hypothesis is the ability of the "intertidal" and "supratidal" environments to produce sediment. The next cycle would accrete once relative sea level rise had submerged the platform in water deep enough for subtidal sedimentation to begin again. Critics of this hypothesis argue that, in order for the sediment surface to intersect the air/water interface on a platform-wide scale, there must be a sea level fall (albeit minor — a metre or less?), because it is unlikely that the seafloor would everywhere build right up to sea level of its own accord. This model is based on examples where shallowing-upward successions are correlated on a regional scale and assumed to be synchronous deposits.

Tidal flat islands are in part aggradational and in part progradational and their location is thought to shift through time in response to changing hydrographic conditions (Fig. 19). During intervals of prolonged static sea level, or slow sea level rise, they would, like the

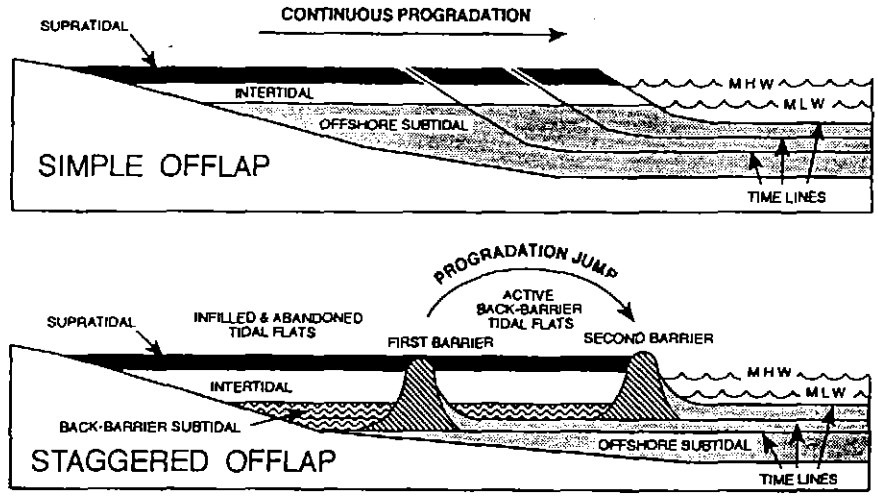

Figure 20 A diagram depicting two styles of tidal flat progradation envisioned from Holocene tidal flats. Simple offlap takes place by continuous progradation. Staggered offlap takes place by formation of an offshore bar which creates a leeward, protected setting in which tidal flat aggradation occurs. Once the flat builds to sea level it becomes dormant until another bar forms seaward and the process of backfilling begins again. Adapted from Hardie (1986).

prograding wedge, gradually choke off local source areas, eventually becoming dormant. For sedimentation to begin again after a period of local stasis and probably protracted exposure of supratidal flats, there must be creation of new accumulation space. Under conditions of more rapid long-term sea level rise, and continually renewed accumulation space, the islands would form a series of laterally discontinuous peritidal units.

These autocyclic models express a basic premise that pervades current thinking about peritidal carbonates. Persistent and ubiquitous stratigraphic repetition of the basic shallowing-upward succession seems to indicate that these systems are, *at least in part*, intrinsically self-governing.

Allocyclicity

The extrinsic factors of subsidence and eustacy, which cause relative sea level change, have long been assumed to exert strong control on *large-scale* peritidal stratal patterns. High-frequency, low-amplitude sea level changes, the fourth- and fifth-order fluctuations of sequence stratigraphy (Chapter 2), are commonly invoked to drive the packaging of metre-scale, shallowing-upward peritidal successions (Grotzinger, 1986; Koerschner and Read, 1989; Read *et al.*, 1991). In this situation, a metre-scale rise in relative sea level provides a *window of opportunity*, in the sense of both time and accumulation space, for the generation of a single shallowing-upward succession (Fig. 21). Deposition occurs while sea level is rising and at its apex, and is arrested by sea level fall.

Formation of the shallowing-upward succession in this window is envisioned in different ways by different workers. All three styles of accretion presented above are viable within this scheme (prograding wedge, Grotzinger, 1986; aggradation, Koerschner and Read, 1989; and tidal flat islands, Strasser, 1988). Extrinsically controlled metre-scale successions of many kinds, including peritidal, have also been called *punctuated aggradational cycles* (PACs; Goodwin *et al.*, 1986) or more recently *metre-scale allocycles* (Anderson and Goodwin, 1990). Such cycles are metre-scale units, bounded by surfaces of abrupt change to deeper or disjunct facies and comprising a suite of contemporaneous facies, all of which shallow upward. The peritidal portions of such cycles are thought to be aggradational, but there is no reason why they could not be progradational (either wedges or islands).

The most commonly postulated external controls to drive, or at least reset, the system at the end of each shallowing-upward succession are rhythmic eustatic change or jerky subsidence. While spasmodic subsidence with the required short frequency has been documented from seismically active areas and for passive margins where listric faulting is common (e.g., Cisne, 1986; Hardie *et al.*, 1991), the importance of subsidence rate changes as a control on stratigraphic rhythmicity in peritidal shallowing-upward successions is unclear. Sudden base level drops have not been observed in modern passive margin platforms, and ancient epeiric settings, where much of the peritidal record is found, seem unlikely to have experienced metre-scale, high-frequency spasms of subsidence. Because there is currently no known frequency to such tectonism, it is difficult to use, and as yet impossible to model this mechanism as a universal control of stratigraphic rhythmicity. Nevertheless, the mechanism should not be dismissed as a potential control, especially in tectonically active regimes (e.g., Fischer, 1964; Knight *et al.*, 1991).

In the early to mid-1970s studies of DSDP sediment cores and relict coral reef terraces demonstrated that the Pleistocene record of eustatic change is one of superimposed orders of sea level variation (orders, in the sense of both magnitude and frequency; Chapter 2). Deep sea sediments were analyzed for oxygen isotopes (as proxy to glacial ice volume) and revealed a long-term (100 k.y.), 100 m-scale, asymmetric sea level oscillation. Pleistocene fossil reef data suggested that a shorter term (20 k.y.) sea level oscillation was superimposed on the longer term fluctuation. These various orders of eustatic change have been correlated to those predicted for icehouse glaciation driven by celestial mechanics, i.e., the Milankovitch rhythm (e.g., Fischer, 1986). It has been postulated that the stratigraphic rhythmicity apparent in ancient peritidal carbonates reflects a similar *composite eustasy* (Goldhammer *et al.*, 1987), both icehouse and greenhouse, of celestial origin. If astronomically forced composite eustasy is indeed the primary driver in the packaging of shallowing-upward successions, then presumably modulation of various orders of superimposed eustatic cycles could have provided potentially limitless rhythms to the stratigraphic record (Bova and Read, 1987; Koerschner and Read, 1989; Read *et al.*, 1991).

The common challenge to allocyclicity is that extrinsic controls on peritidal sedimentation are neither demonstrable in, nor theoretically re-

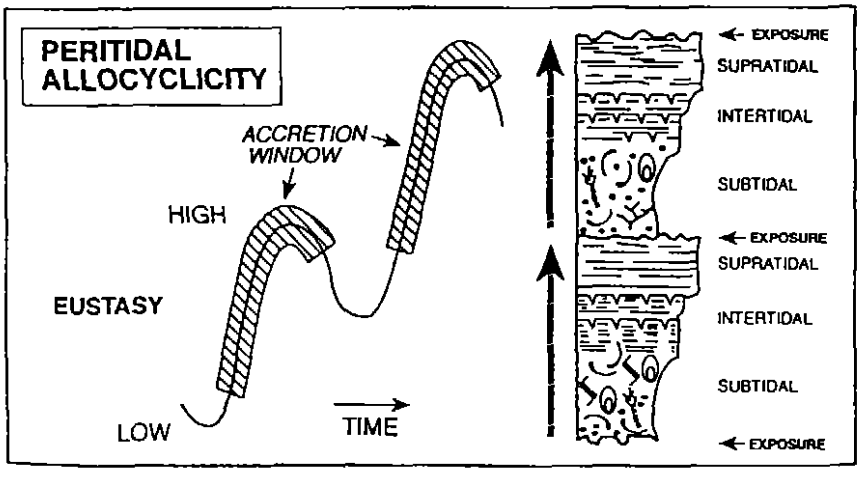

Figure 21 A diagram illustrating the relationship between fluctuating sea level and stacked metre-scale, peritidal, shallowing-upward successions. Sea level rise provides a window of opportunity for the succession to accrete as a prograding wedge, as a simultaneously aggrading sheet or as tidal flat islands. Sea level fall terminates accretion and results in subaerial exposure.

quired to generate metre-scale shallowing-upward successions. It is hard, however, to imagine sea level remaining static for a long period of time, and therefore difficult, if not impossible, to dismiss some extrinsic control on succession development. Allocyclic, platform-wide event stratigraphy should not be underestimated, but its deterministic role in peritidal cyclostratigraphy is still uncertain.

The search for controls and rhythms

Significant effort has recently been devoted to unravelling the meaning of possible stratigraphic rhythms in stacked shallowing-upward successions by numerical analysis. Because peritidal carbonates are so sensitive to changes in climate and sea level, it was widely suspected (hoped?) that this rhythmicity might retain a causative signal of ancient climate and sea level fluctuations. If allocyclic eustatic control on stratal packaging is assumed, then reconstruction of the strata-generating sea level curve can be used as a tool to correlate and explain temporally correlative strata (Read and Goldhammer, 1988).

At the current level of understanding and data base, it is not possible to isolate unequivocal evidence in the rock record for either allocyclic or autocyclic control on most peritidal stratal patterns. Reasonable-looking, synthetic, one-dimensional stratigraphic sections can, however, be generated by varying the critical input parameters of cycle amplitude, duration and asymmetry, bathymetry for each facies, lag time (depth), type of sediment, sedimentation rate, regional and local subsidence, isostatic compensation, wave damping, tidal range, and platform slope and dimension (Grotzinger, 1986; Read *et al.*, 1986; Goldhammer *et al.*, 1987; Spencer and Demicco, 1989). These sections can then be compared to actual examples and eventually a match may be achieved. When similar modelling techniques are used to simulate two-dimensional (multisection) architecture it is often found that the time needed for a peritidal wedge to prograde across the platform is longer than that predicted by Milankovitch rhythms, and the wedges become *stranded*.

Techniques, such as relative time series analysis and *Fischer plotting*, which made a good case for allocyclic forcing of some examples of platform carbonate rhythmicity, i.e., stratigraphic patterns attributable to rhythmic Milankovitch composite eustasy (Goldhammer *et al.*, 1987, 1990), cannot be used for the analysis of metre-scale *peritidal* shallowing-upward successions. Relative time series analysis to reveal the rhythms of sedimentation are invalid for progradational wedges, either local or platform-wide in extent, because such deposits are by nature diachronous, and thicknesses of resultant shallowing-upward successions vary with position on the regional gradient and/or platform topography. Fischer (1964) presented a graphic means of plotting time versus cumulative thickness for laterally continuous, stacked, peritidal shallowing-upward successions. Fischer plots have often been used in recent studies of cyclic strata because they are designed to reveal changes in accumulation space which deviate from that space generated solely by subsidence; these deviations are postulated to result from changes in sea level. However, interpretations of Fischer plots are essentially model driven. For them to be viable two assumptions must be satisfied: 1) each peritidal succession must have been deposited in the same amount of time as every other succession in the chain, and 2) there must be few, if any, missing tidal flat successions. The use of Fischer plots is therefore dubious for any peritidal successions which formed as prograding wedge-shaped tidal flats. It is likely that variations in both the tempo and magnitude of changes in accumulation space, however they are caused, account for stacks of shallowing-upward successions which vary in thickness. Whereas demonstration of allo- or autocyclic control of stratal patterns in stacked shallowing-upward successions appears out of reach at this time, more sophisticated models, particularly those which integrate peritidal rhythms with coeval subtidal and perhaps offplatform stratal patterns, hold promise.

PERITIDAL SEQUENCE STRATIGRAPHY

The concepts of sequence stratigraphy were developed in terrigenous clastic successions and carbonates have only recently been analyzed in this fashion (Chapter 14). *Systematic* packaging of the basic metre-scale shallowing-upward succession is less common and seems less straightforward, or less well developed in carbonates compared to siliciclastics. This difference likely reflects the fundamental differences between carbonate and siliciclastic sediments generally. We have, therefore, avoided the term *parasequence* in this treatment of carbonate tidal flat deposits.

Peritidal deposits are not indicative of any particular systems tract because the controls on tidal flat development, such as climate, platform circulation, wind patterns and tidal range, vary with each platform's unique history and configuration. Nevertheless, tidal flat deposits are potentially useful in delineating sequences and their component systems tracts in two ways, 1) geographic position of the tidal flat on the platform may track long-term changes in sea level, and 2) changes in large-scale accumulation space, and thus sequences, can be recognized through analysis of stacking patterns (packaging) of shallowing-upward successions.

Tracking sea level

Tidal flats can be the first facies overlying a sequence boundary, deposited as the rate of relative sea level fall decreases and the sea slowly floods back across the platform. As third-order sea level fluctuates in response to long-term, large-amplitude driving forces, the location of the strandline on the platform will change. If conditions are favourable for their development, land-fringing tidal flat deposits will mark the position of coastal onlap through the third-order eustatic cycle (i.e., the "onlap-offlap" geometry of Hardie, 1986; Fig. 22). Sarg (1988) documented the utility of tidal flats at the outcrop scale in a sequence stratigraphic context for the Permian of New Mexico, where a sequence boundary and shelf-margin wedge systems tract were recognized in part by the downdip, basinward position of onlapping tidal flat deposits.

Stacking

The stratigraphic patterns of *laterally continuous*, metre-scale, shallowing-upward successions generated by pro-

grading tidal flat wedges, can be envisaged in the framework of long-term changes in relative sea level. Third-order sea level changes are thought to "modulate" the higher-frequency, fourth- and fifth-order sea level cycles represented by the tidal flat successions. This has two consequences.

Long-term, third-order fluctuations in sea level should carry the window of opportunity in which each individual metre-scale succession is formed back and forth across the platform. Depending upon the balance between different rates of subsidence, eustasy and sedimentation, the window will be geographically repositioned during each consecutive fourth or fifth-order change in relative sea level to result in backstepping, offlapping or stacking of peritidal shallowing-upward successions. Figure 22 illustrates, in a conceptual way, how this might work on an inclined shelf. If the rate of change of long-term relative sea level is *low*, the geographic position of successive windows should remain roughly the same. Thus, peritidal successions in lowstand (position 1) and early highstand (position 3) systems tracts will probably be stacked in one place and will be relatively thin because the rate of addition of new accumulation space is low. If the rate of change is *high*, the window should be forced backward and forward across the shelf. This will likely result in either relatively thick, backstepped tidal flat successions (position 2 – transgressive systems tract) or relatively thin successions which offlap in a shingled fashion (position 4 – late highstand or early lowstand systems tracts). It must be stressed that the distance of progradation in each case will be specific to each peritidal package on each shelf.

Long-term sea level rise should accentuate short-term rises and suppress short-term falls; long-term falls in sea level will have the opposite effect. The relative proportions of subtidal, intertidal and supratidal facies in successive shallowing-upward successions may change systematically in response to this long-term modulation of short-term changes in accumulation space. This relationship is as yet hypothetical, and interpretations of such controls in ancient strata are necessarily model driven.

SUMMARY

Peritidal limestones and dolostones exhibit a large number of easily recognized sedimentary and biosedimentary structures. While some of these are individually equivocal bathymetric indicators (stromatolites or wave-rippled beds, for example, can form in subtidal areas), in most cases the features can be used collectively to make a firm environmental conclusion. A boon to interpreting ancient peritidal facies is the wealth of knowledge gained from modern settings. Very often a one-to-one lithologic comparison can be made, leading to a refined understanding of paleoenvironments and paleoclimates in individual cases. A *hierarchy of models* has been formulated that deals with successive levels of interpretation of peritidal carbonate strata.

These kinds of rocks fall into two main depositional systems, low-energy tidal flats and higher-energy beaches. The facies associations are fairly distinctive for each setting: this is the first tier of models to guide basic interpretations.

The vertical record of peritidal facies commonly shows a trend from subtidal limestone through intertidal sediments to supratidal deposits, at a metre scale, as tidal flats aggrade to sea level and prograde laterally. Peritidal models are therefore shown as shallowing-upward successions as a reminder of these dynamic processes.

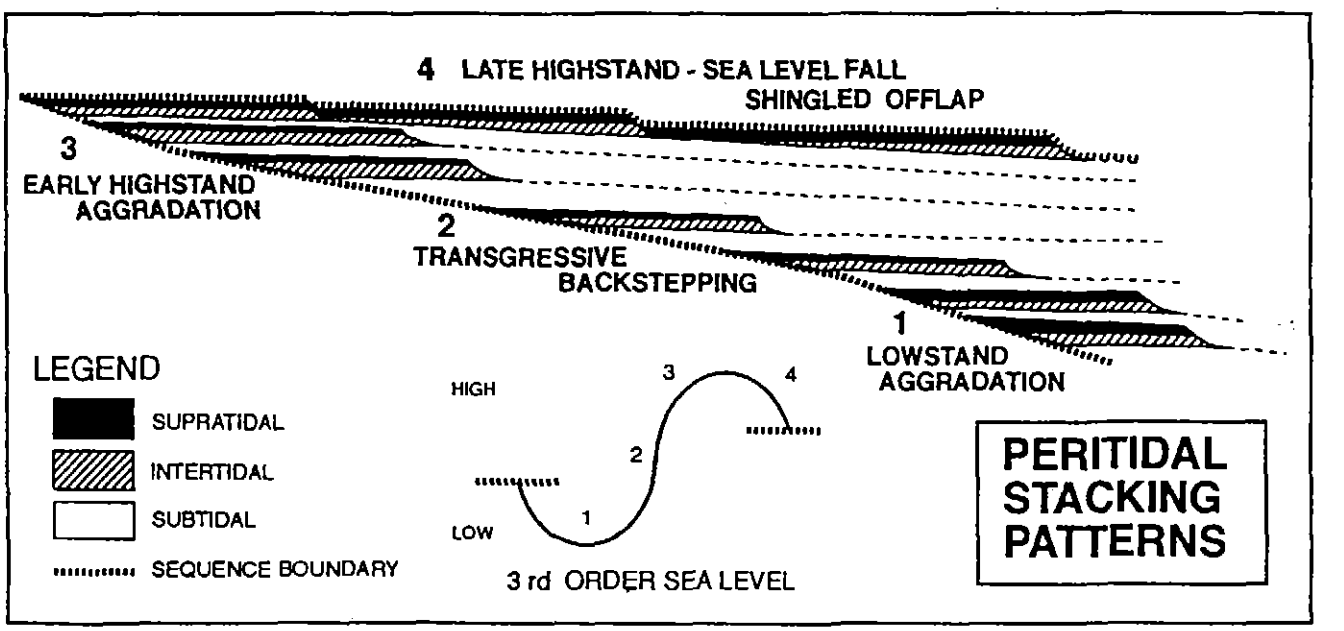

Figure 22 A diagram illustrating the hypothetical stratigraphy of metre-scale, peritidal, successions between two sequence boundaries. Each succession formed by progradation which took place in the window of opportunity produced by short-term fourth- and fifth-order fluctuations in relative sea level during a long-term, third-order rise and fall of sea level. Slow, third-order, sea level-controlled movement of the strandline will dictate where tidal flats develop on the shelf. The balance between sea level changes, sedimentation, and subsidence will dictate how successive tidal flats will stack, backstep or offlap.

These models, as predictors, point to departures from the norm and other irregularities that might have important implications regarding intrinsic or extrinsic controls on deposition. They also provide a framework within which the diagenesis of the sediment can be tracked.

Peritidal carbonates occur repetitively in stratigraphic sequences, often in a seemingly regular, or cyclic, fashion. There is much debate about whether these metre-scale, shallowing-upward successions are platform-wide responses to allogenic forces such as spasmodic subsidence or episodic eustasy, or whether they represent localized tidal flat shorelines and islands shaped by autogenic, i.e., hydrographic, controls. Sedimentologists have their work cut out for them by these models; we are now charged with the job of deciding, if possible, which one best explains our own successions, or if a new approach is necessary. It is an exciting field of research, one that weds careful and precise field observations with increasingly sophisticated numerical modelling.

ACKNOWLEDGEMENTS

This article is an outgrowth of several research projects funded by the Natural Sciences and Engineering Research Council of Canada. An early draft of the text was critically read by E.C. Turner.

REFERENCES

Basic sources of information

Bathurst, R.G.C., 1975, Carbonate sediments and their diagenesis: Amsterdam, Elsevier, 658 p.
Still a good summary of several modern examples.

Ginsburg, R.N., ed., 1975, Tidal deposits: a casebook of Recent examples and fossil counterparts: New York, Springer-Verlag, 428 p.
Many examples of both siliciclastic and carbonate tidal deposits.

Goldhammer, R.K., Dunn, P.A. and Hardie, L.A., 1990, Depositional cycles, composite sea-level changes, cycle stacking patterns, and the hierarchy of stratigraphic forcing: Examples from Alpine Triassic platform carbonates: Geological Society of America, Bulletin, v. 102, p. 535-562.
Manipulation of sedimentological data for computer models to show eustatic effects on a shallow platform.

Hardie, L.A., ed., 1977, Sedimentation on the modern carbonate tidal flats of northwest Andros Island, Bahamas: Johns Hopkins University, Studies in Geology 22, 202 p.
Carbonate tidal flat sediments and biology in a humid setting.

Hardie, L.A. and Shinn, E.A., 1986, Carbonate depositional environments, modern and ancient. Part 3: tidal flats: Colorado School of Mines, Quarterly, v. 81, 74 p.
The place to start, a thorough discussion of peritidal carbonate sediments, facies and depositional models.

Koerschner, W.F. and Read, J.F., 1989, Field and modelling studies of Cambrian carbonate cycles, Virginia Appalachians: Journal of Sedimentary Petrology, v. 59, p. 654-687
Lower Paleozoic peritidal facies and manipulation for computer models trying to show controls by eustasy.

Logan, B.W., Hoffman, P. and Gebelein, C.D., 1974, Evolution and diagenesis of Quaternary carbonate sequences, Shark Bay, Western Australia: American Association of Petroleum Geologists, Memoir 22, 358 p.
Carbonate tidal flat sediments, including stromatolites, in a hypersaline setting.

Pratt, B.R. and James, N.P., 1986, The St George Group (Lower Ordovician) of western Newfoundland: tidal flat island model for carbonate sedimentation in shallow epeiric seas: Sedimentology, v. 33, p. 313-343.
Lower Paleozoic facies and outline of autocyclic island model.

Purser, B.H., ed., 1973, The Persian Gulf: Holocene carbonate sedimentation and diagenesis in a shallow epicontinental sea: Heidelberg, Springer-Verlag, 47 p.
Description of carbonate peritidal sediments in an arid setting.

Shinn, E.A., 1983a, Tidal flats, *in* Scholle, P.A., Bebout, D.G. and Moore, C.H., eds., Carbonate depositional environments: American Association of Petroleum Geologists, Memoir 33, p. 171-210.
Read in conjunction with this article; a colour-illustrated, review of carbonate tidal flat sediments and facies.

Tucker, M.E. and Wright, V.P., 1990, Carbonate sedimentology: Oxford, Blackwell, 482 p.
Succinct review of peritidal carbonate sediments, facies and models.

Wilgus, C.K., Hastings, B.S., Posamentier, H.W., Ross, C.A. and Kendall, C.G.St.C., eds., 1988, Sea level changes: an integrated approach: Society of Economic Paleontologists and Mineralogists, Special Publication 42, 407 p.
Collection of papers emphasizing conceptual basis of sequence stratigraphy plus nimerous case studies of sea level change from the geological record.

Other references

Algeo, T.J. and Wilkinson, B.W., 1988, Periodicity of mesoscale Phanerozoic sedimentary cycles and the role of Milankovitch orbital modulation: Journal of Geology, v. 96, p. 313-322.

Anderson, E.J. and Goodwin, P.W., 1990, The significance of metre-scale allocycles in the quest for a fundamental stratigraphic unit: Journal of the Geological Society of London, v. 147, p. 507-518.

Beales, F.W., 1958, Ancient sediments of Bahaman type: American Association of Petroleum Geologists, Bulletin, v. 42, p. 1845-1880.

Belperio, A.P., Gostin, V.A., Cann, J.H. and Murray-Wallace, C.V., 1988, Sediment-organism zonation and the evolution of Holocene tidal sequences in southern Australia, *in* de Boer, P.L., van Gelder, A. and Nio, S. D., eds., Tide-influenced sedimentary environments and facies: Dordrecht, Reidel Publishing Company, p.475-497.

Bertrand-Sarfati, J. and Moussine-Pouchkine, A., 1988, Is cratonic sedimentation consistent with available models? An example from the Upper Proterozoic of the West African craton: Sedimentary Geology, v. 58, p. 255-276.

Bosellini, A. and Hardie, L.A., 1973, Depositional theme of a marginal marine evaporite: Sedimentology, v. 20, p. 5-27.

Bottjer, D.J. and Ausich, W.I., 1986, Phanerozoic development of tiering in soft substrata suspension-feeding communities: Paleobiology, v. 12, p. 400-420.

Bova, J.A. and Read, J.F., 1987, Incipiently drowned facies within a cyclic peritidal ramp sequence, Early Ordovician Chepultepec interval, Virginia Appalachians: Geological Society of America, Bulletin, v. 98, p. 714-727.

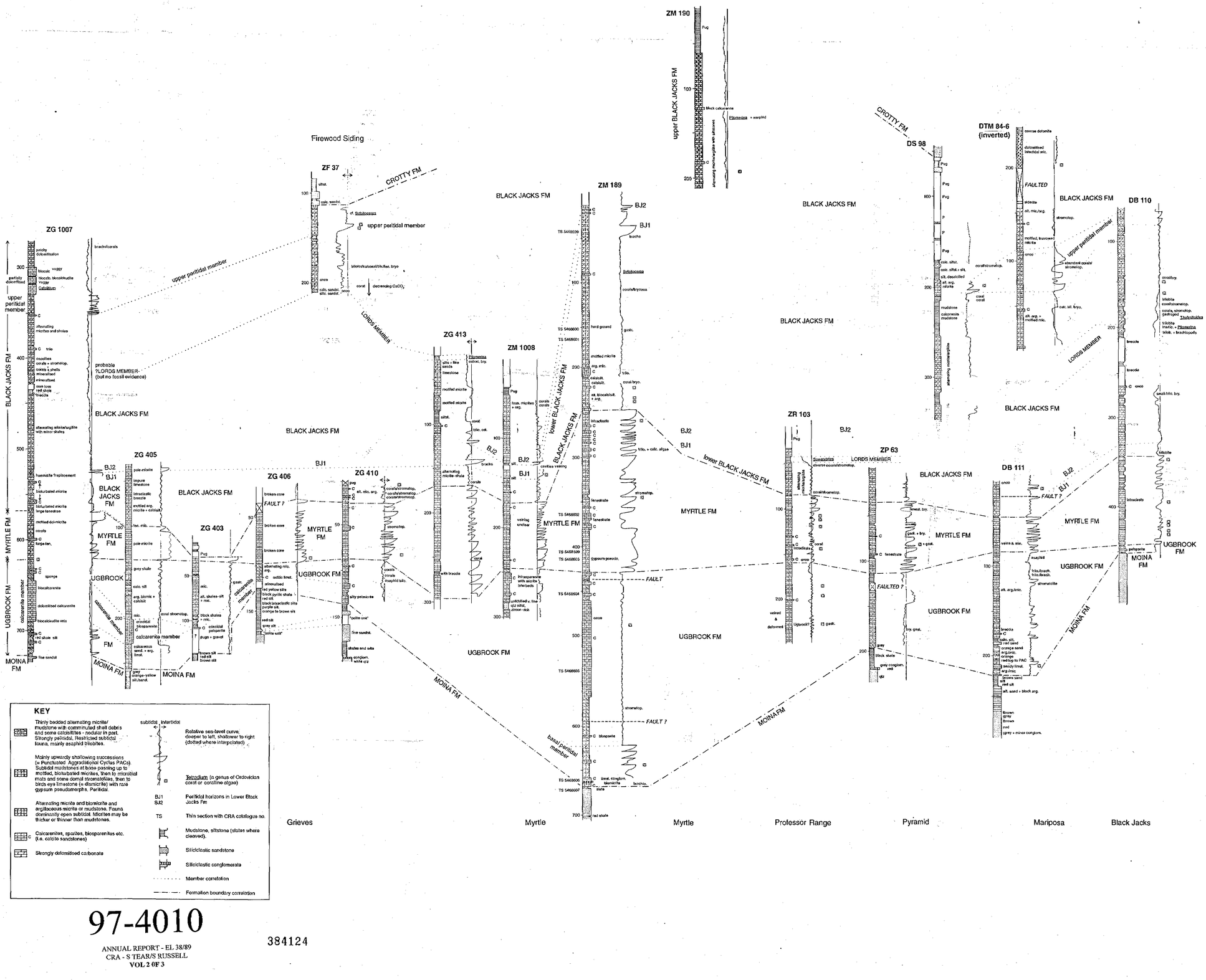

KEY

- Thinly bedded alternating micrite/mudstone with comminuted shell debris and some calcisiltites - nodular in part. Strongly peritidal. Restricted subtidal fauna, mainly esaphid trilobites.
- Mainly upwardly shallowing successions (= Punctuated Aggradational Cycles PACs). Subtidal mudstones at base passing up to mottled, bioturbated micrites, then to microbial mats and some domal stromatolites, then to birds eye limestone (= dismicrite) with rare gypsum pseudomorphs. Peritidal.
- Alternating micrite and biomicrite and argillaceous micrite or mudstone. Fauna dominantly open subtidal. Micrites may be thicker or thinner than mudstones.
- Calcarenites, sparites, biosparenites etc. (i.e. calcite sandstones)
- Strongly dolomitised carbonate

subtidal | intertidal

- Relative sea-level curve, deepen to left, shallower to right (dotted where interpolated)
- Tetradium (a genus of Ordovician coral or coralline algae)
- BJ1 / BJ2 — Peritidal horizons in Lower Black Jacks Fm
- TS — Thin section with CRA catalogue no.
- Mudstone, siltstone (slates where cleaved).
- Siliciclastic sandstone
- Siliciclastic conglomerate
- Member correlation
- Formation boundary correlation

384125

CRA EXPLORATION PTY. LIMITED
ACN 000 057 125

EL 38/89
12 MAY 1997
See folio 85

MICROFILMED
No. 014352-59

Annual Report
For The Period Ending 1 March 1997
EL 38/89 Zeehan No. 4, Tasmania

Volume III of III

Author:	SJ Tear SAJ Russell
Date:	March 1997
Licence Holder:	CRA Exploration Pty. Limited
Submitted to:	Chief Geologist, SE District
Copies to:	Mineral Resources Tasmania CRAE - SE District CRAE - Zeehan CRAE - ETIG Allegiance Mining NL

97-4010

CRAE Report No. 22210

ANNUAL REPORT - EL 38/89
CRA - S TEAR/S RUSSELL
VOL 3 0F 3

Appendix VIII

The Timing and Style of Pb/Zn Mineralisation at Grieves Siding, Western Tasmania

The Timing and Style of Pb-Zn mineralisation at Grieves Siding, Western Tasmania

Darren C. Glover BSc.

Centre for Ore Deposit and Exploration Studies

University of Tasmania

A research thesis submitted in partial fulfilment of the requirements for the degree of Bachelor of Science with Honours

May 1996

Abstract

Base metal mineralisation at Grieves Siding in western Tasmania, is hosted by the 1100m thick Ordovician (Early Caradoc to Ashgill) Gordon Group carbonates. At Grieves Siding the Gordon Group conformably overlies, and interdigitates with, the Ordovician (Llanvirn - Early Caradoc) Moina Sandstone, and is disconformably overlain by the Late Ordovician-Silurian Crotty Quartzite.

Nine lithofacies associations have been recognised in the Gordon Limestone at Grieves Siding, which have been configured into three conformable formations: the Ugbrook, Myrtle, and Black Jacks Formations. The Ugbrook Formation was deposited in protected shallow subtidal to low intertidal waters influenced by a rapidly migrating offshore carbonate bar. The Myrtle Formation was deposited as a tidal flat complex during the mid-Caradoc, recognised by fifteen, 1 to 4 m thick, Punctuated Aggradational Cycles (PACs). Shallow to deep subtidal micrites, argillaceous micrites and biomicrites of the Black Jacks Formation were interrupted during the Late Caradoc by the Lords Siltstone, with further periodic interruptions by peritidal carbonates.

Stratigraphic correlation across 23 diamond drill holes suggests carbonate deposition is related to four main depositional sites on a carbonate platform, developed during an Ordovician marine transgression. Carbonate sedimentation occurred in a tropical environment with a changing Ordovician seawater composition ($\delta^{18}O_{SMOW}$ -6 to -5 ‰, and $\delta^{13}C_{PDB}$ -2.5 to -1.7 ‰), at a temperature of ~25°C. Analogous deposition is seen on the Great Bahama Bank, and in the Persian Gulf.

Mineralisation comprises two stratabound lenses, termed the upper and lower mineralised zones, which contain sphalerite, marcasite and galena within a dolomite-siderite gangue. Sulphide oxidation, dolomite dissolution and remobilisation of HCO_3^- resulted in the precipitation of smithsonite, rhodochrosite and magnesite, with later hemimorphite overprinting other minerals. Significant textural features of the mineralisation include: botryoidal and colloform sphalerite spherules, open-space filling with minor carbonate replacement; possible mineralised bacterial filaments; and evidence for repeated sphalerite dissolution and re-precipitation.

A manganese and barium halo is associated with the lower mineralised zone (LMZ), which also shows a 14 ‰ decrease in $\delta^{13}C_{PDB}$ and a 10 ‰ increase in $\delta^{18}O_{SMOW}$ towards mineralisation. Carbon and oxygen isotopes indicate sedimentary-derived hydrothermal fluids, and wallrock reaction producing decreased carbon and increased oxygen values. A separate H_2CO_3- dominated fluid is indicated for mineralisation of the upper mineralised zone. A wide $\delta^{34}S$ isotopic variation contains high values (31.5 ‰) attributed to Ordovician seawater, whereas lower values (-29.22 ‰) are attributed to bacterial sulphate reduction. Intermediate values around 15 to 22 ‰ represent the hydrothermal fluid composition, consistent with a mixed sulphur source. Lead isotope ratios plot close to the edge of the Cambrian field, and outside (less radiogenic) that attributed to Devonian mineralisation. This implies that the lead source is Late Cambrian, perhaps Ordovician in age. A Late Cambrian source is favoured, with lead and other metals scavenged from underlying Cambrian sediments of the Dundas Group.

A non-magmatic, low temperature (150°C), low salinity (3.5 wt% NaCl), basinal or connate brine, and/or a modified seawater hydrothermal fluid, derived from compaction of Ordovician and Cambrian sediments by the Late Ordovician (Llandovery) Benambran Orogeny, is invoked for Ordovician mineralisation at Grieves Siding in a style consistent with MVT or Irish-type deposits. Remobilisation of Ordovician mineralisation occurred during the Devonian Tabberabberan Orogeny.

Acknowledgements *ii*

There are a number of people I must thank for their help and assistance in making the honours year and my year in Tasmania so rewarding. Most of all I would like to thank all the people of CODES and the Geology Department for being so helpful and approachable. A special thankyou goes to Dr. Paul Kitto for his guidance, motivation and attitude towards this project and its conclusions. Thanks to Clive Burrett for direction and assistance, especially during fieldwork, and thanks also to Dr Prasada Rao for help with sedimentology.

Thanks must also go to Simon Tear, Sandy Menpes and CRA Exploration for lavish logistical support and motivation during the field season. Thanks also to the Department of Tasmanian Development and Resources for much needed financial assistance.

Finally I must acknowledge Dave Cooke for his effort and direction throughout the year, Dr. Garry Davidson, Dr. Tony Crawford, and Peter Wynfield for remodelling some ordinary chapters.

And when it comes time to thank the blokes, I couldn't go past Jonty Maynard, Keen Michael Teen, Jezza, Dougy, CrookMan, Garner and Liam for a memorable and enjoyable year.

Table of Contents

4. MINERALISATION

5. FLUID INCLUSIONS

List of Figures

List of Tables

List of Plates

Plate Set 3.1

Plate 3.1 a : Lithofacies 1. Red beds (R), near the top of a (PAC) sequence. The red bed appears to be oxidised carbonate that formed due to surficial exposure.

Plate 3.1 b : Drill core sample from DDH ZG410 showing an input of red silt into a red bed. Rip up clasts (Rc) and normal grading indicates the sequence is the right way up.

Plate 3.1 c to f : Compositionally zoned dolomites in a red bed of Lithofacies 1. The large zoned crystals occur within finer grained, early diagenetic dolomite. They are interpreted to have formed by mixed marine and meteoric waters.

Plate 3.1 g : Alternating argillaceous limestone and micrite (M) typical of a protected lagoonal environment in the Ugbrook Formation. Small patches of sparry calcite are seen in the micritic material. This sample corresponds to Lithofacies 7.

Plate 3.1 h : Punctuated Agradational Cycle (PAC). The cycle starts at the top of the photomicrograph at (1), in argillaceous subtidal limestone before grading into progressively lighter coloured, high intertidal micrites, dismicrites (D) and algal laminated micrites (AM) before sharply deepening into subtidal argillaceous material near 346 m. A new cycle begins from 346 m to the bottom of the photograph. PACs help define the Myrtle Formation and include Lithofacies 7 and 2.

Plate Set 3.2

Plate 3.2 a : Argillaceous bioturbated calcisiltite of the Ugbrook Formation. Burrows (B) have become elongate with the major cleavage.

Plate 3.2 b : *Tetradium* rich biomicrite in ZM1009

Plate 3.2 c and d: (c) Photomicrograph of *Tetradium sp.* fossils and (d) now replaced with sparry calcite plates.

Plate 3.2 e : Onco-biomicrite of Lithofacies 7. The algal layers of the oncoids (AL) are selectively replaced by dolomite rhombs. Ooids are also found in the sparry calcite matrix

Plate 3.2 f : Biomicrite of Lithofacies 6, containing a brachiopod shell fragment and ooids cemented by a poorly washed calcite matrix

Plate 3.2 g : Dolomitisation of a sparse biomicrite, also showing bituminous films along stylolites

Plate 3.2 h : Massive dolomite of Lithofacies 9 showing compositionally zoned rhombs

Plate Set 3.3

Plate 3.3 a : Oncoid of Lithofacies 5, nucleated around an echinoderm fragment. The concentric algal filaments are assumed to be *Girvanella sp.* Oncoids are deposited in low intertidal to shallow subtidal environments.

Plate 3.3 b : Selectively dolomitised concentric algal layers of an oncoid in a packed onco-biosparite of Lithofacies 3.

Plate 3.3 c : Packed pel-biosparite of Lithofacies 3 containing brachiopods, ooids, and pelloids set in a poorly washed sparry calcite matrix

Plate 3.3 d : Packed biosparite of Lithofacies 3 contains gastropods, corals and elongated ooids (Oo). Opaque material occurs in association with the tectonic stylolites.

Plate 3.3 e : Corraline algae in a micrite of the Ugbrook Formation.

Plate 3.3 f : Pel-bio-oosparites of Lithofacies 3 occurring with a large colonial coral.

Plate 3.3 g and h: Pel-bio-oosparite of Lithofacies 3 in a well washed sparite matrix. Selective dolomitisation of algal ooids occurs. Sparites are associated with the migrating carbonate bar responsible for the calcarenite member.

Plate Set 4.1

Plate 4.1 a : Photomicrograph of the botryoidal, colloform, sphalerite spherules (sp) from the Grieves Prospect.

Plate 4.1 b : Botryoidal, colloform, banded sphalerite from the Grieves Prospect (DDH ZGP1). Pyrite (Py) fills the centre of most spherules, followed by sphalerite (sp) forming the concentric bands. Later stage low Fe sphalerite (sp) infills between spherules.

Plate 4.1 c : Higher magnification view of the botryoidal sphalerite spherules. Early stage pyrite (Py) is overprinted by later spherule growth(sp) producing the dendritic texture.

Plate 4.1 d : Dendritic texture produced by bacteria(?) in sphalerite spherules

Plate 4.1 e : Transmitted light photomicrograph of a sphalerite spherule margin showing dendritic patterns attributed to bacteria(?)

Plate 4.1 f : High magnification photomicrograph of radiating bacteria(?) near the margin of a sphalerite spherule.

Plate 4.1 g : High magnification photomicrograph of the dendritic texture towards the margin of a sphalerite spherule.

Plate 4.1 h : SEM image of bacterial filaments responsible for producing the dendritic textures seen in previous plates. The particles have now been replaced by up to 8 μm sphalerite grains.

Plate Set 4.2

Plate 4.2 a : Euhedral pyrite (Py) showing growth zoning. Later spongy pyrite has filled out into the cavity. Later phase galena (Gn) filled a cavity within pyrite forming cusp and caries textures.

Plate 4.2 b : Fracture and cavity filling pyrite (Py) in dolomite of the Lower Black Jack Formation. Later sphalerite (sp) replaces pyrite.

Plate 4.2 c : Mineralised Ugbrook Formation dolomite showing early pyrite (Py), overprinted by galena (Gn) which forms cusp and caries grain boundaries with both pyrite and later stage sphalerite spherules (sp). Calcite represents the latest stage in the cavity.

Plate 4.2 d : Paragenetic relationships between the first phase pyrite (Py), then galena (Gn) and latest phase sphalerite spherules (sp).

Plate 4.2 e : Quartz-carbonate pressure shadow between pyrite (Py) crystals.

Plate 4.2 f : Higher magnification view of quartz-carbonate pressure shadows between pyrite crystals.

Plate Set 4.3

Plate 4.3 a : Drill core sample from DDH ZG1012 showing a large vug in dolomite of the Lower Black Jack Formation filled by siderite, sphalerite-galena and calcite. The nature of settling of sediment in the bottom of the cavity gives suggests the beds are the right way up.

Plate 4.3 b : Photo of the cavity wall of Plate 4.3a, showing the dolomite wallrock being coated with large euhedral siderite (sid) crystals forming a comb texture. Minor mineralisation (sphalerite and galena) lines the dogtooth siderite terminations. Coarse calcite plates (cal) line the cavity.

Plate 4.3 c, d, e, f, g : High magnification photomicrographs of sphalerite spherules (sp) coating dogtooth siderite crystals and replacing earlier formed galena (Gn). Paragenesis of the spherules involves a fine grained massive sphalerite (sp) first coating the siderite, followed by galena (Gn). Later sphalerite spherules (sp) replace the earlier sphalerite and galena.

Plate Set 4.4

Plate 4.4 a : Angular dolomitised (dol) clasts in a calcite matrix (cal). This angular breccia is a similar lithology to the host rocks of the Oceana deposit.

Plate 4.4 b : Selective silicification of the calcite matrix and the establishment of a cockade texture around dolomite clasts.

Plate 4.4 c and d: Selective silicification (qtz) of the once calcite matrix, producing a classic cockade texture around dolomite clasts (dol).

Plate 4.4 e : Pyrite (Py) comb texture defining the edges of a cavity that has been replaced by radiating hemimorphite (Hm). Hemimorphite replaces the wall-rock and the cavity

Plate 4.4 f and g: Radiating hemimorphite (Hm) nucleating on remnant wall-rock forming a cockade texture.

Plate 4.4 h : Hemimorphite (Hm) veins cross cutting earlier veins and earlier formed hemimorphite.

Plate 5.1

Plate 5.1 a : Photomicrograph of secondary fluid inclusions hosted in Low-Fe sphalerite. Type I inclusions are the large rectangular shaped inclusions occurring in healed fractures. Type II are more isolated, irregular shaped inclusions (DDH ZGP2, transmitted light, field of view ≈ 0.25mm)

Plate 5.1 b : Secondary fluid inclusions occurring in a healed fracture (Type I). The large irregular shaped inclusion (II) is a type II inclusion (DDH ZGP2, transmitted light, field of view ≈ 0.25mm).

Introduction 1

Minor mineralisation at Grieves Siding has made it the target of three separate exploration programs designed to investigate the lead-zinc potential of the Gordon Group limestone south of Zeehan. Exploration elsewhere has uncovered mineralisation previously attributed to Devonian granitoid emplacement; however, recent studies on the southern Oceana deposit, (Taylor and Mathison 1990), 8 km north of Grieves Siding, suggest an older metal source. Emerging evidence indicates the Zeehan Mineral Field may contain Precambrian to Cambrian, as well as Devonian metals. This thesis examines sedimentological and geochemical controls on mineralisation at Grieves Siding in an attempt to outline implications for its timing and style(s).

1.1 AIMS AND PURPOSE

This investigation was undertaken to determine the stratigraphy and diagenetic history of the Ordovician Gordon Group at Grieves Siding, in an effort to delineate horizons most susceptible to mineralisation, and develop a genetic model. Determination of the timing and style of existing mineralisation will assist the formulation of a genetic model and help define exploration targets. Grieves Siding is of particular interest because it possesses both a complete Gordon Group stratigraphy of the Zeehan area, and hosts a small lead-silver prospect, worked during the late 1800's (Fig. 1.1).

1.2 LOCATION AND ACCESS

Grieves Siding is situated in western Tasmania 14.5 km south-southeast of Zeehan, and approximately 23 kms north-northeast of Strahan. The study area covers approximately 15 km^2, centred about 364500,534900 AMG (50); (Fig. 1.1).

Access is provided by the sealed Henty Road (Fig. 1.1), formally the Zeehan-Strahan tramway of the late 1800's, hence Grieves (Rail) Siding. A gravel road provides access from the Henty Road to a disused sandstone quarry used in construction of the Henty Road. An abandoned tramway provides access to the old prospect workings at Grieves Siding.

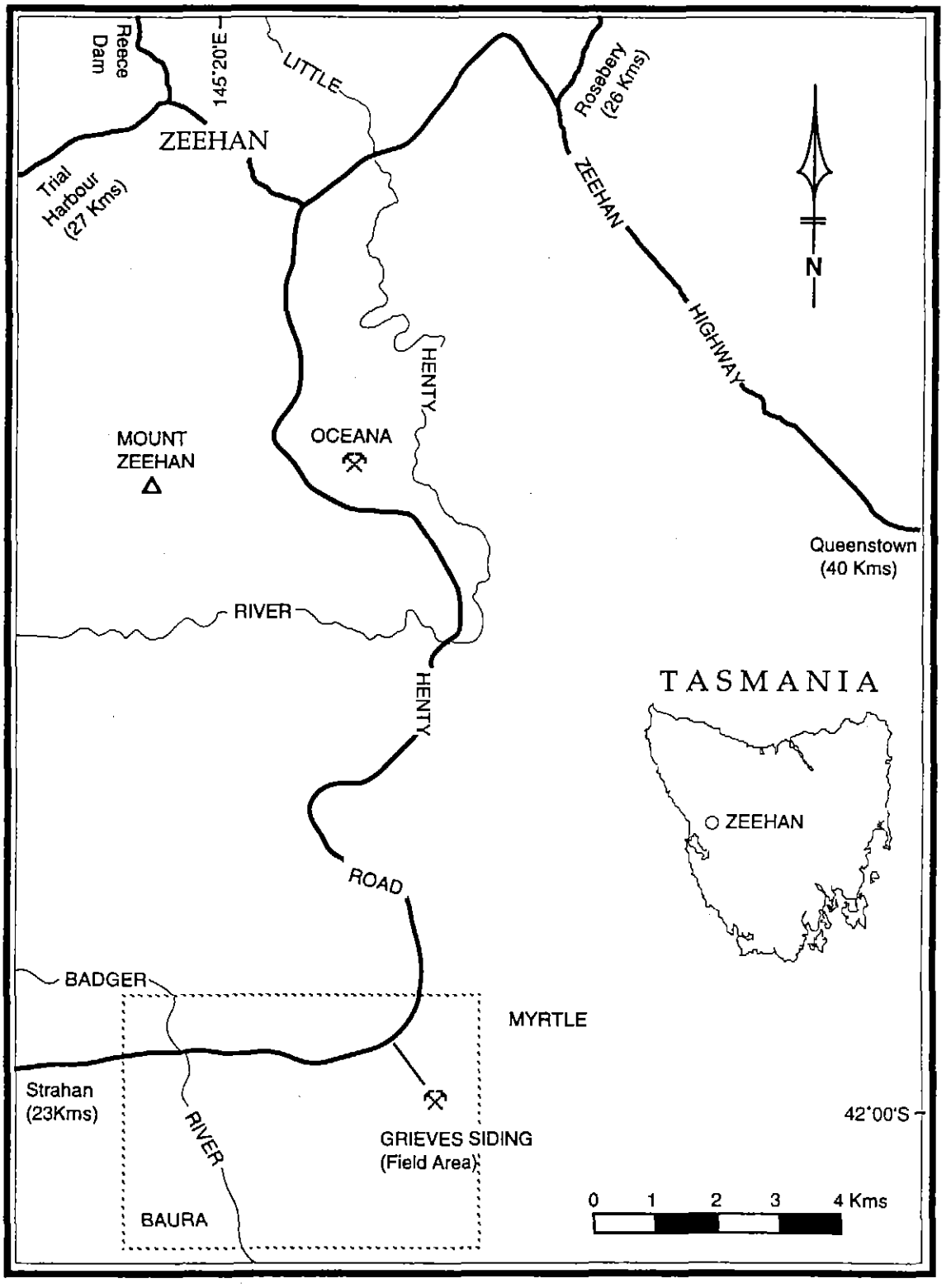

Figure 1.1: Locality of Grieves Siding and surrounding areas. Note the proximity of the Oceana prospect which has been inferred to be an Irish type deposit.

5 cm

1.3 METHODS

Detailed mapping of the area has previously been undertaken by Blissett (1962) and Electrolytic Zinc Co. (E.Z.) geologists in 1985. Consequently, only limited detail, 1:5000 scale surface mapping was undertaken for this thesis (Fig. 1.2). The majority of field work was spent logging thirty six diamond drill holes (combined total length ~ 4500m), (Appendix 1). Ten holes were drilled by CRA Exploration between 1994-5, with the remaining 26 holes drilled by E.Z. between 1984 and 1986. A detailed sedimentological study was undertaken on drill core, and twenty two stratigraphic sections have been compiled (Fig. 3.1 a & b).

Petrographic and geochemical samples were obtained from drill core, outcrop, costeans and the old prospect at Grieves Siding. Thin sections and polished thin sections were made for petrographic, and microscopy studies. Carbon and oxygen stable isotope analysis have been undertaken on carbonate and siderite associated with mineralisation, and systematically sampled within DDH ZG 406. Conventional sulphur isotope studies have also been conducted on pyrite, marcasite, galena and sphalerite, with lead isotope analysis obtained from galena and pyrite. Fluid inclusion studies were undertaken on sphalerite found in a sample from the Grieves prospect, and Scanning Electron Micrographs (SEM) were taken of this same specimen. X-ray diffraction (XRD) has been undertaken on many samples, together with as EM analysis.

1.4 PHYSIOGRAPHY

The topography of the area ranges from gently undulating lowlands, to extremely steep escarpments and plateaus of the Permian 'Henty surface'. Areas underlain by limestone form topographic lows reflecting rapid weathering and decomposition in the wet temperate climate. The limestone decomposes to a decalcified blue/black clay locally known as "pug." Relief in the south-east and north-west is provided by resistant sandstone and quartzite ridges, which rise sharply from contacts with the limestone to form prominent 200 m high plateaus.

Small tributaries of the Badger River drain the immediate Grieves area and join the Badger River proper in the south-west as it drains the swampy buttongrass flats (Fig. 1.1). Zeehan receives 2640 mm of annual average rainfall, most falling between May and September with an average of 23 rainy days per month during that period.

Sedgelands and wet scrub characterise the vegetation at Grieves Siding. The Launceston Field Naturalists Club (1981) suggests that sedgelands occur where heath, scrub and forest has been repeatedly burnt, or on poor peaty, acid soils where the water table is high. Both scenarios exist at Grieves Siding. The marshy sedgelands underlain by limestone are dominated by buttongrass (*Gymnoschoeus sphaerocephalus*) but also host the waratah (*Telopea truncata*) and the pink swamp heath (*Sprengelia incarnata*). The marshy plains provide habitat for freshwater crayfish or yabbies which build elevated mounds up to 35 cm high out of 'pug'. The elevated sandstone and quartzite ridges host a diverse flora encompassing species of *Leptospermum* (tea-tree) including the manuka tea-tree (*Leptospermum scoparium*), species of *Casuarina*, and many other heathland/forest species. Much of the quartzite strata hosts treed and significant understory vegetation which is, however, restricted to pockets within the sandstone units. The dominant eucalypt species is the Smithton Peppermint (*Eucalyptus nitida*). The area has been burned for thousands of years which has served to keep the swampy buttongrass plains open.

1.5 PREVIOUS LITERATURE

1.5.1 Gordon Limestone

Early geological investigations of the region included the reconnaissance work of Strzelecki in 1845, in which he first described the Gordon Limestone. Numerous workers have since studied the stratigraphy and palaeontology of the Gordon Group Limestones. Gill and Banks (1950) described argillaceous, arenaceous, and carbonaceous impurities in the limestone of the Zeehan area. Hill (1955) described Ordovician corals in the limestone, and Banks (1957) reiterated observations of impurities within the limestone of the Zeehan area. Pitt (1962) mapped the Zeehan area in detail, which contributed to the Zeehan 1 mile series map and Geological Survey Explanatory report of Blissett (1962).

The Gordon Limestone was defined as a formation by Banks (1962), and further work by Corbett and Banks (1974) resulted in the limestone being given sub-group status. Burrett (1978) undertook detailed palaeontological work on the limestone and defined a number of conodont assemblages. Subsequently a preliminary biostratigraphy of Ordovician rocks in Tasmania was published by Burrett and Banks (1980). This was amplified by further publications concerning faunal and

lithological successions in the Gordon Group, (Banks et al., 1981; Burrett et al., 1981; Burrett et al., 1984). Work by Burrett et al. (1984) elevated the subgroup to Group status. The Gordon Limestone presently forms part of the Wurawina Supergroup which comprises litho-biostratigraphic correlates throughout the Dundas Trough including the Moina Sandstone and the Crotty Quartzite. Ellis (1984) studied the palaeoenvironments and mineralisation in the Gordon Limestone at Grieves Siding, Myrtle and Oceana prospects; and Rice (1985) examined the environment of deposition and diagenesis of the Gordon Group of the Zeehan area. Considerable information about the entire Gordon Group sequence is complied in the publication "Geology and Mineral Resources of Tasmania" edited by Burrett and Martin (1989).

1.5.2 Zeehan Mineral Field

After the discovery of the Zeehan Mineral Field by Frank Long in 1882, early investigations were undertaken by Montgomery (1891 and 1893) and were published as progress reports presented to the Tasmanian Parliament. Within ten years of discovery, Zeehan "The Silver City of the West" had become the second largest centre in Tasmania, with a population of nearly ten thousand people. Twelvetrees and Ward (1910) produced a further progress report describing the orebodies of the Zeehan mineral field, with further reports and publications being produced as the Zeehan area became heavily worked between the late 1800's and early 1900's. Williams (1968), and Both and Williams (1968) examined hydrothermal zonation of lead-zinc ore deposits around the Heemskirk Granite, and Both et al. (1969), Groves and Loftus-Hills (1968) and Williams (1974) studied the composition of sphalerites from the lead-zinc deposits of the Zeehan area. Ellis (1984) studied mineralisation at the Oceana prospect, which lead to further work by Taylor and Mathison in (1990) and most recently, Peace (1995) studying the origin of the Oceana lead zinc deposit.

Regional Geology and Mineralisation

2

2.1 INTRODUCTION

At Grieves Siding, the Wurawina Supergroup, which contains the Denison Group siliciclastics, the Gordon Group Limestone, and the fine siliciclastics of the Eldon Group, forms a concordant sequence of predominantly shelf-deposited sediment ranging in age from middle-Late Cambrian to Early Devonian (Banks, 1989). These rocks form the upper portion of the Lower Palaeozoic Dundas Trough sequence, which records the marine sedimentary and tectonic evolution of the early Tasman Fold Belt. A late Ordovician deformation correlating with the Benambran Orogeny, preceded the Middle Devonian Tabberabberan Orogeny. Tabberabberan deformation resulted in low grade metamorphism of the Wurawina Supergroup, and regional-scale open folding with north-northwest trending fold axes and associated steep reverse faulting (Berry, 1992). Deformation preceded the intrusion of Devonian granitoids and associated mineralisation between 367 and 332 Ma (Berry, 1992). This chapter is intended as a brief review of the tectonic history, regional geology, and mineralisation of the Zeehan Mineral Field.

2.2 REGIONAL GEOLOGY

Passive rifting of continental crust in the Late Precambrian - Early Cambrian produced a thin continental margin transected by rift basins along the modern day Tasmanian west coast (Crawford and Berry, 1992). Early-Middle Cambrian subduction produced an oceanic arc, east of the passive margin, which by the Middle Cambrian (520 - 525 Ma) underwent arc-continent collision. Subsequent ophiolite emplacement resulted in a downwarping of the foreland, and combined with extension of the Precambrian crust, was responsible for the mid-Middle Cambrian formation of the Dundas Trough (Crawford and Berry, 1992). Crawford and Berry (1992) show Dundas Trough formation during the development of the north-west Tasmanian Terrane (Fig. 2.1).

The Dundas Trough is a northerly trending, 20 - 30 km wide mid-Middle Cambrian trough flanked by the Precambrian Rocky Cape and Tyennan Regions (Corbett, 1989). A schematic map of the Tasmanian terranes (Fig. 2.2) shows the position of the Rocky Cape and the Tyennan Regions relative to the Dundas Trough. Basal Dundas Trough sediments consist of 3500 m of conglomeratic flysch sequences (Jago and Brown, 1989) with ultramafic detritus derived Cambrian volcanics. The Middle to Late Cambrian Mt. Read Volcanics form the eastern-most part of the Dundas Trough, and interfinger westward within the Dundas Trough sequences (Fig. 2.1). This 10 - 15 km wide belt consists of interbedded, subaerial to subaqueous, felsic, intermediate and mafic volcanics (Corbett, 1989) which host a number of world class polymetallic volcanogenic massive sulphide deposits (Mt. Lyell, Rosebery, Hellyer, Hercules, Que River). These deposits are believed to have formed on, or below the sea floor during volcanism, and some appear to be associated with prior changes from subaerial to submarine environments (Corbett and Solomon, 1989).

Cessation of volcanism and uplift in the Tyennan Region in the mid-Late Cambrian - Early Ordovician resulted in rapid deposition of up to 2000 m of Precambrian-derived coarse siliciclastic sediments into the Dundas Trough (Brown, 1989). These sediments belonging to the Denison Group, unconformably overlie the Dundas Group and the Mt. Read Volcanics. The Owen Conglomerate and correlates (including the Mt. Zeehan Conglomerate), basal member of the Denison Group, consists of siliceous siliciclastics, shallow marine to fluvial, pebble to boulder conglomerate and quartz sandstone (Banks, 1989). Thickness and grainsize variations suggest deposition as a series of continental alluvial fans formed as piedmont deposits around the margins of the uplifted Tyennan block in fault-controlled graben structures (Corbett and Turner, 1989). Crawford and Berry (1992) estimate that less than 20 Ma elapsed from the time of arc-continent collision, trough formation, volcanism, and the cessation of sedimentation. The termination of sedimentation correlates with the Cambro-Ordovician Delamarian Orogeny. The presence of worm castings, burrows, brachiopods, and gastropods in the Upper Owen suggests a transgression to a marine environment in the Late Cambrian-Early Ordovician (Banks, 1989).

In the Zeehan area, the Owen Conglomerate correlate is known as the Mt. Zeehan Conglomerate (Blissett, 1962) and reaches a maximum thickness of 450 m.

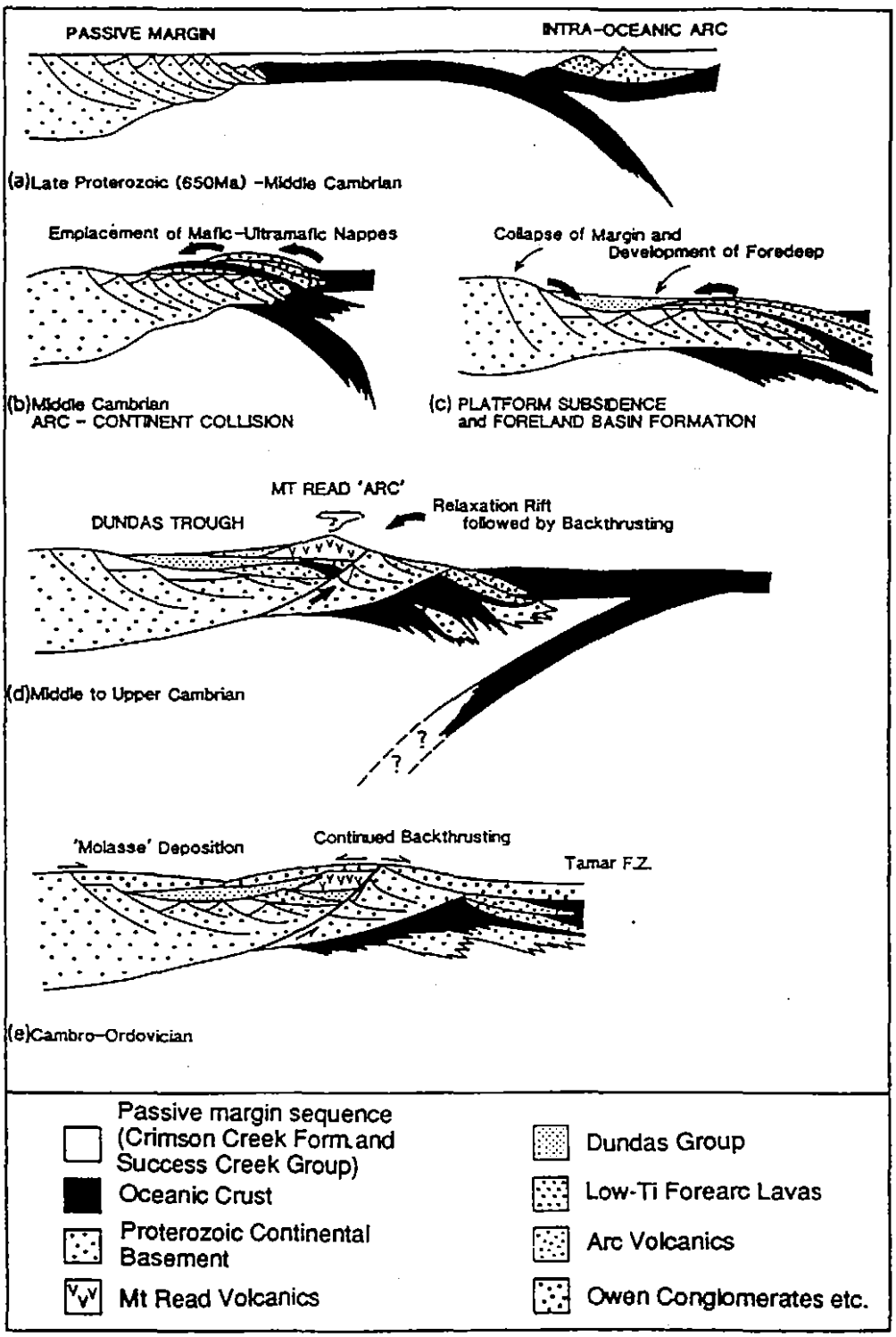

Figure 2.1: Stages in the development of the N-W terrane, including the mid-Middle Cambrian formation of the Dundas Trough (from Crawford and Berry, 1992).

Southwest of Mt. Zeehan, the conglomerate is conformable with the underlying Dundas Group, and ripple marks and palaeocurrent directions indicate south flowing currents (Pitt, 1962). The Mt. Zeehan Conglomerate is thought to have been deposited via a large alluvial fan in a depositional trough in the Zeehan - Professor Range area (Blissett, 1962).

The Owen Conglomerate and correlates are overlain by 10 - 20 m of well-sorted siliceous sandstone of the Pioneer Beds and correlates (Banks, 1989). The Early Ordovician Pioneer Beds are the upper units of the Denison Group and were deposited during a period of quiescence and shallow water sedimentation that lasted from the Ordovician to the Middle Devonian (Banks, 1989). They consist of interbedded sandstone and siltstone units with some conglomeratic beds, and show cross-bedding, ripple markings and bioturbation. Banks (1989) suggests a littoral to sub-littoral marine depositional environment for the Pioneer beds. In the Zeehan area this sandstone unit has been mapped as the Moina Sandstone (Blissett, 1962). Thickness variations in the Zeehan area of approximately 100 m/km from Mt. Zeehan to Professor Range suggests very rapid downwarping or down-faulting contemporaneous with deposition (Banks, 1989).

Conformably overlying and or interdigitating with the Pioneer Beds (and thus the Denison Group) is the Ordovician to Silurian Gordon Group carbonates. The Gordon Limestone was first described by Strzelecki (1845) and consists of a sequence of transgressive shallow marine, ramp-deposited interbedded limestones and dolomitized limestones with minor siliciclastics (Banks and Burrett, 1989). The Gordon Group has a measured thickness of up to 2.0 km and is distributed widely in western Tasmania, west of 147°E (Banks and Burrett, 1989). It is the thickest and most stratigraphically continuous Ordovician (Arenig to Ashgill) sequence in the southern hemisphere (Banks and Burrett, 1979; Banks and Baillie, 1989; Rao, 1990). Deep to medium subtidal limestones form the basal Gordon Group, which are followed by upward shallowing limestones that show cyclicity (punctuated aggradational cycles PACs). Carbonate deposition was relatively rapid, with the dominant carbonate type being micrite (Calver, 1989). The sequence is interrupted by a thin silt layer (Lords Siltstone and correlates) deposited in the Caradoc (Late Ordovician), which is regionally traceable over much of the Tasmanian west coast (Burrett, 1995). The Gordon Group, in places, is richly fossiliferous with the biota present indicating warm, clean, shallow water deposition (Banks and Burrett, 1989). Syngenetic Pb-Zn mineralisation has been

recognised in several places near the northwest and western margins of limestone deposition (Banks, 1989).

The Gordon Group is overlain conformably or disconformably by the shallow marine clastic sequence of the Eldon Group. The disconformity correlates temporally with the Benambran orogeny. The Eldon Group is a Silurian to Early Devonian sequence that contains interbedded quartz sandstone and mudstone with subordinate limestone (Baillie, 1989) and is at least 2.3 km thick.

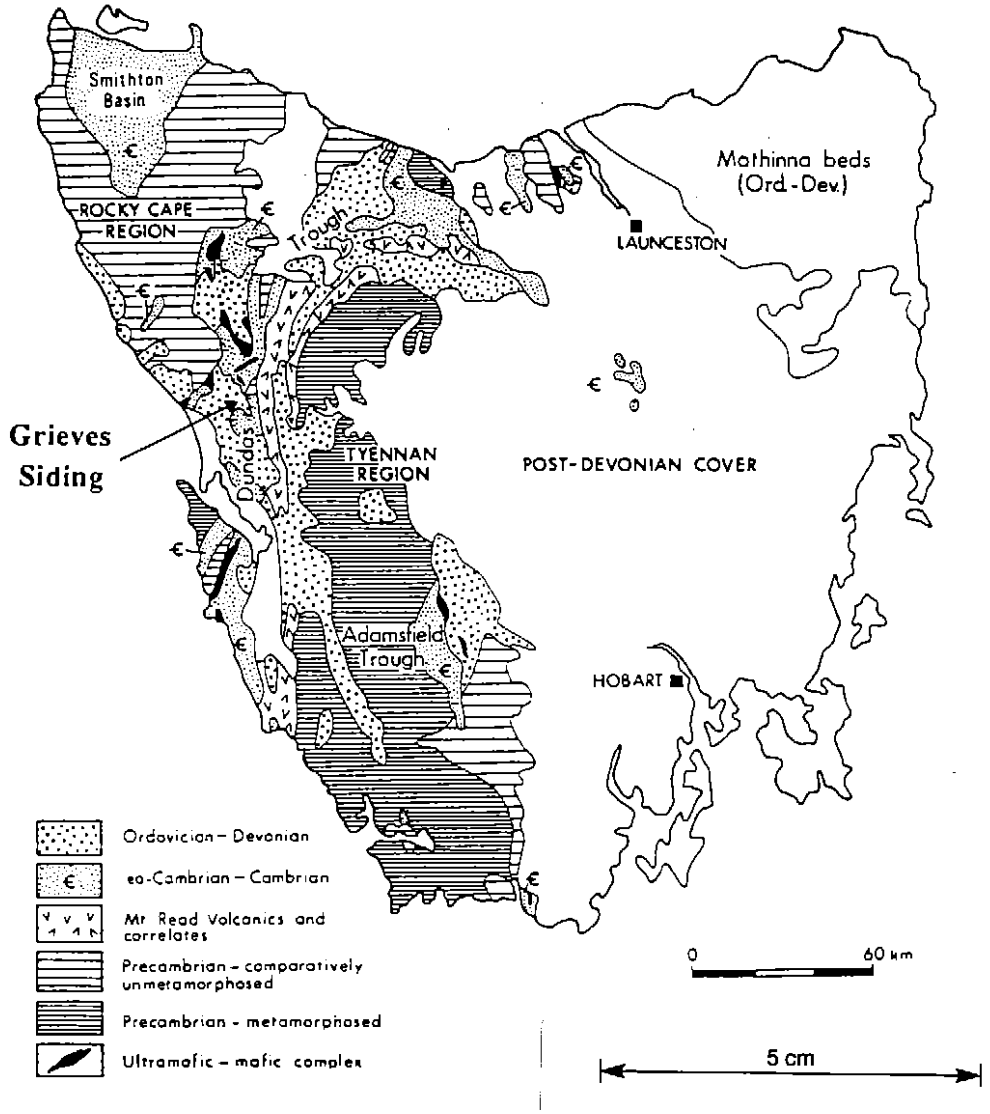

Figure 2.2: Schematic geological map of Tasmania, showing Precambrian and Lower Paleozoic strato-tectonic units in the western Tasmanian terrane (modified from Brown, 1989).

The Eldon Group was formally defined in the Zeehan area where it comprises the following formations (Baillie, 1989):

Bell Shale	420 m (top)
Florence Quartzite	490 m
Keel Quartzite	120 m
Amber Slate	240 m
Crotty Quartzite	490 m

The Eldon Group and correlates are the top sequences of the Wurawina Supergroup of which sedimentation was interrupted by mid-Devonian deformation.

Berry (1992) has argued that the Cambro-Ordovician Delamarian Orogeny caused the cessation of rapid sedimentation of upper Dundas Trough sediments. A period of quiescence and shallow water sedimentation followed from the Ordovician to Middle Devonian times. Two main stages of Devonian deformation are recognised in the Wurawina Supergroup. A Middle Early Devonian deformation resulted in low grade metamorphism (Burrett, 1984). The Middle Devonian Tabberabberan Orogeny produced regional north-northwest trending open folds with steep reverse faults, and later wrench reactivation (Berry, 1989). Devonian granitoids intruded the sequences between 332 and 367 Ma during and after northeast-southwest compression (Berry, 1989). Intrusive lamprophyre dykes which intruded some sequences are thought to be Devonian or younger in age (Reid, 1975).

The Tabberabberan Orogeny was followed by a period of quiescence with minor terrestrial and shallow marine sedimentation. Permian glaciation and associated tillites, together with glaciomarine sequences proceeded Jurassic dolerite intrusions related to Mesozoic wrench faults (Berry, 1992). A widespread unconformity representing a pre-Permian landscape, known as the Henty surface, occurs in the West Coast Range (Colhoun, 1989). Mesozoic and Cenozoic structures are related to the breakup of Gondwana, and were followed by Tertiary basaltic activity. Further glaciation in the Pleistocene added to the modern day topography, otherwise Holocene alluvial deposits can be found on the modern day surface.

2.3 *MINERALISATION*

Low grade sub-economic Pb-Zn-Ag mineralisation is known in three stratigraphic positions (top, middle and bottom) within the Gordon Group sequence (Taylor, 1989). Small quantities of galena have been found in a number of places and significant Pb-Zn-Ag mineralisation occurs at Bub's Hill, and in the Zeehan Mineral Field. Several deposits in the Zeehan Field are large enough to have supported mining operations (Both and Williams, 1968). The following section is a summary of a review of mineralisation in the Gordon Group by Taylor (1989).

Mineralisation at Bub's Hill in western Tasmania occurs in three distinct 2 - 3 m thick, variably dolomitised horizons in the upper part of the Gordon Group sequence. It comprises sphalerite with subordinate galena, barite and dolomite in open space fillings of veinlets, cavities, and intraclastic areas of tectonic breccias. It is suggested that the mineralisation represents a Mississippi Valley style deposit; however, as it is located in the Franklin-Gordon World Heritage listed reserve no resource data has been accumulated.

A number of deposits in the Gordon Group of the Zeehan area, notably Mariposa, Montagu, Despatch, Tasmanian Crown and Austral, were mined for Pb-Ag during the 1890's (Table 2.1). These deposits are predominantly open space in-fillings of veins, cavities, lithological contacts, and tectonic and hydraulic breccias. The mineralising fluids are thought to be derived from the Heemskirk Granite, emplaced at the end of the Devonian Tabberabberan Orogeny. Production in the Zeehan mineral field according to Both et al., (1969) was 200 000 tons of lead, 2700 tons of zinc and 27 000 000 oz (839.8t) of silver.

The most significant and interesting deposit in the Gordon Group sequence is the Oceana deposit, located 3 km south of Zeehan. This prospect was initially mined in 1890 with further intermittent attention up until 1925. In the late 1940's a North Broken Hill / Broken Hill South joint venture rehabilitated the mine and from 1954 to its closure in 1960, Oceana produced 130 843 tons at 11.6% Pb and 14.66 g/t Ag (Taylor, 1989). Renewed exploration in the vicinity of the Oceana workings by Amoco Minerals between 1978 and 1983 defined a resource of 4 million tons at 2% Pb, 8% Zn, and 80 g/t Ag. The mineralisation was defined in two separate areas which were characterised by different styles.

Table 2.1: Characteristics and production from some deposits of the Zeehan Mineral Field hosted in Gordon Group carbonates (after Blissett, 1962; and Taylor,1989).

DEPOSIT	MINERALISATION	PRODUCTION
Tasmanian Crown	Fissure fillings of low grade galena and sphalerite with a siderite gangue.	15 737 ozs Ag 113.34 ton Pb
Austral Valley	Hosted in faulted grits and quartz conglomerates of Moina Sandstone overlain by silicified Gordon Limestone, associated with a ferro - manganiferous gossan.	863 ton of galena (800t Pb) 100 ton of sphalerite (50t Zn) 9 ton of pyrite 33 000 ozs Ag
Despatch	no recorded production	
Montague	Three parallel veins of galena with other smaller veins.	230 ton of galena (115 ton Pb) 1500 ozs Ag
Mariposa	Westerly dipping fissure lodes striking NNW near the contact with the Crotty Quartzite.	Galena ore contained 33-65% Pb 12 to 26 ozs Ag/t

In an area north of the Oceana Fault the mineralisation occurs as massive lenses of generally coarse galena, sphalerite, and siderite with traces of pyrite and chalcopyrite in open space in-fillings of veins, cavities and intraclastic areas of tectonic and hydraulic breccias (Taylor, 1989). The mineralisation is grossly disconcordant with the host rocks, which consist of grey silicified dolomitised limestone.

South of the Oceana Fault the mineralisation comprises two separate stratiform horizons (Fig. 2.3) which strike northwest and dip northeast, conformably with the host sediments (Taylor, 1989). Semi-massive beds of typically fine-grained galena, sphalerite and siderite are found in a distinctive 30 m thick limestone breccia (Taylor and Mathison, 1990). The breccia comprises a chaotic accumulation

of angular to sub-rounded, dolomitised limestone and fossil fragments set either in a matrix or a clast-supported fashion in a fine-grained carbonate mud (Taylor, 1989). They have been interpreted as submarine debris flow breccias caused by gravity slides triggered by periodic movement of the Oceana Fault during carbonate deposition (Taylor, 1989).

The southern mineralisation differs from the northern zone in having a lower Pb/Zn ratio, a lower Cu content, only patchy weak dolomitisation, and possessing textures indicating carbonate replacement rather than open space filling (Taylor, 1989). The carbonate replacement textures and conformable stratiform nature of the southern mineralisation, casts doubt on the previously accepted genetic model proposed for the Oceana mineralisation. This model invoked mineral deposition in structurally controlled fissure veins from mineralising fluids evolved from the Heemskirk Granite at the end of the Devonian Tabberabberan Orogeny. Alternatively, the deposit is now regarded as a variant of the sedimentary exhalative class, possibly Irish-type. The stratiform mineralised layers are therefore interpreted as syndiagenetic replacements of sub-seafloor shallow water carbonate muds prior to lithification.

This is supported by the occurrence of the submarine debris flow breccias associated with the mineralisation. Taylor (1989) suggested that the mineralisation, tectonic setting and host lithologies resemble parts of the Irish type sedimentary exhalative deposits at Silvermines and Navan. Lead isotope determinations from the Oceana southern zone undertaken by Ellis (1984) indicate Oceana Pb is less radiogenic than Pb from Devonian granite-related mineralisation, and suggest, an Ordovician age for the southern zone mineralisation. Ellis (1984) suggested a Precambrian to Cambrian source for Oceana metals. This supports the Irish-type origin for the southern mineralisation (Fig. 2.3).

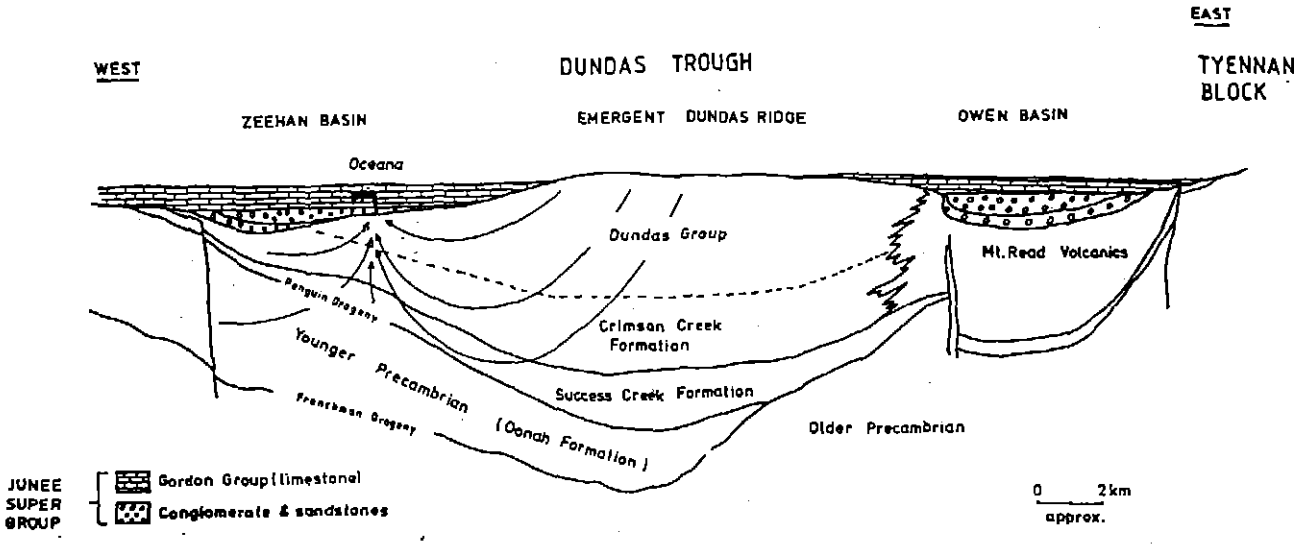

Figure 2.3: One of the genetic models proposed by Ellis (1984) for the development of the Oceana mineralisation. The time period is post Gordon Group (ie. Cincinnatian) and pre-Tabberabberan (ie. Early Devonian). Arrows indicate possible movement patterns for basinal fluids.

2.4 *DISCUSSION*

The western Tasmanian terrane has evolved into a very complex package. The combination of Precambrian passive rifting, Early to Mid Cambrian subduction, Middle Cambrian arc-continent collision, ophiolite emplacement, deformation, and extension leading to the formation of the Dundas Trough contributed to this complexity. The Gordon Group is part of the Wurawina Supergroup, a concordant sequence of middle-Late Cambrian to Early Devonian, predominantly shelf deposited sediments. Devonian (Tabberabberan) deformation and the intrusion of Devonian granitoids served to mobilise fluids responsible for much of the significant mineralisation in the Dundas Trough. Earlier mineralisation, not attributed to these fluids, may occur in the Zeehan field (Taylor and Mathison, 1990). The sedimentology and geochemistry of a small part of the Gordon Group may well confirm the existence of this earlier phase of mineralisation.

Local Geology, Stratigraphy and Basin Analysis

3

3.1 INTRODUCTION

Nine lithofacies associations have been constructed from detailed sedimentological analysis of Gordon Group Limestones at Grieves Siding. Carbonate sedimentation is related to four main depositional sites on a mini-platform which developed during an Early to Mid-Ordovician transgression. Lithostratigraphic units have been established to define these environments and their products. Lithofacies are documented in this chapter in order to assign them to lithostratigraphic units and examine their depositional environments.

3.2 METHODOLOGY

Diamond drill core was sampled for the detailed sedimentological analysis and complimented with outcrop and costean samples (Fig. 1.2). Additional material was also collected from the Grieves Prospect.

Selected samples were split and either thin sectioned or polished for detailed analysis. Thin sections were stained with potassium ferricyanide using an adaptation of Dickson's (1965) method. Staining allows the distinction between calcite, dolomite and ferroan calcite to be made with confidence. Thirty eight thin sections were studied.

The results of handspecimen and thin section analysis is summarised into nine lithofacies (Table 3.1 and 3.2) to allow easy interpretation and recognition of rock types and depositional environment. The carbonate rock classification of Folk (1959 and 1962) was used to define rock types, with lithofacies described according to a criteria described in Appendix 2. Biota were used as indicators of depositional environments by using an adaptation of a scheme produced by Burrett (1978; Appendix 2).

Table 3.1: Summarized lithofacies of the Gordon Limestone at Grieves Siding. Variation in depositional environments are accounted for by inferred boundaries.

DEPOSITIONAL ENVIRONMENT	LITHOFACIES
Peritidal to upper intertidal	1. Red Beds: consist of large compositionally zoned dolomite rhombs in a reddened, oxidised micrite and dolomite matrix. Contains siliciclastic red silt with rip up clasts and scouring.
Upper Intertidal	2. Pale Micrites and dismicrites: Pale grey homogeneous micrites, and irregular (1-4 mm) sparry 'birdseyes' in a micrite matrix.
	3. Sparites and Pelbiosparites: White to light grey unsorted and often poorly washed biosparites, oosparites, oncosparites, and pelbiosparites.
?	
Upper Intertidal to shallow subtidal	4. Calcarenites and Biocalcarenites: Mostly homogeneous calcarenite, strongly crinoidal and contains comminuted shell debris.
	5. Oncobiomicrites: Large 0.5 - 2cms oncoids set in a dark grey-black argillaceous matrix with comminuted shell debris.
?	
Subtidal	6. Biomicrites: Dark grey to black, richly to sparsely fossiliferous micrites. Contains a diverse fossil assemblage with pelloids and ooids.
Low Subtidal	7. Argillaceous micrites and mudstones: Dark grey to black massive, bioturbated, micrites and mudstones with bituminous impurities.
?	
Protected Subtidal	8. Nodular Limestone: light grey micritic and calcisiltite nodules cemented in a dark grey to black argillaceous matrix. Contains well preserved as well as comminuted shell debris.
	9. Dolomites - Selective and persuasive, primary and secondary diagenetic.

Table 3.2: Summarised depositional environments of the nine lithofacies recognised at Grieves Siding. (After Tucker, 1982).

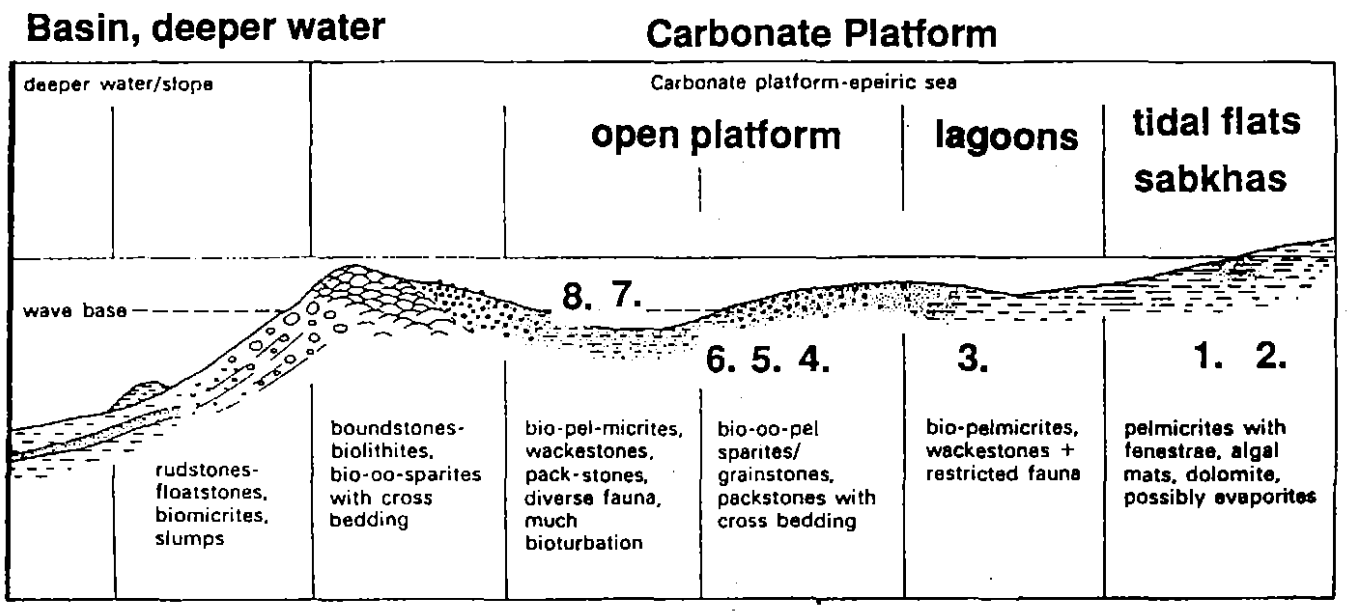

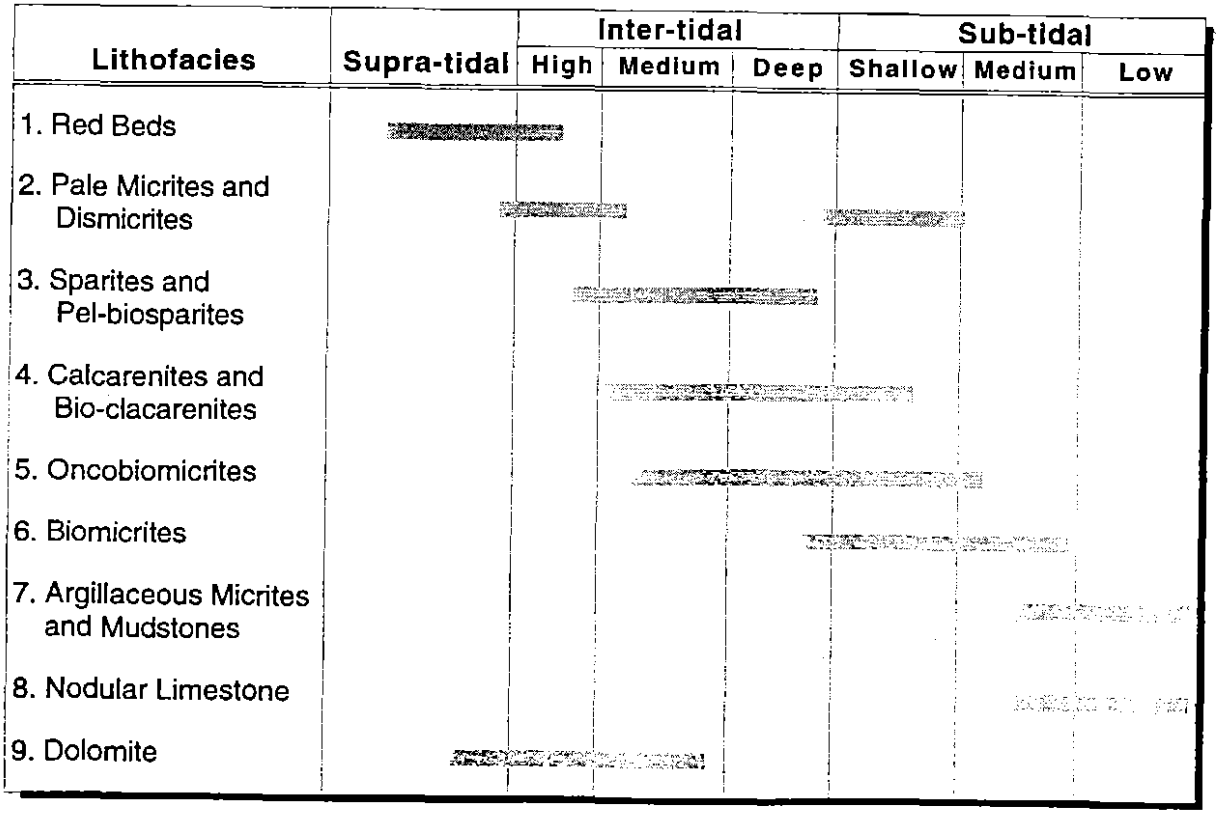

Lithofacies were incorporated into either of three lithostratigraphic formations defined in the Gordon Limestone by Burrett and Geode (1987), Burrett et al., (1989), and Burrett (1995). The Ugbrook, Myrtle and Black Jacks Formations coupled with intra-formational members were overlayed onto 22 stratigraphic sections for Grieves Siding (Fig. 3.1a & b). Formation boundaries and members have been correlated to allow an analysis of basin stratigraphy. Figure 3.2 contains a summary stratigraphic section of Grieves Siding. Sedimentary stylolitisation, and significant deformation, produced pervasive tectostylolitisation with numerous veined, crushed and decomposed intervals. This served to decrease stratigraphic thickness, consequently all thicknesses are uncorrected downhole distances, rather than dip corrected thicknesses. Criteria used to determine depositional environments of each lithofacies are those of Wilson (1975), Rao (1990), Tucker (1981) and Flugel (1982).

3.3 LITHOFACIES DESCRIPTIONS

The Gordon Group comprises a sequence of carbonates and minor siliclastics ranging in age from Early Ordovician to Early Silurian (Banks and Burrett, 1989). It is the thickest (~2.0 km) and most stratigraphically continuous Ordovician (Arenig to Ashgill) sequence in the southern hemisphere (Banks and Burrett, 1979; Banks and Baillie, 1989; Rao, 1990). The Gordon Group conformably overly and/or interdigitates with the Early Ordovician Denison Group, and is overlain conformably or disconformably by the shallow marine clastic sequence of the Silurian-Devonian Eldon Group.

Gordon Group carbonates consist of a sequence of transgressive, shallow marine, ramp deposited, interbedded limestones and dolomitized limestones with minor siliclastics (Banks and Burrett, 1989). They were deposited in subtidal, intertidal, supratidal and tidal channel environments at a palaeolatitude of about 10°N (Rao, 1990). The biota contains abundant corals, oncoids, calcareous algae, and stromatoporids, suggested by Rao (1990) to be similar to the modern tropical *Chlorozoan* assemblages. Non-skeletal grains, including intraclasts, pellets, ooids and aggregates are common with abundant micrite and some sparry calcite. Moderate to deep subtidal limestones form the basal Gordon Group which are overlain by upwardly shallowing cyclic limestones (Punctuated Aggradational Cycles - PACs; Banks & Burrett, 1989). The sequence moves

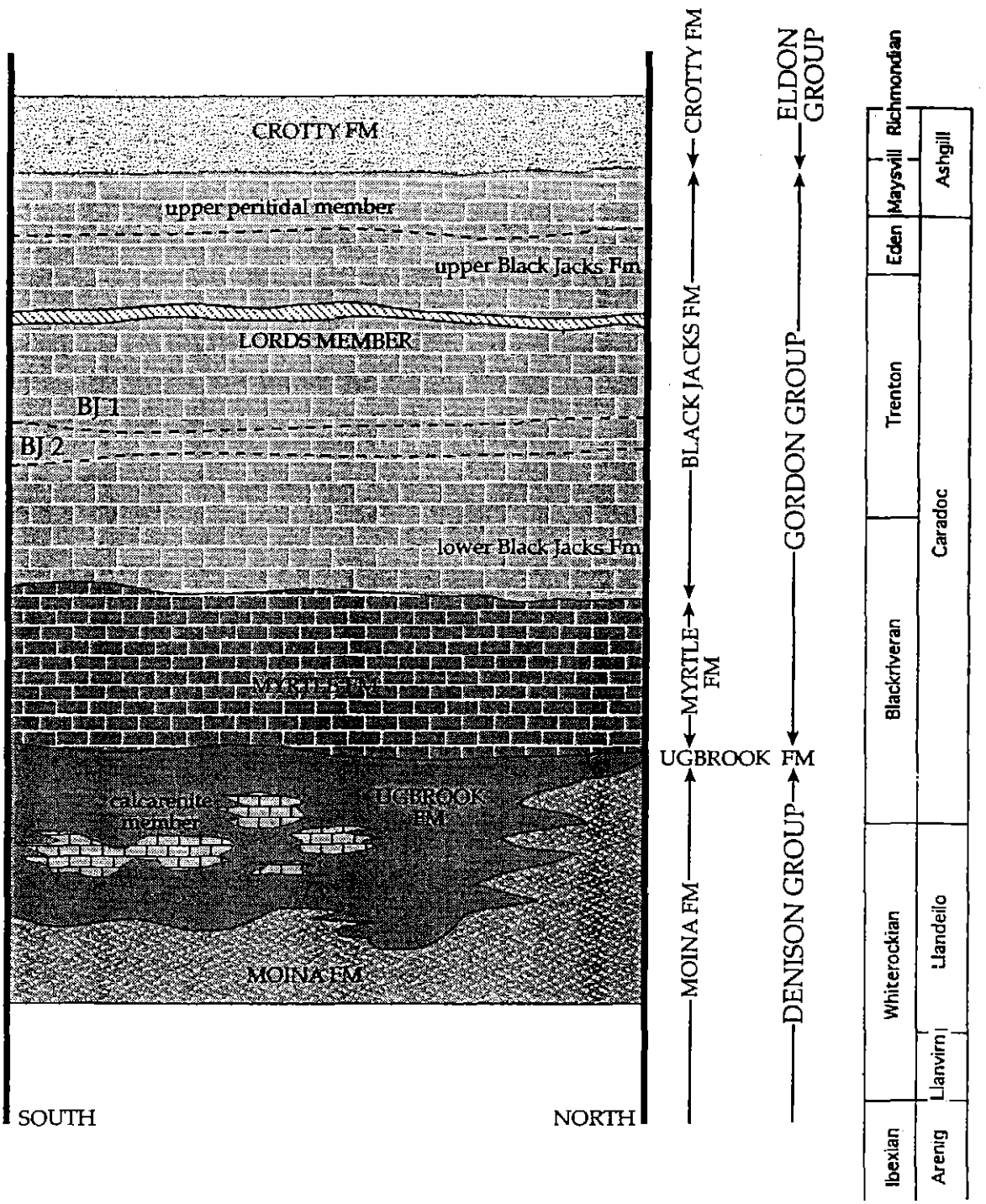

Figure 3.2: Summary of Ordovician stratigraphy at Grieves Siding. Both the American and British time period classification schemes are employed.

towards deeper water lithofacies and biofacies before interruption by the Lords Siltstone. Deeper open subtidal limestones proceed the 'Lords' event.

Work by Burrett et. al., (1987) and Burrett (1995) served to subdivide these sequences into lithostratigraphic units for the interpretation and correlation of depositional environment. These units have been recognised at Grieves Siding and correlated across 22 stratigraphic columns (Fig. 3.1 a & b). The lithostratigraphic units are composed of several lithofacies associations. This section outlines the detailed characteristics of these lithofacies associations before assigning them to the lithostratigraphic units of Burrett et. al., (1987) and Burrett (1995).

3.3.1 **Lithofacies 1**: Red Beds

This lithofacies occurs as rusty red to brown, 5 to 50 cm beds that are well represented in DDH ZG 410 (Plate set 3.1). The red beds are commonly associated with extensive calcite veining on and around bed surfaces (Plate 3.1a). Scoured bedding surfaces, red mudstone rip up clasts and some laminations showing cross-bedding occur (Plate 3.1b). Normal grading, (fining up) is also present.

The red beds are mostly carbonate, containing large primary dolomite rhombs that have been oxidised. Compositional zonation is often seen in dolomite rhombs (Plates 3.1c, d, e, and f) and varying degrees of dolomitisation are seen in the matrix. Strong dolomitisation is observed with large 3-4 mm compositionally zoned euhedral to subhedral rhombs. Smaller equigranular 0.4 mm euhedral to subhedral, strongly zoned rhombs are also evident

Interpretation.

Some red beds represent a very minor siliclastic input of red silt into a shallow, supratidal to peritidal environment. This may signify deposition during storms or may represent siliclastic debris being derived from the uplifted Tyennan and other regions. The scoured bed surfaces and rip up clasts are assumed to have formed during transportation and reworking of sediment into the depositional environment.

Most red beds consist of oxidised, equigranular dolomite rhombs that form a dolomitic mudstone. Where present they represent the very top of PAC

Plate 3.1

Plate 3.1 a : Lithofacies 1. Red beds (R), near the top of a (PAC) sequence. The red bed appears to be oxidised carbonate that formed due to surficial exposure.

Plate 3.1 b : Drill core sample from DDH ZG410 showing an input of red silt into a red bed. Rip up clasts (Rc) and normal grading indicates the sequence is the right way up. (Length of speciman = 10cm)

Plate 3.1 c to f : Compositionally zoned dolomites in a red bed of Lithofacies 1. The large zoned crystals occur within finer grained, early diagenetic dolomite. They are interpreted to have formed by mixed marine and meteoric waters. (DDH ZG410, transmitted light, field of view ≈ 2 mm)

Plate 3.1 g : Alternating argillaceous limestone and micrite (M) typical of a protected lagoonal environment in the Ugbrook Formation. Small patches of sparry calcite are seen in the micritic material. This sample corresponds to Lithofacies 7.

Plate 3.1 h : Punctuated Agradational Cycle (PAC). The cycle starts at the top of the photomicrograph at (1), in argillaceous subtidal limestone before grading into progressively lighter coloured, high intertidal micrites, dismicrites (D) and algal laminated micrites (AM) before sharply deepening into subtidal argillaceous material near 346 m. A new cycle begins from 346 m to the bottom of the photograph. PACs help define the Myrtle Formation and include Lithofacies 7 and 2.

Plate A

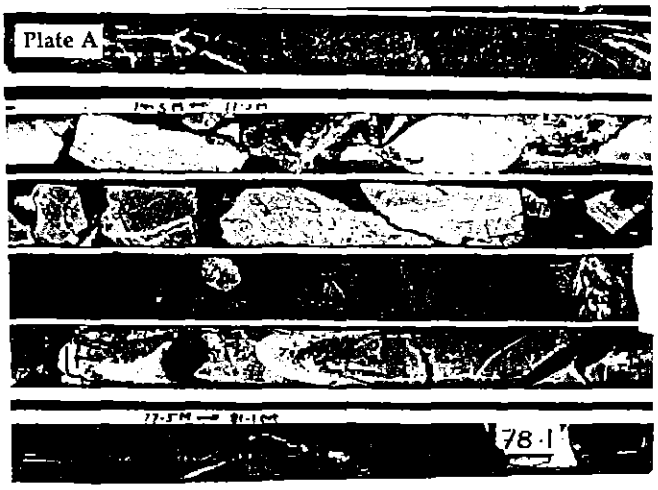

Plate B

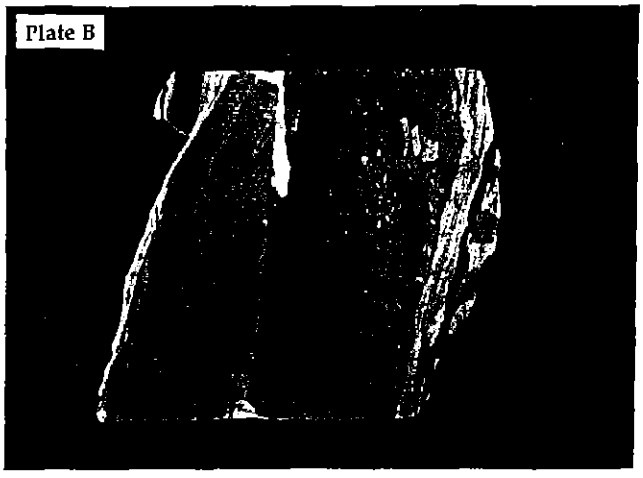

Plate C

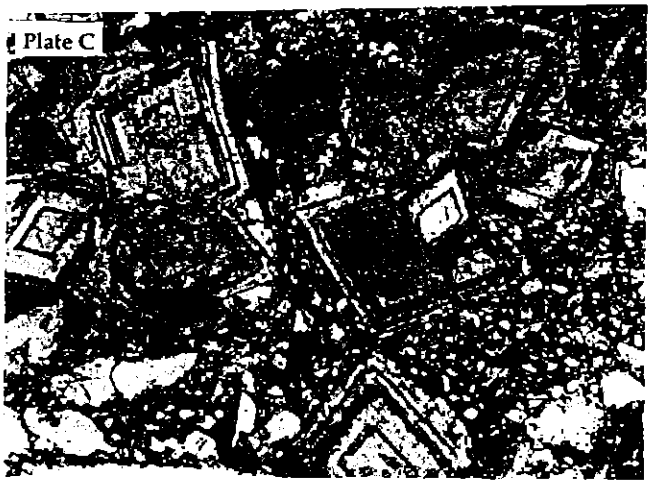

Plate D

Plate E

Plate F

Plate G

Plate H

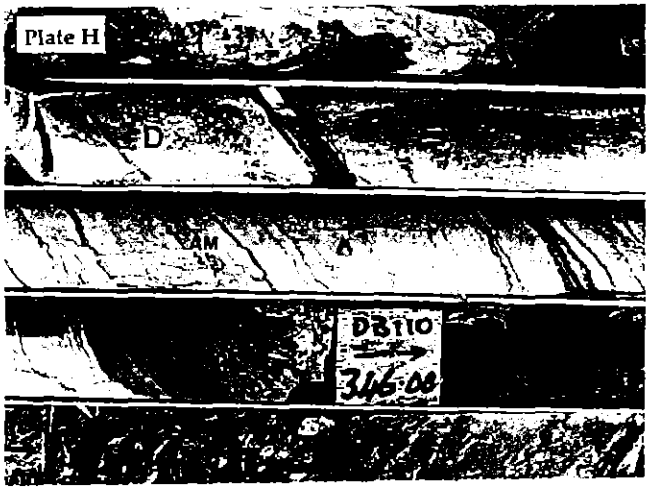

sequences (Plate 3.1a) culminating in a high intertidal to peritidal environment periodically exposed and therefore oxidised. This occurred very close to the shoreline, with surficial exposure occurring as the shallowing up PAC cycles developed. No evaporites are found associated with the red beds. Where red beds mark the top of PAC sequences, they are analogous to the silty grey-green dolomitic mudstones that mark the top of the Duperow cycles of the Devonian Williston Basin, North Dakota, U.S.A. The upper Duperow cycles show intertidal and supratidal sedimentary structures (Wilson, 1975) similar to the scouring, cross-bedding and rip up clasts observed in some red beds. Compositionally zoned dolomite rhombs are indicative of mixed marine and meteoric diagenetic fluids. Calcite veining may be tectonically associated as the oxidised units could have been brittle and susceptible to later calcite veining.

3.3.2 **Lithofacies 2:** Pale micrites and dismicrites

This lithofacies represents an almost pure orthochemical rock composed of white to light grey micrite. It does however, contain very minor bioclastic and sparry intraclasts comprising less than 3% of the rock (Plate 3.1h). It displays a conchoidal to sub-conchoidal fracture pattern, and often shows a strong tectonic stylolitization that overprints a weaker sedimentary stylolitisation. A poorly developed cleavage is sometimes present sub-parallel to bedding although bedding is often obscured and not always obvious.

The homogeneous pale grey micrites are non-fossiliferous and can reach bed thicknesses of up to 20 m. Although not seen in handspecimen, moderate dolomitisation is present with zonal (0.2 mm) subhedral to euhedral rhombs. Minor (2%) pyrite cubes (0.3 mm) occur throughout the dolomitized micrite. Dismicrites rarely exceed 1 m in thickness and are recognised by 'birdseye' structures, composed of circular to irregular (1 - 4 mm) patches of sparry calcite in micrite. They are considered (Tucker, 1981; Flugal, 1982) to be representative of subaerial exposure, and are formed as the sediment undergoes dessication, with escaping gasses leaving pore spaces in the micrite. The pore spaces are later filled with sparry cement.

Interpretation

This lithofacies is autochthonous and was primarily deposited in a shallow marine, low subtidal to high intertidal environment. The massive pale micrites

represent lime mud deposition in a quiet exposed environment, with a noticeable lack of fauna. Studies of recent carbonates (Pratt et al., 1992) show that lime mud precipitates in great volumes on very shallow, quiet platforms as on the Bahama Bank, and in quiet back reef lagoons in the Persian Gulf and in Florida Bay. The dismicrite was deposited in an intertidal to supratidal environment. Dismicrites are especially useful in determining the top of PAC sequences (Plate 3.1h) acting as indicators of intertidal to supratidal environments.

3.3.3 **Lithofacies 3**: Sparites and Pel-bio-oosparites.

This lithofacies occurs in horizons up to 4 m thick and consists of white to light grey, unsorted, rounded and often poorly washed biosparites, oosparites, oncosparites and pel-bio-oosparites (Plate set 3.3 and 3.2). It displays an uneven fracture pattern and appears resistant to stylolitization. Bedding surfaces can be gradational but are mostly uneven, and may be somewhat scoured.

The non-homogeneous, fine to coarse grained matrix consists of moderate and poorly washed sparite with over 50% allochems (Plate set 3.3). It is often mildly dolomitised. Bioclasts include brachiopods, gastropods, bryozoa, crinoids, echinoderms and corals (Plate 3.3e) that can be well preserved, highly fragmented and/or recrystallised to spar. Intraclasts include pelloids, (Plate 3.3h) oncoids and ooids which comprise up to 40% of allochems. Some small (0.2 mm) pyrite cubes and minor (4%) dolomite rhombs are found in the matrix (Plate 3.3b). Sub-rounded to rounded micritic and sparry patches are also present. Ooids can be slightly elongate (Plate 3.3c) and were formed around coral, echinoderm, brachiopod and gastropod fragments as well as dolomite rhombs. Allochems exhibit a range in grain-shapes from sub-angular to rounded, and poorly to well sorted. No grading or imbrication is present.

Interpretation

The removal of lime mud to allow sparry calcite cementation implies a shallow water, moderate to high energy depositional environment (Flugal 1982). Random orientation of fossils confirms a high energy environment of deposition. The ooids formed in such an agitated, shallow subtidal, to intertidal environment, with the presence of such large ooid shoals indicating the influence of tidal currents. The ooid shoals could be associated with a carbonate

Plate 3.2

Plate 3.2 a : Argillaceous bioturbated calcisiltite of the Ugbrook Formation. Burrows (B) have become elongate with the major cleavage.

Plate 3.2 b : *Tetradium* rich biomicrite in ZM1009

Plate 3.2 c and d: (c) Photomicrograph of *Tetradium sp.* fossils and (d) now replaced with sparry calcite plates. (DDH ZG410, transmitted light, field of view ≈ 2 mm)

Plate 3.2 e : Onco-biomicrite of Lithofacies 7. The algal layers of the oncoids (AL) are selectively replaced by dolomite rhombs. Ooids are also found in the sparry calcite matrix (DDH ZG412, transmitted light, field of view ≈ 1 mm).

Plate 3.2 f : Biomicrite of Lithofacies 6, containing a brachiopod shell fragment and ooids cemented by a poorly washed calcite matrix (DDH ZG1012(A), transmitted light, field of view ≈ 2 mm).

Plate 3.2 g : Dolomitisation of a sparse biomicrite, also showing bituminous films along stylolites (DDH ZG1007, transmitted light, field of view ≈ 4 mm)

Plate 3.2 h : Massive dolomite of Lithofacies 9 showing compositionally zoned rhombs (DDH ZG414, transmitted light, field of view ≈ 1 mm)

Plate A

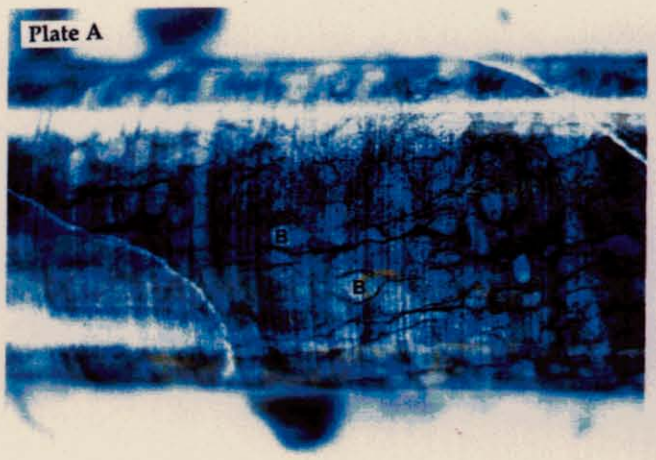

Plate B

Plate C

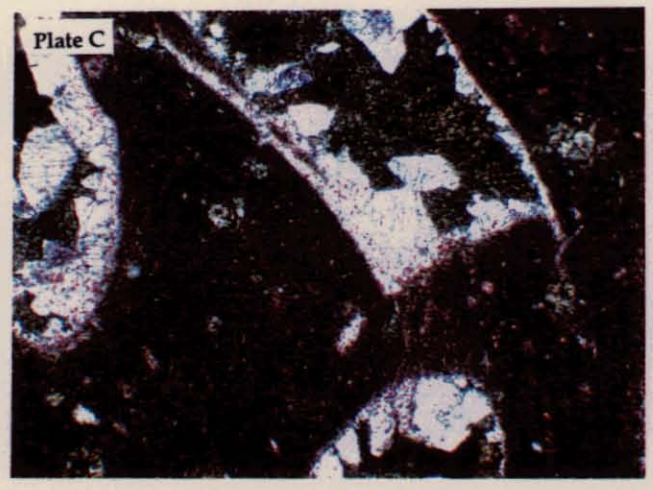

Plate D

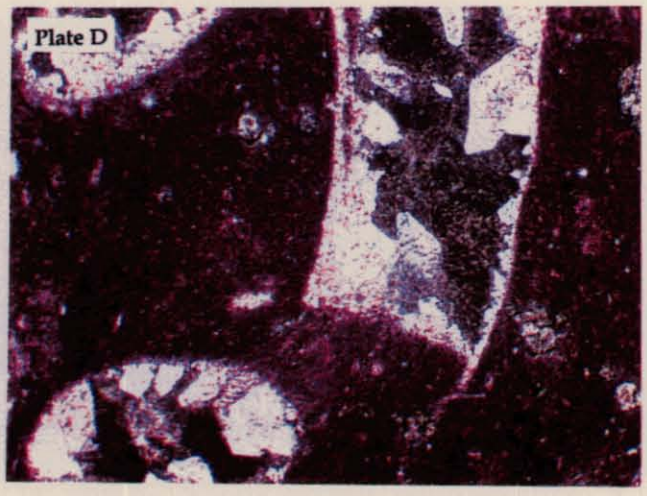

Plate E

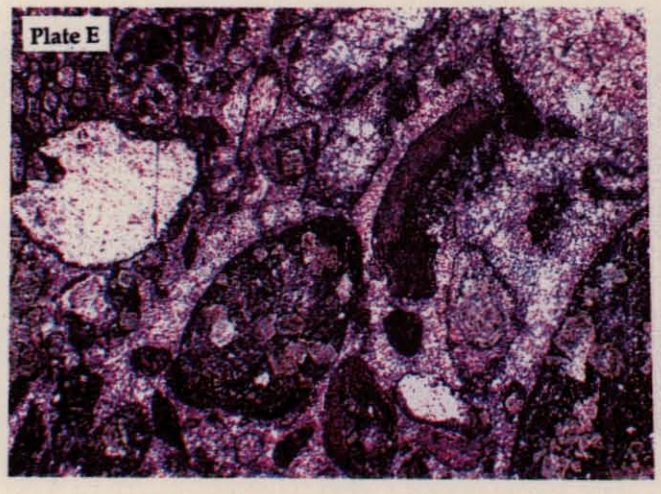

Plate F

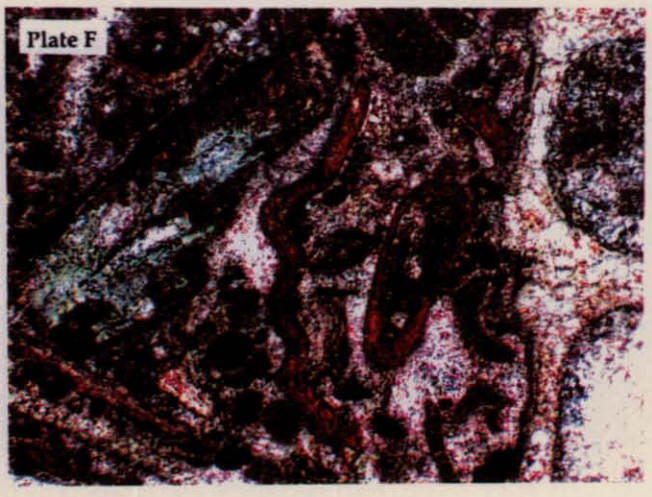

Plate G

Plate H

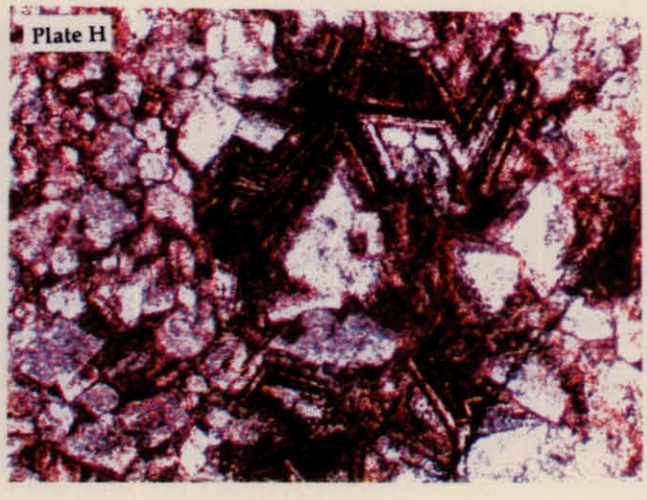

bar that was breached in several locations to allow entry of currents suitable for ooid formation. Pelloids would have also been formed in an intertidal zone and then washed into the shallow subtidal depositional environment. The lithofacies as a whole is most likely represented by a shallow subtidal to intertidal depositional environment. Ooid-dominated sparites may have also formed in intertidal ooid shoals (Tucker, 1981). Those sparites containing highly fractured and/or rounded allochems may have been deposited in tidal channels.

3.3.4 **Lithofacies 4**: Calcarenites and biocalcarenites

This lithofacies occurs as light grey to blue, 0.5 m beds, or as a massive sequence up to 30 m thick. It displays an uneven fracture pattern with very minor stylolitization. Beds sometimes show weak fining up and bedding surfaces can be uneven.

This lithofacies consists of mostly homogeneous calcarenite (0.63 - 2 mm), however it may contain crinoid and echinoderm fragments and some shelly lags. Bioclasts are dominated by crinoid fragments with lesser brachiopod and gastropod fragments. It sometimes contains thin argillaceous lenses, and some sparry calcite patches (5 %) up to 3 mm. It shows either weak (4 %) selective dolomitisation, or pervasive dolomitisation (Plate 3.2g), which commonly results in vuggy porosity. Dolomitisation can persist for up to 7 m. Apart from some normal grading, no sedimentary structures are seen.

Interpretation

The smaller 0.5 m beds are interpreted as tidal channel sediments, deposited into shallow subtidal to high intertidal environments. Such channels truncate the preceding sediments and have negligible lateral extent. They are common towards the top of PAC sequences but occur throughout the entire sequence. The massive calcarenite member was deposited in a medium to shallow subtidal environment, some distance from the micrite producing tidal flats (Burrett, 1995). The calcarenite member is intimately associated with ooid shoals forming a rapidly migrating carbonate bar. The bar was compromised in several locations allowing tidal current to produce extensive ooid shoals (Fig. 3.1a &b).

3.3.5 **Lithofacies** 5: Onco-biomicrites.

The onco-biomicrite lithofacies occurs in beds up to 1.5 m thick and is recognised by large 0.5 - 2 cm oncoids set in a dark grey - black argillaceous matrix (Plate 3.2e and 3.3a). The rocks exhibit an uneven fracture pattern, often with scoured bed surfaces. Oncoids mostly show no orientation, but can be weakly imbricated into layers up to 3 cms thick. These layers are preferentially stylolitised, however stylolitization overall is minimal.

The matrix is non-homogeneous (55%) and composed of dark argillaceous micrite and lesser calcisiltite. A poorly washed sparry matrix is also present. Both matrices can be mildly to strongly dolomitized. Oncoids dominate the allochem component of the lithofacies comprising 50% of the rock, with bioclastic material representing 5%. Fragmented bioclasts include brachiopods, corals, gastropods, trilobite and echinoderm fragments.

The ellipsoidal oncoids are composed of micrite and algal filaments (*Girvanella*?) that have concentrically grown around a coral, brachiopod, gastropod or most a commonly echinoderm nuclei (Plate 3.3a). Some algal filaments show intense selective dolomitisation (Plate 3.3a). The size of the oncoids (0.5 - 2 cm) suggests they may be *Girvanella* oncoids (Flugal, 1982; Banks and Johnston, 1957). The individual concentric layers are wavy and are oriented slightly off centre around the nucleus. The oncoids represent micrite oncoids derived from agglutination of micrite grains on the surface of algal filaments (Flugal, 1982).

Interpretation

The oncoids formed in a shallow marine, agitated, lower intertidal setting. Gastropod, coral, and brachiopod nuclei, important for oncoid formation, were most probably transported into this environment from a nearby shallow subtidal to intertidal environment by the prevailing currents. The large size of the oncoids suggests a depth close to wavebase (Rice, 1985). The argillaceous matrix and weak imbrication of some layers suggest the oncoids have been transported into a deeper subtidal environment and assumed an argillaceous matrix before diagenesis. Preferential dolomitisation of the algal filaments occurs in response to the argillaceous (higher Mn) content of the filaments.

3.3.6 **Lithofacies 6:** Biomicrites

This lithofacies contains up to 55% allochems, of which bioclasts comprise up to 40% followed by lesser intraclasts, pelloids and ooids (Plate 3.2f). Bioclasts are predominantly corals and brachiopods with minor gastropods, ostracods, echinoderms, stromatoporids, bryozoa and trilobite fragments (Plate 3.3e and f). Corals include *Bajgolia contigua*, *Rhombotrypa* sp., *Thamnopora* and *?Monticulipora mammulata*. Most samples are strongly pelloidal with some oncoids and ooids present. Bioclasts are mostly poorly sorted (Plate 3.3c), very angular and not orientated, apart from rare brachiopod geopetal structures (up to 1.5 cm), and some imbrication of brachiopod shells evident in DDH ZG 1011. Comminuted shelly debris layers are also present. Fossil preservation is adequate with little fragmentation, however some sparry recrystallisation of fossils is evident (Plate 3.3d). Calcite veining is common, cross- cutting both matrix and allochems. The matrix is mostly argillaceous micrite and mudstone showing very minor (1%) dolomitisation and is selectively stylolitised (Plate 3.3d). Stylolites are refracted around bioclasts and intraclasts.

Tetradium rich biomicrites

A significant subunit in this lithofacies is the *Tetradium* rich packed biomicrites. They form horizons up to 50cms thick and contain *Tetradium* up to 1 cm long and 2mm in width (Plate 3.2b, c and d). Most *Tetradium* have been recrystallised into sparry calcite (Plate 3.2 c and d), and rarely retain the diagnostic 'tudor rose' cross section revealing the inward pointing septa. *Tetradium* skeletons have been filled with euhedral calcite plates on the margins and a finer grained spar centre.*Tetradium* comprises up to 60% of these packed biomicrite horizons and are cemented by a micrite or argillaceous matrix. Weak dolomitisation has often selectively replaced small portions of the micritic groundmass. Burrows have also been filled with 0.2 mm dolomite rhombs. The sparry recrystallisation results in *Tetradium duplex* being the only identifiable species in thin section. Hand specimen investigation identified *Tetradium cribbiforme.*

Interpretation

The faunal diversity suggests an unrestricted, dominantly medium to shallow subtidal depositional environment. Tucker (1982) suggests biomicrites occur below wavebase, and the comminuted shell debris represent storm reworking. The presence of corals, bryozoa, pelloids, trilobite fragments and *Tetradium*

Plate 3.3

Plate 3.3 a : Oncoid of Lithofacies 5, nucleated around an echinoderm fragment. The concentric algal filaments are assumed to be *Girvanella sp.* Oncoids are deposited in low intertidal to shallow subtidal environments (DDH ZG1001, transmitted light, field of view ≈ 2 mm).

Plate 3.3 b : Selectively dolomitised concentric algal layers of an oncoid in a packed onco-biosparite of Lithofacies 3 (DDH ZG1011, transmitted light, field of view ≈ 4 mm).

Plate 3.3 c : Packed pel-biosparite of Lithofacies 3 containing brachiopods, ooids, and pelloids set in a poorly washed sparry calcite matrix (DDH ZG1012, transmitted light, field of view ≈ 4 mm).

Plate 3.3 d : Packed biosparite of Lithofacies 3 contains gastropods, corals and elongated ooids (Oo). Opaque material occurs in association with the tectonic stylolites (DDH ZG1012(A), transmitted light, field of view ≈ 4 mm).

Plate 3.3 e : Corraline algae in a micrite of the Ugbrook Formation (DDH ZG1001, transmitted light, field of view ≈ 4 mm).

Plate 3.3 f : Pel-bio-oosparites of Lithofacies 3 occurring with a large colonial coral (DDH ZG412, transmitted light, field of view ≈ 4 mm).

Plate 3.3 g and h: Pel-bio-oosparite of Lithofacies 3 in a well washed sparite matrix. Selective dolomitisation of algal ooids occurs. Sparites are associated with the migrating carbonate bar responsible for the calcarenite member (DDH ZG1011, transmitted light, field of view (g) ≈ 2 mm, (h) ≈ 1 mm).

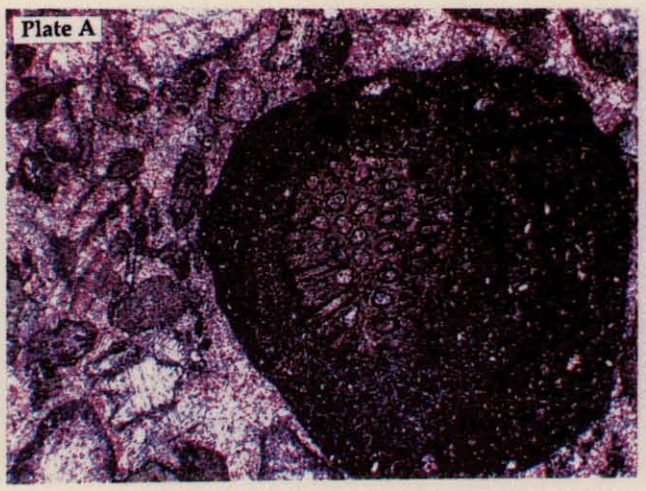

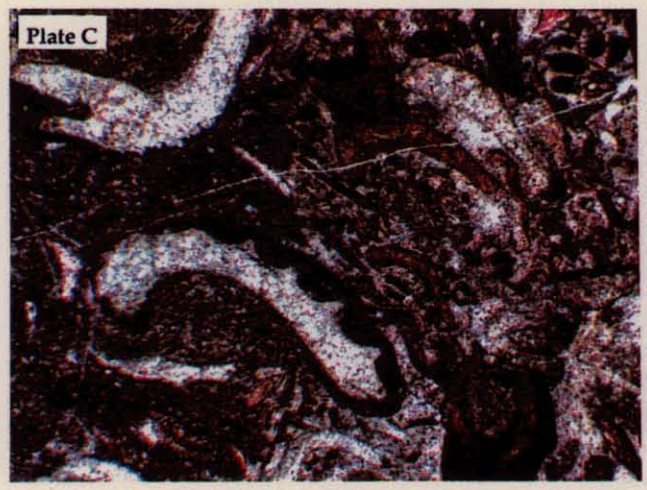

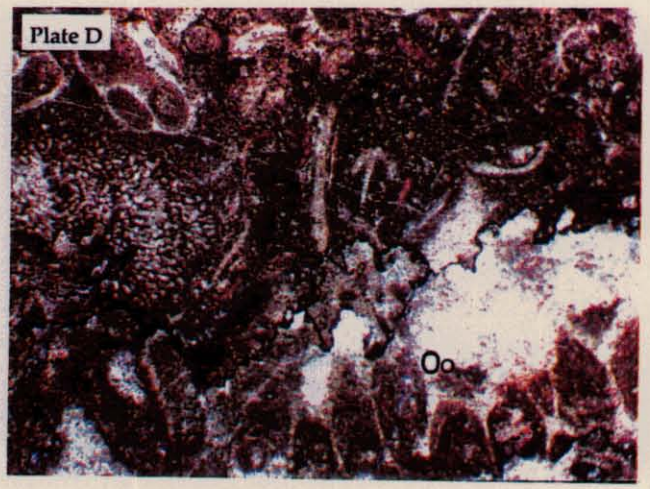

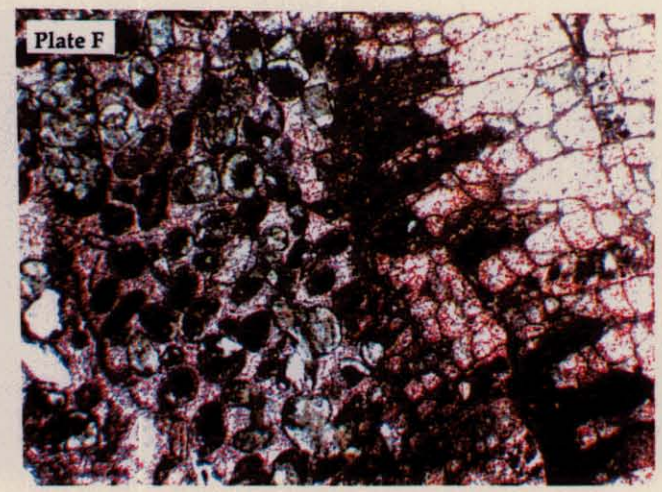

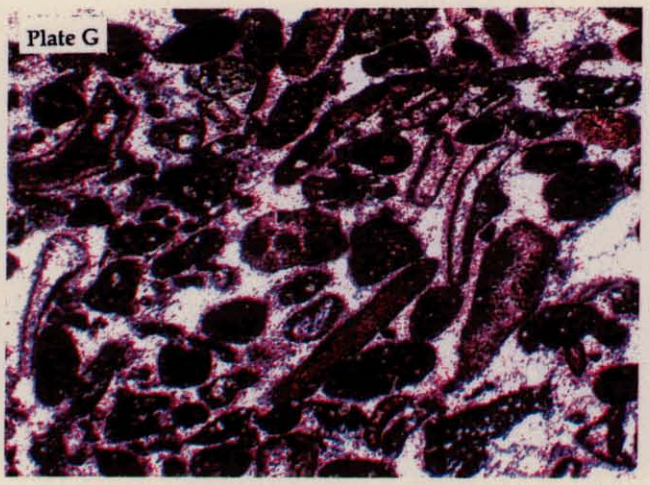

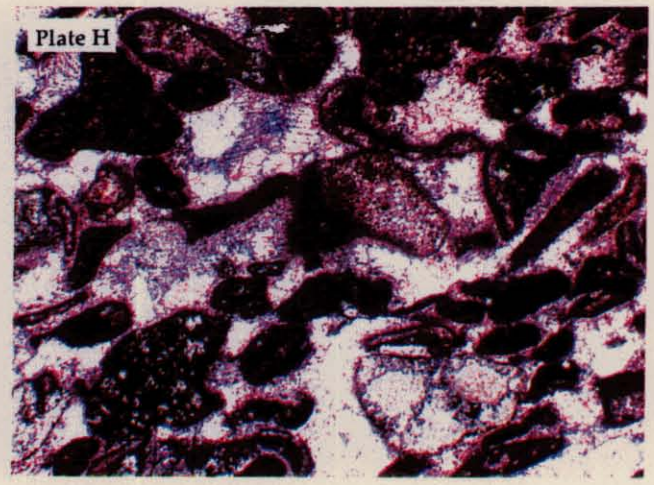

supports with this environmental interpretation. *Tetradium* inhabit medium subtidal to medium intertidal environments. Walker (1972), Calver (1977), Page (1978) and Ellis (1984) agreeing on a shallow subtidal depositional environment for this lithofacies.

3.3.7 **Lithofacies 7**: Argillaceous micrites and mudstones

This dark grey to black lithofacies lacks sedimentary structures and displays an uneven fracture pattern except where cleaved (Plate 3.1g). Cleavage is more pronounced in this unit due to the competency of the argillaceous material which is common in these beds (Plate 3.2a). Allochems are dominated by large bioclasts with lesser intraclasts. Large colonial corals (up to 10 cm), coraline algae, stromatoporids and bryozoa are common with lesser brachiopods, gastropods and trilobites. Fragmented bioclasts are also common, especially in shelly bioclastic lags, which form layers up to 7 cm thick. Intraclasts are predominantly pelloids, and pale micrite fragments.

Bed thickness is highly variable and ranges from centimetre to metre scale (Plate 3.3g). Rare laminations (up to 4 mm) are seen in some mudstone dominated horizons. Bedding surfaces sometimes show load casts, and can be considerably scoured. Some sedimentary boudinage is present with lighter coloured calcisiltite / micrite boudins set in a dark argillaceous matrix.

The mostly homogeneous matrix is composed of dark grey micrite / calcisiltite and/or mudstone, and comprises up to 50% of the lithofacies. Some horizons are purely mudstone or argillaceous micrite and have been heavily bioturbated (Plate 3.2a). Intensely burrowed units persist for up to 7 m, and where cleaved, the burrows elongate to form ellipsoids (Plate 3.3a). Individual burrows are mostly 6 mm in diameter and up to 4 cm in length. Some have been selectively replaced by 0.2 mm dolomite rhombs.

Interpretation

The argillaceous nature of this lithofacies and the presence of a subtidal fauna suggests deposition in a low energy, medium to shallow, subtidal environment. Variation in fossil abundance and diversity separates depositional environments between restricted subtidal or open subtidal. Mudstone intervals may represent a minor siliclastic influx. Argillaceous micrite/mudstone often

forms alternating associations with pale micrite, resulting in repetitious argillaceous-pale micrite sequences. Such a sequence is diagnostic of a high intertidal lagoonal deposits (Burrett, 1995).

3.3.8 **Lithofacies** 8: Nodular Limestone

This lithofacies contains light grey micritic and calcisiltite nodules cemented in a dark grey-black argillaceous matrix. It possesses an uneven fracture pattern even in those samples displaying cleavage. If present, bedding is undulose and grades into loosely packed nodular bodies within the matrix. Bioturbation and the deformational nature of the bedding, obscures bedding surfaces, such that this lithofacies becomes a more massive sequence. Significant stylolitization is preferentially developed in the argillaceous matrix with the micritic and calcisiltite clasts remaining less affected.

The non-homogeneous argillaceous matrix is a finely crystalline (0.03 - 0.06 mm) calcisiltite, and is never sparry. Small (0.3 - 1 mm) rip up clasts of micrite and calcisiltite are present 'floating' within the matrix. It is commonly dolomitic with anhedral to subhedral dolomite rhombs up to 0.4 mm and contains minor sparry ferroan calcite plates up to 3.5 mm. The matrix is often bioclastic, with comminuted shell fragments of brachiopods, gastropods, corals and bryozoa. Well preserved bryozoa are also present. Borrows are commonly filled with dolomite rhombs showing minor imbrication. Bituminous films often occur on the sides of burrows. with pyrite cubes (0.2 mm) also present in some dolomitized burrows.

Micritic and calcisiltite nodules range in size from 3 mm to 10 cm and can be either homogeneous or non-homogeneous calc-bioclastic. Nodular intraclasts contain shell fragments, small (2 - 5 mm) sparry patches, and fragments of calcisiltite and micrite. The nodules are angular and show no noticeable imbrication. They can be either discontinuous seams or exist as fitted nodules. The nodular nature of the limestone has been accentuated by tectonic stylolitization.

Interpretation

A plethora of interpretations exist as to the origins of nodular limestones. The most accepted explanations include slumping of differentially lithified layers (Seyfried, 1980, Weber 1965). Sub-solution during deposition, and late burial diagenesis processes in connection with pressure solution are also proposed for the origin of the nodules. Concretional growth due to diagenetic differentiation of carbonate and argillaceous material was offered by Hildebrand (1929), Schindewolf (1925) to explain the process. The most credible explanation involves sedimentary boudinage and differential compaction (Fig. 3.3) as cited by Born (1921), McCrossan (1958) and Nichols (1966).

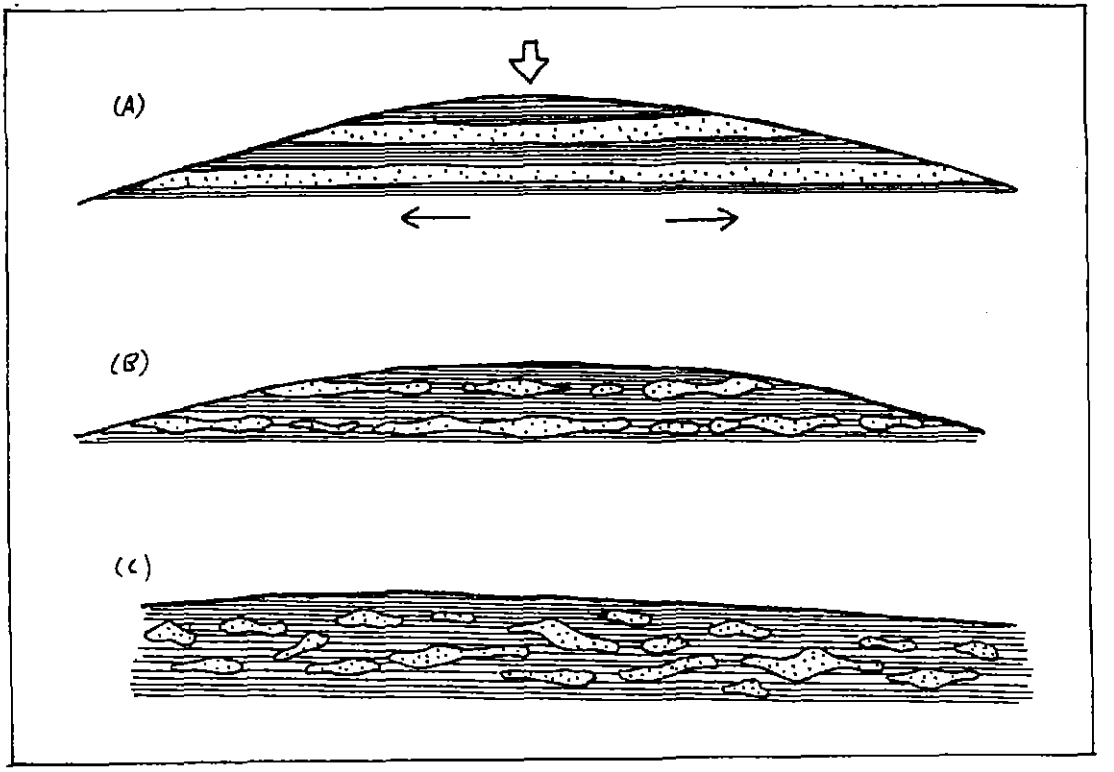

Figure 3.3: Stages in the development of sedimentary boudinage. Modified after McCrossan (1958).

The depositional environment of nodular limestone at Grieves Siding is either medium to deep subtidal, or restricted subtidal. Differentiation between these two environments is achieved by using faunal elements. A restricted subtidal environment contains diverse, and abundant fossils compared to a more open subtidal environment comprising more bioclastic fragments, poorly preserved and less abundant fossils. The nodular lithofacies is proceeded by a gradual deepening of both depositional environment and biofacies.

3.3.9 **Lithofacies 9**: Dolomites.

Although not evident in hand specimen, much of the Gordon Limestone is variably dolomitized. Dolomite is abundant in intertidal and supratidal environments and to a lesser extent in some subtidal carbonates. Small scale dolomite is present along many stylolites and selectively replaces small carbonate patches in argillaceous matrices. Selective dolomitisation of burrows is also present. On a broader scale, dol-biomicrites with selective matrix dolomitisation and dol-oncomicrites with selective algal filament dolomitisation is evident. Fine grained equigranular subhedral to euhedral dolomite rhombs (0.1 - 0.4 mm) are dominant, with larger grains (up to 0.7 mm) showing compositional zonation. Those dolomite rhombs associated with stylolites are often set in a dark bituminous or graphitic matrix. Pervasive dolomitisation is seen in massive micrite and argillaceous carbonates. Limited primary dolomite is observed in association with oxidised red beds.

Interpretation

The selective preservation of sparry calcite patches and calcite veins suggests dolomitisation occurred during early diagenesis, both before and during spar cementation. Four major models of dolomitisation are considered to be significant at Grieves Siding. Hypersaline dolomitisation during intense evaporation in sabkhas, and shallow subtidal dolomitisation by marine and hypersaline fluids are important processes, but the amount of dolomitisation produced by these methods is minimal. Mixing zone dolomitisation and burial dolomitisation is considered more important (Rao, 1990). Marine solutions mixed with meteoric waters, abundant in a tropical environments, are undersaturated with respect to calcite, and supersaturated with respect to dolomite (Rao, 1990). They could act as early diagenetic dolomitising fluids at Grieves Siding. The selective dolomitisation of burrows, oncoids, ooids, algae

and the extensive replacement of micrite, coupled with the preservation of intraclasts and spar patches indicates early diagenetic dolomitisation. Burial dolomitisation and leaching of Mg from argillaceous material (section 3.5.2) could be responsible for pervasive dolomitisation. Texturally destructive dolomitisation is restricted to two stratigraphic positions with thicknesses up to 120 m. These sequences are referred to as the upper and lower dolomite, with minor pyrite and galena mineralisation associated with the lower dolomite.

3.4 *LITHOSTRATIGRAPHIC UNIT DESCRIPTIONS*

3.4.1 *MOINA SANDSTONE*

The Moina Sandstone is the uppermost member of the Denison Group and forms a prominent plateaux along the eastern margin of the field area. It conformably overlies the Mt. Zeehan Conglomerate and forms a sequence 1.2 km thick at Grieves Siding. Thickness increases to the south-west at approximately 100 m/km (Banks, 1989).

Although the nature of the upper contact with the Gordon Limestone is conformable, its exact position is contentious. Burrett (1995) suggests the delineation of the boundary is arbitrary because throughout the Florentine Valley, and areas southwest and north of Mole Creek, the contact exhibits a transitional, interdigitating contact, marked by a siltstone - mudstone transitional zone up to 30 m thick. X-ray diffraction of this transitional zone (Table 3.2) at Grieves Siding shows a high abundance (>60%) of a kaolinite group mineral interpreted as dickite. Dickite ($Al_2Si_2O_5(OH)_4$) usually occurs in hydrothermal veins (Gary et al., 1977; Bottrill, pers. com.) and coupled with the presence of illite, sphalerite, hematite, geothite, and crandallite may suggest that the siltstone - mudstone transitional zone represents hydrothermal alteration of the Gordon Limestone. Major mineralisation at Grieves Siding is situated just above this transitional zone (Fig. 3.1a &b). Siderite gangue associated with the mineralisation is often altered to geothite and hematite (Nesse, 1991), so whether the mineralisation has contaminated the underlying silts or whether they are a pure hydrothermal alteration product remains unconfirmed pending further work. The most likely explanation invokes a combination of silts from an interdigitating contact which have been overprinted by hydrothermal

alteration related to mineralisation. Fluids responsible for the mineralisation would have permeated along the Moina Formation - Gordon Group contact.

The variable interdigitating nature of this contact makes the boundary between of the Denison Group and the Gordon Group difficult to define. It has therefore been placed at the last obvious appearance of consolidated sandstone (Fig. 3.1a &b). In the field (Fig 1.2) the contact is marked by a rapid change in topography as the elevated (500 m) plateaux suddenly drops 100 m into the limestone valley.

The typical Moina Sandstone is a well sorted siliceous sandstone with some conglomeratic beds. Fresh surfaces have a pink colouration weathering to white -grey. Modal grainsize (0.25 - 1.5 mm) is medium to coarse sand with conglomeratic beds containing sub-angular to sub-rounded quartz clasts up to 4 mm. Some clasts are weakly imbricated. Thin (5 cm) laterally discontinuous mudstone interbeds occur within the unit, as well as minor lithic fragments and quartzose beds.

Cross bedding, ripple marking and intensely bioturbated beds are common and indicate beds are right way up (Banks, 1989). Vertical worm burrows perpendicular to bedding have been attributed to *Arenicolites* sp. Anhedral, quartz-filled en-echelon tension gashes are found in association with a poorly developed cleavage, not evident in thick sandstone beds. *Arenicolites* sp. have been interpreted by Banks (1989) as indicating a littoral or sub-littoral depositional environment. Detailed depositional environment interpretation is discussed in Section 3.6.

3.4.2 *GORDON LIMESTONE*

UGBROOK FORMATION

The Ugbrook Formation was first defined at Mole Creek by Burrett et al., (1989). At Grieves Siding the Ugbrook Formation includes alternating micrites, argillaceous micrites, biomicrites and mudstones of Lithofacies 6, 7, and 8. It also contains Lithofacies 3, 4, and 5. The Ugbrook Formation encompasses mineralised sections up to 14 m thick along the contact with the Moina Sandstone. It also includes various sparites, calcarenites and a lower dolomite member, forming a vuggy massive dolomite sequence up to 10 m thick.

Centimetre to decimetre scale alternation of lithofacies occurs forming repetitive sequences up to 20 m thick. Such sequences are strongly pelloidal and show a subtidal fauna dominated by corals, gastropods, and brachiopods. These sequences are commonly nodular (Lithofacies 8) with sparites and pel-biosparites of Lithofacies 3 also common. Development of a calcarenite member (Fig. 3.1a &b) containing features consistent with Lithofacies 3 and 4 occurs sporadically throughout Grieves Siding but intensifies towards the south where the Ugbrook Formation thins.

The calcarenite member is commonly proceeded and preceded by oosparite shoals. The member itself often contains ooids, oncoids corals and comminuted shell debris that can exhibit a sparry matrix. Onco-biosparites and oosparites of Lithofacies 3 are therefore well represented in the calcarenite member. It can be variably dolomitised, with dolomitisation more pronounced in the north. No significant mineralisation is associated with dolomitisation. The calcarenite member signifies an easily recognisable and correlateable member within the Ugbrook Formation. It is often proceeded by subtidal argillaceous micrite and calcisiltite, commonly containing corals, brachiopods and gastropods.

The Ugbrook Formation at Grieves Siding averages 100 m in thickness reaching a maximum thickness in the north of ~230 m. It thins slightly, thickening again, before thinning to 50m in the south (Fig 1.2; Fig. 3.1a &b)

MYRTLE FORMATION

The Myrtle Formation was established by Burrett (1995) and describes a sequence of micrites, argillaceous and bioturbated micrites, biomicrites, dolomitised micrites, minor calcarenites and shales. It contains representatives of Lithofacies 1, 2, 6 and 7. The Myrtle Formation forms upwardly shallowing tidal flat cycles known as Punctuated Aggradational Cycles (PACs), 20 to 160 m thick.

PACs are metre-scale upwardly shallowing units bounded by surfaces of abrupt change to deeper of disjunct facies (Pratt et al., 1992). Minor scouring and rip up clasts are seen on such boundaries. A typical PAC sequence consists of subtidal mudstones and argillaceous micrites grading into bioturbated micrites, pale micrites, intertidal microbial laminated micrites and domal stromatolites. They often terminate in 'birdseye' dismicrites with some terminating in red beds,

(Lithofacies 1). These indicate oxidation in a very shallow, possibly exposed peritidal environment. The peritidal portion of the cycles are thought to be aggradational (Pratt et al., 1992). PAC sequences may be interrupted at any stage by tidal channels (Fig. 3.1a &b) and are thought to be reset by either rhythmic eustatic change or jerky subsidence (Pratt et al., 1992). Calver (1989) suggests the cyclicity was probably developed by the repeated buildup to sea level and progradation of a tidal flat complex.

Fifteen PACs are recognised in the Myrtle Formation. Faulting, stylolitisation, dolomitisation and poor core recovery can collectively act to conceal PACs, making the recognition of all 15 at any one place difficult, and broad correlation between individual PACs unreliable. The Myrtle Formation is intermittently crosscut by tidal channels which also act to conceal PACs.

The Myrtle Formation presently crops out in the north, therefore, without a constrained upper contact, thicknesses are indeterminable. Towards the south the formation thins (Fig. 3.1a &b) such that only 6 of the 15 PACs are clearly recognisable. Whether deformation and stratigraphic loss has hidden these missing PACs or if they were indeed deposited remains in doubt. The formation then thickens again revealing all 15 PACs. Red beds of Lithofacies 1 are also seen on the peritidal tops of some PACs before the sequence becomes dramatically thinned in the very south. In the south, the Myrtle Formation contains two separate, roughly correlateable oo-biosparite and oomicrite shoals with minor oncoids (Fig 3.1b).

BLACK JACKS FORMATION

The Black Jacks Formation consists of alternating micrites, argillaceous micrites and mudstones together with biomicrites, calcarenites and calcisiltites. It has been subdivided into the lower and the upper Black Jacks Formation, which are separated by the Lords Siltstone Member.

lower Black Jacks Formation

The lower Black Jacks Formation contains two peritidal members which include two PACs, labelled as Black Jacks 1 (BJ 1) and Black Jacks 2 (BJ2). Black Jacks 1 and 2 correlate well across the basin (Fig. 3.1a &b). The lower Black Jacks Formation consists of calcarenites, minor sparites, biomicrites, argillaceous micrites, mudstones, and nodular limestone. It contains some silty interbeds and shows weak dolomitisation. It is also crosscut by many (0.5 to 2.5 m) tidal channels with Lithofacies 3, 4, 6, 7, and 8 represented. The lower Black Jacks Formation is conformably overlain by the Lords Siltstone Member, which contains angular rip up clasts presumably of the underlying lower Black Jacks Formation.

LORDS SILTSTONE

Regionally the Lords Siltstone is a thin discontinuous (1-20 m) micaceous siltstone - shale and fine sandstone that appears within the Gordon Limestone over much of Western Tasmania (Burrett, 1995). It sometimes contains calcareous nodules and beds of dark grey to black micritic limestone with bituminous films (Weldon, 1974). It is characterised by a distinctive non- diverse fauna consisting of abundant *Pliomerina* trilobites, strophomenid brachiopods, and the Tasmanian endemic ostracod *Dominina* (Burrett, 1995). Abundant bryozoa, orthids, rhynchonellids, gastropods, bivalves, echinoderms and some large cephalopods and trilobites are present throughout the unit.

At Grieves Siding, the Lords Siltstone forms a discontinuous, however traceable ridge throughout the field area. It ranges in thickness from 5 - 20 m and is faulted in the south (Fig. 3.1a &b). Two distinct traceable ridges are seen for up to 60 m in the south (Fig 1.2), however outcrop is nonexistent so the origin of the second ridge remains questioned. The Lords Siltstone supports a dense and varied heathland vegetation concealing outcrop. In drill core the unit is

predominantly a dark grey to green micaceous siltstone and fine sandstone, which is commonly bioturbated. The lower contact often contains angular rip up clasts of Gordon Limestone (Ellis, 1984) with a sharp upper contact into carbonate. Fossils recorded at Grieves Siding include *Sowerybites* brachiopods, corals and asaphid trilobites.

The Lords Siltstone is thought to have been deposited below wave base, with the silt and sand grains having by-passed the shallower carbonate tidal flats and shallower sea floor (Banks and Burrett, 1989). The Lords lithology and fauna does not appear suddenly, but is proceeded by a gradual deepening of both lithofacies and biofacies.

upper Black Jacks Formation

The upper Black Jacks Formation exhibits massive texturally destructive dolomitisation of Lithofacies 9 (Fig. 3.1a &b). Minor galena and pyrite is associated with the dolomitisation (Chpt. 4). Those sequences not dolomitised consist of pale, argillaceous and bioturbated micrites and alternating biomicrites of Lithofacies 2, 6 and 7. Calcarenites of Lithofacies 4 are also present and show moderate dolomitisation producing vuggy porosity. Calcarenite tidal channels are also present. The upper Black Jacks Formation contains a subtidal to intertidal fauna especially corals, stromatoporids and the large oncoids of Lithofacies 5. Weaker dolomitized peritidal horizons can be distinguished and reveal some PACs. An additional peritidal assemblage, referred to as the upper peritidal member (Fig. 3.1a &b) by Burrett (1995) contains up to 5 PACs.

3.4.3 CROTTY QUARTZITE

The Crotty Quartzite lies on the western side of the mapped area (Fig. 1.2) and forms the basal unit of the Silurian Eldon Group (Baillie, 1989). It exhibits a disconformable basal contact with the underlying Gordon Limestone, and has a gradational conformable upper contact with the Amber Slate. Rolled fragments of *Tetradium* sp. from the Gordon Limestone are used as evidence by Pitt (1962) for the presence of the disconformity. Zeehan is the type area for the Crotty Quartzite where it reaches its maximum thickness of 487 m (Banks, 1989). The unit was named after the Crotty township, established by Irishman James Crotty

in 1891. It outcrops strongly at Grieves Siding, to form a sharp elevated ridge. A dense vegetation cover and surficial weathering conceals exposure to fresh rock, subsequently most fresh exposure is restricted to road cuttings, creeks, and disbanded drill pads.

At Grieves Siding the typical Crotty Quartzite is a relatively homogeneous, well bedded unit consisting of quartz sandstones, quartz clastic pebble conglomerates and minor mudstones. Fresh surfaces exhibit a pink colouration, dulling to white-grey in weathered specimen. Quartzite beds are most commonly pink in colour and display a sugary appearance with grains between 0.5 - 2mm. Quartz clastic pebble conglomerates or 'grits' are matrix supported, moderately sorted, with sub-angular to sub-rounded 1 - 6 mm quartz clasts. The matrix consists of finer sand grains. Quartz sandstones and quartz clastic pebble conglomerates have variable bed thicknesses (10 cm - >1 m), and are often cross bedded, conversely interbedded grey-brown micaceous mudstones - shales are thinly bedded and laminated. Cross bedding occurs up to metre scale and indicates a tentative northerly palaeocurrent direction.

Pitt (1962; p. 62) compiled a complete stratigraphy of the Crotty Quartzite in the Zeehan area, recognising four constituent members (Fig. 3.4). Member A disconformably overlies the Gordon Limestone and consists of current bedded coarse grained silts, calcareous sandstones, quartzose sandstones, and fine pebble conglomerates (Pitt, 1962). Brachiopod moulds were the only fossils recognised. Member A is conformably overlain by Member B which consists of strongly current bedded, poorly sorted quartzose pebble conglomerates, pebbly arenites, thinly bedded well cleaved siltstones, and current bedded pale grey sandstones (Pitt, 1962). Some slump structures occur and some beds contain worm casts sub-parallel to the bedding surface. Other fossils retrieved include *Tetradium* sp. fragments, the brachiopod *Camarotoechia synchoneua*. as seen by Gill (1950), trilobite pygidia, pelecypods, and unidentified brachiopods. Member C consists of homogeneous coarse grained clay rich siltstones, and is overlain by Member D, the uppermost member. It is composed of pale pink strongly cross bedded quartz sandstones, with interbedded silts and muds, and cobble conglomerates (Pitt, 1962). It fines up towards the top of the sequence which indicates these beds are right way up. Arthropod tracks and scattered tubicolar bodies along with planispirally coiled gastropods, cephalopods, and pelecypods are found in this member (Pitt, 1962).

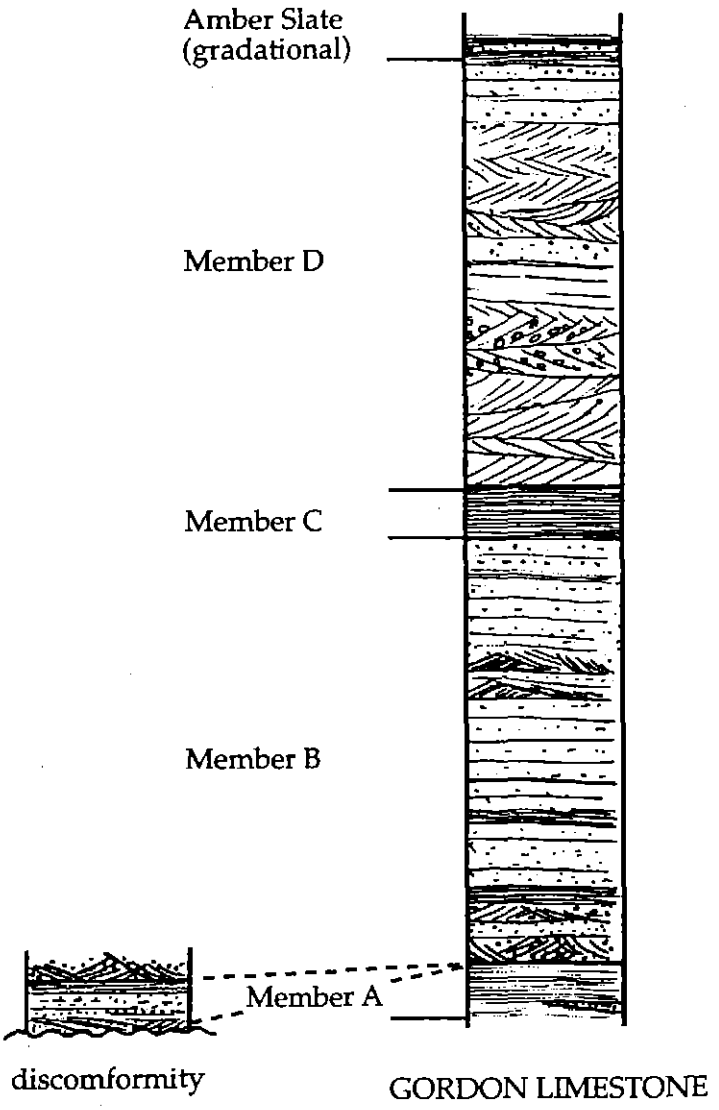

Figure 3.4: Stratigraphic section for the Silurian Crotty Quartzite. The sequence reaches a maximum thickness of 487 m and has been divided into four members by Pitt (1962). (Modified after Pitt, 1962).

Previous work by Gill and Banks (1950) described tubicolar structures normal to bedding planes, with Blissett (1962) noting moulds of large crinoid ossicles in a number of places. Biostratigraphic correlations by Gill (1950) suggested the Crotty Quartzite is Upper Silurian in age.

3.5 *STRATIGRAPHY AND PALAEOENVIRONMENTS*

The Early to Middle Ordovician Moina Sandstone was deposited during a period of quiescence and shallow water sedimentation (Banks, 1989). Cross bedding and ripple marks indicate a southerly palaeocurrent direction on what may have been a shallow, subtidal to peritidal flat. The presence of *Arenicolites* sp. is suggested by Banks (1989) to represent a littoral to sublittoral marine environment. The Moina Sandstone overlies slope or basinal deposits and shallow marine alluvial fans (Mt Zeehan Conglomerate) in a sequence suggested by Banks (1989) as indicating a Late Cambrian regression. Cessation of sandstone deposition and the initiation of limestones may suggest a depleted sandstone source or signify the start of the Early to Middle Ordovician transgression.

Carbonate sedimentation at Grieves Siding occurred on a mini-platform, and was related to 4 main depositional sites: (i) intertidal-supratidal flats, (ii) lagoonal and restricted lagoonal, (iii) intertidal-subtidal bars and shoals, (iv) shallow to medium subtidal open shelves and platforms. Such conditions existed during a marine transgression from the south, west and east towards the Precambrian - Cambrian Tyennan and Rocky Cape regions (Burrett, 1995). The transgression started in the Tremadoc and continued into the Late Caradoc or even Early Ashgill (Burrett, 1995). Carbonate sedimentation occurred in a tropical environment with an Ordovician seawater temperature between 23 and 25°C (Rao, 1990). Modern analogues of this depositional environment can be seen on the Great Bahama Bank and in the Persian Gulf. Suitable depositional models would be that of Irwin-Lees (1965; Fig. 3.5), and Tucker (1981; Fig 3.6a &b).

Carbonate deposition on the Great Bahama Bank occurs on an extensive platform in water depths of less than 8 m. The climate is humid and subtropical with a latitude between 22° and 28°N. It has very little terriginous input which allows the formation of platform carbonates (Rao, in press). Subtidal, intertidal and supratidal carbonates occur on the platform, with the facies present very similar to those at Grieves Siding. The flora is dominated by calcareous algae with fauna including corals, echinoderms. Non-skeletal grains are dominated by ooids, pellets, intraclasts and aggregates (Pratt et al., 1992). Apart from modern day biota and climate, the Bahama bank represents an environment analagous to the lower sequences at Grieves Siding.

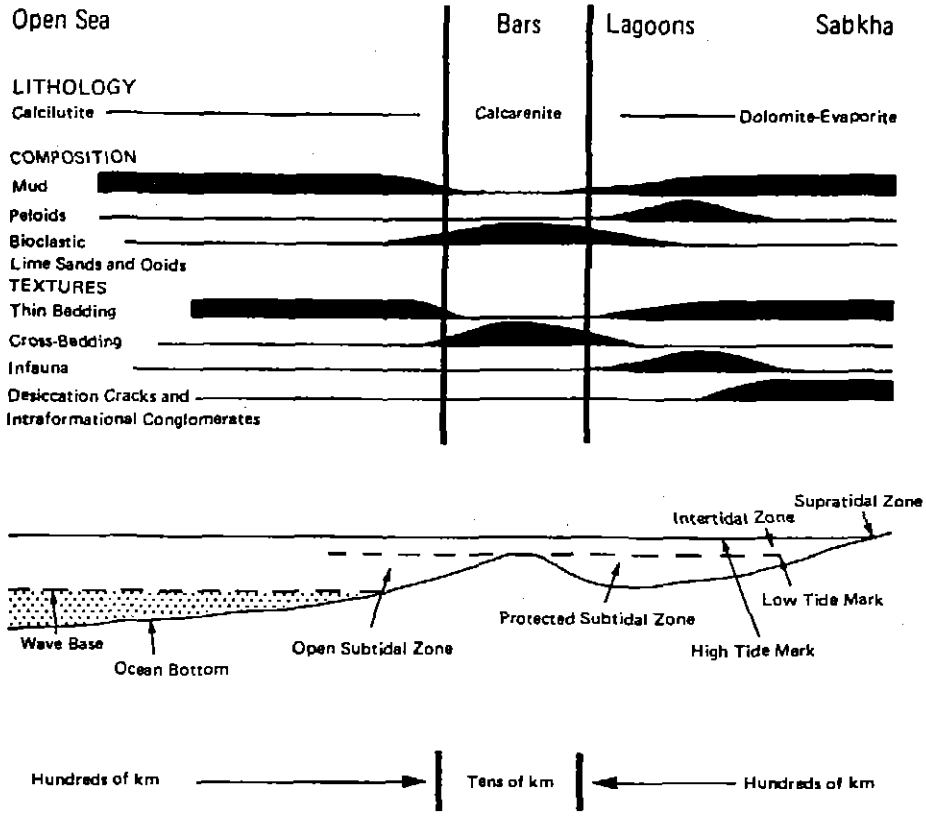

Figure 3.5: Simplified representation of the Irwin model (1965) for carbonate sedimentation, (From Tucker, 1982).

Tidal complex carbonate deposition similar to that inferred responsible for the formation of the middle Grieves sequence (especially the Myrtle Formation) is observed in the Persian Gulf. Although the Persian Gulf is situated in arid subtropical latitudes (24° to 30°N), carbonate deposition is analogous. The Great Pearl Bank acts as a coastal barrier which allows the formation of coastal lagoons, tidal channels, intertidal flats, and a coastal sabkha. Along with modern fauna, lagoons in the Persian Gulf contain gastropods and pellets. Intertidal areas contain abundant algal mats while supratidal areas contain muds, evaporites and algae. The sabkha contains many different forms of gypsum, anhydrite, and halite along with dolomite.

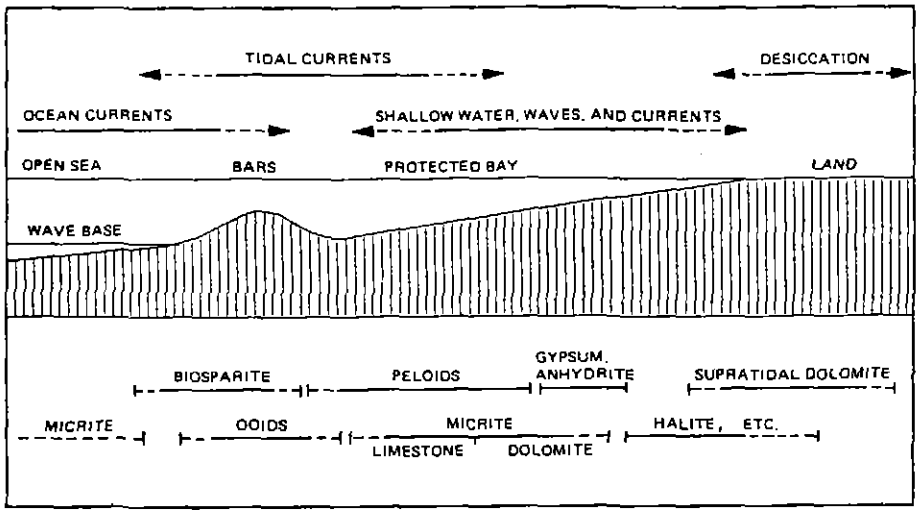

Figure 3.6 (a): Environmental factors and sediment formation according to the Irwin model (1965).

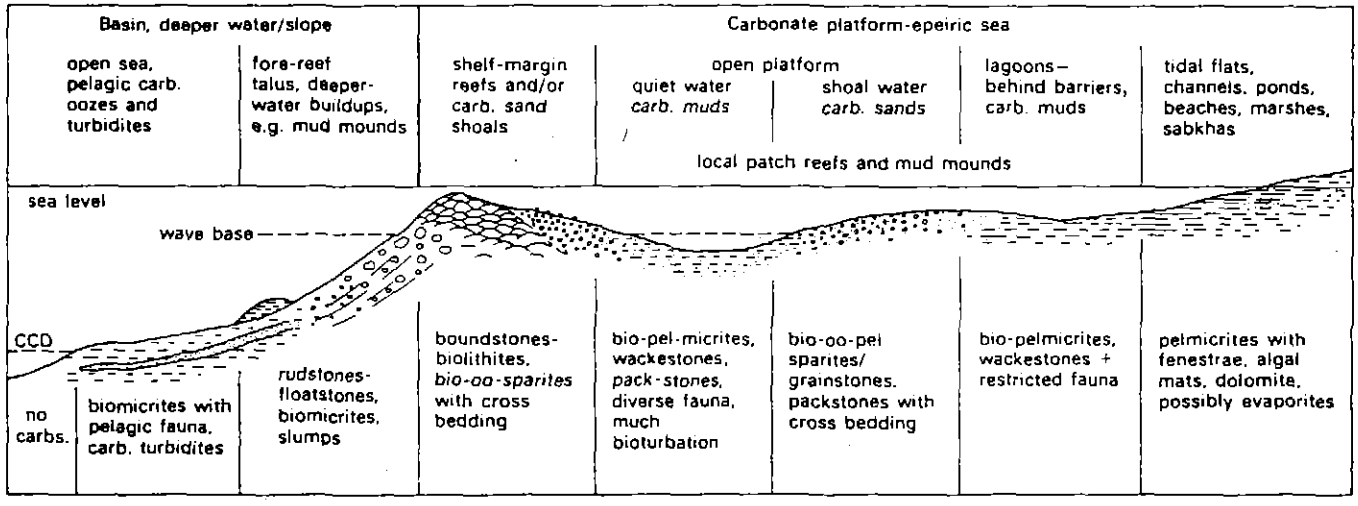

Figure 3.6 (b): Principal marine depositional environments of carbonate sediments and their facies characteristics (From Tucker, 1982).

3.5.1 *Lithostratigraphic Unit deposition*

Lithofacies of the Ugbrook Formation were deposited in subtidal and protected subtidal lagoons formed behind northerly or northeasterly migrating carbonate bars (Burrett, 1995). Pelloidal and bioturbated argillaceous micrites, mudstones and biomicrites of Lithofacies 6 and 7 were deposited in such an environment with nodular limestone of Lithofacies 8 also present. A rich subtidal fauna dominated by corals, stromatoporids and brachiopods was also developed in these lagoons. The calcarenite member and associated oosparites and pelbiosparites formed in association with these migrating bars. Significant ooid shoals associated with the calcarenite member formed at the mouth of tidal channels which connected lagoons and the open shelf. The formation of these isolated sparites and ooid shoals suggests the bars were breached in several locations (Fig. 3.7). Ooids together with skeletal carbonate sands may have also formed barriers and shoals on the carbonate bar (Fig. 3.8). The rounded and subrounded nature of clasts in some sparites suggests deposition in less than 5 - 10 m (Tucker, 1981). Otherwise ocean and tidal currents provided the energy required for a sparry matrix and ooid shoals. Further ooids and minor PACs observed in the Ugbrook Formation were deposited on intertidal, tidal flat islands within the lagoon (Burrett, 1995; Fig. 3.7).

As the transgression continued the carbonate bars moved north from Grieves into Myrtle during Late Ugbrook time (Burrett, 1995). Further work by Burrett (1995) in the north suggests stabilisation of the migrating bars occurred during the Upper Blackriveran (Early Caradoc) which resulted in the Ugbrook Formation being covered by the Myrtle Formation. Radiometric age determinations show a clustering of ages about 445 Ma (Early Caradoc) which could correspond to fault movement (Banks, 1989). Faulting could have ended Ugbrook Formation deposition by producing significant shallowing, thus allowing the formation of PACs. Alternatively faulting assisted or caused the stabilisation of the carbonate bars allowing the development of PAC sequences of the Myrtle Formation.

The Myrtle Formation was deposited on an upper intertidal to supratidal flat during the Blackriveran. With a transgressive sea level and a stabilised carbonate bar, the Ugbrook Formation was soon covered with argillaceous micrites calcisiltites and biomicrites as the carbonate factory kept up.

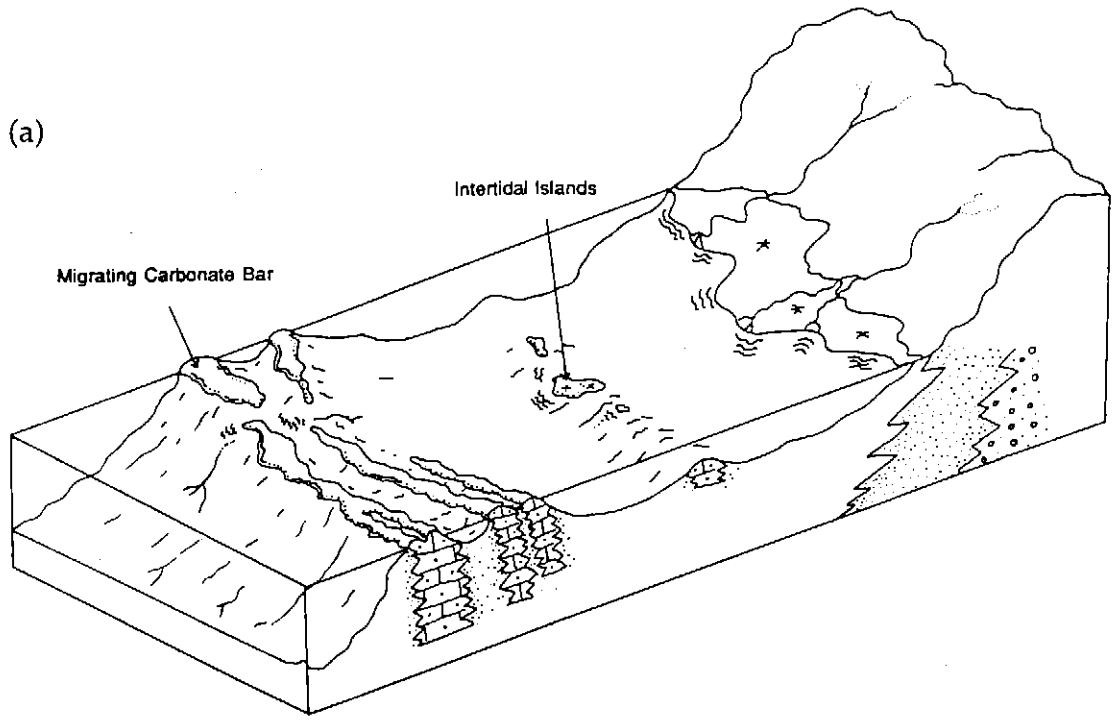

Figure 3.7: Early Caradoc environmental reconstruction of the Ugbrook Formation. Deposition was influenced by a either traditional migrating carbonate bar (a), or an extensive migrating offshore bar complex (b).

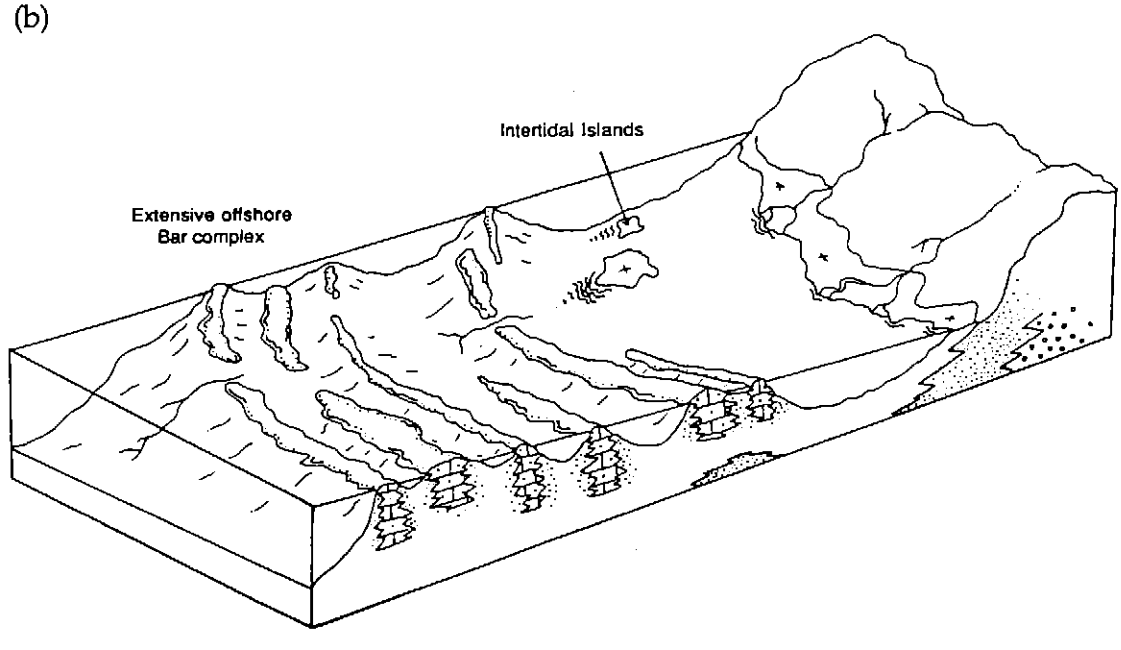

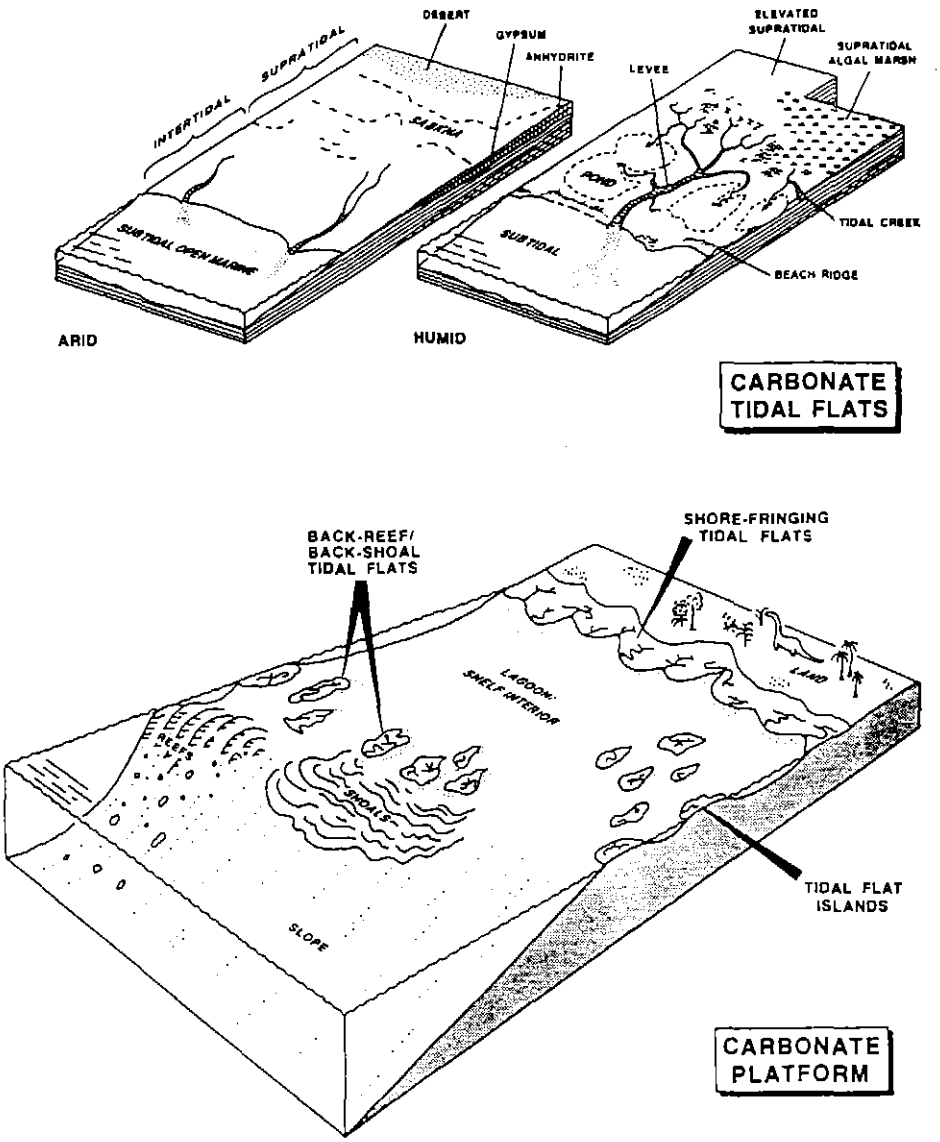

Figure 3.8: Block diagram of a carbonate tidal flat and platform showing locations of tidal flats, carbonate sand shoals, and tidal flat islands. Similar depositional environments are invoked at Grieves Siding for the Ugbrook Formation. (From Pratt et al., 1992).

Burrett (1995) suggests the upper supratidal shoreline at this time had moved north towards Duck Creek and east onto the Tyennan Region. Therefore Grieves Siding would have formed an upper intertidal to peritidal flat allowing the formation of PACs. I suggest a high water mark shoreline close to DDH ZG 410 in which accretion of PAC sequences occurred. Calver (1977) suggests this upper intertidal to peritidal flat represents a prograding tidal flat (Fig. 3.9), repeatedly

renewed by apparently abrupt upward changes in sea level relative to the depositional surface. An upward abrupt change in sea level causes a second prograding tidal flat sequence to be deposited over the first (Calver, 1977), and thereby building the Myrtle Formation.

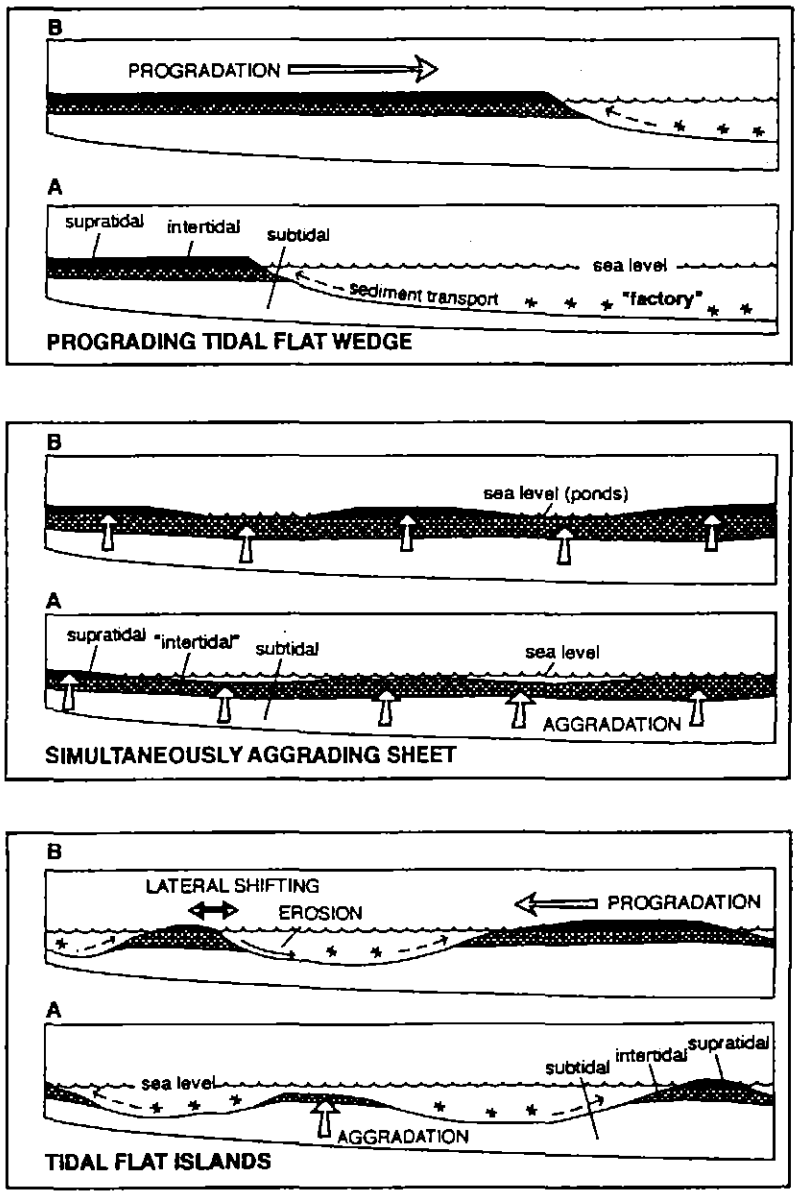

Figure 3.9: Diagrams illustrating various ways in which metre-scale, peritidal, shallowing up successions can form. A prograding wedge may have initiated from a location near DDH ZG 406. (From Pratt et al., 1992)

A significant deepening event ended deposition of the Myrtle Formation. Burrett (1995) suggests an increased rate of basin subsidence or an inability of the carbonate factory to keep up with a rising sea level as a cause of deepening. Alternatively, movement on a fault (Firewood Siding Fault?) could cause a significant deepening. Corbett (1985) suggests activity on the Firewood Siding Fault in the Late Cambrian - Early Ordovician, perhaps movement in the Blackriveran produced this deepening. Radiometric age determinations of faults show multiple movements relevant to the entire sequence at Grieves. Faulting is therefore likely to have initiated and ceased sedimentation of some of the units. The maximum concentration of ages occurs around 475 Ma with another population at 455 Ma (Banks, 1989). These represent significant periods during the deposition of the sequence at Grieves Siding and deserves more attention. The probability of mineralisation being related to such fault activity is high.

Open subtidal argillaceous micrite, biomicrites, oncomicrites and mudstones of the Black Jacks Formation were deposited over the Myrtle Formation. Deposition was largely below wavebase with graded units and shell lags being produced by periodic storms. Open shallow subtidal conditions briefly gave way to lower intertidal deposition of calcarenites and oncoids and brief high intertidal to peritidal deposition of two separate PACs, (BJ1 and BJ2). These could represent deposition on tidal flat islands or a peritidal flat. A deepening in both lithofacies and biofacies occurs in the Black Jacks Formation before the interruption of the Lords Siltstone Member.

The Lords Siltstone was deposited during the mid-Trentonian (Late Caradoc) in response to uplift in the Tyennan region (Burrett, 1995). It is thought to have been deposited below wave base, with the silt and sand grains having by-passed the shallower carbonate tidal flats and shallower sea floor (Banks and Burrett, 1989). It appears over the whole Tasmanian mini-platform, and is thought to represent a significant but short lived tectonic event. Burrett (1995), suggests it could represent an epeirogenic episode during the mid Trentonian.

Shallow subtidal conditions resumed after the Lords event which resulted in the deposition of the remaining Black Jacks Formation consisting of Lithofacies 5,6,7, and 8. A significant interlude within the formation saw the deposition of a peritidal sequence consisting of up to five PACs. This upper peritidal member (Burrett, 1995) is likely to represent deposition on a short lived peritidal flat

before the resumption of shallow subtidal deposition. The development of this peritidal flat may have been fault related as it suddenly appears without shallowing of lithofacies or biofacies.

The entire limestone sequence at Grieves Siding is similar to the shoaling upward sequence of Tucker (1982; Fig. 3.10). Tucker (1981) suggests these sequences are typically several metres thick. Perhaps Grieves Siding represents a very thick shoaling-up sequence.

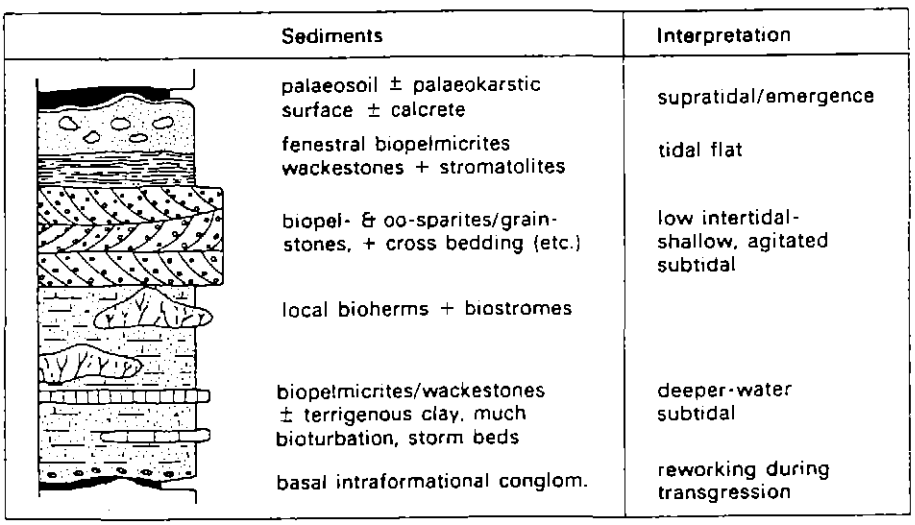

Figure 3.10: Shoaling up limestone sequence of Tucker (1982). Such sequences are typically several to many metres thick. Grieves Siding may represent a shoaling up sequence, 1 km thick, developed during a transgression. (From Tucker, 1982).

Gordon Group carbonates are either conformably or disconformably overlain by the Crotty Quartzite. The disconformity has been correlated by Pitt (1962) to the Late Ordovician (Llandovery) Benambran Orogeny. It signifies the beginning of uplift in the Ashgill that rapidly spread clastic material over the carbonates (Banks, 1989). The Benambran Orogeny was well developed in New South Wales and Victoria, and correlates temporally with the disconformity under the Crotty Quartzite. The Crotty Quartzite was deposited rapidly with little subsequent reworking (Pitt, 1962). Large scale cross bedding and faunal elements indicates a shallow marine, littoral to sublittoral depositional environment. The

deposition of dominantly shallow marine interbedded quartz sandstones, mudstones and subordinate limestones of the Eldon Group continued until the Tabberabberan Orogeny in the Devonian (Banks, 1989).

3.5.2 Dolomitisation

Both syngenetic and epigenetic dolomitisation occurs in the Grieves Siding stratigraphy. Syngenetic dolomitisation was seen with large compositionally zoned dolomite rhombs and finer grained matrix dolomites in supratidal lithofacies. As in the Bahamas, Florida and the Arabian Gulf, these could have precipitated on hard grounds in the supratidal zone and occur to a depth of around one metre (Tucker, 1981). The large rhomb size (3 - 4 mm) and compositional zonation suggests slow recrystallisation rates. Finer grained matrix dolomite in supratidal units is most likely penecontemporaneous or early diagenetic.

Epigenetic dolomitisation occurs as both selective and pervasive dolomite. Various mechanisms could be responsible for producing these dolomites. Evaporative pumping producing evaporative-supratidal dolomitisation could produce a widespread dolomite horizon (Tucker, 1981). Alternatively dolomitisation resulting from mixing of seawater and meteoric water could account for widespread texturally destructive dolomites. The weakly mineralised dolomite horizon immediately below the Lords Siltstone could have formed by a process suggested by Kahle (1965) invoking increasing the Mg/Ca ratio of porewater with no salinity increases. This could occur by leaching of Mg adsorbed on to clays and silts of the Lord Member. Other scattered dolomite rhombs seen in some lithofacies, especially those containing argillaceous material could form from this process. Perhaps the pervasive dolomitisation seen in the upper Black Jacks formation resulted from Mg derived from the argillaceous lagoonal to subtidal lithofacies observed within the formation. In non-argillaceous lithofacies, the scattered rhombs could reflect a local source of Mg from high Mg calcites (Kahle, 1965). Pervasive dolomitisation in the upper Black Jacks Formation and below the Lords Siltstone member could also be related to fluids associated with faulting and perhaps mineralisation. Implications of faulting, dolomitisation and mineralisation is described in Chapter 4.

3.6 SUMMARY

The lithologies occurring at Grieves Siding are contained within the Wurawina Supergroup, which consists of a concordant sequence of predominantly shelf deposited sediment, including the Denison Group, the Gordon Group, and the Eldon Group. The Moina Sandstone, uppermost member of the Denison Group has a conformable, often interdigitating contact with the Gordon Group carbonates. The positioning of this contact is contentious as it is marked by a siltstone-mudstone transitional zone that is often mineralised. This study defines the contact between the Denison Group and the Gordon Group as the last appearance of consolidated silt, and the first appearance of limestone.

Nine lithofacies associations recognised in the Gordon Limestone at Grieves Siding have been configured into three formations, and five intra-formational members. The mid-Ordovician Ugbrook Formation represents subtidal and protected subtidal lagoons influenced by a rapidly migrating carbonate bar. The mid-Caradoc, (Mid to Late Ordovician) Myrtle Formation consists of up to 15 Punctuated Aggradational Cycles (PACs) deposited in shallow subtidal to peritidal conditions. The Myrtle Formation precedes deposition of the dominantly subtidal Black Jacks Formation, which was interrupted during the Late Caradoc by the Lords Siltstone. The Lords 'event' signifies the response to uplift in the Tyennan region, representing a short lived epeirogenetic event. It was proceeded by a return to subtidal limestone deposition, periodically interrupted by peritidal carbonate deposition. Stratigraphic correlation suggests carbonate deposition is related to four main depositional sites on a carbonate platform. Carbonate sedimentation occurred in a tropical environment with an Ordovician seawater temperature of 25°C. Modern analogous depositional environments are seen on the Great Bahama Bahama Bank, and in the Persian Gulf.

Mineralisation 4

4.1 INTRODUCTION

This chapter characterises the setting, morphology, mineralogy and paragenesis of two lenses of mineralisation found in the Gordon Limestone at Grieves Siding. High grade Zn-Pb mineralisation occurs towards the top of the ferruginous and kaolinitic siltstones that mark the contact between the Moina Sandstone and the Gordon Group carbonates (Fig. 4.1). This mineralisation has been intersected in diamond drill core and is exposed on the surface where it supported a small prospect. Further mineralisation has been recognised away from this major zone. Sphalerite, galena and pyrite have been found in dolomites of the lower Black Jacks Formation, marcasite has been recognised in costeans, and minor disseminated pyrite occurs throughout the sequence.

4.2 LOCAL AND STRUCTURAL SETTING OF MINERALISATION

4.2.1 Lower Mineralised Zone

Mineralisation occurring at the contact between the Moina Sandstone and the Gordon Group carbonates is herein referred to as the Lower Mineralised Zone (LMZ). The LMZ is a discontinuous lens that occurs above the lower silt member and appears to be stratabound (Fig. 4.2). The mineralised lenses and the lower silt member occur in beds dipping between 40° and 70° to the north-east and are folded around a large (~3 km) synform with an inferred fold axis orientation of 70-110°. Brittle deformation produced apparent sinistral slip-strike offset on the Grieves Fault displacing the LMZ approximately 40 m. The LMZ crops out on the surface at the abandoned prospect, proximal to the Grieves Fault. Although now totally overgrown, the prospect can still be found by following an abandoned tramway from the Henty Road (Fig 4.2). Minor exploitation of this prospect occurred during the late 1800's, however details of the operation are unknown. Mineralisation above the LMZ occurs in vuggy dolomite of the Ugbrook Formation. Textural and paragenetic similarities results in it being included in the same discussion.

4.2.2 *Upper Mineralised Zone*

Sulphide mineralisation below the Lords Siltstone in dolomites of the lower Black Jacks Formation (Fig 4.2), is herein referred to as the Upper Mineralised Zone (UMZ). The UMZ may occur as conformable discontinuous lenses, however a lack of outcrop and the discontinuous nature of mineralisation has obscured its full extent. Alternatively, it could be a series of isolated occurrences. It is commonly associated with significant siderite alteration.

4.3 *LOWER MINERALISED ZONE (LMZ)*

4.3.1 *INTRODUCTION*

Mineralisation in the lower mineralised zone (LMZ) consists of sphalerite, galena, barite, pyrite and chalcopyrite with a siderite - dolomite - hemimorphite gangue. Smithsonite, rhodochrosite, magnesite, and covellite are also present. The LMZ occupies a lens above the lower silt member that appears to be stratabound (Fig. 4.1). Mineralisation is discontinuous, occurring in lenses that reach a maximum thickness of 24 m in diamond drill hole ZG 406 (Fig 4.1). The lower silts extend laterally north from Grieves Siding for up to 50 m. The best intersections from this zone were 10.6 m @ 17.8% Zn, (including 0.4 m @ 37.4% Zn), and 4 m @ 5.4% Zn, 5.4% Pb, in diamond drill hole ZG 406 (Fig. 4.3).

Comb and cockade textures are common throughout the LMZ (Plate 4.4e), however colloform growth-banded sphalerite spherules are the most common and spectacular sulphide texture (Plate set 4.1). They provide useful insights into the genesis of sulphide mineralisation.

4.3.2 *MINERAL PETROGRAPHY OF THE LMZ*

Mineralogical and textural variations throughout the LMZ necessitates samples collected from different intervals to be discussed separately. Subsequently the mineral petrography of the LMZ intersected in drill core is described first, before describing high grade Zn-carbonate mineralisation and textures seen at the Grieves Siding Prospect. Mineralisation above the LMZ in vuggy dolomite of the Ugbrook Formation is not apart of the LMZ proper, but is included in this discussion.

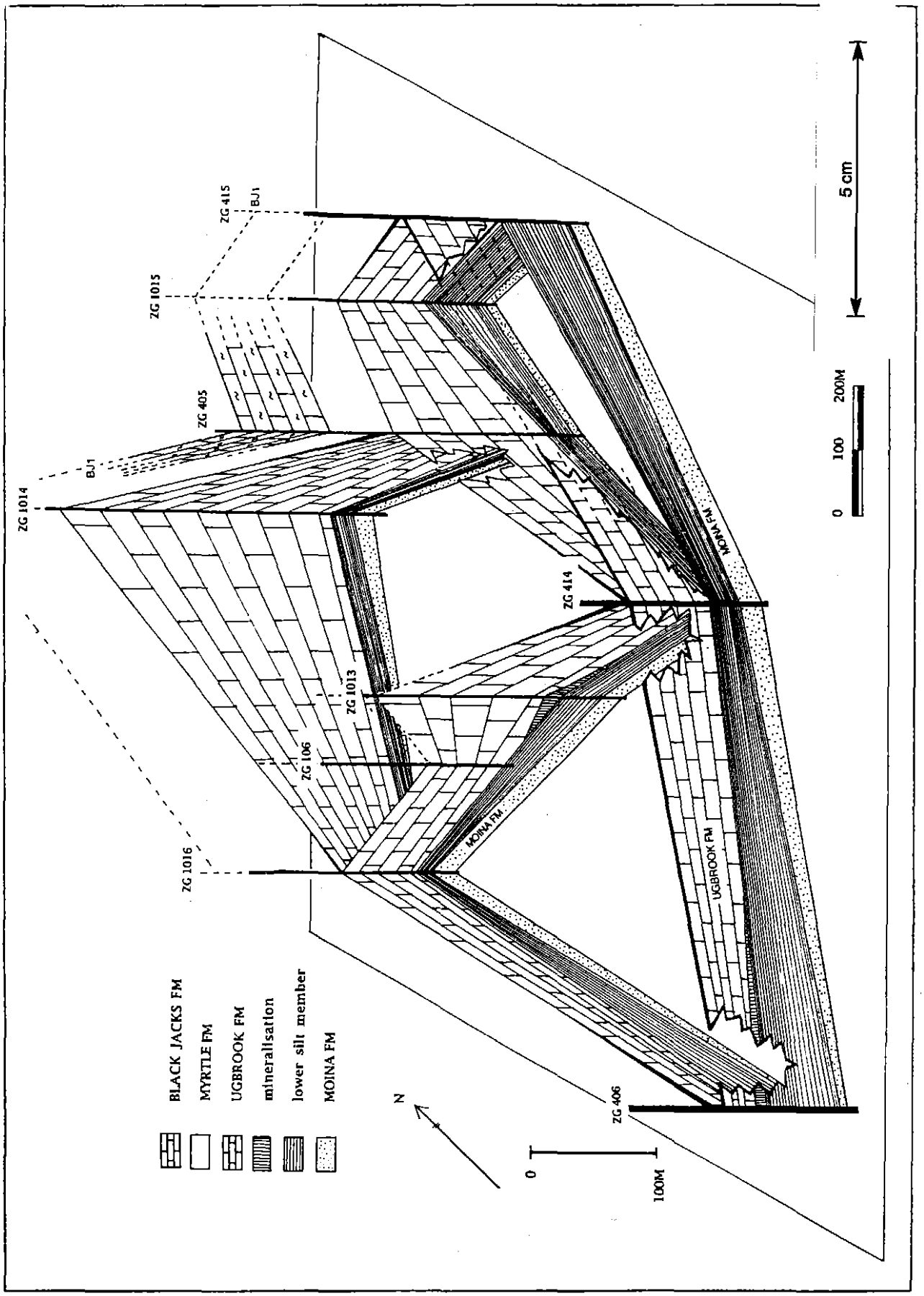

Figure 4.1: Fence diagram showing the stratabound nature of the lower Silt member, and the discontinuous mineralised lenses of the LMZ at North Grieves Siding.

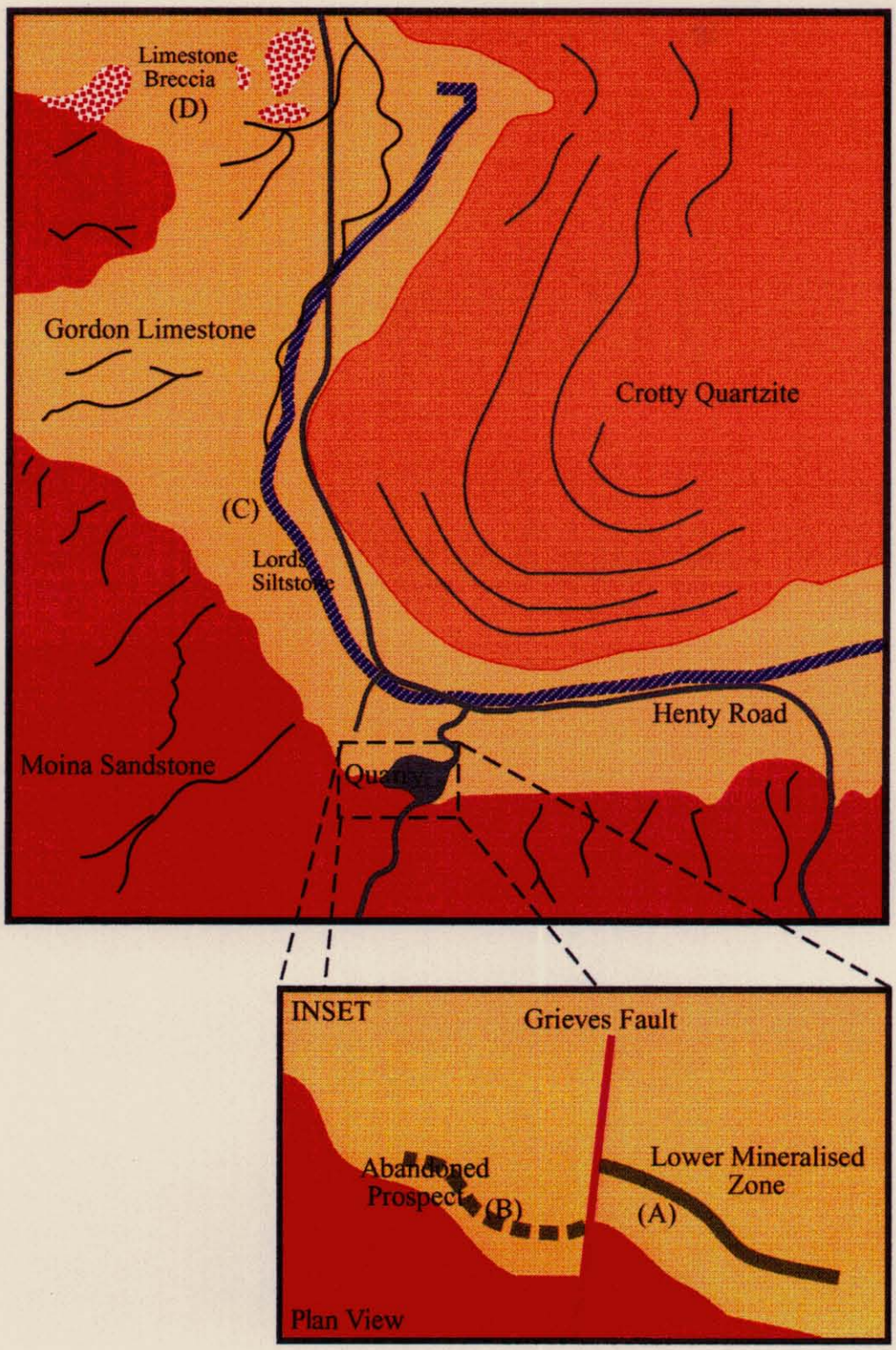

Figure 4.2: Generalised location of mineralisation at Grieves Siding.
(a) Lower Mineralised Zone; (b) Abandoned Grieves Prospect;(c) Marcasite and the UMZ; (d) Silicified dolomite breccia.

4.3.2.1 *Diamond Drill Hole Intersection*

At its thickest point in DDH ZG 406 the LMZ contains white to light grey semi-massive sulphide mineralisation. The semi-massive sulphides contain remnant dolomite and carbonate wall rock in addition to sulphides, siderite and hemimorphite.

1) *Pyrite*

Pyrite occurs as 0.3 mm euhedral crystals growing into cavities, and as 0.1 mm fractured subhedral aggregates (Plate 4.4e). Pyrite framboids are common, and occur as circular, elongate, and as partly recrystallised aggregates or spherical grains up to 0.1 mm in diameter. Disseminated pyrite also occurs throughout remnant dolomite. Pyrite comprises up to 60% of the sulphides present, and together with minor (<1%) galena contributes to the comb texture.

2) *Sphalerite*

Sphalerite exists as small (0.025 mm) spherules occurring around pyrite and into cavities off siderite and other wallrocks. Anhedral, partly replaced sphalerite occurs locally. Sphalerite comprises up to 40% of the sulphides present. The small, circular, honey-coloured spherules of sphalerite have formed tightly packed aggregates between pyrite, accentuating the comb texture.

3) *Calcite*

Fine grained calcite (0.04 mm) has coated the walls of some cavities and occurs on the margins of pyrite and sphalerite crystals that have defined the comb textures. Calcite also occurs as euhedral to subhedral crystals in some cavities. Fine calcite (1μm) commonly coats euhedral (0.04 mm) calcite crystals.

5) *Hemimorphite*

Radiating, fibrous hemimorphite [$Zn_4Si_2O_7(OH)_2.H_2O$] fans and veins cross-cut and replace most of the gangue phases (Plate 4.4h). Hemimorphite needles have replaced the wallrock in some places, and filled cavities elsewhere. It occurs as radiating bow-tie and fan-shaped crystals (Plate 4.4f and g) up to 0.7 mm in diameter. The hemimorphite veins and host carbonate appear to have been folded and fractured during later tectonic activity (Plate 4.4h).

4.3.2.2 *High grade Zn- carbonate mineralisation*

Massive grey to light brown, zinc carbonate mineralisation occurs toward the top of the LMZ. The non-sulphide mineralised zone consists of a fine grained intergrowth of calcite, siderite, dolomite, smithsonite ($ZnCO_3$), rhodochrosite, and magnesite. Altered and mineralised samples have very high specific gravity, are hard, and occur in a 0.4 m interval in DDH ZG 406 that grades at up to 37.4% Zn. Dolomitisation and a siderite overprint obscure remnant carbonate textures, and in many intersections the carbonate mineralised zone has partly decomposed to a distinctive dark grey to brown clay, which retains the high zinc grades. XRD analysis of these clays (Appendix 3) suggests they are dominated by a kaolinite group mineral dickite [$Al_2Si_2O_5(OH)_4$], (>60%), with lesser quartz (50%), illite (30%) and hematite, geothite, crandalite, and rutile (<5%).

4.3.2.3 *The Grieves Prospect*

Excellent examples of colloform textures are found at the surficial expression of the LMZ at the Grieves Prospect (Fig. 4.2). Colloform, growth-banded sphalerite spherules, and botryoidal sphalerite are intimately associated with galena and pyrite (Plate 4.1). Sphalerite is the most abundant sulphide, with XRD analysis suggesting it comprises between 40 and 60 % of mineralisation, with 25 - 40 % galena. Pyrite, chalcopyrite and covellite make up less than 5 % of the rock. Barite comprises 5 - 10 % of the gangue with kaolinite comprising less than 5 wt% (Appendix 3)

1) *Sphalerite*

Sphalerite spherules up to 2 cms project from the wallrock into cavities (Plate set 4.1). The comb textures seen in the LMZ in drill core is also present at the surface, however the large growth of sphalerite spherules has distorted and overprinted the texture (Plate 4.1c). A thin (up to 1 mm) lining of siderite on the dolomite wallrock is overgrown by the 0.1 mm to 2 cm sphalerite spherules. Up to four different phases of sphalerite are present (Plate 4.1a and b). Initial minor massive sphalerite, was preceded by galena precipitation. The second phase resulted in deposition of colloform sphalerite spherules. The third phase produced massive sphalerite which forms cusp and caries textures with galena. The cusp and caries textures grade into well developed relict textures. The third

Plate 4.1

Plate 4.1 a : Photomicrograph of the botryoidal, colloform, sphalerite spherules (sp) from the Grieves Prospect (DDH ZGP1, reflected light, Field of view ≈ 1 mm)

Plate 4.1 b : Botryoidal, colloform, banded sphalerite from the Grieves Prospect (DDH ZGP1). Pyrite (Py) fills the centre of most spherules, followed by sphalerite (sp) forming the concentric bands. Later stage low Fe sphalerite (sp) infills between spherules (DDH ZGP1, transmitted and reflected light, field of view ≈ 4mm).

Plate 4.1 c : Higher magnification view of the botryoidal sphalerite spherules. Early stage pyrite (Py) is overprinted by later spherule growth(sp) producing the dendritic texture (DDH ZGP1, transmitted light, field of view ≈ 1 mm).

Plate 4.1 d : Dendritic texture produced by bacteria(?) in sphalerite spherules (DDH ZGP1, transmitted light, field of view ≈ 1mm).

Plate 4.1 e : Transmitted light photomicrograph of a sphalerite spherule margin showing dendritic patterns attributed to bacteria(?) (DDH ZGP1, transmitted light, field of view ≈ 2mm).

Plate 4.1 f : High magnification photomicrograph of radiating bacteria(?) near the margin of a sphalerite spherule (DDH ZGP1, transmitted light, field of view ≈ 0.5 mm).

Plate 4.1 g : High magnification photomicrograph of the dendritic texture towards the margin of a sphalerite spherule (DDH ZGP1, transmitted light, field of view ≈ 0.5 mm).

Plate 4.1 h : SEM image of what have been interpreted as bacterial filaments responsible for producing the dendritic textures seen in previous plates. The particles have now been replaced by up to 8 μm sphalerite grains.

phase sphalerite has in-filled spaces between spherules and within spherules. A fourth phase of light coloured, semi-translucent (low-Fe) sphalerite occurs on the outside of, and between spherules (Plate 4.1a). It forms fracture in-fill textures between spherules, and contains large (0.05 mm) fluid inclusions.

2) *Pyrite*

The colloform banded spherules contain fibrous, radiating pyrite that have relict and fracture in-fill textures. Anhedral and fractured pyrite occurs as 0.1 - 0.4 mm grains that form a radiating, fibrous pattern in the spherules (Plate 4.1c). Some fractures within the pyrite are filled by massive sphalerite and galena. Others contain 2.5µm circular, deep honey-coloured sphalerite grains that have replaced what have been interpreted as mineralised bacterial filaments (Plate 4.1e to h). These filaments form a dendritic pattern in the pyrite and galena, adding to the fibrous appearance (Plate 4.3d). Scanning electron microscopy of the particles could not positively identify what these structures where, but they are now replaced by fine grained sphalerite (Plate 4.1h). The size and shape are consistent with bacteria, however overprinting by mineralisation makes identification difficult.

3) *Galena*

Galena has formed cusp and caries textures with dendritic pyrite, producing a fracture in-fill texture. Massive to semi-massive galena crystals (up to 1 mm) occur in and around sphalerite spherules (Plate 4.1a), as well as in a distinctive band that has overgrown the first comb texture.

4) *Chalcopyrite*

Chalcopyrite occurs on some fractures within late stage, low Fe sphalerite where it has formed weak cusp and caries textures. Chalcopyrite occurs as subhedral 0.8 mm grains which are typically fractured and contain angular sphalerite inclusions. Chalcopyrite is also found close to the edge of some sphalerite spherules, where it is locally decomposed to contain secondary covellite. Covellite occurs as 2.5 mm grains in fractures with chalcopyrite.

Plate A

Plate B

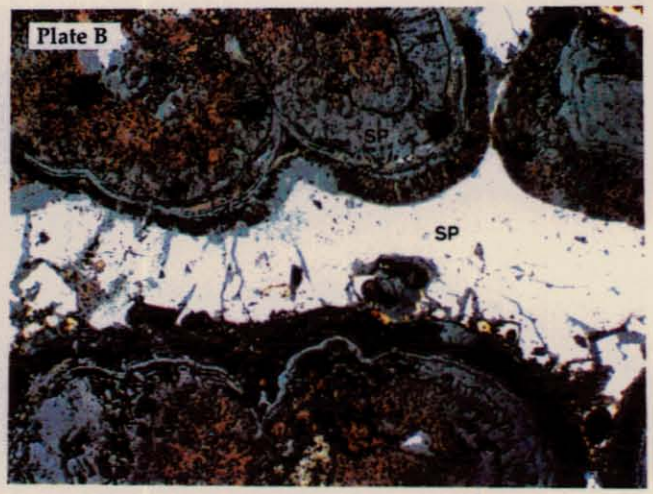

Plate C

Plate D

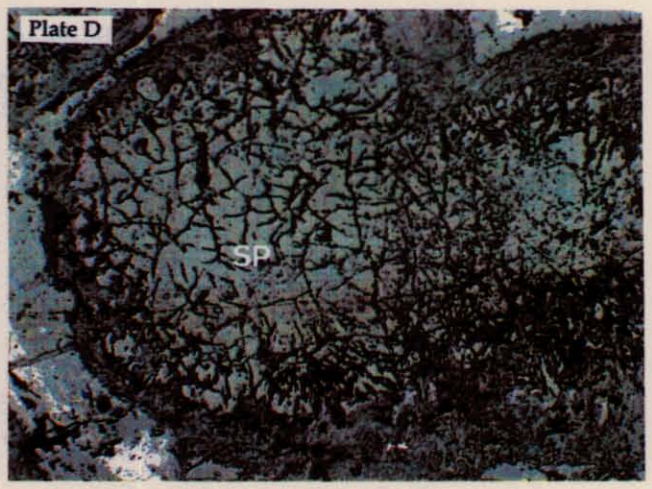

Plate E

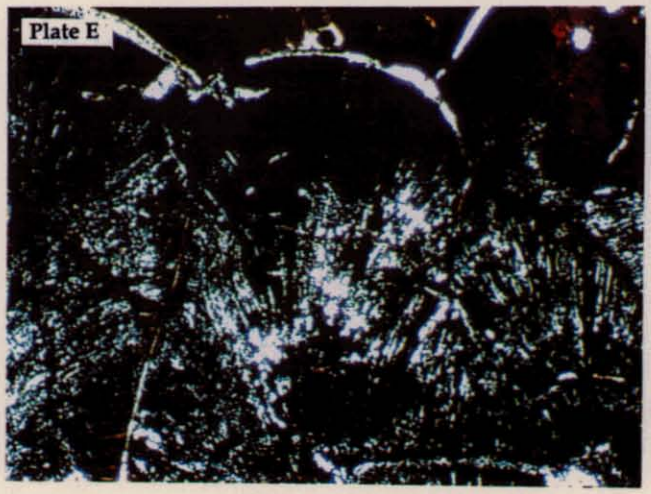

Plate F

Plate G

Plate H

4.3.2.4 *Ugbrook Dolomite Mineralisation*

A vuggy porosity in dolomites of the Ugbrook Formation has been exploited by mineralising fluids (Plate 4.2). Sulphides have filled cavities, fractures, and concentrated along stylolites. This mineralisation occurs above the lower silt member, near the southern LMZ. It is not part of the LMZ proper, but the textures and close proximity to the LMZ see it included within this discussion. Pyrite (80%) dominates the sulphides followed by sphalerite (15%) and galena (5%). Although the amount of sulphide mineralisation is minimal, it assists understanding of the textures of the LMZ.

1) *Sphalerite*

Sphalerite occurs as 0.1 - 0.3 mm anhedral grains in cavities, fractures, along stylolites and as 0.2 mm botryoidal spherules (Plate 4.2c and d). Anhedral sphalerite has cusp and caries textures with galena, and vein - replacement textures with pyrite. Minor botryoidal sphalerite has formed spherules on siderite and dolomite wallrock, and around pyrite grains (Plate 4.2c).

2) *Pyrite*

Pyrite has formed euhedral to subhedral crystals up to 1 mm, some of which have compositional growth rings (Plate 4.2a). Pyrite has filled cavities and fractures in the dolomite and exploits available open spaces, resulting in a stringy set of pyrite veins forming a dendritic texture (Plate 4.2b). Pyrite has also grown in comb textures out from the dolomite and siderite wallrock but it has only completely filled cavities in a few locations. Large (0.8 mm) euhedral to subhedral siderite crystals commonly formed a cavity lining upon which the pyrite cockade textures have grown in larger cavities. Fracturing and dolomite inclusions are common in pyrite which has cusp and caries textures with galena and sphalerite (Plate 4.2c). Pyrite also forms vein and replacement textures within sphalerite crystals. Spongy pyrite occurs on the margins of some euhedral pyrite crystals and in stylolites. It contains many dolomite inclusions and has anhedral grain boundaries.

3) *Galena*

Galena occurs as euhedral crystals up to 1 mm on the margins of euhedral to subhedral pyrite grains. Galena forms part of the cockade texture and comprises

Plate 4.2

Plate 4.2 a : Euhedral pyrite (Py) showing growth zoning. Later spongy pyrite has filled out into the cavity. Later phase galena (Gn) filled a cavity within pyrite forming cusp and caries textures (DDH ZG1007, Reflected light, field of view ≈ 1 mm).

Plate 4.2 b : Fracture and cavity filling pyrite (Py) in dolomite of the Lower Black Jack Formation. Later sphalerite (sp) replaces pyrite (DDH ZG1007, reflected light, field of view ≈ 2mm).

Plate 4.2 c : Mineralised Ugbrook Formation dolomite showing early pyrite (Py), overprinted by galena (Gn) which forms cusp and caries grain boundaries with both pyrite and later stage sphalerite spherules (sp). Calcite represents the latest stage in the cavity (DDH ZG1007, reflected light, field of view ≈ 1mm).

Plate 4.2 d : Paragenetic relationships between the first phase pyrite (Py), then galena (Gn) and latest phase sphalerite spherules (sp) (DDH ZG1007, reflected light, field of view ≈ 0.25mm).

Plate 4.2 e : Quartz-carbonate pressure shadow between pyrite (Py) crystals (DDH ZM1008, transmitted and reflected light, field of view ≈ 2mm)

Plate 4.2 f : Higher magnification view of quartz-carbonate pressure shadows between pyrite crystals (DDH ZM1008, transmitted and reflected light, field of view ≈ 1mm)

384205

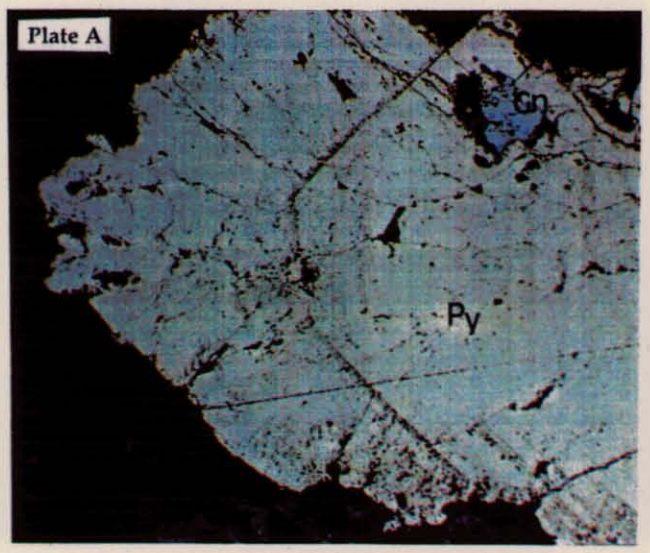
Plate A
Gn
Py

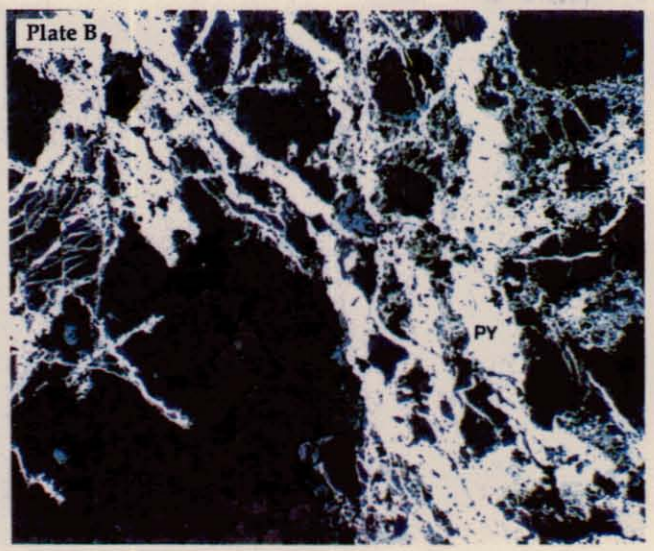
Plate B
PY

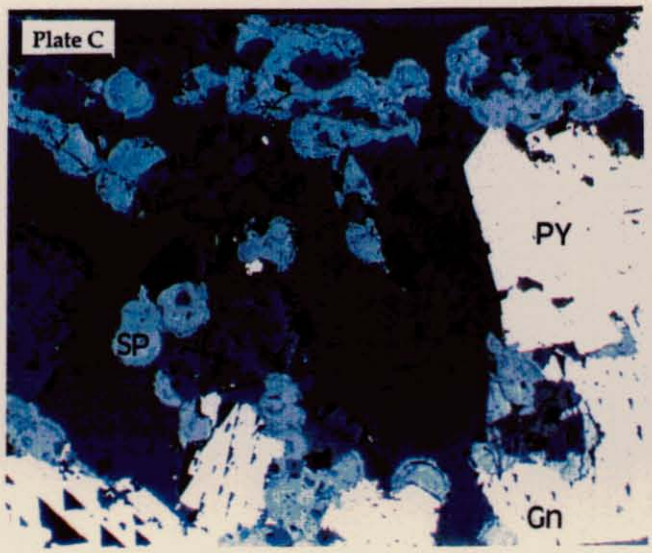
Plate C
PY
SP
Gn

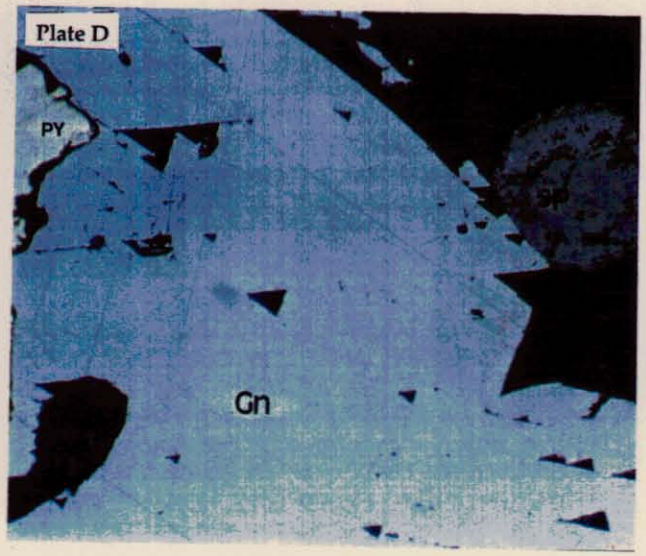
Plate D
PY
SP
Gn


Plate E

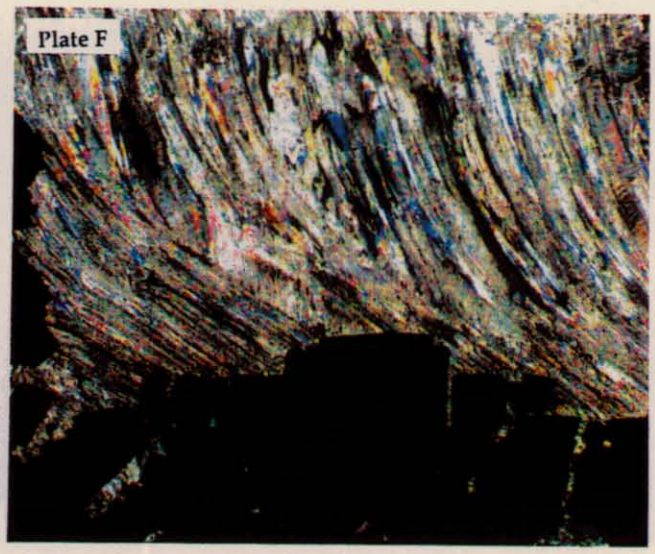
Plate F

up to 5% of the sulphide assemblage (Plate 4.2d). It has cusp and caries grain boundaries with pyrite but the grain boundaries that project into open cavities are euhedral.

4) *Calcite*

Clear calcite rhombs up to 0.4 mm form the innermost lining to some cavities (Plate 4.2c). This lining can be up to 0.6 mm thick and stacked with euhedral to subhedral calcite rhombs.

4.4: UPPER MINERALISED ZONE

4.4.1 INTRODUCTION

Additional mineralisation that appears to be associated with the Lords Siltstone forms the Upper Mineralised Zone (UMZ). The UMZ includes fractured pyrite in calcite veins; isolated massive marcasite; and galena, sphalerite and pyrite associated with pervasive dolomitisation of the lower Black Jacks Formation. The occurrence of a silicified limestone breccia in the south (Fig. 4.2) may also contain sulphide mineralisation, as the Oceana deposit is associated with a similar lithology. The following descriptions outline the characteristics of mineralisation in the UMZ.

4.4.2 MINERAL PETROGRAPHY OF THE UMZ

4.4.2.1 Diamond Drill Hole Intersection

Minor galena and sphalerite associated with the lower Black Jacks Formation was intersected in diamond drill hole ZG 1012 (Plate 4.3a). The sulphides occur below the Lords Siltstone (Fig 4.2). Large vugs and cavities have been filled by a 0.5 - 3 mm thick siderite lining, and coated with minor galena and sphalerite. The sulphide mineralisation is associated with extensive siderite alteration.

1) *Siderite*

Siderite occurs as large (up to 2mm) light brown euhedral crystals that project from the dolomite wall rock into the cavity (Plate 4.3b). They have dogtooth

terminations and define a comb texture. The siderite crystals are coated by small colloidal, sphalerite spherules that range in size between 0.05 - 0.2 mm.

2) *Sphalerite*

Two sphalerite phases are recognised in the UMZ. The first massive phase has nucleated onto siderite crystals and has been partially replaced by small (0.1 mm) anhedral galena crystals, and the second sphalerite phase (Plate 4.3 c,d and e). The massive sphalerite is attached to the siderite and galena grain boundaries, forming cusp and caries textures. A second phase of sphalerite has formed colloidal spheroids up to 0.2 mm in diameter. Spheroids with internal growth banding have overgrown galena grains and formed replacement and relict textures.

3) *Galena*

Galena occurs as 0.01 to 0.2 mm anhedral grains along the outermost sections of the cavity walls (Plate 4.3d). Some grains are partially replaced by sphalerite spheroids, with cusp and caries textures between sphalerite and galena. Relict anhedral galena blebs occur in sphalerite.

4) *Calcite*

Calcite has filled the remaining space in the cavities, forming large (up to 1.2 cm) calcite plates. The plates are subhedral and show no twinning (Plate 4.3e and f).

4.4.2.2 Massive Marcasite

Massive marcasite was found in costeans above and below the Lords Siltstone. Below the Lords Siltstone, marcasite occurs in a costean at 47100N, 61170E (Fig. 1.2). It is cubic, up to 7 mm in diameter and associated with siderite and dolomite. It forms a mineralised matrix surrounding dolomite clasts and has been weathered to geothite and magnesite. A sphalerite clast surrounded by a marcasite matrix was collected by Dr. G. Green of Tasmanian Development and Resources. Above the Lords Siltstone a more radiating form of marcasite occurs with individual blades up to 15 mm in length. It is not associated with siderite or dolomite.

Plate 4.3

Plate 4.3 a : Drill core sample from DDH ZG1012 showing a large vug in dolomite of the Lower Black Jack Formation filled by siderite, sphalerite-galena and calcite. The nature of settling of sediment in the bottom of the cavity gives suggests the beds are the right way up.

Plate 4.3 b : Photo of the cavity wall of Plate 4.3a, showing the dolomite wallrock being coated with large euhedral siderite (sid) crystals forming a comb texture. Minor mineralisation (sphalerite and galena) lines the dogtooth siderite terminations. Coarse calcite plates (cal) line the cavity (DDH ZG1012, transmitted light, field of view ≈ 4mm)

Plate 4.3 c, d, e, f, g : High magnification photomicrographs of sphalerite spherules (sp) coating dogtooth siderite crystals and replacing earlier formed galena (Gn). Paragenesis of the spherules involves a fine grained massive sphalerite (sp) first coating the siderite, followed by galena (Gn). Later sphalerite spherules (sp) replace the earlier sphalerite and galena (DDH ZM1012, transmitted and reflected light, field of view ≈ 1mm)

384209

Plate A

Plate B

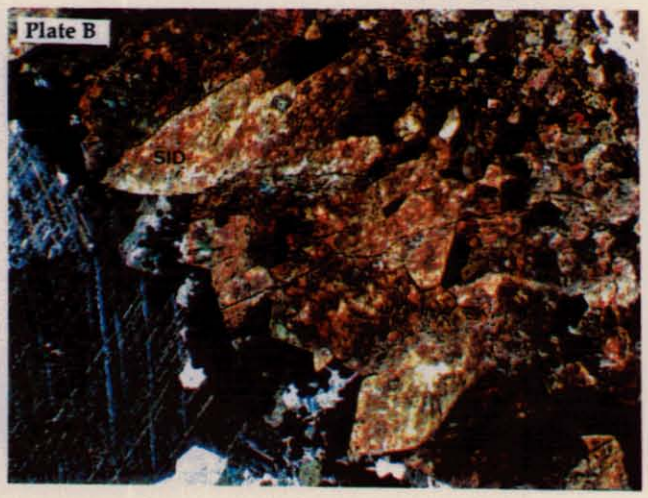

Plate C

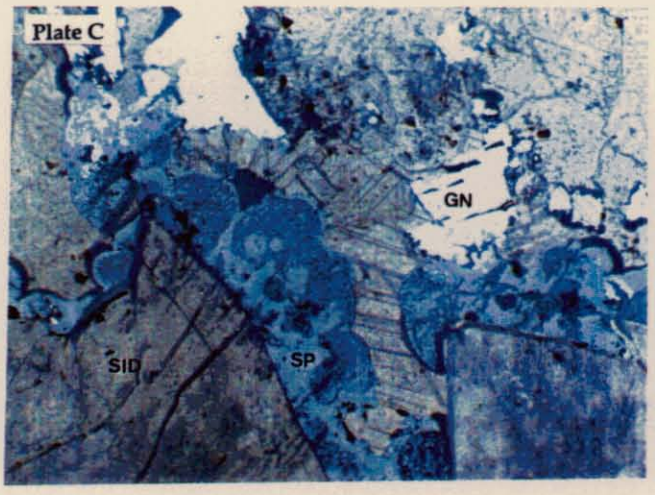

Plate D

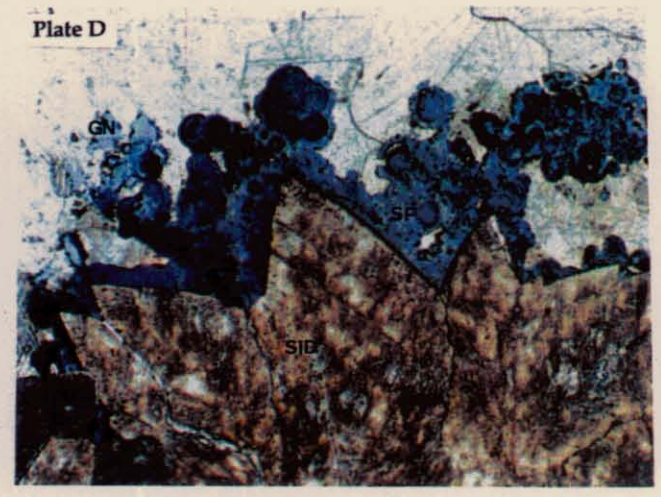

Plate E

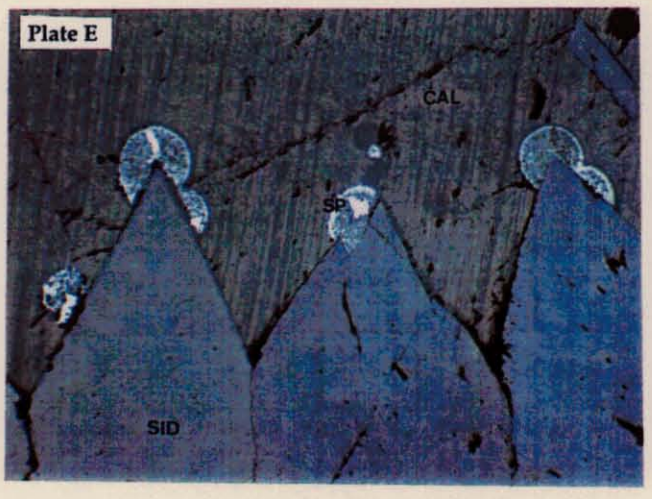

Plate F

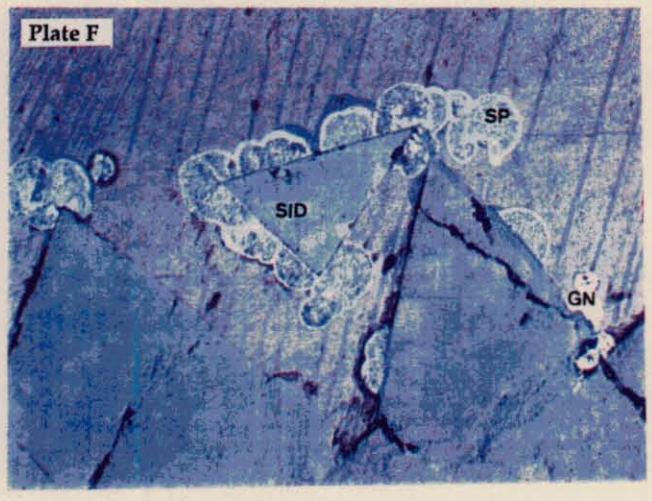

Plate G

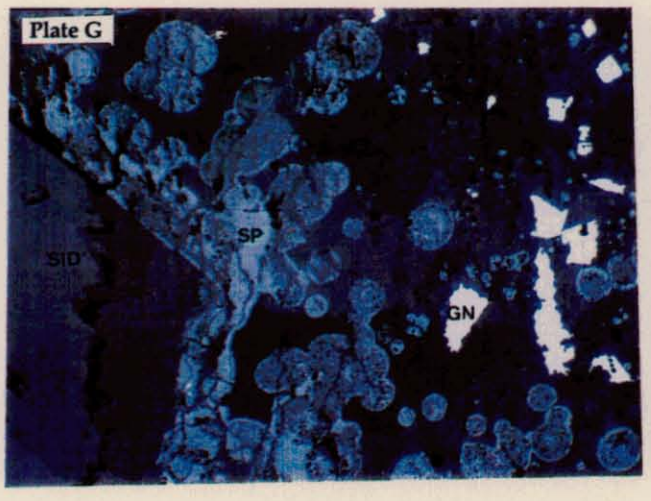

Plate H

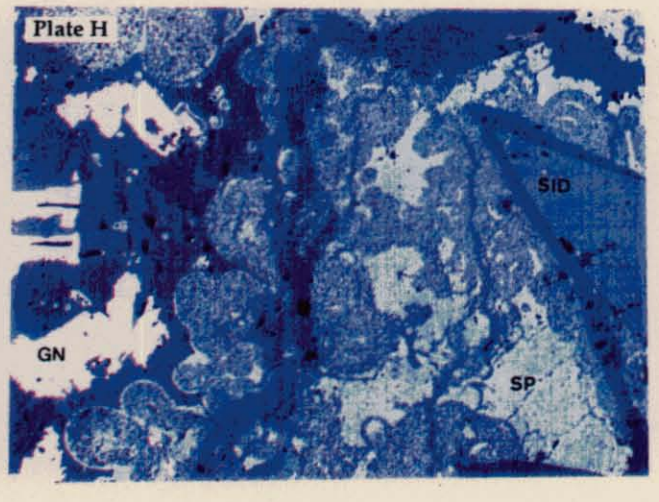

Interpretation

Marcasite below the Lords Siltstone occurs in the Lower Black Jacks Formation, and could be associated with the cavity-filling fine grained galena and sphalerite found in dolomites of the Lower Black Jacks Formation. It may represent the surface expression of the cavity in-filling mineralisation seen in drill core. If this is the case, further mineralisation in a stratabound discontinuous lens may occur between this site, and DDH ZG 1012, forming an intermittently mineralised horizon below the Lords Siltstone (Fig 4.2). The association of this mineralisation with a mineralised breccia, and the close proximity to a black matrix carbonate breccia, gives this area potential.

4.4.2.3 Fractured Pyrite and Calcite Veins

Highly fractured pyrite can occur in some calcite veins parallel or sub-parallel to bedding and along stylolites in all units. Minor dolomitisation has occurred along stylolites that contain pyrite. In some veins, the pyrite is highly fractured (0.3 mm - 1 cm) and filled with pits, tension gashes and calcite grains. Other calcite veins contain less fractured euhedral, (0.2 - 0.7 mm) inclusion-free pyrite that contains partially recrystallised framboids. Undulose quartz-carbonate pressure shadows occur around large pyrite grains as leaf like aggregates (Plate 4.2 e and f)). The calcite veins have mostly cross-cut micrite and at least two separate veins are present. One vein set is associated with pyrite, and is cross-cut by a second barren vein set. Some of the later barren calcite vein sets have crack-seal vein textures, with up to 8 individual crack-seal events recognised. The crack-seal veins may be related to the Tabberabberan Orogeny.

4.4.2.4: Black matrix Dolomite Breccia

Radiating marcasite occurs in close proximity to a black matrix dolomite breccia (Fig. 4.2; and Fig 1.2). The breccia contains highly angular to sub-rounded, unsorted (2 - 20 mm) dolomite clasts set in an argillaceous micritic - dolomitic matrix (Plate 4.4a). The original composition of the clasts is unknown; however they now consist of 0.1 to 0.7 mm, subhedral to anhedral dolomite rhombs. Both matrix and clasts contain small, angular (0.01 mm) anhedral quartz clasts. The matrix is preferentially stylolitised and may shows significant silicification (Plate 4.4 c and d). The argillaceous matrix locally contains 0.05 - 0.1 mm quartz grains that have grown from dolomite clasts into cavities forming classic

Plate 4.4

Plate 4.4 a : Angular dolomitised (dol) clasts in a calcite matrix (cal). This angular breccia is a similar lithology to the host rocks of the Oceana deposit. The proceeding photomicrographs document the progressive silicification of the breccia from north Grieves to south Grieves Siding - Baura prospect (DDH DB110, transmitted light, field of view ≈ 2mm).

Plate 4.4 b : Selective silicification of the calcite matrix and the establishment of a cockade texture around dolomite clasts (Sample BO42600, transmitted light, field of view ≈ 2mm).

Plate 4.4 c and d: Selective silicification (qtz) of the once calcite matrix, producing a classic cockade texture around dolomite clasts (dol) (Sample BO4, transmitted light, field of view ≈ 2mm).

Plate 4.4 e : Pyrite (Py) comb texture defining the edges of a cavity that has been replaced by radiating hemimorphite (Hm). Hemimorphite replaces the wall-rock and the cavity (DDH ZG406, transmitted and reflected light, field of view ≈ 1mm).

Plate 4.4 f and g: Radiating hemimorphite (Hm) nucleating on remnant wall-rock forming a cockade texture.

Plate 4.4 h : Hemimorphite (Hm) veins cross cutting earlier veins and earlier formed hemimorphite (DDH ZG406, transmitted light, field of view ≈ 1mm)

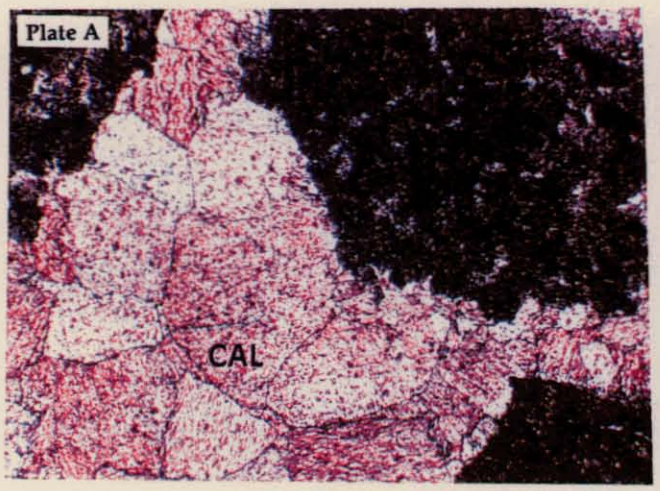
Plate A
CAL

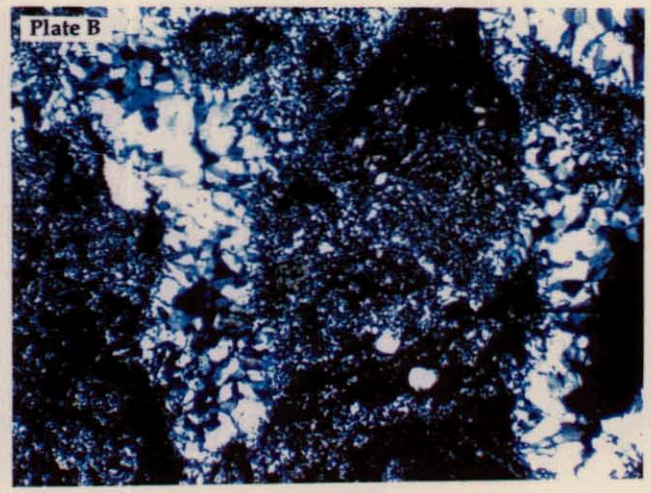
Plate B

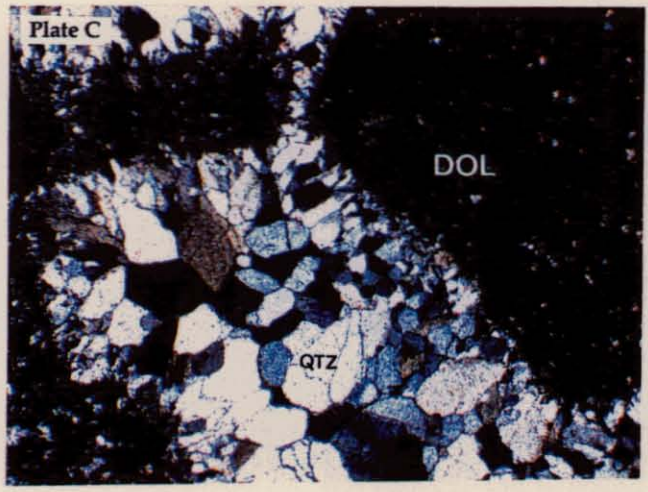
Plate C
DOL
QTZ

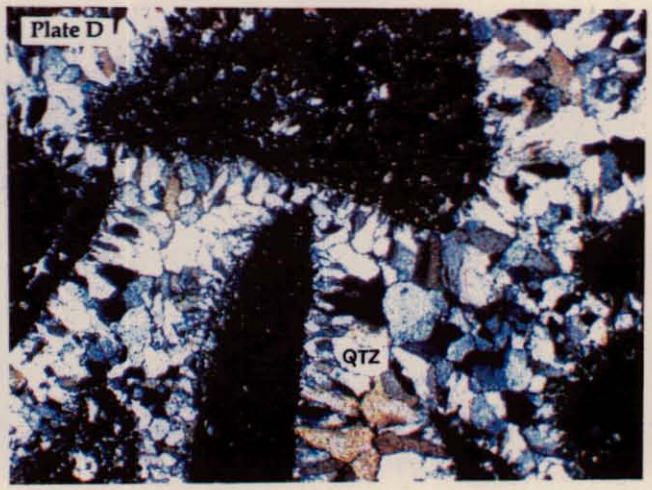
Plate D
QTZ

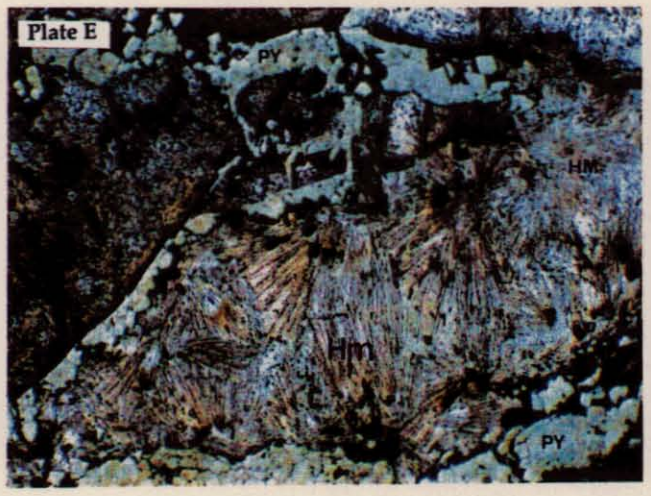
Plate E
PY
HM
Hm
PY

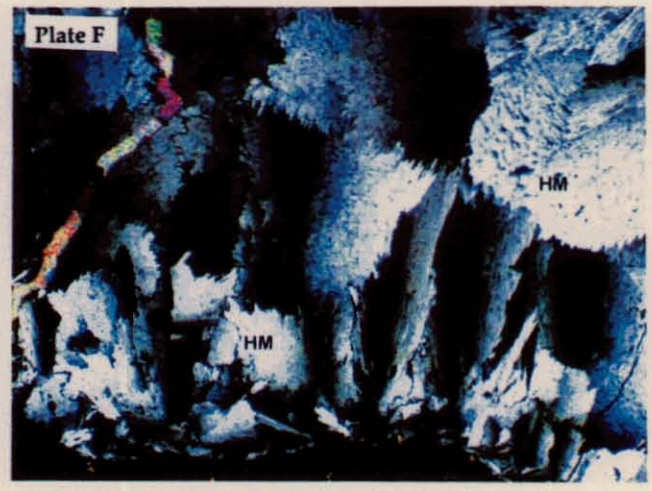
Plate F
HM
HM


Plate G
HM
HM

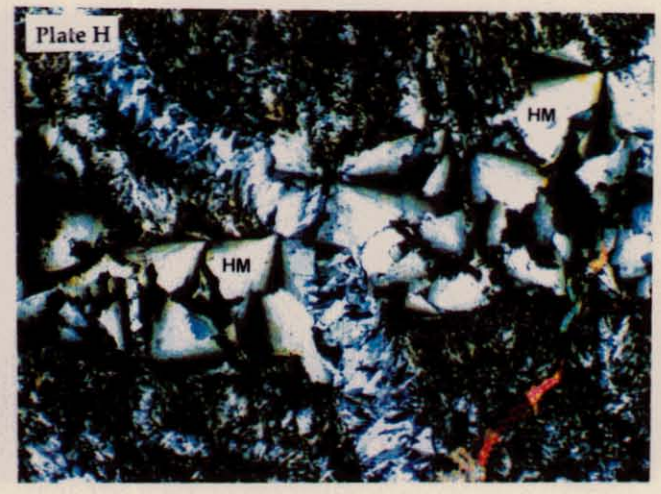
Plate H
HM
HM

cockade textures (Plate 4.4 c and d). Small (up to 0.05 mm) subhedral to euhedral quartz crystals occur closest to the dolomite clasts, grading into coarser (0.1 mm) subhedral to anhedral crystals towards the centre of the cavity. Fine grained quartz veins have cross-cut some dolomite clasts. Varying degrees of silicification are seen in the matrix of the breccia.

Further to the south (Fig 4.2) a completely silicified breccia was found. The matrix retains the cockade textures, and the clasts are completely silicified. The breccia can show remnant bedding however the exact nature of its contact with the Gordon Limestone is unknown. The black matrix breccia occurs to the north of the Firewood Siding Fault, whereas the completely silicified breccia occurs to the south of this fault. (Fig 4.2). The progression from a calcite matrix to a totally silicified unit is illustrated in Plates 4.4a to 4.4d.

4.5: PARAGENESIS

A paragenetic scheme for the Lower Mineralised Zone is summarised in Table 4.1. The paragenesis of mineralisation above the Lower Mineralised Zone in dolomite of the Ugbrook Formation is summarised in Table 4.2. Interpreted paragenetic relationships for the UMZ are summarised in Table 4.3.

4.5.1: Lower mineralised Zone (LMZ)

Sedimentary pyrite framboids were the first sulphides to form in the LMZ. They indicate the presence of sulphur-reducing bacteria in a reduced anoxic environment (Sweeny and Kaplin, 1973). Protected subtidal lagoons of the Ugbrook Formation would have provided a suitable habitat for such organisms.

The sulphide mineralisation in the LMZ formed after diagenic and hydrothermal dolomitisation, as the sulphides occupy cavities formed during dolomitisation. The time elapsed between dolomitisation and mineralisation was discussed in Chapt. 3; However, dolomitisation was probably early diagenetic with some further dolomitisation caused by hydrothermal alteration, prior to the mineralising event (Table 4.1). The resultant cavities were initially filled by euhedral siderite crystals up to 2 mm. They formed the foundation for development of open space filling, and comb textures seen throughout most of the LMZ. The dogtooth siderite terminations were initially coated by minor,

Table 4.1: Interpreted paragenetic relationships of ore and gangue minerals from the Lower Mineralised Zone at Grieves Siding.

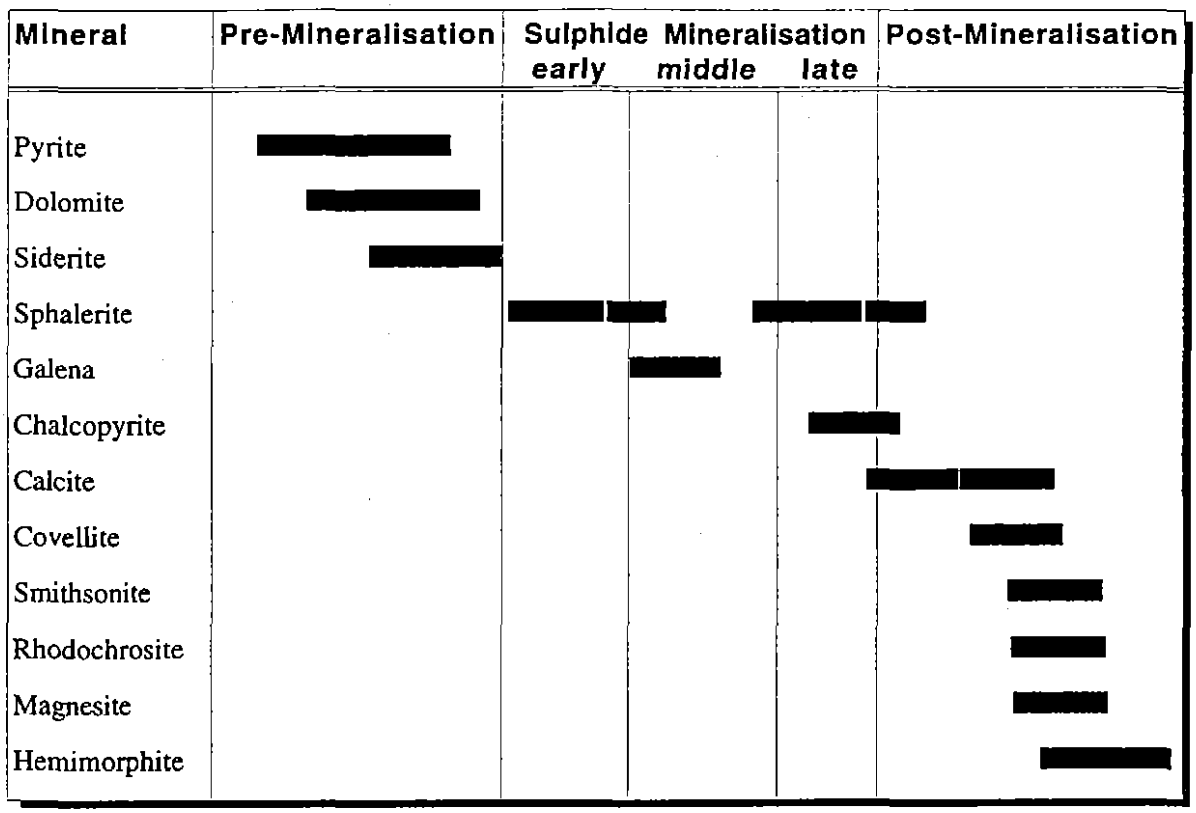

Table 4.2: Interpreted paragenetic relationships of ore and gangue minerals from dolomite in the Ugbrook Formation, just above the Lower Mineralised Zone.

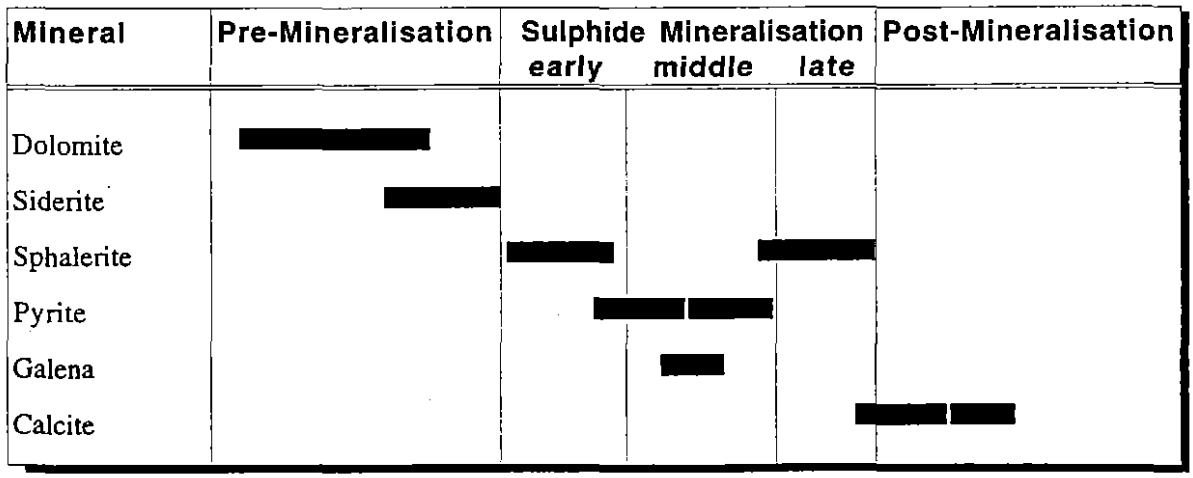

Table 4.3: Interpreted paragenetic relationships of ore and gangue minerals from the Upper Mineralised Zone at Grieves Siding.

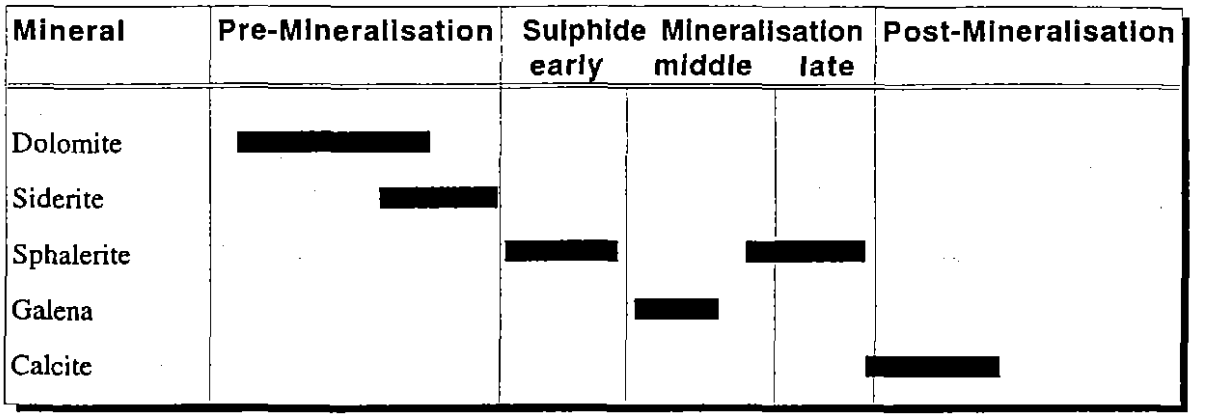

Table 4.4: Generalized paragenetic sequence of mineralisation in the Irish Pb-Zn deposits (After Hitzman, 1995).

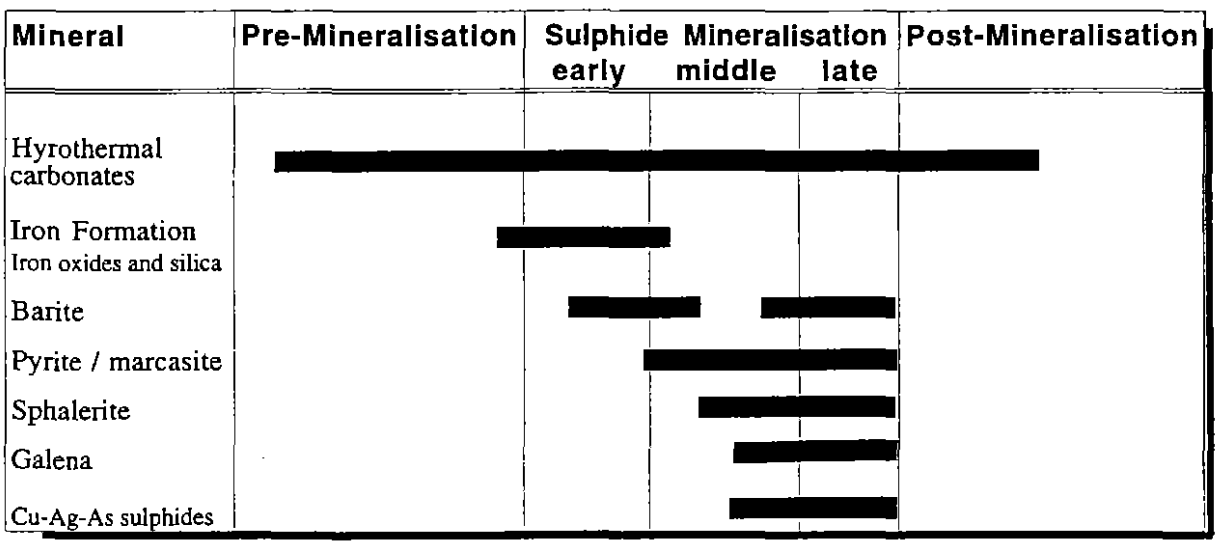

semi-massive sphalerite that formed 0.1 mm anhedral to subhedral crystals. Sphalerite growth was closely followed by the precipitation of galena (Table 4.1).

Deposition of small colloidal textured sphalerite spherules proceeded galena deposition. The galena formed soon after early sphalerite, and has been overprinted by later spherules. Relict pyrite, which formed radiating textures in some spherules from the prospect, may be an early pyrite phase, or may signify the concentration of passively-enriched biogenic pyrite during dissolution of the carbonate (Ellis, 1984). Possible concentration and recrystallisation of framboidal pyrite was seen in DDH ZG 406 where it lined cavity boundaries. Disseminated pyrite in the host carbonate could have recrystallised and mixed with framboidal pyrite to produce this concentrated pyrite. Alternatively, an input of a reduced sulphur-rich fluid could have caused early pyrite precipitation. Relict pyrite observed in spherules would have been produced as the growth-banded spherules grew and overprinted earlier pyrite, thereby producing the radiating textures.

Further colloidal textured sphalerite growth continued after galena deposition (Table 4.1). Spherule growth incorporated the galena such that it now occurs in and around the spheroids. The dendritic texture seen in the cores of some spherules (Plate 4.4d) was probably produced by growth of the colloform banded spherules or by the action of bacterial filaments.

Precipitation of a light honey coloured, translucent, low-Fe sphalerite, around and between spherules, may have resulted from repeated sphalerite dissolution and re-precipitation (Table 4.1). Chalcopyrite occurs along fractures in the light-coloured sphalerite and is interpreted to be younger than sphalerite (Table 4.1). Covellite has partially replaced the chalcopyrite and is interpreted to be supergene in origin. Late stage calcite occurs as an inner lining of the comb textures, and as the final in-fill phase of the cavities. Evidence for two separate episodes of calcite precipitation are seen in DDH ZG 406, with later precipitated, fine grained (3μm) calcite lining the earlier coarser grained (0.04 mm) calcite.

Smithsonite, rhodochrosite, and magnesite along the top of the LMZ may have formed by oxidation of sulphide mineralisation, producing a high grade cap. Oxidised groundwaters may have permeated along the interdigitating Moina Sandstone - Ugbrook Formation contact, allowing the leaching and

precipitation of secondary Zn, Mg and Mn minerals. Sulphide oxidation and remobilisation of HCO_3^- could therefore initiate the precipitation of smithsonite, rhodochrosite, and magnesite. The fibrous, radiating zinc silicate, hemimorphite which typically occurs associated with smithsonite (Nesse, 1991), formed after smithsonite, rhodochrosite, and magnesite, as it occurs in cavities and veins that have cross-cut and replaced all other minerals (Table 4.1). Hemimorphite veins have been fractured and deformed, indicating they have probably been affected by the Devonian (Tabberabberan) orogeny. Weathering and formation of secondary carbonates may therefore have occurred in the Palaeozoic between the Ordovician and mid-Devonian.

4.5.2: Ugbrook Dolomite Mineralisation

Sulphide mineralisation precipitated in the vuggy dolomites of the Ugbrook Formation, above the LMZ, display similar textures to that seen in the LMZ. This mineralisation shows a vaguely similar paragenetic relationships to that of the LMZ, except for the abundance and timing of pyrite (Table 4.2). Therefore, a separate paragenesis has been constructed for this mineralisation.

Sphalerite has formed a cusp and caries, and replacement texture with galena, pyrite, and later stage sphalerite. It is interpreted to have been the first sulphide precipitated after pervasive hydrothermal dolomitisation. An isolated example of siderite that has lined a cavity, suggests it grew before sphalerite, however, in the majority of cases, sphalerite has grown on dolomite wallrock.

Comb textured pyrite has grown outwards from the dolomite wallrock. It has cusp and caries textural relationships with sphalerite, indicating pyrite was deposited after early sphalerite precipitation. Pyrite exploits fractures, vugs and cavities, resulting in a dendritic texture (Plate 4.4b), that grades into compositionally zoned (up to 1 mm) euhedral crystals. A later stage of rapid pyrite precipitation produced spongey textured grains full of small impurities. Pyrite shares cusp and caries grain boundaries with a later stage galena which has euhedral margins into open cavities.

Botryoidal sphalerite spherules occur on siderite, dolomite, sphalerite, pyrite and galena crystals, indicating they precipitated late in the paragenesis. The small spherules are restricted to pockets and fractures within minerals of the

comb texture. Clear 0.4 mm diameter calcite rhombs occur as the innermost lining of some cavities forming bands up to 0.6 mm thick. Calcite was the last phase to precipitate in the cavities (Table 4.2)

4.5.3: Upper mineralised Zone (UMZ)

Interpreted paragenetic relationships of ore and gangue minerals in the UMZ are summarised in Table 4.3.

A vuggy porosity in dolomite of the lower Black Jacks Formation may have been caused by the 13% volume loss incurred when calcite is replaced by dolomite (Tucker, 1982). This reduction only occurs with secondary dolomitisation, subsequently a second hydrothermal dolomitisation is envisaged to have produced the large cavities (Plate 4.3a). Siderite was the next mineral to precipitate, and has coated the vugs.

Fine grained massive sphalerite (Table 4.3) was the first sulphide to precipitate forming the first sulphide lining of the cavity. Contemporaneous or marginally later precipitation of galena produced the second sulphide cavity lining. Renewed sphalerite deposition, perhaps caused by sphalerite dissolution and re-precipitation, formed spherules that overprint galena, and earlier sphalerite (Table 4.3). Late stage calcite was the last mineral to fill the cavity, forming large anhedral plates (Table 4.3).

4.6: GEOCHEMICAL VECTORS

Ten element geochemical analysis of diamond drill hole ZG 406 distinguishes the LMZ from the Gordon Limestone by having elevated Mn, Fe, As, and Ba concentrations and dramatically lower Ca and Mg values (Fig. 4.3). A manganese halo is especially recognisable in a very small alteration envelope defined by geochemical and isotopic evidence (Chapter 5). Manganese halos and Ba halos are also seen in the Irish-type zinc lead deposits (Hitzman, 1994). Abundances of Zn, Ag, Cu, and Pb show expected increases, (Fig. 4.4) especially in two parallel horizons in the LMZ. The lower horizon corresponds to ferruginous and sideritic clays in the lower silt member. The well consolidated 'massive' cap at the top of the LMZ forms the upper horizon which shows high zinc grades.

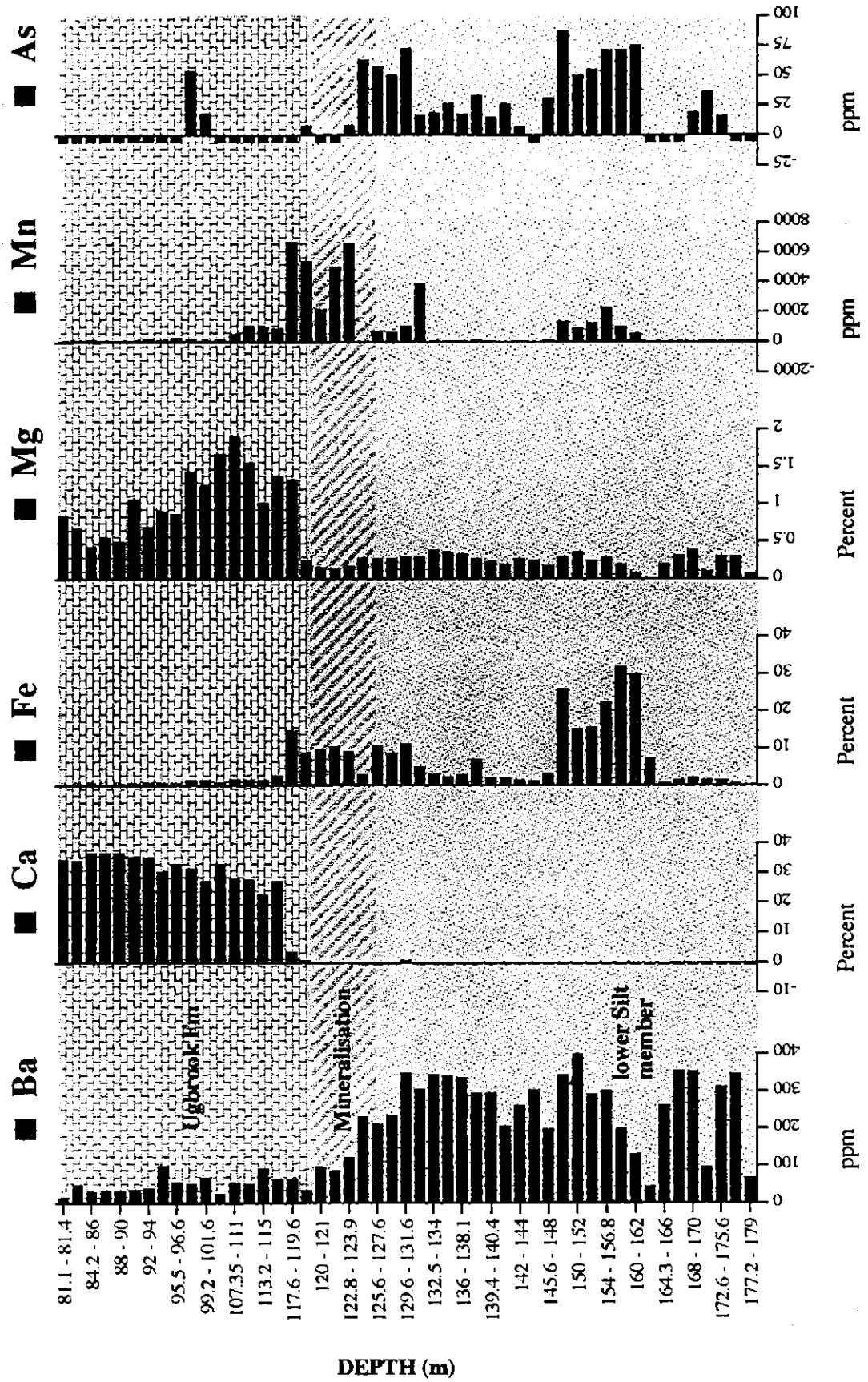

Figure 4.3: Downhole geochemistry of DDH ZG 406. The LMZ is intersected at 119.5 m, corresponding with increases in Ba, Fe, Mn, and As.

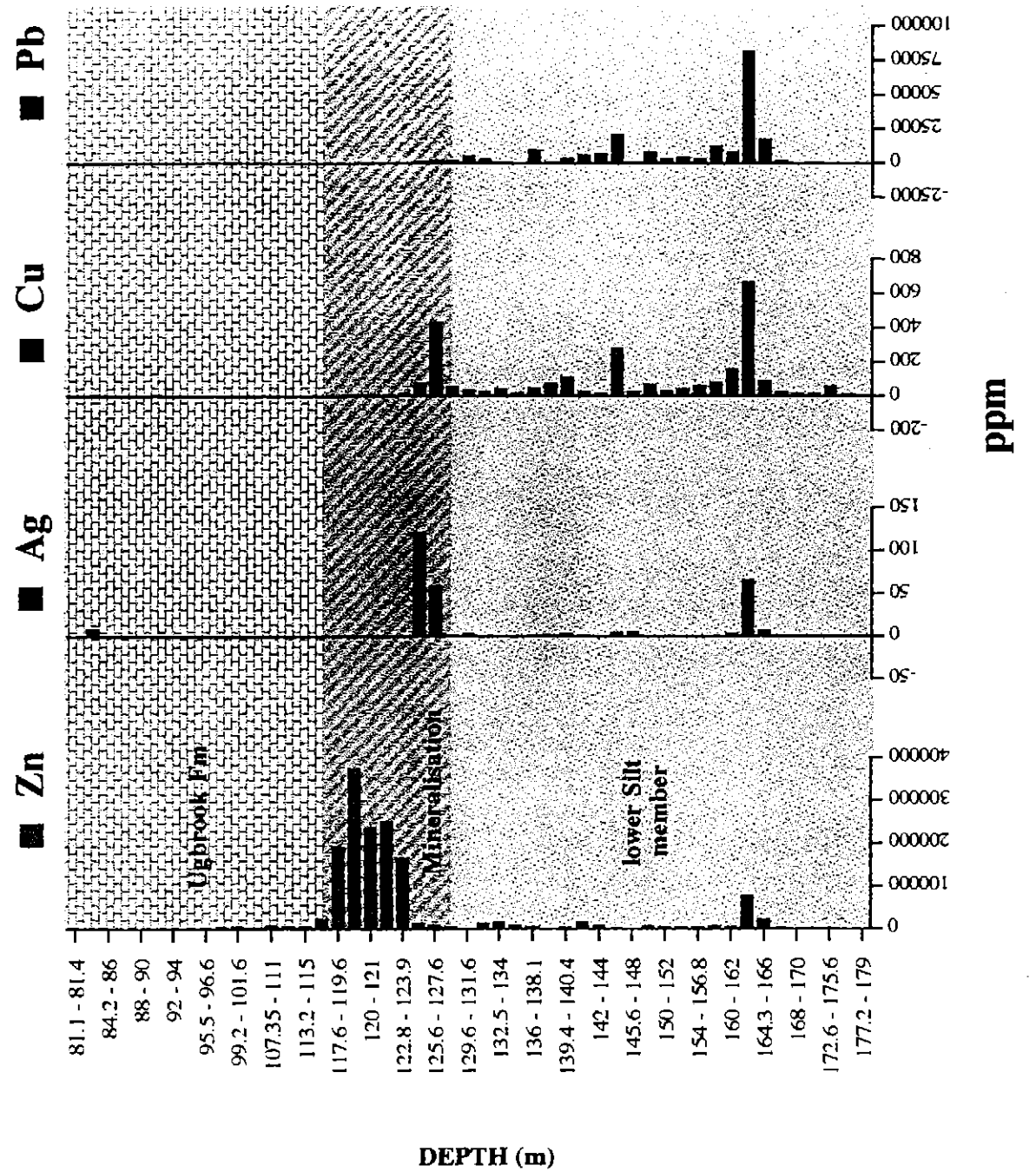

Figure 4.4: Downhole geochemistry of metals in DDH ZG 406. A dramatic increase in zinc associated with secondary mineralised carbonates occurs at the top of the LMZ, whereas lead and copper have the greatest abundance in the lower Silt member.

4.7: *ZINC RATIO*

Comparison of the 'Zinc Ratio' [100 Zn / (Zn + Pb)] (Huston and Large, 1987) of various styles of mineralisation, with the zinc number from this study indicates Grieves Siding data is consistent with ratios in MVT deposits (Fig. 4.5). Leach and Sangster (1994) show most MVT deposits are zinc rich compared to lead, with zinc numbers between 50 and 100%, and a distinct mode at 80%. The Zinc number calculated at Grieves Siding has a mode at 80% and a very similar overall shape to that of MVT deposits. the dominance of zinc in the LMZ is reflected in the zinc ratio. Depending on the position of the LMZ to the hydrothermal feeder zones, the zinc number may be reflecting a distal zinc dominated, lower temperature zone, suggesting a higher temperature lead zone may be in close proximity. Coupled with fluid inclusion data (Chapt. 5), the zinc number provides useful information about the origin of mineralisation. Zinc numbers from Tasmanian Cambrian stratiform sulphides (Fig. 4.6) bear the greatest resemblance to the Grieves Siding data, however the Grieves Siding zinc number is typically unique in Tasmania.

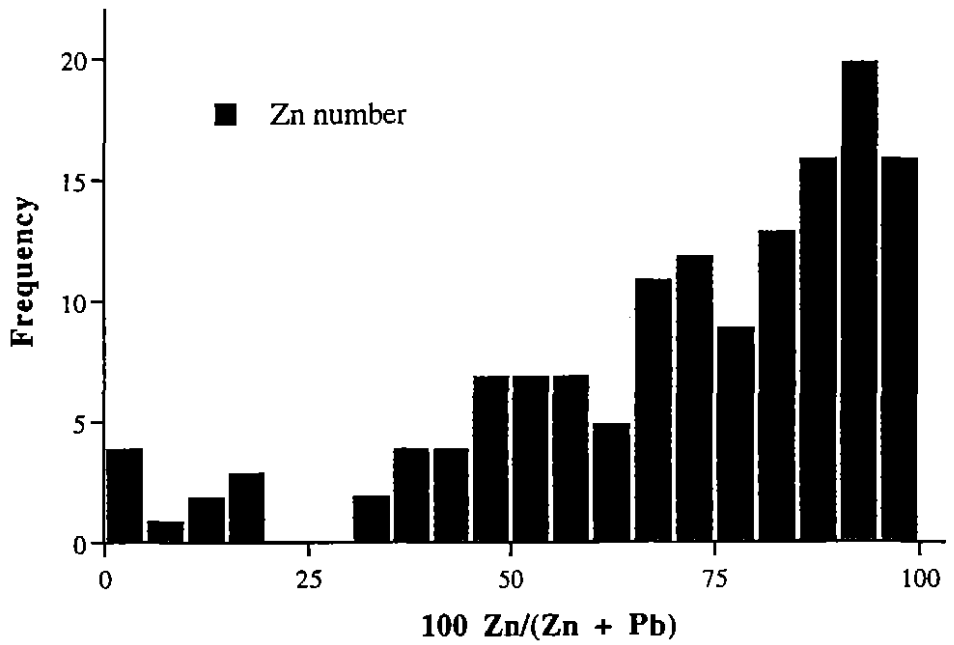

Figure 4.5: Zinc Ratio [100 Zn / (Zn + Pb)] (Huston and Large, 1987) from Grieves Siding is consistent with ratios in MVT deposits.

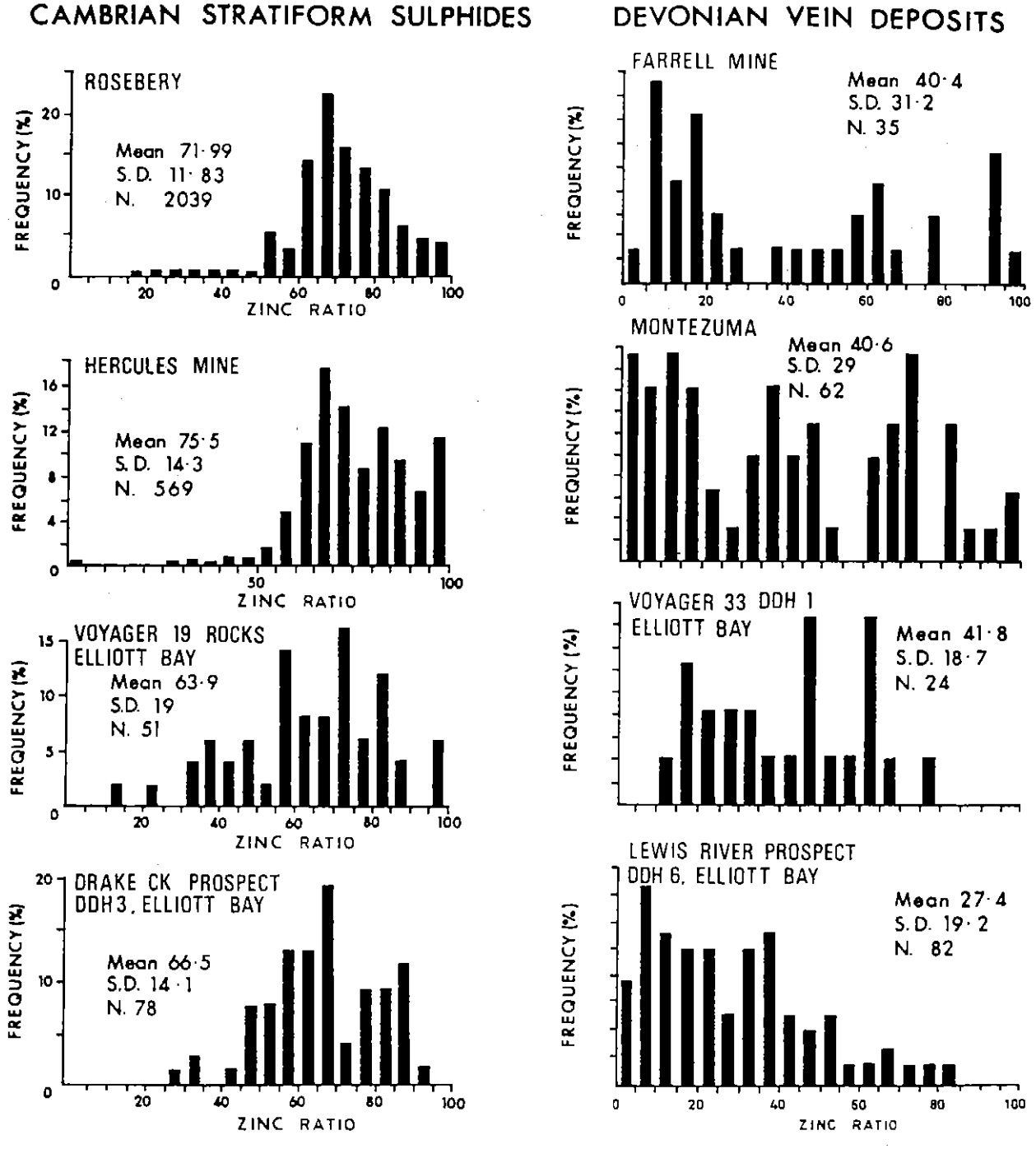

Figure 4.6: Zinc ratio histograms from Tasmanian Cambrian stratiform sulphides and Devonian vein deposits. Data from Grieves Siding resembles Cambrian trends, rather than Devonian signatures.

4.8: *DISCUSSION*

The pattern of dolomitisation and hydrothermal alteration at Grieves Siding is similar to that at the Lisheen Irish-type deposit. Sulphide textures at Grieves Siding are consistent with textures seen in most MVT deposits. The following section relates the sequence of hydrothermal alteration at Lisheen, and sulphide mineral textures in MVT deposits to the paragenetic and textural relationships of mineralisation at Grieves Siding.

Hitzman (1995) indicates regional dolomitisation at Lisheen has been replaced, and brecciated by a series of hydrothermal dolomites spatially associated with massive sulphide bodies. A black matrix dolomite breccia is a distinctive hydrothermal alteration product, and commonly contains disseminated sulphides near massive sulphide lenses.

The black matrix dolomite breccia at Grieves Siding occurs close to massive marcasite and may be related to the UMZ. The marcasite matrix surrounding dolomite and sphalerite clasts may be indicative of a nearby ore lens, similar to patterns seen at Lisheen. Sulphide mineralisation at Lisheen is hosted in the black matrix breccia, with sulphides replacing both matrix and clasts. Silicification of the breccia occurring near southern Grieves Siding close to the Baura prospect (Fig. 1.2), is spatially related to the Firewood Siding Fault. It may represent the product of fluids emanating from the fault, however temporal relationships are unclear.

The sulphide mineral assemblage at Lisheen consists of pyrite, marcasite, sphalerite, galena with minor chalcopyrite and tennantite. Sphalerite forms concentrically zoned colloform masses that commonly enclose early sphalerite spheres. A distinctly later generation of sphalerite is coarser grained and dark to light amber coloured. Gangue minerals are principally dolomite, with some barite, siderite, calcite and very small amounts of quartz and illite (Shearley et al., 1995). The sequence of alteration and mineralisation at Lisheen and other Irish-type deposits is similar to mineralisation at Grieves Siding (Table 4.4). The paragenetic sequence in the Irish Pb-Zn deposits involves: (i) pre-sulphide carbonate precipitation; (ii) iron sulphide deposition; (iii) sphalerite precipitation (iv) mixed sulphide deposition (sphalerite, galena, pyrite, copper sulphides etc); and late carbonate precipitation (Table. 4.4).

A generalised paragenesis for Grieves Siding has: (i) hydrothermal dolomitisation (ii) pre-sulphide siderite precipitation; (iii) pyrite remobilisation and precipitation; (iv) galena and sphalerite deposition and perhaps dissolution and precipitation; (v) and late carbonate (calcite) deposition. Aspects of the paragenetic sequences at Grieves Siding, especially colloform banded sphalerite and repeated sphalerite dissolution and precipitation are similar to Irish-type deposits.

Sulphide textures in Irish-type deposits form in three types: fine grained disseminated ore, coarser grained colloform banded ore; and complex fine grained replacement ore (Shearley et al., 1995). Typical MVT ore formed as open space filling of fractured breccias, and a variety of vugs (Leach and Sangster, 1994). Replacement of carbonate host rocks is generally minor except in areas of high grade mineralisation. Botryoidal colloform sphalerite is commonly intergrown with dendritic galena (Leach and Sangster, 1994).

Open space fill textures and minor carbonate replacement by high grade Zn-carbonate minerals occurs in the LMZ. Botryoidal sphalerite is common throughout the upper and lower mineralised zones, and is well developed at he Grieves Prospect. The paragenetic and textural features of mineralisation at Grieves Siding is consistent with features of Irish-type and MVT deposits.

4.9: SUMMARY

Significant high grade mineralisation at Grieves Siding occurs in a discontinuous stratabound lens referred to as the LMZ. It reaches a maximum thickness of 24 m and is exposed on the surface proximal to the Grieves Fault. Comb and cockade open space fill textures are common and minor carbonate replacement has also been noted. Colloform and botryoidal growth banded spherules of sphalerite and galena are the dominant sulphide texture. There is evidence for multiple periods of sphalerite dissolution and precipitation, with up to four separate sphalerite generations present. Barite could have formed by oxidation caused by the mixing of reduced Ba-rich fluids with fluids containing SO_4 bearing groundwater. Bacterial filaments form the nucleus of some spherules may indicate bacterial sulphate reduction occurred in this sulphur poor, reduced system. These filaments have subsequently been replaced by sphalerite. Pyrite framboids concur with a reduced mineralised environment.

Smithsonite, rhodochrosite and magnesite formed when secondary oxidised sulphur deficient fluids permeated along the interdigitating Moina Sandstone - Ugbrook Formation contact. These minerals form a high grade cap to the sulphide mineralisation. Cross-cutting relationships indicate hemimorphite was the last zinc mineral to precipitate an is an important component of the oxidised cap.

Sulphide mineralisation in the lower Black Jacks Formation is similar to the LMZ, but is distinguished by the abundance and timing of pyrite and the occurrence of marcasite. Colloform sphalerite spherules are present, but are very fine grained. The lateral extent and nature of this mineralisation is obscured by lack of outcrop and drill hole information. It could form stratabound discontinuous lenses below the Lords Siltstone, or isolated mineralised pods in the limestone.

Since deposition, the LMZ has been folded around a large synform, and has undergone brittle deformation on the macro and micro-scale. Mineralogy and mineral textures are unlike those seen in other deposits in the Zeehan Mineral Field. The deformation of mineralisation constrains the timing to prior mid-Devonian (Tabberabberan Orogeny). Geochemical evidence is used in the following chapters to constrain the timing and further define the style of this mineralisation.

Fluid Inclusions 5

5.1 INTRODUCTION

Understanding the physiochemical conditions of ore mineral deposition is essential for determining the timing and style of mineralisation at Grieves Siding. Information about fluid composition have been obtained by microthermometric analysis of fluid inclusions in sphalerite collected from the Grieves Prospect. This chapter documents the data obtained from fluid inclusions before discussing implications for ore genesis.

5.2 CLASSIFICATION OF FLUID INCLUSIONS

The correct interpretation of fluid inclusions relies on the understanding of the temporal relationships between the inclusions and their host minerals. Roedder (1984) recognised that distinguishing between primary and secondary inclusions is critical in understanding such temporal relationships. Criteria listed in Roedder (1984) has been used to classify fluid inclusions obtained from Grieves Siding as secondary inclusions, based on their occurrence in cross-cutting trails.

Two types of fluid inclusions were recognised (Fig. 5.1), with Type I the most common. Type I inclusions are two phase (liquid + vapour), liquid-rich inclusions (Fig 5.1a) that homogenise via vapour disappearance. They comprise 60 % of the fluid inclusions and occur as part of trails outlining healed fractures (Fig 5.2). Type I inclusions average between 3 - 4 μm in size. Type II inclusions are two phase (liquid + vapour), vapour-rich inclusions (Fig 5.1b) that also homogenise via vapour disappearance. Type II inclusions comprise 30 % of those present, and occur as single inclusions that average 8 μm in size.

Fifty percent of both Type I and II fluid inclusions are rectangular in shape, however irregular, amoeboidal, flat and equant shapes were also present. Volume percentage of the vapour phase ranged from 1 to 5% in both inclusion types. Representative Type I and Type II fluid inclusions are illustrated in Plate 5.1.

INCLUSION TYPE		PHASES AT 25°C	HOMOGENISATION BEHAVIOUR
(a)	**Type I** 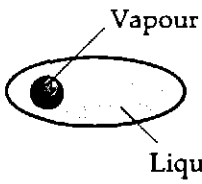	Liquid + Vapour	Vapour disappears
(b)	**Type II** 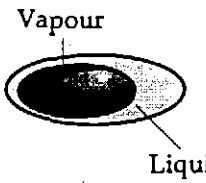	Vapour + Liquid	Vapour disappears

Figure 5.1a & b: Summary of fluid inclusion types, phases present at 25°C, and homogenisation temperature behaviour.

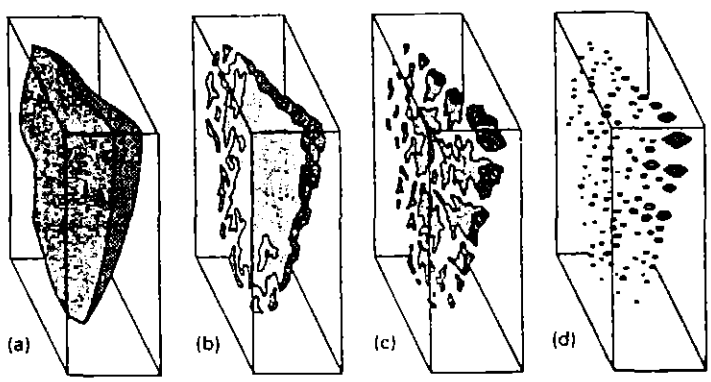

Figure 5.2: Healing of a crack in a crystal resulting in secondary inclusions. If healing occurs with falling temperatures, individual inclusions will have a variety of gas - liquid ratios producing varied results (From Roedder, 1984).

Plate 5.1

Plate 5.1 a : Photomicrograph of secondary fluid inclusions hosted in Low-Fe sphalerite. Type I inclusions are the large rectangular shaped inclusions occurring in healed fractures. Type II are more isolated, irregular shaped inclusions (DDH ZGP2, transmitted light, field of view ≈ 0.25mm)

Plate 5.1 b : Secondary fluid inclusions occurring in a healed fracture (Type I). The large irregular shaped inclusion (II) is a type II inclusion (DDH ZGP2, transmitted light, field of view ≈ 0.25mm).

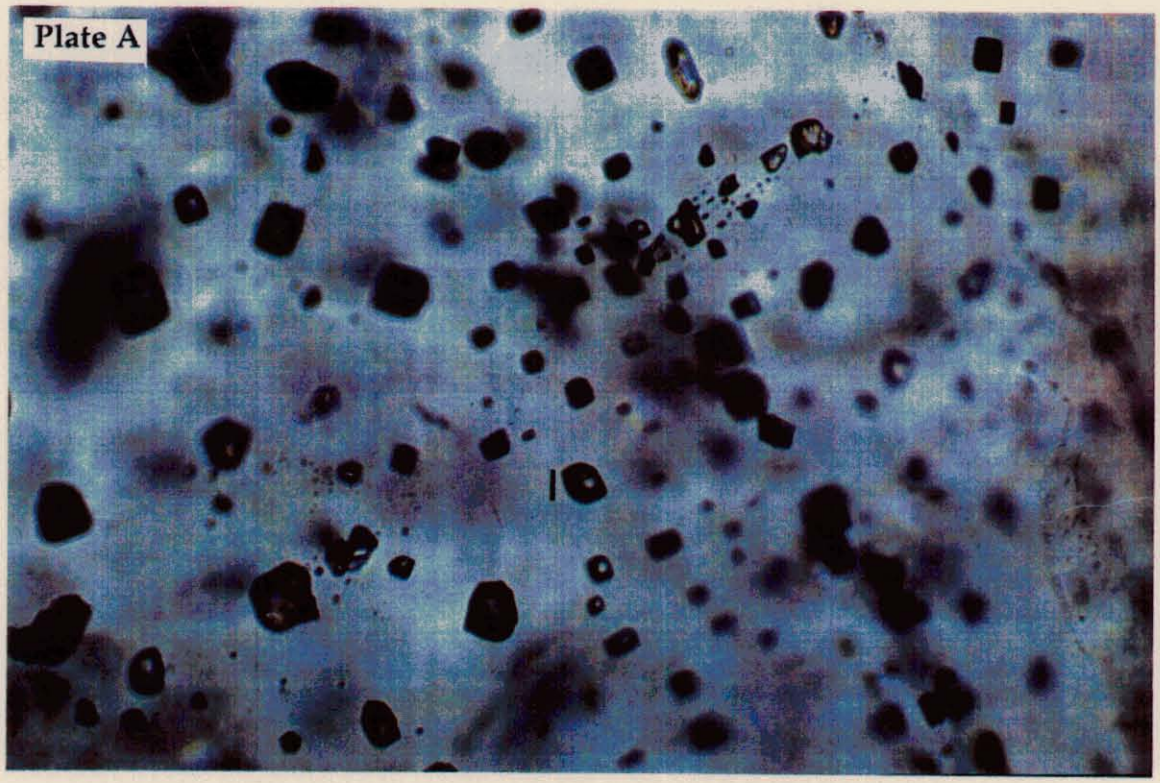

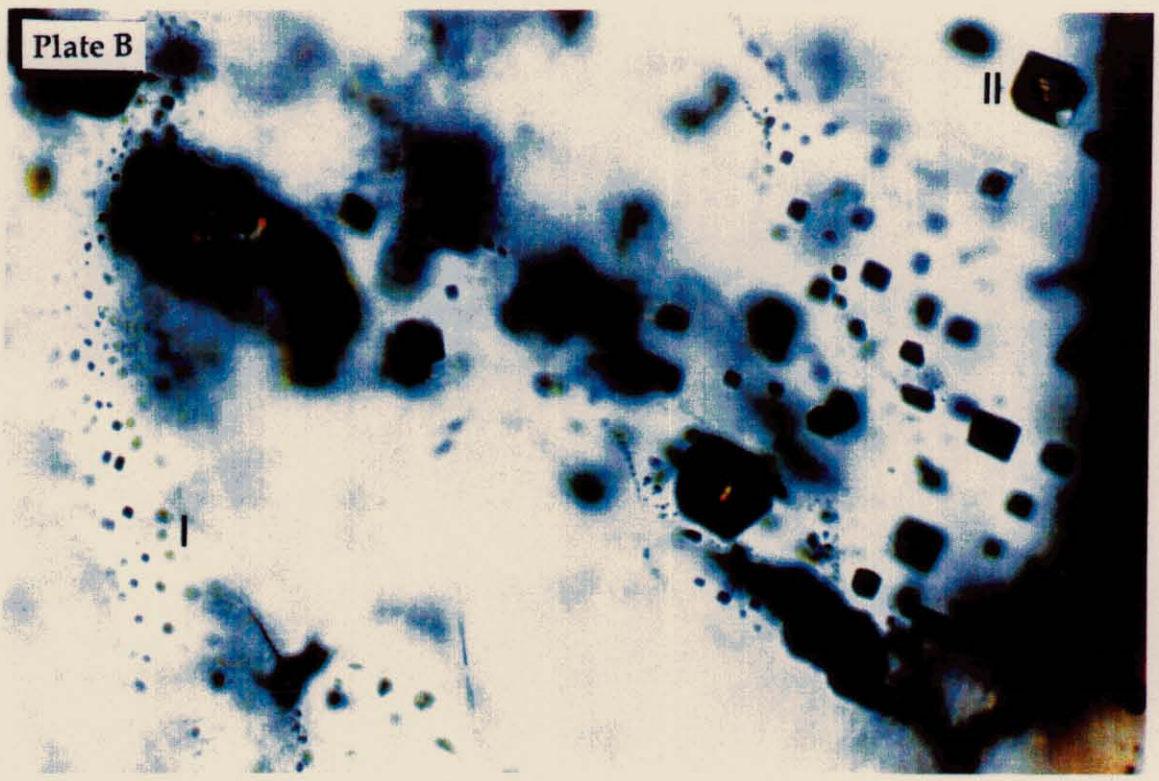

5.3 *MICROTHERMOMETRY*

Heating/freezing microthermometry was performed at the University of Tasmania using a modified version of the Reynolds Stage (Shepherd et al, 1985). The stage was calibrated using synthetic fluid inclusions accurate to within ± 1.0°C for heating and ± 0.3°C for freezing. Salinity estimates were calculated from final melting temperatures using an algorithm of Brown and Lamb (1989). Homogenisation temperatures have not been pressure corrected; therefore homogenisation temperatures are minimum trapping temperature estimates.

The behaviour of Type I and II fluid inclusions during microthermometry was identical, therefore the following results refer to both inclusion types.

5.3.1 Salinity and Temperature of Homogenisation (T_h).

Secondary fluid inclusions found in a sample of honey-coloured (low Fe) sphalerite (ZGP 2) collected from the surface expression of the LMZ had relatively well-constrained temperatures of homogenisation between 130°C and 173°C, averaging 150°C. Freezing point depressions of -2.6°C to -1.5°C (average -2.2°C) correspond to calculated salinities between 2.5 and 4.3 wt% NaCl. Frequency histograms of homogenisation temperatures and salinities are shown in Fig. 5.3 a and b.

Eutectic temperatures were inconsistent, with some inclusions having temperatures around -55°C and others around -37°C. Eutectic temperatures at -55°C are consistent with a fluid containing NaCl, H_2O and $CaCl_2$. Temperatures around -37°C are consistent with a fluid containing K, Na, H_2O, and K_2CO_3, (Sheppard, 1985).

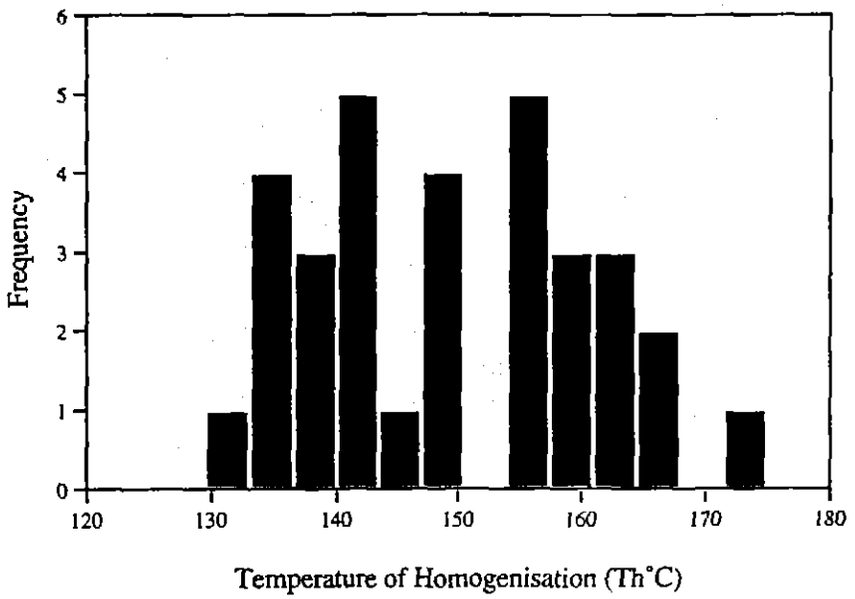

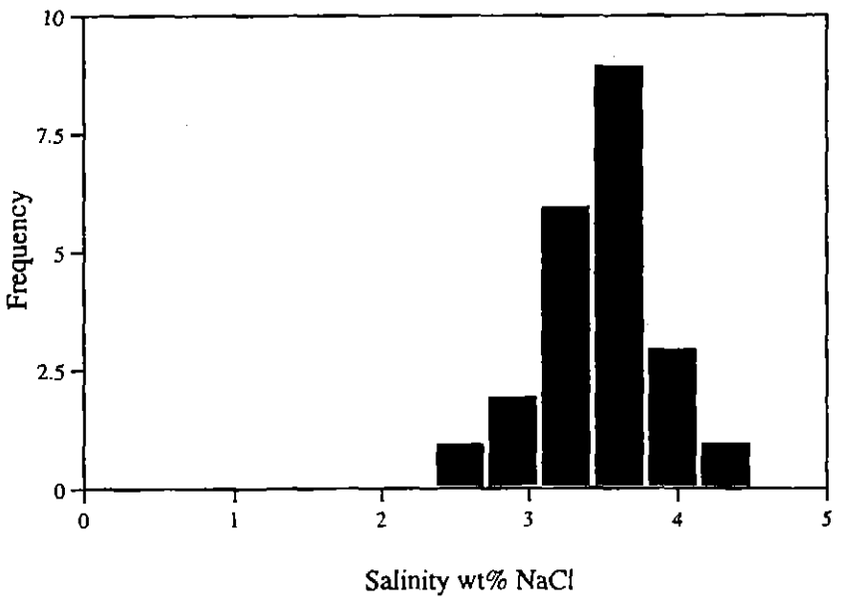

Figure 5.3 (a & b): Frequency Histograms of homogenisation temperatures (a) and salinities (b) observed from secondary fluid inclusions in sphalerite from Grieves Siding.

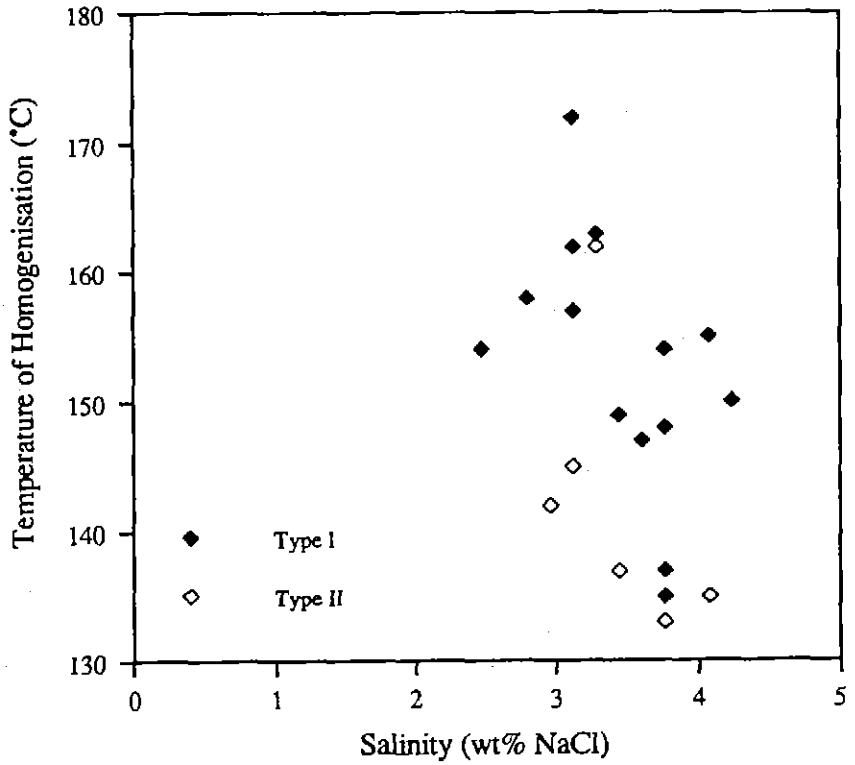

Figure 5.4: Homogenisation vs salinity plot. Type I and Type II fluid inclusions can be weakly distinguished by different temperatures and salinities.

5.4 *DISCUSSION*

Microthermometric studies of secondary fluid inclusions indicates mineralisation at Grieves Siding may have precipitated from low temperature (130-173°C), low salinity (2.5 - 4.3 wt% NaCl) fluids. The fluid contained significant Cl, Ca, Na, and K. Two types of secondary fluid inclusions have been recognised, some occurring in healed fractures and others occurring as single isolated inclusions. Minor variations in the temperature of homogenisation and salinity occurs between these populations.

Low salinity and low homogenisation temperatures are consistent with a mixed meteoric seawater fluid source (Fig 5.5). The data plots just outside values indicative of connate brines, and closest to Sedex and Mississippi Valley Type deposit values (Fig. 5.6).

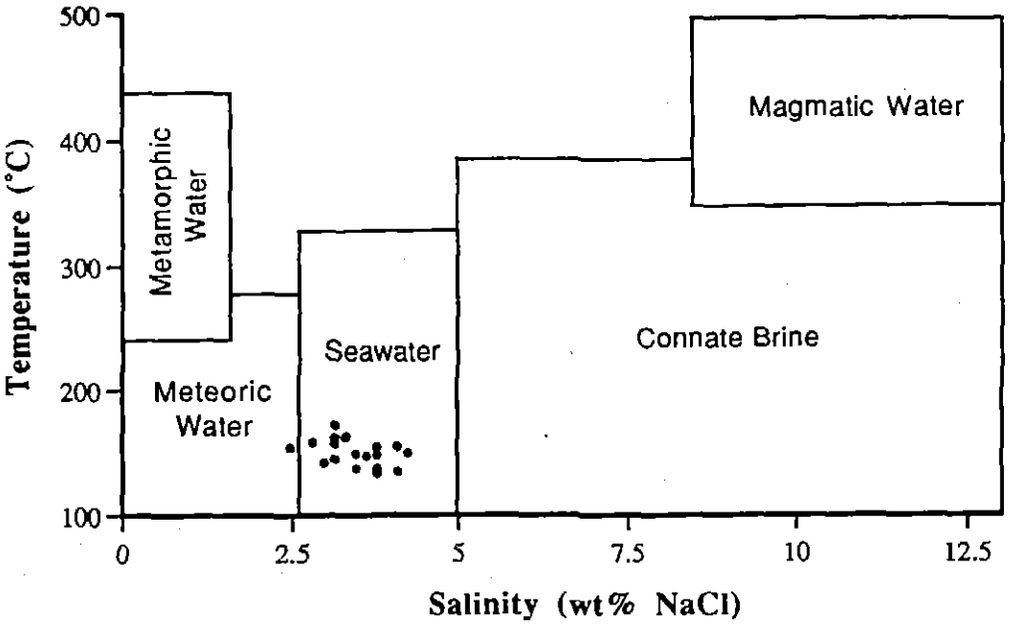

Figure 5.5: Temperature - salinity plot for different fluid sources. Black dots indicate fluid inclusions from Grieves Siding that have a mixed meteoric and seawater source.

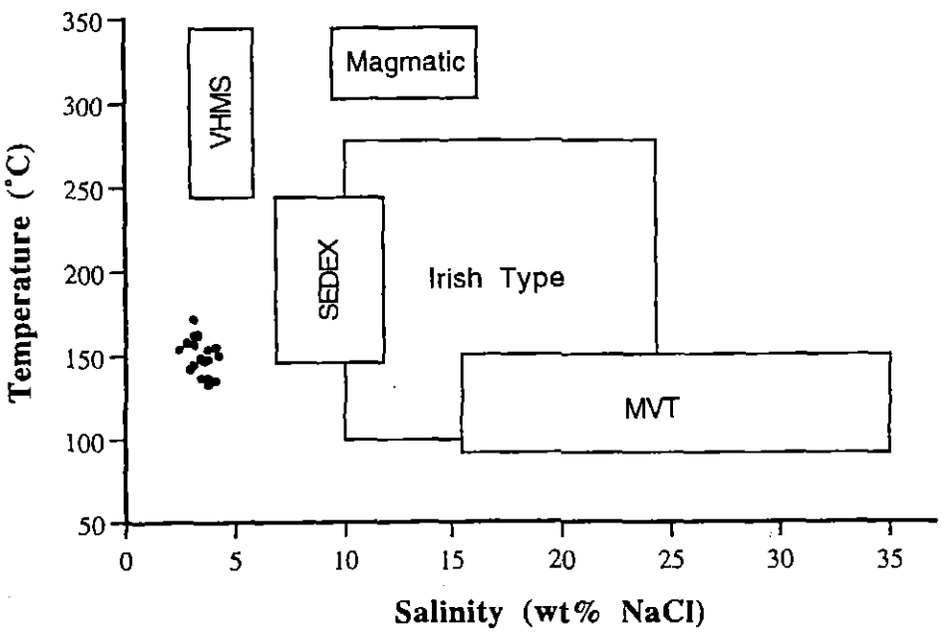

Figure 5.6: Temperature - salinity plot representing values from different styles of mineralisation. Data from Grieves Siding has a similar temperature to Sedex, MVT and Irish Type deposits but has insufficient salinity (Modified after Zaw and Cooke, 1995).

Mississippi Valley Type deposits (MVT) have fluid salinity values between 15 and 35 wt% NaCl, and temperatures of formation between 90 and 150°C. The relative abundance of ions is Cl > Na > Ca > K > Mg > B, in almost all MVT deposits (Roedder, 1985). Sedex deposits have salinities, between 6 and 12 wt% NaCl, and temperatures of formation between 120 and 245°C (Zaw and Cooke, 1995). Irish style deposits formed from moderately saline (7 - 24 wt% NaCl), slightly acid, relatively sulphur poor fluids which had temperatures of 120 to 280°C (Hitzman, 1985).

The temperature and chemical composition of Grieves Siding fluid inclusions are consistent with those seen in MVT deposits. Salinity results are just below those indicative of connate brines, and plot outside those of typical MVT deposits.

The results of fluid inclusion studies have important implications for the timing and style of mineralisation at Grieves Siding. The low salinity of the fluid would equate to low metal solubilities as chloride complexes. Temperatures of formation are consistent with Sedex, MVT and particularly Irish type deposits. The validity of results obtained from secondary inclusions is questionable, however when compared with the Zinc number from Grieves Siding, it appears that the secondary fluid inclusions represent the composition of the original mineralising fluid. A mean zinc number of approximately 80 was obtained from geochemical data at Grieves Siding. Combined with a salinity value of ~3.5 wt % NaCl (corresponding to ~1.5 m NaCl), the temperature estimate derived from Fig. 5.7 of 150°C is consistent with temperatures of homogenisation obtained from fluid inclusions. This indicates a low salinity, low temperature fluid was responsible for precipitation of sphalerite, and presumably other mineralisation at Grieves Siding. The low metal solubility of this fluid therefore contribute the minor amount of mineralisation discovered at Grieves Siding, and has important implications for further exploration.

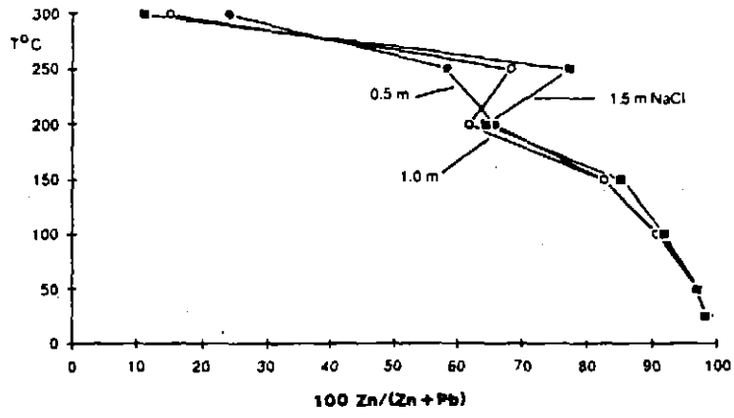

Figure 5.7: Effect of temperature on the zinc ratio for salinities of 0.5, 1.0, 1.5 m NaCl. Grieves Siding has a mean zinc ratio of ~80, a salinity equivalent to 1.5 m NaCl, and therefore a temperature of 150°C.

Stable Isotopes 6

6.1 INTRODUCTION

Stable and radiogenic isotopes have been employed at Grieves Siding to assist in the development of a genetic model, and to determine the likely fluid and metal sources. Transportation and mineral deposition mechanisms, coupled with age determinations have also been eluded to by the application of isotopes. This chapter outlines the use of isotopes in characterising the timing and style of mineralisation at Grieves Siding.

6.2. CARBON AND OXYGEN ISOTOPES

6.2.1 INTRODUCTION

Carbon and oxygen stable isotopes were used to characterise the Gordon Limestone at Grieves Siding, and provide additional information on the conditions at deposition and palaeotemperature. This study was also used to locate isotopic gradients resulting from physiochemical change due to mineralising fluids. Such gradients exist above the Lower Mineralised Zone. Siderite associated with mineralisation was also analysed to characterise the hydrothermal fluids.

Samples were drilled from rocks collected from diamond drill hole ZG 406. Siderite was obtained from the LMZ, and from samples associated with mineralisation in the UMZ. Twenty one carbonate samples were analysed for carbon and oxygen isotopes; fourteen from limestone and seven from siderite.

6.2.2. PROCEDURE

A dentist drill was used to collect calcite and siderite from selected samples. Analyses were derived from whole rock samples which included allochems, intraclasts and matrix carbonate. The resulting fine powder was reacted in 4cc's of 100% phosphoric acid and placed in a water bath at 25°C for 72 hours. The time spent in the water bath depended on the minerals ability to produce CO_2. Some samples liberated H_2S during the reaction. Carbon dioxide released from

the samples was trapped in a liquid nitrogen cooled (-190°C) vacuum line to separate the non-condensables. The remaining sample of frozen gas was heated and refrozen with a mixture of dry ice and acetone to remove any water present. The CO_2 was then frozen separately with liquid nitrogen, and ice remelted and pumped away. Once purified the carbon dioxide was analysed for $^{18}O/^{16}O$ and $^{13}C/^{12}C$ using a VG Micromass 602D mass spectrometer at the Central Science Laboratory, University of Tasmania. The $\delta^{13}C$ and $\delta^{18}O$ values are expressed in conventional per mil δ (‰) notation, relative to PDB and SMOW standards. The precision of data, established with duplicate analyses for both oxygen and carbon is ± 0.1 ‰.

6.2.3. RESULTS

The carbon and oxygen isotopic composition of the Gordon Limestone at Grieves Siding is presented in Table 6.1. Siderite compositions associated with mineralisation are given in Table 6.2, and both limestone and siderite analysis are plotted in Figure 6.1. Three separate populations are disernable on Figure 6.1, which are described separately below.

Population A represents values from unaltered Gordon Limestone sampled systematically down DDH ZG 406. Population A has $\delta^{13}C_{PDB}$ values between -1.8‰ and 0.3‰, with $\delta^{18}O_{SMOW}$ values between 18.4‰ and 23.7‰. Results from previous isotopic investigations of the Gordon Limestone conducted in the Florentine Valley by Rao and Wang, (1990) are overlayed upon data from this study (Fig 6.2).

Population B has $\delta^{13}C_{PDB}$ values that range from 0.9‰ to 4.5‰, with $\delta^{18}O_{SMOW}$ values between 14.6‰ and 22.1‰. These values were derived from siderite associated with sphalerite, galena, and marcasite of the UMZ.

Population C has varying results ranging from $\delta^{13}C_{PDB}$ values between 0.16‰ to -13.3 ‰, and $\delta^{18}O$ values between 22.7‰ and 31.4‰ relative to SMOW. These values were derived from siderite associated with mineralisation in the Lower Mineralised Zone.

The results of systematic sampling down DDH ZG 406 are seen in Fig 6.3. Initial samples were recovered every 10 - 20 m up until a depth of 109.5 m, from which samples were taken every metre to the top of the LMZ at 119 m. Values for the Gordon Limestone remained constant between $\delta^{13}C_{PDB}$ -1.8‰ to 0.3‰, and $\delta^{18}O_{SMOW}$ values of 18.4‰ and 23.7‰. Upon entering the lower mineralised zone, $\delta^{13}C_{PDB}$ values decreased sharply from 0.16 to -13.3 ‰ before increasing slightly to -11.5 ‰ (Fig 6.3). Corresponding $\delta^{18}O_{SMOW}$ values increased dramatically from 22.7 to 31.5, a gain of 8.72 ‰.

Table 6.1: Carbon and oxygen isotopic composition of the Gordon Limestone at Grieves Siding. Samples were collected systematically down DDH ZG 406, from the LMZ to the Myrtle Formation.

Sample No.	Del 13C PDB	Del 18O PDB	Del 18O SMOW
ZG 406 #1	-5.454	-2.348	28.44
ZG 406 #2	0.161	-7.858	22.759
ZG 406 #3	0.384	-7.817	22.802
ZG 406 #4	0.172	-8.719	21.872
ZG 406 #5	-0.193	-7.633	22.991
ZG 406 #6	-0.623	-8.799	21.789
ZG 406 #7	-0.68	-6.927	23.719
ZG 406 #8	-0.457	-9.355	21.216
ZG 406 #9	-0.537	-7.388	23.244
ZG 406 #10	0.174	-7.527	23.101
ZG 406 #20.5	-1.853	-8.563	22.033
ZG 406 #40	-0.121	-12.063	18.424
ZG 406 #55	0.319	-8.173	22.435
ZG 406 #75	0.348	-8.663	21.93

Table 6.2: Carbon and Oxygen isotopic composition of siderite associated with mineralisation at Grieves Siding.

Sample No.	Del 13C PDB	Del 18O PDB	Del 18O SMOW
41700N (A)	1.677	-10.348	20.193
41700N (B)	4.563	-8.495	22.103
ZG 1002 (A)	1.052	-15.69	14.686
ZG 1002 (B)	0.904	-13.573	16.868
LMZ #1 (mine)	-10.952	-2.077	28.718
LMZ #2 (ZG 406-119m)	-13.315	0.186	31.051
LMZ #3 (ZG 406-119.5m)	-11.584	0.603	31.481

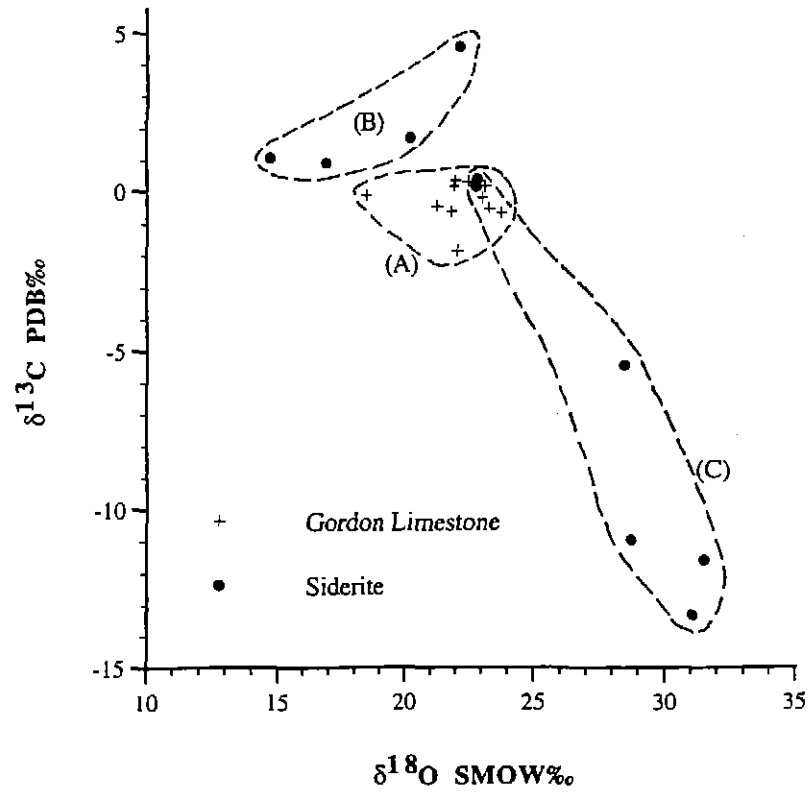

Figure 6.1: Carbon - oxygen isotope plot of siderite and whole rock carbonate at Grieves Siding. Three distinct populations can be defined (a) Unaltered whole rock Gordon Limestone; (b) Siderite from the UMZ; (c) Siderite from the LMZ.

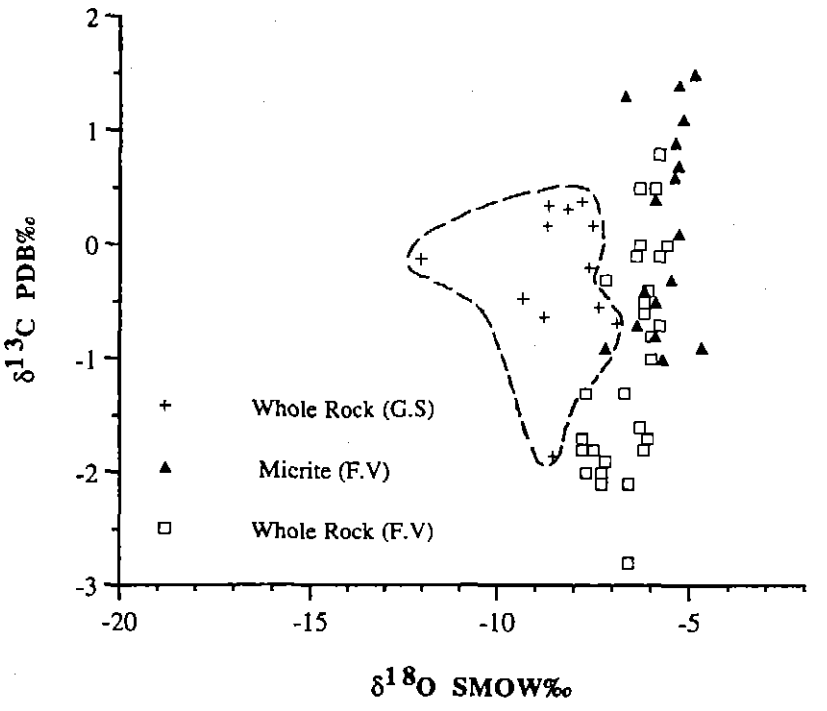

Figure 6.2: Carbon and oxygen isotope graph for whole rock carbonate values for Grieves Siding, overlayed with data from Rao and Wang (1990), for the Florentine Valley.

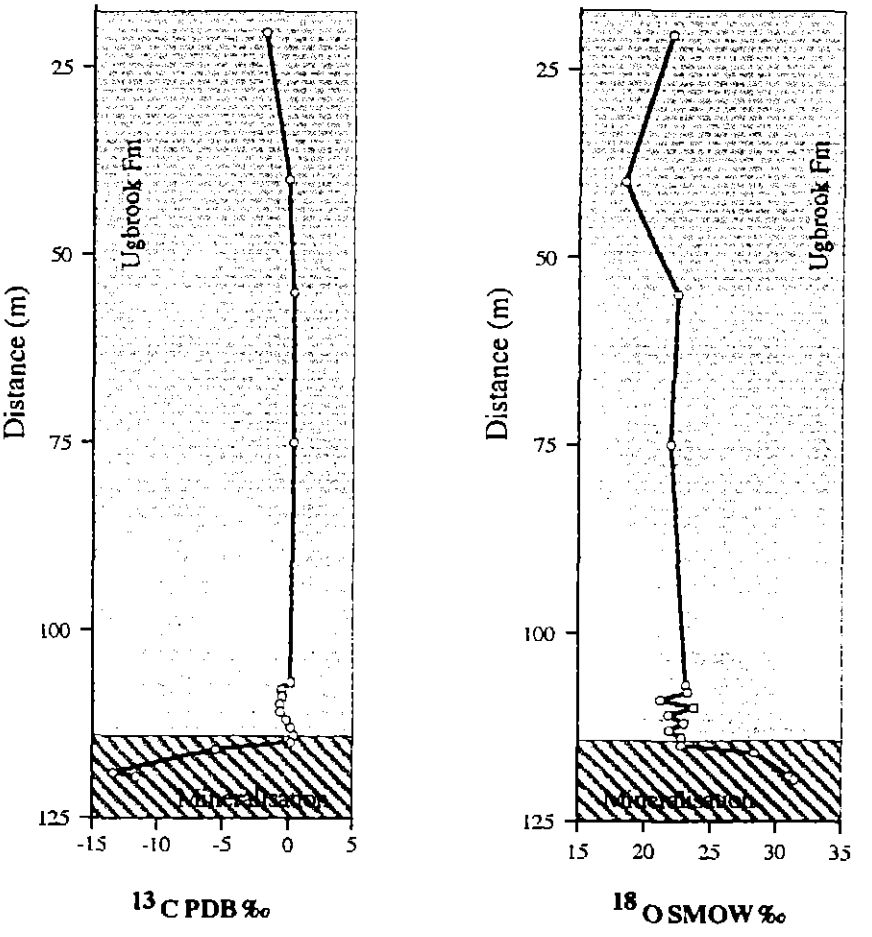

Figure 6.3 Systematic sampling down DDH ZG 406, which is marked by a sharp increase in $\delta^{18}O$, corresponding to a sharp decrease in $\delta^{13}C$ upon entering the LMZ.

6.2.4 *DISCUSSION*

(i) *Gordon Limestone*

The $\delta^{13}C$ and $\delta^{18}O$ data for the Gordon Limestone at Grieves Siding are compared (Fig 6.2) to data for the Gordon Limestone in the Florentine Valley of Rao and Wang, (1990). The tendency for economic geologists to use $\delta^{18}O$ relative to SMOW, whereas sedimentologists use $\delta^{18}O_{PDB}$, can be overcome by using a conversion factor of:

$$\delta^{18}O_{SMOW} = [(1.03086 \times \delta^{18}O_{PDB}) + 30.86]$$

Whole rock limestone data from Grieves Siding can help to quantify changing atmospheric CO_2 concentrations during the Middle to Late Ordovician. Slightly lighter $\delta^{13}C$ and $\delta^{18}O$ (up to 3 ‰ lighter) values from whole rock data in the Florentine Valley can be explained by differing depositional environments and Ordovician seawater values.

Theoretical carbonate (HCO_3^-) curves have been constructed for the Ugbrook and Myrtle Formations, and the average Gordon Group at Grieves Siding (Fig 6.4). These curves assume an Ordovician seawater temperature of 25°C, and were constructed according to the fractionation equation of O'Neil et al., (1969) for $\delta^{13}C$ and the equation of Deines et al., (1974) for $\delta^{18}O$. Estimated fluid values from these curves suggest a Middle Ordovician seawater value responsible for deposition of the Ugbrook Formation of $\delta^{18}O_{SMOW}$ = -6 and $\delta^{13}C_{PDB}$ -2.5. A second curve constructed for the Myrtle formation indicates a Mid to Late Ordovician seawater value of $\delta^{18}O_{SMOW}$ = -5 and $\delta^{13}C_{PDB}$ -1.7. The average Gordon Group sequence at Grieves Siding was deposited from an Ordovician seawater value of $\delta^{18}O_{SMOW}$ = -6 and $\delta^{13}C_{PDB}$ = -2.

Table 6.3 lists Middle, Mid to Late, and Late Ordovician seawater compositions, from this study and work in the Florentine Valley by Rao and Wang, (1990). Middle Ordovician $\delta^{18}O$ values from the Ugbrook Formation at Grieves Siding correspond to values of Rao and Wang, (1990). Differences in carbon values (up

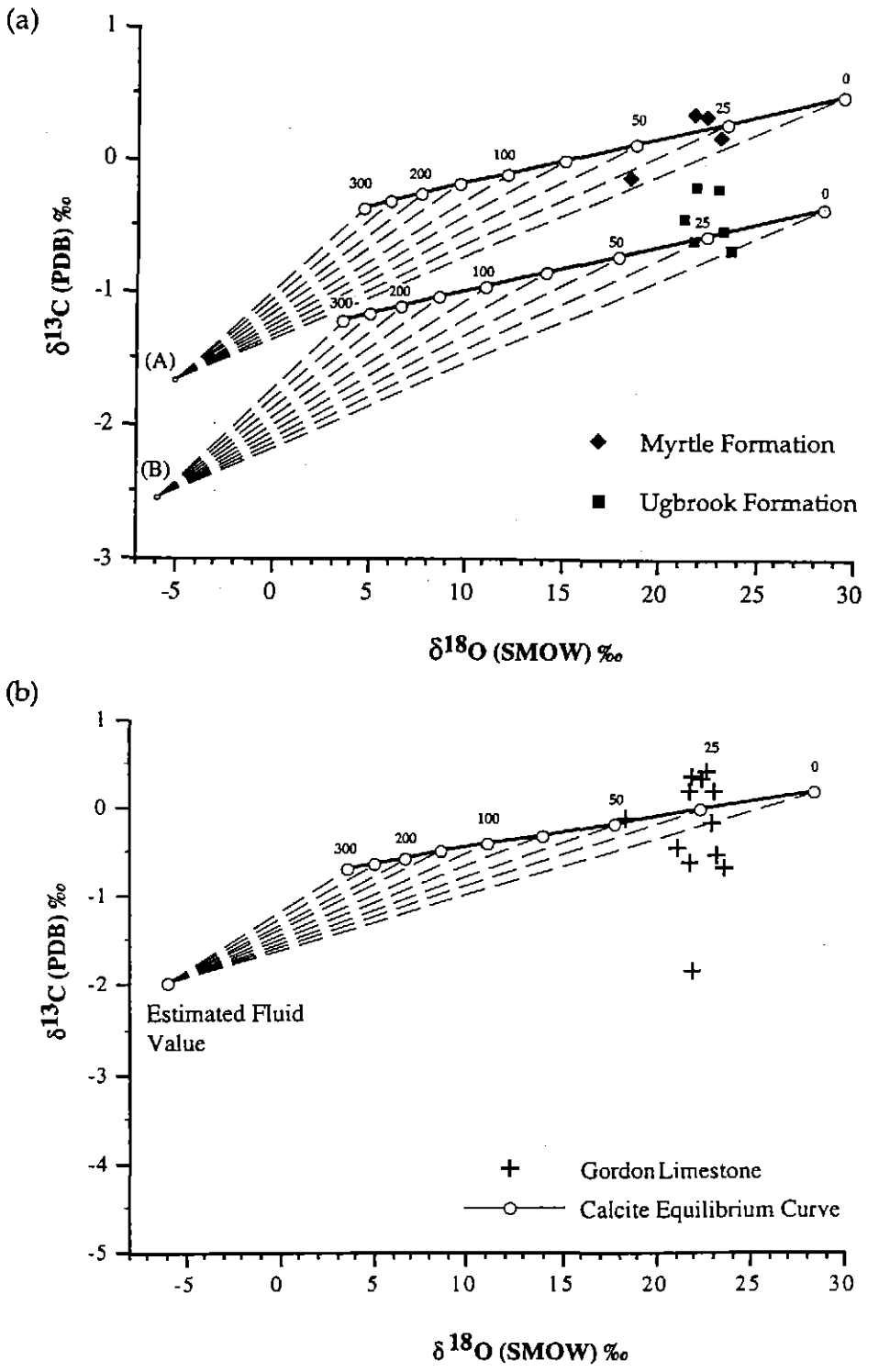

Figure 6.4: (a) Theoretical carbonate (HCO_3^-) curves constructed for comparison of Ordovician seawater compositions, relative to the Myrtle and Ugbrook Formations. (b) and whole rock Gordon Limestone.

to 3.5 ‰) are attributed to argillaceous and organic matter being deposited in protected subtidal lagoons of the Ugbrook Formation, serving to decrease the carbon value. Analyses from the Mid to Late Ordovician Myrtle Formation define an intermediate seawater composition between Middle and Late values published by Rao and Wang (1990). The results confirm an increase in atmospheric CO_2 concentration occurred between the Mid to Late Ordovician, increasing the amount of CO_2 in the sea.

Table 6.3: Middle, Mid to Late, and Late Ordovician seawater compositions, from this study and work in the Florentine Valley by Rao and Wang, (1990). The Myrtle Formation provides an intermediate Mid to Late Ordovician seawater composition between the published Middle and Late Ordovician values of Rao and Wang (1990).

Period	Oxygen (seawater)	Carbon (seawater)	Reference
Middle Ordovician	-6	-2.5	This study
	-5	1	Rao and Wang (1990)
Mid to Late Ordovician	-5	-1.7	This study
Late Ordovician	-3	1	Rao and Wang (1990)

This increase continued until the late Ordovician, producing a seawater composition $\delta^{18}O_{SMOW}$ -3 ‰ and $\delta^{13}C_{PDB}$ +1 ‰. This increase correlates to an icehouse climatic period during the Mid to Late Ordovician (Rao and Wang, 1990) that lead into glaciation during the Late Ordovician (Late Caradoc). Rao and Wang, (1990) suggest atmospheric CO_2 concentrations during Middle and Late Ordovician limestone deposition were similar to present day concentrations. The positive shift of +3.5 ‰ in $\delta^{18}O$ is comparable to the +1.2 ‰ shift during Permian and Quaternary glaciation (Rao and Wang, 1990).

(ii) *Lower Mineralised Zone*

Siderite values in the Lower Mineralised Zone are similar to early phases of ore deposition in the Pine Point MVT deposit. Oxygen values are also consistent with MVT deposits. A theoretical hydrothermal carbonate (H_2CO_3) curve was

calculated for Population C assuming a temperature of mineralisation of 150°C, determined from fluid inclusions (Chapter 5). Fractionation factors were not available for $\delta^{13}C_{PDB}$ siderite-H_2CO_3 therefore the $\delta^{13}C_{PDB}$ calcite-H_2CO_3 fractionation equation of Deines et al., (1974) has been used. The fractionation equation of Carothers et al., (1988) was used for $\delta^{18}O$ siderite values. The estimated fluid value for the LMZ ($\delta^{13}C$ = -14, $\delta^{18}O$ = +18) does not explain the observed trend in values, therefore the mineralising fluid must not have been H_2CO_3 dominated. It indicates the fluid or fluid source interacted with organic matter, imparting an organic carbon signature (~ -25‰). The oxygen fluid value is consistent with a sedimentary carbonate, shale, or sulphate source. Subsequently siderite was precipitated from a sedimentary derived fluid, perhaps similar to basinal or connate brines in MVT deposits.

(iii) *Additional Mineralisation*

Mineralisation away from the LMZ has higher carbon values than those of the LMZ. Higher carbon values (4.5 ‰) are consistent with Mississippi Valley CaCO3, whereas lower values around 0 ‰ are indicative of marine limestones. Oxygen values between 14.6 and 22.1 ‰ relative to SMOW are also consistent with a sedimentary rock source. A theoretical hydrothermal carbonate (H_2CO_3) curve has been calculated for this siderite using the same method as for the LMZ (Fig. 6.5). Estimated fluid values from siderite associated with this mineralisation indicates a fluid composition of $\delta^{13}C_{PDB}$ = -4, and $\delta^{18}O_{SMOW}$ = +1 at 150°C. This data produces a coupled C-O trend (Fig. 6.5), and plots in a marine limestone and marble field. The oxygen fluid value is consistent with oxygen found in hydrothermal quartz, carbonates, and sulphates. The H_2CO_3 dominated fluid cooling curve matches the trend in siderite values producing a positive coupled C-O trend. Mechanisms responsible for producing this curve include: carbonate deposition along a temperature gradient in H_2CO_3 dominated fluids; mixing between two carbonate or fluid sources; and wallrock reaction between a fluid and rock (Davidson, 1990). All of these mechanisms may have occurred, however mineralisation is mostly likely attributed to a separate (Devonian?) fluid or fluid mixing.

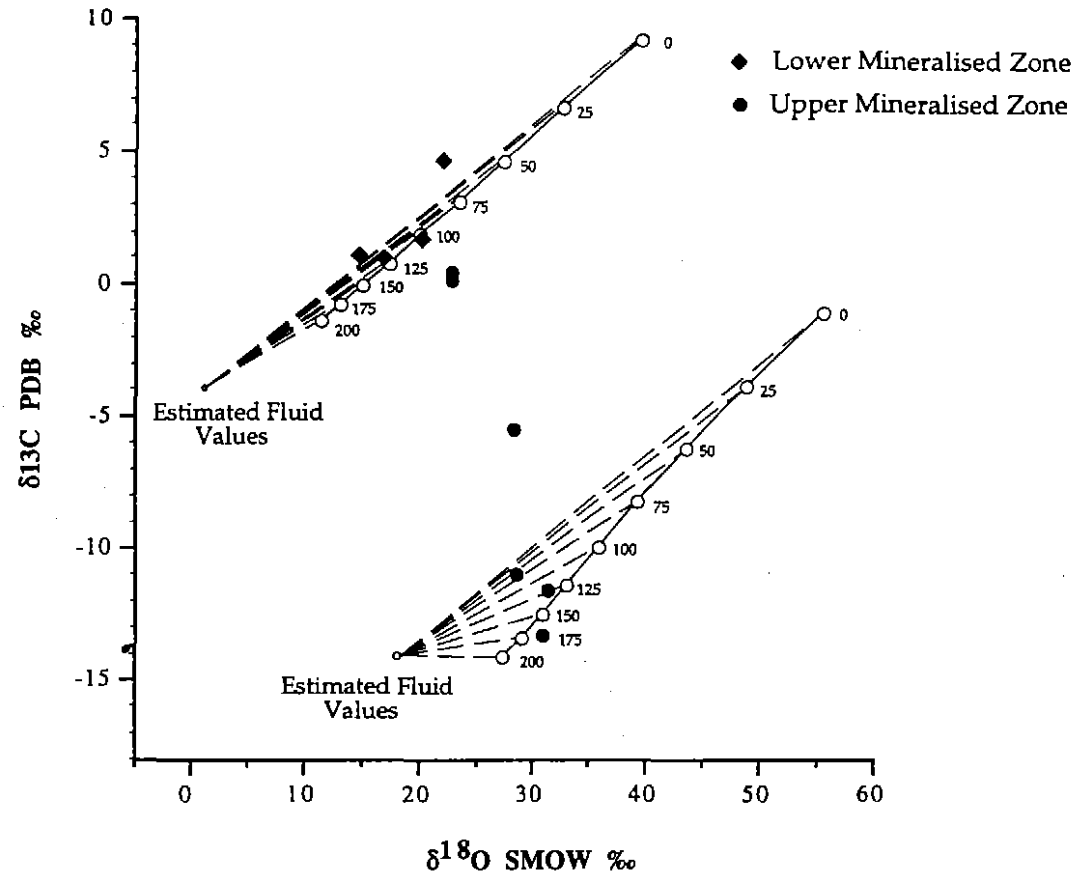

Figure 6.5: Estimated hydrothermal fluid value for the Upper and Lower Mineralised Zones. Fluid values are given in Table 4.6.

Table 6.4: Estimated fluid values for the unaltered Gordon Limestone, and siderite associated the two stratabound mineralised horizons.

FLUID VALUE	GORDON LIMESTONE	UPPER MINERALISATION	LMZ
d13C(PDB)	-2	-4	-14
d18O(SMOW)	-6	1	18

(iv) *Isotopic Halos*

It has been concluded that oxygen - carbon isotopic halos around MVT deposits are usually too small to be of practical use as an ore indicator (Davidson, 1995). In certain instances, however, oxygen - carbon isotopic zonation is the only technique which provides a vector to mineralisation. This is the case at Grieves Siding where a very small alteration halo helps define the LMZ (Fig. 6.3). The

halo is indicative of isotopic exchange between the wall rock carbonate and the mineralising fluid.

Alteration halos up to 60 m wide around two Upper Mississippi Valley deposits are suggested by Hall and Friedman (1969) as representing decreasing temperature gradients away from the orebody. Sverjensky (1981) and Zheng and Hoefs (1993) suggest the halos can be explained as a function of progressively increasing water to rock ratios (W/R).

(v) *Water - Rock Reaction*

Figure 6.5 is a plot of carbon and oxygen isotopes from unaltered Gordon Limestone and siderite of the LMZ. A curved trend is seen in the data that can be explained by progressively increasing water to rock ratios. Calculations were done at 25°C and 150°C for open and closed systems according to an equation modified from Shelton, (1983), after Sverjensky (1981).

The calculated curves are not particularly sensitive to temperature changes up to ±50°C, however they are very sensitive to the initial isotopic composition of the water and rock (Sverjensky, 1981). The initial $\delta^{13}C$ isotopic composition of bicarbonate in the fluid at 23°C is assumed to be -18 ‰, with a siderite value = 0‰. At 150°C the initial $\delta^{13}C$ water value is -18 ‰ and the initial calcite value = 0 ‰. Oxygen values for initial water was +15 ‰, and an initial siderite value of +22‰.

The calculated curves at 25°C and 150°C (Fig 6.5) show a decrease in $\delta^{13}C$ composition of siderite associated with mineralisation as a function of W/R interaction. The shapes of the curves for the data, and the calculated W/R curves are similar (Fig. 6.5) indicating wall rock reaction was responsible for the carbon decrease. The degree of wall rock reaction is expected to decrease away from the mineralisation (Sverjensky, 1981; Fig 6.3). This phenomenon is reflected in the isotope values remaining unaltered (Fig. 6.3) away from the mineralisation as the extent of isotopic exchange decreases. Sverjensky, (1981) suggests the extent of isotopic exchange depends on: the relative proportions of oxygen in the fluid, to that in the rock; on the initial isotope values of the fluid and the rock; and on temperature dependent fluid-rock isotopic fractionation factors. High concentrations of oxygen (+18 ‰), high initial isotope values, and a temperature

of mineralisation of 150°C have undoubtedly influenced isotopic exchange in the LMZ. Water rock reaction can therefore explain isotopic exchange associated with mineralisation, and has helped to understand the origin of the hydrothermal fluid.

The chemical and isotopic compositions of the ore forming fluids have progressively changed during their passage through the wallrocks. The interaction between wallrocks and fluids produces hydrothermal alteration (Sverjensky, 1981). Perhaps the lower silt member above the LMZ which contains dickite, geothite, and illite is indicative of hydrothermal alteration at Grieves Siding. Bones (1987) observed newly formed and recrystallised phyllosilicates (mostly illite) in wallrocks at the Bad Grund MVT deposit, which were attributed to hydrothermal alteration.

The textures and occurrences of ore minerals in the LMZ also support wall rock reaction. Open-space filling of fractures and cavities was important during mineralisation, indicating ore forming fluids could have exploited such openings in the host carbonates.

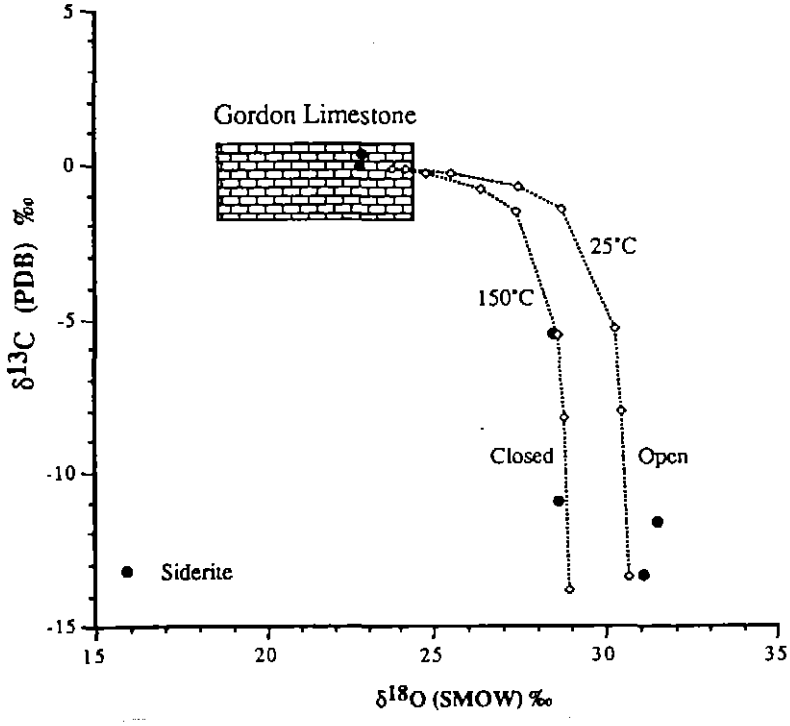

Figure 6.6: Calculated curves at 25°C and 150°C show a decrease in $\delta^{13}C$ composition of siderite associated with mineralisation as a function of W/R interaction.

6.2.5 *SUMMARY*

Carbon and Oxygen stable isotopes have helped record a changing Middle to Late Ordovician seawater composition ($\delta^{18}O_{SMOW}$ -6 to -3 ‰, and $\delta^{13}C_{PDB}$ -2.5 to 1 ‰) corresponding to an icehouse climatic period that preceded glaciation. Mineralisation in the Lower Mineralised Zone was precipitated from a non-magmatic, sedimentary derived fluid perhaps similar to the mineralising basinal and connate brines of MVT deposits. Water rock reaction is assumed to have produced lower carbon isotope values (from $\delta^{13}C_{PDB}$ 0.1 to -13.3 ‰) in siderite, and was perhaps responsible for hydrothermal alteration of the Ugbrook Formation above the LMZ. Mineralisation away from the Lower Mineralised Zone was caused by a separate H_2CO_3 dominated fluid or was produced by mixing of two separate fluids. A Devonian, magmatic fluid could have accessed the same pathways, remobilising Cambrian and Ordovician mineralisation to form the UMZ. The dominance of marcasite in the UMZ, not observed in the LMZ clearly separates these fluids.

6.3 Sulphur Isotopes

6.3.1 INTRODUCTION

A lack of suitable samples has resulted in a limited sulphur isotope study of mineralisation at Grieves Siding. Additional results from the adjacent Myrtle Prospect have been kindly supplied by Dr. G. Green of the Tasmanian Department of Development and Resources. Eight conventional sulphur isotopes analyses were undertaken in order to determine the source(s) of sulphur associated with mineralisation, and to constrain genetic interpretations.

6.3.2 SAMPLING AND ANALYTICAL PROCEDURE

Only six samples from Grieves Siding were suitable for conventional sulphur isotope analyses: two from pyrite of the LMZ (DDH ZG 406); two from massive marcasite; and two from galena and sphalerite found at the abandoned prospect. Two analyses supplied by G. Green, were obtained from galena and barite found in costeans on the Myrtle grid, 5 km south of Grieves Siding.

Samples collected for this study were hand drilled with a dentist drill, and the sulphide material analysed at the Central Science Laboratory (CSL), University of Tasmania. The powdered sulphides were combusted with excess Cu_2O in a *vacuo* to produce SO_2, and the sulphur dioxide gas separated to determine the ^{34}S / ^{32}S ratios. A VG Isogas mass spectrometer was used to determine the sulphur values. Results are expressed as standard δ per mil (‰) relative to the troilite reference standard from the Canon Diablo iron meteorite (CDT). Analytical uncertainty is estimated at $\pm$ 0.2 ‰.

6.3.3 RESULTS

Galena and sphalerite samples from the Grieves Prospect have $\delta^{34}S$ results of 21.4 ‰ and 20.9 ‰ respectively (Fig. 6.7). Large variation was seen in results obtained from pyrite of the lower mineralised zone. Values of 16.4 ‰ and -29.2 ‰ represent a very wide sulphur variation in the LMZ. Further variation was

seen in sulphur values from marcasite above and below the Lords Siltstone. Below the Lords Siltstone marcasite had a $\delta^{34}S$ value of 15.4 ‰, however, above the siltstone, marcasite had a $\delta^{34}S$ value of 31.5 ‰. The results of sulphur isotope analyses of one sulphate and seven sulphide samples are summarised in Table 6.4 (a & b), and Figures 6.7, and 6.8.

The degree of fractionation between $\delta^{34}S_{H2S-\ fluid}$ and sphalerite and galena was calculated from equations given in Ohmoto and Rye (1979). Sphalerite and galena at Grieves Siding were precipitated from a fluid composition of approximately 20.3 ‰ and 17.9 ‰ respectively (Fig. 6.6). This assumes an equilibrium fractionation for sphalerite-H_2S, and galena-H_2S, of 0±1 ‰ and -5 ±1 ‰ respectively.

Table 6.4a: Sulphur Isotope analyses for Grieves Siding.

Location	DDH	Depth	Mineral	d34 S (CDT) ‰
Grieves Siding 42600N	outcrop	-	marcasite	31.5
Grieves Siding 47100N	outcrop	-	marcasite	15.4
LMZ	ZG 406	119 m	pyrite	16.4
LMZ	ZG 406	118.3 m	pyrite	-29.2
Grieves Prospect	outcrop	-	galena	21.4
Grieves Prospect	outcrop	-	sphalerite	20.9

Table 6.4b: Sulphur Isotope analyses supplied by G. Green for the Myrtle prospect.

Location	DDH	Depth	Mineral	d34 S (CDT) ‰
Myrtle 50500N	costean	-	galena	17.6
Myrtle 50600N	costean	-	barite	30.1

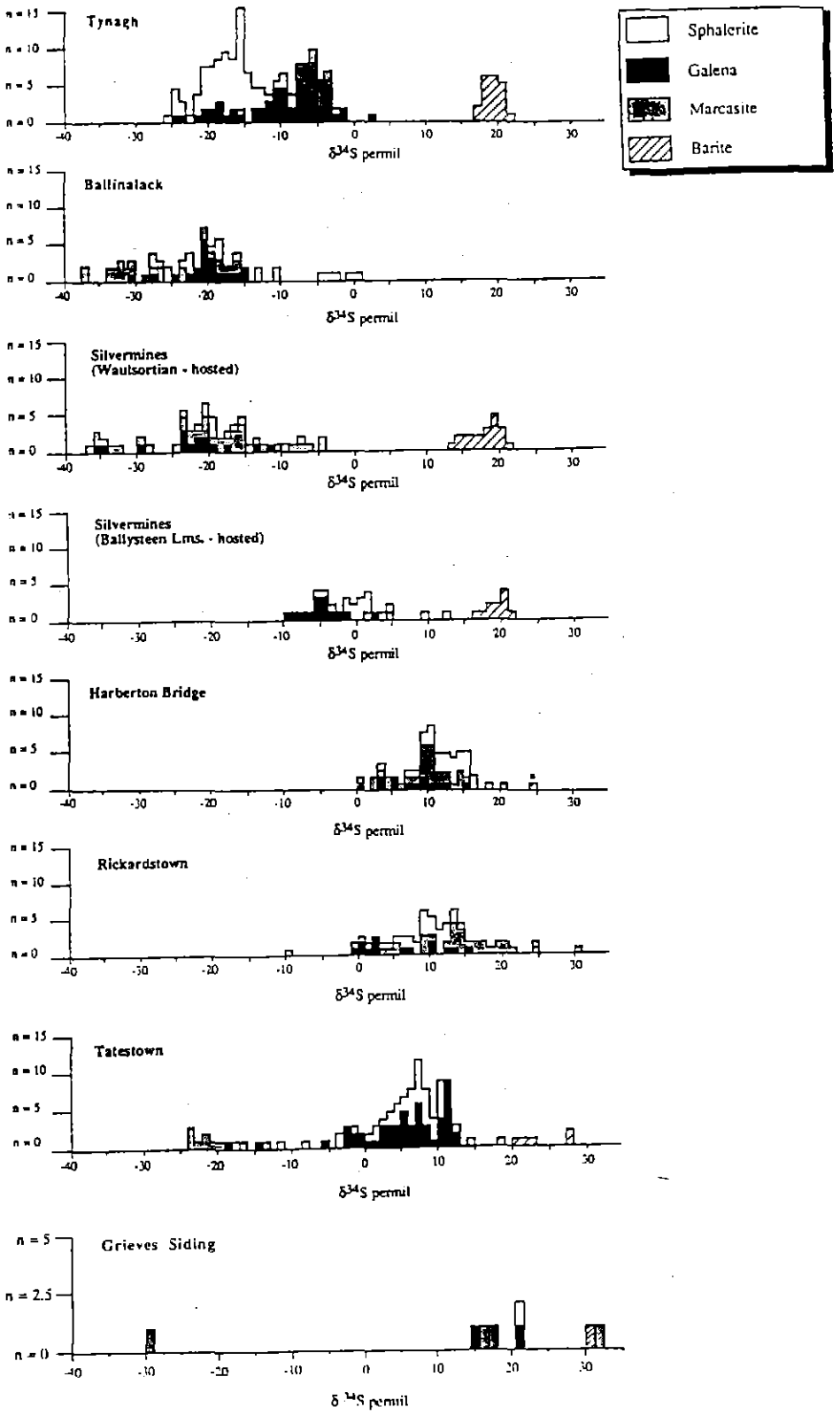

Figure 6.7: Sulphur isotope signatures from Irish-type Zn-Pb deposits relative to values from Grieves Siding. (Modified after Hitzman, 1995).

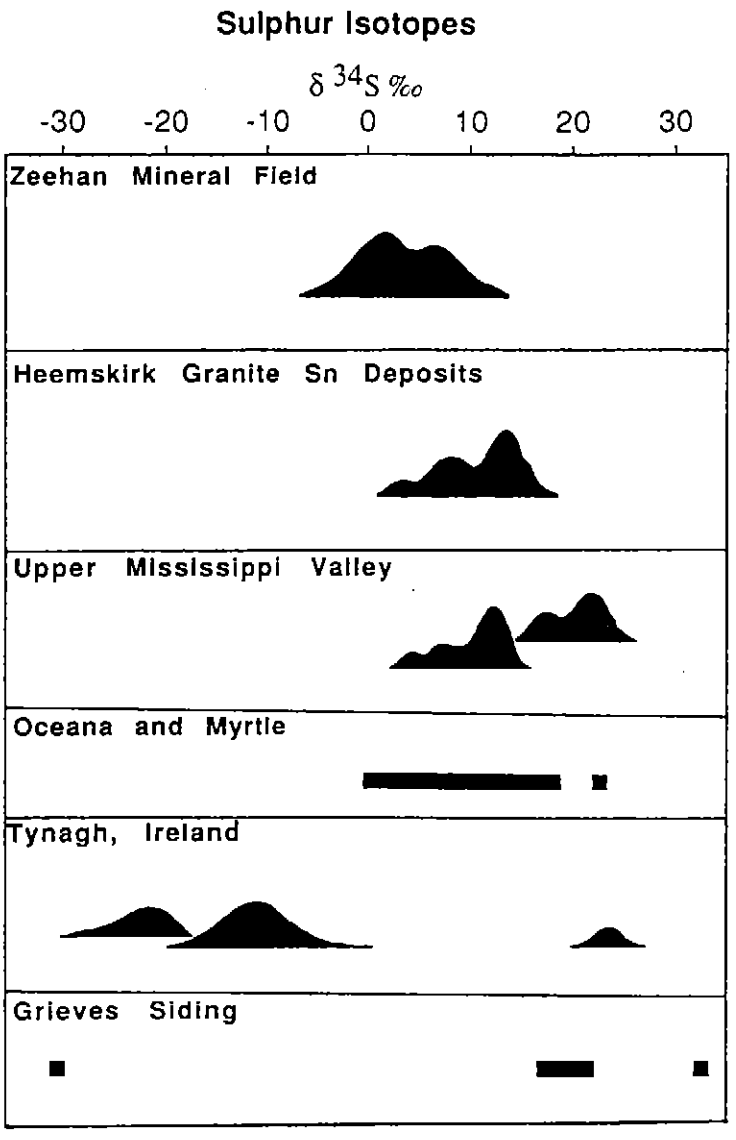

Figure 6.8: $\delta^{34}S$ values from Grieves Siding relative to western Tasmanian deposits, and the Tynagh Irish-type deposit.

5.2.4 DISCUSSION

A very limited sulphur isotope study has yielded results consistent with those from Mississippi Valley Type (MVT) deposits. This discussion relates the main features of this study to those observed in MVT deposits before outlining similarities.

(i) *Variation and Range*

The wide range in sulphur isotope compositions is incompatible with a magmatic source and is similar to patterns seen in MVT deposits (Leech and Sangster, 1994). The sulphur isotope pattern is heavier than those other deposits in the Zeehan Mineral Field, or Heemskirk Granite Sn deposits (Fig. 6.8). Kyser (1987) lists $\delta^{34}S$ isotopic variation in MVT deposits between -8 and +35 ‰. Hitzman (1995) shows isotopic variation in values from the Tatestown Irish-type deposit in Ireland ranging from -24 ‰ to +14 ‰. Grieves Siding has a very wide range between -29.2 and +31.5 ‰ with most sulphide data ranging from 14 - 22‰. Many factors may have contributed to the variation in $\delta^{34}S$ values. The observed range is consistent with derivation of the sulphur from a variety of sources including sulphur bearing organic matter, H_2S reservoir gas, basinal brines, connate seawater and diagenetic sulphides (Leach and Sangster, 1994). Alternatively the wide range may reflect: mixing of sulphur from different sources; isotopic fractionation as a function of mineral species; temperature, and chemical environment (Leach and Sangster, 1994). It is very unlikely that the data can be explained by a single source of sulphur in a homogeneous fluid. Kyser, (1987) suggests that $\delta^{34}S$ variation may be due to reservoir effects (limited supply of H_2S), kinetic isotope fractionation, and reiterates mixing of isotopically different sources. Such a mixing of sources was seen in the Appalachian districts with addition of inorganically reduced seawater sulphate to a fluid dominated by leached biogenic sulphide (Ohmoto et al., 1987).

Biogenic reduction of sulphate is commonly invoked to explain the wide range of $\delta^{34}S$ values, but the temperatures of ore deposition commonly exceed those which can sustain bacterial metabolism. Leach and Sangster, (1994) suggest biogenic reduction must occur separately in time or space from sulphide deposition. The presence of diagenetic pyrite framboids at Grieves Siding concurs with this argument, indicating bacterial sulphate reduction occurred prior to mineralisation.

(ii) *Biogenic Sulphur Reduction*

Bacterial reduction is the principal low temperature control (below 50°C) on sulphur isotope fractionation (Rollinson, 1994). It is used herein to explain the

very low (-29.2 ‰) value obtained from pyrite in the LMZ. Biogenic pyrite framboids seen in the LMZ indicate a reduced environment containing anaerobic sulphate reducing bacteria such as *Desulfuribrio desulfuricans*. Bacteria could have lived in an open sulphur system such as a large body of seawater, eg. a protected subtidal lagoon of the Ugbrook Formation (Chapter 3). Sulphate reducing bacteria operating in such waters would have produced H_2S extremely depleted in ^{34}S (-29.2 ‰) compared to typical Ordovician seawater with $\delta^{34}S$ effectively unchanged (31.5 ‰; Rollinson, 1994). Bacterial filamants which may have been fossilised and later mineralised occuring at the Grieves Prospect is consistent with the presence of sulphate reducing bacteria (Plate 4.1h).

The sulphur composition of Ordovician seawater determined from the sulfate seawater curve was approximately 30 ‰. In a protected subtidal lagoon this seawater value may have elevated slightly, because of progressive closure and removal of sulphate. Therefore the value of 31.5 ‰ recorded from marcasite above the Lords Siltstone is considered indicative of an evolved Ordovician seawater source. Barite at Myrtle has a $\delta^{34}S$ value of 30.1 ‰ which has been interpreted by G. Green (pers. com.) to represent Ordovician seawater. Barite in Irish style deposits records values between +17 ‰ and +22‰, attributed to Carboniferous seawater (Hitzman, 1995), consistent with Green's hypothesis. Barite may not necessarily be giving Ordovician seawater values, instead it could be recording the sulphate value of water derived from Cambro-Ordovician basinal brines.

Bacterial sulphate reduction of this sulphur source could explain lower $\delta^{34}S$ values and contribute to the variation seen in results. Leach and Sangster (1994) suggest the $\delta^{34}S$ values of most MVT sulphides are typically slightly less than those for seawater contemporaneous with the host rocks. They attribute this to isotopic fractionation during various sulphate reduction processes. Mixing of seawater sulphate, perhaps slightly fractionated, with bacterially reduced diagenetic sulphur could therefore help to explain the variation and intermediate range in sulphur isotope results from Grieves Siding. Thermochemical sulphate reduction, which produces a ~7-10 ‰ lighter shift, could also explain intermediate values.

(iii) *Sulphur Sources*

Four out of the six $\delta^{34}S$ results plot between 15.4 and 21.4 ‰. This range is consistent with sediment hosted massive sulphides and MVT deposits. It is also consistent with Tasmanian Cambrian polymetallic massive sulphide deposits which have a spread in $\delta^{34}S$ values in the range of +5 to +20 ‰. These correlations must consider a changing seawater sulphate composition, however they indicate similar sources and processes may have occurred in the genesis of Grieves Siding. As in many sediment hosted deposits, pyrite at Grieves Siding shows the greatest range in $\delta^{34}S$, whereas sphalerite and galena show a restricted range (Large, 1995). Pyrite from Grieves Siding exhibits a very wide variation in $\delta^{34}S$ values, between -29.2 to 16.4 ‰, whereas galena and sphalerite are restricted between 20.9 and 21.4 ‰. A restricted range of $\delta^{34}S$ is often interpreted as indicating an isotopically uniform source of sulphur, however Kyser (1987) suggests, that although sphalerite and galena exhibit a narrow $\delta^{34}S$ range, pyrite often does not. Kyser (1987) interprets this to be due a variety of factors, including admixture of biogenic sulphur (eg. as H_2S, FeS_2).

Application of MVT sulphur isotope theory to Grieves Siding.

At least two sources of locally derived sulphur are inferred at Grieves Siding. These underwent mixing to produce the mineralising fluids. Ordovician seawater sulphate was completely reduced, to produce marcasite with a $\delta^{34}S$ value of 31.5 ‰. Diagenetic pyrite in the form of framboids were formed by bacterial sulphate reduction, most likely of Ordovician seawater sulphate. They are represented by the very low -29.2 ‰ value obtained from the lower mineralised zone. The intermediate sulphur values from pyrite and marcasite (15.4 ‰ and 16.4 ‰) are attributed to either mixing of these sources by the mineralising fluids and/or perhaps an additional input of sulphur from these fluids. Recrystallisation of framboids was observed in thin section from the LMZ, indicating remobilisation of this pyrite by later fluids. This would undoubtedly change $\delta^{34}S$ values perhaps to intermediate values seen in the LMZ. Sverjensky (1986) recognises that not all of the reduced sulphur in MVT deposits was transported with the metal bearing fluids, and suggests some was locally derived. This can help to explain isotopically light sulphur (-29.2 ‰) at

Grieves Siding as being locally derived from diagenetic pyrite in the host rock. Heavier sulphur (around 15 ‰) was brought in by hydrothermal fluids. Speculation can only be made about the source(s) of sulphur in this fluid. An analogy may be in the Kildare District in Ireland, as discussed below.

(iii) Analogies

Analogies can be made between the deep seated sulphur source in the Kildare District, and hydrothermal fluid source at Grieves Siding. Additional comparisons can be drawn between the relatively narrow range in $\delta^{34}S$ for ore fluids that deposited sphalerite and galena in Upper Mississippi Valley deposits.

Consistent $\delta^{34}S$ values from four prospects in the Kildare District ranged between -10 to +30 ‰ with a cluster between +5 to +15 ‰ (Hitzman, 1995). These high $\delta^{34}S$ values are similar to values of sulphides in the 'feeder' zones of other Irish zinc-lead deposits (Hitzman, 1995). They are interpreted by Hitzman (1995) as suggesting sulphides in these deposits were derived from 'deep-seated' sulphur rather than seawater sulphate. Interestingly data from Grieves Siding has a cluster of pyrite and marcasite values around +15 ‰, consistent with these values. Sulphur isotope abundances from twenty three MVT deposits plotted relative to contemporaneous seawater sulphate also cluster around +15 ‰ (Leach and Sangster, 1994). The 'deep seated' source in the Kildare District is of similar composition to the hydrothermal sulphur source at Grieves Siding, perhaps suggesting mineralisation at Grieves represents a feeder zone. The source and evolution of mineralisation could therefore be analogous to that of the Irish Style deposits in the Kildare District.

Sulphur isotope studies in the Upper Mississippi Valley show a relatively narrow range in $\delta^{34}S$ for ore fluids that deposited sphalerite and galena (+22 ‰ and +23 ‰ respectively; Leach and Sangster, 1994). Sphalerite and galena at Grieves Siding were precipitated from a $\delta^{34}S_{H2S}$ fluid composition of 20.3 ‰ and 17.9 ‰ respectively and galena at Myrtle has a mineral value of 17.6 ‰. These results are similar to fluid values for sphalerite and galena deposition in the Pine Point district (+22 ‰ and +23 ‰ respectively). Sverjensky (1986) interpreted these results to represent derivation of sulphur from single sources

or well homogenised multiple sources. Work by Anderson (1990) obtained $\delta^{34}S$ values of -14 ‰ in shales at Queen Hill, north of Zeehan. Values around -14 to -16 could therefore be indicative of sedimentary sulphur sources in the Zeehan area. Subsequently, the source of galena and sphalerite at Grieves Siding is interpreted as being derived from either a single (?sedimentary) source, or well homogenised multiple sources. This source is analogous to the 'deep seated' source suggested by Hitzman (1995) for the Kildare District provinces. The variation in results therefore comes from two sources of sulphur, the mixing of which does not contribute to the sphalerite value, which was derived from one source, with marcasite and pyrite derived from another source.

The uniformity of the calculated values of $\delta^{34}S_{H2S}$ for the Pine Point district is paralleled by the uniform lead isotopic compositions from galena (Sverjensky, 1986). Lead isotopes from galena at Grieves Siding also shows uniformity (Section 6.4).

6.3.5 SUMMARY

Sulphur isotopes from Grieves Siding show a wide variation in $\delta^{34}S$ values consistent with MVT deposits. Although a sulphur poor system was present, the results indicate at least two sulphur sources were exploited. High $\delta^{34}S$ values (31.5 ‰) have been interpreted as representing evolved Ordovician seawater. Low values (-29.2 ‰) are attributed to bacterial sulphate reduction and diagenetic pyrite. Intermediate values around 15 and 20 ‰ are attributed to a hydrothermal fluid perhaps analogous to that in the Kildare District prospects and those seen in feeder zones of some Irish Style deposits. Sphalerite and galena recorded very similar values reflected in many MVT and sediment hosted deposits, with fluid values similar to those of the Pine Point deposit. The source of sulphur in this fluid may have been derived from well homogenised multiple sources, or a single source, perhaps derived from sediments.

These results reflect the variation and complex nature of sulphur sources at Grieves Siding. These characteristics are reflected in many MVT deposits and some Irish Style zinc-lead deposits. They indicate that more work is needed to further constrain sulphur sources to assist genetic interpretations. The initial results are however, very encouraging.

6.4 Lead Isotopes

6.4.1 SAMPLING AND ANALYTICAL TECHNIQUE

Two galena, one pyrite and two marcasite samples were analysed for their radiogenic lead compositions. Pyrite was collected from the LMZ, with galena obtained from both the Grieves Prospect, and mineralisation intersected in DDH ZG 1007, below the Lords Siltstone. Marcasite was obtained from the UMZ. In order to avoid contamination by other sulphides, individual grains were hand-drilled for analysis.

Lead isotope values were analysed by dissolving the samples in 3M HCl and processing through an anion-exchange resin bed to purify the lead. Mass-spectrometric analyses were performed on a VG354 multi-collector mass spectrometer housed at Curtin University, under the supervision of Dr. Neal McNaughton. The data was normalised to NBS-981, and Broken Hill galena Pb used as a reference standard. Analytical uncertainty is ±0.15% (95 % confidence level) in all ratios.

6.4.2: RESULTS

Lead isotopic ratios obtained from samples collected at Grieves Siding are presented in Table 6.5, and plotted in Figure 6.9. Pyrite from the LMZ and marcasite from the UMZ have 206Pb/204Pb values between 18.37 and 18.42; 207Pb/204Pb values between 15.63 and 15.67; and 208Pb/204Pb ratios between 38.33 and 38.44 (Fig. 6.9). Galena from the Grieves Prospect (surface expression of the LMZ) is contained within values from pyrite. Galena from DDH ZG 1007, below the Lords Siltstone also plots within this range.

Table 6.5: Lead isotope sample localities, and ratios.

Sample	Mineral	206Pb / 204 Pb	207Pb / 204Pb	208Pb / 204Pb
Grieves Prospect	galena	18.34	15.62	38.29
ZG 1007	galena	18.36	15.63	38.31
Lower Mineralised Zone	pyrite	18.37	15.66	38.45
Upper Mineralised Zone	marcasite	18.42	15.63	38.33
Upper Mineralised Zone	marcasite	18.38	15.67	38.44

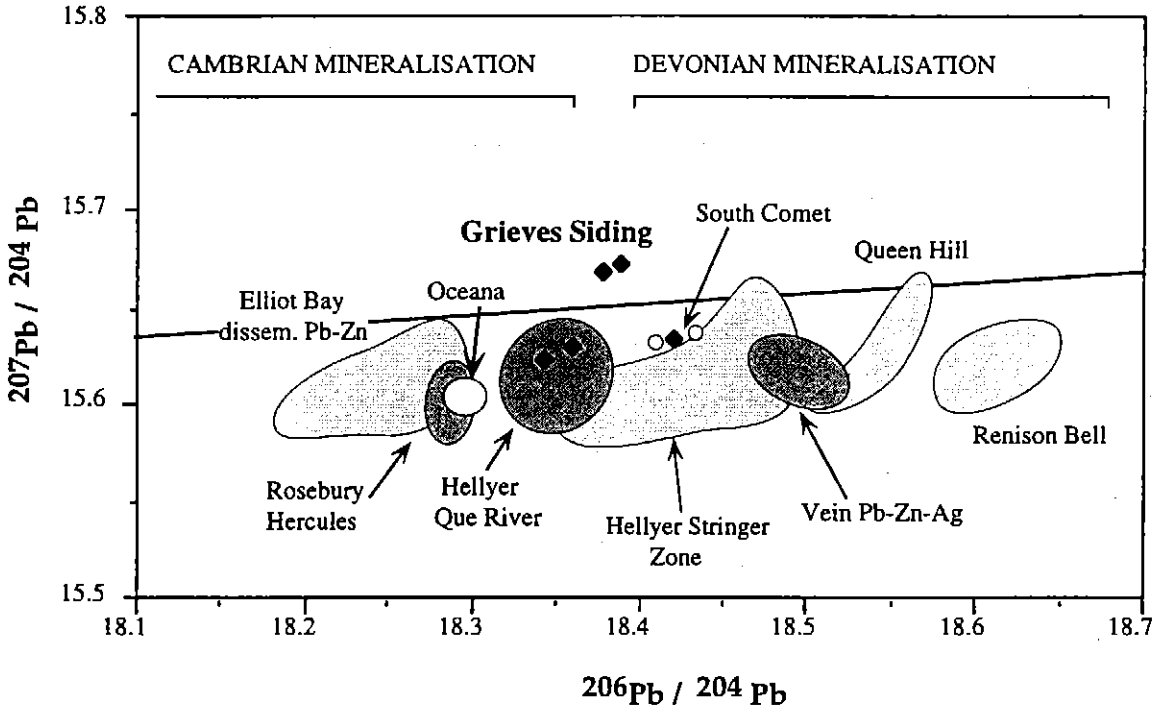

Figure 6.9: Lead isotope compositions of samples obtained from Grieves Siding. Growth curves of Cummings and Richards (1975) are used as a reference. (Modified after Gulson et al., 1987)

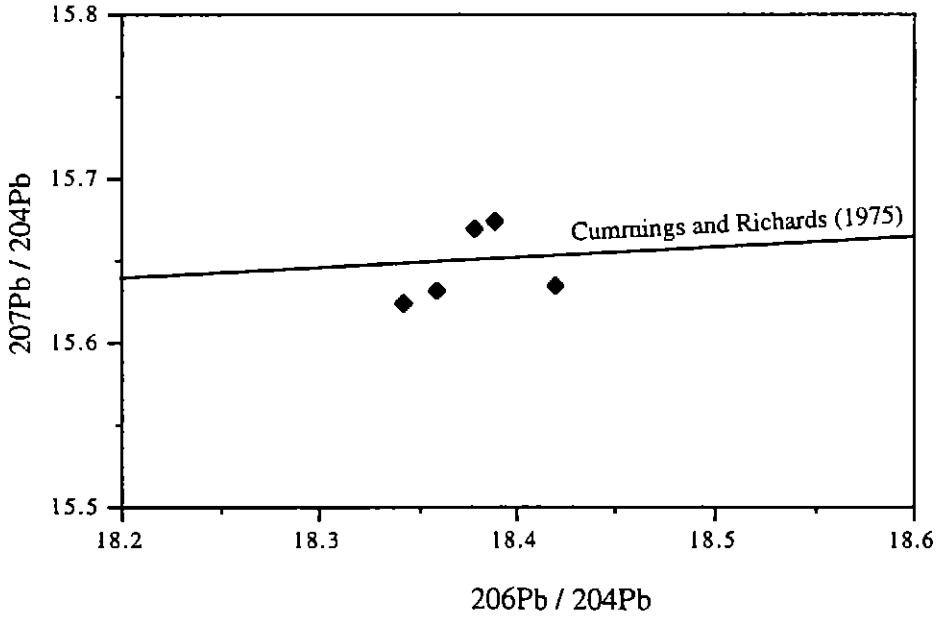

Figure 6.10: Lead Isotope data for western Tasmanian ore deposits (after Gulson et al., 1987). Data from Grieves Siding is less rediogenic than the Devonian Field, and plots towards the edge of the Cambrian field.

Lead isotope ratios from this study are plotted on a $^{207}Pb/^{204}Pb$ vs $^{206}Pb/^{204}Pb$ diagram (Fig. 6.10) together with western Tasmanian lead isotope fields defined by Gulson et al., (1987), and Gemmell et al., (1990). The data plots slightly above the growth curve of Cummings and Richards (1975), and between data considered representative of Cambrian and Devonian mineralisation.

6.4.3 DISCUSSION

Lead isotope signatures of mineralisation in western Tasmania generally fall into two main fields attributed to Cambrian and Devonian mineralisation. A Precambrian source age is implied by Gulson (1984) for Cambrian mineralisation whereas Devonian mineralisation is attributed to granitoid emplacement.

Lead isotope ratios obtained during this study (Fig 6.9) plot towards the edge of the Cambrian field, and well outside (less radiogenic) that attributed to Devonian mineralisation. This implies that the lead was sourced from Late Cambrian sediments, or perhaps an Ordovician source.

Cambrian, Ordovician, and Devonian mineralisation lies on a single linear trend within experimental error. This linear trend on the $^{207}Pb/^{204}Pb$ vs $^{206}Pb/^{204}Pb$ plot intersects the growth curve of Cummings and Richards (1975) for massive sulphide deposits at approximately 1000 Ma. This indicates a similar source for lead, even though the two major phases of mineralisation are Cambrian and Devonian (Ellis, 1984).

The overlap in isotopic signatures from Grieves Siding with Hellyer and Que River may suggest a common source for lead in these deposits. This source is unrelated to Devonian plutonism. In a model explaining the sulphur and lead isotope characters of the Hellyer stringer zone, Gemmell et al., (1990) suggest Cambrian seawater ($\delta^{34}S$ = 30 ‰) entered a convection system that initially scavenged lead from the footwall sequence andesite volcanics. As the convection system intensified it sourced lead derived from clastic sediments and felsic rocks of the Central Volcanic Complex and probably the Precambrian basement (Gemmell et al., 1990). This fluid is considered by Gemmell et al., (1990) to be dominant in the formation of the Hellyer VHMS deposit.

A similar fluid accessing similar sources could have been responsible for mineralisation at Grieves Siding. Metals could be derived from 'deep seated' sources in the Crimson Creek and Oonah Formations. Remobilisation and/or leaching of metals by basinal or connate brines is envisaged to emplace the metals into the Ordovician carbonates.

Taylor and Mathison, (1990), and Large, (1983) suggest the southern Oceana deposit is representative of a sediment hosted stratiform class orebody. Using lead isotopes, Taylor and Mathison, (1990), show that south Oceana leads are less radiogenic than leads from known Tasmanian Devonian (Tabberabberan) granite related mineralisation. This implies that stratiform Oceana mineralisation is Ordovician in age (Taylor and Mathison, 1990). Taylor and Mathison, (1990) suggest the Devonian phase of lead-silver-zinc-tin mineralisation in the Zeehan Mineral Field has been superimposed on an earlier, previously unrecognised mineralising episode in the Ordovician. Lead isotopes in this study would confirm this interpretation.

Lead data from this study is consistent with the interpretation of Taylor and Mathison, (1990). Ordovician mineralisation is seen at Grieves Siding in a style still emerging in sections of the Zeehan Mineral Field.

Evidence from stable and radiogenic isotopes is combined with sedimentological and mineralogical data to develop a genetic model in Chapter 7.

Genetic Model, Summary and Conclusions 7

7.1 INTRODUCTION

The aim of a sedimentological basin analysis and geochemical study of Grieves Siding has been to provide usable information on; (a) the source of the ore-forming components; (b) the mechanisms for metal concentration and transportation, and (c) the mechanism of metal deposition. This chapter summarises the results of this study before proposing a genetic model that attempts to explain the results and outline their implications for exploration.

7.2 GEOLOGICAL SETTING

The lithologies occurring at Grieves Siding are contained within the Wurawina Supergroup, which consists of a concordant sequence of predominantly shelf deposited sediment, including the Denison Group, the Gordon Group, and the Eldon Group. At Zeehan the Moina Sandstone, uppermost member of the Denison Group has a conformable, often interdigitating contact with the Gordon Group carbonates. The positioning of this contact is contentious as it is marked by a siltstone-mudstone transitional zone that is often mineralised. This study defines the contact between the Denison Group and the Gordon Group as the last appearance of consolidated silt, and the first appearance of limestone.

The Gordon Group carbonates are the thickest and most stratigraphically continuous Ordovician (Arenig to Ashgill) sequence in the southern hemisphere. Nine lithofacies associations recognised in the Gordon Limestone at Grieves Siding (Chapter 3) have been configured into three formations, and five intra-formational members. The mid-Ordovician Ugbrook Formation represents subtidal and protected subtidal lagoons influenced by a rapidly migrating carbonate bar. The mid-Caradoc, (Mid to Late Ordovician) Myrtle Formation consists of up to 15 Punctuated Aggradational Cycles (PACs) deposited in shallow subtidal to peritidal conditions. The Myrtle Formation precedes deposition of the dominantly subtidal Black Jacks Formation, which

was interrupted during the Late Caradoc by the Lords Siltstone. The Lords 'event' signifies the response to uplift in the Tyennan region, representing a short lived epirogenetic event (Chapter 3). It was proceeded by a return to subtidal limestone deposition, periodically interrupted by peritidal carbonate deposition. Stratigraphic correlation suggests carbonate deposition is related to four main depositional sites on a carbonate platform. Carbonate was deposited in a tropical environment with a seawater temperature between 23 and 25°C (Chapter 5). Modern analogous depositional environments are seen on the Great Bahama Bahama Bank, and in the Persian Gulf (Pratt, et al., 1992)

Carbon and oxygen stable isotopes from the Ugbrook and Myrtle Formations record a changing Ordovician seawater value (Chapter 5) indicating deposition during an icehouse period from the Mid to Late Ordovician. This proceeds an Early Ordovician greenhouse period, and precedes Late Ordovician to Early Silurian glaciation. Light carbon values at Grieves Siding represent organic material in the depositional environment, (Chapter 6) prevalent in protected subtidal lagoons of the Ugbrook Formation.

The Gordon Group is disconformably overlain by the siliciclastics of the Eldon Group, represented by the Crotty Quartzite at Grieves Siding. The Crotty Quartzite signifies rapid deposition of approximately 500 m of quartz sandstone, clastic pebble conglomerate and minor mudstones in a littoral to sublittoral environment. It represents uplift during the Ashgill (Late Ordovician) that correlates temporally with the Benambran orogeny.

7.3 MINERALISATION

Two mineralised zones are recognised at Grieves Siding. The Lower Mineralised Zone (LMZ) occurs on the interdigitating contact between the Denison and Gordon Groups. It forms a stratiform lens, most pronounced in the north, which has been displaced 40 m by sinistral strike slip movement. Mineral textures in the LMZ are indicative of open-space filling and minor carbonate replacement. Paragenetic studies (Chapter 4) suggest early diagenetic dolomitisation was overprinted by hydrothermal dolomitisation associated with mineralisation. Dolomitisation was followed by iron carbonate (siderite) deposition and pyrite/marcasite in-filling. Sphalerite and galena precipitated almost contemporaneously, followed by repeated sphalerite dissolution and

precipitation producing botryoidal colloform sphalerite spherules (Chapter 4). Four generations of sphalerite are recognised, the latest phase being iron-poor, and containing large fluid inclusions. Minor barite, chalcopyrite, covellite and a late phase calcite are recognised throughout the LMZ. Later sulphide oxidation and remobilisation of HCO3- resulted in the precipitation of smithsonite, rhodochrosite and magnesite. Hemimorphite cross-cuts and replaces all other minerals, and precipitated last.

The Upper Mineralised Zone (UMZ) is associated with the Lords Siltstone which may have acted as a cap for mineralising fluids. Similar mineral textures and paragenetic relationships occur in the UMZ, however massive marcasite and sulphide clasts in a marcasite matrix breccia separates it from the LMZ. Carbon and oxygen isotopes separate the UMZ from the LMZ and suggests a magmatic H_2CO_3 dominated fluid may have been responsible for mineralisation. A Devonian magmatic fluid is perhaps responsible for overprinting and or remobilising the Cambrian metals. The addition of pyrite / marcasite to the upper mineralised zone by well be explained by addition of a magmatic fluid, that exploited the same pathways as Ordovician mineralisation. A Devonian overprint is suggested at Oceana, and at the South Comet mine. remobilisation at Grieves Siding may also be possible. The proximity of a black matrix dolomite breccia in the north, that becomes progressively silicified in the south represents a situation perhaps analogous to the host black matrix breccia in Irish-type deposits and a carbonate breccia associated with mineralisation at Oceana.

Paragenetic studies have defined mineralogies and mineral textures consistent with Irish-type and MVT deposits. Botryoidal colloform sphalerite spherules, open-space filling with minor carbonate replacement; and evidence for repeated sphalerite dissolution and precipitation are consistent with these deposits.

7.4 GEOCHEMICAL ANALYSIS

Stable isotope evidence confirms a non-magmatic source for mineralising fluids. Carbon and oxygen isotopes suggest sedimentary derived fluids, perhaps analogous to mineralising basinal and connate brines in MVT deposits. Wallrock reaction and minor carbonate dissolution is responsible for lower carbon values associated with mineralisation, whereas oxygen values increased.

Table 7.1: Summary of the characteristics of MVT and Irish-type Zn-Pb deposits with respect to mineralisation Grieves Siding. Data from Hitzman (1995), Leach & Sangster (1994) and Russell, (1987); (TSR-thermochemical sulphate reduction).

Feature	MVT	Irish-type	Grieves Siding
Metal Grades	Zn: 2 - 6 wt%; max≈16 wt%	Zn: 2 - 13 wt%	Zn: 10.6m @ 17.8%
	Pb: 1 - 3 wt%	Pb: 0.2 - 6 wt%	Pb: 4m @ 5.4%
	Ag: < 40 g/t	Ag: < 40 g/t	Ag: low
	Cu: low	Cu: low	Cu: low
Mineralogy	Sulphide: low Fe sph, gal, py, marc ± cp, bn	Sulphide: low & high Fe sph, gal, py, marc, minor ten, cp ± bn	Sulphide: low Fe sph, gal, py, marc ± cp, bn, covellite Smithsonite, magnesite, rhodochrosite
	Gangue: dolomite, calcite, minor qtz ± fl, ba	Gangue: dolomite, calcite, minor qtz ± ba, sid	Gangue: dolomite, siderite, ± ba, calcite, hemimorphite
Characteristic Textures	Colloform sulphides, "snow-on-roof", open space fill, carbonate replacement, breccia rims, multiple sph dissolution-precipitation, internal sediments	Massive sulphides, carbonate replacement, colloform sulphides, multiple sph dissolution-precipitation, ± internal sediments	Colloform sulphides, open space fill, minor carbonate replacement, multiple sphalerite dissolution-precipitation
Characteristic Form	Irregular breccias, veins, lesser carbonate replacement and semi-massive stratabound	Massive stratabound to stratiform lenses with associated "feeder" zones typically with halo of veinlet and disseminated mineralisation	Stratabound lenses, with minor Mn, and Ba halo. Black matrix dolomite breccia variably silicified
Association with Dolomitisation	Many districts associated with a pre-mineralisation dolomite	Intimate relationship of regional and alteration dolomitisation	Diagenetic and pre-mineralisation dolomite
Metal Source	Sediments &/or basement	In dispute: sediments or basement	Sediments &/or basement
Sulphur Source	Variable. TSR of evaporites or seawater sulphate; many districts probably had mixing of heavy and light, biogenically reducedsource	Probably two sources: i) isotopically heavy reduced source transported with metals; *ii)* isotopically light biogenically reduced source	Probably three sources: i) modified seawater source; ii) inorganically reduced source; iii) biogenically reduced ?diagenetic source
Temperature of Formation	90°C - 150°C	100°C - 280°C	130°C - 173°C, mean = 150°C
Fluid Salinity	15 – 25 eq.wt% NaCl	10 - 24 eq.wt% NaCl	2.5 - 4.3 eq.wt% NaCl mean = 3.5
Fluid-Flow Mechanisms	Topography, tectonic, episodic, overpressuring, thermal convection	Deep convection or topography (Russell, 1987; Hitzman, 1995)	Convection, topography, diagenetic compaction
Timing of Mineralisation	Late diagenetic or younger; most probably related to tectonic events much younger than depositional age of host successions	Probably diagenetic related to tectonic uplift. Some workers favour a synsedimentary or early diagenetic age	Late diagenetic related to Benambran Orogeny

Sulphur isotopes record a wide $\delta^{34}S$ variation consistent with MVT deposits. high values (31.5 ‰) are attributed to Ordovician seawater as recorded in barite, whereas lower values (-29.22) contributing to the variation in results are attributed to bacterial sulphate reduction. Intermediate values around 15 to 22 ‰ represent the hydrothermal fluid composition. This value signifies a 10‰ shift from Ordovician seawater, due to sulphur isotope fractionation at 150°C via inorganic reduction, or resulted from a separate hydrothermal fluid. The new fluid is derived from either a well homogenised source, or a sediment derived source.

Lead isotope ratios plot towards the edge of the Cambrian field, and well outside (less radiogenic) that attributed to Devonian mineralisation. This implies that the lead is Late Cambrian, perhaps Ordovician in age. A Late Cambrian source is more likely, with lead and other metals scavenged from underlying Cambrian sediments of the Dundas Group.

Secondary fluid inclusions suggest a low salinity (3.5 wt %), low temperature (150°C) fluid was responsible for mineralisation. The temperature of homogenisation is consistent with MVT, and Irish-type deposits (Table 7.1), but low salinity, fluids at Grieves Siding would have low metal solubility of the fluid separates Grieves Siding from these deposits. The zinc number for Grieves Siding is consistent with MVT deposits (mean 80), and suggests the secondary fluid inclusions are indicative of the main mineralising fluid.

7.5: GENETIC MODEL

Sedimentological and geochemical evidence implies the timing of mineralisation at Grieves Siding was Ordovician, and the style is consistent with MVT and Irish-type deposits (Table 7.1)

The source of the mineralising fluids are envisaged as either; (a) basinal and connate brines generated by basinal compaction and dewatering during the Late Ordovician Benambran Orogeny; and/or (b) deep circulating modified seawater. A fluid temperature of 150°C is consistent with a basinal brine, and the low salinity fluid can be explained by a lack of evaporites, and or membrane filtration in the source regions. This maintained the salinity of the brine to 3.5 wt % NaCl, similar to seawater.

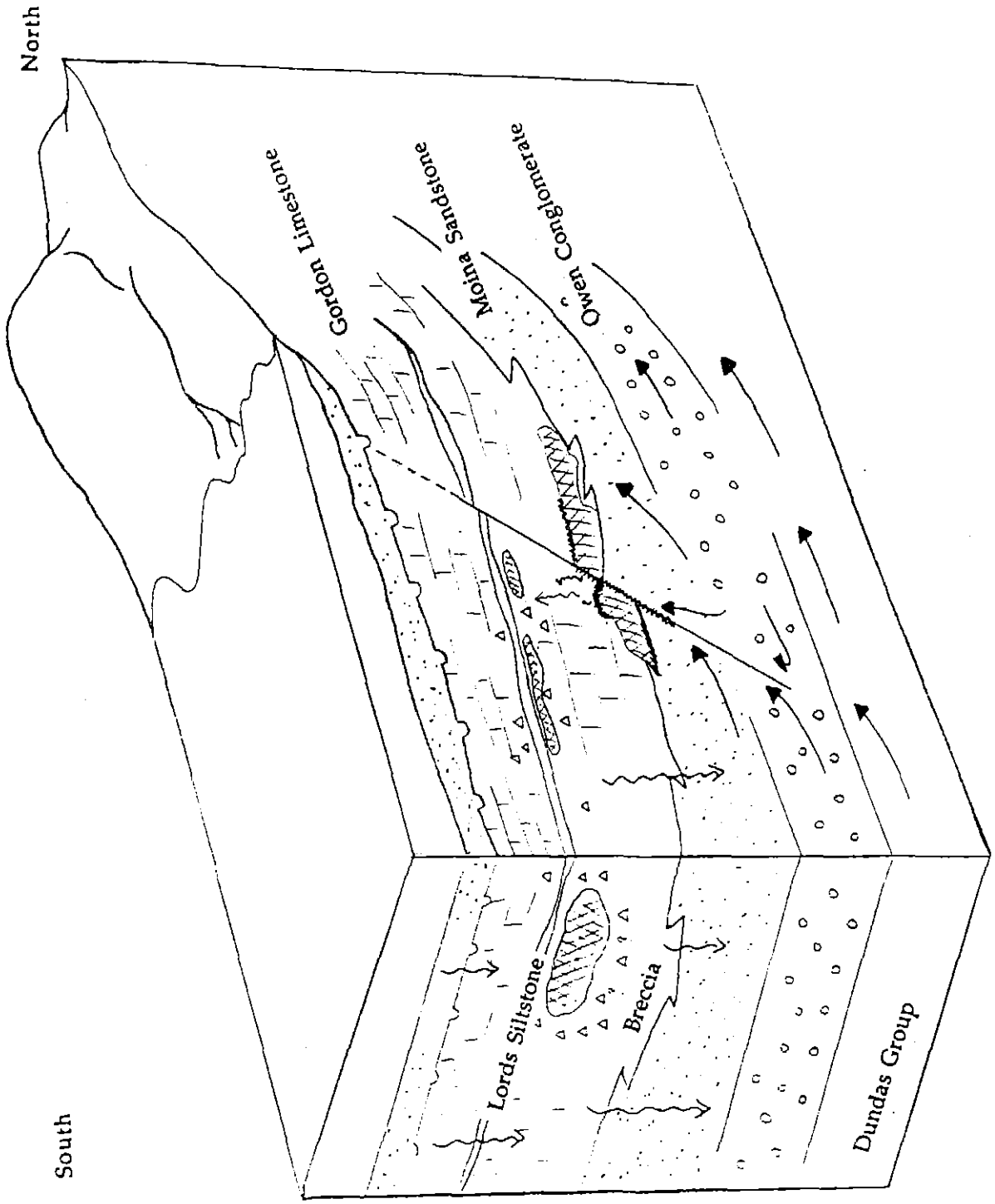

Figure 7.1: Genetic Model for mineralisation in the Lower Mineralised Zone during the Ordovician, and remobilisation during the Devonian responsible for the UMZ. The best exploration target at Grieves Siding is the silicified dolomite breccia to the south.

The metals transported by the the mineralising fluid could be derived from two possible sources. One possibility is an Ordovician source. Lead isotopes plot towards the edge of the Cambrian field, and slightly overlaps into the Devonian. If Ordovician mineralisation exists, it would surely have a lead signature plotting in a similar location to the data from Grieves Siding. A lack of magmatism in the region during the Ordovician, and the occurrence of a stable carbonate platform is unlikely to introduce a new metal source into the system. Subsequently a new Ordovician metal source is unlikely.

Remobilised Cambrian metals accessed by circulating brines or seawater could provide a suitable metal source. Dewatering of the Cambrian sequences below the Wurawina Supergroup may have released some metals before the Ordovician, however the size and thickness of the sequences implies that they contained enough metals to mineralise Grieves Siding. The extent of fluid circulation restricts the accessibility of the fluid to metals. A small convection system could have accessed the Moina Sandstone and underlying Cambrian sediments of the Dundas Group, producing the minor mineralisation at grieves Siding. A larger convection cell, accessing more sediments, such as the Crimson Creek Formation and the Success Creek Formation, would have access to more metals, and produce more mineralisation.

Small convection systems are suspected to produce Irish-type deposits. A similar system is envisaged at Grieves Siding. A small convection system accessing metals from the Dundas Group, and being transported along the Moina Sandstone - Gordon Limestone contact and the Grieves Fault is envisaged to be responsible for mineralisation. A mixture of basinal brines and a modified seawater fluid may have been responsible.

Precipitation primarily occurred by chemical processes and was initiated by either mixing between the hydrothermal fluid and groundwater, or due to an increase in pH caused by interaction with carbonates (Figure 7.2). An increasing pH causes precipitation in the Pb - Zn window. A temperature decrease is also envisaged to have perhaps caused precipitation,

This genetic model implies that mineralisation was emplaced during diagenesis, prior to complete lithification. Mineralisation preceded early diagenetic dolomitisation by mixed marine and meteoric waters. At this time

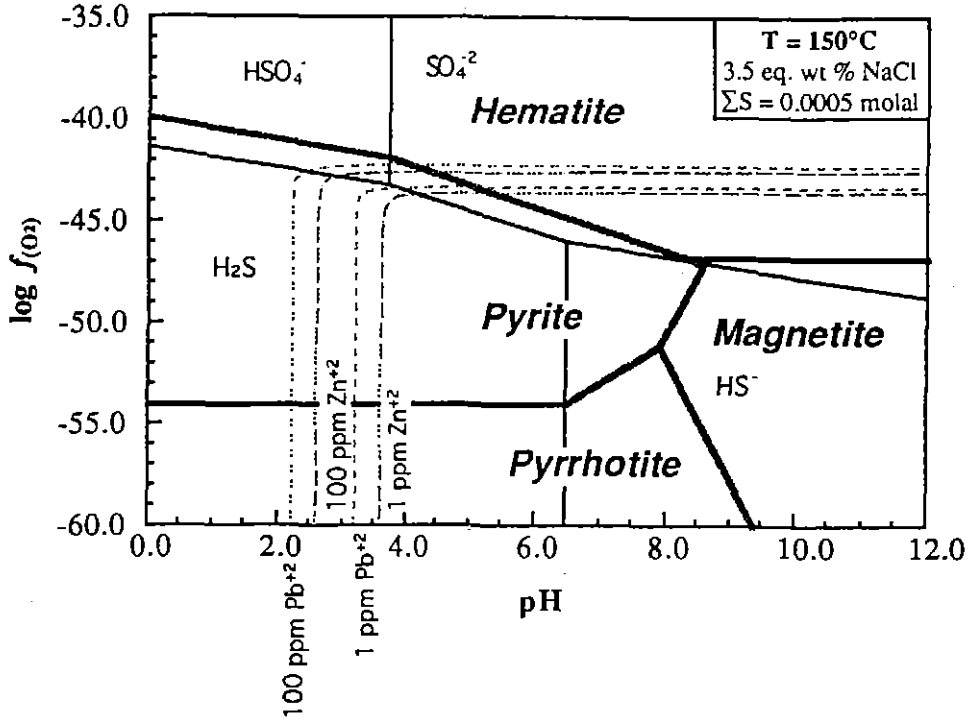

Figure 7.2: Oxygen fugasity - pH diagram illustrating the lead-zinc ore window. Precipitation at Grives Siding is assumed to have occurred in response to increasing pH.

the Moina Sandstone may have been porous enough to act as an aquifer for the brines, that precipitated upon reaching either groundwater or the carbonates of the Ugbrook Formation. Hydrothermal alteration and minor replacement of the Ugbrook Formation by the mineralising fluids is consistent with similar alteration at the Bad Grund MVT deposit. The morphology of the stratiform mineralised lenses is the result of the interdigitating Moina Sandstone-Gordon Limestone contact acting as a conduit to hydrothermal fluid flow (Fig 7.1).

The mineralising system at Grieves Siding shows similarities with MVT and Irish-type deposits (Table 7.1). Metal sources, transportation and deposition mechanisms, mineralogy and mineral textures, and age relationships with the host rocks are consistent with these deposits. The distinction of mineralisation as either Irish-type or MVT cannot be made because of a lack of study material. Investigations to further define metal sources and transportation mechanisms are needed, however for this to occur, further mineralisation must first be

found. The implications for further exploration in the area, provided by this study may yield economic mineralisation.

7.6: EXPLORATION IMPLICATIONS

Although mineralisation at Grieves Siding supported a small prospect during the late 1800's, the deposit is currently uneconomic, with barely enough material collected for this study. Nevertheless the implications of this study to further exploration in the area, and the possibility of further mineralisation at Grieves Siding remain important. The definition of remobilised Cambrian metals emplaced into Ordovician carbonates is a significant recognition for the Zeehan Mineral Field. Exploration models can be modified to account for, and perhaps target MVT and Irish-type mineralisation instead of focussing on mineralisation attributed to Devonian granitoids. The matrix marcasite associated with sulphide clasts near the UMZ, and the close proximity of a progressively silicified dolomite breccia, provides the greatest potential for further mineralisation at Grieves Siding (Fig. 7.1).

Emerging evidence indicates remobilised Cambrian metals are responsible for more significant mineralisation in the Zeehan Mineral Field. By modifying exploration programs to account for this style of mineralisation, a new type of orebody may be found in the Zeehan area.

References

Baillie, P. W. (1989). Silurian and Devonian Sediments. In C. F. Burrett and E.L. Martin. (Ed.), Geology and Mineral resources of Tasmania pp. 224 - 233).

Banks, M. R. (1957). In Hughes, T.D., (ed) 1957, The Stratigraphy of Tasmanian Limestones.

Banks, M. R. (1962). The Ordovician System. In Spry and Banks (eds), The Geology of Tasmania. Journal of the Geological society of Australia, v9 (2), 147 - 176.

Banks, M. R., and Burrett, C.F. (1989). The Gordon Group Mainly Platform Carbonates. , In C. F. Burrett and E.L. Martin. (Ed.), Geology and Mineral resources of Tasmania pp. 201 - 213.

Banks, M. R. (1989). Late Cambrian to Devonian. In C. F. Burrett and E.L. Martin. (Eds.), Geology and Mineral resources of Tasmania (pp. pp. 182 - 237).

Banks, M. R. and Burrett C.F. (1980). A preliminary Ordovician biostratigraphy of Tasmania. Journal of the Geological Society of Australia, v26, pp. 363-376.

Basnayake, S. B. (1975). Geochemistry and Petrology of the Ordovician Gordon Limestone, Mole Creek Area. Honours (unpubl), University of Tasmania,

Berry, R. F., and A.J. Crawford,. (1988). The tectonic significance of the Cambrian allochthonous mafic-ultramafic complexes in Tasmania. Australian Journal of Earth Sciences., v35, pp 161-171.

Berry, R. F. (1992). Structure of Tasmania. In Tectonic and Structural Controls on Ore Deposits, Hobart, Centre for Ore Deposits and Exploration Studies, p. 527-532, ,

Blissett, A. H. (1962). Zeehan - Geological Survey Explanatory Report (K'55-5-50). Tasmania Department of Mines.

Blissett, A. H. (1962b). Geology and Structure of the Zeehan region, West Tasmania. Honours, University of Tasmania,

Both, R. A. and Williams. K. L. (1968). Mineralogical zoning in the lead-zinc ores of the Zeehan Field, Part 2: Paragenetic and Zonal relationships. Journal of the Geological Society of Australia, v 15, pp. 217-243.

Brown, A. V. (1989). Eo-Cambrian - Cambrian. , In C. F. Burrett and E.L. Martin. (Ed.), Geology and Mineral resources of Tasmania pp. 47 - 83.

Brown, L. a. L., J. (1989). P-V-T properties of fluids in the system H2O - CO2 - NaCl: New Graphical presentations and implications for fluid inclusion studies. Geochemica et Cosmochimica Acta, 53, pp. 1209 - 1221.

Burrett, C. F., Laurie, J., and Strait, B. (1981). Gordon Subgroup (Ordovician) carbonates at Precipitous Bluff, and Point Cecil, Southern Tasmania. Pap. Proc. Roy. Soc. Tasm., v 115,

Burrett, C. F., Strait, B., Sharples, C., and Laurie, J. (1984). Middle Upper Ordovician shallow platform to deep basin transect, Southern Tasmania, Australia. in Brunton, D.L. (ed), Aspects of the Ordovician System., no. 295,

Burrett, C. F. (1995 unpubl). Ordovician Gordon Group Carbonates, Zeehan Region, Tasmania, Australia - Stratigraphy and Palaeoenvironments. . Geosea Consultants. pp 15

Burrett, C. F. (1989). In C. F. Burrett and E.L. Martin. (Ed.), Geology and Mineral Resources of Tasmania G.S.A.Inc. 574 pp.

Calver, C. R. (1977). Palaeoecology of the Lower Limestone Member, Benjamin Limestone, Floentine Valley. Honours (Unpub), University of Tasmania,

Club, L. F. N. (1986). Guide to Flowers and Plants of Tasmania . Reed Books.

Cook, H. E., Hine, A.E., and Mullins, H.T., (1983). Platform Margin and Deep Water Carbonates . Society of Economic Palaeontologists and Mineralogists. pp 389.

Corbett, K. D., and Soloman, M. (1989). Cambrian Mt. Read Volcanics and Associated Mineral Deposits . In C. F. Burrett and E.L. Martin. (Ed.), Geology and Mineral resources of Tasmania Geological Society of Australia Incorporated.

Corbett, K. D. (1989). Tectonic Models. , In C. F. Burrett and E.L. Martin. (Ed.), Geology and Mineral resources of Tasmania Geological Society of Australia Incorporated. pp 175 - 181.

Corbett, K. D. and. Banks., M.R. (1974). Ordovician stratigraphy of the Florentine Synclinorium, Tasmania. Pap. Proc. Roy. Soc. Tasm. v 107:, pp. 207 - 238.

Corbett, K. D. and. Turner., N.J. (1989). Early Palaeozoic deformation and tectonics. In C. F. Burrett, Martin, E.L. (Ed.), Geology and Mineral resources of Tasmania , pp. 154 - 181.

Crawford, A. J., and Berry, R.F.,. (1992). Tectonic implications of the late Proterozoic-early Palaeozoic igneous rocks associations in Western Tasmania. Tectonophysics, v214, pp. 1-20.

Ellis, A. P. (1984). Mineralisation and Palaeoenvironments in the Gordon Group Sediments, South of Zeehan, Western Tasmania. Honours (Unpub), University of Tasmania.

Flugel, E. (1982). Microfacies Analysis of Limestones . Springer-Verlag. pp. 632

Gary, M., McAfee, R.Jr., Wolf, C. (eds). (1977). Glossary of Geology (4th edition ed.). American Geological Institute.

Gemmell, B. J., and Large, R.R.,. (1990). Sulphur and Lead isotope study of the stringer zone beneath the Hellyer sulphide deposit, Tasmania. Geochronology, Cosmochronology and Isotope Geology., v 27, pp. 38.

Gill, E. D. and. Banks., M.R. (1949). Silurian and Devonian stratigraphy of the Zeehan area, Tasmania. Pap. Proc. Roy.Soc. Tasm. v262,

Gulson, B. H., and Porritt, P.H. (1987). Base metal exploration of the Mount Read Volcanics, western Tasmania: Lead isotope signatures and genetic implications. Economic Geology, 82, 291 - 307.

Gulson, B. L., Large. R.L., and Porritt, P.M. (1987). Base Metal Exploration of the Mount Read Volcanics: Pt. III. Application of Lead Isotopes at Elliot bay. Economic Geology, 82, pp. 308 - 327.

Gustafason, LB, and Williams, (1981) Sediment hosted stratiform Deposits of Copper, Lead and Zinc. Economic Geology 75th Annaversary Volume, pp. 139 - 178.

Hill, D. (1955). Ordovician corals from Ida Bay, Queenstown and Zeehan, Jour. Proc. Roy. Soc. NSW v 89, pp. 237 - 252.

Hitzman, M. W. (1995). Mineralisation in the Irish Zn-Pb-(Ba-Ag) Orefield. In K. Anderson, Ashton, J., Earls, G., Hitzman, M., and Tear, S. (Eds.), Irish Carbonate Hosted Zn-Pb Deposits (pp. 295 pp.). Society of Economic Geologists.

Jago, J. B. and. Brown, A.V, (1989). Middle to Upper Cambrian fossiliferous sedimentary rocks. In C. F. Burrett and E.L. Martin. (Ed.), Geology and Mineral resources of Tasmania Geological Society of Australia Incorporated. , pp. 74 - 83.

Kahle, C. F. (1965). Possible Roles of Clay minerals in the Formation of Dolomite. Journal of Sedimentary Petrology, 35, pp. 448 - 453.

Kyser, T. K. (1987). Short Course in Stable Isotope Geochemistry of Low Temperature Fluids. Vol. 13. Mineralogical Association of Canada .

Leach, D. L., and Sangster, D.F. (1994). Mississippi Valley type Lead-Zinc Deposits. In R. V. Kirkham (Ed.), Mineral Deposit Midelling Geological Society of Canada.

Nesse, D. N. (1991). Introduction to Optical Mineralogy (2nd Edition ed.). Oxford University Press.

Pitt, R. P. B. (1961). The Geology of the Zeehan area. Honours (unpubl), University of Tasmania,

Pratt, B. R., James, N.P., and Clinton, A. (1992). Facies Models - responses to sea level change . Geological Association of Canada. pp 409

Reid, A. M. (1975). The Dundas Mineral Field. Bulletin of the Geological survey of Tasmania, v 31., 102 pp.

Naughton, P (1995). Forest Trees of Tasmania . Boral Timber.

Rice, P. J. (1985). Environments and Diagenesis of the Gordon Group in the Zeehan area. Honours (unpubl), University of Tasmania,

Roedder, E. (1984). Fluid Inclusions as Samples of Ore Fluids . In Barnes (ed) Geochemistry of Hydrothermal Ore Deposits.(2nd Edition ed.).

Ohmoto, H and Rye, R.O (1979). Isotopes of Sulphur and Carbon . In Geochemistry of Hydrothermal Ore Deposits. Barnes, H.L (ed). pp. 798 Wiley-Interscience, John Wiley and Sons.

Shearley, E., Redmond, P., Goodman, R., and King,M. (1996). A Guide to the Lisheen Zn-Pb Deposit. In K. Anderson, Ashton, J., Earls, G., Hitzman, M., and Tear, S. (Ed.), Irish Carbonate hosted Pb-Zn deposits pp.296

Shepherd, T., Rankin, A.H, and Alderton, D.H.M. (1985). A Practical Guide to Fluid Inclusion Studies . pp 239 Blackie and Son Ltd.

Strzelecki, P. E. v. (1845). Physical description of New South Wales and Van Diemans Land (eds) Longman, Brown and Green, London.

Sverjensky, D. A. (1981). Isotopic Alteration of Carbonate Host Rocks as a function of Water to Rock Ratio - An example from the Upper Mississippi Valley

Zinc-Lead District. Economic Geology, 76, 154 - 172.

Sverjensky, D. A. (1986). Genesis of Mississippi Valley-type Lead Zinc Deposits. Ann.Rev.Earth Planet. Sci 14, 177 - 199.

Taylor, B. E. (1987). Stable isotope Geochemistry of Ore forming Fluids. In T. K. Kyser (Ed.), Stable isotope Geochemistry of Low Temperature Fluids (pp. 410 - 412). Mineralogical Association of Canada.

Taylor, S. (1989). Mineralisation in the Gordon Group Carbonates. In C. F. Burrett and E.L. Martin. (Ed.), Geology and Mineral resources of Tasmania Geological Society of Australia Incorporated. , pp. 221 - 223.

Taylor, S. a. M., I.J. (1990). Oceana Lead-Zinc-Silver Deposit. Geology and Mineral Resources of Australia and Papua New Guinea, , pp. 1253 - 1256.

Tucker, M. E. (1981). Sedimentary Petrology: An Introduction . Blackwell Scientific Publications pp252.

Twelvetrees, W. H., and Ward, L.K.,. (1910). The orebodies of the Zeehan Field. Tas. Geol. Surv. Bull.v8,

Walker, R. G., and James, N.P. (eds). (1992). Facies Models - response to sea level change . Geological Association of Canada.pp 409

Williams, K. L. (1968). Hydrothermal Zoning: A study of the Lead-Zinc Ores of Zeehan, Tasmania. Ph.D. (unpubl), University of Tasmania,

Williams, K. L. (1974). Composition of Sphalerites from Zoned Hydrothermal lead-zinc deposits at Zeehan, Tasmania. Journal of Economic Geology, v. 69, pp. 657 - 672.

Wilson, J. L. (1975). Carbonate Facies in Geological History . pp 745 Springer-Verlag.

Zheng, Y. F., and Hoefs, J. (1993). Carbon and Oxygen isotopic covariations in hydrothermal calcites. Mineral. Deposita. 28, 79 - 89.

Appendix 1
Zeehan, Grieves (ZG) Drill Logs

384279

Location .....

Drill Hole No 26409

Sheet no #1 of #1

Fault / Shear
Vein
Breccia
Disseminated
Massive

Bioturbation
Oolites
Algal Mats
Bioclastic

Brachipods
Corals
Bryozoa
Dismicrite

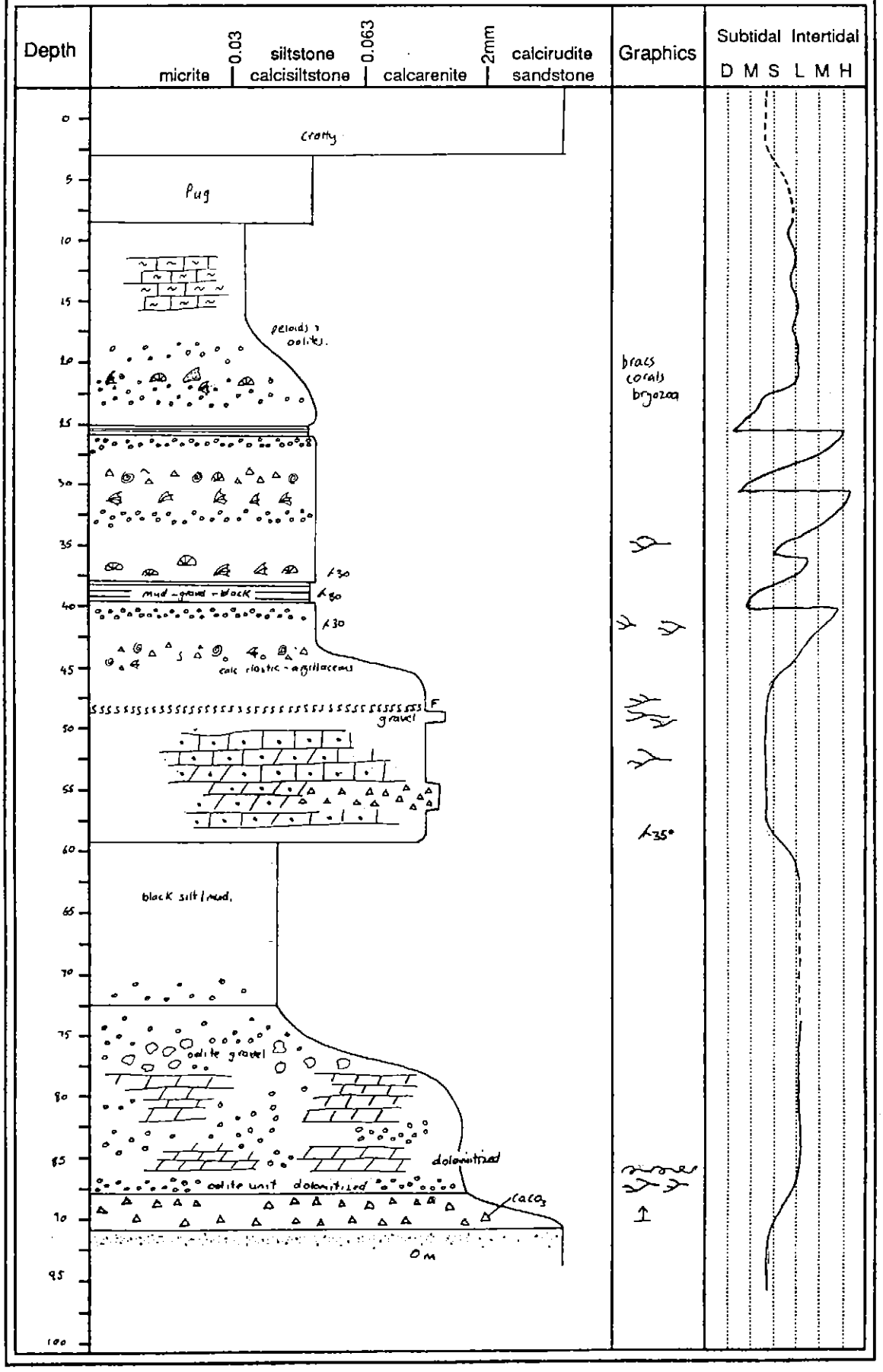

384280

Location .....

Drill Hole No ZG 410

Sheet no #1 of #1

Fault / Shear
Vein
Breccia
Disseminated
Massive

Bioturbation
Oolites
Algal Mats
Bioclastic

Brachipods
Corals
Bryozoa
Dismicrite

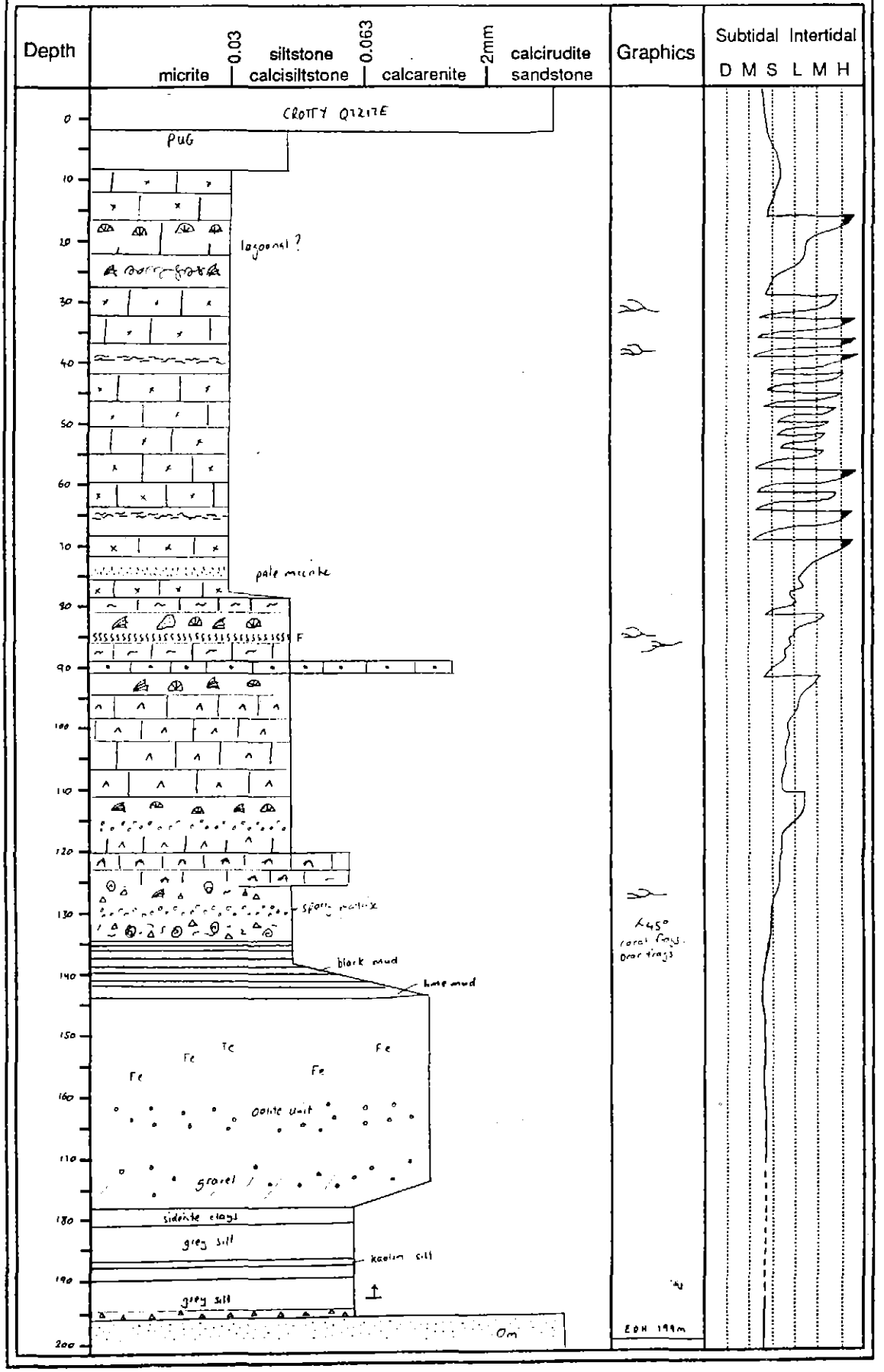

384281

Location .....

Drill Hole No ....26 1001.....

Sheet no ....#1.... of ....#1....

Fault / Shear
Vein
Breccia
Disseminated
Massive

Bioturbation
Oolites
Algal Mats
Bioclastic

Brachiopods
Corals
Bryozoa
Dismicrite

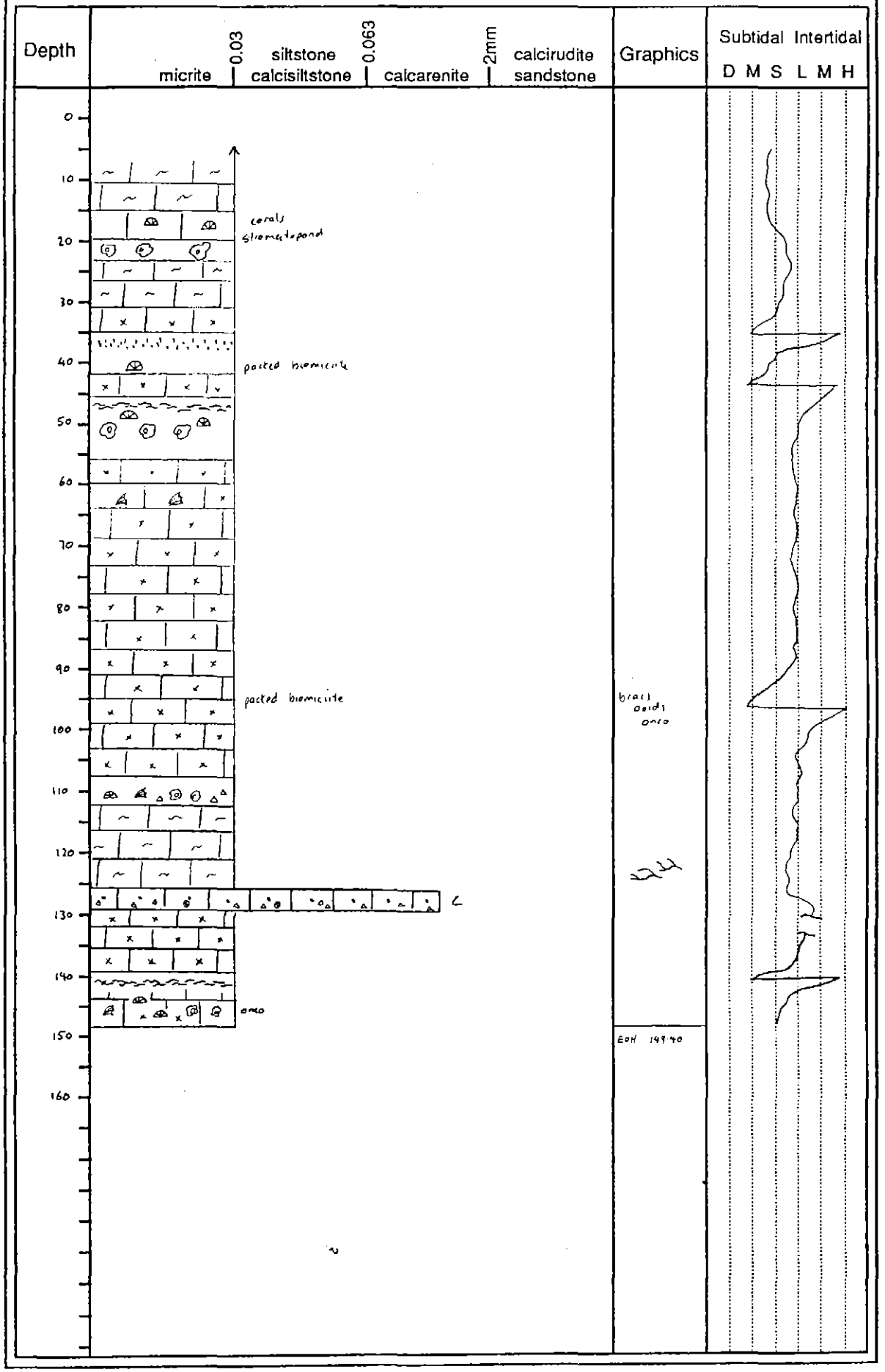

Location 26411

Drill Hole No

Sheet no #1 of #1

384282

Fault / Shear
Vein
Breccia
Disseminated
Massive

Bioturbation
Oolites
Algal Mats
Bioclastic

Brachipods
Corals
Bryozoa
Dismicrite

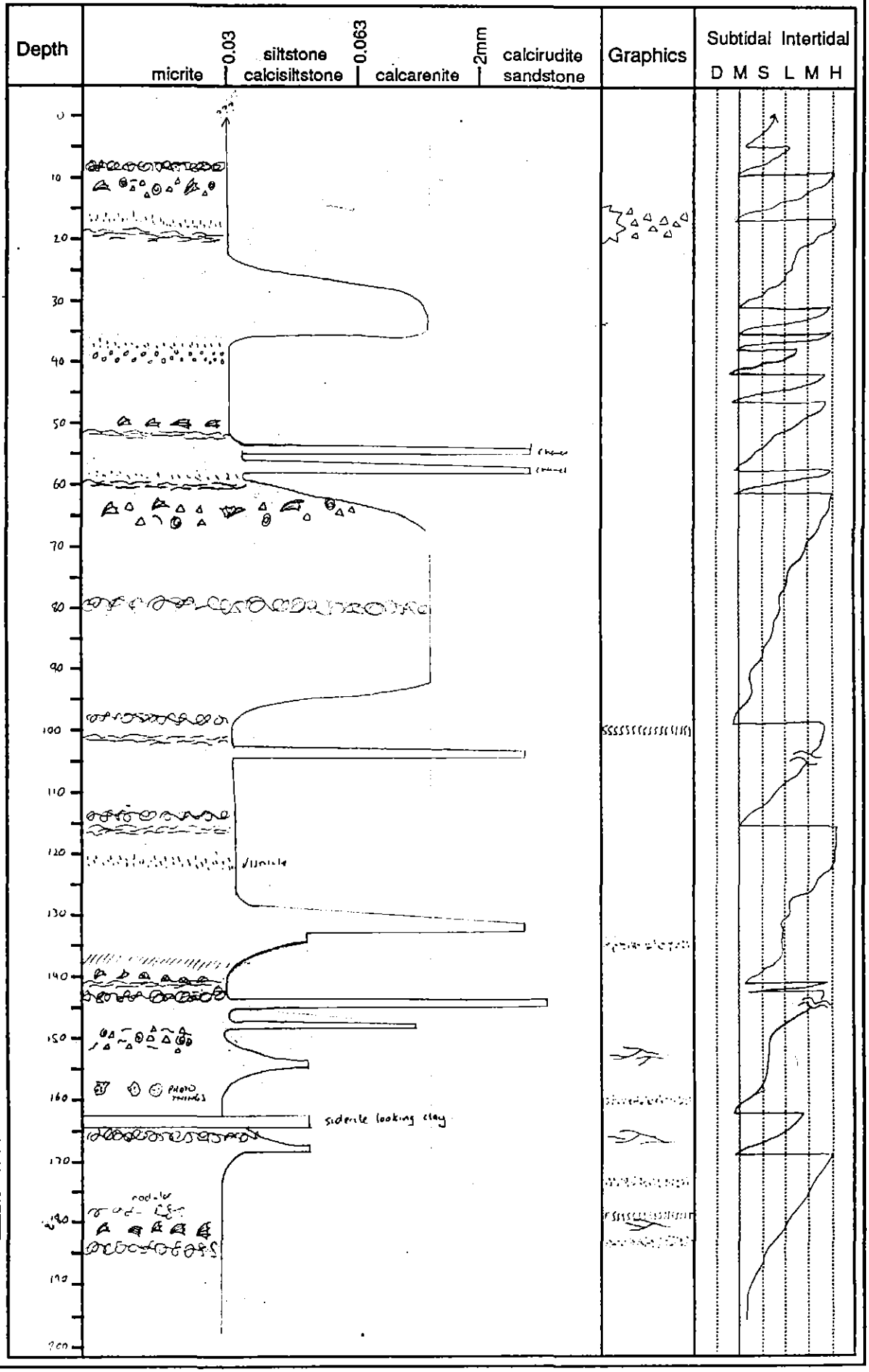

Location .....

Drill Hole No 26 1011

Sheet no #1 of #2

Fault / Shear
Vein
Breccia
Disseminated
Massive

Bioturbation
Oolites
Algal Mats
Bioclastic

Brachipods
Corals
Bryozoa
Dismicrite

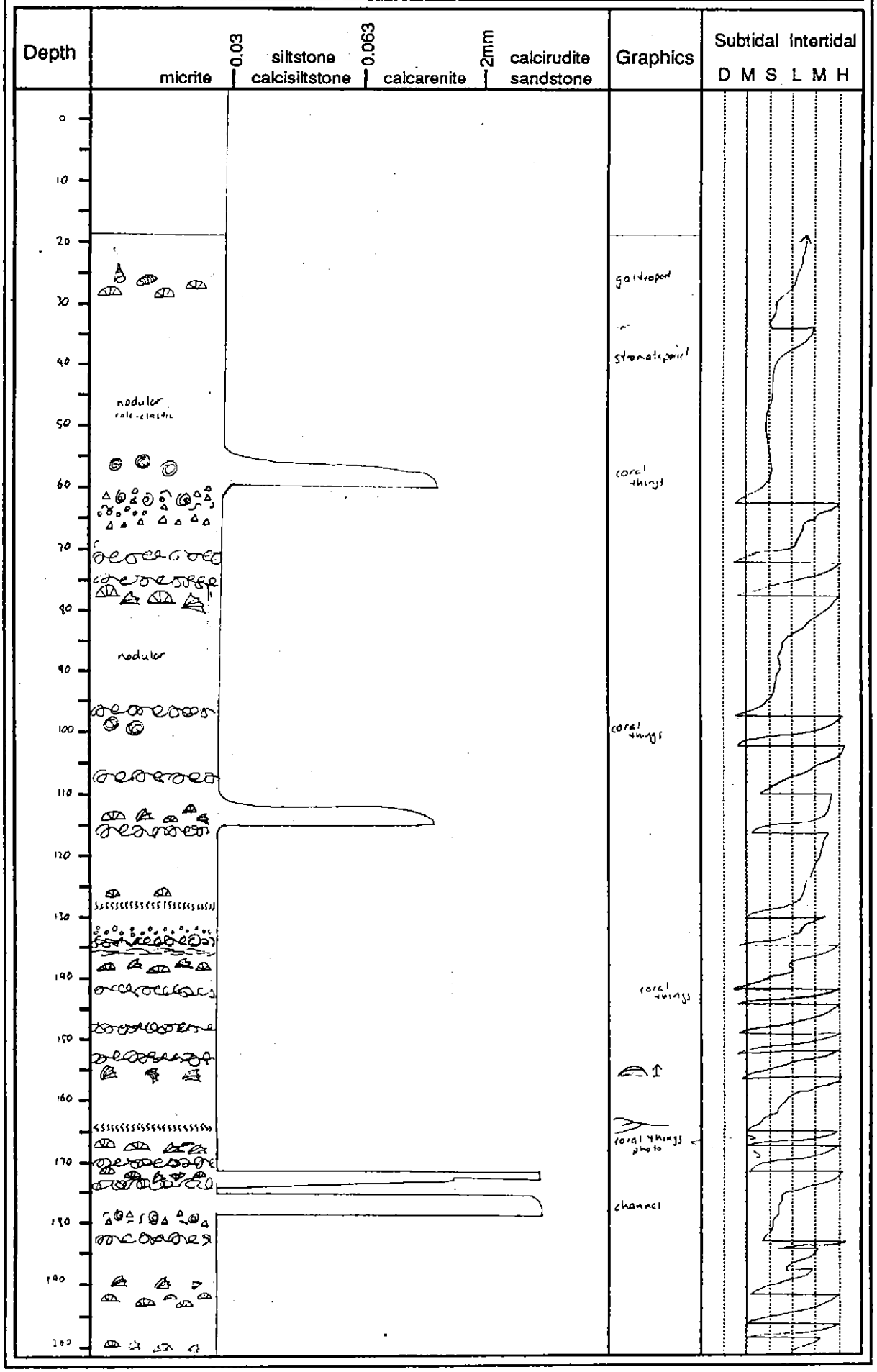

Location .....

Drill Hole No ZG 1011

Sheet no #2 of #2

Fault / Shear
Vein
Breccia
Disseminated
Massive

Bioturbation
Oolites
Algal Mats
Bioclastic

Brachipods
Corals
Bryozoa
Dismicrite

384284

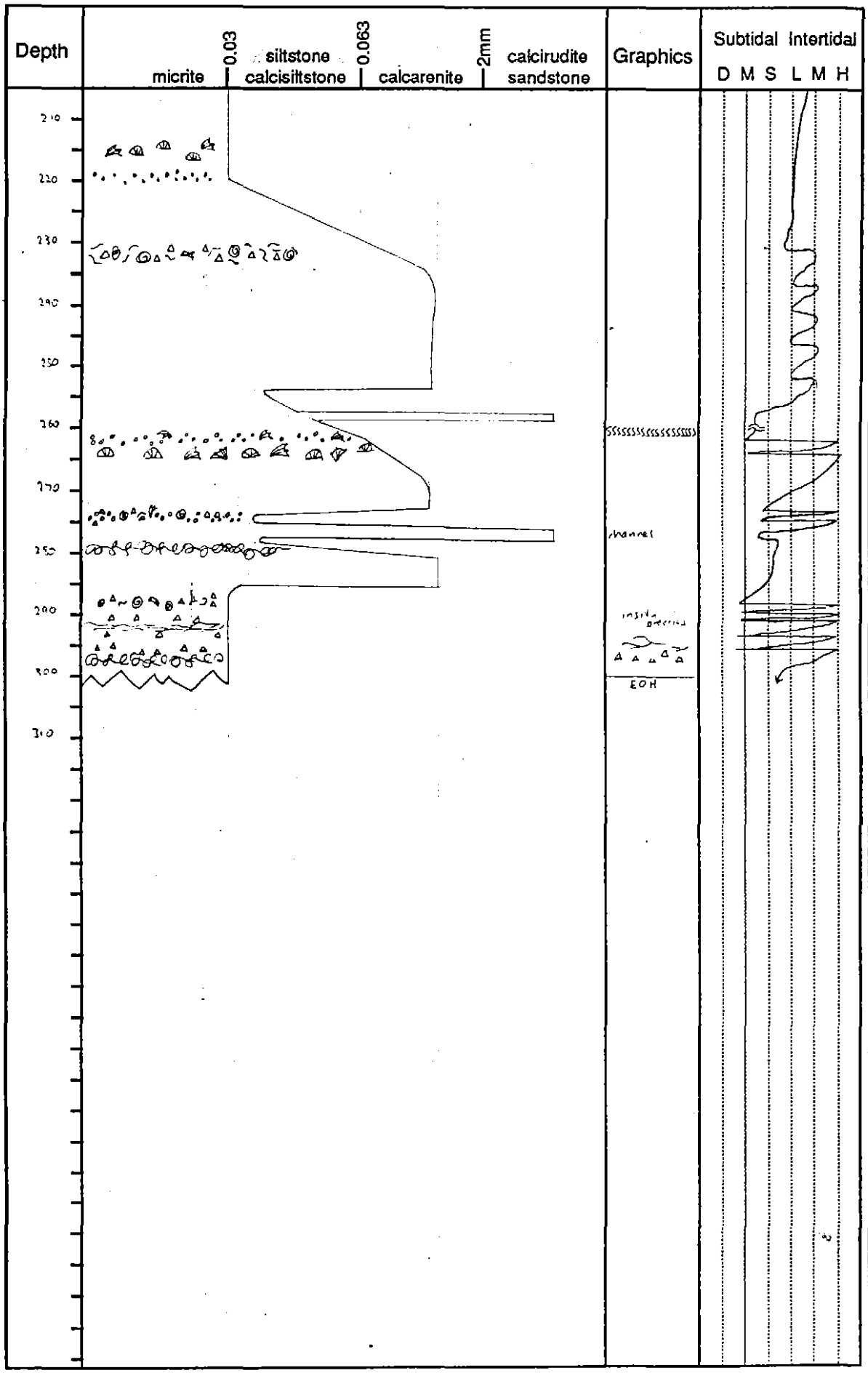

384285

Location .....

Drill Hole No 26 412

Sheet no #1 of #1

Fault / Shear
Vein
Breccia
Disseminated
Massive

Bioturbation
Oolites
Algal Mats
Bioclastic

Brachipods
Corals
Bryozoa
Dismicrite

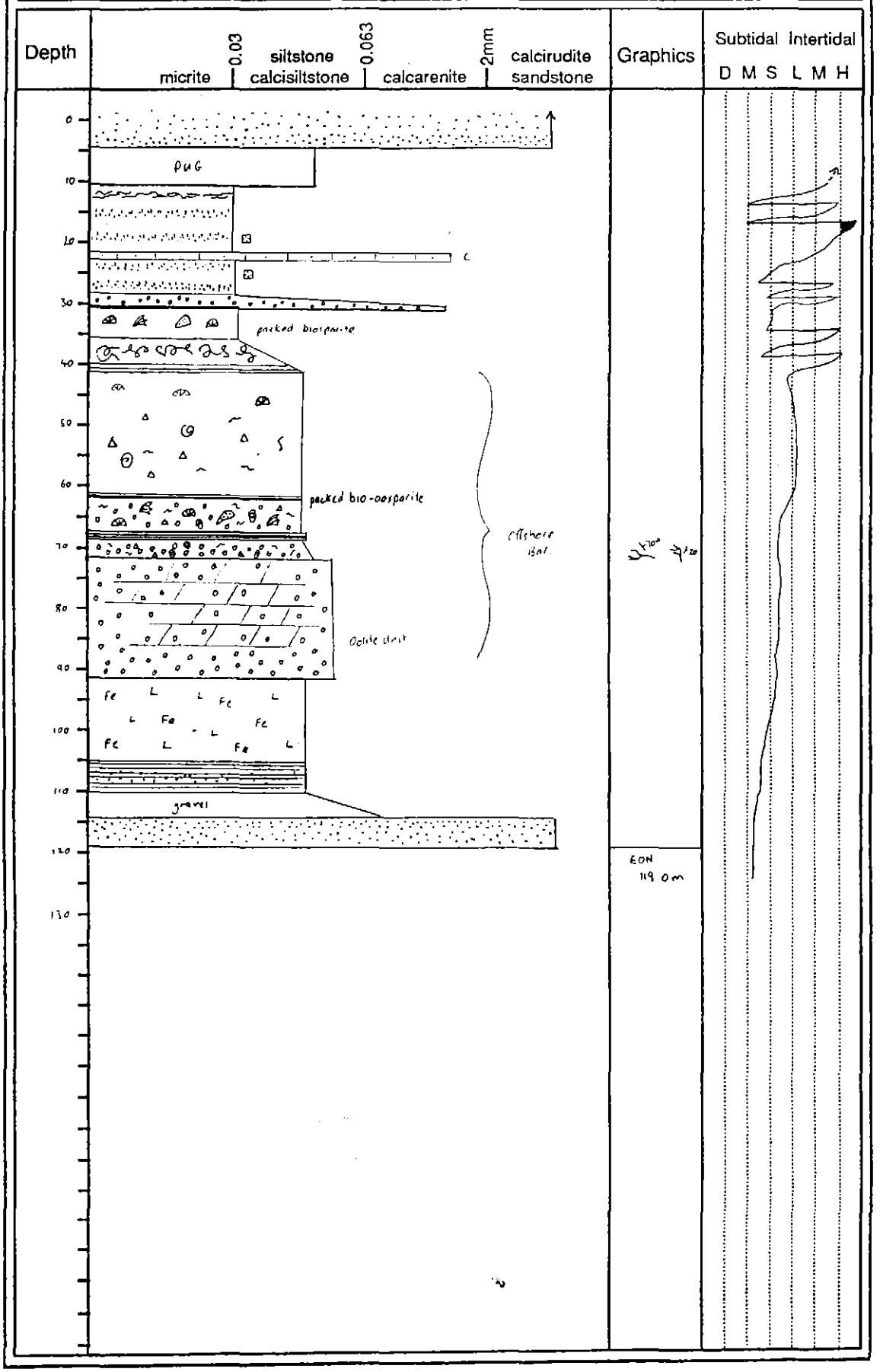

384286

Location .....

Drill Hole No ....26.1010.....

Sheet no ....#1.... of ....#1....

Fault / Shear
Vein
Breccia
Disseminated
Massive

Bioturbation
Oolites
Algal Mats
Bioclastic

Brachipods
Corals
Bryozoa
Dismicrite

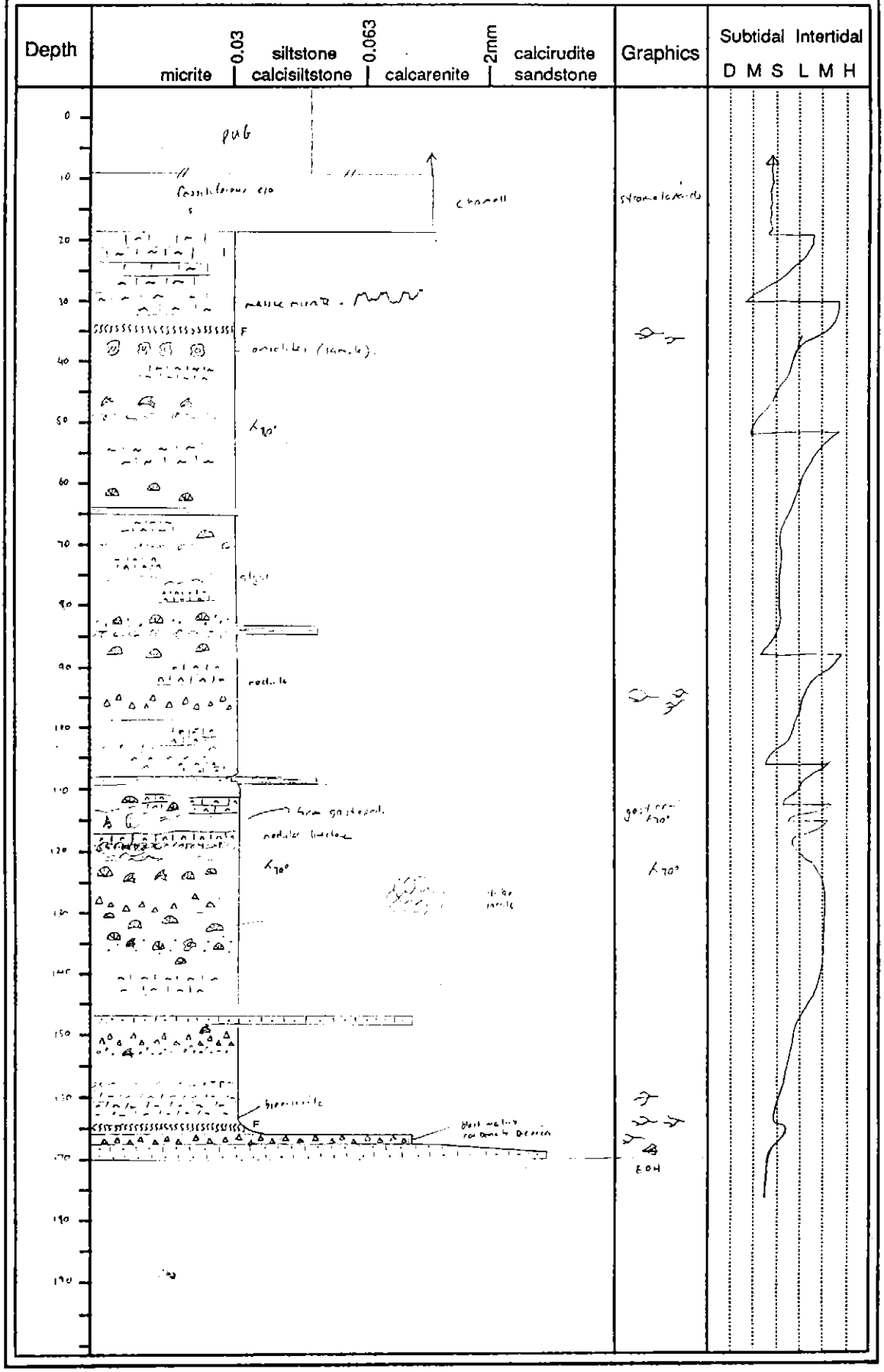

38428

Location .....

Drill Hole No 26 1012

Sheet no # 2 of # 2

Fault / Shear
Vein
Breccia
Disseminated
Massive

Bioturbation
Oolites
Algal Mats
Bioclastic

Brachiopods
Corals
Bryozoa
Dismicrite

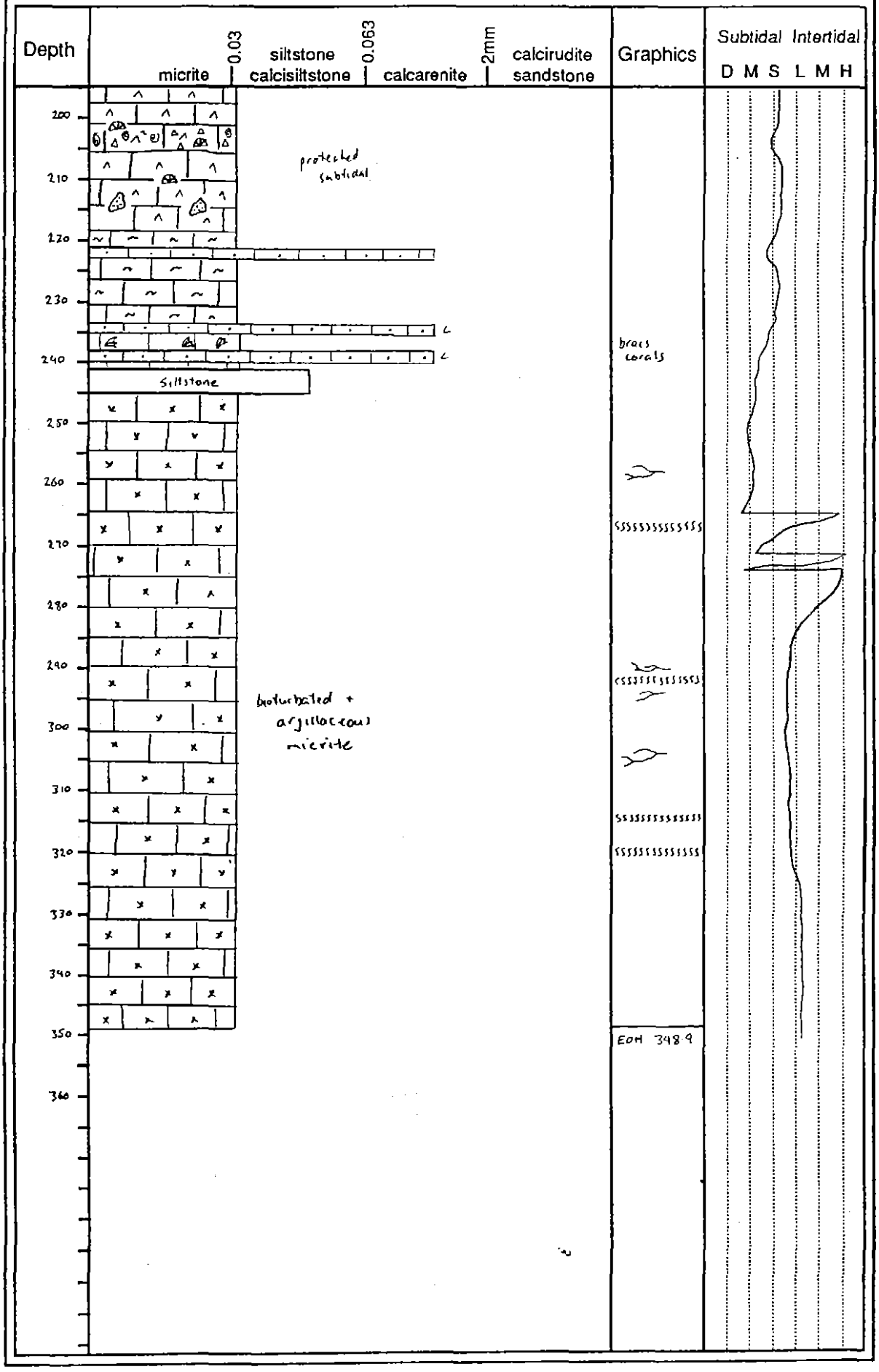

Location .....

Drill Hole No ZB 1007

Sheet no #1 of #4

384288

Fault / Shear
Vein
Breccia
Disseminated
Massive

Bioturbation
Oolites
Algal Mats
Bioclastic

Brachipods
Corals
Bryozoa
Dismicrite

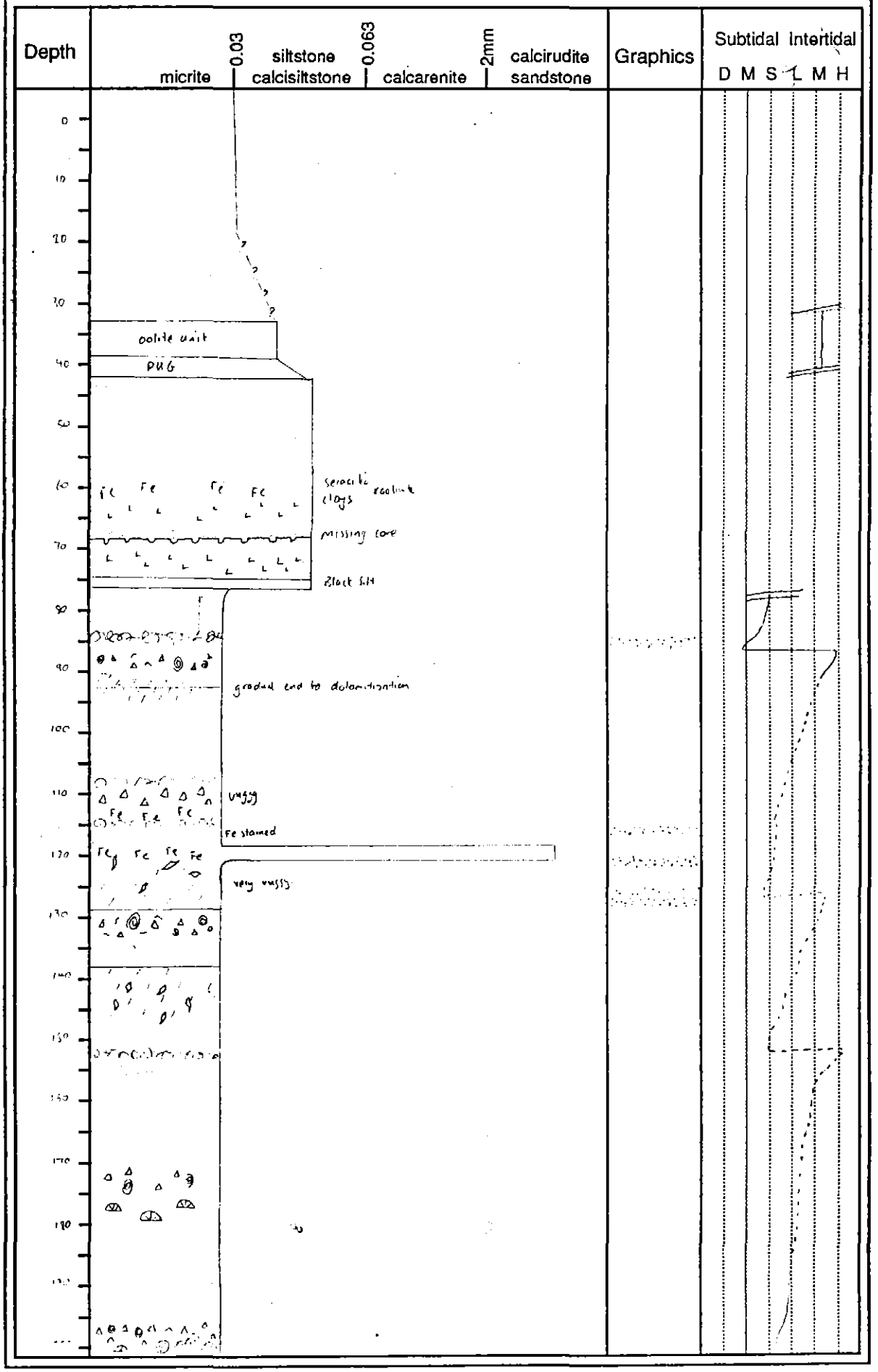

Location .....

Drill Hole No ZB 1007

Sheet no # 2 of # 4

384289

Fault / Shear
Vein
Breccia
Disseminated
Massive

Bioturbation
Oolites
Algal Mats
Bioclastic

Brachipods
Corals
Bryozoa
Dismicrite

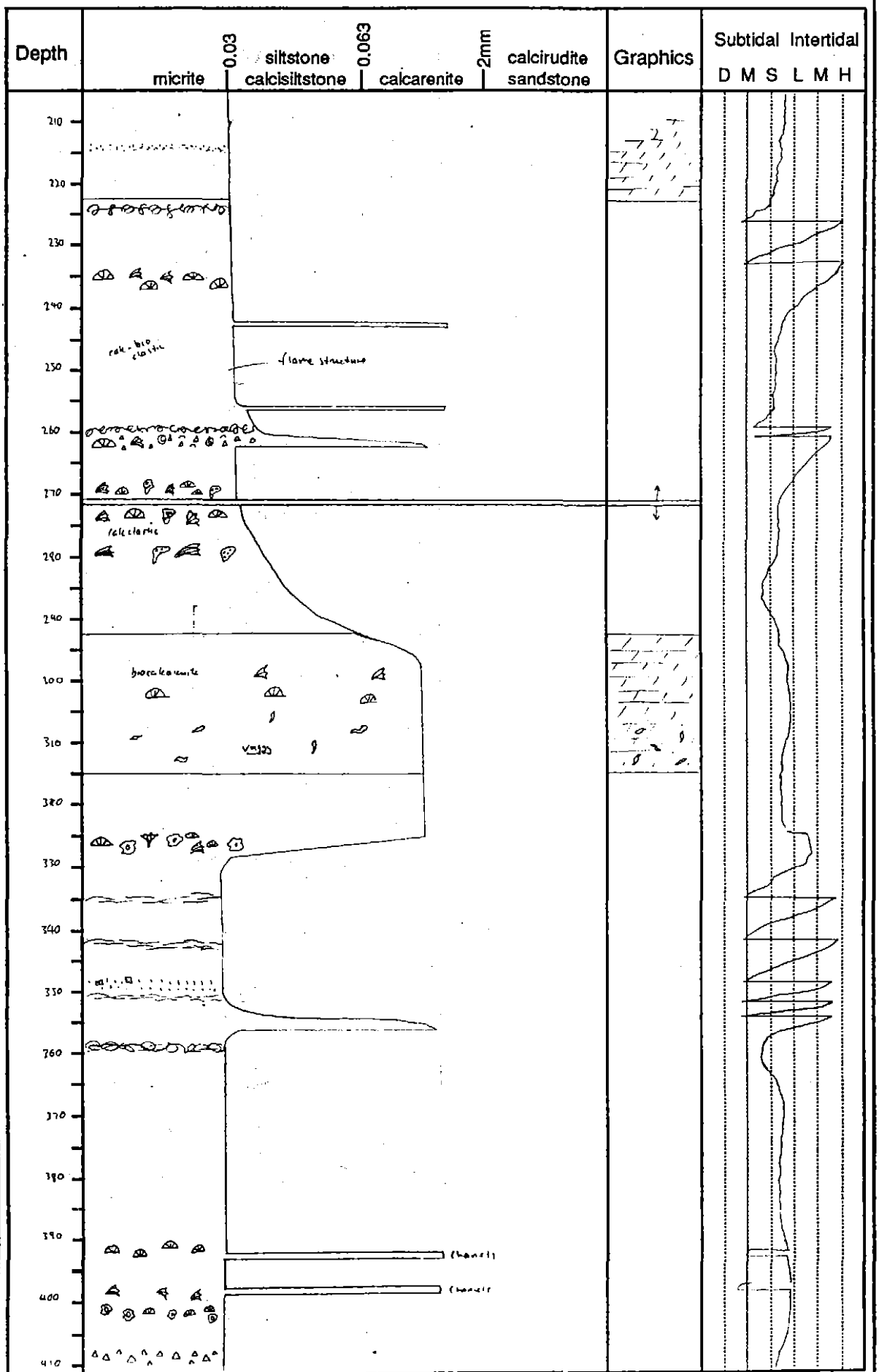

Location .....

Drill Hole No ...ZB 1007.....

Sheet no ...#3..... of ...#4.....

384290

Fault / Shear
Vein
Breccia
Disseminated
Massive

Bioturbation
Oolites
Algal Mats
Bioclastic

Brachipods
Corals
Bryozoa
Dismicrite

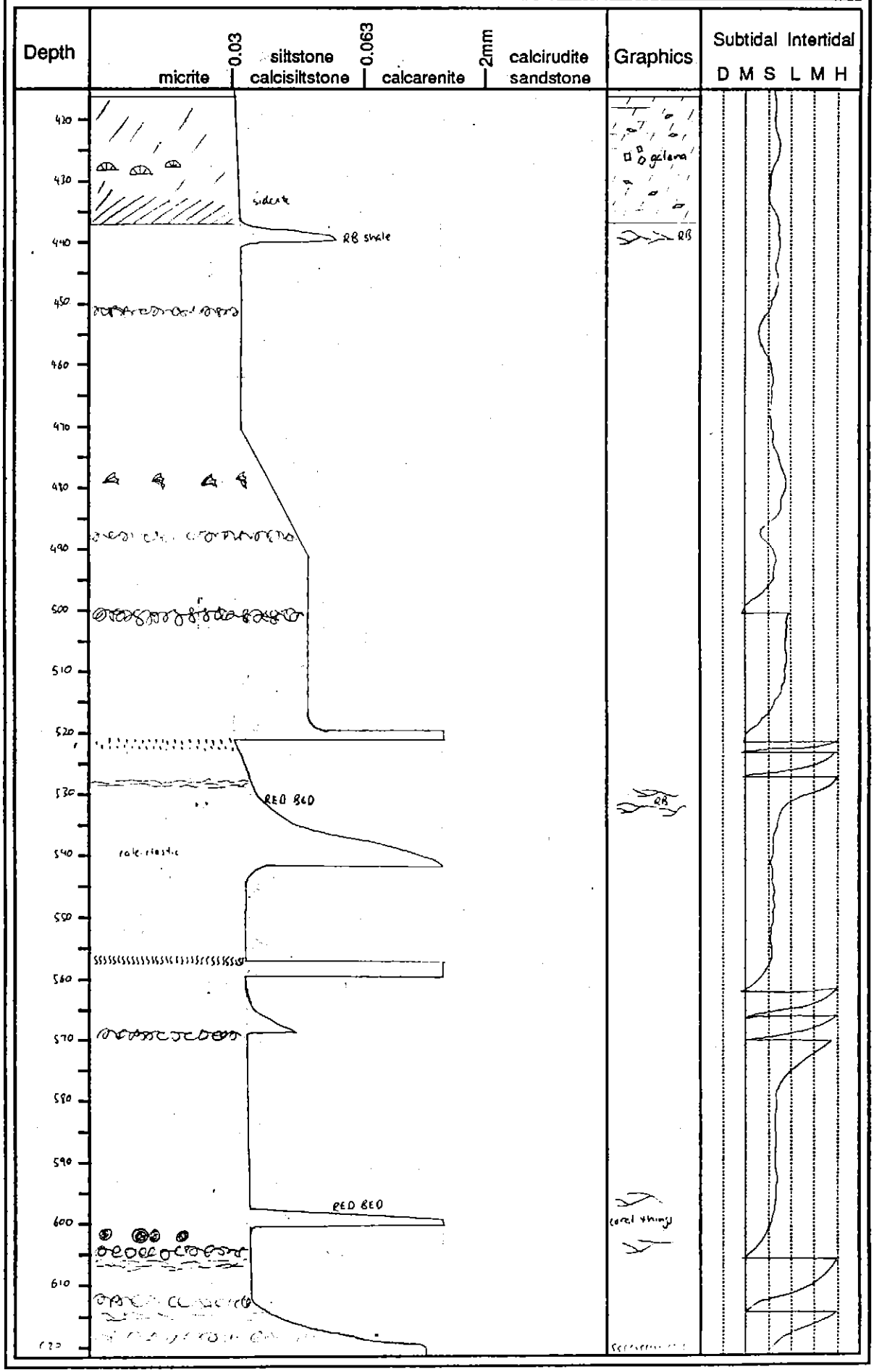

Drill Hole No ZB 1007

Sheet no #4 of #4

Fault / Shear
Cleavage
Fining up grains
Vein
Disseminated
Massive
Bioturbation
Breccia

384291

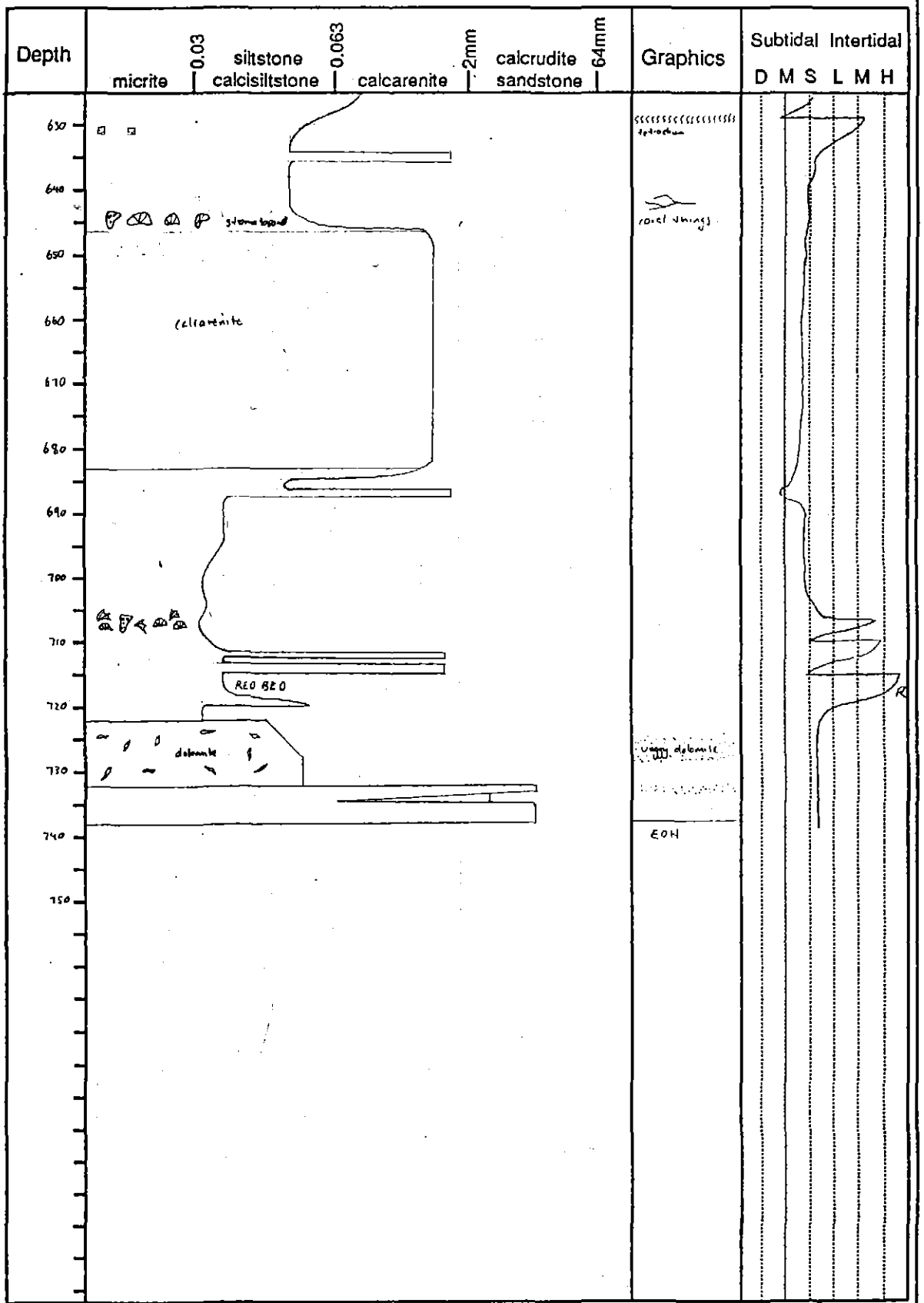

Location .....

Drill Hole No ZG 1009

Sheet no #1 of #1

Fault / Shear
Vein
Breccia
Disseminated
Massive

Bioturbation
Oolites
Algal Mats
Bioclastic

Brachiopods
Corals
Bryozoa
Dismicrite

384292

Depth

micrite | 0.03 | siltstone / calcisiltstone | 0.063 | calcarenite | 2mm | calcirudite / sandstone

Graphics

Subtidal Intertidal
D M S L M H

0
10 pale micrite
Furry corals
20
30
40
50 impure limestone
60
70
80
90
100 packed biomicrite
Furry coral
110
120 calc-bio-clastic
130
140 braces
150 pale micrite
160
170

75°

EOH 151m

Location .....

Drill Hole No .....ZG 1002.....

Sheet no .....#1..... of .....#1.....

Fault / Shear
Vein
Breccia
Disseminated
Massive

Bioturbation
Oolites
Algal Mats
Bioclastic

Brachipods
Corals
Bryozoa
Dismicrite

384293

Depth

micrite | 0.03 | siltstone calcisiltstone | 0.063 | calcarenite | 2mm | calcirudite sandstone

Graphics

Subtidal Intertidal
D M S L M H

0
10
20
30
40
50
60
70
80
90
100
110
120
130
140
150
160
170

START

TOP

nodules

siderite

EOH

384294

Location .....

Drill Hole No ZG 406

Sheet no #1 of #1

Fault / Shear
Vein
Breccia
Disseminated
Massive

Bioturbation
Oolites
Algal Mats
Bioclastic

Brachipods
Corals
Bryozoa
Dismicrite

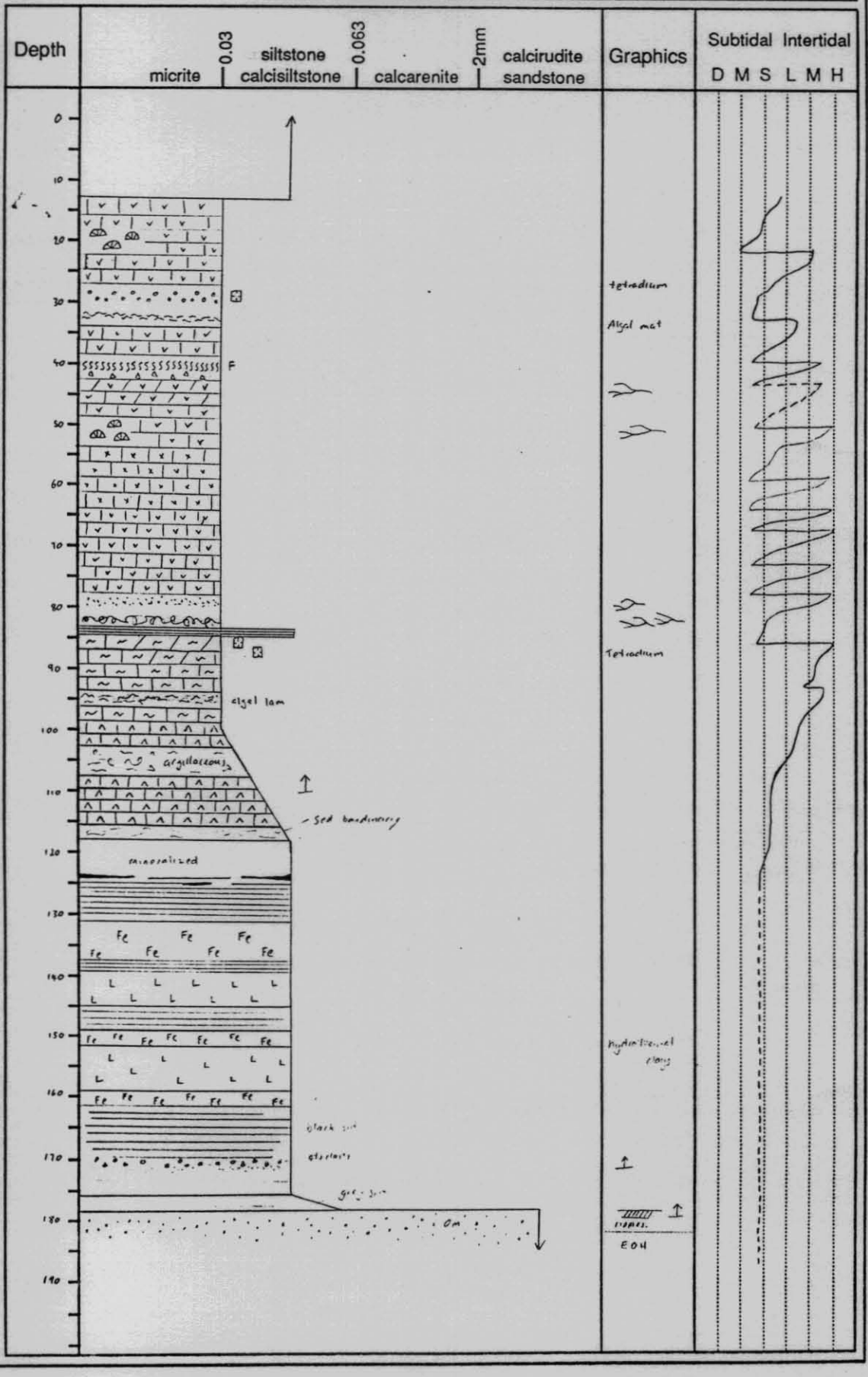

Drill Hole No ....ZG 1016.....

Sheet no ....#1..... of .....

Fault / Shear
Cleavage
Fining up grains
Vein
Disseminated
Massive
Bioturbation
Breccia

384295

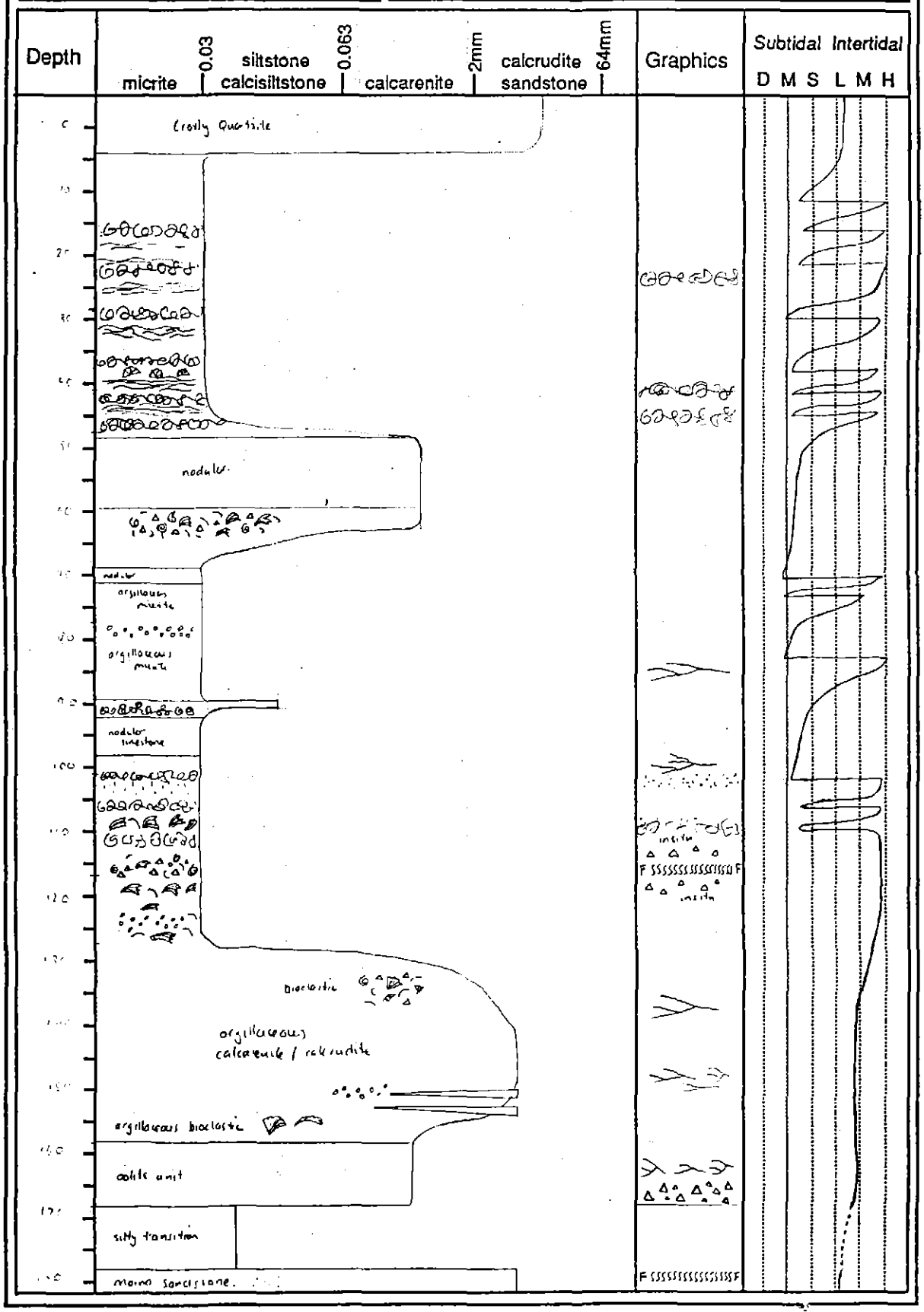

Brachiopods
colites
bioclastic
argillaceous limestone
Algal mats
Nodular

Location .....

Drill Hole No ZG 1006

Sheet no #1 of #1

Fault / Shear
Vein
Breccia
Disseminated
Massive

Bioturbation
Oolites
Algal Mats
Bioclastic

Brachipods
Corals
Bryozoa
Dismicrite

384296

384296

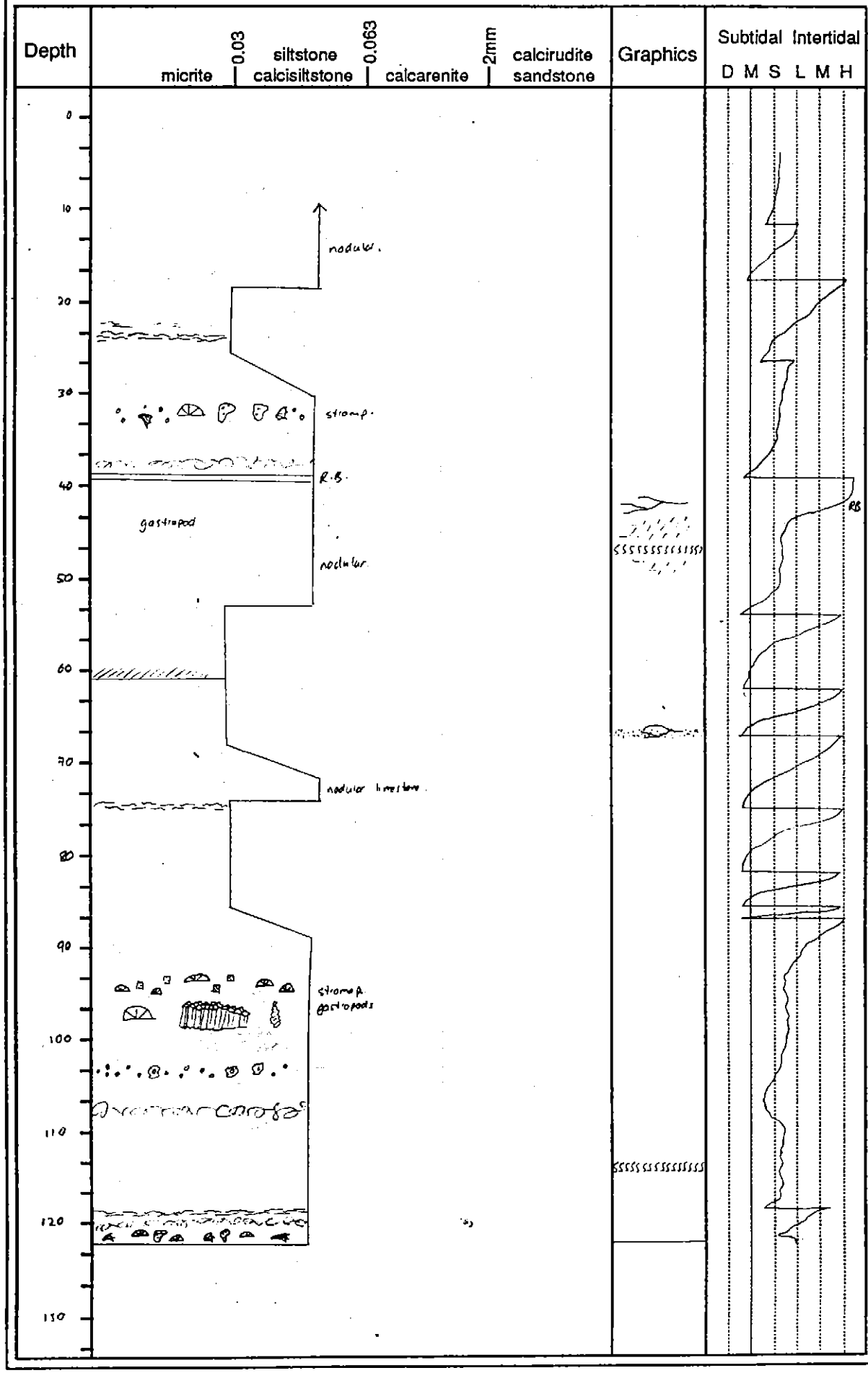

384297

Location .....

Drill Hole No ZG 1013

Sheet no #1 of #1

Fault / Shear
Vein
Breccia
Disseminated
Massive

Bioturbation
Oolites
Algal Mats
Bioclastic

Brachipods
Corals
Bryozoa
Dismicrite

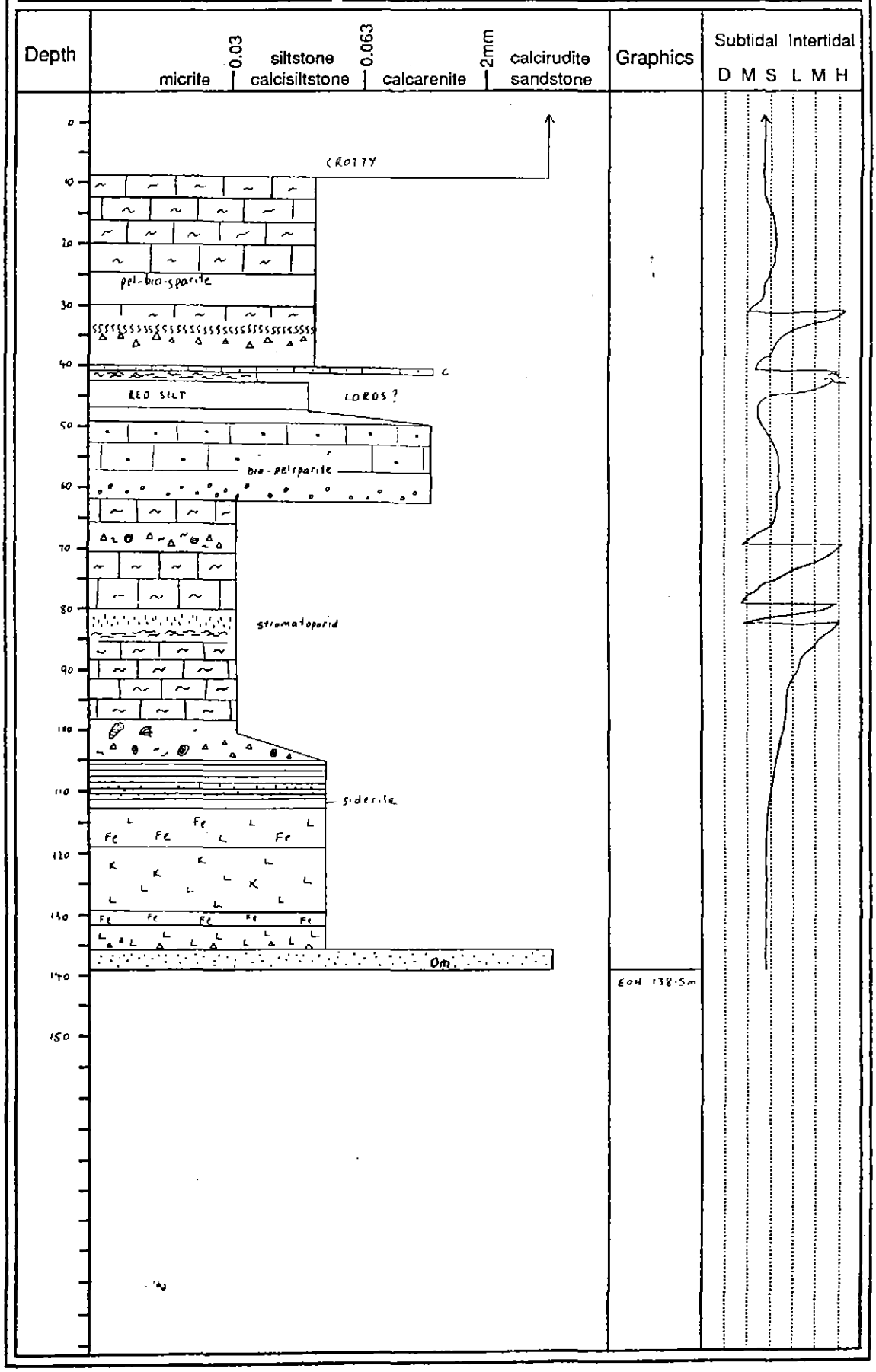

Location .....

Drill Hole No 26414

Sheet no #1 of #1

Fault / Shear
Vein
Breccia
Disseminated
Massive

Bioturbation
Oolites
Algal Mats
Bioclastic

Brachipods
Corals
Bryozoa
Dismicrite

384298

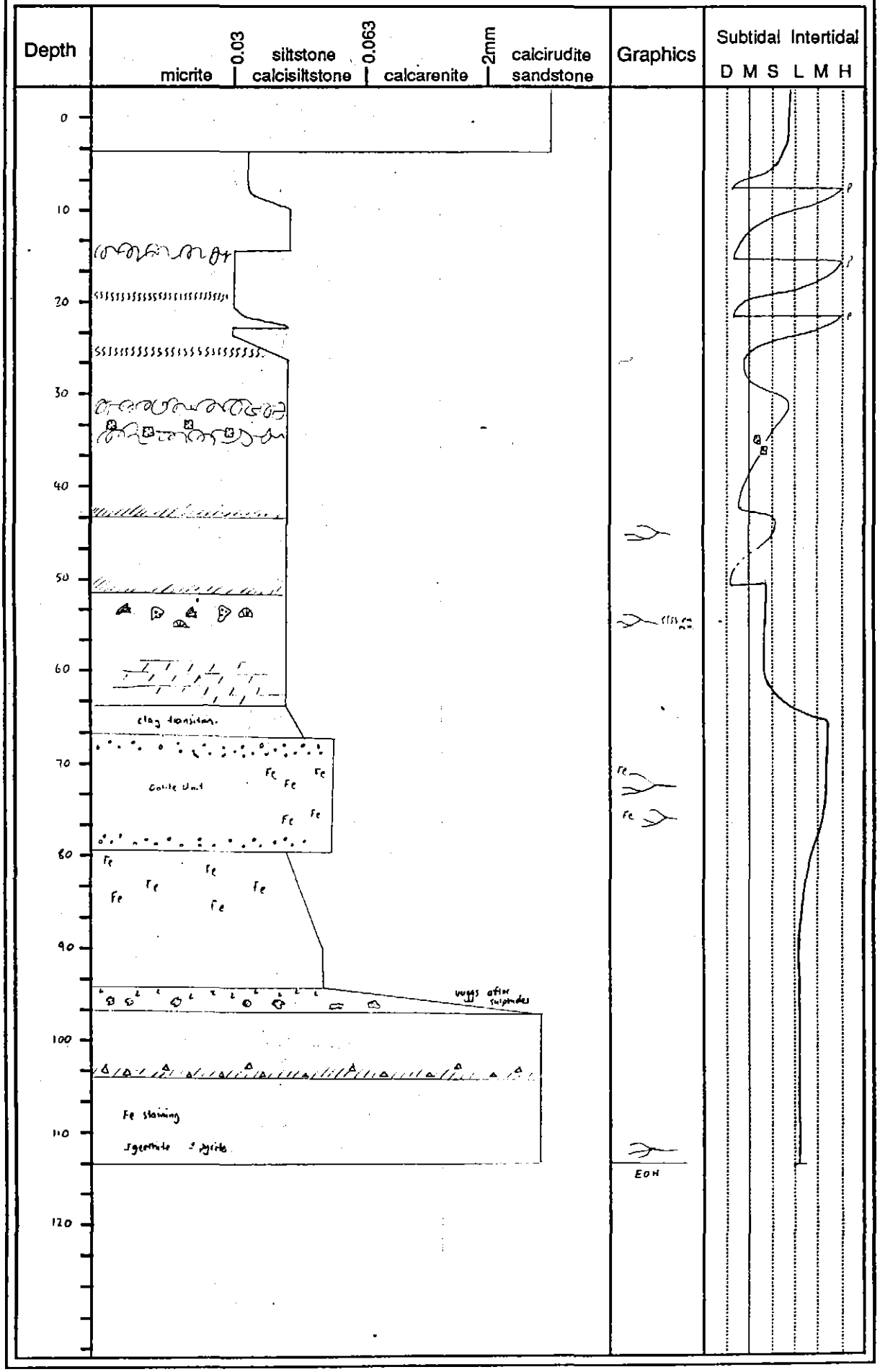

Location .....

Drill Hole No ZG1014

Sheet no #1 of #2

Fault / Shear
Vein
Breccia
Disseminated
Massive

Bioturbation
Oolites
Algal Mats
Bioclastic

Brachipods
Corals
Bryozoa
Dismicrite

384299

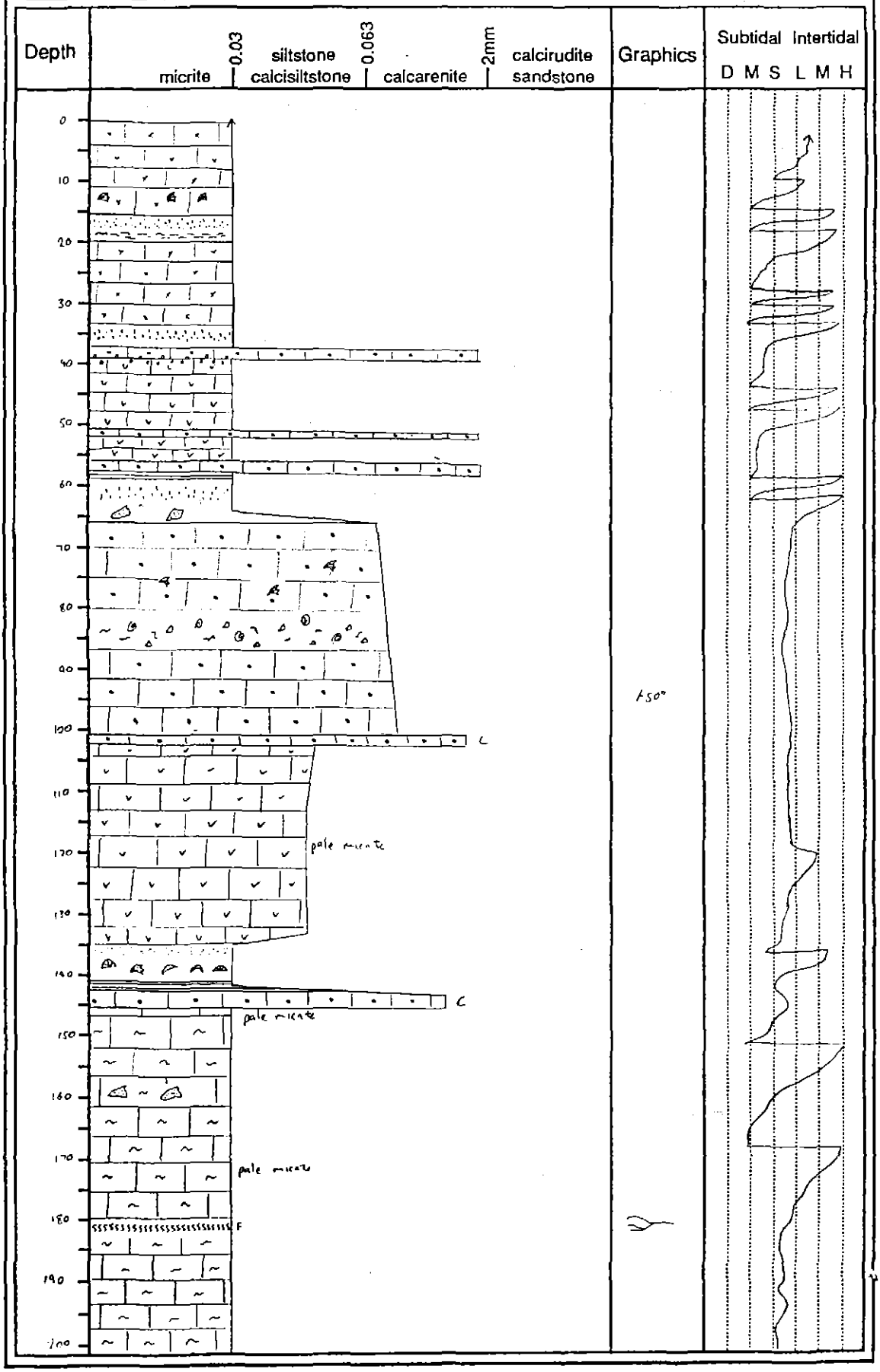

Location .....

Drill Hole No ZG 1014

Sheet no # 2 of # 2

Fault / Shear
Vein
Breccia
Disseminated
Massive

Bioturbation
Oolites
Algal Mats
Bioclastic

Brachipods
Corals
Bryozoa
Dismicrite

384300

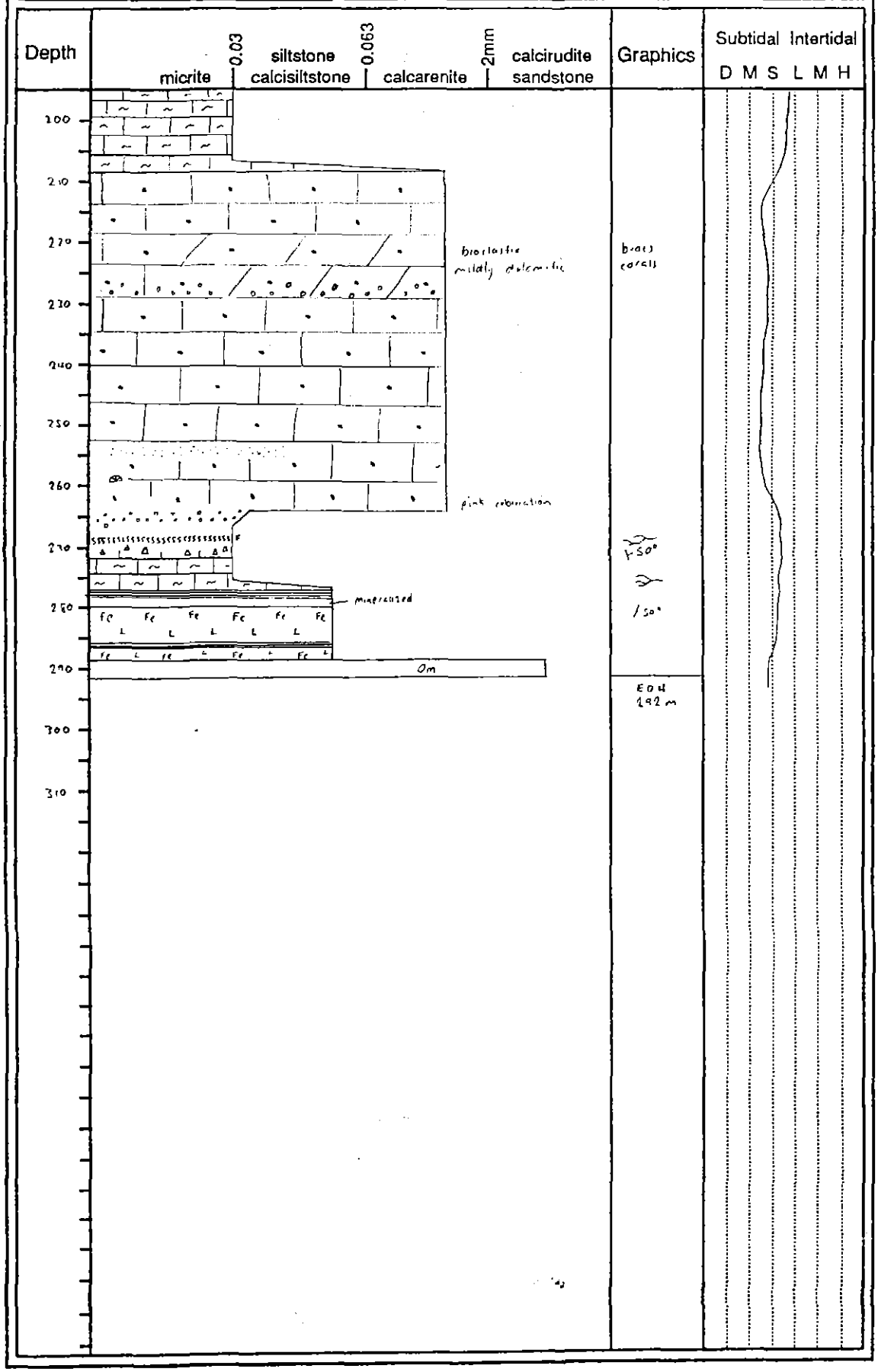

Location .....

Drill Hole No ZG 404

Sheet no #1 of #1

Fault / Shear
Vein
Breccia
Disseminated
Massive

Bioturbation
Oolites
Algal Mats
Bioclastic

Brachipods
Corals
Bryozoa
Dismicrite

384301

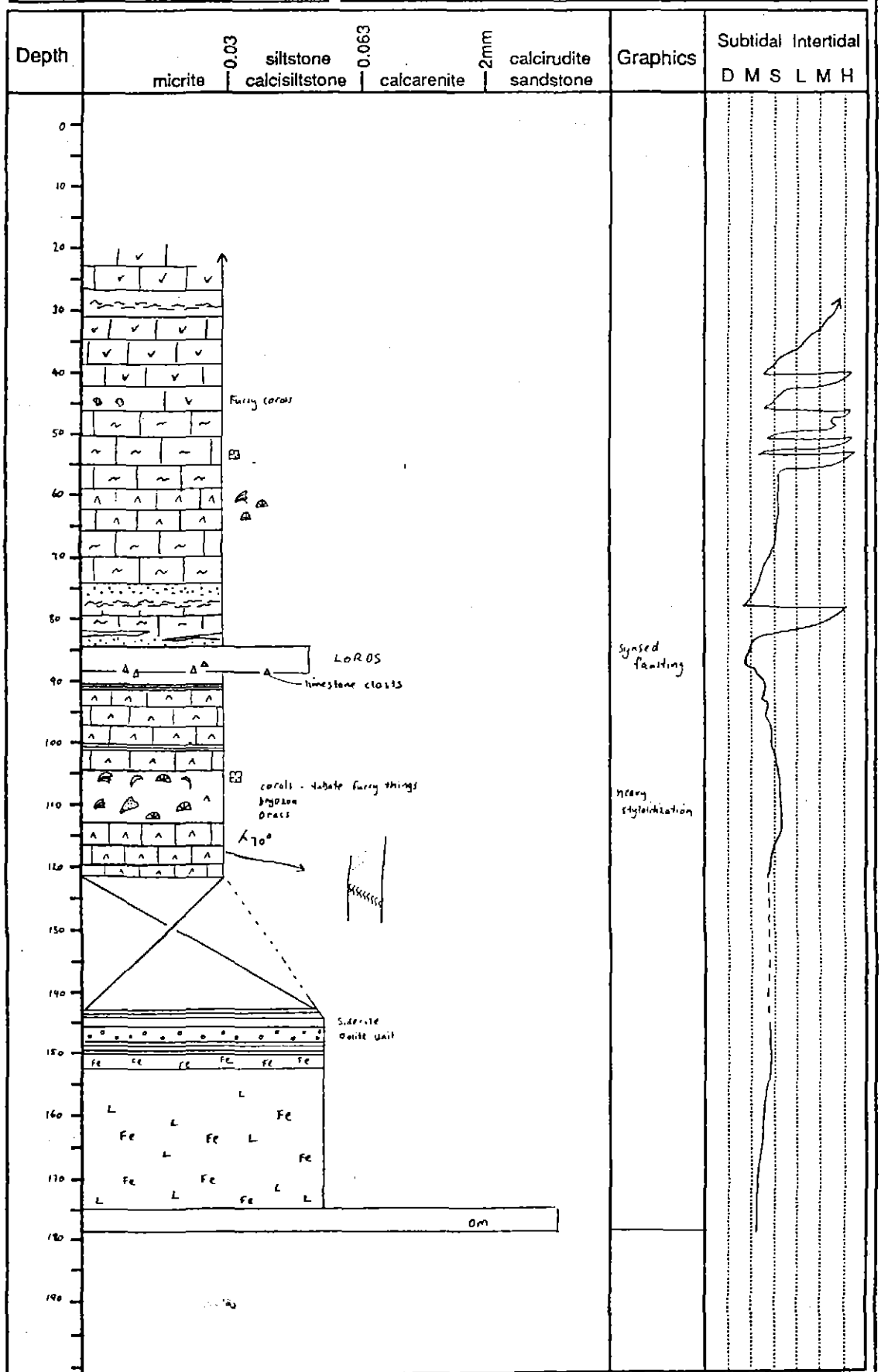

Drill Hole No 26403

Sheet no #1 of #1

Fault / Shear
Cleavage
Fining up grains
Vein
Disseminated
Massive
Bioturbation
Breccia

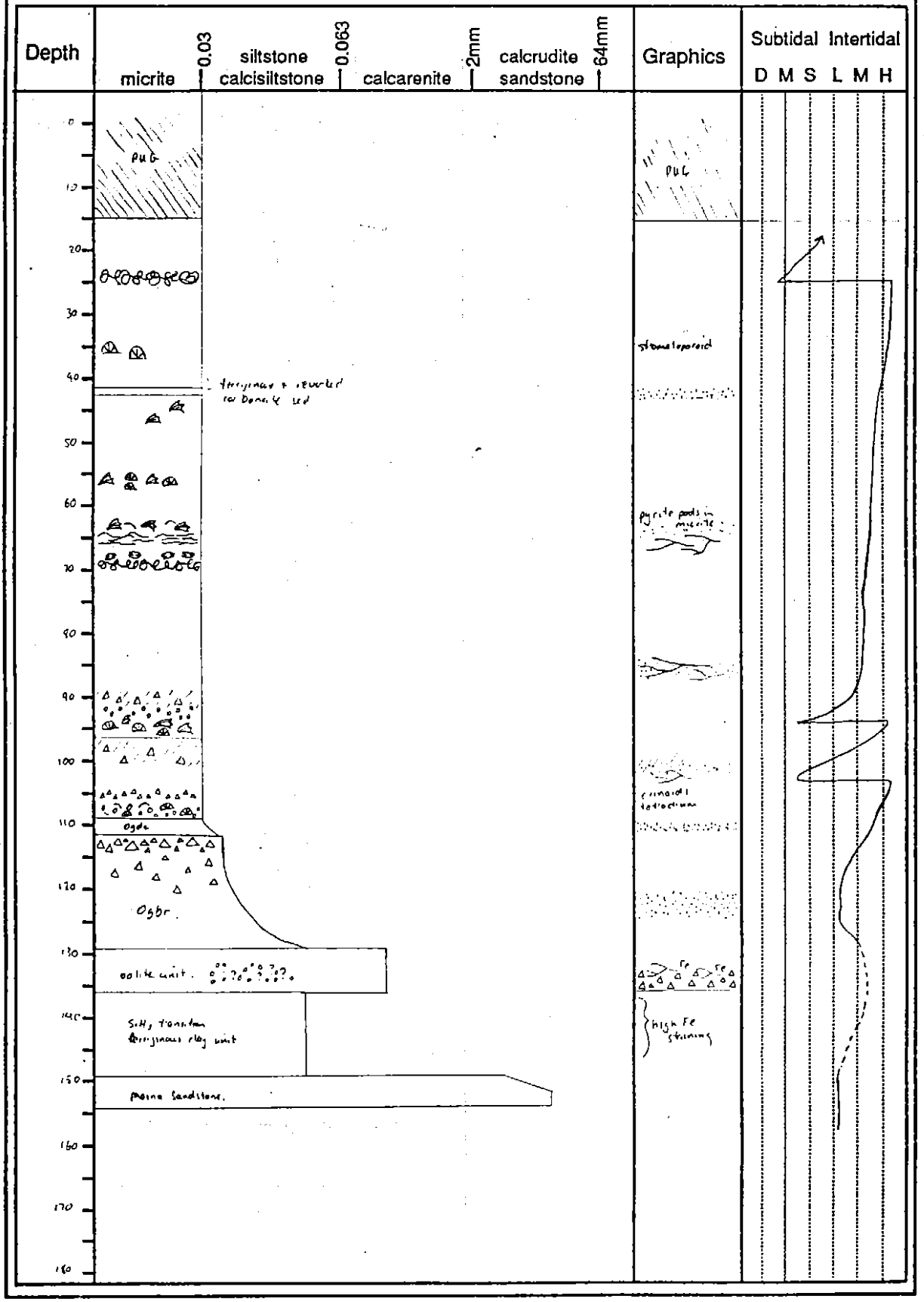

384302

Location .....

Drill Hole No ZG 1015

Sheet no #1 of #1

Fault / Shear
Vein
Breccia
Disseminated
Massive

Bioturbation
Oolites
Algal Mats
Bioclastic

Brachiopods
Corals
Bryozoa
Dismicrite

384303

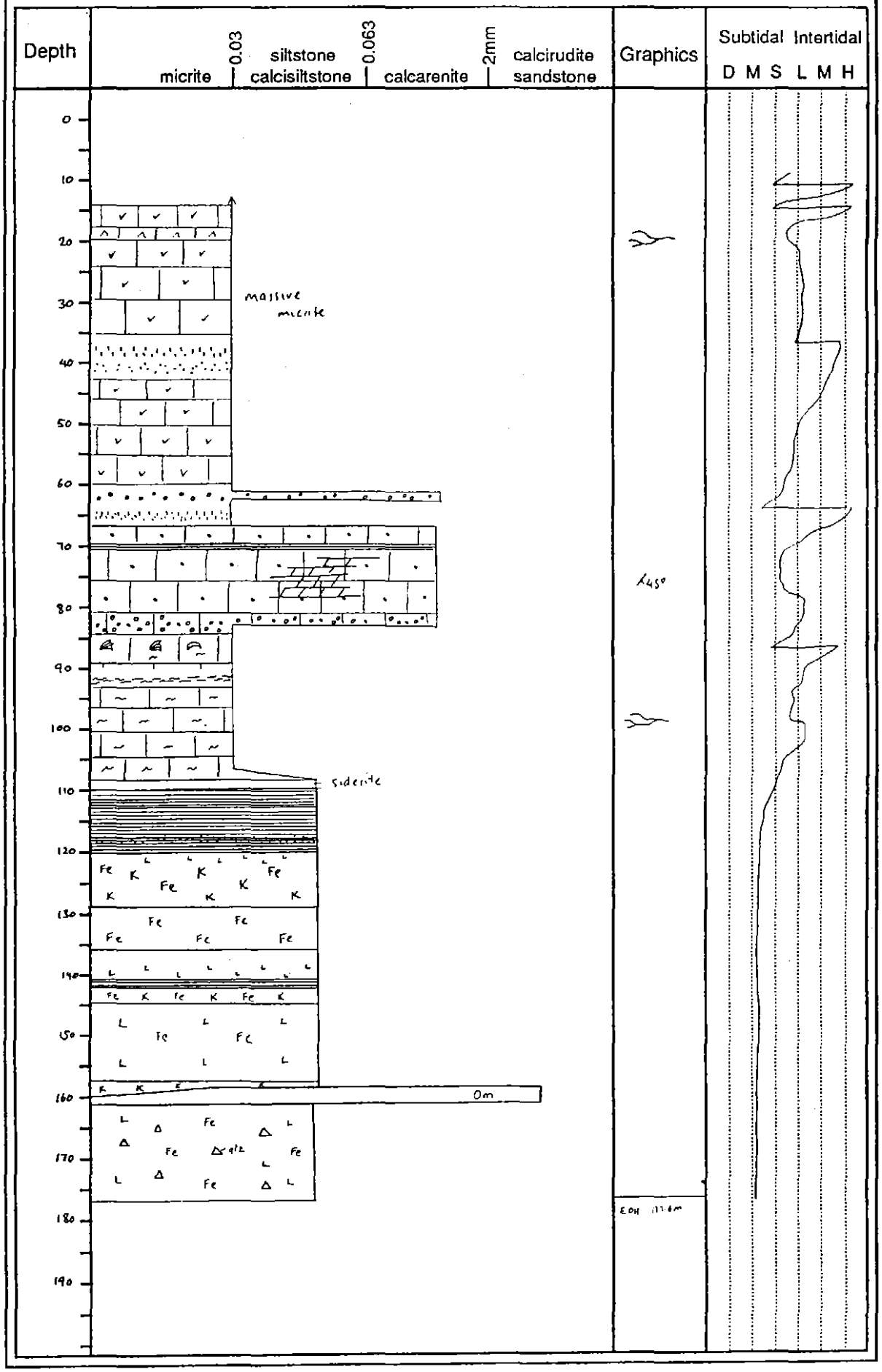

Location .....

Drill Hole No ...26 415.....

Sheet no ...#1..... of ...#1.....

Fault / Shear
Vein
Breccia
Disseminated
Massive

Bioturbation
Oolites
Algal Mats
Bioclastic

Brachipods
Corals
Bryozoa
Dismicrite

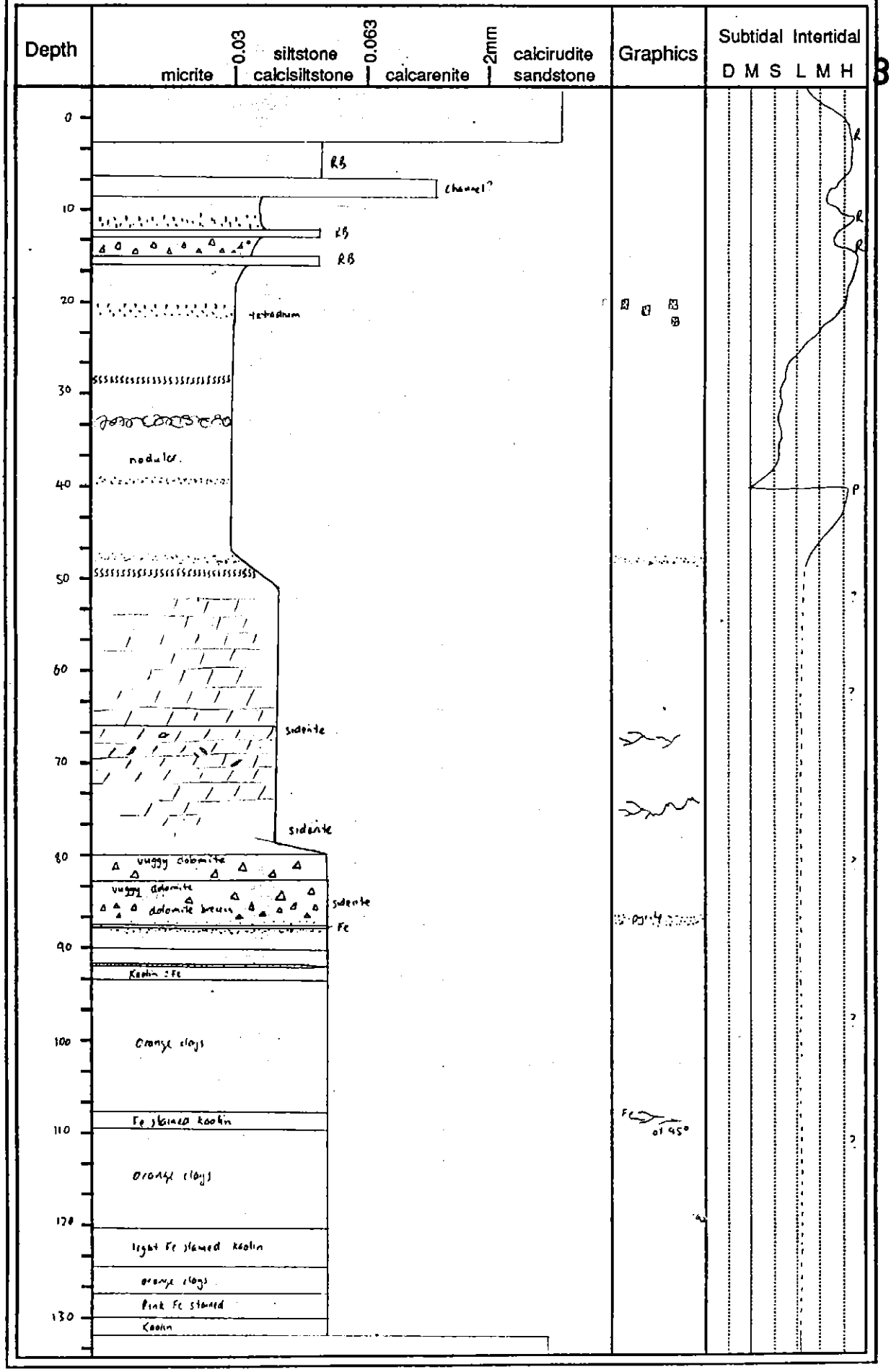

384304

384305

Appendix 2
Sedimentological Data sheets

LITHOFACIES ANALYSIS 384306

COLOUR: Fresh surface:
Weathered surface:

FRACTURE PATTERNS: Conchoidal, Subconchoidal, Uneven, Cleavage

BEDDING AND SEDIMENTARY STRUCTURES:

Bedding types: Horizontal, Biogenic, Cross bedding, Deformational, Lenticular

Bedding Surface: Even, Scour Marks, Load casts, Uneven, Pits, Current marks, Ripple Marks, Imprints

Within Beds: Laminations, Sizes, Bioturbated

Bed Thicknesses and Sed Structures.

MATRIX:

Composition: Lime Mud Matrix, Sparry Calcite Matrix

Homogeneous or Non-homogeneous

Grainsize:
Maximum _____ mm _____ Wentworth
Minimum _____ mm _____ Wentworth
Modal _____ mm _____ Wentworth

ALLOCHEM COMPOSITION:

Type _____ Proportion ____%.

SORTING: Well Sorted, Moderately Sorted, Poorly Sorted

GRAINSHAPE: Well Rounded, Rounded, Subrounded, Subangular, Angular, Very Angular

ORIENTATION: Not Orientated, Imbricated, Graded, etc.

FOSSILS: Species, Abundance, Preservation

MATURITY: Immature, Mature, Submature, Supermature

Dunham Texture: _____.

Folk Texture: _____.

384307

DEPOSITIONAL ENVIRONMENTS

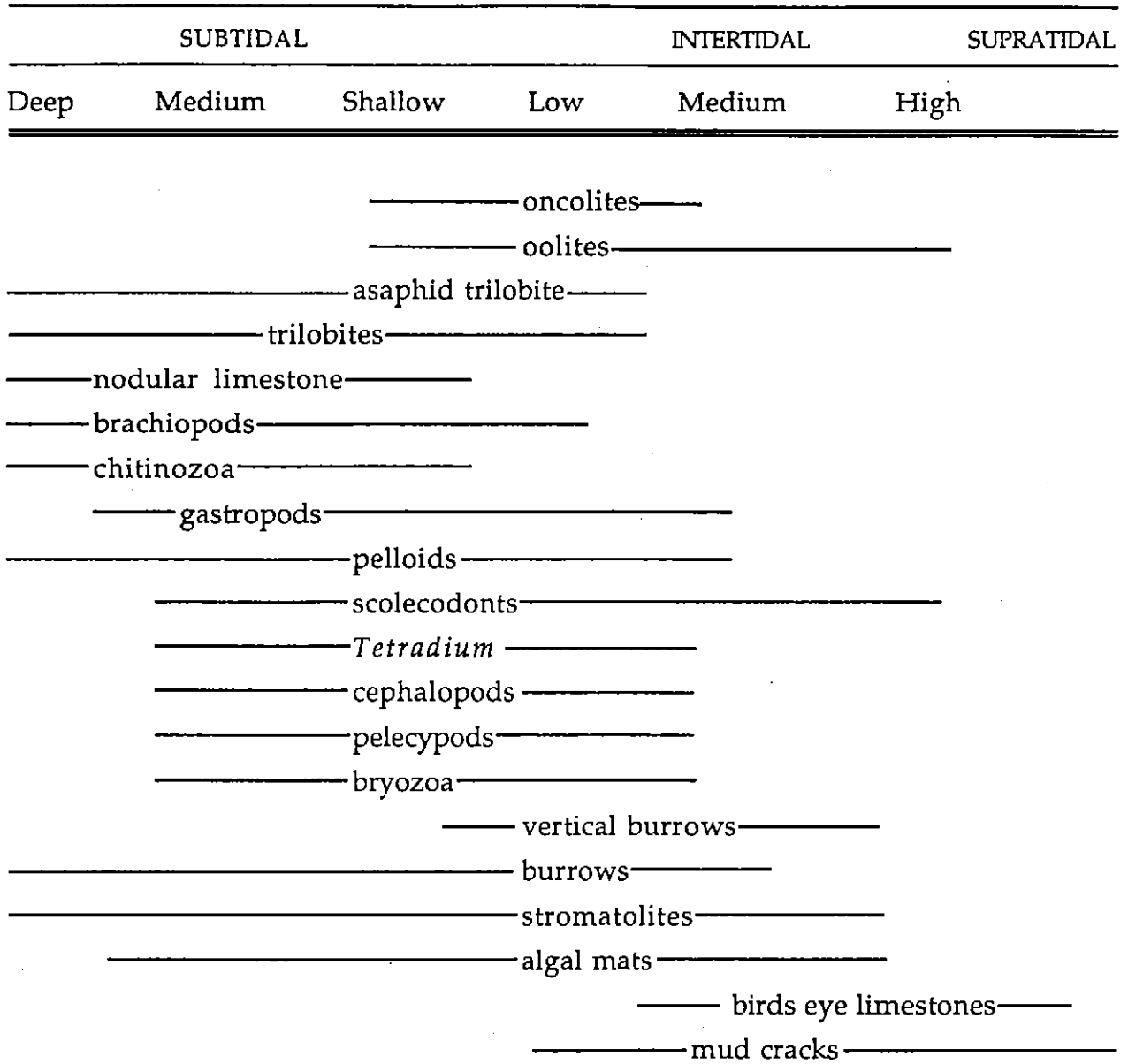

Modified after Burrett, 1978.

GRIEVES SIDING -HAND SPECIMEN DESCRIPTIONS 384308

LOCATION: _____. DATE: _____.
GRID REFERENCE: _____.
SAMPLE No: _____.
OUTCROP: _____.
_____.

100 90 80 70 60 50 40 30 20 10

ORIENTATION: Strike _____. Dip _____.
Folding _____.
_____.
Faulting _____.
_____.

COLOUR: Fresh surface: _____.
_____.
Weathered surface: _____.
_____.

GRAINSIZE: Maximum _____ mm _____ Wentworth
Minimum _____ mm _____ Wentworth
Modal _____ mm _____ Wentworth

SORTING: ☐ Well Sorted ☐ Moderately Sorted ☐ Poorly Sorted

GRAINSHAPE: ☐ Well Rounded ☐ Subrounded ☐ Angular
☐ Rounded ☐ Subangular ☐ Very Angular

INDURATION: ☐ Low ☐ Med ☐ High

ALLOCHEM COMPOSITION: _____.
_____.
_____.

MATRIX COMPOSITION: ☐ Lime Mud Matrix ☐ Sparry Calcite Matrix

MATURITY: ☐ Immature ☐ Submature
☐ Mature ☐ Supermature

MAJOR CLAST TYPES:

Type _____ Proportion ____%.

Rock Fragments ☐ Volcanic ☐ Sedimentary ☐ Metamorphic

Dunham Texture: _____.
Folk Texture: _____.
Structures: _____.
_____.

COMMENTS: _____.
_____.
_____.
_____.

Appendix 3
X-Ray Diffraction Results

TASMANIA DEVELOPMENT AND RESOURCES

Industry Safety and Mines Division

Client: D. Glover
Sample Location: Zeehan
Analysis: Approximate Mineralogy
Method: X-Ray Diffraction

Results (approx wt %)

Sample	*>60%*	*40-60%*	*25-40%*	*15-25%*	*10-15%*	*5-10%*	*<5%*
2G6.2			Kaolinite, Quartz	Illite		Sphalerite	Crandallite-type, 3.25Å, ?
2G6.4		Kaolinite[1]	Illite			Hematite, Goethite	Crandallite-type, 3.25Å
2G6.5	Kaolinite[1]			Illite			Quartz, Crandallite-type, 73.25Å
2G6.6		Quartz	Kaolinite[1]		Illite		Hematite, 73.25Å
2G6.7		Quartz, Kaolinite[1]				Illite	Hematite, Goethite, 73.25Å
2G6.8		Quartz	Illite			Kaolinite	Goethite, Crandallite-type, 3.25Å

[1] probably Dickite
The peak at 3.25Å may represent Rutile or K-Feldspar
Amorphous minerals (e.g. hydrous iron oxides) or minerals present in trace amounts may not be detected

RN Woolley

Analyst: R.N. Woolley
Date: 6 December 1995

384310

384311

TASMANIA DEVELOPMENT AND RESOURCES

Industry Safety and Mines Division

Client: D. Glover
Sample Location: Zeehan
Analysis: Carbonate Composition
Method: X-Ray Diffraction

Sample	*Carbonates (Major Peaks)*
ZB 1007 416m	2.776Å, 3.028Å
ZB UNK 200m	2.794Å
ZWG 1 14.5	2.774Å, 3.033Å
ZG 1014 280m	2.811Å
ZG 6.9 119.4	2.771Å

Quartz used as an internal standard for calibration purposes

Mineral	*Major Peak*
Siderite	2.795Å
Smithsonite	2.75Å
Calcite	3.035Å
Dolomite	2.888Å
Magnesite	2.742Å
Rhodochrosite	2.84Å

R N Woolley

Analyst: R.N. Woolley
Date: 13 December 1995

384312

TASMANIA DEVELOPMENT AND RESOURCES

Mineral Resources Tasmania

Client: D. Glover
Sample Location: Grieve's Siding, Zeehan
Analysis: Approximate Mineralogy
Method: X-Ray Diffraction

Results - Small Chip (approx wt %)

40%-60%	*25%-40%*	*15%-25%*	*10%-15%*	*5%-10%*	*<5%*
Sphalerite	Galena			Barite	Kaolinite

Peak overlap may interfere with identifications
Minerals present in trace amounts, or amorphous minerals, may not be detected

Large Specimen
Circled area - confirmed as Sphalerite

Sample peaks:

d Å	Intensity
3.122	100
2.704	8
1.913	58
1.632	30
1.562	2

Standard values:

d Å	Intensity
3.123	100
2.705	10
1.912	50
1.633	30
1.561	2

R N Woolley

Analyst: R.N. Woolley
Date: 17 April 1996

GEOLOGY OF THE GRIEVES SIDING AREA, WESTERN TASMANIA

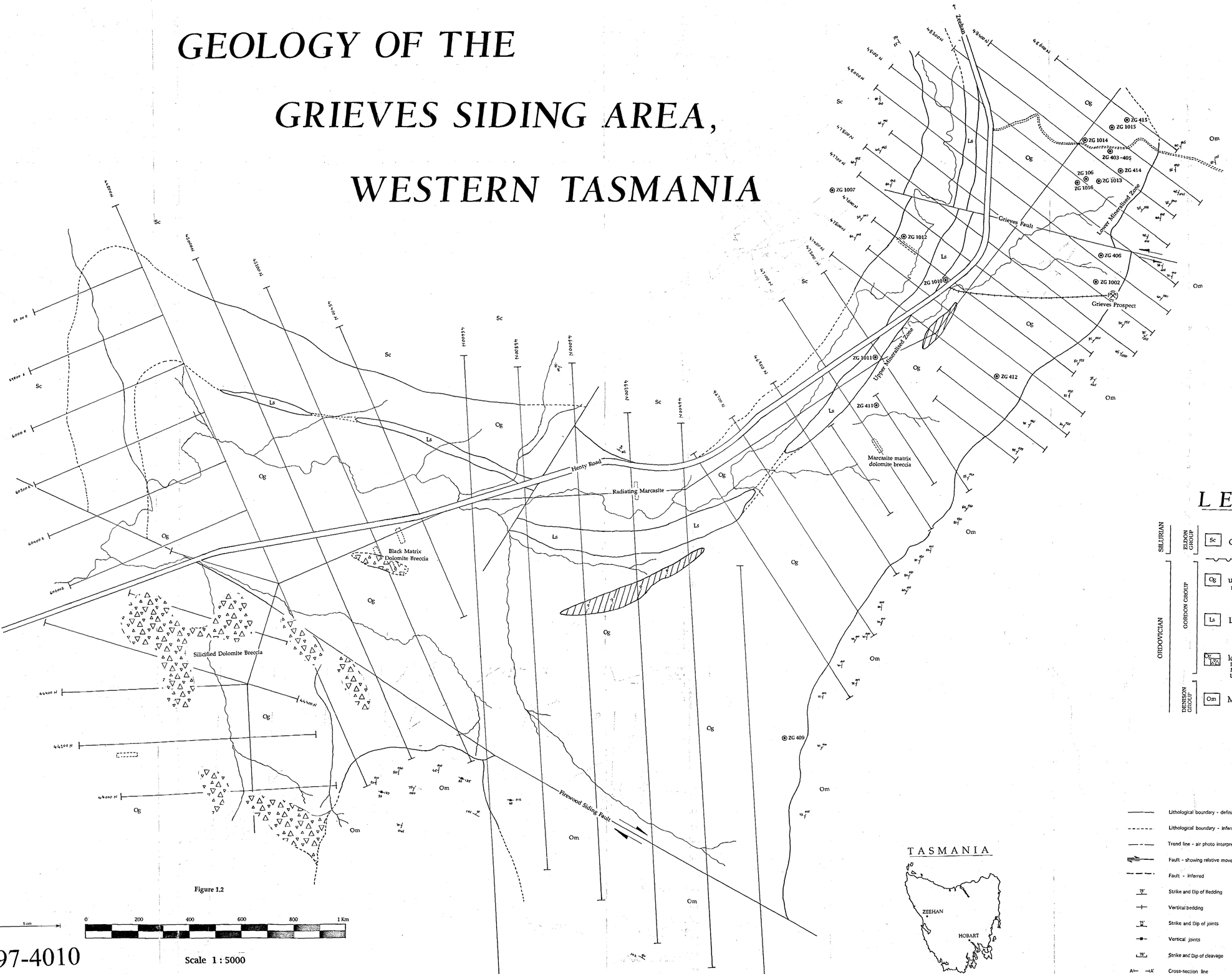

Figure 1.2

Scale 1 : 5000

MN

TN

TASMANIA

LEGEND

SILURIAN	ELDON GROUP	Sc	Crotty Quartzite — Quartz sandstones, quartz clastic conglomerates and minor mudstones
ORDOVICIAN	GORDON GROUP	Og	upper limestone, Upper Black Jacks Fm — Alternating micrite, biomicrite, and argillaceous micrite. Open subtidal fauna. Minor dolomitisation
		Ls	Lords Siltstone — Micaceous siltstone - shale and fine sandstone. Weakly fossiliferous.
		Xc, Xa	lower limestone, Lower Black Jacks Fm, Myrtle Formation, Ugbrook Formation — Micrite, biomicrite, argillaceous micrite, biosparites, sparites and calcarenites, bioturbated and weakly dolomitized. Localised Limestone Breccia.
	DENISON GROUP	Om	Moina Sandstone — Well sorted siliceous sandstone, minor conglomeratic beds, cross bedding, ripples, and vertically burrowed.

- Lithological boundary - definite
- Lithological boundary - inferred
- Trend line - air photo interpreted.
- Fault - showing relative movement
- Fault - inferred
- Strike and Dip of Bedding
- Vertical bedding
- Strike and Dip of joints
- Vertical joints
- Strike and Dip of cleavage
- A — A' Cross-section line
- Axial trace of syncline (-form) with plunge
- Axial trace of anticline (-form) with plunge
- Vergence of mesoscopic folds
- Costean
- Younging Direction
- 1st Class Sealed Road
- Gravel Road
- Tramway (abandoned)
- Prospect disbanded
- Mineralisation
- Silicification
- ZG 408 DDH

97-4010

ANNUAL REPORT - EL 38/89
CRA - S TEAR/S RUSSELL
VOL 3 OF 3

384313

Darren Glover BSc. 1996

Stratigraphy of the North Grieves Siding Area, Western Tasmania

KEY

Argillaceous micrite, calcisiltite and minor mudstone with comminuted shell debris. Nodular in part with a predominant subtidal fauna. Includes Lithofacies 7 and 8.

Nodular limestone, consisting of micrite and calcisiltite nodules in an argillecous matrix. Contains some comminuted shell debris and represents Lithofacies 8.

Upwardly shallowing Punctuated Aggrigational Cycles (PACs), representing Lithofacies 1,2,6 and 7. Consists of subtidal mudstones grading into bioturbated micrites, pale micrites, microbial laminated micrites and domal stromatolites, terminating in dismicrites.

Micrites, argillaceous and bioturbated micrites, and alternating biomicrites of Lithofacies 2,5,6 and 7. Contains subtidal to low intertidal fauna .

Calcarenites, sparites, bio-pel-oosparites etc. corresponding to Lithofacies 3 and 4. Includes insitu and tidal channel (C) deposits.

Dolomitized carbonate of Lithofacies 9.

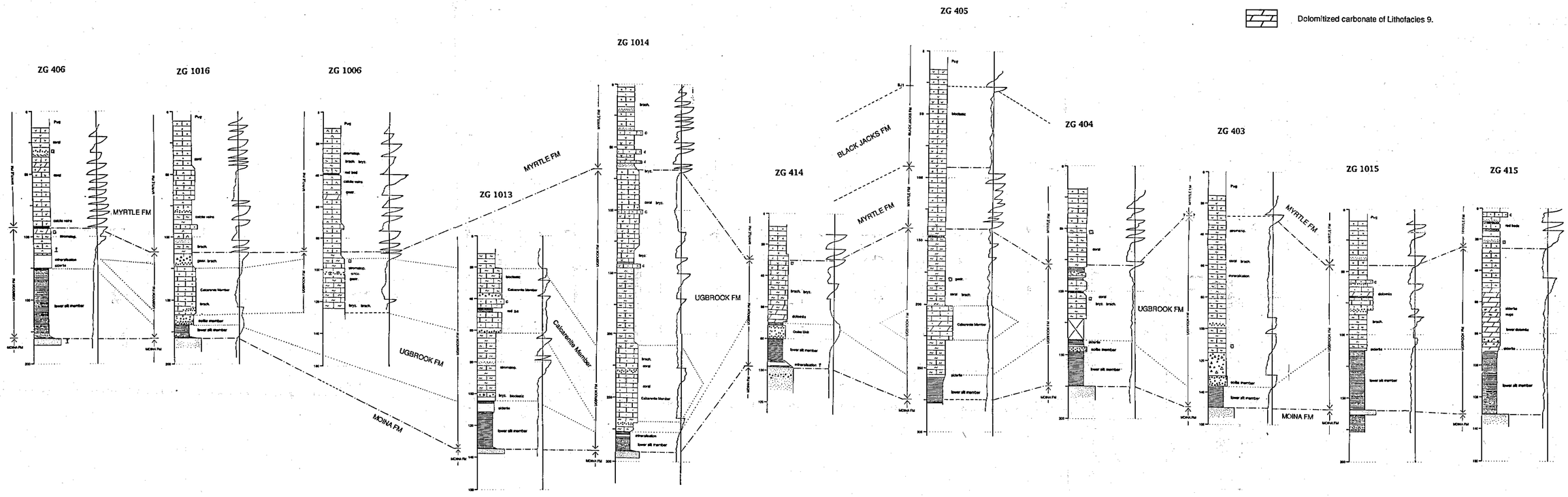

subtidal | intertidal

Relative sea-level curve, deeper to left, shallower to right.

Tetradium (a genus of Ordovician coral or coralline algae).

BJ1, BJ2 — Peritidal horizons in Black Jacks Fm

Member correlation

Formational boundary correlation

Ooids

Oncoids

Siltstones and mudstones

Pug — Decalcified and decomposed limestone

Siliclastic sandstone

97-4010

ANNUAL REPORT - EL 38/89
CRA - S TEAR/S RUSSELL
VOL 3 0F 3

384314

Figure 3.1 (b)

Compiled and drafted by Darren Glover Bsc. 1995/6

Stratigraphy of the South Grieves Siding Area, Western Tasmania

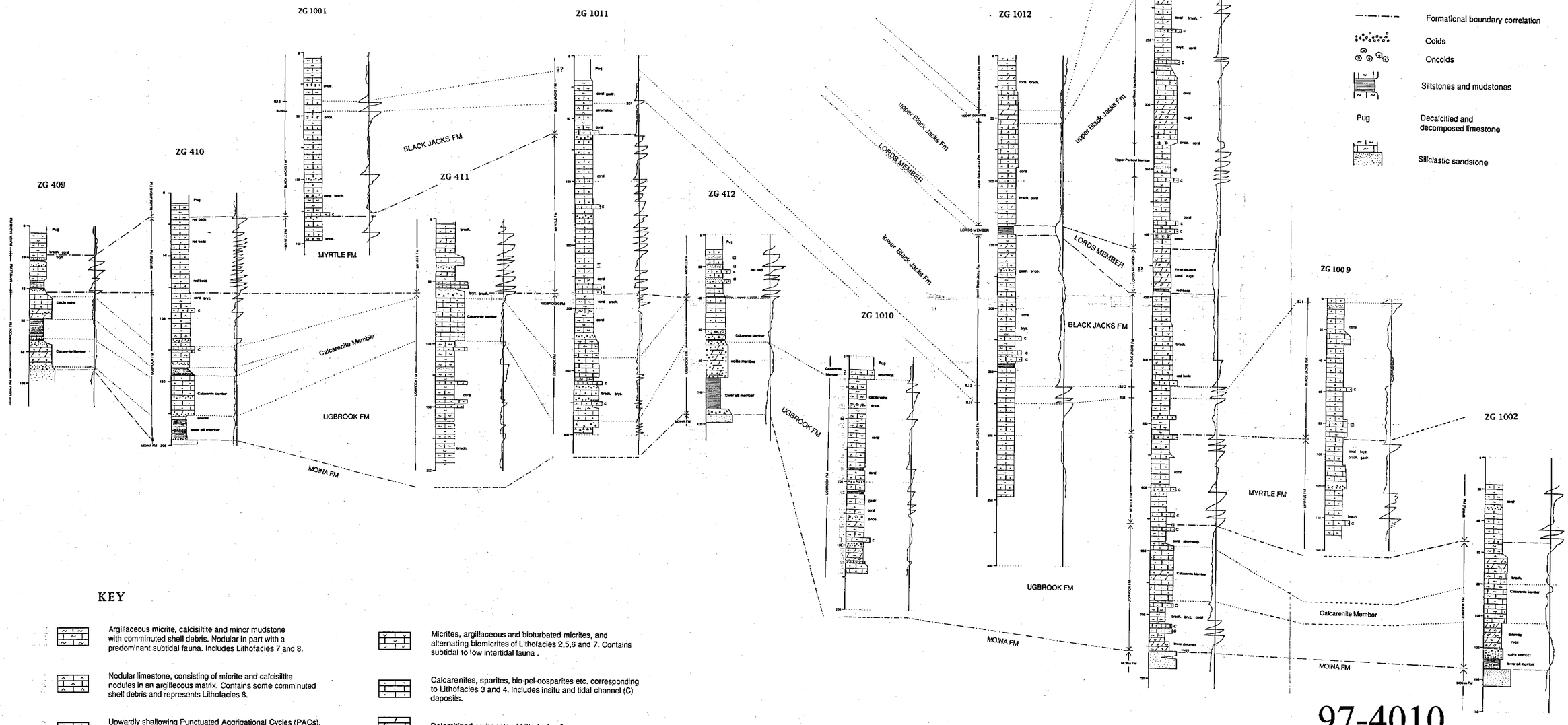

subtidal Intertidal

Relative sea-level curve, deeper to left, shallower to right.

Tetradium (a genus of Ordovician coral or coralline algae).

BJ1 BJ2 — Peritidal horizons in Black Jacks Fm

Member correlation

Formational boundary correlation

Ooids

Oncoids

Siltstones and mudstones

Pug — Decalcified and decomposed limestone

Siliclastic sandstone

KEY

Argillaceous micrite, calcisiltite and minor mudstone with comminuted shell debris. Nodular in part with a predominant subtidal fauna. Includes Lithofacies 7 and 8.

Nodular limestone, consisting of micrite and calcisiltite nodules in an argillecous matrix. Contains some comminuted shell debris and represents Lithofacies 8.

Upwardly shallowing Punctuated Aggrigational Cycles (PACs), representing Lithofacies 1,2,6 and 7. Consists of subtidal mudstones grading into bioturbated micrites, pale micrites, microbial laminated micrites and domal stromatolites, terminating in dismicrites.

Micrites, argillaceous and bioturbated micrites, and alternating biomicrites of Lithofacies 2,5,6 and 7. Contains subtidal to low intertidal fauna .

Calcarenites, sparites, bio-pel-oosparites etc. corresponding to Lithofacies 3 and 4. Includes insitu and tidal channel (C) deposits.

Dolomitized carbonate of Lithofacies 9.

97-4010

ANNUAL REPORT - EL 38/89
CRA - S TEAR/S RUSSELL
VOL 3 OF 3

384315

Compiled and drafted by Darren Glover Bsc. 1995/6

Figure 3.1 (a)

Appendix IX

Nanotem Work

384317

CRA Exploration Pty. Ltd.
N.S.W. District

Memorandum

To: R. Parkinson

Copy to: A. Doe
T. McConacy

From: J. M. Tesselaar

Date: 26 October 1995

Summary of Grieves NANOTEM

Summary:

One line of NANOTEM was conducted by Zonge Engineering over the Grieves prospect, near Zeehan during May of this year.

The NANOTEM was conducted as a trial survey to determine if it could detect variations in the thickness of the black pug layer. It has been found that where this layer is the thickest, mineralisation is the most well developed.

Extensive drilling on this line enables me to make a comparison between the geological section and the NANOTEM inversion.

The NANOTEM inversion proved successful in determining the thickness of the black pug layer.

This technique I believe could be used in similar areas as an exploration tool.

Details

During May of this year Zonge Engineering undertook a NANOTEM survey over line 48200N of the Grieves prospect.

NANOTEM is an EM system designed for high resolution near the surface. In order to do this, small loops are used and the system is designed to read the EM signal from very early times. The main use for this system is in environmental geophysics.

This survey was designed to determine the thickness of the Black Pug layer. This layer is very shallow (often <5m deep), and relatively thin (5-20 m thick). Mineralisation is best developed in the thickest zone of this clay layer (plan Tv1006).

The NANOTEM was ran as a trial survey to determine if it could resolve the thickness of these clays. It was ran over Line 48200N because ths line had a lot of geological control, obtained from drilling.

The NANOTEM was inverted by Zonge Engineering to produce a conductivity depth section. The inverted section and geological cross section are presented in plan Tv1006.

The NANOTEM inversion has been successful in determining the thickest (mineralised) clay zone. A conductivity low is evident between 61100E and 61140E. This zone corresponds to the thickest clay zone. The most conductive point on the NANOTEM however does not match the deepest point on the clays.

Discussion/Recommendations

The NANOTEM has been very successful in determining the thickest zone of the black pug clays.

On the bass of this test line, I believe that the NANOTEM would prove useful for determining the thickness of the black pug clays in other areas near Grieves.

Regards,

J.M. Tesselaar

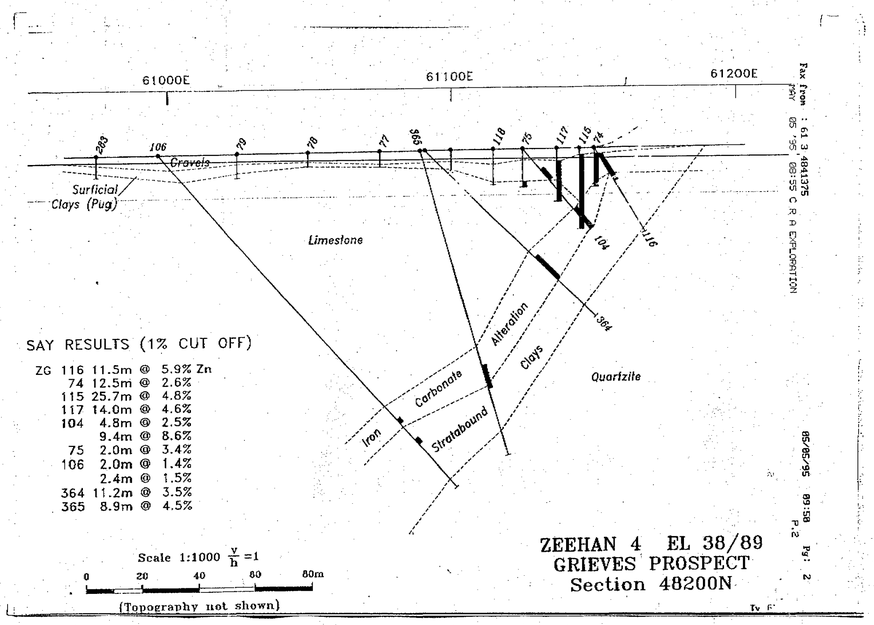

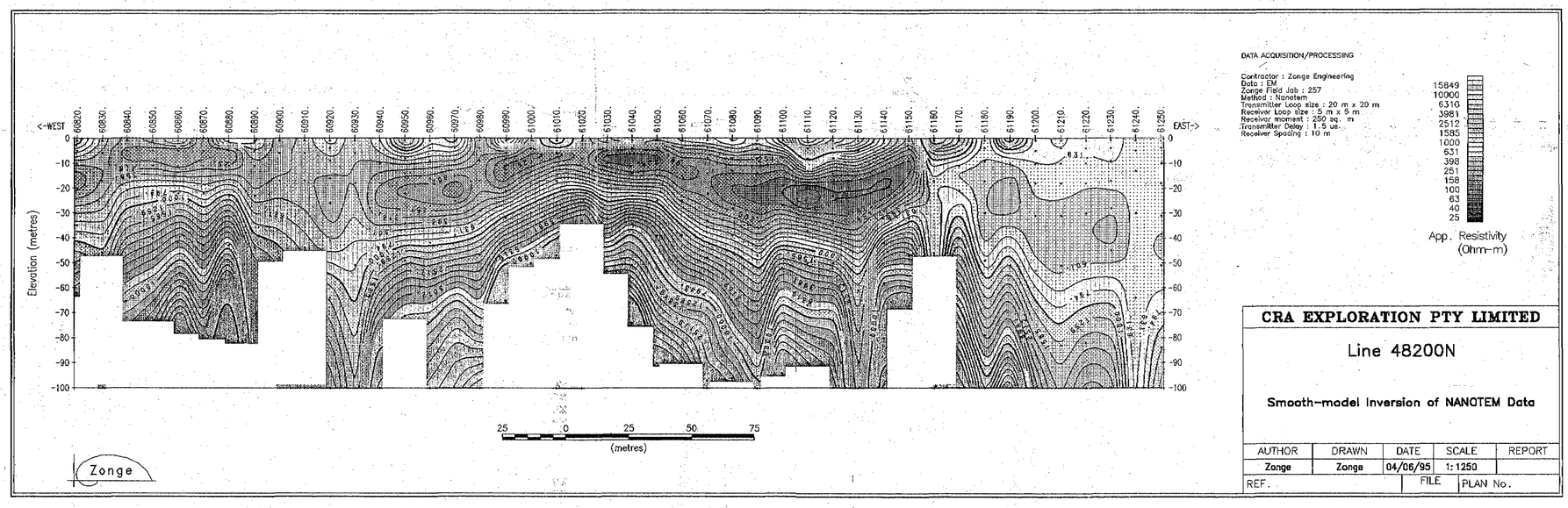

Grieves Prospect
NANOTEM Inversion & Geological section
Line 48200 N
Tasmania NE Sk-55 Dundas 3636
Scale 1:1000 5cm
Plan no: Tv1006

Appendix X

Zinc Mineralisation in the Gordon Limestone

Zinc Mineralisation of the Gordon Limestone

CRAE's exploration and research activities directed at locating carbonate-hosted Zn-Pb mineralisation within Gordon Limestone at Zeehan have led to a number of mineralisation styles being recognised. The following discussion is a synthesis of CRAE's current level of knowledge, grained from work throughout the Zeehan area.

CRAE's exploration activities in the Zeehan area have indicated that Zn-Pb mineralisation within the Gordon Limestone may be pre-Devonian in age, and therefore unrelated to the Tabberabberan Orogeny. On this basis, it is possible that carbonate-hosted Zn-Pb mineralisation may be more widespread than that presently under evaluation at Zeehan.

The Gordon Limestone originally occupied a large area, deposited at the close of a major period of tectonic activity that produced the metal-rich Mount Read Volcanics. During and immediately before carbonate deposition the tectonic regime was still unstable, evidenced by rapid changes in stratigraphic thickness of Ordovician strata. Hydrothermal systems may have continued to emit metals into this system, focused by basement irregularities and syn-sedimentary faults. Basin-bounding syn-sedimentary faults in the Zeehan area are WNW-trending, and include the Firewood Siding Fault on the SW side, and Professor Range and Balstrup Faults on the NE side.

The present Gordon Limestone exposure is a vestige of Devonian deformation. Ordovician mineralisation may have a distribution totally independent of the well-documented Devonian systems.

Five targets are recognised for the carbonate-hosted Zn mineralisation in Gordon Limestone at Zeehan, subdivided by the stratigraphic interval in which they are hosted (Figure):-

- stratabound at the lower limestone-sandstone contact
- stratabound at the upper limestone-quartzite contact
- stratabound within a sub-unit in the middle of the limestone sequence
- structurally controlled discordant mineralisation
- surficial "clay-hosted" accumulations developed above primary mineralisation.

Stratabround at the lower limestone-sandstone contact
Mineralisation at Grieves and Mariposa falls into this category. Alteration located at Blackjacks, Pyramid and Professor Range may also belong to this deposit type.

This position is characterised by carbonaceous and/or ferruginous clays resting on the Moina Sandstone, in turn overlain by a massive siderite zone. The siderite zones passes stratigraphically upward either gradationally or abruptly into unaltered and unmineralised limestone. The clay layer may be up to 50m thick and the siderite zone up to 25m thick. Both may contain Zn mineralisation up to several percent. The clay and siderite zone are laterally quite uniform and it may be that the mineralisation is actually stratiform.

Mineralisation of this style has an alteration halo that is both visually and geochemically distinct. This halo, characterised by vughy, broken or massive recrystallised Fe-carbonate and Fe-rich clays, may extend laterally hundreds of metres beyond the main Zn mineralisation, and thus present a considerably larger target than the mineralised core. Lateral alteration geochemistry is reflected by Fe-Mn-As-Zn. Stratigraphy above the mineralised core is a weaker halo of elevated Zn ($\pm$ As).

Ore mineralogy, based on work at Grieves, is complex with a mixture of zincian siderite and minor sphalerite in the siderite zone, and a Zn-clay with minor to moderate amounts of sphalerite in the siderite zone, and a Zn-clay with minor to moderate amounts of sphalerite in the clay zone. It is not known whether this is a regional characteristic of this position. It could be possible that the complex clay mineralogy is a supergene weathering process acting on an original sphalerite-pyrite mineralised black shale. The siderite may be capping the sulphide systems, preserved in its primary form due to its low porosity and permeability.

The stratiform character, replacive style of alteration/mineralisation, intense Fe-Mn alteration, and reasonably predictable geometry suggest similarities to Navan or Reocin.

Stratabound at the upper limestone-quartzite contact
Low-grade but widely anomalous zones from Firewood Siding, Grieves, Professor Range, Sunny Corner, and Mariposa are examples of this type.

Upper zone mineralisation occurs near the contact between the limestone and overlying Crotty Quartzite. Mineralisation is not closely bound to the upper quartzite contact, but may "wander" up to 100m stratigraphically below the contact.

Mineralisation appears characterised by widespread but low-level Zn in the 0.1% to 2% Zn range. None of the prospects tested has revealed a higher-grade core, although given the limited drilling it is entirely possible high-grade cores may exist. Limited mineralogy suggests all Zn to be as sphalerite.

Aircore drilling shows the mineralised zones to be comprised of clays and decomposed carbonate. Rare fresher material is usually a granular recrystallised dolomite, and can be ferroan. Intense siderite alteration is absent. A detailed geochemical study of the alteration has not been completed.

The upper zone style may be occurring within karstic structures formed by Ordovician weathering before deposition of the Crotty Quartzite. This setting is analogous to Bleiberg or Cracow-Silesia.

Stratabround in a middle sub-unit of the limestone sequence
Currently two occurrences fall into this grouping, Grieves middle zone, and Oceana. Apart from their stratigraphic concurrence, these two deposits may not share many other similarities.

The mineralised middle sub-unit is equidistant from the upper and lower contacts, although facies variations may affect the location at other prospects. Mineralisation is breccia hosted, and in the case of Grieves has a linear aspect. For Grieves there is very little indication of proximity to mineralisation as there is virtually no alteration outside the breccia zone itself.

Mineralogy at Grieves is a mixture of zincian siderite and sphalerite. Oceana is dominated by galena with subordinate (?) sphalerite. There is also intense siderite alteration at Oceana, presumably containing Zn?

Zinc grades at both prospects are high, locally forming massive sulphide.

There has been insufficient work completed at Grieves middle zone to suggest any controlling mechanisms.

Structurally controlled discordant mineralisation
Most mineralisation in the Zeehan area is structurally controlled. Mineralisation at the historic Mariposa mine, and at Myrtle belong to this type. Possibly some of the mineralisation at Oceana is also structurally controlled.

Structurally controlled mineralisation may occur at any stratigraphic level. It appears to be late-stage filling of brittle fractures. Alteration of wall-rocks is absent, and the gangue to mineralisation may be pure calcite. Mineralisation within the structures is patchily distributed. Ore minerals are coarse-grained sulphides.

Devonian deformation is the likely cause of the fracturing and mineralisation. Potential deposit size is small, although the presence of discordant mineralisation may indicate a nearby stratabound source. Late-stage structurally controlled deposits *per se* are not currently considered a valid CRAE target.

Surficial "clay-hosted" accumulations developed above primary mineralisation
Surficial Zn accumulations within decomposed carbonate was CRAE's original target for carbonate exploration in Zeehan. All currently tested prospects were selected due to the presence of known surficial mineralisation.

It has now been conclusively demonstrated that the surficial mineralisation occupies the surface trace of underlying stratabound mineralisation. Geometry of the surficial deposits are therefore dependent on the shape and extent of this underlying mineralisation. Depth extent of the Zn-rich clays and decomposed carbonates averages 10m to 20m, but have been reported to be over 100m at Oceana.

A thin layer of decomposed carbonate exists over large areas of limestone, but this layer only thickens and becomes substantially Zn-rich as "basement" mineralisation is approached. Areas of +0.1% Zn in the clay layer are regionally extensive, indicating substantial dispersions from the primary zone. Clay thickness and Zn grade may be useful vectors toward primary zones. Geochemically inert peat and gravels up to 5m thick obscure the clays and limestone over virtually the entire trace of the Gordon Limestone.

Zinc ore mineralogy is dominantly to exclusively sphalerite.

Because of their restriction to the surface zone, the potential size of the surficial deposit is somewhat limited. They are probably unlikely to be a CRA target in themselves. Their main attraction is their usefulness as an indicator of the underlying primary mineralisation. If a large primary deposit suitable to CRAE's requirements can be identified, then the surficial deposits would possible be an easy way to generate short-term cash-flow whilst the major deposit was being developed.

Zinc-rich clay deposits overlying primary carbonate mineralisation have been described at Tynagh and Silvermines.

R.G.Parkinson